

# The pivotal role of oral microbiota dysbiosis and microbiota-host interactions in diseases

**Edited by**

Yulong Niu, Huizhi Wang, Xin Xu and Jin Xiao

**Published in**

Frontiers in Cellular and Infection Microbiology



## FRONTIERS EBOOK COPYRIGHT STATEMENT

The copyright in the text of individual articles in this ebook is the property of their respective authors or their respective institutions or funders. The copyright in graphics and images within each article may be subject to copyright of other parties. In both cases this is subject to a license granted to Frontiers.

The compilation of articles constituting this ebook is the property of Frontiers.

Each article within this ebook, and the ebook itself, are published under the most recent version of the Creative Commons CC-BY licence. The version current at the date of publication of this ebook is CC-BY 4.0. If the CC-BY licence is updated, the licence granted by Frontiers is automatically updated to the new version.

When exercising any right under the CC-BY licence, Frontiers must be attributed as the original publisher of the article or ebook, as applicable.

Authors have the responsibility of ensuring that any graphics or other materials which are the property of others may be included in the CC-BY licence, but this should be checked before relying on the CC-BY licence to reproduce those materials. Any copyright notices relating to those materials must be complied with.

Copyright and source acknowledgement notices may not be removed and must be displayed in any copy, derivative work or partial copy which includes the elements in question.

All copyright, and all rights therein, are protected by national and international copyright laws. The above represents a summary only. For further information please read Frontiers' Conditions for Website Use and Copyright Statement, and the applicable CC-BY licence.

ISSN 1664-8714  
ISBN 978-2-83251-122-0  
DOI 10.3389/978-2-83251-122-0

## About Frontiers

Frontiers is more than just an open access publisher of scholarly articles: it is a pioneering approach to the world of academia, radically improving the way scholarly research is managed. The grand vision of Frontiers is a world where all people have an equal opportunity to seek, share and generate knowledge. Frontiers provides immediate and permanent online open access to all its publications, but this alone is not enough to realize our grand goals.

## Frontiers journal series

The Frontiers journal series is a multi-tier and interdisciplinary set of open-access, online journals, promising a paradigm shift from the current review, selection and dissemination processes in academic publishing. All Frontiers journals are driven by researchers for researchers; therefore, they constitute a service to the scholarly community. At the same time, the *Frontiers journal series* operates on a revolutionary invention, the tiered publishing system, initially addressing specific communities of scholars, and gradually climbing up to broader public understanding, thus serving the interests of the lay society, too.

## Dedication to quality

Each Frontiers article is a landmark of the highest quality, thanks to genuinely collaborative interactions between authors and review editors, who include some of the world's best academicians. Research must be certified by peers before entering a stream of knowledge that may eventually reach the public - and shape society; therefore, Frontiers only applies the most rigorous and unbiased reviews. Frontiers revolutionizes research publishing by freely delivering the most outstanding research, evaluated with no bias from both the academic and social point of view. By applying the most advanced information technologies, Frontiers is catapulting scholarly publishing into a new generation.

## What are Frontiers Research Topics?

Frontiers Research Topics are very popular trademarks of the *Frontiers journals series*: they are collections of at least ten articles, all centered on a particular subject. With their unique mix of varied contributions from Original Research to Review Articles, Frontiers Research Topics unify the most influential researchers, the latest key findings and historical advances in a hot research area.

Find out more on how to host your own Frontiers Research Topic or contribute to one as an author by contacting the Frontiers editorial office: [frontiersin.org/about/contact](https://frontiersin.org/about/contact)



# The pivotal role of oral microbiota dysbiosis and microbiota-host interactions in diseases

## Topic editors

Yulong Niu — Sichuan University, China

Huizhi Wang — Virginia Commonwealth University, United States

Xin Xu — Sichuan University, China

Jin Xiao — University of Rochester Medical Center, United States

## Citation

Niu, Y., Wang, H., Xu, X., Xiao, J., eds. (2023). *The pivotal role of oral microbiota dysbiosis and microbiota-host interactions in diseases*.

Lausanne: Frontiers Media SA. doi: 10.3389/978-2-83251-122-0

# Table of contents

- 05 **Editorial: The Pivotal Role of Oral Microbiota Dysbiosis and Microbiota-Host Interactions in Diseases**  
Xin Xu, Jin Xiao and Yulong Niu
- 09 **Alteration in Oral Microbiome Among Men Who Have Sex With Men With Acute and Chronic HIV Infection on Antiretroviral Therapy**  
Shuang Li, Junping Zhu, Bin Su, Huanhuan Wei, Fei Chen, Hongshan Liu, Jiaqi Wei, Xiaodong Yang, Qiuyue Zhang, Wei Xia, Hao Wu, Qiushui He and Tong Zhang
- 20 **Machine Learning Approach Identified Multi-Platform Factors for Caries Prediction in Child-Mother Dyads**  
Tong Tong Wu, Jin Xiao, Michael B. Sohn, Kevin A. Fiscella, Christie Gilbert, Alex Grier, Ann L. Gill and Steve R. Gill
- 30 **Effects of *Helicobacter pylori* Infection on the Oral Microbiota of Reflux Esophagitis Patients**  
Tian Liang, Fang Liu, Lijun Liu, Zhiying Zhang, Wenxue Dong, Su Bai, Lifeng Ma and Longli Kang
- 43 **Taxonomic and Functional Dysregulation in Salivary Microbiomes During Oral Carcinogenesis**  
Jiung-Wen Chen, Jer-Horng Wu, Wei-Fan Chiang, Yuh-Ling Chen, Wei-Sheng Wu and Li-Wha Wu
- 59 **Oral Osteomicrobiology: The Role of Oral Microbiota in Alveolar Bone Homeostasis**  
Xingqun Cheng, Xuedong Zhou, Chengcheng Liu and Xin Xu
- 78 **Effect of Cavity Cleanser With Long-Term Antibacterial and Anti-Proteolytic Activities on Resin–Dentin Bond Stability**  
Yaping Gou, Wei Jin, Yanning He, Yu Luo, Ruirui Si, Yuan He, Zhongchi Wang, Jing Li and Bin Liu
- 91 **Comparative Analysis of Salivary Mycobiome Diversity in Human Immunodeficiency Virus-Infected Patients**  
Shenghua Chang, Haiying Guo, Jin Li, Yaoting Ji, Han Jiang, Lianguo Ruan and Minquan Du
- 100 **Protein Tyrosine and Serine/Threonine Phosphorylation in Oral Bacterial Dysbiosis and Bacteria-Host Interaction**  
Liang Ren, Daonan Shen, Chengcheng Liu and Yi Ding
- 112 **Raman Spectroscopy: A Potential Diagnostic Tool for Oral Diseases**  
Yuwei Zhang, Liang Ren, Qi Wang, Zhining Wen, Chengcheng Liu and Yi Ding
- 129 **The Application of Small Molecules to the Control of Typical Species Associated With Oral Infectious Diseases**  
Sirui Yang, Xiaoying Lyu, Jin Zhang, Yusen Shui, Ran Yang and Xin Xu

- 146 **Influence of Fluoride-Resistant *Streptococcus mutans* Within Antagonistic Dual-Species Biofilms Under Fluoride *In Vitro***  
Keke Zhang, Yangfan Xiang, Youjian Peng, Fengyu Tang, Yanfan Cao, Zhenjie Xing, Yejian Li, Xiangyan Liao, Yan Sun, Yan He and Qingsong Ye
- 158 ***Porphyromonas gingivalis* Induces Increases in Branched-Chain Amino Acid Levels and Exacerbates Liver Injury Through *livh/livk***  
Leng Wu, Rui Shi, Huimin Bai, Xingtong Wang, Jian Wei, Chengcheng Liu and Yafei Wu
- 170 **Probiotic Species in the Management of Periodontal Diseases: An Overview**  
Yuwei Zhang, Yi Ding and Qiang Guo
- 185 **Oral Microbiota-Host Interaction Mediated by Taste Receptors**  
Hao Dong, Jiaxin Liu, Jianhui Zhu, Zhiyan Zhou, Marco Tizzano, Xian Peng, Xuedong Zhou, Xin Xu and Xin Zheng



# Editorial: The Pivotal Role of Oral Microbiota Dysbiosis and Microbiota-Host Interactions in Diseases

Xin Xu<sup>1\*</sup>, Jin Xiao<sup>2</sup> and Yulong Niu<sup>3</sup>

<sup>1</sup> State Key Laboratory of Oral Diseases, National Clinical Research Center for Oral Diseases, West China Hospital of Stomatology, Sichuan University, Chengdu, China, <sup>2</sup> Eastman Institute for Oral Health, University of Rochester Medical Center, Rochester, NY, United States, <sup>3</sup> Key Laboratory of Bio-Resources and Eco-Environment of Ministry of Education, College of Life Sciences, Sichuan University, Chengdu, China

**Keywords:** oral diseases, dental caries, periodontitis, oral microbiota, probiotics, HIV - human immunodeficiency virus, Raman spectroscopy

## Editorial on the Research Topic

### The Pivotal Role of Oral Microbiota Dysbiosis and Microbiota-Host Interactions in Diseases

## OPEN ACCESS

### Edited and reviewed by:

Benoit Chassaing,  
Institut National de la Santé et de la  
Recherche Médicale (INSERM),  
France

### \*Correspondence:

Xin Xu  
xin.xu@scu.edu.cn

### Specialty section:

This article was submitted to  
Microbiome in Health and Disease,  
a section of the journal  
Frontiers in Cellular and  
Infection Microbiology

**Received:** 19 May 2022

**Accepted:** 30 May 2022

**Published:** 14 June 2022

### Citation:

Xu X, Xiao J and Niu Y (2022) Editorial:  
The Pivotal Role of Oral Microbiota  
Dysbiosis and Microbiota-Host  
Interactions in Diseases.  
Front. Cell. Infect. Microbiol. 12:947638.  
doi: 10.3389/fcimb.2022.947638

The oral microbiome is an important constituent of human microbiome, playing a pivotal role in human health. Oral microbial dysbiosis is the major causative factor of oral diseases such as dental caries and periodontal diseases, and it is also closely associated with systemic diseases such as cardiovascular diseases, diabetes, and gastrointestinal diseases, etc (Hajishengallis, 2015; Hajishengallis and Chavakis, 2021). The last two decades have witnessed tremendous progress in the field of oral microbiota and its related human diseases, largely due to the advancement in high throughput “-omics” techniques such as metagenomics and metatranscriptomics. In addition, the development of non-invasive detection methods such as Raman Spectroscopy also makes the dynamic detection of microbial metabolic activity possible (Su et al., 2020). Oral microbiota can be recognized as the “fingerprint” of human health, and tools and models developed based on metadata and comprehensive bioinformatics can be utilized to robustly predict the occurrence and prognosis of oral diseases as well as the related systemic diseases (Xu et al., 2017). In addition, identification of *Porphyromonas gingivalis* as the keystone pathogen of periodontitis has greatly advanced the knowledge on the pathogenesis of this disease (Hajishengallis et al., 2012). Novel approaches that can specifically target key pathogens are promising for the ecological management of oral diseases. In this Research Topic, we have included eight original research articles as well as six comprehensive reviews, covering the novel findings in oral microbiota dysbiosis and microbiota-host interactions, and new compounds or novel approaches in the diagnosis and treatment of diseases associated with oral microbial dysbiosis.

The relationship between oral cancer and microbiome has been suggested, but with controversial conclusions (Kamarajan et al., 2020; Sepich-Poore et al., 2021). Chen et al. investigated the salivary microbiome in the cohorts of orally healthy, non-recurrent oral verrucous hyperplasia, and oral verrucous hyperplasia-associated oral cancer at taxonomic and function levels. They demonstrated that predicted functional profiles were more related to the alterations of oral health status as compared to taxonomic data. In addition to oral cancer, increasing evidence has suggested the association of HIV infection and oral microbiota (Annavaiah et al., 2020; Fulcher, 2020). However,



the impact of antiretroviral therapy (ART) on oral microbiome of HIV-infected patients has yet to be investigated. Li et al. performed a longitudinal comparative study, and investigated the oral microbial alterations in the men who have sex with men with acute/chronic HIV infections. They found that microbial diversity was significantly decreased in patients with acute and chronic HIV infections compared with those HIV-free individuals before and after ART. Specific genera with altered abundance were also identified to be associated with HIV infection and ART administration. In addition to bacterial dysbiosis, HIV-infected individuals are more susceptible to fungal infections (Patil et al., 2018). The longitudinal study by Chang et al. identified an increased diversity and richness of salivary mycobiome in HIV-infected individuals as compared to the HIV-free controls. After ART, the diversity and richness of salivary mycobiome in HIV-infected patients were reduced significantly. These findings suggest that both HIV infection and ART administration have significantly impact on salivary mycobiome, which might mirror the immune state of the body. In addition to viral infection that can alter oral microbiome, translocation of specific pathogens also contributes to the microbial alterations in the oral cavity. A cross-sectional study on reflux esophagitis patients by Liang et al. demonstrated that reflux esophagitis significantly disturbed oral microbiome with an increased beta diversity, and *Helicobacter pylori* infection could inhibit this disorderly trend.

As the occurrence, progression and prognosis of oral diseases are accompanied with compositional and metabolic alterations of oral microbiota, development of non-invasive, high throughput detection tools with single-cell resolutions are promising in the diagnosis, treatment planning and outcome evaluation of oral diseases. Raman spectroscopy detects molecular vibration information by collecting inelastic scattering light, which provides rapid, sensitive, accurate, and minimally invasive detection (Xu et al., 2017). Zhang et al. reviewed the application of Raman spectroscopy in the early diagnosis, treatment and prognosis evaluation of oral diseases including dental caries, periodontal diseases and oral cancer. Although Raman spectroscopy is promising, the authors suggested that future efforts to increase signal-to-noise ratios and develop robust tools for data analysis are still needed.

Bacterial protein phosphorylation systems have been suggested to be involved in microbial dysbiosis and microbes-host interaction (Lamont et al., 2018). Ren et al. discussed the roles of tyrosine and serine/threonine phosphorylation systems in keystone species *P. gingivalis*, with a particular focus on their involvement in bacterial metabolism and virulence, community development, and bacteria-host interactions. In addition to its association with periodontitis, *P. gingivalis* can increase the risk of systemic diseases such as type 2 diabetes mellitus (T2DM), cardiovascular diseases, nonalcoholic fatty liver disease (NAFLD), rheumatoid arthritis, and gut inflammation (Hajishengallis, 2015; Kitamoto et al., 2020; Hajishengallis and Chavakis, 2021). Previous study by Xu' group demonstrated that *P. gingivalis* was able to induce insulin resistance by increasing the serum level of branched-chain amino acid (BCAA) in high

fat diet (HFD)-fed mice (Tian et al., 2020). Work by Wu et al. further demonstrated that *P. gingivalis* elevated serum level of BCAA and exacerbated liver injury in HFD-fed mice, and this effect was dependent on the bacterial BCAA transport system genes *livh/livk*.

*Streptococcus mutans* is the main aciduric and acidogenic species in the oral cavity, and its persistence within the multispecies oral biofilms may antagonize commensal bacteria and drive compositional shift of oral microbiota towards a more cariogenic community that favors the development of dental caries (Lamont et al., 2018; Du et al., 2021). Fluoride is an effective anti-caries agent. However, widespread application of fluoride may induce fluoride-resistance in *S. mutans* (Li et al., 2021). Zhang et al. established an antagonistic dual-species biofilm consisting of *S. mutans* and *Streptococcus sanguinis*, and demonstrated that fluoride-resistant strain of *S. mutans* gained a survival advantage over *S. sanguinis* with an excessive production of extracellular polysaccharides after fluoride exposure, challenging the control of dental plaque biofilm. Dental caries is a multifactorial disease, and its progression is closely associated with ecological shift of oral microbiota towards a more cariogenic community that favors the demineralization of tooth hard tissue (Lamont et al., 2018). Wu et al. created a multifactorial machine learning model using oral microbiome of mother-child dyads in combination with demographic-environmental factors and relevant fungal information. By using this model, they identified specific caries-associated oral bacteria, *Candida*, and other multi-source factors for preschool children and their mothers.

The interactions between host and microbes play pivotal role in the development of oral diseases. Osteomicrobiology is a novel terminology that refers to the role of microbiota in bone homeostasis. Recent studies have shown the roles of oral microbiota in modulating host defense systems and alveolar bone homeostasis. Cheng et al. proposed the terminology "oral osteomicrobiology" and discussed the regulation of alveolar bone development and bone loss by oral microbiota under physiological and pathological conditions. Signaling pathways involved in oral osteomicrobiology and critical techniques for related investigations were also introduced. The recognition of pathogen-associated molecular patterns (PAMP) or damage-associated molecular patterns (DAMP) by the pattern-recognition receptors (PRRs) such as Toll-like receptors (TLRs) and nucleotide-binding oligomerization domain-like receptors (NLRs) has been well documented as the main molecular mechanisms for the host-microbial interactions (Akira et al., 2006; Kanneganti et al., 2007). Recent studies have identified a wide expression of extra-gustatory taste receptors in tissues/organs including airways, nasopharyngeal cavities, gastrointestinal tract and gingivae, and demonstrated their pivotal role in host immune responses and infectious diseases (O'Leary et al., 2019; Schneider et al., 2019; Ting and Von Moltke, 2019; Zheng et al., 2019). A review article from Dong et al. discussed how taste receptors, particularly bitter and sweet taste receptors, mediated the oral microbiota-host interaction and the development of oral diseases. The taste

receptor-mediated signaling and host immune responses may provide novel treatment targets for the management of oral infectious diseases such as periodontal diseases.

Since frequent use of wide-spectrum antimicrobials may cause microbial dysbiosis and drug resistance, novel approaches that can restore microecology without necessarily killing the bacteria are promising (Kuang et al., 2018). Zhang et al. reviewed the application of probiotics in the management of periodontal diseases. Probiotic bacteria derived from the genera *Lactobacillus*, *Bifidobacterium*, *Streptococcus*, and *Weissella* have shown effectiveness in the prevention and treatment of periodontal diseases. Competition for adhesion sites, antagonism against growth, biofilm formation and virulence expression of periodontopathogens, and regulation on host immune responses are the most recognized mechanisms. Nevertheless, more well-controlled clinical trials are still needed to provide solid evidence for their clinical usage. Small molecules which can either selectively inhibit keystone microbes or suppress the key virulence of the microbial community, are promising for the ecological management of oral diseases. Yang et al. discussed the research progress in the development of antimicrobial small molecules and delivery systems, with a particular focus on their antimicrobial activity against typical species such as *S. mutans*, *P. gingivalis* and *Candida albicans*. Although future work is still needed to delineate its molecular mechanisms and the exact drug targets, the authors believed that small molecules with potent antimicrobial activity, high selectivity, and low toxicity are promising for the ecological management of oral diseases. In addition to probiotics and small molecules, poly(amidoamine) dendrimers with amino terminal groups (PAMAM-NH<sub>2</sub>) have been identified as promising antimicrobial agents (Mintzer et al., 2012). Secondary caries caused by microbial leakage and hybrid layer degradation is one of the major causes of treatment failure of dental caries. Gou et al. developed a novel dentin cavity cleanser

that contains PAMAM-NH<sub>2</sub>. Although the exact molecular mechanisms are still unclear, the PAMAM-NH<sub>2</sub> showed long-term antimicrobial and anti-proteolytic activities, which are crucial for the maintenance of resin-dentin bond durability and thus promote the prevention of secondary caries.

A recurring theme in the current topic is the microbial diversity of oral microbiota and its association with oral and systemic health status. Although we have seen several submissions with longitudinal studies that showed dynamic microbial alterations during the treatment process, the key factors and underlying mechanisms that drive the microbial shift have yet to be investigated. In addition, although functional profiles have been suggested to be more related to diseases as compared to taxonomic alterations, current submissions mainly include data obtained from 16S and 18S rRNA amplicon sequencing. Future studies with metagenomic, meta-transcriptomic and meta-metabolomic approaches are still needed to better delineate the robust interactions between host and microbiota, and thus provide molecular basis for the development of new diagnostics and treatment modalities that target keystone pathogens in oral diseases.

## AUTHOR CONTRIBUTIONS

XX drafted the editorial and JX, YN contributed to the final submitted version. All authors contributed to the article and approved the submitted version.

## FUNDING

This work was supported by a grant from Health Commission of Sichuan Province (21PJ058).

## REFERENCES

- Akira, S., Uematsu, S., and Takeuchi, O. (2006). Pathogen Recognition and Innate Immunity. *Cell* 124 (4), 783–801. doi: 10.1016/j.cell.2006.02.015
- Annajhala, M. K., Khan, S. D., Sullivan, S. B., Shah, J., Pass, L., Kister, K., et al. (2020). Oral and Gut Microbial Diversity and Immune Regulation in Patients With HIV on Antiretroviral Therapy. *mSphere* 5 (1), e00798–19. doi: 10.1128/mSphere.00798-19
- Du, Q., Ren, B., He, J., Peng, X., Guo, Q., Zheng, L., et al. (2021). Candida Albicans Promotes Tooth Decay by Inducing Oral Microbial Dysbiosis. *ISME J.* 15 (3), 894–908. doi: 10.1038/s41396-020-00823-8
- Fulcher, J. A. (2020). Is the Oral Microbiome Important in HIV-Associated Inflammation? *mSphere* 5 (1), e00034–20. doi: 10.1128/mSphere.00034-20
- Hajishengallis, G. (2015). Periodontitis: From Microbial Immune Subversion to Systemic Inflammation. *Nat. Rev. Immunol.* 15 (1), 30–44. doi: 10.1038/nri3785
- Hajishengallis, G., and Chavakis, T. (2021). Local and Systemic Mechanisms Linking Periodontal Disease and Inflammatory Comorbidities. *Nat. Rev. Immunol.* 21 (7), 426–440. doi: 10.1038/s41577-020-00488-6
- Hajishengallis, G., Darveau, R. P., and Curtis, M. A. (2012). The Keystone-Pathogen Hypothesis. *Nat. Rev. Microbiol.* 10 (10), 717–725. doi: 10.1038/nrmicro2873
- Kamarajan, P., Ateia, I., Shin, J. M., Fenno, J. C., Le, C., Zhan, L., et al. (2020). Periodontal Pathogens Promote Cancer Aggressivity via TLR/MyD88 Triggered Activation of Integrin/FAK Signaling That Is Therapeutically Reversible by a Probiotic Bacteriocin. *PLoS Pathog.* 16 (10), e1008881. doi: 10.1371/journal.ppat.1008881
- Kanneganti, T. D., Lamkanfi, M., and Nunez, G. (2007). Intracellular NOD-Like Receptors in Host Defense and Disease. *Immunity* 27 (4), 549–559. doi: 10.1016/j.immuni.2007.10.002
- Kitamoto, S., Nagao-Kitamoto, H., Jiao, Y., Gilliland, M. G.3rd, Hayashi, A., Imai, J., et al. (2020). The Intermucosal Connection Between the Mouth and Gut in Commensal Pathobiont-Driven Colitis. *Cell* 182 (2), 447–462.e14. doi: 10.1016/j.cell.2020.05.048
- Kuang, X., Chen, V., and Xu, X. (2018). Novel Approaches to the Control of Oral Microbial Biofilms. *BioMed. Res. Int.* 2018, 6498932. doi: 10.1155/2018/6498932
- Lamont, R. J., Koo, H., and Hajishengallis, G. (2018). The Oral Microbiota: Dynamic Communities and Host Interactions. *Nat. Rev. Microbiol.* 16 (12), 745–759. doi: 10.1038/s41579-018-0089-x
- Li, C., Qi, C., Yang, S., Li, Z., Ren, B., Li, J., et al. (2021). F0F1-ATPase Contributes to the Fluoride Tolerance and Cariogenicity of Streptococcus Mutans. *Front. Microbiol.* 12, 777504. doi: 10.3389/fmicb.2021.777504
- Mintzer, M. A., Dane, E. L., O'Toole, G. A., and Grinstaff, M. W. (2012). Exploiting Dendrimer Multivalency to Combat Emerging and Re-Emerging Infectious Diseases. *Mol. Pharm.* 9 (3), 342–354. doi: 10.1021/mp2005033
- O'Leary, C. E., Schneider, C., and Locksley, R. M. (2019). Tuft Cells-Systemically Dispersed Sensory Epithelia Integrating Immune and Neural Circuitry. *Annu. Rev. Immunol.* 37, 47–72. doi: 10.1146/annurev-immunol-042718-041505

- Patil, S., Majumdar, B., Sarode, S. C., Sarode, G. S., and Awan, K. H. (2018). Oropharyngeal Candidosis in HIV-Infected Patients-An Update. *Front. Microbiol.* 9, 980. doi: 10.3389/fmicb.2018.00980
- Schneider, C., O'Leary, C. E., and Locksley, R. M. (2019). Regulation of Immune Responses by Tuft Cells. *Nat. Rev. Immunol.* 19 (9), 584–593. doi: 10.1038/s41577-019-0176-x
- Sepich-Poore, G. D., Zitvogel, L., Straussman, R., Hasty, J., Wargo, J. A., and Knight, R. (2021). The Microbiome and Human Cancer. *Science* 371 (6536), eabc4552. doi: 10.1126/science.abc4552
- Su, X., Gong, Y., Gou, H., Jing, X., Xu, T., Zheng, X., et al. (2020). Rational Optimization of Raman-Activated Cell Ejection and Sequencing for Bacteria. *Anal. Chem.* 92 (12), 8081–8089. doi: 10.1021/acs.analchem.9b05345
- Tian, J., Liu, C., Zheng, X., Jia, X., Peng, X., Yang, R., et al. (2020). Porphyromonas Gingivalis Induces Insulin Resistance by Increasing BCAA Levels in Mice. *J. Dent. Res.* 99 (7), 839–846. doi: 10.1177/0022034520911037
- Ting, H. A., and Von Moltke, J. (2019). The Immune Function of Tuft Cells at Gut Mucosal Surfaces and Beyond. *J. Immunol.* 202 (5), 1321–1329. doi: 10.4049/jimmunol.1801069
- Xu, J., Ma, B., Su, X., Huang, S., Xu, X., Zhou, X., et al. (2017). Emerging Trends for Microbiome Analysis: From Single-Cell Functional Imaging to Microbiome Big Data. *Engineering* 3 (1), 66–70. doi: 10.1016/J.ENG.2017.01.020
- Zheng, X., Tizzano, M., Redding, K., He, J., Peng, X., Jiang, P., et al. (2019). Gingival Solitary Chemosensory Cells Are Immune Sentinels for Periodontitis. *Nat. Commun.* 10 (1), 4496. doi: 10.1038/s41467-019-12505-x

**Conflict of Interest:** The authors declare that the research was conducted in the absence of any commercial or financial relationships that could be construed as a potential conflict of interest.

**Publisher's Note:** All claims expressed in this article are solely those of the authors and do not necessarily represent those of their affiliated organizations, or those of the publisher, the editors and the reviewers. Any product that may be evaluated in this article, or claim that may be made by its manufacturer, is not guaranteed or endorsed by the publisher.

Copyright © 2022 Xu, Xiao and Niu. This is an open-access article distributed under the terms of the Creative Commons Attribution License (CC BY). The use, distribution or reproduction in other forums is permitted, provided the original author(s) and the copyright owner(s) are credited and that the original publication in this journal is cited, in accordance with accepted academic practice. No use, distribution or reproduction is permitted which does not comply with these terms.



# Alteration in Oral Microbiome Among Men Who Have Sex With Men With Acute and Chronic HIV Infection on Antiretroviral Therapy

Shuang Li<sup>1†</sup>, Junping Zhu<sup>2†</sup>, Bin Su<sup>1†</sup>, Huanhuan Wei<sup>2</sup>, Fei Chen<sup>2</sup>, Hongshan Liu<sup>2</sup>, Jiaqi Wei<sup>1</sup>, Xiaodong Yang<sup>1</sup>, Qiuyue Zhang<sup>1</sup>, Wei Xia<sup>1</sup>, Hao Wu<sup>1</sup>, Qiushui He<sup>2,3\*</sup> and Tong Zhang<sup>1\*</sup>

<sup>1</sup> Beijing Key Laboratory for HIV/AIDS Research, Center for Infectious Diseases, Beijing Youan Hospital, Capital Medical University, Beijing, China, <sup>2</sup> Department of Medical Microbiology, Capital Medical University, Beijing, China, <sup>3</sup> Institute of Biomedicine, Research Center for Infections and Immunity, University of Turku, Turku, Finland

## OPEN ACCESS

### Edited by:

Yulong Niu,  
Sichuan University, China

### Reviewed by:

Pengfan Zhang,  
Max Planck Institute for Plant Breeding  
Research, Germany  
Keke Zhang,  
Wenzhou Medical University, China

### \*Correspondence:

Tong Zhang  
zt\_doc@ccmu.edu.cn  
Qiushui He  
qiuhe@utu.fi

<sup>†</sup>These authors have contributed  
equally to this work

### Specialty section:

This article was submitted to  
Microbiome in Health and Disease,  
a section of the journal  
Frontiers in Cellular and  
Infection Microbiology

**Received:** 15 April 2021

**Accepted:** 24 June 2021

**Published:** 14 July 2021

### Citation:

Li S, Zhu J, Su B, Wei H, Chen F, Liu H,  
Wei J, Yang X, Zhang Q, Xia W, Wu H,  
He Q and Zhang T (2021) Alteration in  
Oral Microbiome Among Men  
Who Have Sex With Men  
With Acute and Chronic HIV  
Infection on Antiretroviral Therapy.  
Front. Cell. Infect. Microbiol. 11:695515.  
doi: 10.3389/fcimb.2021.695515

Despite the antiretroviral therapy (ART), human immunodeficiency virus (HIV)-related oral disease remains a common problem for people living with HIV (PLWH). Evidence suggests that impairment of immune function in HIV infection might lead to the conversion of commensal bacteria to microorganisms with increased pathogenicity. However, limited information is available about alteration in oral microbiome in PLWH on ART. We performed a longitudinal comparative study on men who have sex with men (MSM) with acute HIV infection (n=15), MSM with chronic HIV infection (n=15), and HIV-uninfected MSM controls (n=15). Throat swabs were collected when these subjects were recruited (W0) and 12 weeks after ART treatment (W12) from the patients. Genomic DNAs were extracted and 16S rRNA gene sequencing was performed. Microbiome diversity was significantly decreased in patients with acute and chronic HIV infections compared with those in controls at the sampling time of W0 and the significant difference remained at W12. An increased abundance of *unidentified Prevotellaceae* was found in patients with acute and chronic HIV infections. Moreover, increased abundances of *Prevotella* in subjects with acute HIV infection and *Streptococcus* in subjects with chronic HIV infection were observed. In contrast, greater abundance in *Lactobacillus*, *Rothia*, *Lautropia*, and *Bacteroides* was found in controls. After effective ART, *Bradyrhizobium* was enriched in both acute and chronic HIV infections, whereas in controls, *Lactobacillus*, *Rothia*, *Clostridia*, *Actinobacteria*, and *Ruminococcaceae* were enriched. In addition, we found that lower CD4<sup>+</sup> T-cell counts (<200 cells/mm<sup>3</sup>) were associated with lower relative abundances of *Haemophilus*, *Actinomyces*, *unidentified Ruminococcaceae*, and *Rothia*. This study has shown alteration in oral microbiome resulting from HIV infection and ART. The results obtained warrant further studies in a large number of subjects with different ethnics. It might contribute to improved oral health in HIV-infected individuals.

**Keywords:** human immunodeficiency virus, oral microbiome, 16S rRNA sequencing, antiretroviral therapy, men who have sex with men



## INTRODUCTION

Human immunodeficiency virus (HIV) infection is characterized by rapid and substantial loss of CD4<sup>+</sup> T cells that impairs host defense and increases the risk of opportunistic microbial infections. Worldwide, there are approximately 38 million people living with HIV infection (PLWH), with about 25.4 million receiving antiretroviral therapy (ART). Although PLWH with ART might achieve a stable virus suppression, several oral diseases, such as oropharyngeal candidiasis (OPC), oral hairy leukoplakia, periodontitis, oral warts, ulcers, herpes, and Kaposi's sarcoma, are frequently reported (Goldberg et al., 2015; Heron and Elahi, 2017; El Howati and Tappuni, 2018).

It has been shown that impairment of immune function in HIV infection might lead to the conversion of commensal bacteria to microorganisms with increased pathogenicity and contributes to opportunistic infections (Saxena et al., 2016; Griffen et al., 2019). Several studies reported the changes of gut microbiota composition observed in HIV infection (Sun et al., 2016; Zhou et al., 2018; Rocafort et al., 2019), including the increase in *Prevotella* and decrease in *Bacteroides* (Dillon et al., 2014; Mutlu et al., 2014). Alterations in the gut microbiota will eventually lead to an imbalance between microbes and their metabolites and could result in HIV-associated immune activation and inflammation (Dinh et al., 2015; Zevin et al., 2016). In addition, various studies have demonstrated that microbial translocation is a cause of HIV-associated immune activation and inflammation (Brenchley et al., 2006; Marchetti et al., 2013; Koay et al., 2018). Early in HIV infection, the observed loss of Th17 cells results in impaired integrity of the mucosal epithelial barriers, leading to microbial translocation from the gut lumen into the systemic circulation (Brenchley et al., 2006; Mudd and Brenchley, 2016). Although a great number of studies have focused on the contribution of gut microbiota to HIV infection, a handful of studies have also characterized the oral microbiome in HIV-infected individuals (Fulcher, 2020). Li et al reported that in comparison to the HIV-negative individuals, PLWH had higher levels of total cultivable microbes in saliva, including oral *streptococci*, *Streptococcus mutans*, *lactobacilli*, and *Candida* (Li et al., 2014). Recently Annavajhala et al. have shown that oral microbiome communities likely contribute to systemic inflammation and immune activation in PLWH (Annavajhala et al., 2020). However, data are still limited about alterations in oral microbiome in HIV infection on ART.

Previous studies have also demonstrated that the abundance and diversity of oral microbiomes in PLWH were significantly different from those observed in healthy controls. Indeed after ART, the oral microbiome composition was not completely

recovered, although it turned to be similar to that observed in healthy controls (Presti et al., 2018; Li et al., 2020). It is known that the composition and homeostasis of oral microbiome are affected by multiple factors, such as diet, medication, and host responses (Samaranayake and Matsubara, 2017). It has been shown that *Prevotella*-rich microbiomes in the gut are associated with MSM and with HIV infection status (Noguera-Julian et al., 2016; Armstrong et al., 2018). Therefore, HIV-uninfected MSM could serve as useful controls when the effect of HIV infection itself on the oral microbiomes is studied. Further, to explore the impact of ART treatment on oral microbiomes, longitudinal studies and serial samples are needed. In this longitudinal study, we aimed to compare and identify changes in the oral microbiome in MSM with acute and chronic HIV infection before and after ART. Paired throat swab samples were collected within an interval of 12 weeks.

## MATERIALS AND METHODS

### Study Subjects and Sample Collection

Participants with acute HIV infection or chronic HIV infection (both were from MSM population) were recruited from Beijing Youan Hospital, Beijing, China from May to November 2019. All acute HIV-infected individuals (referred as A0, n=15) and chronic HIV-infected individuals (B0, n=15) had not initiated ART. Fifteen HIV-uninfected MSM (D, n=15) were selected and included as controls. Throat swabs were collected from controls and all HIV-infected ART-naïve individuals at the time of recruitment. Thereafter, all acute HIV-infected individuals (A12, n=15) and chronic HIV-infected individuals (B12, n=15) received ART, and throat swabs were collected at 12 weeks of ART. Acute HIV infection was defined as a positive HIV RNA but with negative or indeterminate HIV antibody results. Participants who have used antibiotics, probiotics, and prebiotics within the previous 4 weeks were excluded. In addition, the patients accompanied by active opportunistic infection and HBV/HCV were also excluded. The demographic and clinical characteristics of the study subjects are shown in **Table 1**. This study received approval from the ethics committee of the Beijing Youan Hospital ([2018]025), and all participants provided written informed consents.

### 16S rRNA Gene Sequence Analysis

Altogether 73 throat swabs from PLWH (except two patients at 12 weeks of ART were lost to follow-up), and controls were collected. The clean throat swabs were used by the clinical nurses

**TABLE 1 |** Demographic and clinical characteristics of the study subjects.

1	Acute HIV infection (n = 15)	Chronic HIV infection (n = 15)	Controls (n = 15)
Age (years, IQR)	29.4 (19–50)	37.3 (23–55)	40.1 (26–55)
Nadir CD4 <sup>+</sup> T-cell count (cells/mm <sup>3</sup> , IQR)	387 (293.8–531)	376.2 (303.8–532)	—
CD4 <sup>+</sup> T-cell count (cells/mm <sup>3</sup> , IQR)	397.4 (259–562.7)	486.5 (402–543)	—
Viral load (copies/ml)	56407 (7,156–97,871)	36592 (6,112–39,112)	—

All study subjects were male and had sex with men. IQR indicates interquartile range.

to collect oral samples from the posterior throat and tonsil areas. The swabs were used to repeatedly wipe the sampling site two times and quickly transported and stored at  $-20^{\circ}\text{C}$  in the laboratory before polymerase chain reaction (PCR). Genomic DNAs were extracted from swabs using the QIAamp Fast DNA Stool Mini Kit (50) and amplified by PCR for the sequencing of 16S rRNA V4-V5 region. Sequencing libraries were generated using Illumina TruSeq DNA PCR-Free Library Preparation Kit (Illumina, USA). The library quality was assessed on the Qubit@ 2.0 Fluorometer (Thermo Scientific) and Agilent Bioanalyzer 2100 system. At last, the library was sequenced on an Illumina NovaSeq platform and 250 bp paired-end reads were generated.

Paired-end reads were assigned to samples based on the unique barcodes and merged by using FLASH (V1.2.7). The raw tags were obtained, and the quality filtering was performed under specific filtering conditions to obtain the high-quality clean tags according to the QIIME (V1.9.1, [http://qiime.org/scripts/split\\_libraries\\_fastq.html](http://qiime.org/scripts/split_libraries_fastq.html)) quality control process. Then the tags were compared with the reference database (Silva database, <https://www.arb-silva.de/>) using UCHIME algorithm (UCHIME algorithm, [http://www.drive5.com/usearch/manual/uchime\\_algo.html](http://www.drive5.com/usearch/manual/uchime_algo.html)) to detect chimera sequences. The chimera sequences were removed, and the effective tags were finally obtained. Operational taxonomic units (OTUs) were clustered by Uparse software (Uparse v7.0.1001), and representative sequence for each OTU was screened for further annotation. For each representative sequence, the Silva Database was used based on Mothur algorithm to annotate taxonomic information. Alpha diversity is applied in analyzing complexity of species diversity for a sample, including Observed-species, Chao1, Shannon, Simpson, ACE, Good-coverage, and PD whole tree. All these indices in our samples were calculated with QIIME (Version 1.7.0) and displayed with R software (Version 2.15.3). Beta diversity analysis was used to evaluate differences of samples in species complexity. Beta diversity on both weighted and unweighted unifrac was calculated by QIIME software (Version 1.9.1). Principal Coordinate Analysis (PCoA) analysis was displayed by WGCNA package, stat packages, and ggplot2 package in R software (Version 2.15.3).

## Statistical Analysis

Alpha diversity and beta diversity in oral microbiome among groups were tested by the Wilcoxon rank-sum test. To assess the differences in the microbial abundance between samples, significance test was conducted with some statistical analysis methods, including *t*-test and LEfSe. Mann-Whitney test and Kruskal Wallis test were used for comparing continuous variables. Two sides of  $p < 0.05$  were considered statistically significant.

## RESULTS

### Study Population

Samples were collected from 15 patients with acute HIV infection, 15 patients with chronic HIV infection, and 15

healthy controls. All participants ( $\geq 18$  years old) were MSM, and all PLWH with acute and chronic HIV infection had not initiated ART. Throat swabs were collected from controls and HIV-infected patients at baseline and 12 weeks of ART. The baseline  $\text{CD4}^+$  T-cell count was  $387 \text{ cells/mm}^3$  in acute HIV infection and  $376.2 \text{ cells/mm}^3$  in chronic HIV infection. After ART for 12 weeks, all patients had increased  $\text{CD4}^+$  T-cell counts, with  $397.4 \text{ cells/mm}^3$  in acute HIV infection and  $486.5 \text{ cells/mm}^3$  in chronic HIV infection (Table 1).

### Oral Microbiome Diversity in Study Subjects

Sequencing resulted in an average of 59,794 high-quality sequences after quality checks. Rarefaction curves and rank abundance showed a great sequencing depth and an even species distribution of the samples in our study (Supplementary Figures S1A, B). By clustering the sequences into OTUs with 97% similarity, an average of 683 OTUs were identified in controls. The corresponding numbers were 298 and 276 OTUs in the A0 and B0 groups, respectively. Following 12 weeks of ART, the corresponding numbers were 299 and 300 OTUs in the A12 and B12 groups. The following dominant phyla were observed in the oral microbiome: *Proteobacteria*, *Firmicutes*, *Bacteroidetes*, *Fusobacteria*, *Actinobacteria*, and *Spirochaetes*, etc (Figure 1A). These six dominant bacterial phyla accounted for more than 98% of the total oral microbiome. The most abundantly detected bacterial genus in the oral microbiome were *Streptococcus*, *Neisseria*, *unidentified Prevotellaceae*, with lower relative abundance of *Veillonella*, *Haemophilus*, *Actinobacillus*, *Alloprevotella*, and *Fusobacterium* in controls and the HIV-infected patients prior to ART. In addition, the abundance of *Bradyrhizobium* in both acute and chronic HIV infection groups was increased following 12 weeks of ART (Figure 1B).

We next used richness estimators (Chao) and diversity index (Shannon index) to compare microbial alpha diversity among different groups of samples. Compared with the control group D, the Chao1 index and Shannon index of oral microbiomes in both A0 group and B0 group were significantly decreased (Figures 1C, D) (all  $p < 0.001$ ). Although after 12 weeks of ART, the Chao1 index and Shannon index were still significantly lower in acute and chronic HIV-treated groups when compared with healthy controls (Figures 1C, D) (Supplementary Table S1) (all  $p < 0.001$ ). However, the Chao1 index of oral microbiomes in B12 group was significantly increased compared to B0 group (Figure 1C) ( $p < 0.001$ ). In addition, the Chao1 index in B0 group was significant decreased compared to A0 group ( $p < 0.01$ ), whereas the differences was not significant between the A12 and B12 (Figure 1C) ( $p = 0.75$ ). To identify the differences in microbial community composition of participants in these groups, the Principal Co-ordinates Analysis (PCoA) was used for beta diversity analysis. A conspicuous separation between HIV infection groups and control group was observed, beta diversity of oral microbiomes was significantly different between HIV-infected individuals and controls (Figures 1E, F)

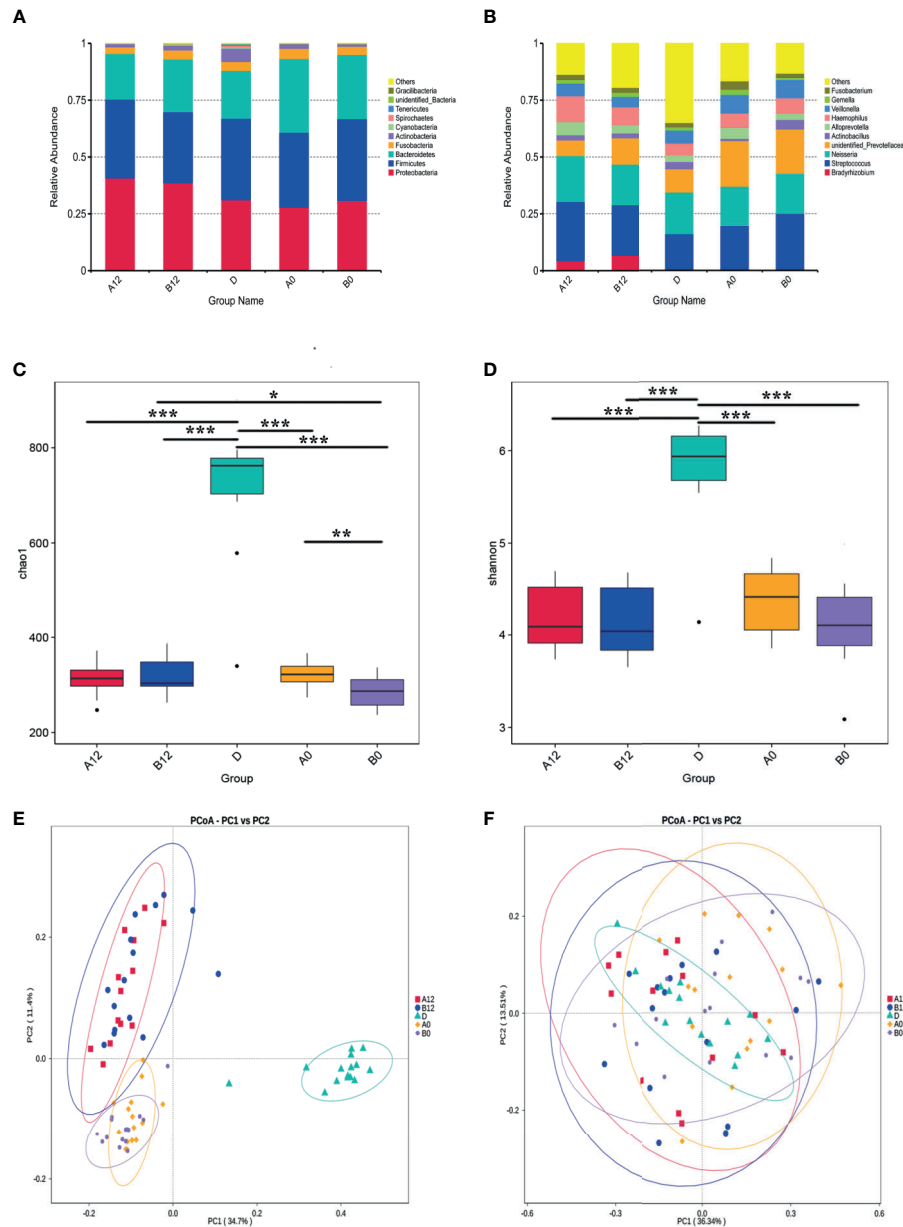


**FIGURE 1** | The composition, relative abundance, and diversity of oral microbiota in HIV-infected groups and controls **(A)** at the phylum level; **(B)** at the genus level; **(C)** Alpha diversity exemplified by the Chao1 index; **(D)** Alpha diversity exemplified by the Shannon index; **(E)** Beta diversity represented by Principal coordinate analysis (PcoA) of unweighted UniFrac distances; **(F)** Beta diversity represented by Principal coordinate analysis (PcoA) of weighted UniFrac distances. A0, people living with acute HIV infection at baseline; B0, people living with chronic HIV infection at baseline; D, HIV-uninfected controls; A12, people living with acute HIV infection after 12 weeks of ART; B12, people living with chronic HIV infection after 12 weeks of ART. \* $p < 0.05$ ; \*\* $p < 0.01$ ; \*\*\* $p < 0.001$ .

( $p < 0.001$ ). There was no significant difference in beta diversity represented by PcoA of weighted UniFrac distances when comparing A0 group and B0 group ( $p = 0.58$ ), but there was a significant difference between groups A12 and B12 ( $p < 0.001$ ) (**Figure 1F**). Likewise, no significant difference in beta diversity of weighted UniFrac distances was observed between A0 and A12 groups ( $p = 0.32$ ), but there was a significant difference between groups B0 and B12 (**Figure 1F**) ( $p < 0.001$ ).

## Oral Microbiome Dysbiosis in People Living With Acute and Chronic HIV Infection

Differences in the composition of oral microbiome between controls and PLWH were analyzed. At the genus level, we observed the increased abundance of *unidentified Prevotellaceae* in both A0 and B0 groups. The abundances of *Prevotella* in the A0 group and *Streptococcus* in the B0 group

were significantly increased. In contrast, several groups of bacteria, such as *Lactobacillus*, *Rothia*, *Lautropia*, and *Bacteroides* were found in greater abundance in D group (Figures 2A, B).

## Effects of ART on the Oral Microbiome

All of the PLWH included in this study received ART after the swab samples at baseline were taken. The second swabs were taken after 12 weeks of ART. LEfSe analyses showed that *Bradyrhizobium*

was enriched in both A12 and B12 groups, whereas *Clostridia*, *Actinobacteria*, *Lactobacillus*, *Ruminococcaceae*, *Rothia* were enriched in the D group (Figures 3A–D).

Moreover, *Prevotella histicola*, *Prevotella melaninogenica*, *Bacteroidales*, and unidentified *Prevotellaceae* were enriched in the A0 group, while *Bradyrhizobium* were enriched in the A12 group (Figures 4A, B). In the chronic HIV-infected patients, *Prevotella histicola*, *Prevotella melaninogenica*, *Veillonellaceae*, and unidentified *Prevotellaceae* were enriched in the B0 group,

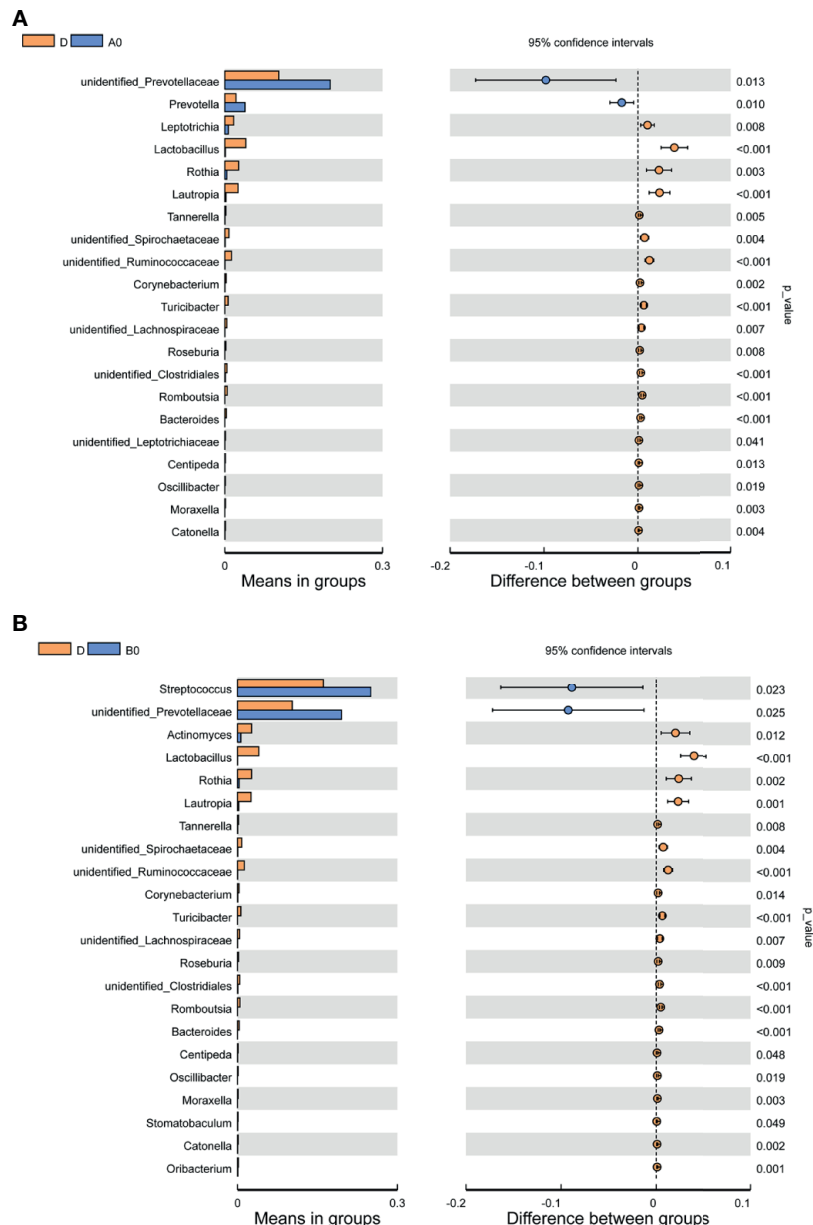


**FIGURE 2** | Comparisons of the relative abundance in oral microbiota at the genus level (A) Between A0 and D groups; (B) Between B0 and D groups. A0, people living with acute HIV infection at baseline; B0, people living with chronic HIV infection at baseline; D, HIV-uninfected controls; A12, people living with acute HIV infection after 12 weeks of ART; B12, people living with chronic HIV infection after 12 weeks of ART.



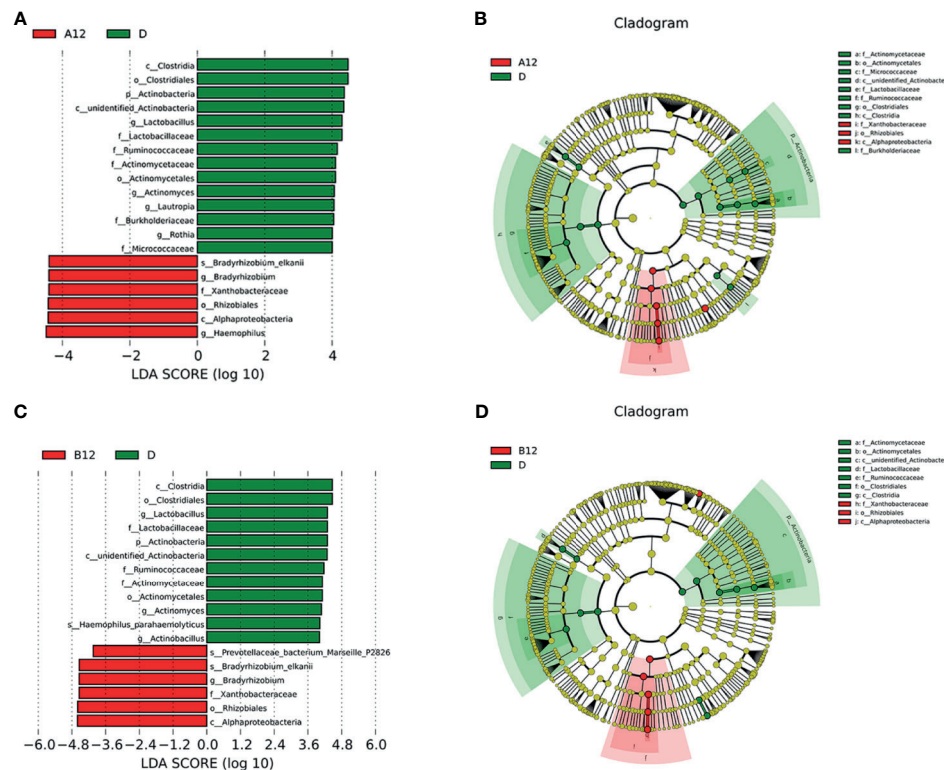


**FIGURE 3 |** Linear discriminative analysis (LDA) effect size (LefSe) at the genus level. **(A, B)** shown between A12 and D groups and **(C, D)** between B12 and D groups. In **(A, B)**, LDA scores for the significant taxa in D group are represented on the positive scale (green), and LDA-negative scores represent enriched taxa in A12 group (red); and in **(C, D)**, LDA scores for the significant taxa in D group are represented on the positive scale (green), and LDA-negative scores represent enriched taxa in B12 group (red). A12, people living with acute HIV infection after 12 weeks of ART; B12, people living with chronic HIV infection after 12 weeks of ART; D, HIV-uninfected controls.

whereas the relative abundance of *Bradyrhizobium* in the B12 group was significantly higher (Figures 4C, D).

Additionally, we also compared the composition of oral microbiome in people living with acute HIV infection and chronic HIV infection. Compared with A0 group, we noticed lower abundances of *Oribacterium* in the B0 group (Figure 4E). However, after 12 weeks of ART, we found that the abundance of *Campylobacter* in the B12 group was significantly higher than those in the A12 group (Figure 4F).

## Association of the Oral Microbiome With CD4<sup>+</sup> T-Cell Count

To study whether there is relationship between the alteration observed in oral microbiome and CD4<sup>+</sup> T-cell count of patients, we performed analyses of these parameters. We found that the abundance of *Haemophilus* in patients with CD4<200 cells/mm<sup>3</sup> was significantly decreased when comparing with HIV-uninfected controls and patients with CD4>200 cells/mm<sup>3</sup>. However, there was no significant difference between controls and patients with CD4>200 cells/mm<sup>3</sup>. In addition, the abundances of *Actinomyces*, *unidentified Ruminococcaceae*, and *Rothia* collected from both subjects with CD4 <200 cells/mm<sup>3</sup> and subjects with CD4>200 cells/mm<sup>3</sup> were significantly lower

than those in HIV-uninfected subjects. Furthermore, lower CD4<sup>+</sup> T-cell counts (<200 cells/mm<sup>3</sup>) were associated with lower relative abundances of *Haemophilus*, *Actinomyces*, *unidentified Ruminococcaceae*, and *Rothia* (Figures 5A–D).

## Differences in Microbiota Metabolic Pathways Between HIV Infections and Healthy Controls

According to the functional annotation, we used PICRUSt metagenome prediction to estimate the functional role of oral microbiome in PLWH and healthy controls. Compared with the D group, we noticed that pathways involved in cell growth and death, glycan biosynthesis, and metabolism increased in HIV-infected patients prior to ART ( $p<0.05$ ). Moreover, replication and repair of DNA, genetic information processing, and translation-related pathways also increased in both A0 and B0 groups ( $p<0.05$ ). In contrast, pathways related to xenobiotics biodegradation and metabolism, signal transduction, and cell motility ( $p<0.05$ ) were decreased in both A0 and B0 groups (Figure 6 and Supplementary Figures S2A, B).

After 12 weeks of ART, comparison of pathways between HIV-infected groups and healthy controls showed that ART could partly reverse the changes of pathways in the acute and

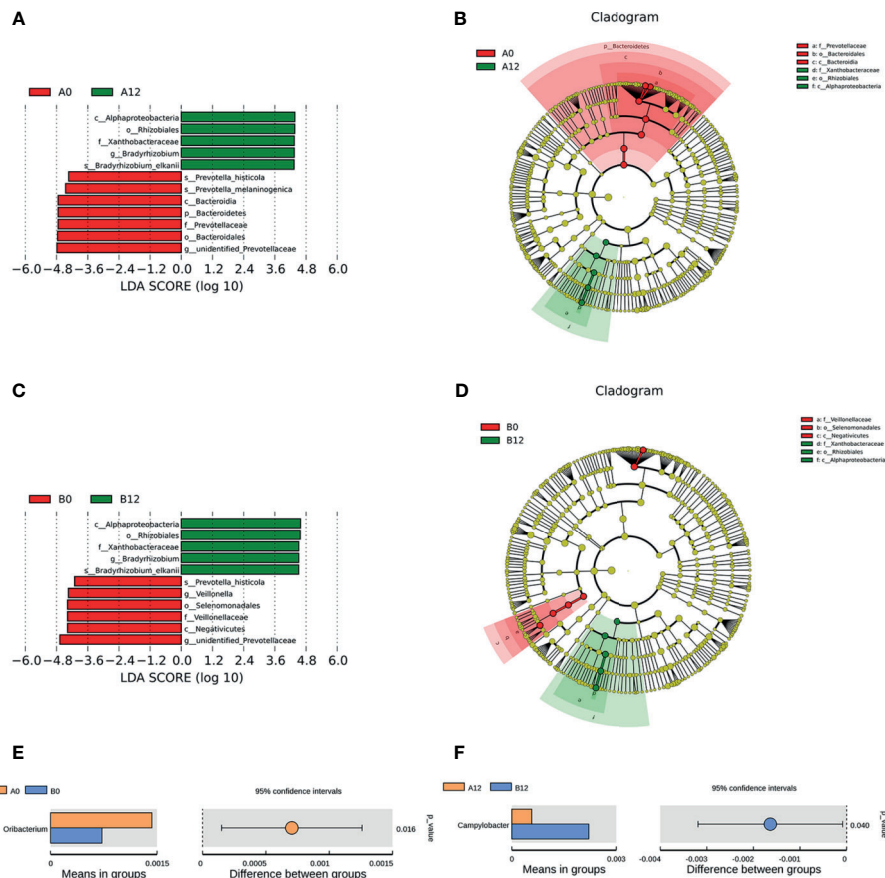


**FIGURE 4 |** Linear discriminative analysis (LDA) effect size (LefSe) at the genus level. **(A, B)** shown between A0 and A12 groups and **(C, D)** between B0 and B12 groups. In **(A, B)**, LDA scores for the significant taxa in A12 group are represented on the positive scale (green), and LDA-negative scores represent enriched taxa in A0 group (red); and in **(C, D)**, LDA scores for the significant taxa in B12 group are represented on the positive scale (green), and LDA-negative scores represent enriched taxa in B0 group (red). Comparisons of the relative abundance in oral microbiota at the genus level **(E)** Between A0 and B0 groups; **(F)** Between A12 and B12 groups. A0, people living with acute HIV infection at baseline; B0, people living with chronic HIV infection at baseline; D, HIV-uninfected controls; A12, people living with acute HIV infection after 12 weeks of ART; B12, people living with chronic HIV infection after 12 weeks of ART.

chronic HIV infection, but pathways related to metabolism, cell growth and death were still significantly increased ( $p < 0.05$ ), whereas transcription was significantly decreased in both A12 and B12 groups ( $p < 0.05$ ) (**Figure 6** and **Supplementary Figures S2C, D**).

## DISCUSSION

Our present study clearly showed that the OTUs identified in oral microbiome in people living with acute or chronic HIV infection were significantly lower compared with those in controls, and the number of OTUs in patients did not return to normal level even after 12 weeks of ART. Moreover, the alpha diversity of oral microbiomes in the patients was decreased significantly. In addition, beta diversity was also found to be different between patients and controls. Our results were in line with an earlier finding in which a decrease in microbial diversity in HIV-infected individuals was observed (Li et al., 2014). The

decreased alpha diversity may be attributed to the increased proportions of opportunistic microbes as a result of immunocompromised state of patients (Li et al., 2014). Recently, Jiménez-Hernández et al. reported an increase of diversity parameters in salivary microbiota in HIV-infected individuals, mainly in those viremic ART-naïve patients (Jimenez-Hernandez et al., 2019). It is conceivable that the impaired immune function resulting from HIV infection can disrupt the normally constituted commensal oral bacterial colonization, and the elevated viremia in untreated PLWH is associated with significantly higher proportions of potentially pathogenic *Veillonella*, *Prevotella*, *Megasphaera*, and *Campylobacter* species than in healthy controls (Dang et al., 2012).

In this study, the Chao1 index and Shannon index of oral microbiomes in both A0 group and B0 group were significantly decreased when compared with HIV-uninfected controls, and the significant difference remained after 12 weeks of ART. We also found that before the ART, the Chao1 index in chronic HIV-

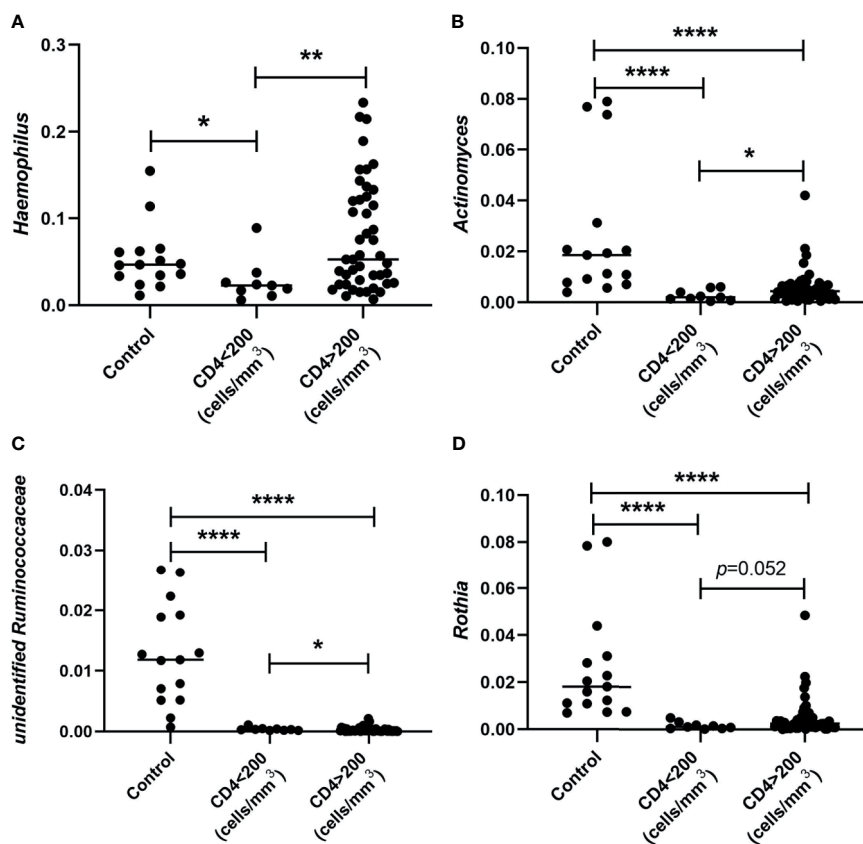


**FIGURE 5** | Comparison of relative abundances of *Haemophilus* (A), *Actinomyces* (B), unidentified *Ruminococcaceae* (C), and *Rothia* (D) collected from subjects whose CD4<sup>+</sup> T cells were defined < and CD4>200 cells/mm<sup>3</sup> and HIV-uninfected MSM controls. \**p* < 0.05; \*\**p* < 0.01; \*\*\*\**p* < 0.0001.

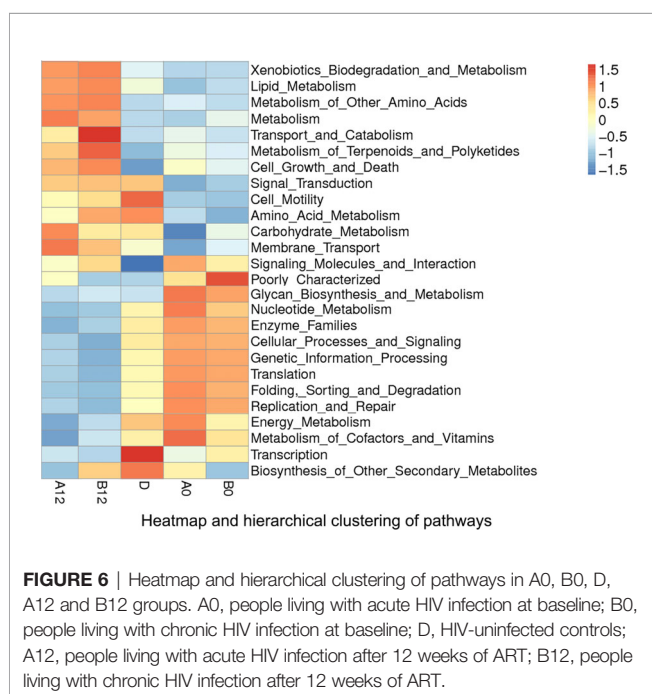


**FIGURE 6** | Heatmap and hierarchical clustering of pathways in A0, B0, D, A12 and B12 groups. A0, people living with acute HIV infection at baseline; B0, people living with chronic HIV infection at baseline; D, HIV-uninfected controls; A12, people living with acute HIV infection after 12 weeks of ART; B12, people living with chronic HIV infection after 12 weeks of ART.

infected patients B0 group was significantly lower than that in the acute HIV-infected individuals A0 group, whereas after 12 weeks of the ART, the differences was not significant. Further, after 12 weeks of ART, the Chao1 index in B12 group significantly increased compared with the B0 group. These results suggested that the richness and diversity of oral microbiomes decreased with the progression of HIV infection. Although such reduction can be improved by ART, the oral microbiota dysbiosis cannot be fully restored after the 12-week ART in PLWH (Saxena et al., 2016; Presti et al., 2018). Moreover, there was no significant difference observed in beta diversity when comparing A0 group with B0 group, but a significant difference was noticed between groups A12 and B12. Likewise, no significant difference in beta diversity was found between A0 and A12 groups, whereas there was a significant difference between groups B0 and B12. These results further indicated that the dysbiosis in oral microbiome in people living with acute HIV infection could be partially restored if the ART is early initiated. Recent studies have also revealed that ART initiated in acute HIV infection can limit reservoir size and mitigate systemic chronic immune activation (Cheret et al., 2015; Hey-Cunningham et al., 2015). Altogether, these findings suggested that ART initiated during acute HIV infection might play an

important role in protecting commensal bacterial colonization and preventing the occurrence of HIV-related oral diseases.

Alterations in oral microbiota have been noted in individuals with HIV. However, the mechanisms remain unclear and the compromised mucosal immunity might contribute to the dysbiosis of the oral microbiota in PLWH (Heron and Elahi, 2017). It is well documented that Th17 cells are depleted in HIV infection (Cote et al., 2019), however, other studies have shown that oral-resident Th17 cells can play an important role in controlling oral fungal colonization (Conti et al., 2014; Kirchner and LeibundGut-Landmann, 2021). Additionally, salivary components, such as salivary IgA, lactoferrin, defensins, and epithelial cell-mediated cytokines, are altered in PLWH, resulting in the occurrence of frequent oral infections (Muller et al., 1992). A recent study reported that the changes of salivary microbiome in HIV infection and found that *Streptococcus* was enriched in HIV-infected individuals, whereas the richness of *Neisseria* was high in healthy controls (Li et al., 2020). In present study, we observed that the abundance of unidentified *Prevotellaceae* in both groups of patients with acute and chronic HIV infection was increased as well as the abundances of *Prevotella* in acute HIV individuals and *Streptococcus* in chronic HIV individuals.

Interestingly, the changes observed in the oral microbiomes were similar to those in the gut microbiomes in HIV-infected patients. One possible explanation is that oral microbiome could indirectly impact gut bacteria by eating and dispersing (Schmidt et al., 2019). The gut microbes might also in turn affect the oral microbiome through microbial translocation or systemic immune regulation. In addition, it has been shown that *Prevotella* exhibit an increased ability to induce inflammatory mediators, such as IL-6, IL-8, and tumor necrosis factor- $\alpha$  (TNF- $\alpha$ ), when compared with strict commensal oral bacteria (Larsen, 2017). The *Prevotella* can also promote periodontitis by driving the recruitment of neutrophil via Th17 immune responses (Uriarte et al., 2016). Another study also found that *Streptococcus* was enriched in AIDS patients with periodontitis (Zhang et al., 2015). Moreover, a recent study revealed a significant enrichment of *Streptococcus* in the saliva of HIV-infected individuals with high sCD14 levels, which might contribute to HIV-associated immune activation (Annavaajhala et al., 2020). In contrast, several groups of bacteria, such as *Lactobacillus*, *Rothia*, *Lautropia*, and *Bacteroides*, were found in greater abundance in healthy controls. It has been demonstrated that *Lactobacillus* species can produce various antimicrobial factors including hydrogen peroxide, acetic acid, lactic acid, and bacteriocins (Spinler et al., 2008). Salari et al. also demonstrated in an *in vitro* study that the *lactobacilli* have antifungal effects on different oral *Candida* species isolated from HIV/AIDS patients (Salari and Ghasemi Nejad Almani, 2020). It therefore seems that HIV-induced oral microbiota dysbiosis might be characterized by an increased abundance of bacteria that are potentially inflammatory or pathogenic and a decreased abundance of bacteria that are anti-inflammatory or protective.

Although the similar oral microbiome composition has been reported between the HIV-infected individuals undergoing ART

and healthy controls, there are significant differences (Li et al., 2020). In the longitudinal study, we collected samples from acute and chronic HIV-infected MSM at baseline and 12 weeks of ART. We found that *Bradyrhizobium* was enriched in both acute and chronic HIV-infected individuals after 12 weeks of ART, whereas *Clostridia*, *Actinobacteria*, *Lactobacillus*, *Ruminococcaceae*, and *Rothia* were enriched in controls. Yang et al. reported that *Bradyrhizobium* was enriched in the proximal gut of PLWH (Yang et al., 2016). They also found that *Lactobacillus* species might have a co-avoidant relationship with *Bradyrhizobium pachyrrhizi* in the duodenum. However, little is known about the mechanisms of *Bradyrhizobium* colonization in PLWH, and the exact effects of ART on *Bradyrhizobium* colonization remain to be shown. Furthermore, we found that the abundances of potentially pathogenic bacteria, such as *Prevotella histicola*, *Prevotella melaninogenica*, and *Veillonellaceae*, were decreased when comparing samples collected at baseline with those collected following 12 weeks of ART in PLWH. Our data indicated that ART can partially reverse the effects of HIV on the oral bacteriome, whereas the commensal bacteria with “protective capacity in the oral cavity have been not fully recovered (Moyes et al., 2016).

After 12 weeks of ART, comparing the composition of oral microbiome in people living with acute HIV infection with that of chronic HIV infection, we found that the abundance of *Campylobacter* in the chronic HIV-infected individuals was significantly higher than those in acute HIV-infected individuals. *Campylobacter* spp are gram-negative bacteria with predominant enteric pathogenicity (Manfredi et al., 2002). Molina et al. showed that *Campylobacter* can cause acute diarrhea in PLWH (Molina et al., 1995). In untreated PLWH, *Campylobacter* species in the lingual microbiome was associated with high-level viremia (Dang et al., 2012). However, another study showed that ART increased the risk for recovering *Campylobacter* species in saliva of HIV-positive women (Navazesh et al., 2005).

Of note, we also observed that alterations in the oral microbiome are associated with CD4<sup>+</sup> T-cell count in patients. The abundances of *Haemophilus*, *Actinomyces*, unidentified *Ruminococcaceae*, and *Rothia* were significantly decreased in subjects with lower CD4<sup>+</sup> T-cell counts (<200 cells/mm<sup>3</sup>) when comparing with subjects with CD4>200 cells/mm<sup>3</sup>. It is known that *Haemophilus* bacteria can implicate in various opportunistic infections. A previous study reported that *Haemophilus parainfluenzae* was significantly associated with HIV-positive individuals, and it was positively correlated with CD4<sup>+</sup> T cell counts within the HIV-positive group (Kistler et al., 2015). However, a recent study found that the genus *Haemophilus* was correlated negatively with CD4<sup>+</sup> T cell count (Li et al., 2020). The possible reasons for the different results might include the different study subjects, samples, the small sample sizes, and other possible factors not involved in the analysis.

One of the limitations of this study was the small sample size. Clearly, studies with large sample size are required. Other factors, such as age, might also affect the results of our study. In addition,



previous studies have indicated that oral fungal colonization is altered in HIV-infected individuals (Mukherjee et al., 2014; Hager and Ghannoum, 2018). Although the occurrence of OPC in HIV infection has significantly declined since the introduction of ART, it remains a common opportunistic infection in AIDS diseases (Thompson et al., 2010; Patil et al., 2018). The present study was focused on the oral bacterial community in HIV infection, future studies should also address how the oral mycobiome shifts in the setting of HIV infection and ART initiation.

In conclusion, this longitudinal study has shown important alterations in oral microbiome resulting from HIV infection as well as among MSM with acute and chronic HIV infection before and after ART. The findings might contribute to improved oral health in HIV-infected individuals and provide some clues to exploring the association of the oral and the intestinal microbiome during the disease courses.

## DATA AVAILABILITY STATEMENT

The datasets presented in this study can be found in online repositories. The names of the repository/repositories and accession number(s) can be found below: NCBI SRA PRJNA739016.

## ETHICS STATEMENT

The studies involving human participants were reviewed and approved by the Ethics Committee of the Beijing Youan Hospital ([2018]025). The patients/participants provided their written informed consent to participate in this study.

## REFERENCES

- Annavaiahala, M. K., Khan, S. D., Sullivan, S. B., Shah, J., Pass, L., Kister, K., et al. (2020). Oral and Gut Microbial Diversity and Immune Regulation in Patients with HIV on Antiretroviral Therapy. *mSphere* 5 (1), e00798-19. doi: 10.1128/mSphere.00798-19
- Armstrong, A. J. S., Shaffer, M., Nusbacher, N. M., Griesmer, C., Fiorillo, S., Schneider, J. M., et al. (2018). An Exploration of Prevotella-Rich Microbiomes in HIV and Men Who Have Sex With Men. *Microbiome* 6, 198. doi: 10.1186/s40168-018-0580-7
- Brenchley, J. M., Price, D. A., Schacker, T. W., Asher, T. E., Silvestri, G., Rao, S., et al. (2006). Microbial Translocation is a Cause of Systemic Immune Activation in Chronic HIV Infection. *Nat. Med.* 12, 1365–1371. doi: 10.1038/nm1511
- Cheret, A., Bacchus-Souffan, C., Avettand-Fenoel, V., Melard, A., Nembot, G., Blanc, C., et al. (2015). Combined ART Started During Acute HIV Infection Protects Central Memory CD4+ T Cells and can Induce Remission. *J. Antimicrob. Chemother.* 70, 2108–2120. doi: 10.1093/jac/dkv084
- Conti, H. R., Peterson, A. C., Brane, L., Huppler, A. R., Hernandez-Santos, N., Whibley, N., et al. (2014). Oral-Resident Natural Th17 Cells and Gammadelta T Cells Control Opportunistic Candida Albicans Infections. *J. Exp. Med.* 211, 2075–2084. doi: 10.1084/jem.20130877
- Cote, S. C., Stilla, A., Burke Schinkel, S. C., Berthoud, T. K., and Angel, J. B. (2019). IL-7-Induced Proliferation of Peripheral Th17 Cells Is Impaired in HAART-Controlled HIV Infection. *AIDS* 33, 985–991. doi: 10.1097/QAD.0000000000002164
- Dang, A. T., Cotton, S., Sankaran-Walters, S., Li, C. S., Lee, C. Y., Dandekar, S., et al. (2012). Evidence of an Increased Pathogenic Footprint in the Lingual Microbiome of Untreated HIV Infected Patients. *BMC Microbiol.* 12:153. doi: 10.1186/1471-2180-12-153

## AUTHOR CONTRIBUTIONS

All authors made a substantial, direct, and intellectual contribution to the work, including the study design, subject recruitment, sample collection, laboratory experiments, data analysis, and manuscript drafting. All authors contributed to the article and approved the submitted version.

## FUNDING

This work was supported by the National Natural Science Foundation of China (82072271, 81772165, and 81974303), the National 13<sup>th</sup> Five-Year Grand Program on Key Infectious Disease Control (2017ZX10202101-004-001, 2017ZX10202102-005-003), Beijing Natural Science Foundation (7172016), the NSFC-NIH Biomedical collaborative research program (81761128001), the Beijing Key Laboratory for HIV/AIDS Research (BZ0089), and Beijing Natural Science Foundation and Handian Innovation Joint Project (19L2043).

## ACKNOWLEDGMENTS

We thank all of the staff from Beijing Youan Hospital, Capital Medical University, and Novogene who worked on this study.

## SUPPLEMENTARY MATERIAL

The Supplementary Material for this article can be found online at: <https://www.frontiersin.org/articles/10.3389/fcimb.2021.695515/full#supplementary-material>

- Dillon, S. M., Lee, E. J., Kotter, C. V., Austin, G. L., Dong, Z., Hecht, D. K., et al. (2014). An Altered Intestinal Mucosal Microbiome in HIV-1 Infection Is Associated With Mucosal and Systemic Immune Activation and Endotoxemia. *Mucosal Immunol.* 7, 983–994. doi: 10.1038/mi.2013.116
- Dinh, D. M., Volpe, G. E., Duffalo, C., Bhalchandra, S., Tai, A. K., Kane, A. V., et al. (2015). Intestinal Microbiota, Microbial Translocation, and Systemic Inflammation in Chronic HIV Infection. *J. Infect. Dis.* 211, 19–27. doi: 10.1093/infdis/jiu409
- El Howati, A., and Tappuni, A. (2018). Systematic Review of the Changing Pattern of the Oral Manifestations of HIV. *J. Investig. Clin. Dent.* 9, e12351. doi: 10.1111/jicd.12351
- Fulcher, J. A. (2020). Is the Oral Microbiome Important in HIV-Associated Inflammation? *mSphere* 5 (1), e00034-20. doi: 10.1128/mSphere.00034-20
- Goldberg, B. E., Mongodin, E. F., Jones, C. E., Chung, M., Fraser, C. M., Tate, A., et al. (2015). The Oral Bacterial Communities of Children With Well-Controlled HIV Infection and Without HIV Infection. *PLoS One* 10, e0131615. doi: 10.1371/journal.pone.0131615
- Griffen, A. L., Thompson, Z. A., Beall, C. J., Lilly, E. A., Granada, C., Treas, K. D., et al. (2019). Significant Effect of HIV/HAART on Oral Microbiota Using Multivariate Analysis. *Sci. Rep.* 9, 19946. doi: 10.1038/s41598-019-55703-9
- Hager, C. L., and Ghannoum, M. A. (2018). The Mycobiome in HIV. *Curr. Opin. HIV AIDS* 13, 69–72. doi: 10.1097/COH.0000000000000432
- Heron, S. E., and Elahi, S. (2017). HIV Infection and Compromised Mucosal Immunity: Oral Manifestations and Systemic Inflammation. *Front. Immunol.* 8:241. doi: 10.3389/fimmu.2017.00241
- Hey-Cunningham, W. J., Murray, J. M., Natarajan, V., Amin, J., Moore, C. L., Emery, S., et al. (2015). Early Antiretroviral Therapy With Raltegravir Generates Sustained Reductions in HIV Reservoirs But Not Lower T-Cell Activation Levels. *AIDS* 29, 911–919. doi: 10.1097/QAD.0000000000000625

- Jimenez-Hernandez, N., Serrano-Villar, S., Domingo, A., Pons, X., Artacho, A., Estrada, V., et al. (2019). Modulation of Saliva Microbiota through Prebiotic Intervention in HIV-Infected Individuals. *Nutrients* 11 (6), 1346. doi: 10.3390/nu11061346
- Kirchner, F. R., and LeibundGut-Landmann, S. (2021). Tissue-Resident Memory Th17 Cells Maintain Stable Fungal Commensalism in the Oral Mucosa. *Mucosal Immunol.* 14, 455–467. doi: 10.1038/s41385-020-0327-1
- Kistler, J. O., Arirachakaran, P., Poovorawan, Y., Dahlen, G., and Wade, W. G. (2015). The Oral Microbiome in Human Immunodeficiency Virus (HIV)-Positive Individuals. *J. Med. Microbiol.* 64, 1094–1101. doi: 10.1099/jmm.0.000128
- Koay, W. L. A., Siems, L. V., and Persaud, D. (2018). The Microbiome and HIV Persistence: Implications for Viral Remission and Cure. *Curr. Opin. HIV AIDS* 13, 61–68. doi: 10.1097/COH.0000000000000434
- Larsen, J. M. (2017). The Immune Response to Prevotella Bacteria in Chronic Inflammatory Disease. *Immunology* 151, 363–374. doi: 10.1111/imm.12760
- Li, J., Chang, S., Guo, H., Ji, Y., Jiang, H., Ruan, L., et al. (2020). Altered Salivary Microbiome in the Early Stage of HIV Infections among Young Chinese Men Who Have Sex with Men (MSM). *Pathogens* 9 (1), 960. doi: 10.3390/pathogens9110960
- Li, Y., Saxena, D., Chen, Z., Liu, G., Abrams, W. R., Phelan, J. A., et al. (2014). HIV Infection and Microbial Diversity in Saliva. *J. Clin. Microbiol.* 52, 1400–1411. doi: 10.1128/JCM.02954-13
- Manfredi, R., Calza, L., and Chiodo, F. (2002). Enteric and Disseminated Campylobacter Species Infection During HIV Disease: A Persisting But Significantly Modified Association in the HAART Era. *Am. J. Gastroenterol.* 97, 510–511. doi: 10.1111/j.1572-0241.2002.05522.x
- Marchetti, G., Tincati, C., and Silvestri, G. (2013). Microbial Translocation in the Pathogenesis of HIV Infection and AIDS. *Clin. Microbiol. Rev.* 26, 2–18. doi: 10.1128/CMR.00050-12
- Molina, J., Casin, I., Hausfater, P., Giretti, E., Welker, Y., Decazes, J., et al. (1995). Campylobacter Infections in HIV-Infected Patients: Clinical and Bacteriological Features. *AIDS* 9, 881–885. doi: 10.1097/00002030-199508000-00008
- Moyes, D. L., Saxena, D., John, M. D., and Malamud, D. (2016). The Gut and Oral Microbiome in HIV Disease: A Workshop Report. *Oral. Dis.* 22 Suppl 1, 166–170. doi: 10.1111/odi.12415
- Mudd, J. C., and Brenchley, J. M. (2016). Gut Mucosal Barrier Dysfunction, Microbial Dysbiosis, and Their Role in HIV-1 Disease Progression. *J. Infect. Dis.* 214 Suppl 2, S58–S66. doi: 10.1093/infdis/jiw258
- Mukherjee, P. K., Chandra, J., Retuerto, M., Sikaroodi, M., Brown, R. E., Jurevic, R., et al. (2014). Oral Mycobiome Analysis of HIV-Infected Patients: Identification of Pichia as an Antagonist of Opportunistic Fungi. *PloS Pathog.* 10, e1003996. doi: 10.1371/journal.ppat.1003996
- Muller, F., Holberg-Petersen, M., Rollag, H., Degre, M., Brandtzaeg, P., and Froland, S. S. (1992). Nonspecific Oral Immunity in Individuals With HIV Infection. *J. Acquir. Immune Defic. Syndr.* (1988) 5 (1), 46–51.
- Mutlu, E. A., Keshavarzian, A., Losurdo, J., Swanson, G., Siewe, B., Forsyth, C., et al. (2014). A Compositional Look at the Human Gastrointestinal Microbiome and Immune Activation Parameters in HIV Infected Subjects. *PloS Pathog.* 10, e1003829. doi: 10.1371/journal.ppat.1003829
- Navazesh, M., Mulligan, R., Pogoda, J., Greenspan, D., Alves, M., Phelan, J., et al. (2005). The Effect of HAART on Salivary Microbiota in the Women's Interagency HIV Study (WIHS). *Oral. Surg. Oral. Med. Oral. Pathol. Oral. Radiol. Endod.* 100, 701–708. doi: 10.1016/j.tripleo.2004.10.011
- Noguera-Julian, M., Rocafor, M., Guillen, Y., Rivera, J., Casadella, M., Nowak, P., et al. (2016). Gut Microbiota Linked to Sexual Preference and HIV Infection. *EBioMedicine* 5, 135–146. doi: 10.1016/j.ebiom.2016.01.032
- Patil, S., Majumdar, B., Sarode, S. C., Sarode, G. S., and Awan, K. H. (2018). Oropharyngeal Candidosis in HIV-Infected Patients-An Update. *Front. Microbiol.* 9:980. doi: 10.3389/fmicb.2018.00980
- Presti, R. M., Handley, S. A., Droit, L., Ghannoum, M., Jacobson, M., Shiboski, C. H., et al. (2018). Alterations in the Oral Microbiome in HIV-Infected Participants After Antiretroviral Therapy Administration Are Influenced by Immune Status. *AIDS* 32, 1279–1287. doi: 10.1097/QAD.0000000000001811
- Rocafor, M., Noguera-Julian, M., Rivera, J., Pastor, L., Guillen, Y., Langhorst, J., et al. (2019). Evolution of the Gut Microbiome Following Acute HIV-1 Infection. *Microbiome* 7, 73. doi: 10.1186/s40168-019-0687-5
- Salari, S., and Ghasemi Nejad Almani, P. (2020). Antifungal Effects of Lactobacillus Acidophilus and Lactobacillus Plantarum Against Different Oral Candida Species Isolated From HIV/AIDS Patients: An *In Vitro* Study. *J. Oral. Microbiol.* 12:1769386. doi: 10.1080/20002297.2020.1769386
- Samaranayake, L., and Matsubara, V. H. (2017). Normal Oral Flora and the Oral Ecosystem. *Dent. Clin. North Am.* 61, 199–215. doi: 10.1016/j.cden.2016.11.002
- Saxena, D., Li, Y., Devota, A., Pushalkar, S., Abrams, W., Barber, C., et al. (2016). Modulation of the Orodigestive Tract Microbiome in HIV-Infected Patients. *Oral. Dis.* 22 Suppl 1, 73–78. doi: 10.1111/odi.12392
- Schmidt, T. S., Hayward, M. R., Coelho, L. P., Li, S. S., Costea, P. I., Voigt, A. Y., et al. (2019). Extensive Transmission of Microbes Along the Gastrointestinal Tract. *Elife* 8, e42693. doi: 10.7554/eLife.42693
- Spinler, J. K., Taweetchotipatr, M., Rognerud, C. L., Ou, C. N., Tumwasorn, S., and Versalovic, J. (2008). Human-Derived Probiotic Lactobacillus Reuteri Demonstrate Antimicrobial Activities Targeting Diverse Enteric Bacterial Pathogens. *Anaerobe* 14, 166–171. doi: 10.1016/j.anaerobe.2008.02.001
- Sun, Y., Ma, Y., Lin, P., Tang, Y. W., Yang, L., Shen, Y., et al. (2016). Fecal Bacterial Microbiome Diversity in Chronic HIV-Infected Patients in China. *Emerg. Microbes Infect.* 5, e31. doi: 10.1038/emi.2016.25
- Thompson, G. R.3rd, Patel, P. K., Kirkpatrick, W. R., Westbrook, S. D., Berg, D., Erlandsen, J., et al. (2010). Oropharyngeal Candidiasis in the Era of Antiretroviral Therapy. *Oral. Surg. Oral. Med. Oral. Pathol. Oral. Radiol. Endod.* 109, 488–495. doi: 10.1016/j.tripleo.2009.11.026
- Uriarte, S. M., Edmisson, J. S., and Jimenez-Flores, E. (2016). Human Neutrophils and Oral Microbiota: A Constant Tug-of-War Between a Harmonious and a Discordant Coexistence. *Immunol. Rev.* 273, 282–298. doi: 10.1111/imr.12451
- Yang, L., Poles, M. A., Fisch, G. S., Ma, Y., Nossa, C., Phelan, J. A., et al. (2016). HIV-Induced Immunosuppression Is Associated With Colonization of the Proximal Gut by Environmental Bacteria. *AIDS* 30, 19–29. doi: 10.1097/QAD.0000000000000935
- Zevin, A. S., McKinnon, L., Burgener, A., and Klatt, N. R. (2016). Microbial Translocation and Microbiome Dysbiosis in HIV-Associated Immune Activation. *Curr. Opin. HIV AIDS* 11, 182–190. doi: 10.1097/COH.0000000000000234
- Zhang, F., He, S., Jin, J., Dong, G., and Wu, H. (2015). Exploring Salivary Microbiota in AIDS Patients With Different Periodontal Statuses Using 454 GS-FLX Titanium Pyrosequencing. *Front. Cell Infect. Microbiol.* 5:55. doi: 10.3389/fcimb.2015.00055
- Zhou, Y., Ou, Z., Tang, X., Zhou, Y., Xu, H., Wang, X., et al. (2018). Alterations in the Gut Microbiota of Patients With Acquired Immune Deficiency Syndrome. *J. Cell Mol. Med.* 22, 2263–2271. doi: 10.1111/jcmm.13508

**Conflict of Interest:** The authors declare that the research was conducted in the absence of any commercial or financial relationships that could be construed as a potential conflict of interest.

Copyright © 2021 Li, Zhu, Su, Wei, Chen, Liu, Wei, Yang, Zhang, Xia, Wu, He and Zhang. This is an open-access article distributed under the terms of the Creative Commons Attribution License (CC BY). The use, distribution or reproduction in other forums is permitted, provided the original author(s) and the copyright owner(s) are credited and that the original publication in this journal is cited, in accordance with accepted academic practice. No use, distribution or reproduction is permitted which does not comply with these terms.



# Machine Learning Approach Identified Multi-Platform Factors for Caries Prediction in Child-Mother Dyads

Tong Tong Wu<sup>1</sup>, Jin Xiao<sup>2\*</sup>, Michael B. Sohn<sup>1</sup>, Kevin A. Fiscella<sup>3</sup>, Christie Gilbert<sup>4</sup>, Alex Grier<sup>4</sup>, Ann L. Gill<sup>4</sup> and Steve R. Gill<sup>4\*</sup>

<sup>1</sup> Department of Biostatistics and Computational Biology, University of Rochester Medical Center, Rochester, NY, United States, <sup>2</sup> Eastman Institute for Oral Health, University of Rochester Medical Center, Rochester, NY, United States, <sup>3</sup> Department of Family Medicine, University of Rochester Medical Center, Rochester, NY, United States, <sup>4</sup> Microbiology and Immunology, University of Rochester Medical Center, Rochester, NY, United States

## OPEN ACCESS

### Edited by:

Xin Xu,  
Sichuan University, China

### Reviewed by:

Jiyao Li,  
Sichuan University, China  
Yuan Liu,  
University of Pennsylvania,  
United States

### \*Correspondence:

Jin Xiao  
Jin\_Xiao@urmc.rochester.edu  
Steve R. Gill  
steven\_gill@urmc.rochester.edu

### Specialty section:

This article was submitted to  
Microbiome in Health and Disease,  
a section of the journal  
Frontiers in Cellular and  
Infection Microbiology

**Received:** 19 June 2021

**Accepted:** 09 July 2021

**Published:** 19 August 2021

### Citation:

Wu TT, Xiao J, Sohn MB, Fiscella KA, Gilbert C, Grier A, Gill AL and Gill SR (2021) Machine Learning Approach Identified Multi-Platform Factors for Caries Prediction in Child-Mother Dyads. *Front. Cell. Infect. Microbiol.* 11:727630. doi: 10.3389/fcimb.2021.727630

Untreated tooth decays affect nearly one third of the world and is the most prevalent disease burden among children. The disease progression of tooth decay is multifactorial and involves a prolonged decrease in pH, resulting in the demineralization of tooth surfaces. Bacterial species that are capable of fermenting carbohydrates contribute to the demineralization process by the production of organic acids. The combined use of machine learning and 16s rRNA sequencing offers the potential to predict tooth decay by identifying the bacterial community that is present in an individual's oral cavity. A few recent studies have demonstrated machine learning predictive modeling using 16s rRNA sequencing of oral samples, but they lack consideration of the multifactorial nature of tooth decay, as well as the role of fungal species within their models. Here, the oral microbiome of mother-child dyads (both healthy and caries-active) was used in combination with demographic-environmental factors and relevant fungal information to create a multifactorial machine learning model based on the LASSO-penalized logistic regression. For the children, not only were several bacterial species found to be caries-associated (*Prevotella histicola*, *Streptococcus mutans*, and *Rothia mucilaginosa*) but also *Candida* detection and lower toothbrushing frequency were also caries-associated. Mothers enrolled in this study had a higher detection of *S. mutans* and *Candida* and a higher plaque index. This proof-of-concept study demonstrates the significant impact machine learning could have in prevention and diagnostic advancements for tooth decay, as well as the importance of considering fungal and demographic-environmental factors.

**Keywords:** machine learning, statistical approaches, dental caries, multiplatform analysis, candida, oral microbiome

## INTRODUCTION

Poor maternal and child oral health is a public health crisis with potential intergenerational health impacts. With oral disease affecting 50% of the global population (3.9 billion) and untreated tooth decay (dental caries) impacting almost half of the world's population (44%), oral disease has become

the most prevalent of all the 291 conditions included in the Global Burden of Disease Study (FDI World Dental Federation. <https://www.fdiworlddental.org/oral-health/ask-the-dentist/facts-figures-and-stats>. Accessed September 5, 2020). Significantly, children younger than 5 years and their mothers, who together comprise 22% of the whole population, are profoundly affected by dental caries. Unmet oral health needs worsen among minority women and children who are from low-income families (Marchi et al., 2010; Thompson et al., 2013; Singhal et al., 2014).

Dental caries is multifactorial infectious disease, initiated from the virulent dental biofilms/plaque formed on tooth surfaces (Tanzer, 1995). Within dental biofilms/plaque, oral cariogenic bacteria metabolize dietary carbohydrates resulting in acid production and initiating demineralization of tooth enamel (Bowen, 2016). Remineralization, or restoration of mineral ions, is mediated through salivary calcium, phosphate, and fluoride ions. In a healthy (caries-free) mouth, the remineralization and demineralization rates are at equilibrium; when the demineralization rate exceeds the remineralization rate, tooth decay occurs (Takahashi and Nyvad, 2011; Abou Neel et al., 2016). Often, this shift from equilibrium is caused by a disruption in the ecology of the oral microbiome from a largely commensal community to a community dominated by cariogenic bacteria.

Recognizing the essential contribution of oral microorganisms to dental caries, the development of effective predictive models that utilize sensitive microbial markers would offer substantial opportunities to predict and prevent caries. However, because of the multifactorial etiology of dental caries, developing effective predictive models is also challenging. The current dental caries prediction model falls into two categories: 1) one utilizing classical statistical models that assess the contribution of demographic and environmental factors, either without consideration of microbial factors or only including a limited number of traditional caries risk markers, e.g., *Streptococcus mutans* and *Lactobacillus* (Caufield et al., 1993; Klein et al., 2004; Li et al., 2005; Kanasi et al., 2010; Slayton, 2011; Zhan et al., 2012; Klinke et al., 2014); 2) the other utilizing statistical/machine learning models that identify caries-related taxa and its differential abundance based on caries status, with limited adjusting of demographic, environmental, and other contributing factors (Teng et al., 2015; Grier et al., 2020). The approaches mentioned above do not take caries multifactorial etiology into account. Furthermore, in the past decade, studies have also indicated the potential cariogenic role of *Candida albicans* in children, together with *S. mutans* (Hossain et al., 2003; de Carvalho et al., 2006; Rozkiewicz et al., 2006; Raja et al., 2010; Srivastava et al., 2012; Yang et al., 2012; Klinke et al., 2014; Qiu et al., 2015; Alkhars et al., 2021). However, the existing caries prediction models have not assessed the contribution of *Candida*. Therefore, developing a statistical/machine learning model that assesses all caries-related risk factors, including bacteria, *Candida*, and demographic-environmental factors, is urgently needed.

To address this research gap, as a proof-of-concept study, we developed statistical/machine learning (ML) models to identify

caries-related oral microbes in cross-sectional mother-child dyads from a low-income underserved background.

## MATERIALS AND METHODS

### Study Population, Sample Collection, and 16S Ribosomal RNA Sequencing Data

A cohort of mother-child dyads with a balanced distribution of children with or without early childhood caries (ECC) was enrolled at the Eastman Institute for Oral Health, University of Rochester, detailed previously (Xiao et al., 2018a). Ethical approval of the study was obtained from the University of Rochester Research Subject Review Board (RSRB00056870). Children were younger than 6 years. Subjects who had severe systematic diseases or antibiotic treatment within the previous 3 months were excluded. Non-stimulated whole saliva was collected from subjects through a saliva jet connected to a suction pump at least 2 h after any tooth brushing, eating, or drinking. Supragingival dental plaque was collected from the whole dentition with a standard dental scaler. Previous established methods were used to isolate and identify *Candida species* (Xiao et al., 2016), and to perform oral microbiome sequencing and related bioinformatics analysis (Merkley et al., 2015; Grier et al., 2017). The results of the 16S ribosomal RNA (16s rRNA) sequencing data were detailed previously (Xiao et al., 2018a). Sequencing data that passed quality controls were included in this study to develop caries predictive model and were assigned to operational taxonomic units (OTUs) using the 2014 release of the closed reference OSU CORE database (Griffen et al., 2011). DESeq2-negative binomial Wald test was used to compare the microbial differential abundance at species level between caries and caries-free groups among the children and their mothers.

### Variables

The primary outcome is caries status (Y/N). The independent variables were as follows: (1) race (Black/African American or other), (2) years of age (ordinal), (3) ethnicity (Hispanic or non-Hispanic), (4) tooth brushing frequency (0, not every day; 1, once per day; 2, two times per day), (5) daycare attendance (Y/N), (6) inhaler use (for children only), (7) Plaque index (ordinal), (8) oral *Candida* status (Y/N), (9) relative abundance of taxa. Demographic-socioeconomic and oral hygiene behavior characteristics were collected through questionnaires.

### Transformation of Relative Abundance

The centered log-ratio (CLR) transformation was applied to the relative abundance of taxa, where for each subject, the sample vector undergoes a transformation based on the logarithm of the ratio between the individual elements and the geometric mean of the vector. CLR removes the value-range restriction of percentages (relative abundance is a percentage) but keeps the sum constraint of compositional data.



## LASSO-Penalized Logistic Regression

Our goal is to build a model that could explain and predict the probability of having caries based on a small set of factors. Therefore, logistic regression model was fitted for the response variable whether the subject has caries or not, on a large pool of candidate input variables, including demographic and clinical factors and CLR-transformed relative abundance of taxa. Because the number of candidate variables (~360) far exceeds the number of subjects (~40 in each model), regularization is needed to avoid overfitting and to identify a small set of relevant variables. Variable selection technique, specifically LASSO penalty, was applied. K-fold cross-validation (K=4) was used to determine the optimal value of the tuning parameters for the

LASSO penalty, i.e., the strength of the selection. Using this tuning parameter, the model was fitted and the solution path was calculated to show the order of variables entering the model.

## RESULTS

### Caries Prediction Models for Children

For the children's model, species-level sequencing data of 37 salivary samples and 36 plaque samples were used. The salivary and plaque microbial profiling is shown in **Figure 1**. *Veillonella atypica\_dispar\_parvula* and *Streptococcus ET\_G\_4D04* are the

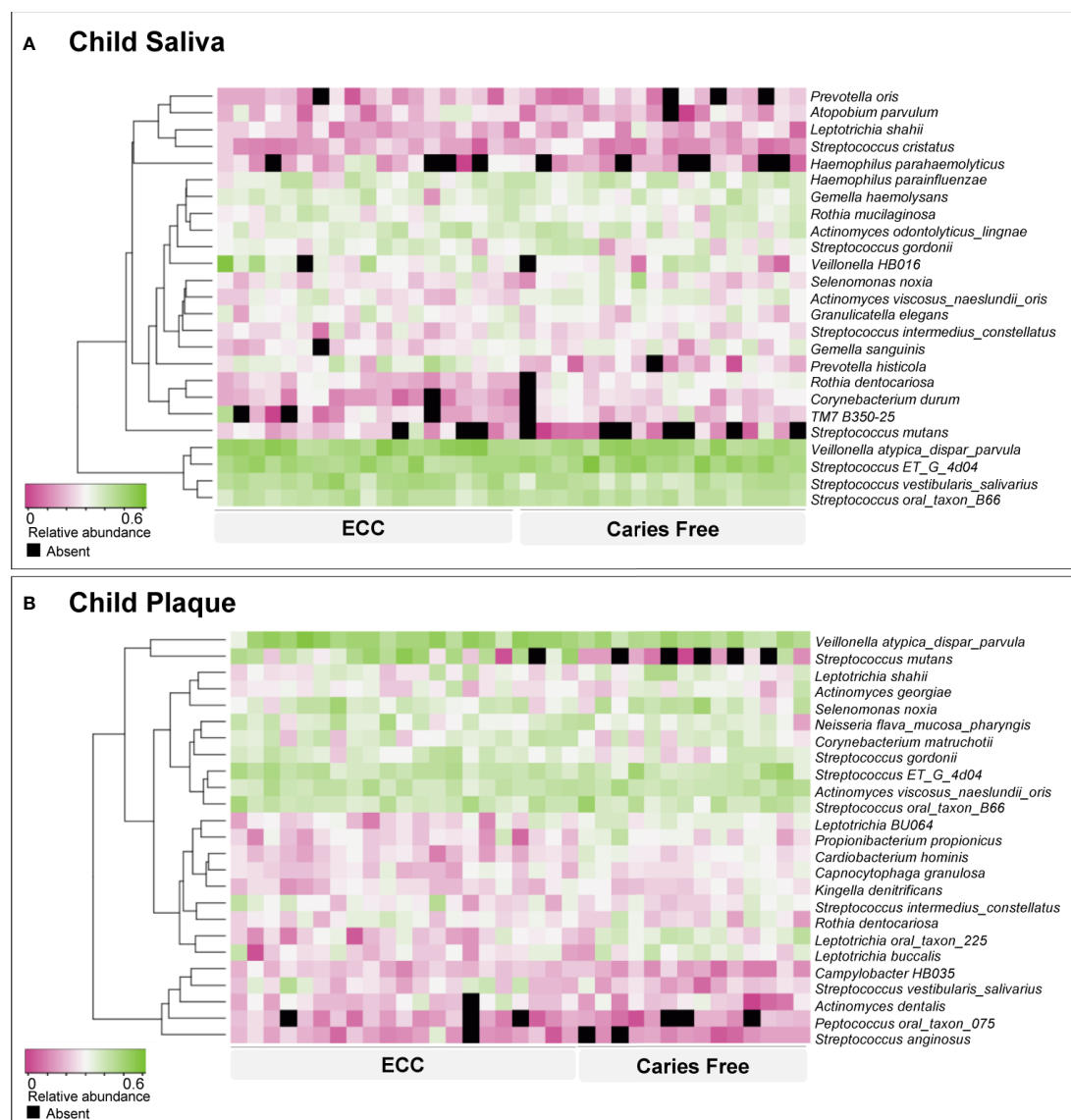


**FIGURE 1** | Early childhood caries-associated and caries-free-associated oral microbiome in children. Based on relative abundance, the salivary (A) and plaque (B) microorganisms were clustered into ECC-associated and caries-free-associated groups, as shown by the dendrogram on the left. Relative abundance is indicated by a gradient of shades from pink to green. Black spots indicate no detection of the species.

most abundant species in children's saliva and plaque. Not surprisingly, *S. mutans* is more abundant and with a higher detection among children with ECC.

### Saliva Model

Using 37 children's saliva taxa data (relative species abundance), we ran a LASSO-penalized logistic regression model on having

caries (1) or not (0) on a pool of candidate variables including 353 species in the microbiome data, four demographic variables (age, gender, race, ethnicity), four medical-dental-behavior characteristics (frequency of toothbrushing per day, attending daycare, inhaler use, and plaque index), and one fungal-related parameter (*Candida* detection status). Seven variables were identified to be associated with caries. The LASSO solution

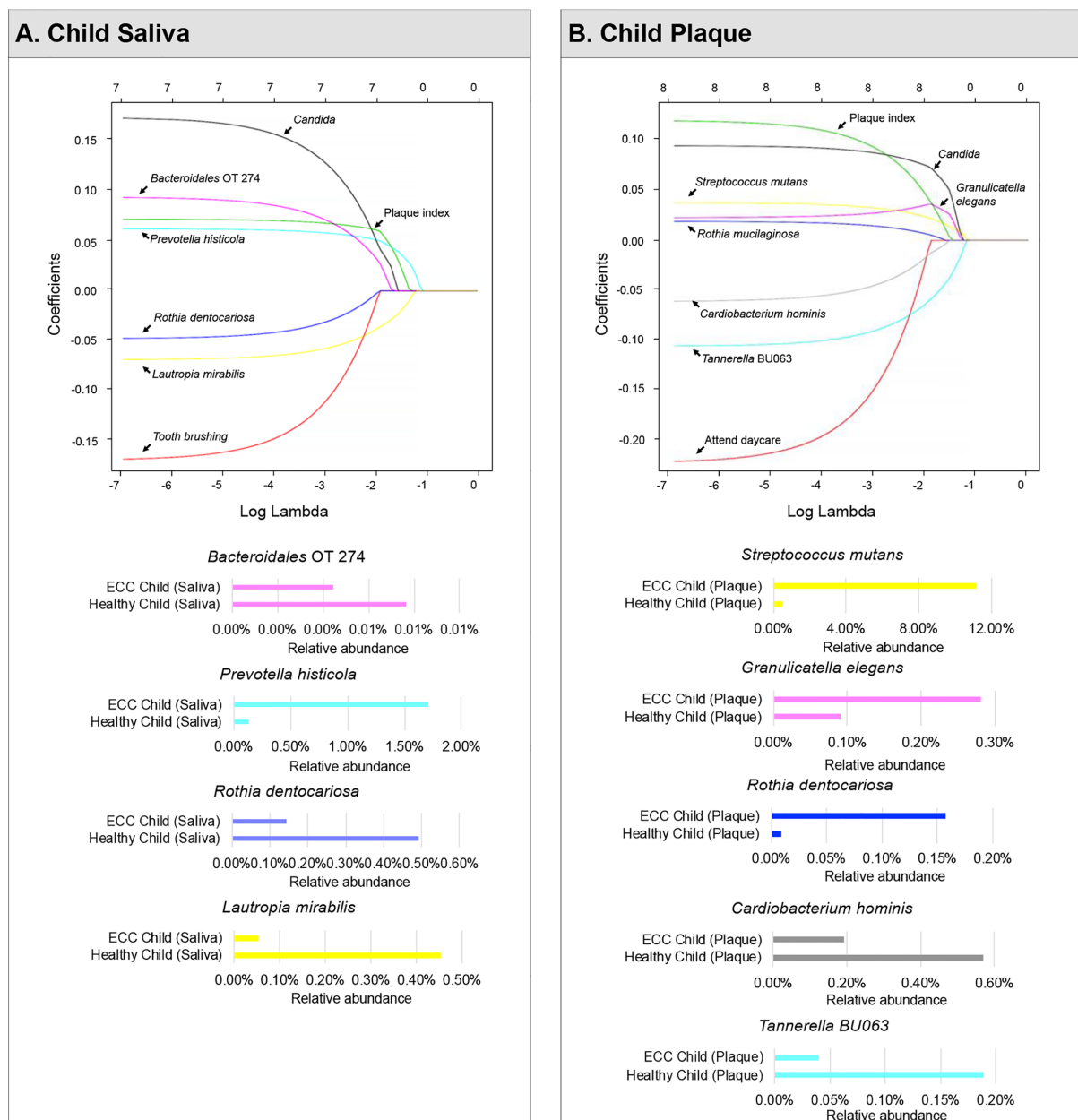


**FIGURE 2 |** Identified factors associated with child's caries risk using machine Learning model. LASSO-penalized logistic regression modeling was used for caries predictor selection for children's saliva and plaque samples. Specifically, seven variables for models using salivary microorganisms (A) and eight variables for models using plaque microorganisms (B) were identified as predictive factors for dental caries in preschool children. The LASSO solution path above shows how the model is built sequentially by adding one variable at a time to the active set.



path (**Figure 2A**) shows how the model is built sequentially by adding one variable at a time to the active set (i.e., set of variables with non-zero coefficients).

In a sequential order, *Prevotella histicola* (1.7% in ECC children and 0.12% in caries-free children) was the first variable that enters the saliva model, indicating that if a model with only one variable is desired, *P. histicola* would be the one to be used. As lambda decreases, *Lautropia mirabilis* entered the model as the second variable. Then plaque index and *Candida* were selected into the model, followed by an unclassified *Bacteroidales* oral taxon 274, *Rothia dentocariosa*, and toothbrushing frequency.

Moreover, *P. histicola*, plaque index, *Candida*, and *Bacteroidales* Oral Taxon 274 were predicted to be associated with an increased risk for caries; whereas, *L. mirabilis*, toothbrushing, and *R. dentocariosa* were associated with a decreased risk for caries in children. When lambda reached an extremely small number (e.g.,  $10^{-7}$  in the far left of the solution path), the coefficient estimates are approximately the same as those in the unpenalized logistic regression model. The predictive model using childrens' saliva samples is given by:

$$\begin{aligned} \text{logit}(p) = X\beta = & 0.641 + 0.174\text{Candida} - 0.170\text{toothbrush} + \\ & 0.072\text{plaque} - 0.048\text{Rothia dentocariosa} + 0.062\text{Prevotella} \\ & \text{histicola} + 0.094\text{Bacteroidales oral taxon 274} - 0.069 \\ & \text{Lautropia mirabilis}, \end{aligned}$$

where the probability of having caries can be estimated by

$$p(\text{caries}) = \frac{\exp(X\beta)}{1 + \exp(X\beta)}$$

Using the variable “toothbrush” as an example, the interpretation of the coefficient is that for individuals who brush their teeth for one or more times per day, the odds of having caries will be  $\exp(-0.170)=0.84$  times the odds for those who do not, which will result in an approximately 16% reduction. Similarly, individuals who brush their teeth twice per day will have an odds of 30% lower than those who do not brush teeth every day.

Furthermore, the differential abundance of three selected species (*L. mirabilis*, *R. dentocariosa*, *P. histicola*) was statistically significant ( $p<0.05$ ) (see **Figure 3A**).

### Plaque Model

In the plaque model (**Figure 2B**), eight variables were selected, with five of them being the relative abundance of bacterial taxa, one fungal-related (*Candida* status), one oral hygiene index, and one behavior parameter. In sequential order, *S. mutans* entered the model as the first variable with an increased risk for caries (11.14% in ECC and 0.47% in caries-free children). *Tannerella BU063* entered the model as the second variable with a reduced caries risk, more abundant in caries-free children (0.18%), and less abundant in ECC children (0.04%). *Candida* (increased caries risk) was the third variable selected,

followed by *Granulicatella elegans* (increased caries risk), plaque index, *Cardiobacterium hominis* (reduced caries risk), *Rothia mucilaginosa* (increased caries risk), and daycare attendance (reduced caries risk). The differential abundance of four selected species (*T. BU063*, *R. mucilaginosa*, *C. hominis*, and *G. elegans*) was statistically significant ( $p<0.05$ ) (see **Figure 3B**).

The predictive model that used childrens' plaque samples is the follows:

$$\begin{aligned} \text{logit}(p) = X\beta \\ = & 0.459 + 0.098\text{Candida} - 0.231\text{daycare attendance} + 0.125\text{plaque} \\ & + 0.020\text{Rothia mucilaginosa} - 0.110\text{Tannerella BU063} \\ & + 0.024\text{Granulicatella elegans} + 0.039\text{Streptococcus mutans} \\ & - 0.063\text{Cardiobacterium hominis} \end{aligned}$$

### Caries Prediction Model for Mothers

For the mothers' model, species-level sequencing data of 32 plaque samples were used. The plaque microbial profiling of each sample is shown in **Figure 4**. For the mothers, the LASSO solution path that demonstrates how the model is built sequentially is shown in **Figure 5**. Nine taxa, one fungal parameter (*Candida* status) and oral hygiene index were selected into the model. *Streptococcus intermedius constellatus* (increased caries risk) and *Neisseria* AP085 (decreased caries risk) entered the model closely as the top 2 variables. Plaque index (increased risk) was selected as the third variable in the model. The remaining variables were selected in an order as follows: *Peptococcus* OT 075 (increased risk), *Streptococcus* GU045364 (increased risk), *Anaeroglobus* BS073\_CS025 (increased risk), *Catonella* GQ106843 (decreased risk), *Candida* (increased risk), *Corynebacterium durum* (decreased risk), *Streptococcus cristatus* (increased risk), and *Tannerella forsythia* (decreased risk).

The predictive model that used mothers' plaque samples is the following:

$$\begin{aligned} \text{logit}(p) = X\beta \\ = & 0.459 + 0.006\text{Candida} + 0.012\text{plaque} \\ & - 0.022\text{Corynebacterium durum} - 0.002\text{Tannerella forsythia} \\ & + 0.018\text{Streptococcus GU045364} + 0.003\text{Streptococcus cristatus} \\ & + 0.033\text{Streptococcus intermedius constellatus} \\ & - 0.023\text{Catonella GQ106843} + 0.052\text{Peptococcus oral taxon 075} \\ & + 0.014\text{Anaeroglobus BS073_CS025} - 0.009\text{Neisseria AP085} \end{aligned}$$

### Performance of Caries Prediction Model

The caries prediction models achieved desirable performance that was assessed by area under the ROC curve (AUC), see **Figure 6**. The average AUC over 20 random four-fold cross-validation was 0.82 for the child's saliva model, 0.78 for the child's plaque model, and 0.73 for the mother's plaque model.

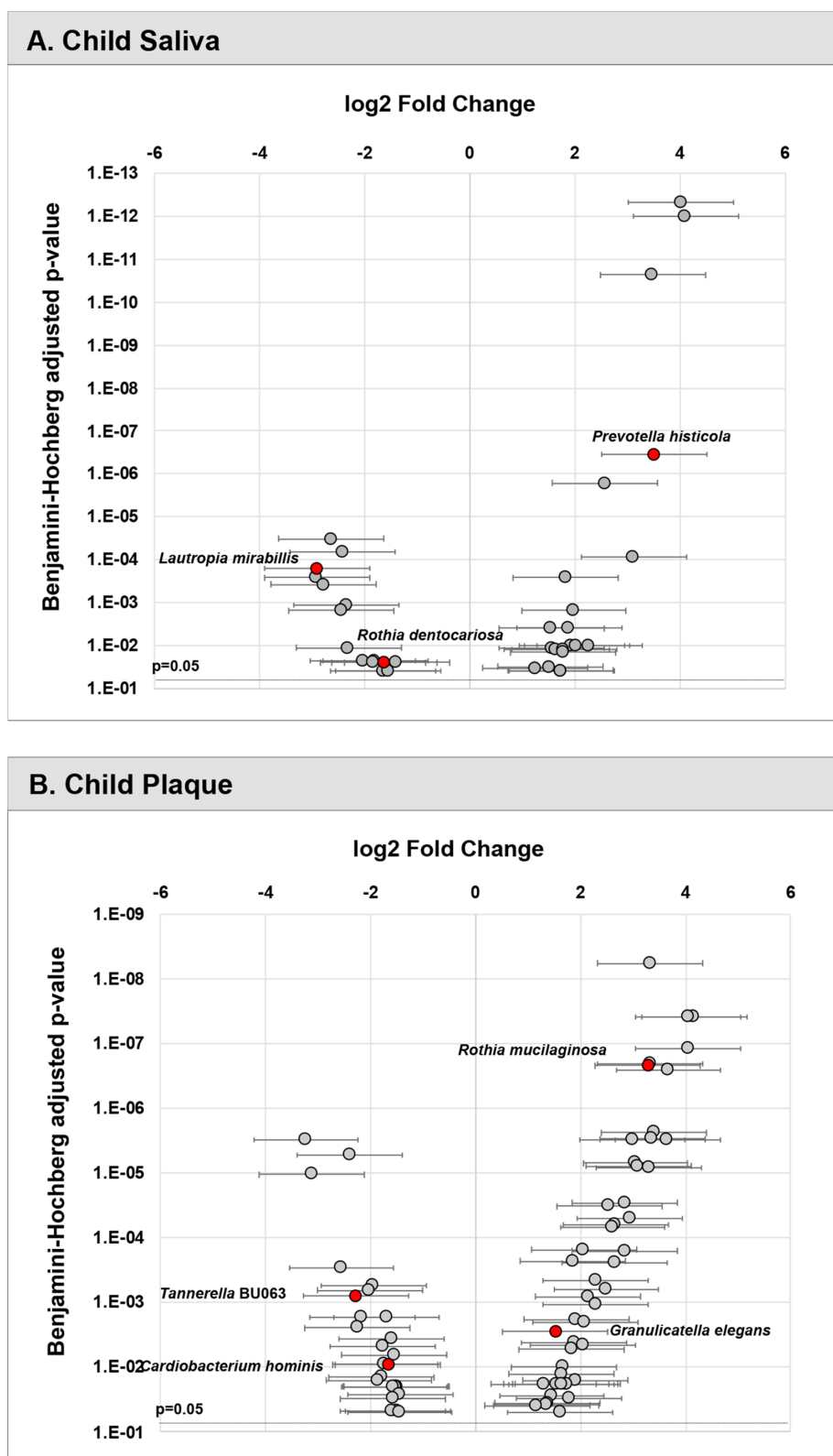
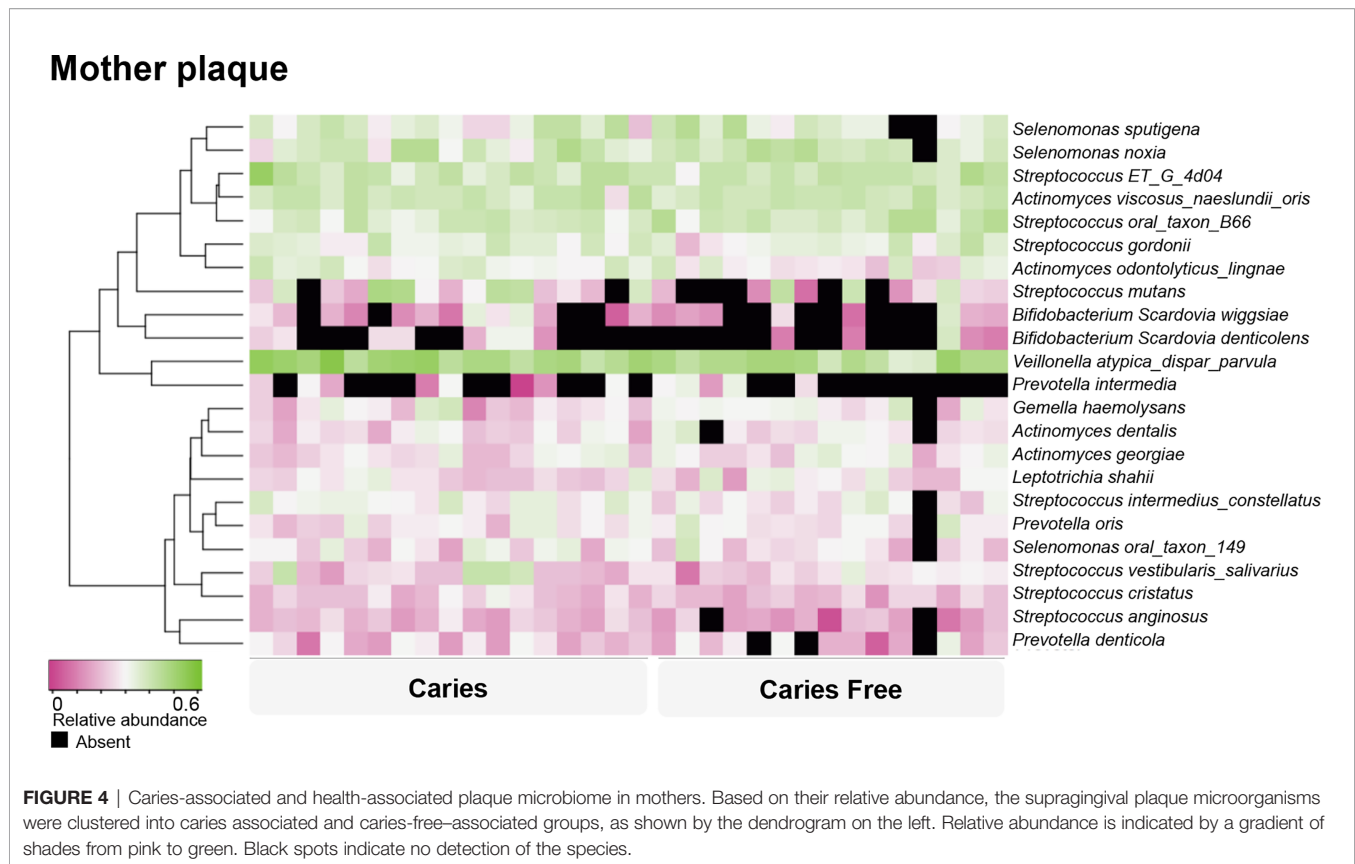


**FIGURE 3** | Differential abundance of taxa in children's saliva and plaque. Relative fold change in abundance of species in saliva (A) and plaque (B) from children with ECC vs. caries-free. All species plotted with a p value <0.05.



## DISCUSSION

ML modeling of the oral microbiome has the potential to identify microbial biomarkers and aid in the prediction of dental caries. This proof-of-concept study is the first study to our knowledge that used an enhanced ML approach to incorporate multi-source variables with microbial data for dental caries prediction. The developed models have the following features:

1. The models considered the multifactorial etiology of dental caries by incorporating demographic-medical-dental characteristics, oral hygiene practice, daycare attendance, together with 16s relative species abundance, and oral *Candida* status. A meta-analysis indicates that children with oral *C. albicans* have (>5 times) higher odds of having ECC compared with those without *C. albicans* (Xiao et al., 2018b) and children with early-life oral *Candida* colonization are at higher risk for *S. mutans* emergence in the mouth by 1 year of age (Alkhars et al., 2021). However, no caries risk models have reflected the potential contribution from *Candida*. Our study demonstrated the consistent contribution from *Candida* in both child's and mother's prediction model.
2. The sequential order of the variables that entered the model reflects the contribution of the variables to predicting dental caries.
3. Intercept of the variables in the model would enable quantification of caries risk assessment, which has important clinical use implication.

Teng et al. (2015) used temporal patterns of the salivary and plaque microbiome to predict onset of ECC among children followed up from 4 to 6 years of age. The most discriminate species in Teng's predictive model included *S. mutans* and *P. histicola*. Our model also included *P. histicola* as a discriminate species with an increased abundance in caries-active children, this is supported by previous findings of the association of *P. histicola* and caries (Hurley et al., 2019). Although *P. histicola* has been identified in several studies as being associated with caries and lower pH values, its direct function and role in the oral microbiome has not been elucidated. Additionally, Grier et al. (2020) developed a ML model to identify species in saliva that is associated with the onset of ECC among 56 preschool children. *R. mucilaginosa*, *Streptococcus* sp. and *Veillonella parvula* were selected as discriminatory markers for ECC onset. Both *Streptococcus* sp. and *Veillonella parvula* were highly abundant in the plaque and saliva samples of children with caries in our study. The early colonizer *R. mucilaginosa* was not a discriminatory microbe in our salivary model; this may be reflective of the age of our cohort and demonstrates a need for studies at earlier timepoints (and longitudinally).

Despite having a smaller sample size in our model, the performance of our ML was comparable or better than models of these studies. Potentially, this could be because of the advantages of our multifactorial approach. This is exemplified by *Candida* presence (increased risk) and toothbrushing frequency (decreased risk) as strong discriminatory factors in our model, which would have been otherwise missed if our ML relied solely on 16s rRNA data. In addition, our model was able to utilize both cariogenic and

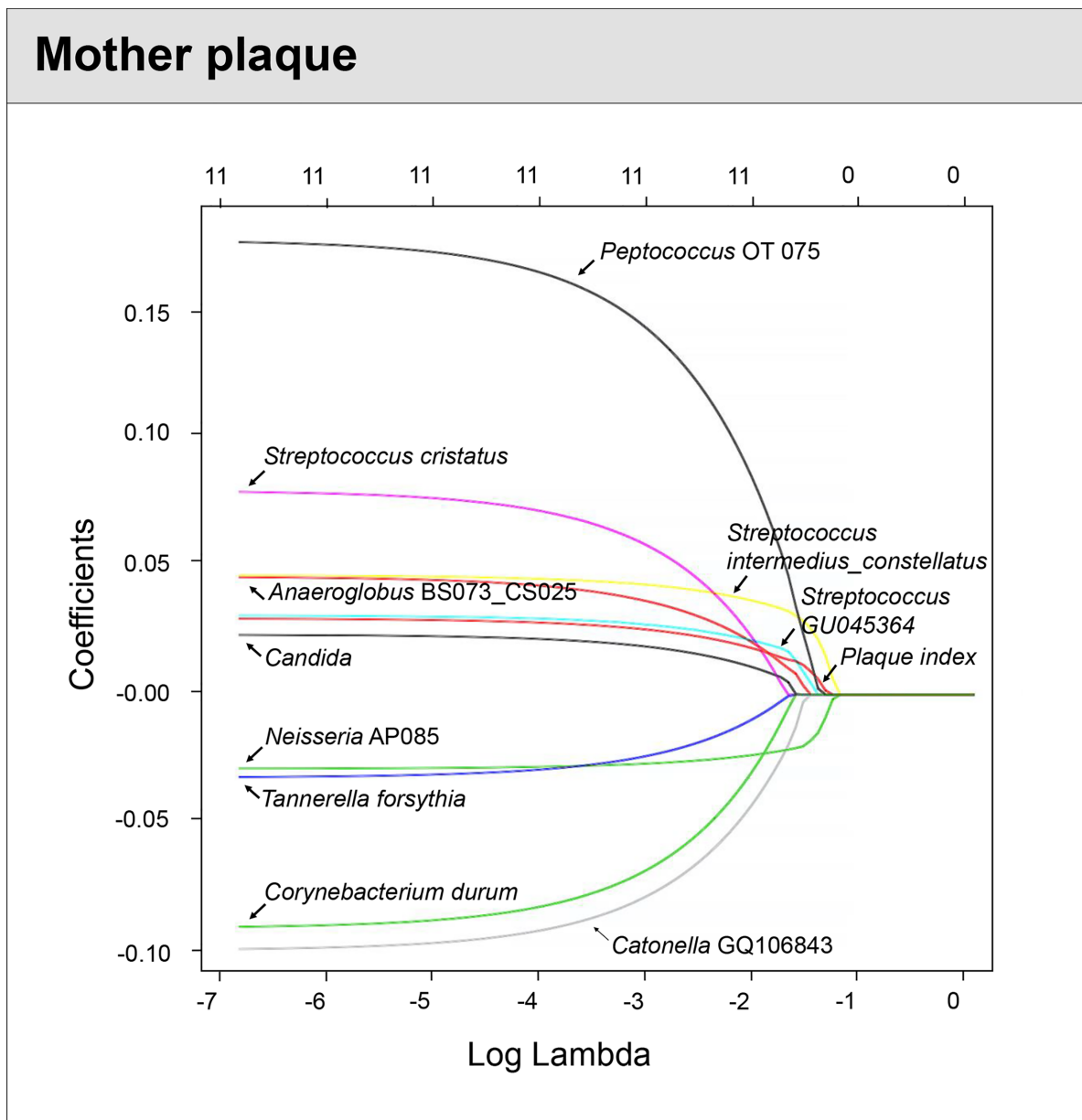


**FIGURE 5** | Identified factors associated with mother's caries risk using machine Learning model. LASSO-penalized logistic regression modeling was used for caries predictor selection for children's saliva and plaque samples. Eleven variables for models using plaque microorganisms were identified as predictive factors for dental caries in mothers. The LASSO solution path above shows how the model is built sequentially by adding one variable at a time to the active set.

protective bacteria as discriminatory markers. *Lautropia mirabilis* and *Rothia dentocariosa* were found to be protective markers in the salivary microbiome of the children in this study. In a comparison of caries-free and caries-active children of 6 to 9 years old, *L. mirabilis* was found to have a significantly higher abundance in the caries-free children (Qudeimat et al., 2021). Future *in vitro* assays would be helpful to determine whether *L. mirabilis* functions to create a healthier (neutral pH) oral environment, or if a higher abundance of *L. mirabilis* implies an indirect consequence of an

already neutral pH. Additionally, a higher abundance of *R. dentocariosa* has been found in children with caries in some studies (Jiang et al., 2016; Inquimbert et al., 2019), which is contrary to our results.

Using the proposed ML models, we identified specific caries-related oral bacteria, *Candida*, together with other multi-source factors for preschool children and their mothers. Prediction models for both children and their mothers achieved desirable performance. Fine-tuning and further validation are needed

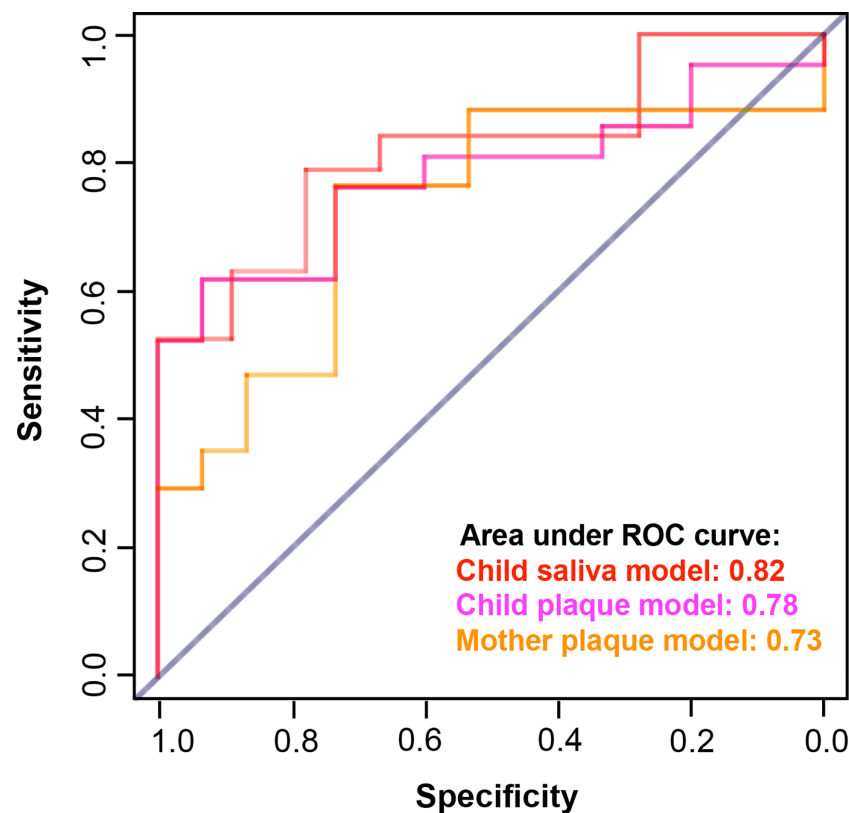


**FIGURE 6 |** Performance of caries prediction models. The caries prediction models achieved desirable performance that was assessed by area under the ROC curve (AUC). The AUC for the child saliva model was 0.82; The AUC for the child plaque model was 0.78; and the AUC for the mother plaque model was 0.73.

using larger and longitudinal caries onset sample set. Future models will consider incorporating more diverse biological and environmental variables, including children's diet, parent's education, oral hygiene, health, and oral microbiome. Experimental and clinical confirmation of the predicted microbial signatures for caries risk prediction and the translation into clinically measurable parameters of antigen and bacterial abundance will enhance our ability to identify at-risk children and promote the development of preventative therapeutics.

The following limitations need to be considered when interpreting the study results: (1) limited sample size; (2) conducted in one US city. Thus, generalization to other populations is unreliable because of the small convenient sample size; (3) with the data set being cross-sectional data set, the models are built upon the existing caries status, not through the longitudinal onset of caries. Future validations of our models are warranted using longitudinal data set.

## DATA AVAILABILITY STATEMENT

The original contributions presented in the study are included in the article material. Further inquiries can be directed to the corresponding authors.

## ETHICS STATEMENT

The studies involving human participants were reviewed and approved by University of Rochester Research Subject Review Board. Written informed consent to participate in this study was provided by the participants or the participants' legal guardian.

## AUTHOR CONTRIBUTIONS

TTW, JX, MBS, KAF, CG, and SRG contributed to the conception, design, data acquisition, analysis, and interpretation, drafting, and critically revising the manuscript. AG and ALG contributed to data acquisition, analysis, and critically revising the manuscript. All authors contributed to the article and approved the submitted version.

## FUNDING

JX's research was supported by the National Institute of Dental and Craniofacial Research grant K23DE027412. TT's work is supported by grant from the National Science Foundation NSF-CCF-1934962.



## REFERENCES

- Abou Neel, E. A., Aljabo, A., Strange, A., Ibrahim, S., Coathup, M., Young, A. M., et al. (2016). Demineralization-Remineralization Dynamics in Teeth and Bone. *Int. J. Nanomed.* 11, 4743–4763. doi: 10.2147/ijn.S107624
- Alkhars, N., Zeng, Y., Alomeir, N., Al Jallad, N., Wu, T. T., Abaelmagd, S., et al. (2021). Oral Candida Predicts Streptococcus Mutans Emergence in Underserved US Infants. *J. Dent. Res.*, 220345211012385. doi: 10.1177/00220345211012385
- Bowen, W. H. (2016). Dental Caries - Not Just Holes in Teeth! A Perspective. *Mol. Oral Microbiol.* 31 (3), 228–233. doi: 10.1111/omi.12132
- Caufield, P. W., Cutter, G. R., and Dasanayake, A. P. (1993). Initial Acquisition of Mutans Streptococci by Infants: Evidence for a Discrete Window of Infectivity. *J. Dent. Res.* 72 (1), 37–45. doi: 10.1177/00220345930720010501
- de Carvalho, F. G., Silva, D. S., Hebling, J., Spolidorio, L. C., and Spolidorio, D. M. (2006). Presence of Mutans Streptococci and Candida Spp. In Dental Plaque/Dentine of Carious Teeth and Early Childhood Caries. *Arch. Oral Biol.* 51 (11), 1024–1028. doi: 10.1016/j.archoralbio.2006.06.001
- FDI World Dental Federation (2020). Available at: <https://www.fdiworlddental.org/oral-health/ask-the-dentist/facts-figures-and-stats> (Accessed September 5).
- Grier, A., Myers, J. A., O'Connor, T. G., Quivey, R. G., Gill, S. R., and Kopycka-Kedzierawski, D. T. (2020). Oral Microbiota Composition Predicts Early Childhood Caries Onset. *J. Dent. Res.* 100 (6), 599–607. doi: 10.1177/0022034520979926
- Grier, A., Qiu, X., Bandyopadhyay, S., Holden-Wiltse, J., Kessler, H. A., Gill, A. L., et al. (2017). Impact of Prematurity and Nutrition on the Developing Gut Microbiome and Preterm Infant Growth. *Microbiome* 5 (1), 158. doi: 10.1186/s40168-017-0377-0
- Griffen, A. L., Beall, C. J., Firestone, N. D., Gross, E. L., Difrancio, J. M., Hardman, J. H., et al. (2011). CORE: A Phylogenetically-Curated 16S rDNA Database of the Core Oral Microbiome. *PLoS One* 6 (4), e19051. doi: 10.1371/journal.pone.0019051
- Hossain, H., Ansari, F., Schulz-Weidner, N., Wetzel, W. E., Chakraborty, T., and Domann, E. (2003). Clonal Identity of Candida Albicans in the Oral Cavity and the Gastrointestinal Tract of Pre-School Children. *Oral Microbiol. Immunol.* 18 (5), 302–308. doi: 10.1034/j.1399-302X.2003.00086.x
- Hurley, E., Barrett, M. P. J., Kinirons, M., Whelton, H., Ryan, C. A., Stanton, C., et al. (2019). Comparison of the Salivary and Dentinal Microbiome of Children With Severe-Early Childhood Caries to the Salivary Microbiome of Caries-Free Children. *BMC Oral Health* 19 (1), 13. doi: 10.1186/s12903-018-0693-1
- Inquimbert, C., Bourgeois, D., Bravo, M., Viennot, S., Tramini, P., Llodra, J. C., et al. (2019). The Oral Bacterial Microbiome of Interdental Surfaces in Adolescents According to Carious Risk. *Microorganisms* 7 (9), 319–342. doi: 10.3390/microorganisms7090319
- Jiang, S., Gao, X., Jin, L., and Lo, E. C. (2016). Salivary Microbiome Diversity in Caries-Free and Caries-Affected Children. *Int. J. Mol. Sci.* 17 (12), 1978–1990. doi: 10.3390/ijms17121978
- Kanasi, E., Johansson, I., Lu, S. C., Kressin, N. R., Nunn, M. E., Kent, R. Jr., et al. (2010). Microbial Risk Markers for Childhood Caries in Pediatricians' Offices. *J. Dent. Res.* 89 (4), 378–383. doi: 10.1177/0022034509360010
- Klein, M. I., Florio, F. M., Pereira, A. C., Hofling, J. F., and Goncalves, R. B. (2004). Longitudinal Study of Transmission, Diversity, and Stability of Streptococcus Mutans and Streptococcus Sobrinus Genotypes in Brazilian Nursery Children. *J. Clin. Microbiol.* 42 (10), 4620–4626. doi: 10.1128/JCM.42.10.4620-4626.2004
- Klinke, T., Urban, M., Luck, C., Hannig, C., Kuhn, M., and Kramer, N. (2014). Changes in Candida Spp., Mutans Streptococci and Lactobacilli Following Treatment of Early Childhood Caries: A 1-Year Follow-Up. *Caries Res.* 48 (1), 24–31. doi: 10.1159/000351673
- Li, Y., Caufield, P. W., Dasanayake, A. P., Wiener, H. W., and Vermund, S. H. (2005). Mode of Delivery and Other Maternal Factors Influence the Acquisition of Streptococcus Mutans in Infants. *J. Dent. Res.* 84 (9), 806–811. doi: 10.1177/154405910508400905
- Marchi, K. S., Fisher-Owens, S. A., Weintraub, J. A., Yu, Z., and Braveman, P. A. (2010). Most Pregnant Women in California do Not Receive Dental Care: Findings From a Population-Based Study. *Public Health Rep.* 125 (6), 831–842. doi: 10.1177/003335491012500610
- Merkley, M. A., Bice, T. C., Grier, A., Strohl, A. M., Man, L. X., and Gill, S. R. (2015). The Effect of Antibiotics on the Microbiome in Acute Exacerbations of Chronic Rhinosinusitis. *Int. Forum Allergy Rhinol.* 5 (10), 884–893. doi: 10.1002/alr.21591
- Qiu, R., Li, W., Lin, Y., Yu, D., and Zhao, W. (2015). Genotypic Diversity and Cariogenicity of Candida Albicans From Children With Early Childhood Caries and Caries-Free Children. *BMC Oral Health* 15 (1), 144. doi: 10.1186/s12903-015-0134-3
- Qudeimat, M. A., Alyahya, A., Karched, M., Behbehani, J., and Salako, N. O. (2021). Dental Plaque Microbiota Profiles of Children With Caries-Free and Caries-Active Dentition. *J. Dent.* 104, 103539. doi: 10.1016/j.jdent.2020.103539
- Raja, M., Hannan, A., and Ali, K. (2010). Association of Oral Candidal Carriage With Dental Caries in Children. *Caries Res.* 44 (3), 272–276. doi: 10.1159/000314675
- Rozkiewicz, D., Daniluk, T., Zaremba, M. L., Cylwik-Rokicka, D., Stokowska, W., Pawinska, M., et al. (2006). Oral Candida Albicans Carriage in Healthy Preschool and School Children. *Adv. Med. Sci.* 51 (Suppl 1), 187–190.
- Singhal, A., Chattopadhyay, A., Garcia, A. I., Adams, A. B., and Cheng, D. (2014). Disparities in Unmet Dental Need and Dental Care Received by Pregnant Women in Maryland. *Matern. Child Health J.* 18 (7), 1658–1666. doi: 10.1007/s10995-013-1406-7
- Slayton, R. L. (2011). Reducing Mutans Streptococci Levels in Caregivers may Reduce Transmission to Their Children and Lead to Reduced Caries Prevalence. *J. Evid. Based Dent. Pract.* 11 (1), 27–28. doi: 10.1016/j.jebdp.2010.11.014
- Srivastava, B., Bhatia, H. P., Chaudhary, V., Aggarwal, A., Kumar Singh, A., and Gupta, N. (2012). Comparative Evaluation of Oral Candida Albicans Carriage in Children With and Without Dental Caries: A Microbiological *In Vivo* Study. *Int. J. Clin. Pediatr. Dent.* 5 (2), 108–112. doi: 10.5005/jp-journals-10005-1146
- Takahashi, N., and Nyvad, B. (2011). The Role of Bacteria in the Caries Process: Ecological Perspectives. *J. Dent. Res.* 90 (3), 294–303. doi: 10.1177/0022034510379602
- Tanzer, J. M. (1995). Dental Caries is a Transmissible Infectious Disease: The Keyes and Fitzgerald Revolution. *J. Dent. Res.* 74 (9), 1536–1542. doi: 10.1177/00220345950740090601
- Teng, F., Yang, F., Huang, S., Bo, C., Xu, Z. Z., Amir, A., et al. (2015). Prediction of Early Childhood Caries via Spatial-Temporal Variations of Oral Microbiota. *Cell Host Microbe* 18 (3), 296–306. doi: 10.1016/j.chom.2015.08.005
- Thompson, T. A., Cheng, D., and Strobino, D. (2013). Dental Cleaning Before and During Pregnancy Among Maryland Mothers. *Matern. Child Health J.* 17 (1), 110–118. doi: 10.1007/s10995-012-0954-6
- Xiao, J., Grier, A., Faustoferri, R. C., Alzoubi, S., Gill, A. L., Feng, C., et al. (2018a). Association Between Oral Candida and Bacteriome in Children With Severe ECC. *J. Dent. Res.* 97 (13), 1468–1476. doi: 10.1177/0022034518790941
- Xiao, J., Huang, X., Alkhers, N., Alzamil, H., Alzoubi, S., Wu, T. T., et al. (2018b). Candida Albicans and Early Childhood Caries: A Systematic Review and Meta-Analysis. *Caries Res.* 52 (1-2), 102–112. doi: 10.1159/000481833
- Xiao, J., Moon, Y., Li, L., Rustchenko, E., Wakabayashi, H., Zhao, X., et al. (2016). Candida Albicans Carriage in Children With Severe Early Childhood Caries (S-ECC) and Maternal Relatedness. *PLoS One* 11 (10), e0164242. doi: 10.1371/journal.pone.0164242
- Yang, X. Q., Zhang, Q., Lu, L. Y., Yang, R., Liu, Y., and Zou, J. (2012). Genotypic Distribution of Candida Albicans in Dental Biofilm of Chinese Children Associated With Severe Early Childhood Caries. *Arch. Oral Biol.* 57 (8), 1048–1053. doi: 10.1016/j.archoralbio.2012.05.012
- Zhan, L., Tan, S., Den Besten, P., Featherstone, J. D., and Hoover, C. I. (2012). Factors Related to Maternal Transmission of Mutans Streptococci in High-Risk Children-Pilot Study. *Pediatr. Dent.* 34 (4), e86–e91.

**Conflict of Interest:** The authors declare that the research was conducted in the absence of any commercial or financial relationships that could be construed as a potential conflict of interest.

**Publisher's Note:** All claims expressed in this article are solely those of the authors and do not necessarily represent those of their affiliated organizations, or those of the publisher, the editors and the reviewers. Any product that may be evaluated in this article, or claim that may be made by its manufacturer, is not guaranteed or endorsed by the publisher.

Copyright © 2021 Wu, Xiao, Sohn, Fiscella, Gilbert, Grier, Gill and Gill. This is an open-access article distributed under the terms of the Creative Commons Attribution License (CC BY). The use, distribution or reproduction in other forums is permitted, provided the original author(s) and the copyright owner(s) are credited and that the original publication in this journal is cited, in accordance with accepted academic practice. No use, distribution or reproduction is permitted which does not comply with these terms.



# Effects of *Helicobacter pylori* Infection on the Oral Microbiota of Reflux Esophagitis Patients

Tian Liang<sup>1,2†</sup>, Fang Liu<sup>1,2†</sup>, Lijun Liu<sup>1,2</sup>, Zhiying Zhang<sup>1,2</sup>, Wenxue Dong<sup>1,2</sup>, Su Bai<sup>1,2</sup>, Lifeng Ma<sup>1,2\*</sup> and Longli Kang<sup>1,2\*</sup>

<sup>1</sup> Key Laboratory for Molecular Genetic Mechanisms and Intervention Research on High Altitude Disease of Tibet Autonomous Region, School of Medicine, Xizang Minzu University, Xianyang, China, <sup>2</sup> Key Laboratory of High Altitude Environment and Genes Related to Diseases of Tibet Autonomous Region, School of Medicine, Xizang Minzu University, Xianyang, China

## OPEN ACCESS

### Edited by:

Yulong Niu,  
Sichuan University, China

### Reviewed by:

Takuichi Sato,  
Niigata University, Japan  
Yuan Wang,  
Zhejiang University, China

### \*Correspondence:

Lifeng Ma  
xzmymf@163.com  
Longli Kang  
longli\_kang@163.com

<sup>†</sup>These authors have contributed  
equally to this work

### Specialty section:

This article was submitted to  
Microbiome in Health and Disease,  
a section of the journal  
Frontiers in Cellular and  
Infection Microbiology

**Received:** 29 June 2021

**Accepted:** 11 August 2021

**Published:** 16 September 2021

### Citation:

Liang T, Liu F, Liu L, Zhang Z,  
Dong W, Bai S, Ma L and Kang L  
(2021) Effects of *Helicobacter pylori*  
Infection on the Oral Microbiota of  
Reflux Esophagitis Patients.  
Front. Cell. Infect. Microbiol. 11:732613.  
doi: 10.3389/fcimb.2021.732613

The human oral microbiota plays a vital role in maintaining metabolic homeostasis. To explore the relationship between *Helicobacter pylori* (*Hp*) and reflux esophagitis, we collected 86 saliva samples from reflux esophagitis patients (RE group) and 106 saliva samples from healthy people (C group) for a high-throughput sequencing comparison. No difference in alpha diversity was detected between the RE and the C groups, but beta diversity of the RE group was higher than the C group. Bacteroidetes was more abundant in the RE group, whereas Firmicutes was more abundant in the C group. The linear discriminant analysis effect size analysis demonstrated that the biomarkers of the RE group were *Prevotella*, *Veillonella*, *Leptotrichia*, and *Actinomyces*, and the biomarkers of the C group were *Lautropia*, *Gemella*, *Rothia*, and *Streptococcus*. The oral microbial network structure of the C group was more complex than that of the RE group. Second, to explore the effect of *Hp* on the oral microbiota of RE patients, we performed the <sup>14</sup>C-urea breath test on 45 of the 86 RE patients. We compared the oral microbiota of 33 *Hp*-infected reflux esophagitis patients (REHpp group) and 12 non-*Hp*-infected reflux esophagitis patients (REHpn group). No difference in alpha diversity was observed between the REHpn and REHpp groups, and beta diversity of the REHpp group was significantly lower than that of the REHpn group. The biomarkers in the REHpp group were *Veillonella*, *Haemophilus*, *Selenomonas*, *Megasphaera*, *Oribacterium*, *Butyrivibrio*, and *Campylobacter*; and the biomarker in the REHpn group was *Stomatobaculum*. *Megasphaera* was positively correlated with *Veillonella* in the microbial network of the REHpp group. The main finding of this study is that RE disturbs the human oral microbiota, such as increased beta diversity. *Hp* infection may inhibit this disorderly trend.

**Keywords:** Reflux esophagitis, oral microbiota, *Helicobacter pylori*, alpha diversity, beta diversity

## INTRODUCTION

The oral microbiota is closely related to the esophageal microbiota, and the esophageal microbiota is largely affected by the oral microbiota (Lv et al., 2019). Reflux esophagitis (RE) can cause disorder of the host oral microbiota (Wang et al., 2020). Disturbances in the oral microbiota are influential in inducing diseases of the upper and lower gastrointestinal tract (Schmidt et al., 2019). The esophagus and oral mucosa are damaged during acid reflux, and the oral microbiota of RE patients differs from that of healthy people (Wang et al., 2020). In addition, oral bacteria may migrate to the esophagus, thereby indirectly affecting the esophageal microorganisms and promoting the occurrence and development of esophageal diseases (Gao et al., 2018). Human oral microbiota disorders can induce chronic inflammation through immune pathways, leading to the occurrence of RE, Barrett's esophagus, and esophageal adenocarcinoma (Snider et al., 2016).

*Helicobacter pylori* (*Hp*) is one of the most important causes of chronic gastritis, gastric atrophy, and gastric cancer (Ding, 2020). Previous studies have reported that *Hp* infection can induce disorders of the oral and stomach microbiota in humans (Zhao et al., 2019). However, *Hp* infection has a protective effect on patients with esophageal diseases (Sugimoto et al., 2020). The oral and esophageal mucosa and microbiota of RE patients are damaged by acid reflux. Gastric atrophy occurs when the body is infected with *Hp*, which, in turn, decreases gastric acid, thereby indirectly protecting the oral mucosa (Ding, 2020). The incidence of esophageal disease may increase after eradicating *Hp*. Serum ghrelin levels increase during *Hp* eradication, affecting gastric emptying, and ultimately leading to an increased risk of esophageal reflux disease. Other studies have found that *Hp* infection is negatively correlated with the incidence of esophageal diseases, such as Barrett's esophagus and esophageal adenocarcinoma (Anderson et al., 2008).

Only a few studies have assessed the effect of *Hp* infection on the oral microbiota of patients with RE, so we carried out this study. The purpose of this study is to reveal the effect of *Hp* infection on the oral microbiota of patients with RE and to lay the foundation for investigating the interaction mechanism between *Hp* and RE.

## MATERIALS AND METHODS

### Sample Collection

We recruited 86 RE patients and 106 healthy volunteers at Xizang Minzu University Affiliated Hospital from May 2018 to July 2019. All participants were diagnosed by endoscopy using the Los Angeles classification method. All RE patients had typical symptoms of heartburn and reflux. The inclusion criteria were no treatment with glucocorticoids, antibiotics, proton pump inhibitors, or other drugs within 3 months; no gastrointestinal diseases or cancer; no gastrointestinal surgery; no oral diseases, and no pregnancy. The  $^{14}\text{C}$ -urea breath test was used to identify

whether patients with RE were infected with *Hp*. We collected 10 mL of saliva from volunteers in a 50 mL sterile tube and stored it at  $-80^{\circ}\text{C}$  until further use. We also collected information on gender, age, height, weight, body mass index (BMI), and eating habits. All participants signed informed consent and the purpose of the study was understood by all. This study was reviewed and approved by the Ethics Committee of Xizang Minzu University before the participants were recruited (ID: 201702). The experiments followed the standard biosecurity and safety procedures of Xizang Minzu University.

### DNA Extraction and High-Throughput Sequencing

The TIANamp Swab DNA Kit (Shanghai, China) was used to extract total microbial DNA. The V3-V4 region of the 16S rRNA gene was amplified with universal 341F and 805R primers. Polymerase chain reaction amplification, purification, and quantification were performed as described previously (Liu F. et al., 2021). The DNA library was merged into equimolar concentrations and sequenced using an Illumina MiSeq platform with a  $2 \times 250$  paired-end protocol. The raw sequence data were deposited at the Genome Sequence Archive at the Data Center, Beijing Institute of Genomics, Chinese Academy of Sciences, under Accession number CRA: CRA004395, which is publicly accessible at <https://ngdc.cnbc.ac.cn/gsa>.

### Bioinformatics and Statistical Analysis

Raw FASTQ files were demultiplexed, quality-filtered using Trimmomatic v0.39 (Bolger et al., 2014), and merged with FLASH v1.2.11 (Magoc and Salzberg, 2011) as described previously (Liu F. et al., 2021). Operational taxonomic units (OTUs) were defined at 97% similarity by UPARSE v7.1 (Edgar, 2013), and chimeric sequences were detected and removed with UCHIME v4.1 (Edgar et al., 2011). Taxonomy was assigned by the RDP Classifier algorithm v2.2 against the Silva (SSU123) 16S rRNA database using a confidence threshold of 80%. Species accumulation curves were constructed with the 'vegan' package (Oksanen et al., 2013). Alpha diversity was calculated using the Chao 1 and Shannon indices (Schloss et al., 2009). Principal coordinate analysis (PCoA) and permutational multivariate analysis of variance were performed to determine beta diversity (Bray-Curtis distance) (Lozupone and Knight, 2005; Kelly et al., 2015). A linear discriminant effect size analysis (LEfSe software v1.0, Segata et al., 2011) was used to discover biomarkers between different groups (LDA score  $> 2.0$ ). The demographic information of the different groups was compared with Student's *t*-test. The chi-square test was used to verify the difference in eating habits between the groups. The relative abundance of bacterial phyla and genera between the different groups was compared using the Wilcoxon rank-sum test. The false discovery rate (FDR) was used to correct the *P*-values, and  $P\text{-FDR} < 0.05$  was considered significant. SparCC and 100 bootstraps were used to calculate the correlation of each oral bacteria genus in the co-occurrence network between different groups (correlation value  $> 0.4$ , *P* value  $< 0.05$ ). Centrality of the co-occurrence network was calculated using closeness and

eigenvector of the node (Friedman and Alm, 2012; Wang et al., 2018). Gephi software was used to visualize the oral microbiota co-occurrence networks (Wang et al., 2018).

## RESULTS

A total of 192 participants were recruited between May 2018 and July 2019, including 86 RE patients and 106 healthy subjects, and a total of 192 saliva samples were collected. No significant differences in height, weight, or BMI were observed between the RE and C groups ( $P > 0.05$ ). The dietary habits of the groups were similar, but the RE group consumed less fiber and had a higher smoking rate ( $P < 0.05$ ), as shown in **Table 1**.

### Comparison of Community Composition of the Oral Microbiota Between the RE and C Groups

A total of 4,785,985 sequences were obtained after quality control, and the average reads per sample were 71,432 (range 43,299–98,661 reads per sample), and 71,261 OTUs were obtained. The rarefaction curve showed that sequencing depth captured most of the bacterial species in the oral microbiota sample (**Supplementary Figure 1**). The human oral microbiota was dominated by Firmicutes (36.01%), Bacteroidetes (23.66%), Proteobacteria (19.80%), Actinobacteria (9.59%), Fusobacteria (7.40%), and Spirochaetes (1.31%) (**Figure 1A**).

At the genus level, the oral microbiota was composed primarily of *Streptococcus* (19.15%), *Prevotella* (11.71%), *Neisseria* (10.16%), *Porphyromonas* (6.15%), *Rothia* (6.12%), *Haemophilus* (5.48%), *Veillonella* (4.60%), *Fusobacterium* (4.49%), *Alloprevotella* (4.05%), *Leptotrichia* (2.78%),

*Granulicatella* (2.18%), *Actinomyces* (2.08%), and *Gemella* (2.03%) (**Figure 1B**).

### Diversity of the Oral Microbiota in the RE and C Groups

All 86 RE patients were compared to the 106 controls to test the potential effect of RE on the oral microbiota. No significant difference in alpha diversity was observed between the RE and C groups ( $P = 0.61$ , **Figures 1C, D**). However, the beta diversity of the C group was significantly lower than that of the RE group ( $P = 0.0015$ ,  $R^2 = 0.041$ , **Figure 1E**). The PCoA plots revealed significantly different community structures between the RE and C groups (**Figure 1F**).

### Comparison of Oral Bacterial Abundance Between the RE and C Groups

Bacteroidetes were more abundant in the RE group, whereas Firmicutes were more abundant in the C group (**Figures 2A, B**). **Supplementary Figure 2A** indicates no significant differences at the genus level between the RE and C groups. The LEfSe analysis screened out biomarkers with significant abundance between the RE and C groups. The abundance rates of *Prevotella*, *Veillonella*, *Leptotrichia*, and *Actinomyces* were higher in the RE group; and those of *Lautropia*, *Gemella*, *Rothia*, and *Streptococcus* were higher in the C group ( $LDA > 2$ ,  $P < 0.05$ , **Figure 2C**).

### Comparison of the Oral Microbial Network Between the RE and C Groups

We compared the oral microbial network of the RE and C groups to explore the effect of RE on the oral microbial network (**Figure 3**). As results, the microbial network of the RE group (40 nodes, 38 edges) had more edges than the microbial network of the C group (38

**TABLE 1 |** Basic information of Reflux Esophagitis (RE) patients and healthy controls.

Characteristics	Healthy controls	RE patients	$\chi^2$	P value
Gender				
Male	49	50	1.09	$P > 0.05$
Female	57	36	1.09	$P > 0.05$
Height	165.38 ± 7.38	164.9 ± 7.13		$P > 0.05$
Weight	63.96 ± 10.2	63.76 ± 10.83		$P > 0.05$
Body mass index (BMI)	23.3 ± 2.66	23.35 ± 2.9		$P > 0.05$
Age	50.81 ± 13.9	56.27 ± 13.6		$P > 0.05$
Smoking				
None or occasionally	90	50	7.79	$P < 0.05$
sometimes or frequently	16	36	7.79	$P < 0.05$
Alcohol drinking				
None or occasionally	85	58	1.5	$P > 0.05$
sometimes or frequently	21	28	1.5	$P > 0.05$
Fiber intake				
Low fiber intake	47	64	7.05	$P < 0.05$
High fiber intake	59	22	7.05	$P < 0.05$
Salt intake				
Low salt intake	104	81	1.76	$P > 0.05$
High salt intake	2	5	1.76	$P > 0.05$
Fat and meat intake				
Low fat intake	94	70	1.1	$P > 0.05$
High fat intake	12	16	1.1	$P > 0.05$



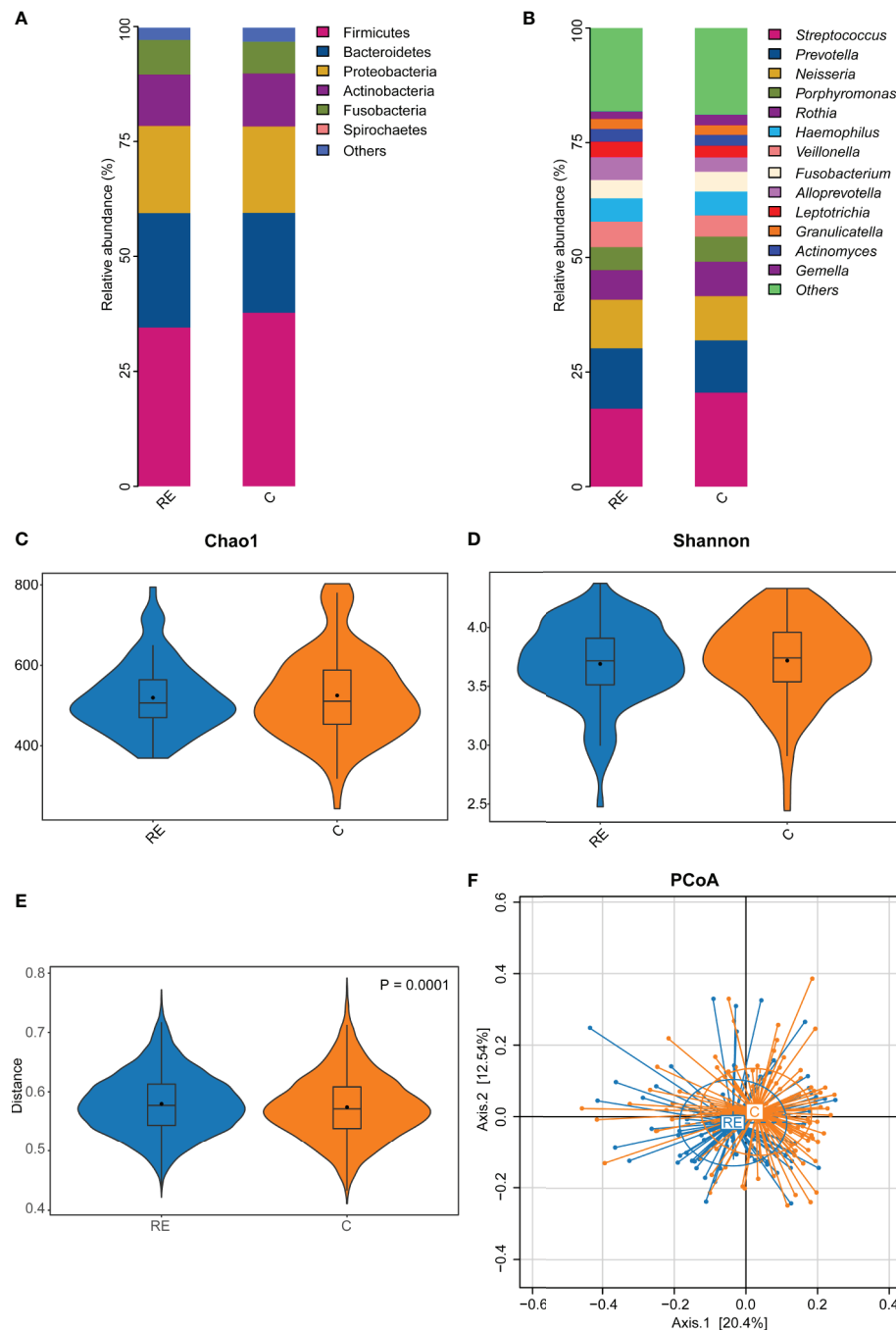


**FIGURE 1** | The effect of reflux esophagitis on the human oral microbiota. The oral bacterial community composition in reflux esophagitis patients (RE group) and healthy people (C group) at the phylum level (A), and the genus level (B). The alpha diversity of the RE group tended to be lower than that of the C group, but it was not significantly different,  $P > 0.05$  (C, D). The beta diversity of RE group was significantly higher than that of the C group,  $R^2 = 0.009$ ,  $P = 0.0001$  (E, F).

nodes, 71 edges). *Prevotella* was positively correlated with *Veillonella*, while *Neisseria* was negatively correlated with *Atopobium* in the RE group. *Streptococcus* was negatively correlated with *Selenomonas* and *Campylobacter* in the C group (Figure 3). These results suggest that the microbial network of the human oral microbiota was affected by reflux esophagitis.

## Diversity of the Oral Microbiota in the REHp and REHp Groups

We further explored the effect of *Hp* infection on the oral microbiota of RE patients and compared 33 RE patients with *Hp* infection (REHp) and 12 RE patients without *Hp* infection (REHp<sup>-</sup>). As a result, no significant difference in alpha diversity



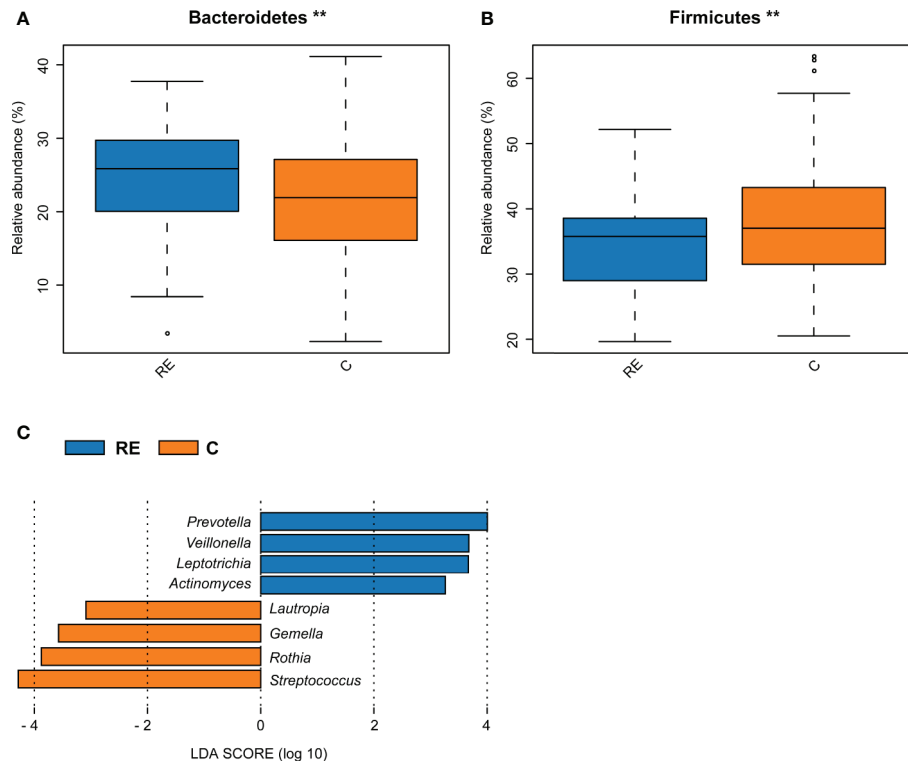


**FIGURE 2** | Comparison of bacterial abundance between the reflux esophagitis and the healthy groups. The abundance of Bacteroidetes in the RE group was higher, while the abundance of Firmicutes in the C group was higher,  $**P < 0.01$  (A, B). LefSe analysis results of the RE and C groups (C).

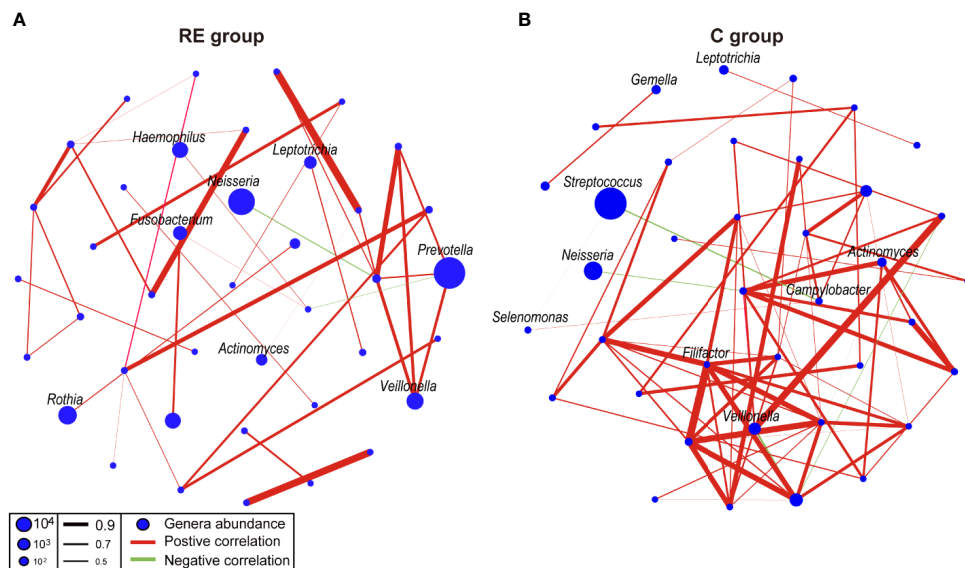


**FIGURE 3** | Co-occurrence networks of the reflux esophagitis and healthy groups (A, B). The co-occurrence network was inferred by the pairwise correlation of the relative abundances of all genera. Each node in the network represents a bacterial genus. The node size represents the mean relative abundance of a genus in the oral microbiota. Red line: positive correlation; green line: negative correlation. Relative thickness of the lines represents the degree of the correlation (greater thickness of the edges means a stronger correlation).

was observed between the REHpn and REHpp groups ( $P = 0.5$ , **Figures 4A, B** and **Supplementary Figures 2B, C**). However, the beta diversity of the REHpp group was significantly lower than that of the REHpn group ( $P = 0.006$ ,  $R^2 = 0.053$ , **Figure 4C**). The PCoA plots revealed separation of the samples in the REHpp and REHpn groups (**Figure 4D**).

### Comparison of Oral Bacterial Abundance Between the REHpp and REHpn Groups

No significant differences in bacteria phyla were observed between the REHpp and REHpn groups (**Supplementary Figure 2D**). At the genus level, the relative abundance rates of *Veillonella* and *Selenomonas* were higher in the REHpp group

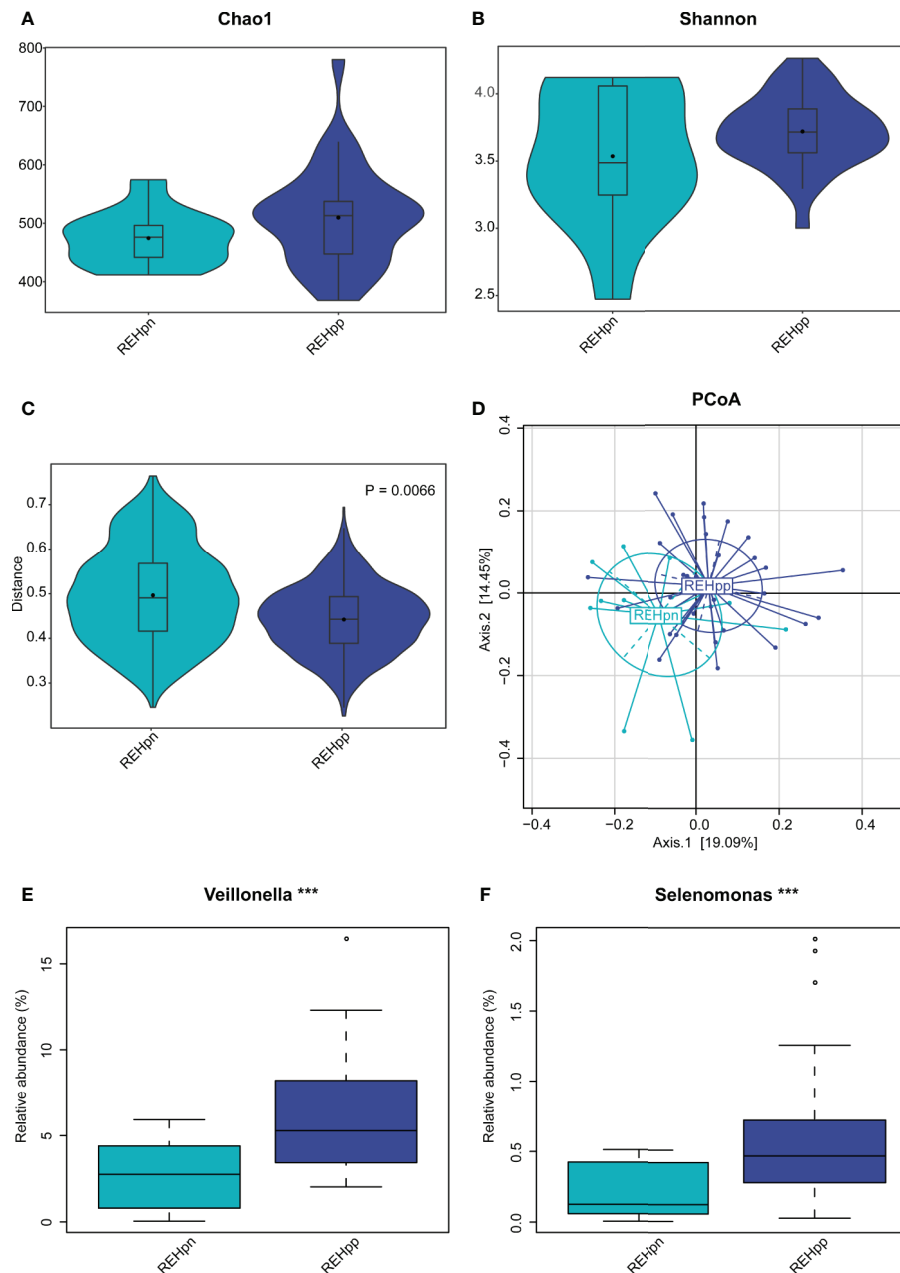


**FIGURE 4** | The influence of *Hp* infection on the oral microbiota of reflux esophagitis patients. The alpha diversity of the REHpp group tended to be higher than that of the REHpn group, but it was not significant,  $P > 0.05$  (**A, B**), and the beta diversity was significantly lower than that of the REHpn group,  $R^2 = 0.053$ ,  $P = 0.0066$  (**C, D**). Comparison of bacterial abundance between the REHpn and REHpp groups at the genus level (**E, F**), the abundances of *Veillonella* and *Selenomonas* in the REHpp group were significantly higher than those in the REHpn group,  $***P < 0.005$ .

( $P < 0.05$ , **Figures 4E, F**). We performed LEfSe analysis to further confirm the differentially abundant taxa in the REHpn and REHpp groups. At the genus level, the biomarker in the REHpn group was *Stomatobaculum*, while those in the REHpp group were *Veillonella*, *Haemophilus*, *Selenomonas*, *Megasphaera*, *Oribacterium*, *Butyrivibrio*, and *Campylobacter* (**Figure 5**).

## Comparison of the Oral Microbial Network Between the REHpn and REHpp Groups

We compared the oral microbial network of the REHpn and REHpp groups to explore the effect of *Hp* infection on the oral microbial network of RE patients. The microbial network structure of the REHpp group (9 nodes, 5 sides) was similar to

the REHpn group (7 nodes, 5 sides). *Megasphaera* was positively correlated with *Veillonella* in the microbial network of the REHpp group. *Solobacterium* was positively correlated with *Peptostreptococcus* in the microbial network of the REHpn group (**Figure 6**). Overall, these results indicate that the microbial network of the oral microbiota of RE patients was affected by *Hp* infection.

## DISCUSSION

The oral microbiota plays a fundamental role in maintaining normal physiology (Gao et al., 2018). Disorders of the oral

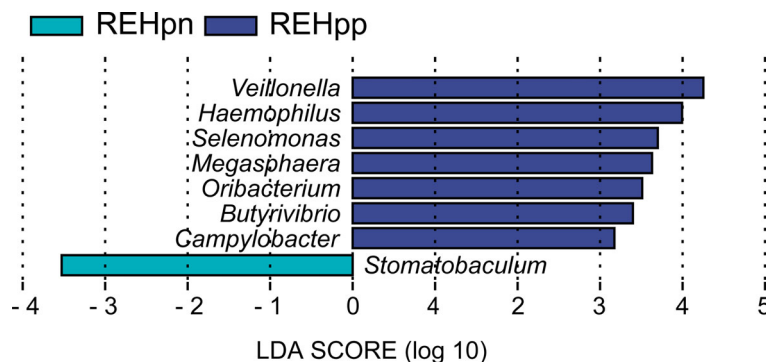


**FIGURE 5** | LEfSe analysis shows that the relative abundance rates of *Veillonella*, *Haemophilus*, *Selenomonas*, *Megasphaera*, *Oribacterium*, *Butyrivibrio*, and *Campylobacter* were higher in the REHpp group, while the abundance of *Stomatobaculum* was higher in the REHpn group.

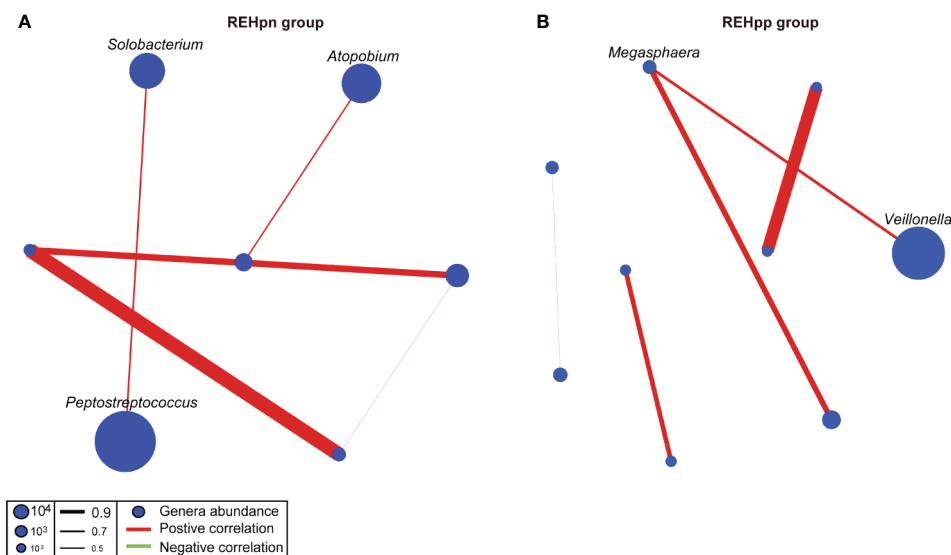


**FIGURE 6** | Co-occurrence networks of the REHpn and REHpp groups (**A, B**). Each node in the network represents a bacterial genus. The node size represents the mean relative abundance of a genus in the oral microbiota. Red line: positive correlation; green line: negative correlation. Relative thickness of the lines represents the degree of correlation (greater thickness of the edges means a stronger correlation).

microbiota may be essential for inducing digestive tract diseases, such as RE, chronic gastritis, and indigestion (Coker et al., 2018; Wang et al., 2020). Wang et al. (2020) reported that oral microbiota disorders are closely related to RE. Many studies have shown a negative association between *Hp* infection and the incidence of RE (Lv et al., 2019; Sugimoto et al., 2020). Recent research suggests that *Hp* is negatively correlated with the incidence of esophageal disease (Anderson et al., 2008). Some scholars hold the view that *Hp* is protective against RE (Nie et al., 2014; Neto et al., 2016). In addition, *Hp* eradication treatment may worsen RE, and promote the occurrence and development of esophageal diseases, such as Barrett's esophagus (Zhou et al., 2020). In this study, we report a comprehensive characterization of the microbial characteristics that distinguished RE patients from healthy people and emphasize the effect of *Hp* infection on the oral microbiota of RE patients. The results of our study show that RE increases oral microbiota disorders and that *Hp* may inhibit these disorders.

### Effect of Reflux Esophagitis on Alpha Diversity of the Oral Microbiota

The alpha diversity of the oral microbiota of RE patients was similar to that of the healthy control group. Following the present results, previous studies have demonstrated no significant difference between alpha diversity of the oral microbiota of patients with upper gastrointestinal diseases and that of healthy people (Wang et al., 2020). No differences in alpha diversity of the esophageal microbiota are observed between healthy people, Barrett's esophagus patients, and esophageal adenocarcinoma patients (Lopetuso et al., 2020). Snider's studies also reported that the alpha diversity of oral microbes in patients with Barrett's esophagus is not significantly different from that of healthy people (Snider et al., 2018). Hence, we hypothesized that RE may not affect the alpha diversity of the human oral microbiota.

According to these data, we infer that a *Hp* infection slightly increases the alpha diversity of the oral microbiota of RE patients. Current research suggests that the alpha diversity of human oral microbiota may not be affected by *Hp* infection (Chua et al., 2019). Gudra's research revealed no significant difference in the alpha diversity of the oral and gut microbiota between RE patients and healthy control subjects (Gudra et al., 2020). The alpha diversity of the human intestinal microbiota does not seem to be affected by *Hp* eradication treatment (Gudra et al., 2020). Therefore, *Hp* infection may not be a crucial factor affecting the alpha diversity of oral microbial communities. We suggest that *Hp* infection does not affect the alpha diversity of the oral microbiota in RE patients.

Our results show that the alpha diversity of the oral microbiota in RE patients was slightly lower than that of healthy people. We also observed that the alpha diversity of the REHpp group increased slightly compared with the REHpn group. *Hp* infection may be a protective factor for RE patients, which is consistent with an earlier study (Anderson et al., 2008). Taken together, we speculate that RE may lead to a slight decrease in the alpha diversity of the human oral microbiota, but *Hp* infection may inhibit this decrease. *Hp* infection slightly

increased the alpha diversity of the oral microbiota of RE patients, which may stabilize the bacterial community structure.

### Effect of Reflux Esophagitis on Beta Diversity of the Oral Microbiota

This study demonstrated that the beta diversity of RE patients was significantly higher than that of healthy people. Previous studies have reported that RE is a key factor affecting the beta diversity of the human oral microbiota (Wang et al., 2020). Zhou's study clarified that the oral microbiota community structure of patients with Barrett's esophagitis is significantly different from that of healthy people, which is consistent with our research results (Zhou et al., 2020). Thus, we consider that the beta diversity of human oral microbiota is affected by RE.

The beta diversity of the REHpp group was significantly lower than that of the REHpn group. *Hp* infection may affect oral microbial community structure, as the beta diversity of the oral microbiota of *Hp* infected patients is significantly different from that of healthy people (Chua et al., 2019; Ji et al., 2020). Beta diversity of the intestinal microbiota changes significantly in humans after *Hp* eradication treatment (Gudra et al., 2020). UniFrac distance is significantly different between patients who have not undergone *Hp* eradication and those who have undergone *Hp* eradication treatment (Gudra et al., 2020). *Hp* causes chronic gastritis to deteriorate into gastric atrophy, intestinal metaplasia, and gastric cancer (Gantuya et al., 2020). The community structure of the gastric microbiota in patients with gastric atrophy, intestinal metaplasia, or gastric cancer is significantly different from that of healthy people (Gantuya et al., 2020). Our results show that the beta diversity of the oral microbiota of RE patients was significantly higher than that of healthy people. However, the beta diversity of oral microbiota of the REHpp group was significantly lower than that of the REHpn group due to *Hp* infection. We speculate that this may have been due to the *Hp* infection, which led to a decrease in beta diversity of the oral microbiota of patients with RE.

### Effect of Reflux Esophagitis on the Abundance of Oral Bacterial Phyla

Our results show that the abundance of Bacteroidetes was higher in the RE group, while the abundance of Firmicutes was higher in the C group. The abundance of Bacteroidetes is lower in the oral and esophageal microbiota of healthy people (Gantuya et al., 2020). Previous studies reported that the abundance of Bacteroides is higher, while the abundance of Firmicutes is lower in the oral and esophageal microbiota of RE and Barrett's esophagus patients (Gantuya et al., 2020; Lopetuso et al., 2020). Zhou et al. (2020) reported that Bacteroidetes may promote the deterioration of RE into esophageal adenocarcinoma.

The abundance of Firmicutes in the esophagus of healthy people is significantly higher than that in RE patients (Liu et al., 2013). According to one recent report, the abundance of Firmicutes decreases with the severity of esophageal disease (Liu et al., 2013). Compared with patients with high-grade

dysplasia of Barrett's esophagus, the abundance of Firmicutes in patients with Barrett's esophagus increases significantly in those with non-dysplasia and low-grade dysplasia (Park and Lee, 2020). Liu J. et al. (2021) confirmed that the abundance of Firmicutes is negatively correlated with ROR $\gamma$ t, but positively correlated with FoxP3. ROR $\gamma$ t and FoxP3 are important transcription factors for Th17 and Treg cells, respectively (Liu J. et al., 2021). An increase in the number of Th17 cells and a decrease in Treg cells are also observed in patients with RE (Liu J. et al., 2021).

Yang's research suggests that the human esophageal microbiota can be divided into type I and type II (Yang et al., 2009). The healthy people's esophagus is the type I microbiota, mainly Firmicutes and Gram-negative anaerobes. In contrast, the RE patient's esophagus is a type II microbiome, and Bacteroides and Gram-negative anaerobes account for high (Yang et al., 2009; Lv et al., 2019). Most of the bacteria from Firmicutes belong to Gram-positive bacteria, and bacteria from Bacteroides belong to Gram-negative bacteria. The abundance of Gram-positive bacteria is higher in *Hp*-infected patients, whereas the abundance of Gram-negative bacteria is higher in non-infected-*Hp* patients (Park and Lee, 2020). The current study argues that the human disease state may promote a change in the body's microbial community from Gram-positive bacteria to Gram-negative bacteria (Yang et al., 2009). Healthy people have a higher abundance of Gram-positive bacteria in the oral cavity (Okereke et al., 2019). RE causes the numbers of Gram-positive and Gram-negative bacteria in the human oral microbiota to decrease and increase, respectively (Deshpande et al., 2018). The DNA and RNA of Gram-negative bacteria and their metabolite lipopolysaccharide stimulate upregulation of TLR4 expression (Deshpande et al., 2018). TLR4 plays a vital role in the pathogenesis of esophageal diseases (Deshpande et al., 2018). Activation of TLR4 triggers the nuclear factor kappa-B pathway, which leads to inflammation. Moreover, the toxins produced by Gram-negative bacteria can damage the stability of the genome and cause DNA damage and inflammation (Deshpande et al., 2018). We speculate that this may due to RE-induced chronic inflammation, resulting in a decrease in the abundance of Firmicutes and an increase in the abundance of Bacteroidetes.

## Effect of Reflux Esophagitis on the Abundance of Oral Bacterial Genera

Our study shows that the biomarkers in the RE group were *Prevotella*, *Veillonella*, *Leptotrichia*, and *Actinomyces*. It has been assumed that the abundance of *Veillonella* is negatively correlated with the degree of exacerbation of esophageal disease (Snider et al., 2018). Compared with non-dysplastic Barrett's esophagus patients, patients with high-grade dysplasia Barrett's esophagus have a lower abundance of *Veillonella* in the oral microbiota (Lopetuso et al., 2020). The abundance of *Prevotella*, *Veillonella*, and *Leptotrichia* in the esophagus of esophageal adenocarcinoma patients increases significantly (Lopetuso et al., 2020). There is some evidence to suggest that *Prevotella*, *Veillonella*, and *Leptotrichia* can interact to induce cancer (Lopetuso et al., 2020). *Leptotrichia* is an opportunistic

pathogen associated with many cancers, such as colon cancer, stomach cancer, and pancreatic tumors (Fan et al., 2018; Kim et al., 2018). *Leptotrichia* stimulates immune response and indirectly promotes esophageal tumors (Lopetuso et al., 2020). Bronswijk et al. (2019) suggested that *Actinomyces* is a key genus that induces RE.

Our research found that the biomarkers of the C group were *Lautropia*, *Gemella*, *Rothia*, and *Streptococcus*. *Lautropia* is a key bacterial genus in the oral microbiota that plays an anti-inflammatory effect, and its reduced abundance may lead to the proliferation of other pro-inflammatory bacteria (Vincent et al., 2013; Desai et al., 2016). The abundance of *Lautropia* in the oral cavity of healthy people increases significantly compared to patients with head and neck squamous cell carcinoma (Guerrero-Preston et al., 2016). The abundance of *Lautropia*, *Gemella*, *Rothia*, and *Streptococcus* in the oral microbiota of healthy people is higher compared with patients with RE (Wang et al., 2020). A high abundance of Gram-negative bacteria may promote biofilm formation (Blackett et al., 2013). A high-abundance of Gram-negative bacteria produce lipopolysaccharides and activate the natural immune response, which subsequently stimulates the expression of nuclear factor kappa-B to promote the release of interleukin-1 $\beta$ , -6, -8, and tumor necrosis factor- $\alpha$  (Yang et al., 2012; Kährström et al., 2016). Lipopolysaccharides produced by microorganisms enter the blood circulation through the digestive tract mucosa, thereby inducing local and systemic inflammatory reactions, particularly in patients with digestive tract diseases (Zhao et al., 2019).

Our study showed that the biomarker of the oral microbiota in the REHp group was *Stomatobaculum*; and those in the REHpp group were *Veillonella*, *Haemophilus*, *Selenomonas*, *Megasphaera*, *Oribacterium*, *Butyrivibrio*, and *Campylobacter*. *Hp* infection reduces gastric acid secretion, thereby increasing the abundance of Gram-negative bacteria, such as *Veillonella* and *Haemophilus* (Miyata et al., 2019). *Haemophilus* and *Veillonella* produce more lipopolysaccharides than *Hp* (Sharma and Rao, 2012). Lipopolysaccharides activate TLR4 and promote the nuclear translocation of nuclear factor kappa-B, leading to increased IL-8 gene expression (Smith et al., 2003; Yang et al., 2012). The abundance of other bacterial genera in the bacterial community is affected by the presence of *Hp* (Peng et al., 2017). The abundance of *Veillonella* in the human stomach increases after *Hp* infection (Peng et al., 2017). Other studies have reported that the abundance of *Veillonella* decreases significantly after *Hp* eradication (Tanaka et al., 2005). *Haemophilus* has a function similar to that of *Hp* and is a potentially pathogenic bacterium of non-*Hp* infection gastritis (Gantuya et al., 2019). *Haemophilus* is also the dominant bacteria in the gastric microbiota of gastric cancer patients (Gantuya et al., 2019). Importantly, *Haemophilus* causes the accumulation of nitrite, which promotes the production of carcinogens (Gantuya et al., 2019). *Selenomonas* has been detected on the tongue coating of gastric cancer patients and has been considered a potential biomarker (Rodriguez et al., 2020). The abundance of *Oribacterium* in the human oral cavity increases significantly after *Hp* infection (Ji et al., 2020). The relative abundance of *Stomatobaculum* in the oral microbiota of



RE patients is significantly higher (Wang et al., 2020). As a result, we speculate that the abundance of bacterial genera in RE patients is affected by *Hp*.

## Influence of *Hp* Infection on the Oral Microbial Network of Reflux Esophagitis Patients

In our study, *Prevotella* was positively correlated with *Veillonella* in the RE group. *Streptococcus* was negatively correlated with *Selenomonas* and *Campylobacter* in the C group. Smoking is a risk factor leading to RE (Wang K. et al., 2019), and the proportion of smokers in the RE group was significantly higher than that in the C group. Smoking increases nitrate intake, and *Veillonella* converts nitrate into carcinogenic nitrosamines and pro-inflammatory nitric oxide (Jia et al., 2021). Vanhatalo's studies reported that *Prevotella* and *Veillonella* are positively correlated and are essential markers of early inflammation, leading to an increase in the number of lymphocytes and centrioles (Hérivaux et al., 2021; Vanhatalo et al., 2021). Several recent studies have shown that lactic acid and glucose are metabolized into short-chain fatty acids by *Veillonella*, which promotes mucin synthesis (Chen et al., 2020). *Prevotella* is one of the main bacterial genera that decompose mucin (Ilhan et al., 2020). The findings reported here suggest that *Veillonella* and *Prevotella* may be positively correlated through metabolites.

The relationship between *Streptococcus*, *Selenomonas*, and *Campylobacter* may partly be explained by the fact that *Streptococcus* plays a positive role in reducing the production of peroxides, acids, and lipopolysaccharides in the body (Zhou et al., 2020). *Streptococcus salivarius* inhibits the release of inflammatory factors and exerts an anti-inflammatory effect (Di Giacinto et al., 2005; Laws et al., 2021). *Selenomonas* and *Campylobacter* are potential pathogenic bacteria, which promote the release of IL-6, IL-17, and IL-33 and induce the inflammatory response (Di Pilato et al., 2016; Volgenant et al., 2017; Li et al., 2019). *Streptococcus* competitively inhibits the growth of other bacterial genera in the same community through the metabolite H<sub>2</sub>O<sub>2</sub> (Zhou et al., 2017; Zhou et al., 2020). Therefore, it is likely that connections exist between *Streptococcus*, *Selenomonas*, and *Campylobacter* in the microbial network of the C group.

Another important finding is that *Solobacterium* was positively correlated with *Peptostreptococcus* in the microbial network of the REHpn group. *Megasphaera* was positively correlated with *Veillonella* in the microbial network of the REHpp group. *Solobacterium* degrades cysteine to produce methyl mercaptan using  $\beta$ -galactosidase and protease (Tanabe and Grenier, 2012; Suzuki et al., 2019). Methyl mercaptan is transported and utilized by *Peptostreptococcus* (Tang-Larsen et al., 1995). *Peptostreptococcus* and *Solobacterium* produce various acids, which lower the pH of the environment, induce local inflammation, and induce digestive tract cancer (Senneby et al., 2017). Current studies suggest that the high abundance of *Peptostreptococcus* may increase the risk of esophageal squamous cell carcinoma (Sung et al., 2020). Thus, *Solobacterium* and *Peptostreptococcus* are positively correlated in the microbial network of the REHpn group.

The lactic acid content and the abundance of lactic acid-producing bacteria are both higher in the esophagus of esophageal cancer patients (Lertpiriyapong et al., 2014; Vinasco et al., 2019; Zhou et al., 2020). Disorders of lactate metabolism can aggravate esophagitis to become esophageal cancer (Lin et al., 2020). Several reports have shown that the abundances of *Megasphaera* and *Veillonella* increase in the oral and stomach microbiota of healthy people after *Hp* infection (Castaño-Rodríguez et al., 2017; Miyata et al., 2019; Wu et al., 2020). Excess acetic acid is converted into acetate and propionate by *Megasphaera* and *Veillonella* via the acrylate pathway and the methylmalonyl-CoA pathway, respectively (Canfora et al., 2019; Scheiman et al., 2019). A strong interaction exists between *Hp* and *Veillonella*, and this may be related to gastric lesions or cancer (Guo et al., 2020). We speculate that the abundances of *Megasphaera* and *Veillonella* in the REHpp group were positively correlated, which may be affected by the *Hp* infection.

## CONCLUSION

Taken together, our research reveals a trend that RE leads to an increase in the beta diversity of the human oral microbiota, an increase in the abundance of Gram-negative bacteria, and a decrease in the abundance of Gram-positive bacteria. However, *Hp* infection inhibits the change in diversity, and the oral microbiota tends to be normal. However, our study had some limitations. We did not compare the oral microbes before and after *Hp* infection in patients with RE, which may only reflect part of the picture. Future research should focus on the use of transcriptomic, proteomic, metabolomic, and other multi-omics approaches to explore the relationship between the oral microbiota, reflux esophagitis, and *Hp*. It is extremely important to explore the role of the oral microbiota in the occurrence and development of RE.

## DATA AVAILABILITY STATEMENT

The datasets presented in this study can be found in online repositories. The names of the repository/repositories and accession number(s) can be found below: <https://ngdc.cnbc.ac.cn/gsa>, accession number: CRA (CRA004395).

## ETHICS STATEMENT

The studies involving human participants were reviewed and approved by Ethics Committee of Xizang Minzu University. The patients/participants provided their written informed consent to participate in this study.

## AUTHOR CONTRIBUTIONS

LK: attributed to the study design. TL, FL, ZZ, LL, WD, SB, and LM: performed the sample collection and experimental work. TL:

finished the date analyses and drafted the manuscript. All authors contributed to the article and approved the submitted version.

## FUNDING

This research was supported by National Natural Science Foundation of China (31660307), Science and Technology Department Project of Tibet Autonomous Region (No. XZ201801-GB-03).

## REFERENCES

- Anderson, L. A., Murphy, S. J., Johnston, B. T., Watson, R. G., Ferguson, H. R., Bamford, K. B., et al. (2008). Relationship Between *Helicobacter Pylori* Infection and Gastric Atrophy and the Stages of the Oesophageal Inflammation, Metaplasia, Adenocarcinoma Sequence: Results From the FINBAR Case-Control Study. *Gut* 57 (6), 734–739. doi: 10.1136/gut.2007.132662
- Blackett, K. L., Siddhi, S. S., Cleary, S., Steed, H., Miller, M. H., Macfarlane, S., et al. (2013). Oesophageal Bacterial Biofilm Changes in Gastro-Oesophageal Reflux Disease, Barrett's and Oesophageal Carcinoma: Association or Causality? *Aliment. Pharmacol. Ther.* 37 (11), 1084–1092. doi: 10.1111/apt.12317
- Blaser, M. J., and Falkow, S. (2009). What are the Consequences of the Disappearing Human Microbiota? *Nat. Rev. Microbiol.* 7, 887–894. doi: 10.1038/nrmicro2245
- Bolger, A. M., Lohse, M., and Usadel, B. (2014). Trimmomatic: A Flexible Trimmer for Illumina Sequence Data. *Bioinformatics (Oxford, England)* 30 (15), 2114–2120. doi: 10.1093/bioinformatics/btu170
- Bronswijk, M., Victor, J., and Cuyle, P. J. (2019). Deep Ulcerative Esophagitis: A Rare Presentation of Gastrointestinal Actinomycosis. *Dig. Liver. Dis.* 51 (6), 907. doi: 10.1016/j.dld.2019.01.026
- Canfora, E. E., Meex, R., Venema, K., and Blaak, E. E. (2019). Gut Microbial Metabolites in Obesity, NAFLD and T2DM. *Nat. Rev. Endocrinol.* 15 (5), 261–273. doi: 10.1038/s41574-019-0156-z
- Castaño-Rodríguez, N., Goh, K. L., Fock, K. M., Mitchell, H. M., and Kaakoush, N. O. (2017). Dysbiosis of the Microbiome in Gastric Carcinogenesis. *Sci. Rep.* 7 (1), 15957. doi: 10.1038/s41598-017-16289-2
- Chen, X., Sun, H., Jiang, F., Shen, Y., Li, X., Hu, X., et al. (2020). Alteration of the Gut Microbiota Associated With Childhood Obesity by 16S rRNA Gene Sequencing. *PeerJ* 8, e8317. doi: 10.7717/peerj.8317
- Chua, E. G., Chong, J. Y., Lamichhane, B., Webberley, K. M., Marshall, B. J., Wise, M. J., et al. (2019). Gastric *Helicobacter Pylori* Infection Perturbs Human Oral Microbiota. *PeerJ* 7, e6336. doi: 10.7717/peerj.6336
- Coker, O. O., Dai, Z., Nie, Y., Zhao, G., Cao, L., Nakatsu, G., et al. (2018). Mucosal Microbiome Dysbiosis in Gastric Carcinogenesis. *Gut* 67 (6), 1024–1032. doi: 10.1136/gutjnl-2017-314281
- Desai, M. S., Seekatz, A. M., Koropatkin, N. M., Kamada, N., Hickey, C. A., Wolter, M., et al. (2016). A Dietary Fiber-Deprived Gut Microbiota Degrades the Colonic Mucus Barrier and Enhances Pathogen Susceptibility. *Cell* 167 (5), 1339–1353 e1321. doi: 10.1016/j.cell.2016.10.043
- Deshpande, N. P., Riordan, S. M., Castano-Rodríguez, N., Wilkins, M. R., and Kaakoush, N. O. (2018). Signatures Within the Esophageal Microbiome are Associated With Host Genetics, Age, and Disease. *Microbiome* 6 (1), 227. doi: 10.1186/s40168-018-0611-4
- Di Giacinto, C., Marinaro, M., Sanchez, M., Strober, W., and Boirivant, M. (2005). Probiotics Ameliorate Recurrent Th1-Mediated Murine Colitis by Inducing IL-10 and IL-10-Dependent TGF- $\beta$ -Bearing Regulatory Cells. *J. Immunol.* 174 (6), 3237–3246. doi: 10.4049/jimmunol.174.6.3237
- Ding, S. Z. (2020). Global Whole Family Based-*Helicobacter Pylori* Eradication Strategy to Prevent its Related Diseases and Gastric Cancer. *World J. Gastroenterol.* 26 (10), 995–1004. doi: 10.3748/wjg.v26.i10.995
- Pilato, V., Freschi, G., Ringressi, M. N., Pallecchi, L., Rossolini, G. M., and Bechi, P. (2016). The Esophageal Microbiota in Health and Disease. *Ann. N. Y. Acad. Sci.* 1381 (1), 21–33. doi: 10.1111/nyas.13127

## ACKNOWLEDGMENTS

We sincerely thank the Editor and reviewers for their contributions and suggestions.

## SUPPLEMENTARY MATERIAL

The Supplementary Material for this article can be found online at: <https://www.frontiersin.org/articles/10.3389/fcimb.2021.732613/full#supplementary-material>

- Edgar, R. C. (2013). UPARSE: Highly Accurate OTU Sequences From Microbial Amplicon Reads. *Nat. Methods* 10, 996–998. doi: 10.1038/nmeth.2604
- Edgar, R. C., Haas, B. J., Clemente, J. C., Quince, C., and Knight, R. (2011). UCHIME Improves Sensitivity and Speed of Chimera Detection. *Bioinformatics* 27, 2194–2200. doi: 10.1093/bioinformatics/btr381
- Fan, X., Alekseyenko, A. V., Wu, J., Peters, B. A., Jacobs, E. J., Gapstur, S. M., et al. (2018). Human Oral Microbiome and Prospective Risk for Pancreatic Cancer: A Population-Based Nested Case-Control Study. *Gut* 67 (1), 120–127. doi: 10.1136/gutjnl-2016-312580
- Friedman, J., and Alm, E. J. (2012). Inferring Correlation Networks From Genomic Survey Data. *PLoS Comput. Biol.* 8 (9), e1002687. doi: 10.1371/journal.pcbi.1002687
- Gantuya, B., El-Serag, H. B., Matsumoto, T., Ajami, N. J., Oyuntsetseg, K., Azzaya, D., et al. (2019). Gastric Microbiota in *Helicobacter Pylori*-Negative and -Positive Gastritis Among High Incidence of Gastric Cancer Area. *Cancers (Basel)* 11 (4), 504. doi: 10.3390/cancers11040504
- Gantuya, B., El-Serag, H. B., Matsumoto, T., Ajami, N. J., Uchida, T., Oyuntsetseg, K., et al. (2020). Gastric Mucosal Microbiota in a Mongolian Population With Gastric Cancer and Precursor Conditions. *Aliment. Pharmacol. Ther.* 51 (8), 770–780. doi: 10.1111/apt.15675
- Gao, L., Xu, T., Huang, G., Jiang, S., Gu, Y., and Chen, F. (2018). Oral Microbiomes: More and More Importance in Oral Cavity and Whole Body. *Protein Cell* 9 (5), 488–500. doi: 10.1007/s13238-018-0548-1
- Gudra, D., Pupola, D., Skenders, G., Leja, M., Radovica-Spalvina, I., Gorskis, H., et al. (2020). Lack of Significant Differences Between Gastrointestinal Tract Microbial Population Structure of *Helicobacter Pylori*-Infected Subjects Before and 2 Years After a Single Eradication Event. *Helicobacter* 25 (5), e12748. doi: 10.1111/hel.12748
- Guerrero-Preston, R., Godoy-Vitorino, F., Jedlicka, A., Rodríguez-Hilario, A., González, H., Bondy, J., et al. (2016). 16s rRNA Amplicon Sequencing Identifies Microbiota Associated With Oral Cancer, Human Papilloma Virus Infection and Surgical Treatment. *Oncotarget* 7 (32), 51320–51334. doi: 10.18632/oncotarget.9710
- Guo, Y., Zhang, Y., Gerhard, M., Gao, J. J., Mejias-Luque, R., Zhang, L., et al. (2020). Effect of *Helicobacter Pylori* on Gastrointestinal Microbiota: A Population-Based Study in Linqu, a High-Risk Area of Gastric Cancer. *Gut* 69 (9), 1598–1607. doi: 10.1136/gutjnl-2019-319696
- Hérivaux, A., Willis, J. R., Mercier, T., Lagrou, K., Gonçalves, S. M., Gonçalves, R. A., et al. (2021). Lung Microbiota Predict Invasive Pulmonary Aspergillosis and its Outcome in Immunocompromised Patients. *Thorax. thoraxjnl-2020-216179*. doi: 10.1136/thoraxjnl-2020-216179
- Ilhan, Z. E., Łaniewski, P., Tonachio, A., and Herbst-Kralovetz, M. M. (2020). Members of *Prevotella* Genus Distinctively Modulate Innate Immune and Barrier Functions in a Human Three-Dimensional Endometrial Epithelial Cell Model. *J. Infect. Dis.* 222 (12), 2082–2092. doi: 10.1093/infdis/jiaa324
- Jia, Y., Liao, Y., He, Y. Q., Zheng, M. Q., Tong, X. T., Xue, W. Q., et al. (2021). Association Between Oral Microbiota and Cigarette Smoking in the Chinese Population. *Front. Cell Infect. Microbiol.* 11, 658203. doi: 10.3389/fcimb.2021.658203
- Ji, Y., Liang, X., and Lu, H. (2020). Analysis of by High-Throughput Sequencing: *Helicobacter Pylori* Infection and Salivary Microbiome. *BMC Oral. Health* 20 (1), 84. doi: 10.1186/s12903-020-01070-1
- Kährström, C., Pariente, N., and Weiss, U. (2016). Intestinal Microbiota in Health and Disease. *Nature* 535 (7610), 47. doi: 10.1038/535047a

- Kanehisa, M., and Goto, S. (2000). KEGG: Kyoto Encyclopedia of Genes and Genomes. *Nucleic Acids Res.* 28, 27–30. doi: 10.1093/nar/28.1.27
- Kelly, B. J., Bittinger, R. G. K., Sherrill-Mix, S., Lewis, J. D., Collman, R. G., Bushman, F. D., et al. (2015). Power and Sample-Size Estimation for Microbiome Studies Using Pairwise Distances and PERMANOVA. *Bioinformatics* 31, 2461–2468. doi: 10.1093/bioinformatics/btv183
- Kim, K., Castro, E. J. T., Shim, H., Advincula, J. V. G., and Kim, Y. W. (2018). Differences Regarding the Molecular Features and Gut Microbiota Between Right and Left Colon Cancer. *Ann. Coloproctol.* 34 (6), 280–285. doi: 10.3393/ac.2018.12.17
- Langille, M. G. I., Zaneveld, J., Caporaso, J. G., McDonald, D., Knights, D., Reyes, J. A., et al. (2013). Predictive Functional Profiling of Microbial Communities Using 16S rRNA Marker Gene Sequences. *Nat. Biotechnol.* 31, 814–821. doi: 10.1038/nbt.2676
- Laws, G. L., Hale, J., and Kemp, R. A. (2021). Human Systemic Immune Response to Ingestion of the Oral Probiotic *Streptococcus Salivarius* BLIS K12. *Probiotics. Antimicrob. Proteins.* doi: 10.1007/s12602-021-09822-3
- Lertpiriyapong, K., Whary, M. T., Muthupalani, S., Lofgren, J. L., Gamazon, E. R., Feng, Y., et al. (2014). Gastric Colonisation With a Restricted Commensal Microbiota Replicates the Promotion of Neoplastic Lesions by Diverse Intestinal Microbiota in the *Helicobacter Pylori* INS-GAS Mouse Model of Gastric Carcinogenesis. *Gut* 63 (1), 54–63. doi: 10.1136/gutjnl-2013-305178
- Lin, C. C., Huang, W. C., Su, C. H., Lin, W. D., Wu, W. T., Yu, B., et al. (2020). Effects of Multi-Strain Probiotics on Immune Responses and Metabolic Balance in *Helicobacter Pylori*-Infected Mice. *Nutrients* 12 (8), 2476. doi: 10.3390/nu12082476
- Liu, N., Ando, T., Ishiguro, K., Maeda, O., Watanabe, O., Funasaka, K., et al. (2013). Characterization of Bacterial Biota in the Distal Esophagus of Japanese Patients With Reflux Esophagitis and Barrett's Esophagus. *BMC Infect. Dis.* 13, 130. doi: 10.1186/1471-2334-13-130
- Liu, F., Liang, T., Zhang, Z., Liu, L., Li, J., Dong, W., et al. (2021). Effects of Altitude on Human Oral Microbes. *AMB. Express* 11 (1), 41. doi: 10.1186/s13568-021-01200-0
- Liu, J., Luo, Y., Wang, J., Xi, C., Chen, Y., Yang, G., et al. (2021). Key Molecules Involved in the Th17/Treg Balance are Associated With the Pathogenesis of Reflux Esophagitis and Barrett's Esophagus. *Esophagus* 18 (2), 388–397. doi: 10.1007/s10388-020-00773-2
- Li, Y., Wang, H. F., Li, X., Li, H. X., Zhang, Q., Zhou, H. W., et al. (2019). Disordered Intestinal Microbes are Associated With the Activity of Systemic Lupus Erythematosus. *Clin. Sci. (Lond)*. 133 (7), 821–838. doi: 10.1042/CS20180841
- Lopetuso, L. R., Severgnini, M., Pecere, S., Ponziani, F. R., Boskoski, I., Larghi, A., et al. (2020). Esophageal Microbiome Signature in Patients With Barrett's Esophagus and Esophageal Adenocarcinoma. *PloS One* 15 (5), e0231789. doi: 10.1371/journal.pone.0231789
- Lozupone, C., and Knight, R. (2005). UniFrac: A New Phylogenetic Method for Comparing Microbial Communities. *Appl. Environ. Microbiol.* 71 (12), 8228–8235. doi: 10.1128/AEM.71.12.8228-8235.2005
- Lv, J., Guo, L., Liu, J. J., Zhao, H. P., Zhang, J., and Wang, J. H. (2019). Alteration of the Esophageal Microbiota in Barrett's Esophagus and Esophageal Adenocarcinoma. *World J. Gastroenterol.* 25 (18), 2149–2161. doi: 10.3748/wjg.v25.i18.2149
- Magoc, T., and Salzberg, S. L. (2011). FLASH: Fast Length Adjustment of Short Reads to Improve Genome Assemblies. *Bioinformatics* 27, 2957–2963. doi: 10.1093/bioinformatics/btr507
- Miyata, N., Hayashi, Y., Hayashi, S., Sato, K., Hirai, Y., Yamamoto, H., et al. (2019). Lipopolysaccharides From Non-*Helicobacter Pylori* Gastric Bacteria Potently Stimulate Interleukin-8 Production in Gastric Epithelial Cells. *Clin. Transl. Gastroenterol.* 10 (3), e00024. doi: 10.14309/ctg.0000000000000024
- Muto, M., Hitomi, Y., Ohtsu, A., Shimada, H., Kashiwase, Y., Sasaki, H., et al. (2000). Acetaldehyde Production by non-Pathogenic *Neisseria* in Human Oral Microflora: Implications for Carcinogenesis in Upper Aerodigestive Tract. *Int. J. Cancer* 88 (3), 342–350. doi: 10.1002/1097-0215(20001101)88:3<342::AID-IJCA>3.0.CO;2-I
- Nardone, G., and Compare, D. (2015). The Human Gastric Microbiota: Is it Time to Rethink the Pathogenesis of Stomach Diseases? *United. Eur. Gastroenterol. J.* 3 (3), 255–260. doi: 10.1177/2050640614566846
- Neto, A. G., Whitaker, A., and Pei, Z. (2016). Microbiome and Potential Targets for Chemoprevention of Esophageal Adenocarcinoma. *Semin. Oncol.* 43 (1), 86–96. doi: 10.1053/j.seminoncol.2015.09.005
- Nie, S., Chen, T., Yang, X., Huai, P., and Lu, M. (2014). Association of *Helicobacter Pylori* Infection With Esophageal Adenocarcinoma and Squamous Cell Carcinoma: A Meta-Analysis. *Dis. Esophagus*. 27 (7), 645–653. doi: 10.1111/dote.12194
- Okereke, I., Hamilton, C., Reep, G., Krill, T., Booth, A., Ghouri, Y., et al. (2019). Microflora Composition in the Gastrointestinal Tract in Patients With Barrett's Esophagus. *J. Thorac. Dis.* 11 (Suppl 12), S1581–S1587. doi: 10.21037/jtd.2019.06.15
- Oksanen, J., Blanchet, F. G., Kindt, R., Legendre, P., Minchin, P. R., O'hara, R. B., et al. (2013). Vegan: Community Ecology Package. *R. Package Version*. 2, 0–7.
- Park, C. H., and Lee, S. K. (2020). Exploring Esophageal Microbiomes in Esophageal Diseases: A Systematic Review. *J. Neurogastroenterol. Motil.* 26 (2), 171–179. doi: 10.5056/jnm19240
- Peng, X., Zhou, L., Gong, Y., Song, Z., He, L., Lin, S., et al. (2017). Non-*Pylori Helicobacters* (NHPHs) Induce Shifts in Gastric Microbiota in *Helicobacter Pylori*-Infected Patients. *Front. Microbiol.* 8, 1038. doi: 10.3389/fmicb.2017.01038
- Rodriguez, R. M., Hernandez, B. Y., Menor, M., Deng, Y., and Khadka, V. S. (2020). The Landscape of Bacterial Presence in Tumor and Adjacent Normal Tissue Across 9 Major Cancer Types Using TCGA Exome Sequencing. *Comput. Struct. Biotechnol. J.* 18, 631–641. doi: 10.1016/j.csbj.2020.03.003
- Scheiman, J., Luber, J. M., Chavkin, T. A., MacDonald, T., Tung, A., Pham, L. D., et al. (2019). Meta-Omics Analysis of Elite Athletes Identifies a Performance-Enhancing Microbe That Functions via Lactate Metabolism. *Nat. Med.* 25 (7), 1104–1109. doi: 10.1038/s41591-019-0485-4
- Schloss, P. D., Westcott, S. L., Ryabin, T., Hall, J. R., Hartmann, M., Hollister, E. B., et al. (2009). Introducing Mothur: Open-Source, Platform-Independent, Community-Supported Software for Describing and Comparing Microbial Communities. *Appl. Environ. Microbiol.* 75 (23), 7537–7541. doi: 10.1128/AEM.01541-09
- Schmidt, T. S., Hayward, M. R., Coelho, L. P., Li, S. S., Costea, P. I., Voigt, A. Y., et al. (2019). Extensive Transmission of Microbes Along the Gastrointestinal Tract. *Life* 8, e42693. doi: 10.7554/eLife.42693
- Segata, N., Izard, J., Waldron, L., Gevers, D., Miropolsky, L., Garrett, W. S., et al. (2011). Metagenomic Biomarker Discovery and Explanation. *Genome Biol.* 12, R60. doi: 10.1186/gb-2011-12-6-r60
- Senneby, A., Davies, J. R., Svensäter, G., and Neilands, J. (2017). Acid Tolerance Properties of Dental Biofilms *In Vivo*. *BMC Microbiol.* 17 (1), 165. doi: 10.1186/s12866-017-1074-7
- Sharma, R., and Rao, D. N. (2012). Functional Characterization of UvrD Helicases From *Haemophilus Influenzae* and *Helicobacter Pylori*. *FEBS J.* 279 (12), 2134–2155. doi: 10.1111/j.1742-4658.2012.08599.x
- Smith, M. F. Jr., Mitchell, A., Li, G., Ding, S., Fitzmaurice, A. M., Ryan, K., et al. (2003). Toll-Like Receptor (TLR) 2 and TLR5, But Not TLR4, are Required for *Helicobacter Pylori*-Induced NF-Kappa B Activation and Chemokine Expression by Epithelial Cells. *J. Biol. Chem.* 278 (35), 32552–32560. doi: 10.1074/jbc.M305536200
- Snider, E. J., Compres, G., Freedberg, D. E., Giddins, M. J., Khiabani, H., Lightdale, C. J., et al. (2018). Barrett's Esophagus is Associated With a Distinct Oral Microbiome. *Clin. Transl. Gastroenterol.* 9 (3), 135. doi: 10.1038/s41424-018-0005-8
- Snider, E., Compres, G., Freedberg, D., Khiabani, H., Nobel, Y., Stump, S., et al. (2019). Alterations to the Esophageal Microbiome Associated With Progression From Barrett's Esophagus to Esophageal Adenocarcinoma. *Cancer Epidemiol. Biomarkers Prev.* 28 (10), 1687–1693. doi: 10.1158/1055-9965.EPI-19-0008
- Snider, E. J., Freedberg, D. E., and Abrams, J. A. (2016). Potential Role of the Microbiome in Barrett's Esophagus and Esophageal Adenocarcinoma. *Dig. Dis. Sci.* 61 (8), 2217–2225. doi: 10.1007/s10620-016-4155-9
- Sugimoto, M., Murata, M., Mizuno, H., Iwata, E., Nagata, N., Itoi, T., et al. (2020). Endoscopic Reflux Esophagitis and Reflux-Related Symptoms After *Helicobacter Pylori* Eradication Therapy: Meta-Analysis. *J. Clin. Med.* 9 (9), 3007. doi: 10.3390/jcm9093007
- Sung, J. J. Y., Coker, O. O., Chu, E., Szeto, C. H., Luk, S. T. Y., Lau, H. C. H., et al. (2020). Gastric Microbes Associated With Gastric Inflammation, Atrophy and Intestinal Metaplasia 1 Year After *Helicobacter Pylori* Eradication. *Gut* 69 (9), 1572–1580. doi: 10.1136/gutjnl-2019-319826
- Suzuki, N., Yoneda, M., Takeshita, T., Hirofuji, T., and Hanioka, T. (2019). Induction and Inhibition of Oral Malodor. *Oral Microbiol.* 34 (3), 85–96. doi: 10.1111/omi.12259

- Tanabe, S., and Grenier, D. (2012). Characterization of Volatile Sulfur Compound Production by *Solobacterium Moorei*. *Arch. Oral. Biol.* 57 (12), 1639–1643. doi: 10.1016/j.archoralbio.2012.09.011
- Tanaka, J., Fukuda, Y., Shintani, S., Hori, K., Tomita, T., Ohkusa, T., et al. (2005). Influence of Antimicrobial Treatment for *Helicobacter Pylori* Infection on the Intestinal Microflora in Japanese Macaques. *J. Med. Microbiol.* 54 (Pt 3), 309–314. doi: 10.1099/jmm.0.45814-0
- Tang-Larsen, J., Claesson, R., Edlund, M. B., and Carlsson, J. (1995). Competition for Peptides and Amino Acids Among Periodontal Bacteria. *J. Periodontal. Res.* 30 (6), 390–395. doi: 10.1111/j.1600-0765.1995.tb01292.x
- Vanhatalo, A., L'Heureux, J. E., Kelly, J., Blackwell, J. R., Wylie, L. J., Fulford, J., et al. (2021). Network Analysis of Nitrate-Sensitive Oral Microbiome Reveals Interactions With Cognitive Function and Cardiovascular Health Across Dietary Interventions. *Redox Biol.* 41, 101933. doi: 10.1016/j.redox.2021.101933
- Vinasco, K., Mitchell, H. M., Kaakoush, N. O., and Castaño-Rodríguez, N. (2019). Microbial Carcinogenesis: Lactic Acid Bacteria in Gastric Cancer. *Biochim. Biophys. Acta Rev. Cancer* 1872 (2), 188309. doi: 10.1016/j.bbcan.2019.07.004
- Vincent, C., Stephens, D., Loo, V., Edens, T., Behr, M., Dewar, K., et al. (2013). Reductions in Intestinal Clostridiales Precede the Development of Nosocomial *Clostridium Difficile* Infection. *Microbiome* 1 (1), 18. doi: 10.1186/2049-2618-1-18
- Volgenant, C. M., Zaura, E., Brandt, B. W., Buijs, M. J., Tellez, M., Malik, G., et al. (2017). Red Fluorescence of Dental Plaque in Children -A Cross-Sectional Study. *J. Dent.* 58, 40–47. doi: 10.1016/j.jdent.2017.01.007
- Wang, N., Guo, D., Tian, X., Lin, H., Li, Y., Chen, S., et al. (2016). Niacin Receptor GPR109A Inhibits Insulin Secretion and is Down-Regulated in Type 2 Diabetic Islet Beta-Cells. *Gen. Comp. Endocrinol.* 237, 98–108. doi: 10.1016/j.ygcen.2016.08.011
- Wang, Q., Rao, Y., Guo, X., Liu, N., Liu, S., Wen, P., et al. (2019). Oral Microbiome in Patients With Oesophageal Squamous Cell Carcinoma. *Sci. Rep.* 9 (1), 19055. doi: 10.1038/s41598-019-55667-w
- Wang, K., Zhang, L., He, Z. H., Liu, Z. J., Zhang, L., Hu, N., et al. (2019). A Population-Based Survey of Gastroesophageal Reflux Disease in a Region With High Prevalence of Esophageal Cancer in China. *Chin. Med. J. (Engl.)* 132 (13), 1516–1523. doi: 10.1097/CM9.0000000000000275
- Wang, B., Zhang, Y., Zhao, Q., Yan, Y., Yang, T., Xia, Y., et al. (2020). Patients With Reflux Esophagitis Possess a Possible Different Oral Microbiota Compared With Healthy Controls. *Front. Pharmacol.* 11, 1000. doi: 10.3389/fphar.2020.01000
- Wang, J., Zheng, J., Shi, W., Du, N., Xu, X., Zhang, Y., et al. (2018). Dysbiosis of Maternal and Neonatal Microbiota Associated With Gestational Diabetes Mellitus. *Gut* 67 (9), 1614–1625. doi: 10.1136/gutjnl-2018-315988
- Wu, J., Zhang, C., Xu, S., Xiang, C., Wang, R., Yang, D., et al. (2020). Fecal Microbiome Alteration May Be a Potential Marker for Gastric Cancer. *Dis. Markers* 2020, 3461315. doi: 10.1155/2020/3461315
- Yang, L., Francois, F., and Pei, Z. (2012). Molecular Pathways: Pathogenesis and Clinical Implications of Microbiome Alteration in Esophagitis and Barrett Esophagus. *Clin. Cancer Res.* 18 (8), 2138–2144. doi: 10.1158/1078-0432.CCR-11-0934
- Yang, L., Lu, X., Nossa, C. W., Francois, F., Peek, R. M., and Pei, Z. (2009). Inflammation and Intestinal Metaplasia of the Distal Esophagus are Associated With Alterations in the Microbiome. *Gastroenterology* 137 (2), 588–597. doi: 10.1053/j.gastro.2009.04.046
- Zhao, Y., Gao, X., Guo, J., Yu, D., Xiao, Y., Wang, H., et al. (2019). *Helicobacter Pylori* Infection Alters Gastric and Tongue Coating Microbial Communities. *Helicobacter* 24 (2), e12567. doi: 10.1111/hel.12567
- Zhou, P., Li, X., Huang, I. H., and Qi, F. (2017). *Veillonella* Catalase Protects the Growth of *Fusobacterium Nucleatum* in Microaerophilic and *Streptococcus Gordonii*-Resident Environments. *Appl. Environ. Microbiol.* 83 (19), e01079–e01017. doi: 10.1128/AEM.01079-17
- Zhou, J., Shrestha, P., Qiu, Z., Harman, D. G., Teoh, W. C., Al-Sohaily, S., et al. (2020). Distinct Microbiota Dysbiosis in Patients With Non-Erosive Reflux Disease and Esophageal Adenocarcinoma. *J. Clin. Med.* 9 (7), 2162. doi: 10.3390/jcm9072162

**Conflict of Interest:** The authors declare that the research was conducted in the absence of any commercial or financial relationships that could be construed as a potential conflict of interest.

**Publisher's Note:** All claims expressed in this article are solely those of the authors and do not necessarily represent those of their affiliated organizations, or those of the publisher, the editors and the reviewers. Any product that may be evaluated in this article, or claim that may be made by its manufacturer, is not guaranteed or endorsed by the publisher.

Copyright © 2021 Liang, Liu, Liu, Zhang, Dong, Bai, Ma and Kang. This is an open-access article distributed under the terms of the Creative Commons Attribution License (CC BY). The use, distribution or reproduction in other forums is permitted, provided the original author(s) and the copyright owner(s) are credited and that the original publication in this journal is cited, in accordance with accepted academic practice. No use, distribution or reproduction is permitted which does not comply with these terms.





# Taxonomic and Functional Dysregulation in Salivary Microbiomes During Oral Carcinogenesis

Jiung-Wen Chen<sup>1</sup>, Jer-Horng Wu<sup>1\*</sup>, Wei-Fan Chiang<sup>2,3</sup>, Yuh-Ling Chen<sup>4</sup>, Wei-Sheng Wu<sup>5</sup> and Li-Wha Wu<sup>6\*</sup>

<sup>1</sup> Department of Environmental Engineering, National Cheng Kung University, Tainan, Taiwan, <sup>2</sup> Department of Oral & Maxillofacial Surgery, Chi-Mei Medical Center, Liouying, Taiwan, <sup>3</sup> School of Dentistry, National Yang-Ming University, Taipei, Taiwan, <sup>4</sup> Institute of Oral Medicine, College of Medicine, National Cheng Kung University, Tainan, Taiwan, <sup>5</sup> Department of Electrical Engineering, National Cheng Kung University, Tainan, Taiwan, <sup>6</sup> Institute of Molecular Medicine, College of Medicine, National Cheng Kung University, Tainan, Taiwan

## OPEN ACCESS

### Edited by:

Huizhi Wang,  
Virginia Commonwealth University,  
United States

### Reviewed by:

Alison Ravenscraft,  
University of Texas at Arlington,  
United States  
Juhi Bagaikar,  
University of Louisville, United States

### \*Correspondence:

Jer-Horng Wu  
enewujh@ncku.edu.tw  
Li-Wha Wu  
liwhawu@mail.ncku.edu.tw

### Specialty section:

This article was submitted to  
Microbiome in Health and Disease,  
a section of the journal  
Frontiers in Cellular and  
Infection Microbiology

**Received:** 02 February 2021

**Accepted:** 23 August 2021

**Published:** 16 September 2021

### Citation:

Chen J-W, Wu J-H, Chiang W-F,  
Chen Y-L, Wu W-S and Wu L-W  
(2021) Taxonomic and Functional  
Dysregulation in Salivary Microbiomes  
During Oral Carcinogenesis.  
Front. Cell. Infect. Microbiol. 11:663068.  
doi: 10.3389/fcimb.2021.663068

Exploring microbial community compositions in humans with healthy versus diseased states is crucial to understand the microbe-host interplay associated with the disease progression. Although the relationship between oral cancer and microbiome was previously established, it remained controversial, and yet the ecological characteristics and their responses to oral carcinogenesis have not been well studied. Here, using the bacterial 16S rRNA gene amplicon sequencing along with the *in silico* function analysis by PICRUSt2 (Phylogenetic Investigation of Communities by Reconstruction of Unobserved States 2), we systematically characterized the compositions and the ecological drivers of saliva microbiome in the cohorts of orally healthy, non-recurrent oral verrucous hyperplasia (a pre-cancer lesion), and oral verrucous hyperplasia-associated oral cancer at taxonomic and function levels, and compared them with the re-analysis of publicly available datasets. Diversity analyses showed that microbiome dysbiosis in saliva was significantly linked to oral health status. As oral health deteriorated, the number of core species declined, and metabolic pathways predicted by PICRUSt2 were dysregulated. Partitioned beta-diversity revealed an extremely high species turnover but low function turnover. Functional beta-diversity in saliva microbiome shifted from turnover to nestedness during oral carcinogenesis, which was not observed at taxonomic levels. Correspondingly, the quantitative analysis of stochasticity ratios showed that drivers of microbial composition and functional gene content of saliva microbiomes were primarily governed by the stochastic processes, yet the driver of functional gene content shifted toward deterministic processes as oral cancer developed. Re-analysis of publicly accessible datasets supported not only the distinctive family taxa of *Veillonellaceae* and *Actinomycetaceae* present in normal cohorts but also that *Flavobacteriaceae* and *Peptostreptococcaceae* as well as the dysregulated metabolic pathways of nucleotides, amino acids, fatty acids, and cell structure were related to oral cancer. Using predicted functional profiles to elucidate the correlations to the oral health status



shows superior performance than using taxonomic data among different studies. These findings advance our understanding of the oral ecosystem in relation to oral carcinogenesis and provide a new direction to the development of microbiome-based tools to study the interplay of the oral microbiome, metabolites, and host health.

**Keywords:** oral cancer, microbiome dysbiosis, machine learning, oral verrucous hyperplasia, saliva

## 1 INTRODUCTION

Oral cavity is a dynamic and complex ecosystem, harboring more than 1,000 species of microorganisms (Lamont et al., 2018). The ecological balance of the host-microbiome symbiosis benefits human health by supporting the host immune system, maintaining physiological functions, and providing additional metabolic potentials (Kilian et al., 2016) to inhibit the growth of exogenous/opportunistic pathogens (Kreth et al., 2005; Wescombe et al., 2009) and regulate the host-microbe homeostasis such as systemic nitrate metabolism that is linked to cardiovascular diseases (Govoni et al., 2008; Farah et al., 2018). Recent studies have shown that the oral microbiome plays an essential role in the etiology of oral and systemic diseases, such as caries, periodontitis, and oral cancer (Socransky and Haffajee, 2005; Costalonga and Herzberg, 2014; Gao et al., 2018). Among these diseases, oral cancer is of particular concern because it causes approximately 180,000 deaths a year worldwide (Ferlay et al., 2019). Oral bacteria, along with other known risk factors (smoking, alcohol, and betel quid chewing), have been reported to be associated with oral cancers (Katz et al., 2011; Lin et al., 2011; Zhao et al., 2017). Oral carcinogenesis has been considered a pivotal factor to alter the oral microbiome, while the microbiome dysbiosis may exacerbate the disease progression in the host. For example, using the gnotobiotic mouse model of oral cancer, research demonstrated that the oral microbiome regulated a specific signaling pathway to promote tumorigenesis in oral cancer (Stashenko et al., 2019). A recent study further provides causal evidence in promoting oral tumorigenesis *via* crosstalk between signaling pathways by periodontal pathogens (Kamarajan et al., 2020). Although the relationship between microbiome and cancer is still controversial and complicated (Sepich-Poore et al., 2021), these studies have pointed out the complex mutual interplay between the oral microbiome and oral carcinogenesis.

Oral potentially malignant disorders (OPMDs) describe a diverse group of lesions or conditions, including leukoplakia, erythroplakia, oral submucous fibrosis, and oral verrucous hyperplasia (OVH), that may precede the development of oral squamous cell carcinoma (OSCC), accounting for more than 90% of oral cancers (Markopoulos, 2012; Warnakulasuriya, 2020). Though oral cavity can be easily accessed for oral cancer screening, more than 60% of patients were detected at a late stage of OSCC partly due to the unawareness of patients and healthcare practitioners for the asymptomatic lesions (Mashberg, 2000; Mager et al., 2005; Lingen et al., 2008; Kaur et al., 2018). Conventional oral examination (COE) followed by confirmatory tissue biopsy is the gold standard for oral cancer diagnosis

(Lingen et al., 2008). However, COE may not be able to identify all OPMD lesions or lesions that are prone to progress to OSCC (Lingen et al., 2008). Besides, the tissue biopsy is invasive, painful, and time-consuming (Kaur et al., 2018). Although other clinical diagnostic tools were available for oral cancer detection (Mashberg, 1983; Eisen, 2002), patients are still diagnosed in the late stages of OSCC (Kaur et al., 2018). Therefore, early detection and diagnosis technology for OPMD and oral cancer are necessary, and saliva serves as an ideal reservoir for non-invasive biomarker exploration.

Studies have suggested that the oral microbiome changed during the progression of OSCC (Zhao et al., 2017; Hashimoto et al., 2019; Chen et al., 2020). These studies mainly focused on two cohorts (healthy control/OSCC or OPMD/OSCC) instead of three (healthy control/OPMD/OSCC) without a follow-up.

However, the progress of OPMD malignancy usually takes years to more than decades, with malignant transformation rates ranging from less than 1% to over 30% (Chiang et al., 2020; Warnakulasuriya, 2020). Although a few oral microbiome studies did include OPMD samples (Hernandez et al., 2017; Lee et al., 2017), the inclusion of a wide variety of OPMDs may confound the results. Among OPMDs, OVH is commonly detected in the oral cavity of betel quid chewers and has high transformation rates of up to 21.3% (Chiang et al., 2020; Warnakulasuriya, 2020). So far, the interaction between the oral microbiome and OVH carcinogenesis has not yet been reported.

The microbial community structure of the oral cavity remains compositionally stable to ecological determinants (e.g., pH, redox, and nutrients) due to its capability of resistance and resilience (Richards et al., 2017; Marsh, 2018). The stability may be substantially perturbed by stressors, driving the microbial communities into distinct patterns in taxonomical and functional components (Zaneveld et al., 2017), and this concept was captured in several hypotheses regarding the microbial ecology and oral diseases. For example, the ecological plaque hypothesis postulated that caries and periodontal diseases are a consequence of a taxonomic profile change of plaque microbiota driven by an altered environment (Marsh, 2003). For the host-microbiome ecosystem of OSCC, the oral microbiome may initially comprise species with competitive advantage *via* host selection, followed by a functional dysbiosis and enhancement of OSCC development as virulence factors of selected microbes are expressed (Al-Hebshi et al., 2019). To decipher how microbiomes respond to stressors, the patterns of microbial composition and the underlying ecological drivers were usually studied using taxonomic data. A recent systemic review of studies on the microbiome of OSCC patients reported

that the tumor-associated microbiome presented similar functional potentials regardless of variations in taxonomic profiles (Al-Hebshi et al., 2019). Thus, taxonomic information in conjugation with functional profiles may shed some light on the variation of the oral microbiome.

The between-sample diversity (beta diversity) is often used to measure the differences between samples and can be disentangled into nestedness and turnover components: the former is a non-random process of species loss or gain, while the latter is the replacement of some species by others (Baselga, 2010). These patterns are microbial responses to deterministic processes, stochastic processes, or combinations of the two (Chase and Myers, 2011; Stegen et al., 2013; Zhou and Ning, 2017). As such, the quantitative determination of the ecological drivers influencing community composition in an ecosystem is important for explicitly elucidating the community dynamics. By quantifying the stochasticity ratio using the pattern-oriented null model (Ning et al., 2019), our previous study showed the dominance of stochastic perturbations in shaping the oral microbiomes of oral submucous fibrosis (one of the OPMDs) and OSCC cohorts (Chen et al., 2020). The influence of stochastic perturbations might also be crucial in the healthy group, given that the oral microbiome was highly personalized and time-varied (Mukherjee et al., 2018). Since highly diverse microorganisms would survive in similar ecosystems (i.e., oral cavity of healthy individuals, OPMD, and OSCC cohorts), we, therefore, were interested in exploring whether the disease stressor can shape the functional gene content of oral microbiome and the functional dysbiosis would occur in response to the development of oral carcinogenesis.

In the present study, we hypothesized that the alteration of oral microbiomes of orally healthy (normal), OPMD (specifically OVH), and OSCC cohorts were associated with oral health status. To investigate the role of ecological patterns in healthy and diseased oral microbiomes, both taxonomic profiles and functional potentials were studied in terms of the dichotomy of beta diversity (nestedness and turnover), along with the stochasticity ratio. To our knowledge, this is the first report to disentangle the contribution of the turnover and nestedness of both taxonomic and functional compositions in three different states of the oral cavity ecosystem (orally healthy, OPMD, and OSCC). We further validated our results with publicly available data using the same pipeline and the machine learning prediction.

## 2 MATERIALS AND METHODS

### 2.1 Study Participants and Sample Collection

All participants were recruited from Chi Mei Medical Center (CMMC), Liouying, Taiwan, with the approval of the Institutional Review Board of CMMC (IRB No.: 10612-L02). Participants were interviewed to ensure no antibiotics or surgical treatments for at least one month to enrollment and instructed to refrain from eating, drinking, or using oral hygiene products for at least one hour prior to saliva collection and to rinse their

mouth with drinking water. Five minutes after oral rinsing, participants were instructed to spit into a 50 mL centrifuge tube, which was kept on ice, and were cautioned not to cough up sputum. A total of 5 mL of saliva was collected from each participant within a 30-minute time frame. Saliva samples were then centrifuged at  $2,600 \times g$  at  $4^{\circ}\text{C}$  for 15 min. One milliliter of the supernatant was transferred to a new centrifuge tube for other research, and the rest of the saliva supernatant was treated with RNase Inhibitor (Ambion, Austin, TX, USA) and stored at  $-80^{\circ}\text{C}$  for further analysis. The samples were processed and frozen within 30 minutes after collection.

### 2.2 DNA Extraction, PCR, and 16S rRNA Gene Sequencing

Bacterial genomic DNA was extracted from saliva samples using a QIAamp DNA Mini Kit (Qiagen, Germany) according to the manufacturer's spin column protocol. The extracted DNA was amplified using a barcoded *Bacteria*-specific primer set (341F/806R) that targets the V3–V4 hypervariable region of the 16S rRNA gene. The PCR amplicons were sequenced on a MiSeq platform (Illumina, USA) using v3 Chemistry Kits ( $2 \times 300$  bp). The detailed sequencing protocol has been described previously (Chen et al., 2017).

### 2.3 Bioinformatics Analyses

#### 2.3.1 16S rRNA Sequence Processing

High-throughput amplicon sequencing data were analyzed on the QIIME 2 platform (v2019.4) (Bolyen et al., 2019). After the primers at both ends were trimmed, raw sequences were quality filtered, denoised, merged, and chimera filtered using DADA2 to produce ASVs (Callahan et al., 2016), which provides a finer resolution of sequence variants down to single nucleotide differences compared to traditional 97% similarity of operational taxonomic units. The maximum number of expected errors was set at 3. The denoised ASVs with lengths outside the interval between 400 and 450 nt were excluded from the subsequent analysis. To obtain taxonomy at the species level with a focus on bacteria present in oral cavity, taxonomic annotation of ASVs was performed by a customized naïve Bayes classifier trained on the expanded Human Oral Microbiome Database (version 15.1) (Escapa et al., 2018) using the q2-feature-classifier plugin (Bokulich et al., 2018b) with default settings. "Unclassified" was appended to the lowest available taxonomic level for ASVs that were not resolved to the species level.

#### 2.3.2 Diversity Analysis

Alpha and beta diversity indices were calculated at a rarefaction depth of 43,313 reads per sample using the QIIME2 plugin q2-diversity. A phylogenetic tree was constructed using the QIIME2 plugin q2-fragment-insertion (Matsen et al., 2010; Eddy, 2011; Matsen et al., 2012; Janssen et al., 2018) for phylogenetic alpha (Faith's phylogenetic diversity) and beta diversity (UniFrac) measurements. Kruskal–Wallis rank-sum test was used to compare the differences between the alpha diversity indices among cohorts. The contribution of participant age, oral health

status (healthy, OVH, and OSCC), and lifestyle factors (alcohol, betel nut, or cigarette consumption) were analyzed using Adonis with 9999 permutations. Distance-based permutational multivariate analysis of variance (PERMANOVA) was used to test the significant difference levels of the centroid of beta diversity metrics among cohorts in the ordination space of PCoA. For the observed significant PERMANOVA results, PERMDISP was then performed with 9999 permutations to determine the within-group homogeneity of dispersion. The Benjamini-Hochberg procedure was applied to control the FDR for multiple testing by statsmodels (0.10.2) (Seabold and Perktold, 2010). To evaluate the respective contribution of turnover and nestedness components to beta-diversity as a whole, we calculated the multiple-site dissimilarity (Sørensen-based,  $\beta_{SOR}$ ), and the partitioning dissimilarities that accounted only for turnover (Simpson-based,  $\beta_{SIM}$ ) and for nestedness ( $\beta_{NES}$ ) components, respectively (Baselga, 2010).

### 2.3.3 Core Microbiome Analysis

Core microbiome analysis was performed using a customized Python script and visualized using matplotlib-venn (0.11.5). The feature table was first converted to incidence data (presence/absence), and the prevalence of each taxon in each cohort was calculated. If the prevalence of a given taxon was greater than 75%, it was considered a core species in a cohort (Takeshita et al., 2016; Willis et al., 2018). A Venn diagram was used to illustrate the distinct and shared core species between cohorts.

### 2.3.4 *In Silico* Metagenome Prediction

The metagenomic content was developed *in silico* from the denoised 16S rRNA genes using PICRUSt2 (Douglas et al., 2020). HMMER (www.hmm.org), EPA-NG, and GAPP were performed to place ASVs into reference phylogeny (Barbera et al., 2018; Czech and Stamatakis, 2019). The functional profiles of oral microbiome were predicted in accordance with the community-wide abundance method. The castor R package was subsequently used for hidden state prediction to infer gene family copy numbers (Louca and Doebeli, 2017). Finally, the EC number abundances were predicted based on the adjusted gene family abundances. To infer pathway abundances, MinPath was applied to identify a set of minimum pathways based on the predicted gene families (Ye and Doak, 2009). Default settings were used to regroup EC numbers to MetaCyc reactions and further inferred to MetaCyc pathway abundances (Caspi et al., 2020).

### 2.3.5 Statistical Testing of Differential Abundance

LEfSe was applied to identify differentially abundant species and metabolic pathways among cohorts (Segata et al., 2011). The input of the frequency matrix was rarefied to the same depth and then transformed into a relative abundance matrix. The significance level was 0.05 for the Kruskal-Wallis test, and the cutoff of the logarithmic LDA scores was 3.

### 2.3.6 Stochasticity Ratio Estimation

To evaluate the drivers of the community composition and functional profile, the null-model-based approach was used to

calculate the normalized ratio of the difference between the actual and expected similarity, referring to as a selection strength (SS), to assess the strength of determinism acting against the stochastic forces (Ning et al., 2019). In this method, the actual Bray-Curtis similarity of any two samples in the metacommunity of a cohort was first calculated based on taxonomic and pathway data and compared with the mean of null expected similarity that was obtained by averaging the similarity of 1,000 times of randomization of the two samples in the metacommunity. The stochasticity ratio was calculated as  $(1 - SS)$ . The ratio ranges from 0 to 100%, with 0 for the community composition/functional profile solely shaped by deterministic processes, and 100% for the community composition/functional profile purely influenced by the stochastic forces. For the null model algorithm, proportional taxa/pathway occurrence frequency and richness were applied to generate random microbial/functional communities (Gotelli, 2000). Samples in each cohort shared the sample regional taxa/pathway pool in the null model algorithm.

## 2.4 Public Data Acquisition, Processing, and Re-Analysis

Academic search systems, including Google Scholar and PubMed, were used to find studies published in the last five years (2015–2020) with the search terms “oral microbiome”, “saliva microbiome”, and “OSCC”. We included 16S rRNA amplicon-based studies with publicly available sequences and metadata indicating OSCC or control for each sample. To compare the results, we only included studies with samples collected by non-invasive collection methods (oral swab, oral rinse, or saliva samples), while excluding the studies of using tissue biopsies and those without sample metadata. Studies with the OSCC cohort consisting of both the oral cavity and oropharynx types were also included. The raw sequence processing, diversity analysis, and core species/metabolic pathway analysis were performed as described in previous sections.

## 2.5 Prediction Using Machine Learning Analysis

The QIIME2 q2-sample-classifier plugin (Bokulich et al., 2018a) was used to predict sample health statuses based on taxonomic and functional profiles generated from this study, and the publicly available dataset was re-analyzed. Input data were randomly split into 80% for training and 20% for testing. The Random Forest classifier was applied for supervised machine learning. Cross-validated recursive feature elimination was applied for feature selection, with 5% of features eliminated at each iteration. Hyperparameters were automatically tuned using a random grid search with 5-fold cross-validation. Based on taxonomic and functional profiles, respectively, we performed the analysis procedure 100 times with different random seeds and recorded the testing accuracy ratio for each iteration. The resulting accuracy ratio data was tested using an independent *t*-test to determine the statistical significance of the machine learning prediction results. AUROC metrics were calculated using the scikit-learn package (Pedregosa et al., 2011). For



multi-class classification, micro-average was used. The data in each study were trained and validated separately to minimize the experimental batch effects.

### 3 RESULTS

#### 3.1 Cohort Descriptions and Sequencing Quality

Saliva samples collected from 75 male participants, including healthy controls (normal,  $n = 27$ ), non-recurrent OVH patients with > 8-year follow-up (2011 December–2019 November) (OVH,  $n = 21$ ), and patients having primary OVH followed by OSCC development within eight years follow-up (OSCC,  $n = 27$ ), were included in this study (Table S1). Statistical analysis of the participants' metadata (age and lifestyle factors) showed that the differences in the studied cohorts were significant for age between normal and OSCC cohorts, and for betel nut chewing habits between OVH and OSCC cohorts (Table S2). Illumina high-throughput sequencing generated a total of 14,261,633 raw sequences targeting the V3–V4 region of the 16S rRNA gene. After sequence denoising, 8,522,211 denoised reads were retained from 75 samples, with an average of  $113,629 \pm 33,379$  high-quality sequences per library. The plateau rarefaction curves indicated that the sequencing depth was sufficient for downstream analysis (Figure S1).

#### 3.2 Phylogenetic Diversity Was Slightly Reduced in the Microbiomes of Diseased Cohorts

In the assessment of ASVs detected within samples, the results revealed that the four alpha diversity indices were not significantly different between the studied cohorts ( $q > 0.05$  after false discovery rate (FDR) adjustment, Table S3). To evaluate the effects of risk factors, including participant age, oral health status, and lifestyle, on the changes of the oral microbial community, UniFrac distance-based Adonis analysis was performed with the host health status as the last variables (Alcohol+BetelNut+Cigarette+Age+HealthStatus). As shown in Figures 1A, B, oral health status was detected as the strongest explanatory power (Adonis  $R^2 = 0.037$  for unweighted UniFrac and 0.057 for weighted UniFrac) to significantly differentiate the cohorts (FDR-adjusted  $p < 0.05$ ). Although age and betel nut chewing habit exhibited significant distinction between some cohorts (Table S2), the variable, betel nut chewing, was not significantly associated with changes in oral microbial communities. However, age as a variable may confound the change of oral microbiome with the unweighted UniFrac distance (Adonis  $R^2 = 0.021$ , FDR-adjusted  $p < 0.05$ ). The UniFrac-based beta diversity distribution of salivary microbiomes from the cohorts was visualized using a principal co-ordinate analysis (PCoA) plot (Figures 1C, D), and showed random distribution on the ordination space. Pairwise permutation analyses of multivariate dispersions (PERMDISP) analysis further confirmed that the dispersion effect was not found among cohorts based on the unweighted UniFrac metric

( $p_{\text{PERMDISP}} = 0.1669$ ); however, this effect was observed between normal and diseased (OVH/OSCC) cohorts. In particular, the dispersion effect reached a significant level between the normal and OVH cohorts (FDR-adjusted  $p_{\text{PERMDISP}} = 0.0362$ ) in the weighted UniFrac distance measurement, suggesting heterogeneous dispersion of abundant taxa in salivary microbiota in correspondence with the oral health status.

#### 3.3 Oral Carcinogenesis Altered Core Microbiomes

To further compare the differences in salivary microbiomes among cohorts, we investigated the “core” species, defined as the taxa commonly present in the saliva of each cohort with a prevalence > 75% (Takeshita et al., 2016; Willis et al., 2018). The number of core species was 55 ( $67.14 \pm 11.06\%$  of total abundance), 39 ( $47.24 \pm 14.96\%$  of total abundance), and 30 ( $44.52 \pm 12.81\%$  of total abundance) in normal, OVH, and OSCC cohorts, respectively, and 24 species taxa were universal in the saliva samples from all cohorts, even when the oral health status altered (Figure 2A). Five species (*Anaeroglobus geminatus*, *Porphyromonas gingivalis*, *Prevotella oulorum*, *Saccharibacteria* (TM7) [G5] bacterium HMT-356, and *Tannerella forsythia*) were specific to the OVH cohort. In comparison, two species (*Capnocytophaga sputigena* and *Catonella morbi*) were specific to the OSCC cohort. One species (*Dialister invisus*) was specific to the OVH and OSCC cohort. Interestingly, a decreased trend in overall core species richness (gamma diversity) was clearly observed with deteriorating oral health status (Figure 2B) from 12.53% in the normal cohort to 6.34% in the OSCC cohort.

The linear discriminant analysis effect size (LEfSe) analysis revealed the core species with significant abundance in each group ( $p < 0.05$ , LDA score >  $10^3$ ) (Figure 2C). A total of 15 species taxa were enriched in the normal cohort compared to 2–4 species in the two diseased cohorts. In the normal cohort, they included two unclassified taxa related to *Prevotella* and *Selenomonas* genera, three uncultured species (*Saccharibacteria* (TM7) [G-1] bacterium HMT-352, *Leptotrichia* sp. HMT-417, and *Actinomyces* sp. HMT-180), and 10 known species within 7 genera: *Prevotella* (*Prevotella melaninogenica*, *Prevotella salivae*, and *Prevotella pallens*), *Veillonella* (*Veillonella atypica*, and *Veillonella dispar*), *Streptococcus salivarius*, *Haemophilus parainfluenzae*, *Megasphaera micronuciformis*, *Campylobacter concisus*, and *Rothia mucilaginosa*. For the OVH cohort, only *Veillonella parvula* and *Rothia dentocariosa* were significantly abundant ( $p < 0.05$ , LDA score >  $10^3$ ), while four species, *Capnocytophaga sputigena*, *Prevotella oris*, *Peptostreptococcus stomatis*, and *Parvimonas micra* were specifically abundant in the OSCC cohort (abundance see Table S4). Furthermore, LEfSe conducted with higher rank data showed that the species variation converges at specific family-level taxa in different cohorts. When prevalence taken into account, the enriched family taxa in the normal cohort were *Actinomycetaceae* (mean  $\pm$  SD;  $1.55\% \pm 1.16\%$ ), *Veillonellaceae* ( $12.50\% \pm 7.41\%$ ), and *Prevotellaceae* ( $20.60\% \pm 10.00\%$ ). *Leptotrichiaceae* ( $3.05\% \pm 3.92\%$ ) was the only family specifically enriched in the OVH cohort. The saliva microbiome, however, shifted to

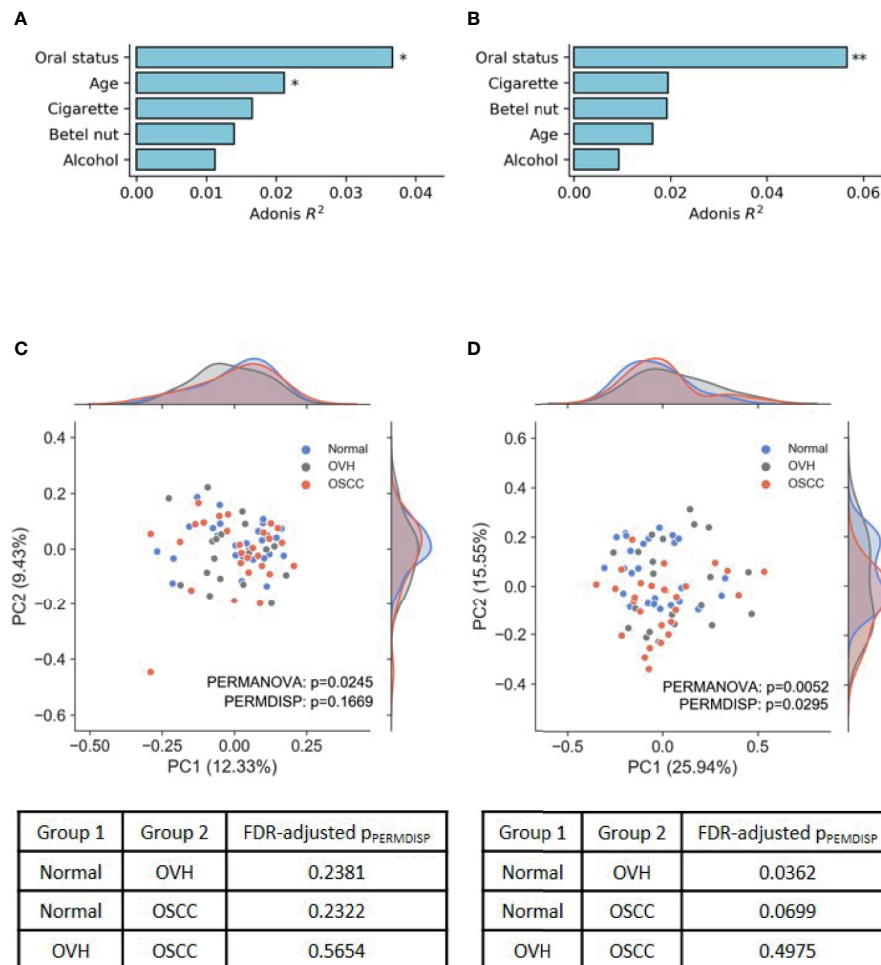


**FIGURE 1** | Differences in oral microbiomes among normal, OVH, and OSCC cohorts. **(A, B)** Adonis analysis based on **(A)** unweighted and **(B)** weighted UniFrac distance metrics shows the effect ( $R^2$ ) of factors with the oral microbiome. \* indicates FDR-adjusted  $p < 0.05$  and \*\* indicates FDR-adjusted  $p < 0.01$ . **(C, D)** Principal coordinate analysis (PCoA) plots of taxonomic profiles based on **(C)** unweighted and **(D)** weighted UniFrac distance metrics. Marginal kernel densities visualize the distribution of microbial diversity along both axes. The pairwise PERMDISP reveals the dispersion effect (FDR-adjusted  $p < 0.05$ ) between normal and OVH cohorts.

*Flavobacteriaceae* (8.61%  $\pm$  11.36%), *Peptostreptococcaceae* (2.37%  $\pm$  1.61%), *Mycoplasmataceae* (1.46%  $\pm$  2.36%), *Carnobacteriaceae* (1.65%  $\pm$  2.12%), *Lachnospiraceae* (2.19%  $\pm$  1.83%), and *Peptoniphilaceae* (0.53%  $\pm$  0.51%) as abundant taxa specific to the OSCC cohort (**Figure 2D** and **Figure S2**).

### 3.4 Distinct Metabolic Pathways Were Dysregulated Among Three Cohorts

We applied PICRUSt2, an updated version of a widely used metagenomic prediction tool (Langille et al., 2013), to infer the functional profiles of the microbial communities using denoised ASVs. The nearest-sequenced taxon index (NSTI) of 81.68% of reads was less than 0.15 (**Figure S3A**), suggesting the high-quality metagenome predicted (Langille et al., 2013). LEfSe analysis identified 26, 7, and 24 inferred pathways that were significantly abundant specific to normal, OVH, and OSCC cohorts, respectively (**Figure S3B**). By categorizing these pathways to higher classes, we found that most of them belong

to amino acid biosynthesis (10 pathways), and cofactor, prosthetic group, electron carrier, and vitamin biosynthesis (8 pathways) for the normal cohort. The pathways for cell structure biosynthesis (5 pathways), fatty acid and lipid biosynthesis (4 pathways), and nucleoside and nucleotide metabolism (3 for biosynthesis; 2 for degradation) were abundant in the OSCC cohort (**Figure 3**). Only three pathways belonging to TCA cycles and nucleic acid processing were found to be significantly higher in abundance in specific relation to the OVH cohort.

### 3.5 Though a High Taxonomic Turnover, Functional Nestedness Evolved During Oral Carcinogenesis

To determine the differentiation of beta diversity in the saliva microbiome, we compared the dissimilarities of the salivary microbiomes quantitatively based on taxonomic and functional profiles. For community composition data, the species nestedness was 0.042, 0.058, and 0.043 (sustainably lower than



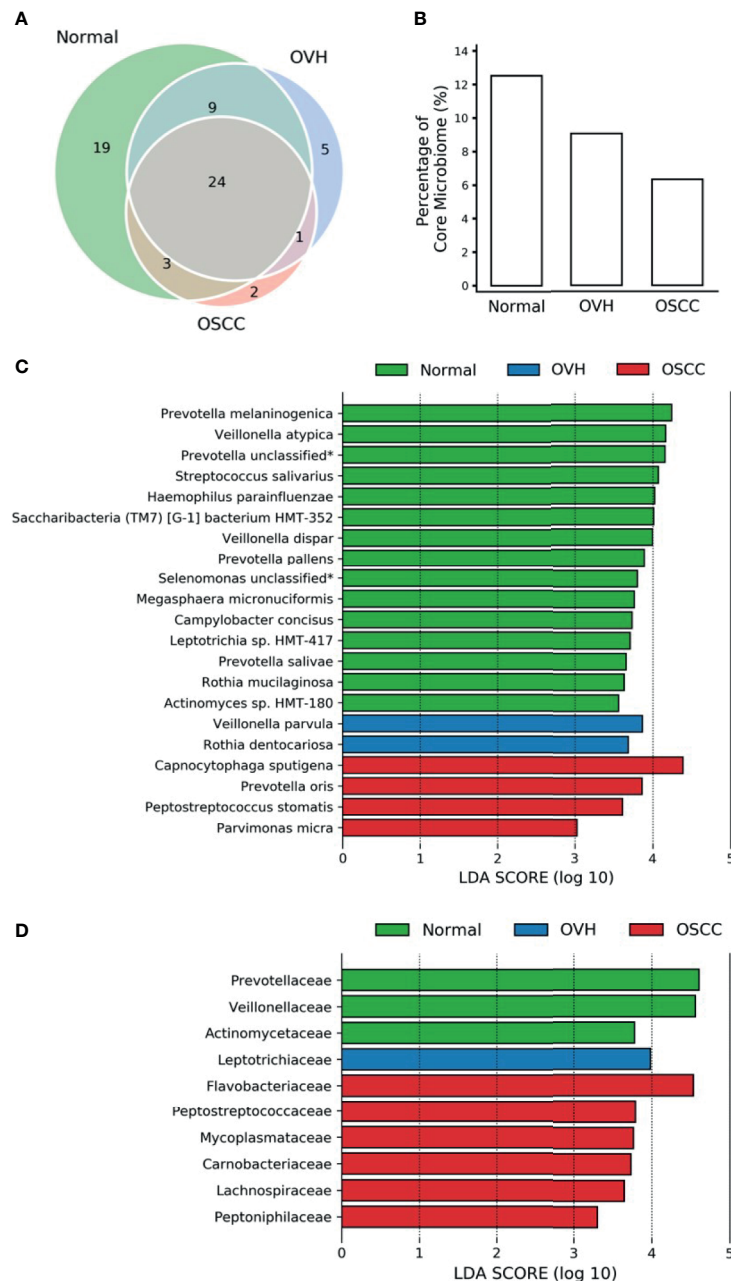


**FIGURE 2** | Core microbiome analysis. **(A)** Venn diagram of core microbiomes among cohorts. The core is defined as the species taxa present in saliva with  $\geq 75\%$  prevalence. **(B)** The fraction of core species number to overall species richness in each cohort. **(C)** LefSe reveals the distribution of core species displaying the abundance significantly higher ( $LDA > \log_{10}^3$ ) among cohorts. The asterisk (\*) indicates a taxon that was annotated only to the genus level. **(D)** Same as **(C)** but at the family level.

the turnover: 0.822, 0.802, and 0.841) for the normal, OVH, and OSCC cohorts, respectively (**Figure 4**), showing that the differentiation of salivary microbiomes was predominantly influenced by the species turnover. The high taxonomic turnover rate (low prevalence ( $< 33\%$ ) and high variation of species) among closely related species within these distinct family taxa could be visualized *via* a taxonomic tree

(**Figure S4**). By contrast, the functional profiles of the salivary microbiomes were relatively stable: the mean multi-site Sørensen dissimilarity related to pathways ( $0.456 \pm 0.044$ ) was lower than that related to species taxa ( $0.869 \pm 0.013$ ) by approximately 50%. Notably, the numerical distributions of function nestedness (0.180, 0.187, and 0.295) and function turnover (0.291, 0.209, and 0.204) were relatively similar in each of the three cohorts

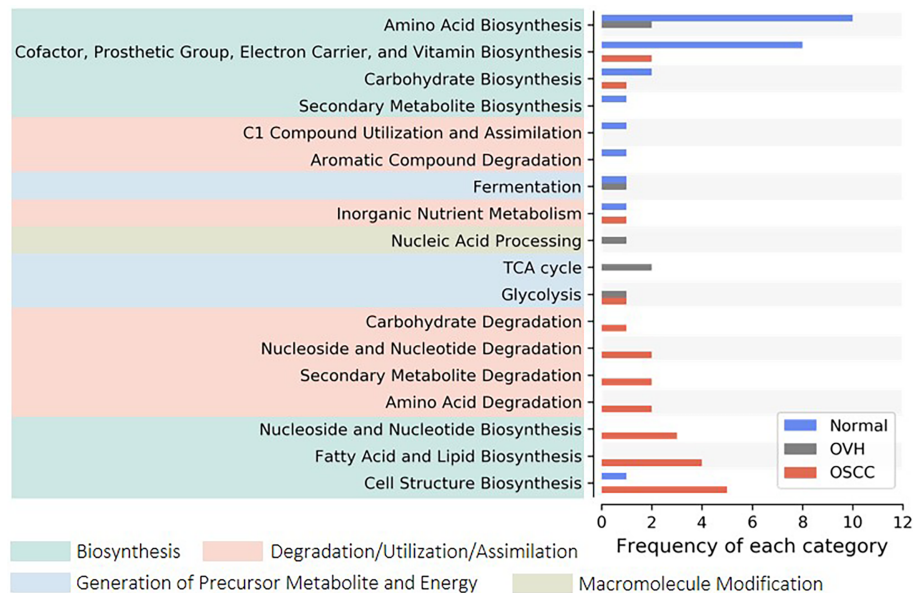


**FIGURE 3** | Distribution of signature pathways. The signature pathways, which abundances are significantly higher concerning each studied cohort, are detected using LEfSe. The inferred pathways are collapsed to each category based on Metacyc's pathway ontology. Colored boxes indicate a higher rank of the categories.

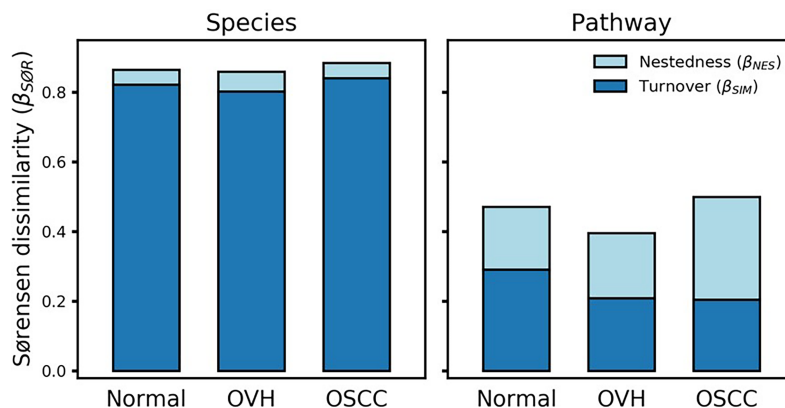


**FIGURE 4** | Multiple-site beta diversity (Sørensen dissimilarity) and corresponding nestedness and turnover components. The dissimilarities were analyzed in terms of species and metabolic pathway profiles in each cohort.

(normal, OVH, and OSCC, respectively), as compared to species-based Sørensen dissimilarity (Figure 4). Conspicuously, the ratio of the function nestedness to turnover increased from 0.620 for normal or 0.896 for OVH, to 1.449 for OSCC, suggesting that nestedness emerges with the functional differentiation of salivary microbiomes during the process of oral carcinogenesis. Regardless of the observed high species turnover of the salivary ecosystem, the dominance of functional nestedness in the OSCC cohort suggests that a set of distinct microbial functions, which may be associated with oral carcinogenesis, evolved accordingly in the oral cavity.

### 3.6 Deterministic Processes Influence Functional Profiles but Not Taxonomic Variations

To better understand the driving forces in shaping the salivary microbiomes, a null model-based quantitative analysis of stochasticity with taxonomic and functional profiles was performed (Ning et al., 2019), respectively. The resulting stochasticity ratio serves as an index to assess the partition and contribution of the deterministic and stochastic processes in shaping the microbiome structure. In the quantitative assessment of the relative importance of the two ecological drivers, the

deterministic and stochastic influence is summed to a total of 100%. Thus, the higher the stochasticity ratio, the stronger influence of stochastic processes or the less influence of deterministic forces. **Figure 5** shows that the stochastic process dominated the drivers of the bacterial community composition and functional gene content in saliva, with a stochastic ratio of inferred pathways ( $85.97 \pm 16.73\%$  to  $93.04 \pm 4.02\%$ ) higher than that of species taxa ( $61.88 \pm 13.75\%$  to  $64.44 \pm 13.11\%$ ). This finding suggests that the stochastic process played a more critical role in structuring the saliva microbiome at the functional level than the taxonomic level. Remarkably, the distribution patterns of taxa-based stochastic ratio among cohorts were relatively similar, showing stable stochastic and deterministic influences on taxonomic variations in the microbiomes of these three cohorts. By contrast, far broader distribution spectra for the function-based stochastic ratios were displayed in the strong association with the progression of oral carcinogenesis. Corresponding to the results of partitioning turnover and nestedness (**Figure 4**), this finding differentiates the stochastic influences from deterministic ones on shaping the saliva microbiome of different cohorts. It also supports a shift of the underlying driving force of the functional alternation towards the deterministic process corresponding to changes in oral health status from healthy through OPMD to OSCC.

### 3.7 Meta-Analysis Validates the Relation of Dysregulation Consistently to Several Taxa and Pathways

To test our findings' generalizability, we compared the taxonomic and functional data of this study with two previous studies [(Wolf et al., 2017; Zhao et al., 2017); see justifications in **Table S5**]. Because all the previous studies focused on the analysis of 16S rRNA sequences with a 97% similarity threshold using a clustering approach to resolve the signature taxa at the genus level, we re-analyzed the sequences with our

analytical pipeline to achieve phylogenetic resolution down to the species level. Although the signature species with specific abundances related to the study cohorts were found in each study, none was shared across all three studies for the normal and OSCC cohorts (**Figures 6A, B**), suggesting inconsistency among different studies. LEfSe was then conducted with family taxa. Similar to our data, re-analyzing Zhao's data at the family level revealed that *Actinomycetaceae* ( $1.82\% \pm 1.79\%$ ) and *Veillonellaceae* ( $8.09\% \pm 6.89\%$ ) were enriched in the normal control, whereas *Flavobacteriaceae* ( $7.06\% \pm 7.01\%$ ), *Peptostreptococcaceae* ( $2.04\% \pm 1.80\%$ ), and *Peptoniphilaceae* ( $0.06\% \pm 0.95\%$ ) were abundant in the OSCC group. *Prevotellaceae* ( $28.39\% \pm 15.67\%$ ) and *Carnobacteriaceae* ( $1.29\% \pm 1.62\%$ ) were also enriched in their OSCC. The differential abundance of either family in normal versus OSCC cohorts between ours and Zhao's data suggests that microbial turnover in saliva, albeit moderate, can still be detected even at the family level. For the re-work of Wolf's data, the abundance of *Pasteurellaceae* and *Bifidobacteriaceae* was specific to normal and OSCC cohorts, respectively. The discrepancy between Wolf's data and the other two studies (Zhao's data and ours) could likely attribute to a low sample number and different cancer types (11 samples; oropharynx = 7, oral cavity = 4) studied.

Nevertheless, we found a comparatively high number of pathways between studies when comparing functional profiles. For the normal cohort, no common pathway across studies was detected (**Figure 6C**). For the OSCC cohort, four pathways involved in nucleotide biosynthesis (UMP biosynthesis I) and cell structure biosynthesis (UDP-N-acetylmuramoyl-pentapeptide biosynthesis I and II, and peptidoglycan biosynthesis I) were prevalent across the studies (**Figure 6D**). Importantly, we obtained consistent results in a functional meta-analysis (**Figure S5**). In Zhao's and our datasets, amino biosynthesis pathways (arginine, ornithine, or histidine) were more abundant in normal control and pre-cancer groups,

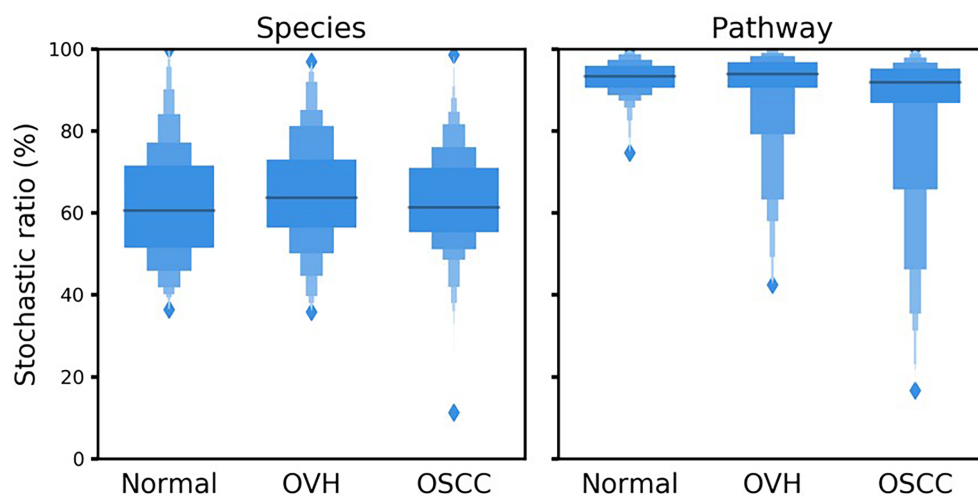


**FIGURE 5** | Boxplots illustrate the null-model-based stochastic ratio of microbial taxonomic composition and functional profile based on Bray-Curtis dissimilarities. The simulated procedure was repeated 999 times with proportional occurrence frequency and richness.

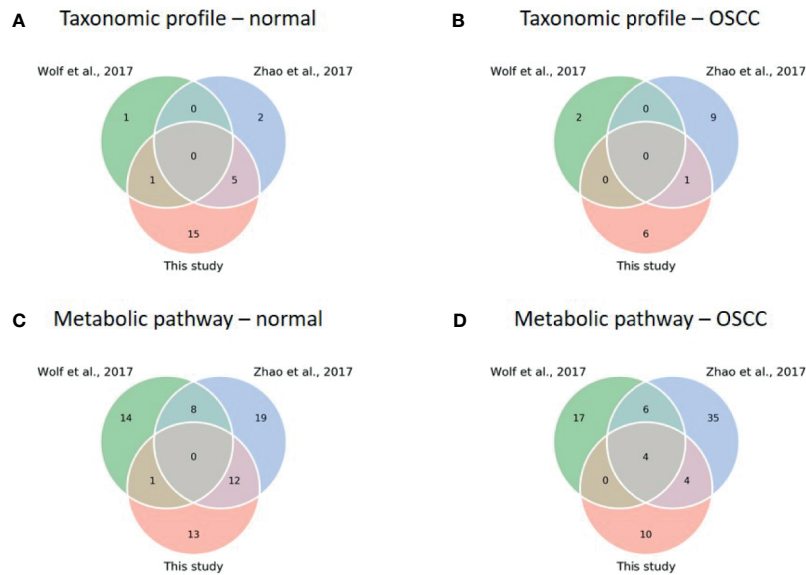


**FIGURE 6** | Comparison of diversity and core analysis between taxonomic and functional profiles from this study and previous studies (Wolf et al., 2017; Zhao et al., 2017). **(A–D)** Venn diagrams reveal common core species/pathways (prevalence > 75%) in normal and OSCC cohorts, respectively. (Taxonomic profiles of normal **(A)** and OSCC **(B)** cohorts; metabolic pathway profiles of normal **(C)** and OSCC **(D)** cohorts).

whereas the potentials of arginine and/or histidine degradation pathways were predicted higher in the OSCC cohort. In addition, two unsaturated fatty acid biosynthesis pathways (cis-vaccenate and gondoate) were abundant in the OSCC group, whereas no common pathway enriched in the cofactor or vitamin biosynthesis category was found. The meta-analysis results generalized our findings that microbiome dysbiosis in OSCC patients was dysregulated by the aforementioned distinctive functions. Because the PICRUSt2 predicted the functionality based on the abundance of the detected taxa, the functionality consequences are thus associated with the collective abundance of the contributing taxa. The family taxa, *Veillonellaceae* and *Actinomycetaceae* for the healthy cohort, and *Flavobacteriaceae* and *Peptostreptococcaceae* for the cancer cohort (**Figure S2**) might contribute to functional variations such as cofactor, prosthetic group, electron carrier, and vitamin biosynthesis, nucleoside and nucleotide biosynthesis, and cell structure biosynthesis (**Table S6**).

### 3.8 Using Functional Profiles Complements Using Taxonomic Data for Microbiome Analysis Among Different Studies

To compare the performance of using taxonomic and functional profiles for predicting the occurrence of oral cancer, we trained random forest models with the profiles separately. The datasets from each study were independently processed in accordance with the analytical process illustrated in **Figure S6**. The mean accuracy ratio (the mean of the ratios of predicted accuracy to the accuracy of random guess, 100 iterations) was higher when using the functional profile than using the taxonomic profile

(**Figure 7A** and **Figure S7**), although statistical significance was only detected in Wolf et al. (2017) ( $t$ -test,  $p = 0.043$ ) and Zhao et al. (2017) ( $t$ -test,  $p = 0.001$ ). Besides, we bootstrapped the receiver-operating characteristic (ROC) analysis 100 times. The area under the receiver operating characteristic curve (AUROC) was higher with functional profiles to distinguish OSCC samples from healthy controls, compared with that using taxonomic profiles (**Figures 7B, C**), suggesting the potential of using the (predicted) functional profiles can complement the use of taxonomic data in detecting the associations of the oral microbiome and health status.

## 4 DISCUSSION

Previous studies have reported that the change of oral microbiome was associated with the influences mixed with oral diseases and risk factors (betel nut chewing, cigarette smoking, and alcohol consumption) (Sampaio-Maia et al., 2016; Wu et al., 2016; Hernandez et al., 2017; Fan et al., 2018; Debelius et al., 2020). In this study, however, by analyzing the saliva from 8-year follow-up cohorts, we found that the OVH carcinogenesis was identified as the main contributor to the altered oral microbiome. The age may be confounding, in particular for the changes in minor taxa in accordance with the significant level achieved by the Adonis analysis with unweighted UniFrac distance. Several studies have reported the association between age and salivary microbiome (Xu et al., 2015; Takeshita et al., 2016; Lira-Junior et al., 2018). This can partly be attributed to the functional decline of the immune system due to natural aging (Feres et al., 2016), and different levels of daily activities and metabolism

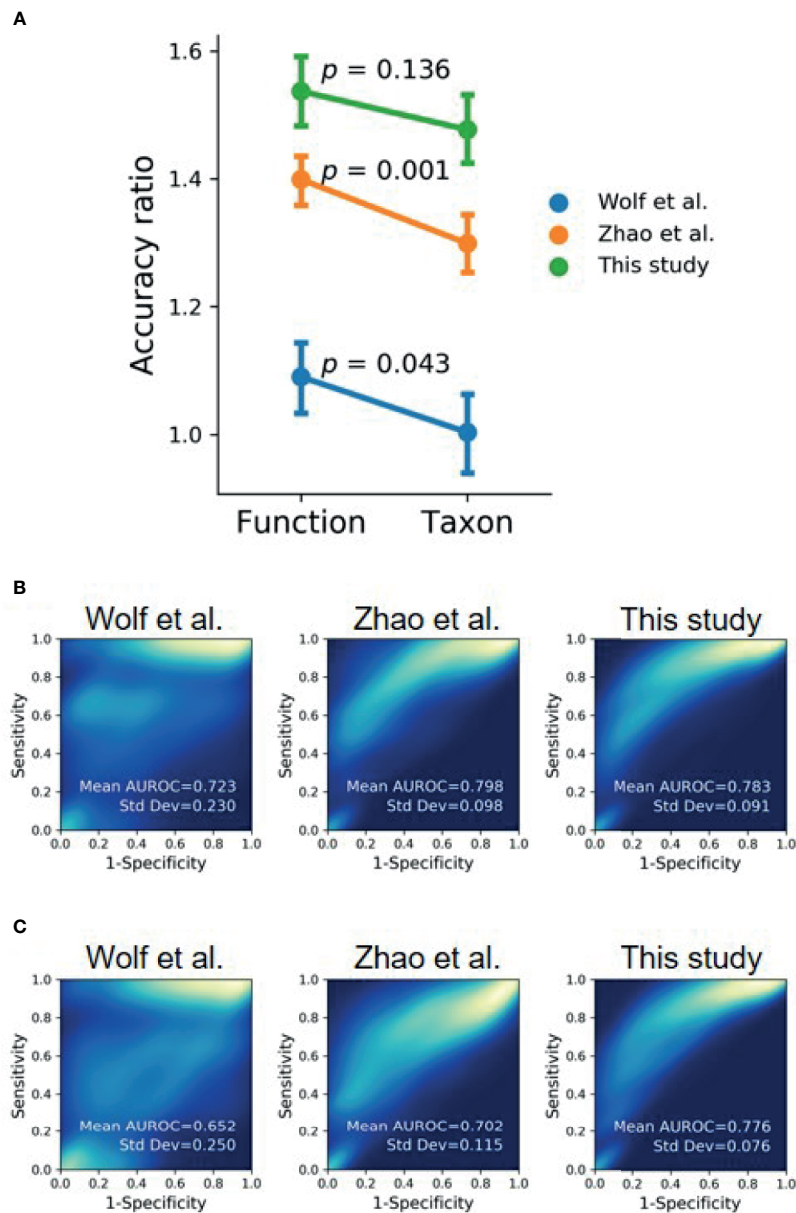


**FIGURE 7** | Evaluating functional profile as an alternative signature for OSCC detection using machine learning with the datasets of this study and previous studies (Wolf et al., 2017; Zhao et al., 2017). **(A)** The mean accuracy ratios of 100 iterations of the randomly split dataset (80% training and 20% testing) were based on taxonomic and functional profiles. The accuracy ratio is defined as the predicted accuracy to the accuracy of a random guess. Vertical bars indicate 95% confidence intervals. **(B, C)** The 2D-density plots of ROC curves from 100 iterations demonstrate a higher mean AUROC using **(B)** functional profiles to distinguish OSCC from normal cohorts compared to that using **(C)** taxonomic profiles.

between younger and elder people (Liu et al., 2020). Although the within-group diversity was not significantly different among cohorts, a decreased trend of core microbiome from healthy or OVH to OSCC was observed when the total diversity of each cohort (gamma diversity) was considered. Consistent with the previous studies that the richness of core species among healthy individuals was 9.6–13.1% (Takeshita et al., 2016; Willis et al., 2018) and it decreased to 5.96% in the OSCC patients with oral submucous fibrosis (Chen et al., 2020), our study also showed the

decrease of richness from 12.53% in the normal cohort to 6.34% in the OSCC cohort. Together, the gamma diversity as an indication reflecting dysbiosis of the core salivary microbiome is effectually linked to the progression of oral cancer.

The altered oral microbiomes might be in part attributed to the host inflammation and immune responses to OPMD and OSCC. In periodontitis, the inflammatory environment was considered to be a source of host-derived nutrients for the microbes and thus altered the microbial community



(Abusleme et al., 2013; Gaffen and Moutsopoulos, 2020). The change of micron-scale habitats in the oral cavity may subsequently alter the microbial composition and its related functional potentials. Common clinical features of OSCC including roughness and hardening of soft tissue, irregular ulcers, and exophytic tumors in the oral cavity (Bagan et al., 2010). The OVH was reported to form slightly elevated plaque-like lesions or protruding masses with the verrucous or papillary surface (Wang et al., 2009). The difference of the “landscape” in the oral cavity influences temperature, moisture, pH, oxygen, and nutrients availability and thus shapes the resident microbiota and, in turn, the neighboring microbes (Mark Welch et al., 2020; Wilbert et al., 2020).

Though we identified several enriched species that were associated with the health status of the oral cavity, the generalizability of these taxa as universal signatures for OSCC was suboptimal (**Figures 6A, B**). The signature taxa specifically related to the health status found in one study were not reported or even exhibited contradictory results to those in another study. For example, *P. melaninogenica*, *S. salivarius*, and *R. mucilaginosa* were highly abundant in patients with OPMD or OSCC (Mager et al., 2005; Pushalkar et al., 2012; Amer et al., 2020), but were identified as signatures for the healthy cohort in our dataset. Perera et al. reported that, at the species level, *Campylobacter concisus*, *Prevotella salivae*, *Prevotella loeschii*, and *Fusobacterium* oral taxon 204 were enriched in OSCC (Perera et al., 2018); however, the first two species were associated with healthy individuals in the present study. The genus *Actinomyces* was linked to tumor development in one study (Mukherjee et al., 2017), but the opposite microbial pattern was identified in another study (Zhao et al., 2017). The lack of consistency between studies could be attributed to the experimental design [e.g., sample types or hypervariable regions of the 16S rRNA gene (Tremblay et al., 2015)], the bioinformatics analysis pipeline [e.g., sequence denoising approaches (Nearing et al., 2018) and reference databases (Knight et al., 2018)], the genetics of studied cohorts [e.g., racial factors (Yang et al., 2019), and the complexity of oral carcinogenesis (Tanaka and Ishigamori, 2011)]. Alternatively, our results suggest that the inconsistencies may be due to the extremely high species turnover, which may be a consequence of the stochastic process (contributing to about 60%; **Figure 5**) in primarily shaping microbial communities in saliva (**Figure 4** and **Figure 5**). In addition to the host selection effect (contributing to about 40%; **Figure 5**), the high microbial species variation can be attributed to diet, lifestyles, hygiene habits, salivary dysfunction, frequent exposure to exogenous bacteria, and rapid changes in environmental factors (Marsh, 2003; Wade, 2013; Grassl et al., 2016; Lamont et al., 2018), eventually leading to high turnover rates of salivary microbiota, regardless of oral health status. Although the identified signature species were consistently related to several distinct family taxa, such as *Veillonellaceae* and *Actinomycetaceae*, in the healthy cohort; *Flavobacteriaceae*, *Peptostreptococcaceae*, and *Lachnospiraceae* in the OSCC cohort, the differential abundance of some signatures (e.g., *Prevotellaceae* and *Carnobacteriaceae*) showed opposite patterns in diseased

versus normal cohorts when compared the previous studies with the meta-analysis in the present study (Zhang et al., 2020; Zhong et al., 2021). Taken together, microbes in saliva are subject to a high population dynamic at the taxonomic level, representing an extraordinarily dynamic ecosystem. Thus, it would be a challenging task to identify universal taxa signatures for OSCC.

The function profiles of saliva microbiomes remained distinguishable, despite the high taxonomic variation and abundance fluctuation in the saliva microbiome. This stable function profile but highly varied species composition in the salivary ecosystem may be likely due to functional redundancy, which has been proposed for other microbial ecosystems like soil and the human gut (Mendes et al., 2015; Vieira-Silva et al., 2016). Unlike the microbial composition, the functional profile is sensitive to the host oral carcinogenesis, as the proportion of driving forces shifted toward the deterministic process (**Figure 5**). This shift of drivers for the functional gene content may also reciprocally affect the primary contribution to the differences in functional profiles (**Figure 4**). Since nestedness reflects the effect of environmental filtering (Chase and Myers, 2011; Daniel et al., 2019), a possible explanation is that the diseased status of the oral cavity (OVH and OSCC) was a more influential environmental filtering factor than the healthy one, leading to the loss/gain of specific metabolic niches and an increase in nestedness components during the shift from healthy to diseased states. As a whole, oral carcinogenesis of OVH does not seem to impact the taxonomic composition but tilts the balance of functional gene content toward the deterministic process, making the functional profiles mirror oral cancer development more meritoriously than the taxonomic composition.

Through the re-analysis of publicly accessible OSCC-associated oral microbiomes datasets, we obtained more consistent results from the functional analysis. Although different hypervariable regions among studies may impact the analysis results to some extent, the advance in novel bioinformatics tool enables meta-analysis among multiple hypervariable regions (Callahan et al., 2017). The consistency can be explained by previous metabolomics studies (Lohavanichbutr et al., 2018; Song et al., 2020), which show dysregulated metabolite profiles in saliva between healthy and OSCC cohorts. Song et al. directly characterized the saliva metabolic profiles of healthy, precancerous, and OSCC cohorts, showing the specific down-regulated metabolites, including spermine, arginine, ornithine, and histidine, and the up-regulated metabolites, including putrescine, cadaverine, thymidine, adenosine, and 5-aminopentanoate, in the OSCC cohort (Song et al., 2020). Several amino acid biosynthesis pathways (isoleucine, tryptophan, arginine, ornithine, valine, and methionine) were enriched in the normal group, particularly in Zhao's and our datasets (**Figure S5**), suggesting potential up-regulation of those amino acids in the healthy cohort (and correspondingly down-regulation in the OSCC cohort), which is consistent with previous studies (Yang et al., 2018). Several previous studies also suggested the dysregulation of ornithine, arginine, and polyamine synthesis in the salivary microbiome during oral carcinogenesis from the

healthy or precancerous stage (Chen et al., 2020; Sharma et al., 2020). In addition, Zhao's and our study showed that the biosynthesis of lipids and fatty acids, especially *cis*-vacenate and gondoate are enriched in the OSCC cohort (Figure 3). In the same line of the observations, the increase of *cis*-vacenate would decrease the production of anti-inflammatory palmitoleic acid (Schirmer et al., 2016), leading to the increase of inflammatory cytokines like TNF- $\alpha$  required for the oral cancer stemness and aggressiveness (Lee et al., 2012; Krishnan et al., 2014). Although gondoate is often found in plants, it can also be anaerobically produced by microbes. Whether gondoate and the microbes responsible for the biosynthesis play any role in oral carcinogenesis remains characterized. The dysregulated metabolisms of amino acids, polyamines, long-chain fatty acids, and corresponding derivatives potentially underline the interplay among host oral carcinogenesis and oral microbiota and their metabolites. However, because the microbiome functions were analyzed with DNA samples through the PICRUSt2 prediction in this study, it is necessary to validate whether the corresponding pathways are expressed differentially in the salivary environments in accordance with the health status using paired DNA and RNA samples. Future studies would be warranted to address the dynamic interactions of the host, oral microbiome and metabolome, and how the microbial-host co-modulation of gene expressions and metabolites relate to the OSCC development.

In several previous studies, machine learning-aided models were trained for disease prediction using taxonomic profiles derived from 16S rRNA genes (Teng et al., 2015; Tremblay et al., 2015; Ai et al., 2017; Xu et al., 2018). Since the saliva microbiome was characterized as a highly dissimilar, high species-turnover, and stochasticity-dominated entity in this study, using taxonomic data as input features for classification and prediction tasks can be suboptimal and study-dependent. The predicted functional profiles from OSCC-associated individuals were reported similar despite the variation of the taxonomic profiles (Al-Hebshi et al., 2019). This study and a recent shotgun metagenomic study (Baker et al., 2021) suggest a high predictive accuracy for the health status using the functional profiles. These results suggest that the use of functional profiles may complement the use of taxa data to study the interplay of oral microbiome and OSCC. One limitation of using predicted functional profiles is the loss of function data attributed to a fraction of microbes without genomic information. This can be improved in the future by incorporating both metagenomics and culturomics to expand the microbiome database (Bilen et al., 2018). Raw sequence sharing, along with completely publicly available metadata, will also enable us to reproduce, compare, and validate results across studies through meta-analysis. This is especially crucial to untangle the roles of microbiomes in the progression from the healthy oral cavity through OPMD to OSCC.

Overall, this study has revealed the altered bacterial community composition with the specific functional dysregulation in saliva during OVH carcinogenesis. From the perspective of microbial ecology, any attempt to discover oral microbial consortia as biomarkers for oral cancer would be a daunting task due to the high taxonomic turnover (i.e., high variance and fluctuation) of the oral ecosystems. Functional gene content is relatively stable but

susceptible to oral carcinogenesis, thus making functional profiles, although obtained by a prediction analysis in this study, a complement to taxa data in reflecting the oral cancer development. The dysregulated pathways identified in this study provided clues to study the interplay of the oral microbiome, metabolites, and oral cancer in the future.

## DATA AVAILABILITY STATEMENT

The datasets presented in this study can be found in online repositories (<https://github.com/mft-lab/OVH-study>). The names of the repository/repositories and accession number(s) can be found below: <https://www.ebi.ac.uk/ena>, PRJEB39064.

## ETHICS STATEMENT

The studies involving human participants were reviewed and approved by Institutional Review Board of Chi Mei Medical Center (IRB No.: 10612-L02). The patients/participants provided their written informed consent to participate in this study.

## AUTHOR CONTRIBUTIONS

J-HW, Y-LC, and L-WW conceived the study. J-HW designed the analysis. W-FC collected and processed the saliva samples. J-WC performed experiments and data analysis. J-WC and J-HW drafted the manuscript. J-HW and L-WW revised the manuscript and edited the final version. All authors contributed to the article and approved the submitted version.

## FUNDING

This study was supported by the Ministry of Science and Technology, Taiwan (grant numbers 107-2321-B-006-007, 108-2321-B-006-010, and 108-2221-E-006 -160 -MY3). The research was supported in part by Higher Education Sprout Project, Ministry of Education to the Headquarters of University Advancement at National Cheng Kung University (NCKU).

## ACKNOWLEDGMENTS

We thank Gina Lee's assistance in sample collection, and Dr. Wei-Yu Chen and Mr. Han-De Chen for technical assistance in the microbiome analysis.

## SUPPLEMENTARY MATERIAL

The Supplementary Material for this article can be found online at: <https://www.frontiersin.org/articles/10.3389/fcimb.2021.663068/full#supplementary-material>

## REFERENCES

- Abusleme, L., Dupuy, A. K., Dutzan, N., Silva, N., Burleson, J. A., Strausbaugh, L. D., et al. (2013). The Subgingival Microbiome in Health and Periodontitis and its Relationship With Community Biomass and Inflammation. *ISME J.* 7, 1016–1025. doi: 10.1038/ismej.2012.174
- Ai, L. Y., Tian, H. Y., Chen, Z. F., Chen, H. M., Xu, J., and Fang, J. Y. (2017). Systematic Evaluation of Supervised Classifiers for Fecal Microbiota-Based Prediction of Colorectal Cancer. *Oncotarget* 8, 9546–9556. doi: 10.18632/oncotarget.14488
- Al-Hebshi, N. N., Borgnakke, W. S., and Johnson, N. W. (2019). The Microbiome of Oral Squamous Cell Carcinomas: A Functional Perspective. *Curr. Oral Health Rep.* 6, 145–160. doi: 10.1007/s40496-019-0215-5
- Amer, A., Whelan, A., Al-Hebshi, N. N., Healy, C. M., and Moran, G. P. (2020). Acetaldehyde Production by *Rothia Mucilaginosa* Isolates From Patients With Oral Leukoplakia. *J. Oral. Microbiol.* 12, 1743066. doi: 10.1080/20002297.2020.1743066
- Bagan, J., Sarrion, G., and Jimenez, Y. (2010). Oral Cancer: Clinical Features. *Oral Oncol.* 46, 414–417. doi: 10.1016/j.oraloncology.2010.03.009
- Baker, J. L., Morton, J. T., Dinis, M., Alvarez, R., Tran, N. C., Knight, R., et al. (2021). Deep Metagenomics Examines the Oral Microbiome During Dental Caries, Revealing Novel Taxa and Co-Occurrences With Host Molecules. *Genome Res.* 31, 64–74. doi: 10.1101/gr.265645.120
- Barbera, P., Kozlov, A. M., Czech, L., Morel, B., Darriba, D., Flouri, T., et al. (2018). EPA-NG: Massively Parallel Evolutionary Placement of Genetic Sequences. *Systematic Biol.* 68, 365–369. doi: 10.1093/sysbio/syy054
- Baselga, A. (2010). Partitioning the Turnover and Nestedness Components of Beta Diversity. *Global Ecol. Biogeography* 19, 134–143. doi: 10.1111/j.1466-8238.2009.00490.x
- Bilen, M., Dufour, J. C., Lagier, J. C., Cadoret, F., Daoud, Z., Dubourg, G., et al. (2018). The Contribution of Culturomics to the Repertoire of Isolated Human Bacterial and Archaeal Species. *Microbiome* 6, 94. doi: 10.1186/s40168-018-0485-5
- Bokulich, N. A., Dillon, M. R., Bolyen, E., Kaehler, B. D., Huttley, G. A., and Caporaso, J. G. (2018a). Q2-Sample-Classifer: Machine-Learning Tools for Microbiome Classification and Regression. *J. Open Res. Software* 3, 934. doi: 10.21105/joss.00934
- Bokulich, N. A., Kaehler, B. D., Rideout, J. R., Dillon, M., Bolyen, E., Knight, R., et al. (2018b). Optimizing Taxonomic Classification of Marker-Gene Amplicon Sequences With QIIME 2's Q2-Feature-Classifer Plugin. *Microbiome* 6, 90. doi: 10.1186/s40168-018-0470-z
- Bolyen, E., Rideout, J. R., Dillon, M. R., Bokulich, N., Abnet, C. C., Al-Ghalith, G. A., et al. (2019). Reproducible, Interactive, Scalable and Extensible Microbiome Data Science Using QIIME 2. *Nat. Biotechnol.* 37, 852–857. doi: 10.1038/s41587-019-0209-9
- Callahan, B. J., McMurdie, P. J., and Holmes, S. P. (2017). Exact Sequence Variants Should Replace Operational Taxonomic Units in Marker-Gene Data Analysis. *ISME J.* 11, 2639–2643. doi: 10.1038/ismej.2017.119
- Callahan, B. J., McMurdie, P. J., Rosen, M. J., Han, A. W., Johnson, A. J. A., and Holmes, S. P. (2016). DADA2: High-Resolution Sample Inference From Illumina Amplicon Data. *Nat. Methods* 13, 581–583. doi: 10.1038/Nmeth.3869
- Caspi, R., Billington, R., Keseler, I. M., Kothari, A., Krummenacker, M., Midford, P. E., et al. (2020). The MetaCyc Database of Metabolic Pathways and Enzymes - a 2019 Update. *Nucleic Acids Res.* 48, D445–D453. doi: 10.1093/nar/gkz862
- Chase, J. M., and Myers, J. A. (2011). Disentangling the Importance of Ecological Niches From Stochastic Processes Across Scales. *Philos. Trans. R. Soc. Lond. B. Biol. Sci.* 366, 2351–2363. doi: 10.1098/rstb.2011.0063
- Chen, M. Y., Chen, J. W., Wu, L. W., Huang, K. C., Chen, J. Y., Wu, W. S., et al. (2021). Carcinogenesis of Male Oral Submucous Fibrosis Alters Salivary Microbiomes. *J. Dent. Res.* 100, 397–405. doi: 10.1177/0022034520968750
- Chen, W.-Y., Ng, T. H., Wu, J.-H., Chen, J.-W., and Wang, H.-C. (2017). Microbiome Dynamics in a Shrimp Grow-Out Pond With Possible Outbreak of Acute Hepatopancreatic Necrosis Disease. *Sci. Rep.* 7, 9395. doi: 10.1038/s41598-017-09923-6
- Chiang, W. F., Liu, S. Y., Lin, J. F., Chiu, S. F., Gou, S. B., Chiou, C. T., et al. (2020). Malignant Development in Patients With Oral Potentially Malignant Disorders Detected Through Nationwide Screening: Outcomes of 5-Year Follow-Up at a Single Hospital. *Head Neck* 42, 67–76. doi: 10.1002/hed.25973
- Costalonga, M., and Herzberg, M. C. (2014). The Oral Microbiome and the Immunobiology of Periodontal Disease and Caries. *Immunol. Lett.* 162, 22–38. doi: 10.1016/j.imlet.2014.08.017
- Czech, L., and Stamatakis, A. (2019). Scalable Methods for Analyzing and Visualizing Phylogenetic Placement of Metagenomic Samples. *PLoS One* 14, e0217050. doi: 10.1371/journal.pone.0217050
- Daniel, J., Gleason, J. E., Cottenie, K., and Rooney, R. C. (2019). Stochastic and Deterministic Processes Drive Wetland Community Assembly Across a Gradient of Environmental Filtering. *Oikos* 128, 1158–1169. doi: 10.1111/oik.05987
- Debelius, J. W., Huang, T. T., Cai, Y. L., Ploner, A., Barrett, D., Zhou, X. Y., et al. (2020). Subspecies Niche Specialization in the Oral Microbiome is Associated With Nasopharyngeal Carcinoma Risk. *mSystems* 5, e00065–20. doi: 10.1128/mSystems.00065-20
- Douglas, G. M., Maffei, V. J., Zaneveld, J. R., Yurgel, S. N., Brown, J. R., Taylor, C. M., et al. (2020). PICRUSt2 for Prediction of Metagenome Functions. *Nat. Biotechnol.* 38, 685–688. doi: 10.1038/s41587-020-0548-6
- Eddy, S. R. (2011). Accelerated Profile HMM Searches. *PLoS Comput. Biol.* 7, e1002195. doi: 10.1371/journal.pcbi.1002195
- Eisen, D. (2002). Brush Biopsy 'Saves Lives'. *J. Am. Dent. Assoc.* 133, 668–692. doi: 10.14219/jada.archive.2002.0249. 688, 690, 692.
- Escapa, I. F., Chen, T., Huang, Y., Gajare, P., Dewhirst, F. E., and Lemon, K. P. (2018). New Insights Into Human Nostril Microbiome From the Expanded Human Oral Microbiome Database (eHOMD): A Resource for the Microbiome of the Human Aerodigestive Tract. *mSystems* 3, e00187–18. doi: 10.1128/mSystems.00187-18
- Fan, X. Z., Peters, B. A., Jacobs, E. J., Gapstur, S. M., Purdue, M. P., Freedman, N. D., et al. (2018). Drinking Alcohol is Associated With Variation in the Human Oral Microbiome in a Large Study of American Adults. *Microbiome* 6, 59. doi: 10.1186/s40168-018-0448-x
- Farah, C., Michel, L. Y. M., and Balligand, J. L. (2018). Nitric Oxide Signalling in Cardiovascular Health and Disease. *Nat. Rev. Cardiol.* 15, 292–316. doi: 10.1038/nrcardio.2017.224
- Feres, M., Teles, F., Teles, R., Figueiredo, L. C., and Faveri, M. (2016). The Subgingival Periodontal Microbiota of the Aging Mouth. *Periodontol.* 2000 72, 30–53. doi: 10.1111/prd.12136
- Ferlay, J., Colombet, M., Soerjomataram, I., Mathers, C., Parkin, D. M., Pineros, M., et al. (2019). Estimating the Global Cancer Incidence and Mortality in 2018: GLOBOCAN Sources and Methods. *Int. J. Cancer* 144, 1941–1953. doi: 10.1002/ijc.31937
- Gaffen, S. L., and Moutsopoulos, N. M. (2020). Regulation of Host-Microbe Interactions at Oral Mucosal Barriers by Type 17 Immunity. *Sci. Immunol.* 5, eaau4594. doi: 10.1126/sciimmunol.aau4594
- Gao, L., Xu, T. S., Huang, G., Jiang, S., Gu, Y., and Chen, F. (2018). Oral Microbiomes: More and More Importance in Oral Cavity and Whole Body. *Protein Cell.* 9, 488–500. doi: 10.1007/s13238-018-0548-1
- Gotelli, N. J. (2000). Null Model Analysis of Species Co-Occurrence Patterns. *Ecology* 81, 2606–2621. doi: 10.1890/0012-9658(2000)081[2606:NMAOSC]2.0.CO;2
- Govoni, M., Jansson, E. A., Weitzberg, E., and Lundberg, J. O. (2008). The Increase in Plasma Nitrite After a Dietary Nitrate Load is Markedly Attenuated by an Antibacterial Mouthwash. *Nitric. Oxide* 19, 333–337. doi: 10.1016/j.niox.2008.08.003
- Grassl, N., Kulak, N. A., Pichler, G., Geyer, P. E., Jung, J., Schubert, S., et al. (2016). Ultra-Deep and Quantitative Saliva Proteome Reveals Dynamics of the Oral Microbiome. *Genome Med.* 8, 44. doi: 10.1186/s13073-016-0293-0
- Hashimoto, K., Shimizu, D., Hirabayashi, S., Ueda, S., Miyabe, S., Oh-Iwa, I., et al. (2019). Changes in Oral Microbial Profiles Associated With Oral Squamous Cell Carcinoma vs Leukoplakia. *J. Investig. Clin. Dent.* 10, e12445. doi: 10.1111/jicd.12445
- Hernandez, B. Y., Zhu, X. M., Goodman, M. T., Gatewood, R., Mendiola, P., Quinata, K., et al. (2017). Betel Nut Chewing, Oral Premalignant Lesions, and the Oral Microbiome. *PLoS One* 12, e0172196. doi: 10.1371/journal.pone.0172196
- Janssen, S., McDonald, D., Gonzalez, A., Navas-Molina, J. A., Jiang, L., Xu, Z. Z., et al. (2018). Phylogenetic Placement of Exact Amplicon Sequences Improves Associations With Clinical Information. *mSystems* 3, e00021–18. doi: 10.1128/mSystems.00021-18



- Kamarajan, P., Ateia, I., Shin, J. M., Fenno, J. C., Le, C., Zhan, L., et al. (2020). Periodontal Pathogens Promote Cancer Aggressivity via TLR/MyD88 Triggered Activation of Integrin/FAK Signaling That is Therapeutically Reversible by a Probiotic Bacteriocin. *PLoS Pathogens* 16, e1008881. doi: 10.1371/journal.ppat.1008881
- Katz, J., Onate, M. D., Pauley, K. M., Bhattacharyya, I., and Cha, S. (2011). Presence of Porphyromonas Gingivalis in Gingival Squamous Cell Carcinoma. *Int. J. Oral. Sci.* 3, 209–215. doi: 10.4248/IJOS11075
- Kaur, J., Jacobs, R., Huang, Y., Salvo, N., and Politis, C. (2018). Salivary Biomarkers for Oral Cancer and Pre-Cancer Screening: A Review. *Clin. Oral. Investig.* 22, 633–640. doi: 10.1007/s00784-018-2337-x
- Kilian, M., Chapple, I. L., Hannig, M., Marsh, P. D., Meuric, V., Pedersen, A. M., et al. (2016). The Oral Microbiome - an Update for Oral Healthcare Professionals. *Br. Dent. J.* 221, 657–666. doi: 10.1038/sj.bdj.2016.865
- Knight, R., Vrbanc, A., Taylor, B. C., Aksenov, A., Callewaert, C., Debelius, J., et al. (2018). Best Practices for Analysing Microbiomes. *Nat. Rev. Microbiol.* 16, 410–422. doi: 10.1038/s41579-018-0029-9
- Kreth, J., Merritt, J., Shi, W., and Qi, F. (2005). Competition and Coexistence Between Streptococcus Mutans and Streptococcus Sanguinis in the Dental Biofilm. *J. Bacteriol.* 187, 7193–7203. doi: 10.1128/JB.187.21.7193-7203.2005
- Krishnan, R., Thayalan, D. K., Padmanaban, R., Ramadas, R., Annasamy, R. K., and Anandan, N. (2014). Association of Serum and Salivary Tumor Necrosis Factor-Alpha With Histological Grading in Oral Cancer and its Role in Differentiating Premalignant and Malignant Oral Disease. *Asian Pac. J. Cancer Prev.* 15, 7141–7148. doi: 10.7314/APJCP.2014.15.17.7141
- Lamont, R. J., Koo, H., and Hajishengallis, G. (2018). The Oral Microbiota: Dynamic Communities and Host Interactions. *Nat. Rev. Microbiol.* 16, 745–759. doi: 10.1038/s41579-018-0089-x
- Langille, M. G. I., Zaneveld, J., Caporaso, J. G., McDonald, D., Knights, D., Reyes, J. A., et al. (2013). Predictive Functional Profiling of Microbial Communities Using 16S rRNA Marker Gene Sequences. *Nat. Biotechnol.* 31, 814–821. doi: 10.1038/nbt.2676
- Lee, W.-H., Chen, H.-M., Yang, S.-F., Liang, C., Peng, C.-Y., Lin, F.-M., et al. (2017). Bacterial Alterations in Salivary Microbiota and Their Association in Oral Cancer. *Sci. Rep.* 7, 1–11. doi: 10.1038/s41598-017-16418-x
- Lee, S. H., Hong, H. S., Liu, Z. X., Kim, R. H., Kang, M. K., Park, N. H., et al. (2012). TNFalpha Enhances Cancer Stem Cell-Like Phenotype via Notch-Hes1 Activation in Oral Squamous Cell Carcinoma Cells. *Biochem. Biophys. Res. Commun.* 424, 58–64. doi: 10.1016/j.bbrc.2012.06.065
- Lingen, M. W., Kalmr, J. R., Karrison, T., and Speight, P. M. (2008). Critical Evaluation of Diagnostic Aids for the Detection of Oral Cancer. *Oral. Oncol.* 44, 10–22. doi: 10.1016/j.oraloncology.2007.06.011
- Lin, W. J., Jiang, R. S., Wu, S. H., Chen, F. J., and Liu, S. A. (2011). Smoking, Alcohol, and Betel Quid and Oral Cancer: A Prospective Cohort Study. *J. Oncol.* 2011:525976. doi: 10.1155/2011/525976
- Lira-Junior, R., Akerman, S., Klinge, B., Bostrom, E. A., and Gustafsson, A. (2018). Salivary Microbial Profiles in Relation to Age, Periodontal, and Systemic Diseases. *PLoS One* 13, e0189374. doi: 10.1371/journal.pone.0189374
- Liu, S., Wang, Y., Zhao, L., Sun, X., and Feng, Q. (2020). Microbiome Succession With Increasing Age in Three Oral Sites. *Aging (Albany NY)* 12, 7874–7907. doi: 10.18632/aging.103108
- Lohavanichbutr, P., Zhang, Y. Z., Wang, P., Gu, H. W., Gowda, G. A. N., Djukovic, D., et al. (2018). Salivary Metabolite Profiling Distinguishes Patients With Oral Cavity Squamous Cell Carcinoma From Normal Controls. *PLoS One* 13, e0204249. doi: 10.1371/journal.pone.0204249
- Louca, S., and Doebeli, M. (2017). Efficient Comparative Phylogenetics on Large Trees. *Bioinformatics* 34, 1053–1055. doi: 10.1093/bioinformatics/btx701
- Mager, D. L., Haffajee, A. D., Devlin, P. M., Norris, C. M., Posner, M. R., and Goodson, J. M. (2005). The Salivary Microbiota as a Diagnostic Indicator of Oral Cancer: A Descriptive, Non-Randomized Study of Cancer-Free and Oral Squamous Cell Carcinoma Subjects. *J. Transl. Med.* 3, 27. doi: 10.1186/1479-5876-3-27
- Markopoulos, A. K. (2012). Current Aspects on Oral Squamous Cell Carcinoma. *Open Dent. J.* 6, 126–130. doi: 10.2174/1874210601206010126
- Mark Welch, J. L., Ramirez-Puebla, S. T., and Borisy, G. G. (2020). Oral Microbiome Geography: Micron-Scale Habitat and Niche. *Cell Host Microbe* 28, 160–168. doi: 10.1016/j.chom.2020.07.009
- Marsh, P. D. (2003). Are Dental Diseases Examples of Ecological Catastrophes? *Microbiology-Sgm* 149, 279–294. doi: 10.1099/mic.0.26082-0
- Marsh, P. D. (2018). In Sickness and in Health-What Does the Oral Microbiome Mean to Us? An Ecological Perspective. *Adv. Dent. Res.* 29, 60–65. doi: 10.1177/0022034517735295
- Mashberg, A. (1983). Final Evaluation of Tolonium Chloride Rinse for Screening of High-Risk Patients With Asymptomatic Squamous Carcinoma. *J. Am. Dent. Assoc.* 106, 319–323. doi: 10.14219/jada.archive.1983.0063
- Mashberg, A. (2000). Diagnosis of Early Oral and Oropharyngeal Squamous Carcinoma: Obstacles and Their Amelioration. *Oral. Oncol.* 36, 253–255. doi: 10.1016/s1368-8375(00)00006-3
- Matsen, F. A., Hoffman, N. G., Gallagher, A., and Stamatakis, A. (2012). A Format for Phylogenetic Placements. *PLoS One* 7, e31009. doi: 10.1371/journal.pone.0031009
- Matsen, F. A., Kodner, R. B., and Armbrust, E. V. (2010). Pplacer: Linear Time Maximum-Likelihood and Bayesian Phylogenetic Placement of Sequences Onto a Fixed Reference Tree. *BMC Bioinf.* 11, 538. doi: 10.1186/1471-2105-11-538
- Mendes, L. W., Tsai, S. M., Navarrete, A. A., de Hollander, M., van Veen, J. A., and Kuramae, E. E. (2015). Soil-Borne Microbiome: Linking Diversity to Function. *Microbial. Ecol.* 70, 255–265. doi: 10.1007/s00248-014-0559-2
- Mukherjee, C., Beall, C. J., Griffen, A. L., and Leys, E. J. (2018). High-Resolution ISR Amplicon Sequencing Reveals Personalized Oral Microbiome. *Microbiome* 6, 153. doi: 10.1186/s40168-018-0535-z
- Mukherjee, P. K., Wang, H., Retuerto, M., Zhang, H., Burkey, B., Ghannoum, M. A., et al. (2017). Bacteriome and Mycobiome Associations in Oral Tongue Cancer. *Oncotarget* 8, 97273–97289. doi: 10.18632/oncotarget.21921
- Nearing, J. T., Douglas, G. M., Comeau, A. M., and Langille, M. G. I. (2018). Denoising the Denoisers: An Independent Evaluation of Microbiome Sequence Error-Correction Approaches. *PeerJ* 6, e5364. doi: 10.7717/peerj.5364
- Ning, D. L., Deng, Y., Tiedje, J. M., and Zhou, J. Z. (2019). A General Framework for Quantitatively Assessing Ecological Stochasticity. *Proc. Natl. Acad. Sci. USA* 116, 16892–16898. doi: 10.1073/pnas.1904623116
- Pedregosa, F., Varoquaux, G., Gramfort, A., Michel, V., Thirion, B., Grisel, O., et al. (2011). Scikit-Learn: Machine Learning in Python. *J. Mach. Learn. Res.* 12, 2825–2830.
- Perera, M., Al-Hebshi, N. N., Perera, I., Ipe, D., Ulett, G. C., Speicher, D. J., et al. (2018). Inflammatory Bacteriome and Oral Squamous Cell Carcinoma. *J. Dent. Res.* 97, 725–732. doi: 10.1177/0022034518767118
- Pushalkar, S., Ji, X., Li, Y., Estilo, C., Yegnanarayana, R., Singh, B., et al. (2012). Comparison of Oral Microbiota in Tumor and Non-Tumor Tissues of Patients With Oral Squamous Cell Carcinoma. *BMC Microbiol.* 12, 144. doi: 10.1186/1471-2180-12-144
- Richards, V. P., Alvarez, A. J., Luce, A. R., Bedenbaugh, M., Mitchell, M. L., Burne, R. A., et al. (2017). Microbiomes of Site-Specific Dental Plaques From Children With Different Caries Status. *Infect. Immun.* 85, e00106–17. doi: 10.1128/IAI.00106-17
- Sampaio-Maia, B., Caldas, I. M., Pereira, M. L., Perez-Mongiovi, D., and Araujo, R. (2016). The Oral Microbiome in Health and its Implication in Oral and Systemic Diseases. *Adv. Appl. Microbiol.* 97, 171–210. doi: 10.1016/b.s.aambs.2016.08.002
- Schirmer, M., Smekens, S. P., Vlamakis, H., Jaeger, M., Oosting, M., Franzosa, E. A., et al. (2016). Linking the Human Gut Microbiome to Inflammatory Cytokine Production Capacity. *Cell* 167, 1125–1136.e8. doi: 10.1016/j.cell.2016.11.046
- Seabold, S., and Perktold, J. (2010). Statsmodels: Econometric and Statistical Modeling With Python. In *Proceedings of the 9th Python in Science Conference*. 92–96. doi: 10.25080/Majora-92b1f922-011
- Segata, N., Izard, J., Waldron, L., Gevers, D., Miropolsky, L., Garrett, W. S., et al. (2011). Metagenomic Biomarker Discovery and Explanation. *Genome Biol.* 12, R60. doi: 10.1186/gb-2011-12-6-r60
- Sepich-Poore, G. D., Zitvogel, L., Straussman, R., Hasty, J., Wargo, J. A., and Knight, R. (2021). The Microbiome and Human Cancer. *Science* 371, eabc4552. doi: 10.1126/science.abc4552
- Sharma, A. K., DeBusk, W. T., Stepanov, I., Gomez, A., and Khariwala, S. S. (2020). Oral Microbiome Profiling in Smokers With and Without Head and Neck Cancer Reveals Variations Between Health and Disease. *Cancer Prev. Res.* 13, 463–474. doi: 10.1158/1940-6207.Capr-19-0459

- Socransky, S. S., and Haffajee, A. D. (2005). Periodontal Microbial Ecology. *Periodontol.* 2000 38, 135–187. doi: 10.1111/j.1600-0757.2005.00107.x
- Song, X. W., Yang, X. H., Narayanan, R., Shankar, V., Ethiraj, S., Wang, X., et al. (2020). Oral Squamous Cell Carcinoma Diagnosed From Saliva Metabolic Profiling. *Proc. Natl. Acad. Sci. USA* 117, 16167–16173. doi: 10.1073/pnas.2001395117
- Stashenko, P., Yost, S., Choi, Y., Danciu, T., Chen, T., Yoganathan, S., et al. (2019). The Oral Mouse Microbiome Promotes Tumorigenesis in Oral Squamous Cell Carcinoma. *mSystems* 4, e00323–19. doi: 10.1128/mSystems.00323-19
- Stegen, J. C., Freestone, A. L., Crist, T. O., Anderson, M. J., Chase, J. M., Comita, L. S., et al. (2013). Stochastic and Deterministic Drivers of Spatial and Temporal Turnover in Breeding Bird Communities. *Global Ecol. Biogeography* 22, 202–212. doi: 10.1111/j.1466-8238.2012.00780.x
- Takeshita, T., Kageyama, S., Furuta, M., Tsuboi, H., Takeuchi, K., Shibata, Y., et al. (2016). Bacterial Diversity in Saliva and Oral Health-Related Conditions: The Hisayama Study. *Sci. Rep.* 6, 22164. doi: 10.1038/srep22164
- Tanaka, T., and Ishigamori, R. (2011). Understanding Carcinogenesis for Fighting Oral Cancer. *J. Oncol.* 2011:603740. doi: 10.1155/2011/603740
- Teng, F., Yang, F., Huang, S., Bo, C. P., Xu, Z. Z., Amir, A., et al. (2015). Prediction of Early Childhood Caries via Spatial-Temporal Variations of Oral Microbiota. *Cell Host Microbe* 18, 296–306. doi: 10.1016/j.chom.2015.08.005
- Tremblay, J., Singh, K., Fern, A., Kirton, E. S., He, S. M., Woyke, T., et al. (2015). Primer and Platform Effects on 16S rRNA Tag Sequencing. *Front. Microbiol.* 6, 771. doi: 10.3389/fmicb.2015.00771
- Vieira-Silva, S., Falony, G., Darzi, Y., Lima-Mendez, G., Yunta, R. G., Okuda, S., et al. (2016). Species-Function Relationships Shape Ecological Properties of the Human Gut Microbiome. *Nat. Microbiol.* 1, 16088. doi: 10.1038/nmicrobiol.2016.88
- Wade, W. G. (2013). The Oral Microbiome in Health and Disease. *Pharmacol. Res.* 69, 137–143. doi: 10.1016/j.phrs.2012.11.006
- Wang, Y. P., Chen, H. M., Kuo, R. C., Yu, C. H., Sun, A., Liu, B. Y., et al. (2009). Oral Verrucous Hyperplasia: Histologic Classification, Prognosis, and Clinical Implications. *J. Oral. Pathol. Med.* 38, 651–656. doi: 10.1111/j.1600-0714.2009.00790.x
- Warnakulasuriya, S. (2020). Oral Potentially Malignant Disorders: A Comprehensive Review on Clinical Aspects and Management. *Oral. Oncol.* 102, 104550. doi: 10.1016/j.oraloncology.2019.104550
- Wescombe, P. A., Heng, N. C., Burton, J. P., Chilcott, C. N., and Tagg, J. R. (2009). Streptococcal Bacteriocins and the Case for Streptococcus Salivarius as Model Oral Probiotics. *Future Microbiol.* 4, 819–835. doi: 10.2217/fmb.09.61
- Wilbert, S. A., Mark Welch, J. L., and Borisy, G. G. (2020). Spatial Ecology of the Human Tongue Dorsum Microbiome. *Cell Rep.* 30, 4003–4015.e3. doi: 10.1016/j.celrep.2020.02.097
- Willis, J. R., Gonzalez-Torres, P., Pitts, A. A., Bejarano, L. A., Cozzuto, L., Andreu-Somavilla, N., et al. (2018). Citizen Science Charts Two Major “Stomatotypes” in the Oral Microbiome of Adolescents and Reveals Links With Habits and Drinking Water Composition. *Microbiome* 6, 218. doi: 10.1186/s40168-018-0592-3
- Wolf, A., Moissl-Eichinger, C., Perras, A., Koskinen, K., Tomazic, P. V., and Thurnher, D. (2017). The Salivary Microbiome as an Indicator of Carcinogenesis in Patients With Oropharyngeal Squamous Cell Carcinoma: A Pilot Study. *Sci. Rep.* 7, 5867. doi: 10.1038/s41598-017-06361-2
- Wu, J., Peters, B. A., Dominianni, C., Zhang, Y. L., Pei, Z. H., Yang, L. Y., et al. (2016). Cigarette Smoking and the Oral Microbiome in a Large Study of American Adults. *Isme J.* 10, 2435–2446. doi: 10.1038/ismej.2016.37
- Xu, X., He, J., Xue, J., Wang, Y., Li, K., Zhang, K., et al. (2015). Oral Cavity Contains Distinct Niches With Dynamic Microbial Communities. *Environ. Microbiol.* 17, 699–710. doi: 10.1111/1462-2920.12502
- Xu, H., Tian, J., Hao, W. J., Zhang, Q., Zhou, Q., Shi, W. H., et al. (2018). Oral Microbiome Shifts From Caries-Free to Caries-Affected Status in 3-Year-Old Chinese Children: A Longitudinal Study. *Front. Microbiol.* 9, 2009. doi: 10.3389/fmicb.2018.02009
- Yang, C. Y., Yeh, Y. M., Yu, H. Y., Chin, C. Y., Hsu, C. W., Liu, H., et al. (2018). Oral Microbiota Community Dynamics Associated With Oral Squamous Cell Carcinoma Staging. *Front. Microbiol.* 9, 862. doi: 10.3389/fmicb.2018.00862
- Yang, Y. H., Zheng, W., Cai, Q. Y., Shrubsole, M. J., Pei, Z. H., Brucker, R., et al. (2019). Racial Differences in the Oral Microbiome: Data From Low-Income Populations of African Ancestry and European Ancestry. *mSystems* 4, e00323–19. doi: 10.1128/mSystems.00639-19
- Ye, Y., and Doak, T. G. (2009). A Parsimony Approach to Biological Pathway Reconstruction/Inference for Genomes and Metagenomes. *PLoS Comput. Biol.* 5, e1000465. doi: 10.1371/journal.pcbi.1000465
- Zaneveld, J. R., McMinds, R., and Thurber, R. V. (2017). Stress and Stability: Applying the Anna Karenina Principle to Animal Microbiomes. *Nat. Microbiol.* 2, 17121. doi: 10.1038/nmicrobiol.2017.121
- Zhang, L., Liu, Y., Zheng, H. J., and Zhang, C. P. (2020). The Oral Microbiota may Have Influence on Oral Cancer. *Front. Cell. Infection Microbiol.* 9, 476. doi: 10.3389/fcimb.2019.00476
- Zhao, H. S., Chu, M., Huang, Z. W., Yang, X., Ran, S. J., Hu, B., et al. (2017). Variations in Oral Microbiota Associated With Oral Cancer. *Sci. Rep.* 7, 11773. doi: 10.1038/s41598-017-11779-9
- Zhong, X., Lu, Q., Zhang, Q., He, Y., Wei, W., and Wang, Y. (2021). Oral Microbiota Alteration Associated With Oral Cancer and Areca Chewing. *Oral. Dis.* 27, 226–239. doi: 10.1111/odi.13545
- Zhou, J. Z., and Ning, D. L. (2017). Stochastic Community Assembly: Does it Matter in Microbial Ecology? *Microbiol. Mol. Biol. Rev.* 81, e00002–17. doi: 10.1128/MMBR.00002-17

**Conflict of Interest:** The authors declare that the research was conducted in the absence of any commercial or financial relationships that could be construed as a potential conflict of interest.

**Publisher's Note:** All claims expressed in this article are solely those of the authors and do not necessarily represent those of their affiliated organizations, or those of the publisher, the editors and the reviewers. Any product that may be evaluated in this article, or claim that may be made by its manufacturer, is not guaranteed or endorsed by the publisher.

Copyright © 2021 Chen, Wu, Chiang, Chen, Wu and Wu. This is an open-access article distributed under the terms of the Creative Commons Attribution License (CC BY). The use, distribution or reproduction in other forums is permitted, provided the original author(s) and the copyright owner(s) are credited and that the original publication in this journal is cited, in accordance with accepted academic practice. No use, distribution or reproduction is permitted which does not comply with these terms.





# Oral Osteomicrobiology: The Role of Oral Microbiota in Alveolar Bone Homeostasis

Xingqun Cheng, Xuedong Zhou, Chengcheng Liu\* and Xin Xu\*

State Key Laboratory of Oral Diseases, National Clinical Research Center for Oral Diseases, West China Hospital of Stomatology, Sichuan University, Chengdu, China

## OPEN ACCESS

### Edited by:

Yolanda López-Vidal,  
Universidad Nacional Autónoma de  
México, Mexico

### Reviewed by:

J. Christopher Fenno,  
University of Michigan, United States  
Joseph Selvin,  
Pondicherry University, India

### \*Correspondence:

Chengcheng Liu  
liuchengcheng519@163.com  
Xin Xu  
xin.xu@scu.edu.cn

### Specialty section:

This article was submitted to  
Microbiome in Health and Disease,  
a section of the journal  
Frontiers in Cellular and Infection  
Microbiology

**Received:** 01 August 2021

**Accepted:** 29 October 2021

**Published:** 17 November 2021

### Citation:

Cheng X, Zhou X, Liu C and Xu X  
(2021) Oral Osteomicrobiology:  
The Role of Oral Microbiota in  
Alveolar Bone Homeostasis.  
*Front. Cell. Infect. Microbiol.* 11:751503.  
doi: 10.3389/fcimb.2021.751503

Osteomicrobiology is a new research field in which the aim is to explore the role of microbiota in bone homeostasis. The alveolar bone is that part of the maxilla and mandible that supports the teeth. It is now evident that naturally occurring alveolar bone loss is considerably stunted in germ-free mice compared with specific-pathogen-free mice. Recently, the roles of oral microbiota in modulating host defense systems and alveolar bone homeostasis have attracted increasing attention. Moreover, the mechanistic understanding of oral microbiota in mediating alveolar bone remodeling processes is undergoing rapid progress due to the advancement in technology. In this review, to provide insight into the role of oral microbiota in alveolar bone homeostasis, we introduced the term “oral osteomicrobiology.” We discussed regulation of alveolar bone development and bone loss by oral microbiota under physiological and pathological conditions. We also focused on the signaling pathways involved in oral osteomicrobiology and discussed the bridging role of osteoimmunity and influencing factors in this process. Finally, the critical techniques for osteomicrobiological investigations were introduced.

**Keywords:** oral microbiota, alveolar bone, osteomicrobiology, osteoimmunology, RANKL signaling, Notch signaling, Wnt signaling, synthetic microbial community

## 1 INTRODUCTION

Humans are inhabited by a diverse milieu of microorganisms, referred to as the commensal microbiota. They mostly reside in five body regions: the gut, oral cavity, skin, nose, and vagina, and are essential for human development, nutrition, and immune status. Accumulating evidence has indicated a close connection between the commensal microbiota and bone health. In 2012, Sjögren et al. demonstrated an increased bone mass in germ-free (GF) mice compared to controls raised in conventional conditions. This phenotype was reversed by colonization with gut flora from conventionally raised mice, providing evidence that the results were not due to innate abnormalities of the GF mice (Sjögren et al., 2012). That was the first report to suggest that the gut microbiota is a critical regulator of bone mass. Two years later, Ohlsson and Sjögren introduced

**Abbreviations:** CD, cluster of differentiation; DM, diabetes mellitus; GF, germ-free; IL, interleukin; LPS, lipopolysaccharide; NF- $\kappa$ B, nuclear factor kappa B; NLRP3, nucleotide oligomerization domain-like receptor family pyrin domain-containing 3; OPG, osteoprotegerin; RANKL, receptor activator of nuclear factor kappa B ligand; SCC, solitary chemosensory cell; SPF, specific pathogen-free; TNF- $\alpha$ , tumor necrosis factor- $\alpha$ ; Wnt, Wingless-integrated.

a new term, “osteomicrobiology”, to refer to the study of the role of microbiota in health and disease, and the mechanisms by which microbiota regulate post-natal skeletal maturation, bone aging, and pathological bone loss (Ohlsson and Sjögren, 2015).

Recently, numerous links have been suggested between the gut microbiota and bone remodeling (Ohlsson and Sjögren, 2018; Yan et al., 2018). In general, the effect of the gut microbiota on bone depends on various factors, such as the composition of the microbiome, human diet, and age (Yan et al., 2018). However, the mechanisms by which the gut microbiota participate in bone regulation require further investigation. The oral cavity houses the second largest and second-most diverse microbiota after the gut in the body, with over 700 species of bacteria, fungi, viruses, archaea, and protozoa currently known (Paster et al., 2006). The alveolar bone is that part of the maxilla and mandible that supports the teeth, and the association of the oral microbiota with alveolar bone homeostasis has also received considerable attention (Costalonga and Herzberg, 2014; Hathaway-Schrader and Novince, 2021). In 1969, Brown et al. first reported that alveolar bone loss is statistically significantly stunted in GF mice compared with specific-pathogen-free (SPF) mice (Brown et al., 1969). More recently, Hajishengallis et al. validated those results (Hajishengallis et al., 2011). Moreover, an interplay between the oral microbiota and immune and bone cells was demonstrated by Horton et al. in 1972. Specifically, human peripheral blood leukocytes stimulated by dental plaque derived from patients with periodontitis produced osteoclast-activating factors (calcium-45) and increased the number of active osteoclasts (Horton et al., 1972). Collectively, these studies indicate that there is a complex, reciprocal relationship between the oral microbiota and alveolar bone homeostasis. Depending on the conditions, oral microbiota may have either a protective or a pathological effect on alveolar bone. However, the available data suggest that such interaction is limited, and the mechanism underlying alveolar bone regulation by the oral microbiota remains to be elucidated. Thus, we propose the term “oral osteomicrobiology” to denote the rapidly emerging field of study of the role of oral microbes in alveolar bone health and disease, aiming to bridge the gaps in the interplay between oral microbiology, immunology, and the alveolar bone.

Patients with severe periodontitis are estimated to swallow  $10^{12}$ – $10^{13}$  bacteria in their saliva daily (Sender et al., 2016). Swallowed indigenous oral bacteria can change the composition of the gut microbiota and induce gut dysbiosis (Kitamoto et al., 2020; Kobayashi et al., 2020). Moreover, intestinal microorganisms can indirectly affect the structure of the oral microbiome. Inflammatory bowel disease is an inflammatory response caused by intestinal flora disorders. Inflammatory bowel disease is often accompanied by changes in the composition of the salivary microbiota and corresponding oral symptoms, suggesting that the intestinal microbiota in the pathological state may directly or indirectly affect the composition of the oral microbiome (Said et al., 2014). Probiotics can also alter the composition and/or metabolic activity of gut microbiota, which can result in modulatory effects on the host immune response as well as oral microbiota

(Abboud and Papandreou, 2019; Mishra et al., 2020). Therefore, oral and gut osteomicrobiota seemingly interact with each other. For example, mice with gut dysbiosis induced by orally administered *Porphyromonas gingivalis* have an increased immune response, worse arthritis, and substantially lower bone mineral density than do controls (Arimatsu et al., 2014; Sato et al., 2017). Trinitrobenzene sulphonic acid and dextran sodium sulphate treatment in mice elicited gut dysbiosis and caused alveolar bone loss in both maxillae and mandibles, worsening over time (Oz and Ebersole, 2010). Berberine ameliorates periodontal bone loss in rats by regulating the gut microbiota (Jia et al., 2019). Although there are similarities in the mechanisms involved in alveolar bone loss mediated by the oral and gut microbiota, there are also unique characteristics. Both the oral and gut microbiota regulate bone homeostasis by inducing the host immune response and sustained changes in receptor activator of nuclear factor kappa B (NF- $\kappa$ B) ligand (RANKL)-mediated osteoclastogenesis (Hsu and Pacifici, 2018). The gut microbiota can alter the production of insulin-like growth factor 1, and regulate nutrient absorption and metabolism, affecting the hormone production critical for bone health such as sex steroids, vitamin D, and serotonin (Markle et al., 2013; Hsu and Pacifici, 2018). The oral microbiota causes alveolar bone resorption when the ecological equilibrium is disturbed. During the pathological process, virulence factors of pathobionts play important roles (Costalonga and Herzberg, 2014). However, the direct linkages and differences between oral and gut osteomicrobiology have not been elucidated.

In the present article, to contribute to the understanding of oral osteomicrobiology, we review the roles of the oral microbiota in alveolar bone formation and loss, discuss the role of osteo-immunomodulatory effects as a bridge between the oral microbiota and the alveolar bone, and inspect the mechanisms by which the oral microbiota modulate alveolar bone. We focused on RANKL, Notch, and Wntless-integrated (Wnt) signaling, as well as the nucleotide oligomerization domain-like receptor family pyrin domain-containing 3 (NLRP3) inflammasome. We also summarize the factors that influence the interaction between the oral microbiota and alveolar bone loss, as well as techniques that are critical for oral osteomicrobiology research.

## 2 ORAL MICROBIOTA IN ALVEOLAR BONE FORMATION AND BONE LOSS

### 2.1 Oral Microbiota in Post-Natal Jawbone Development

The gut commensal microbiota have been demonstrated to affect bone remodeling. For instance, GF mice have a general growth defect reflected by a slower gain in body weight as well as decreased longitudinal and radial bone growth compared to conventionally raised mice. This is due to growth hormone resistance and a reduced concentration of insulin-like growth factor 1 concentrations, both associated with the gut microbiota;

their phenotype can be normalized by treatment with a specific *Lactobacillus plantarum* strain (Schwarzer et al., 2016). As for the oral microbiota, several lines of evidence have suggested that they participate in regulating post-natal jawbone development. SPF mice reportedly have a larger body size with a lower alveolar bone mineral density and alveolar bone volume fraction compared with GF mice (Uchida et al., 2018). Further analysis suggested that the oral commensal microbiota prevent excessive mineralization by enhancing the expression of osteocalcin, an inhibitor of bone mineralization, in osteoblasts, and directs the activity of osteoblasts and osteoclasts by regulating specific transcription factors (Uchida et al., 2018). For example, the expression of *androgen receptor* and *alkaline phosphatase* was activated in SPF mice, which increased long bone growth and size, and enhanced differentiation of osteoblasts, respectively (Huang et al., 2007; Manolagas et al., 2013). Existing data indicate that the commensal microbiota is responsible for both anabolic and catabolic activities in alveolar bone formation and physiological skeletal growth (Sjögren et al., 2012; Novince et al., 2017; Irie et al., 2018). Further investigations are required to clarify the regulation of post-natal jawbone development by the oral microbiota.

## 2.2 Oral Microbiota in Physiological Alveolar Bone Loss

The alveolar bone “lives and dies” with the teeth, as it forms during teeth development and eruption but is resorbed after tooth loss. In the physiological state, the alveolar bone is renewed through a succession of apposition-resorption cycles, with osteoclasts responsible for tissue resorption and osteoblasts for matrix deposition (Preshaw et al., 2007). The balance between those two opposite functions results in a dynamic equilibrium of constantly remodeled healthy bone. Disturbance of this delicate balance leads to excess bone loss (Harris and Heaney, 1969).

Aging is a process of physiological involution. Although alveolar bone loss is not a natural consequence of aging, both clinical and animal studies have indicated a positive correlation between alveolar bone loss and aging in physiological conditions. For example, Hajishengallis et al. revealed that aged, healthy GF mice (18-month-old) showed increased alveolar bone loss and concentrations of inflammatory mediators compared with young GF mice (5-week-old) (Hajishengallis et al., 2011). They also demonstrated that the commensal microbiota was necessary for and directly contributed to the non-pathological bone loss observed in their model. In agreement, Liang et al. reported that old mice displayed a statistically significant increase in alveolar bone destruction, accompanied by an elevated expression of proinflammatory cytokines, in comparison with young mice, suggesting that alveolar bone is resorbed to a greater extent with age (Liang et al., 2010). A more recent study of the effects of aging on periodontal tissues revealed that SPF but not GF mice exhibited an age-related increase in alveolar bone loss (Irie et al., 2018). In healthy humans, a modest but not critical loss of periodontal support has been discovered with age (Huttner et al., 2009). This “natural” bone loss is associated with an increase in periodontal cell response to the oral

microbiota, alterations in differentiation and proliferation of the osteoblasts and osteoclasts, and endocrine alterations (Nishimura et al., 1997; Abiko et al., 1998; Okamura et al., 1999; Huttner et al., 2009). The specific mechanisms of physiological alveolar bone loss remain unknown. Gut microbiota have an anti-anabolic effect by inhibiting osteoblastogenesis and a pro-catabolic effect by stimulating osteoclastogenesis, ultimately driving bone loss (Novince et al., 2017); oral commensal microbiota may have the same effects on physiological alveolar bone loss. Natural bone loss seems to be a manifestation of the homeostatic relationship between the host and its oral microbial community. Moreover, further study is required to determine whether the oral commensal microbiota directly affects physiological alveolar bone loss, and which features of the oral microbiome predispose individuals to bone loss. The techniques needed to study these issues will be introduced in section 5.

## 2.3 Oral Microbiota as Regulator of Pathological Alveolar Bone Loss

The dysbiosis of the oral microbiota results in an increase in pathogenic microorganisms or in the pathogenicity of the microbiota. The oral microbiota has a catabolic effect, impacting osteoclast-osteoblast-mediated alveolar bone remodeling, leading to pathological bone loss. Most cases of pathological alveolar bone loss are associated with oral infectious diseases (e.g., periodontitis, apical periodontitis, and peri-implantitis) driven by the oral microbiota. The results of relevant studies have been summarized in **Table 1**.

### 2.3.1 Periodontitis

Periodontitis is a chronic inflammatory disease affecting tooth-supporting tissues. It is initiated by microbial communities but requires disruption of the normal host immune-inflammatory state (Curtis et al., 2020). Moreover, periodontitis is a dysbiosis disease, reliant upon an entirely dysfunctional oral microbiome, not a conventional infectious disease caused by select periodontal pathogens (Hajishengallis et al., 2011; Hajishengallis and Lamont, 2021). Polymicrobial communities induced a dysregulated host response and resulted in periodontal tissue destruction (Lamont et al., 2018). GF mice administered with *P. gingivalis* did not develop any detectable pathogenic changes, while *P. gingivalis* induced bone loss and substantial changes in the oral commensal microbial community in SPF mice, indicating that an oral microbial shift is critical for *P. gingivalis*-induced alveolar bone loss (Hajishengallis et al., 2011; Sato et al., 2018). Consistent with that result, Darveau et al. discovered that *P. gingivalis* could modulate the complement function, facilitating a marked change in both the quantity and composition of the commensal oral microbiota, ultimately contributing to pathological bone loss in mice (Darveau et al., 2012). Interestingly, the ability of *P. gingivalis* to cause oral microbiota-mediated alveolar bone loss is strain-dependent. For instance, *P. gingivalis* W83 can reportedly initiate periodontitis, while *P. gingivalis* TDC60-treated mice experience only moderate lesions. *P. gingivalis* W83-treated mice reportedly

**TABLE 1 |** Summary of the dysbiosis of oral microbiota associated with pathological alveolar bone loss.

Diseases associated with alveolar bone loss	Principle findings of pathogens associated with alveolar bone loss	Animal model or clinical study	References
Periodontitis	<i>P. gingivalis</i> colonization facilitated a change in quantity and composition of the commensal oral microbiota.	Mouse models	Hajishengallis et al., 2011; Sato et al., 2018; Darveau et al., 2012
	Oral microbiota in <i>P. gingivalis</i> -treated mice exhibited lower concentrations and an imbalance, with decreased proportions of taxa associated with good oral health.	Mouse model	Boyer et al., 2020
	Concentrations of antibodies against <i>P. gingivalis</i> W83 and/or 381, <i>E. corrodens</i> , and <i>P. gingivalis</i> 33277 were positively correlated with alveolar bone loss, while the number of enteric bacteria and concentrations of antibodies against <i>F. nucleatum</i> and <i>P. intermedia</i> were negatively correlation with alveolar bone height.	Clinical study	Wheeler et al., 1994
	<i>P. gingivalis</i> and <i>T. denticola</i> concentrations were associated with the degree of alveolar bone loss.	Clinical study	Pradhan-Palikhe et al., 2013
	Healthy participants had higher concentrations of <i>Streptococcus</i> and <i>Actinomyces</i> sp., while participants with bone loss had higher concentrations of <i>A. actinomycetemcomitans</i> , <i>S. parasanguinis</i> , <i>F. alocis</i> , <i>P. micra</i> , and <i>Peptostreptococcus</i> sp. human oral taxon 113.	Clinical study	Fine et al., 2013
Apical periodontitis	A spectrum of 300 species colonizing the healthy human mouth have been consistently isolated from infected root canals of teeth with periapical destruction.	Clinical study	Nair, 1997
	The prominent isolates in apical periodontitis included <i>Enterococcus</i> , <i>Eubacterium</i> , <i>Fusobacterium</i> , <i>Campylobacter</i> , <i>Porphyromonas</i> , <i>Prevotella</i> , <i>Peptostreptococcus</i> , <i>Propionibacterium</i> , and <i>Streptococcus</i> strains.	Clinical studies	Farber and Seltzer, 1988; Sundqvist et al., 1989
	The root canal microbiome is dominated by aerobic and facultative anaerobic bacteria during the early course of pulpal infection; thereafter, obligate anaerobes become more abundant.	Clinical studies	Tani-Ishii et al., 1994; Stashenko et al., 1994
	Proper endodontic treatment resulted in substantial or complete radiographic regression of apical periodontitis, whereas persisting symptoms were associated with either incomplete closure of the root canal chamber or improper disinfection.	Clinical studies	Orstavik, 1996; Sundqvist, 1994
Peri-implantitis	The most commonly reported bacteria associated with peri-implantitis were obligate anaerobe Gram-negative bacteria, asaccharolytic anaerobic Gram-positive rods, and other Gram-positive species.	Clinical study	Kensara et al., 2021
	The peri-implantitis microbiome is commensal-microbe-depleted and pathogen-enriched, with increased concentrations of <i>Porphyromonas</i> and <i>Treponema</i> sp.	Clinical study	Sanz-Martin et al., 2017
	The core peri-implantitis-related species were <i>Fusobacterium</i> , <i>Parvimonas</i> , and <i>Campylobacter</i> sp., as well as organisms often associated with periodontitis ( <i>T. denticola</i> , <i>P. gingivalis</i> , <i>F. alocis</i> , <i>F. fastidiosum</i> , and <i>T. maltophilum</i> ).	Clinical study	Sanz-Martin et al., 2017
	<i>S. moorei</i> and <i>P. denticola</i> were core taxa specific to peri-implantitis.	Clinical study	Komatsu et al., 2020
	Implants caused bone loss at remote periodontal sites due to microbial dysbiosis induced by the implants.	Clinical study	Heyman et al., 2020
	<i>Firmicutes</i> decreased and <i>Bacteroides</i> increased in the peri-implantitis group at the phylum level, and <i>Peptostreptococcus</i> decreased and <i>Porphyromonas</i> increased at the genus level.	Canine model	Qiao et al., 2020

*P. gingivalis*, *Porphyromonas gingivalis*; *E. corrodens*, *Eikenella corrodens*; *F. nucleatum*, *Fusobacterium nucleatum*; *P. intermedia*, *Prevotella intermedia*; *T. denticola*, *Treponema denticola*; *A. actinomycetemcomitans*, *Aggregatibacter actinomycetemcomitans*; *S. parasanguinis*, *Streptococcus parasanguinis*; *F. alocis*, *Filifactor alocis*; *P. micra*, *Parvimonas micra*; *F. fastidiosum*, *Fretibacterium fastidiosum*; *T. maltophilum*, *Treponema maltophilum*; *S. moorei*, *Solobacterium moorei*; *P. denticola*, *Prevotella denticola*.

exhibit a substantial reduction, imbalance, and shift in the proportions of microbial taxa compared to healthy mice (Boyer et al., 2020).

In the disrupted periodontal microenvironment, Gram-negative bacteria dominate. This dysbiosis induces inflammation and a loss of the periodontal tissues. A cross-sectional periodontal study indicated that the concentrations of antibodies to *P. gingivalis* W83 and/or 381, *Eikenella corrodens*, and *P. gingivalis* 33277 were all positively correlated with alveolar bone loss, while the number of enteric bacteria and concentrations of antibodies to *Fusobacterium nucleatum* and *Prevotella intermedia* were all negatively correlated with alveolar bone height (Wheeler et al., 1994). The concentrations of microbial species considered etiologically related to periodontitis, such as *P. gingivalis* and *Treponema denticola*, were statistically significantly associated with the degree of

alveolar bone loss (Pradhan-Palikhe et al., 2013). In a longitudinal study, it was demonstrated that a test for *Aggregatibacter actinomycetemcomitans* was positive in 91.7% of participants presenting with vertical periodontal bone loss, highlighting the destructive pathological impact of that microorganism on the tooth-alveolar bone complex (Fine et al., 2013). Higher concentrations of *Streptococcus* and *Actinomyces* species were discovered in *A. actinomycetemcomitans*-positive participants who remained healthy, while higher concentrations of *A. actinomycetemcomitans*, *Filifactor alocis*, *Parvimonas micra*, and *Peptostreptococcus* sp. human oral taxon 113 were discovered in those with bone loss (Fine et al., 2013). At vulnerable sites, *A. actinomycetemcomitans*, *Streptococcus parasanguinis*, and *F. alocis* concentrations were elevated prior to bone loss. Taken together, data from that study reinforced the importance of *A. actinomycetemcomitans* in localized aggressive



periodontitis and indicated a potential synergistic partnership of that microorganism with *F. alocis* and *S. parasanguinis* in non-junctophilin-2-related disease, as that consortium was strongly associated with alveolar bone loss (Fine et al., 2013). Fascinatingly, some human skulls, more than one thousand years of age, had pathogenic alveolar bone lesions in the tooth areas, characteristic of periodontitis (Philips et al., 2020). Microbiome analysis derived from the periodontitis sites indicated that the same pathogenic species were responsible for the development of periodontitis in those samples as are today (Philips et al., 2020). Taken together, there is strong evidence that the oral microbiota is closely associated with periodontitis-related alveolar bone loss. In particular, the shift of the oral flora to a predominance of gram-negative anaerobic bacteria plays a pivotal role in this process.

### 2.3.2 Apical Periodontitis

Apical periodontitis is a prevalent infectious and inflammatory disorder that involves inflammation of periapical tissues and bone resorption surrounding the root apex (Wei et al., 2021). Ample clinical and experimental evidence indicates that apical periodontitis is initiated primarily by the mixed microflora of infected root canals (Márton and Kiss, 2000). A spectrum of 300 species colonizing the healthy human mouth have been consistently isolated from infected root canals of teeth with periapical destruction (Nair, 1997). The prominent isolates include *Enterococcus*, *Eubacterium*, *Fusobacterium*, *Campylobacter*, *Porphyromonas*, *Prevotella*, *Peptostreptococcus*, *Propionibacterium*, and *Streptococcus* strains (Farber and Seltzer, 1988; Sundqvist et al., 1989). The root canal microbiome is mainly dominated by aerobic and facultative anaerobic bacteria during the early course of pulpal infection, with obligate anaerobes increasing as a result of local consumption of oxygen (Stashenko et al., 1994; Tani-Ishii et al., 1994). Accumulating clinical follow-up studies have disclosed that proper endodontic treatment resulted in substantial or complete radiographic regression in 85% to 90% of apical periodontitis cases, whereas persisting symptoms were associated most frequently either with incomplete closure of the root canal chamber or improper disinfection, indicating the pathogenic role of the mixed bacterial flora of the pulp chamber in periapical infection (Sundqvist, 1994; Orstavik, 1996).

### 2.3.3 Peri-implantitis

Peri-Implantitis is an infection of the tissue around an implant, resulting in the loss of supporting bone. A history of periodontitis, dental plaque, poor oral hygiene, smoking, diabetes, and alcohol consumption are risk factors for peri-implantitis (Nguyen-Hieu et al., 2012). Microbial involvement is one of the most important proposed etiological factors for bone loss around an implant (Bousdras et al., 2006). Mechanical treatment combined with antiseptics or antibiotics reportedly yields clinical attachment and bone reconstruction (Bousdras et al., 2006).

Microbial diversity and richness vary during peri-implantitis. The microbes most associated with peri-implantitis are obligate anaerobe Gram-negative bacteria, asaccharolytic anaerobic

Gram-positive rods, and other Gram-positive species (Kensara et al., 2021). The peri-implantitis microbiome is commensal-depleted and pathogen-enriched, with an abundance of *Porphyromonas* and *Treponema* (Sanz-Martin et al., 2017) sp. The core peri-implantitis-related microbes were *Fusobacterium*, *Parvimonas*, and *Campylobacter* sp., as well as microbes often associated with periodontitis (*T. denticola*, *P. gingivalis*, *F. alocis*, *Fretibacterium fastidiosum*, and *Treponema maltophilum*) (Sanz-Martin et al., 2017). Komatsu et al. also deemed *Solobacterium moorei* and *Prevotella denticola* core taxa specific to peri-implantitis (Komatsu et al., 2020).

The immune response is triggered by the dysbiosis of the oral microbiota. The most frequently reported pro-inflammatory mediators associated with peri-implantitis are interleukin (IL)-1 $\beta$ , IL-6, IL-17, and tumor necrosis factor- $\alpha$  (TNF- $\alpha$ ). Osteolytic mediators such as receptor of NF- $\kappa$ B, RANKL, and Wnt5a, as well as proteinases such as matrix metalloproteinase-2, matrix metalloproteinase-9, and cathepsin-K are also reportedly upregulated in peri-implantitis sites compared to controls (Kensara et al., 2021). It is worth noting that implants have an impact on remote periodontal sites, as elevated inflammation and accelerated bone loss have been detected in intact, distant teeth (Heyman et al., 2020). That impact was due to microbial dysbiosis induced by the implants, since antibiotic treatment was demonstrated to prevent periapical bone loss. However, antibiotic treatment does not prevent the loss of implant-supporting bone, highlighting the distinct mechanisms mediating bone loss at each site (Heyman et al., 2020).

In experimental studies, placement of ligatures together with plaque formation causes resorption of supporting tissues and considerable inflammatory cell infiltration around implants and teeth (Berglundh et al., 2011). Using a canine peri-implantitis model, researchers observed that *Firmicutes* decreased and *Bacteroides* increased over time at the phylum level, and *Peptostreptococcus* decreased and *Porphyromonas* increased at the genus level (Qiao et al., 2020). They also identified several potential keystone species during peri-implantitis development using species-level and co-occurrence network analyses (Qiao et al., 2020). In summary, peri-implantitis is associated with a complex and distinct microbial community that includes bacteria, archaea, fungi, and viruses (Belibasakis and Manoil, 2021). The ecosystem shift from healthy to diseased includes an increase in microbial diversity and a gradual depletion of commensal microbes, along with an enrichment of classical and emerging periodontal pathogens. This change in the microbiota could provoke an inflammatory response and osteolytic activity, contributing to the physiopathology of peri-implantitis.

## 3 OSTEOMICROBIAL MECHANISMS OF ALVEOLAR BONE LOSS

Pathological alveolar bone loss is net bone loss caused by increased osteoclastogenesis-mediated bone resorption and decreased osteoblastogenesis-mediated bone formation, a process that is



mediated dynamically by both osteoclasts and osteoblasts. Under pathological conditions, oral pathogenic microbes or microbial dysbiosis induce catabolic disruption of osteoclast-osteoblast-mediated bone remodeling, which leads to alveolar bone loss. According to clinical, animal, and *in vitro* studies, microbial virulence factors and toxic derivatives could interfere with humoral or cellular anti-bacterial defense mechanisms, eliciting alveolar bone resorption (Márton and Kiss, 2000; Wei et al., 2021). As summarized in **Table 2**, the most typical such factor is lipopolysaccharide (LPS). It has been reported that  $10^{-3}$  g/L LPS can directly stimulate bone loss, while a tiny concentration of LPS ( $10^{-9}$  g/L) can indirectly promote bone loss by activating the production of bone resorptive cytokines and prostaglandins (Beuscher et al., 1987; Paula-Silva et al., 2020). Interestingly, the indirect involvement of endotoxins in the process of alveolar bone loss is a million times more likely than a direct pathogenic role for this bacterial cell wall component (Beuscher et al., 1987; Tatakis

et al., 1988). In particular, LPS could inhibit the differentiation and proliferation while promoting the apoptosis of osteoblasts *via* the following mechanisms: (1) inhibiting the expression of bone differentiation markers in osteoblast cells, including alkaline phosphatase, bone sialoprotein, and osteocalcin (Tachikake-Kuramoto et al., 2014); (2) substantially stunting synthesis of DNA and collagen (Wilson et al., 1988; Meghji et al., 1992); (3) elevating pro-inflammatory cytokine production of osteoblasts (Albus et al., 2016); and (4) inducing production of nitric oxide (Sosroseno et al., 2009). Moreover, a high concentration of *P. gingivalis* LPS could also reduce mesenchymal stem cell proliferation and osteogenic differentiation, and inhibit activated T cells (Tang et al., 2015). In addition, the capsular-like polysaccharide antigen from serotype c of *A. actinomycetemcomitans* inhibited osteoblast cell line proliferation through a pro-apoptotic mechanism (Yamamoto et al., 1999). It is more complex to determine how

**TABLE 2 |** Summary of microbial virulence factors involved in alveolar bone loss.

Microbial virulence factors	Principle findings	References
LPS	<p><math>10^{-3}</math> g/L of LPS could directly stimulate bone loss, while a tiny concentration of LPS (<math>10^{-9}</math> g/L) could indirectly promote bone loss by activating the production of bone resorptive cytokines and prostaglandins.</p> <p>LPS could inhibit differentiation and proliferation while promoting apoptosis of osteoblasts <i>via</i> various mechanisms.</p> <p>High concentrations of <i>P. gingivalis</i> LPS could reduce mesenchymal stem cell proliferation and osteogenic differentiation, and have the capacity to inhibit activated T cells.</p> <p><i>P. gingivalis</i> LPS increased the expression of RANKL <i>via</i> TLR2 in osteoblasts.</p> <p>LPS of oral bacteria could stimulate Notch signaling, thus inducing IL-6 expression in macrophages. Macrophages stimulated by LPS <i>in vitro</i> showed increased expression of JAG1, implying that LPS and Notch signaling are involved in bone loss.</p> <p><i>P. gingivalis</i> LPS could modulate the expression of Wnt signaling, regulating alveolar bone health.</p>	<p>Paula-Silva et al., 2020; Beuscher et al., 1987; Tatakis et al., 1988</p> <p>Wilson et al., 1988; Meghji et al., 1992; Tachikake-Kuramoto et al., 2014; Albus et al., 2016; Sosroseno et al., 2009</p> <p>Tang et al., 2015</p> <p>Kassem et al., 2015</p> <p>Wongchana and Palaga, 2012; Skokos and Nussenzweig, 2007; Tsao et al., 2011</p> <p>Nanbara et al., 2012; Maekawa et al., 2017; Tang et al., 2014</p> <p>Yamamoto et al., 1999</p>
CPA	CPA from serotype c (CPA-c) of <i>A. actinomycetemcomitans</i> inhibited osteoblast cell line proliferation through a pro-apoptotic mechanism.	
Protease	Red complex pathobionts damage the epithelial tissue through the production of high protease activity which allows for the translocation of immunostimulatory molecules into tissues.	Bamford et al., 2007; Saito et al., 1997
Gingipains	Gingipains of <i>P. gingivalis</i> cleaved and degraded OPG and increased the RANKL/OPG ratio, contributing to bone loss by inducing osteoclast formation.	Tsukasaki and Takayanagi, 2019; Yasuhara et al., 2009; Akiyama et al., 2014
RagA	The expression of RagA and RagB of <i>P. gingivalis</i> was increased after exposure to smoking, which could facilitate the invasion of <i>P. gingivalis</i> to the periodontium.	Bagaitkar et al., 2009
RagB		
OMP29	Surface RANKL on T cells primed with <i>A. actinomycetemcomitans</i> -derived OMP29 was essential for osteoclastogenesis.	Lin et al., 2011
Td92	Td92, the surface protein of <i>T. denticola</i> , activates NLRP3 in macrophages and induces caspase-1-dependent cell death	Jun et al., 2012
	Td92 induces osteoclastogenesis <i>via</i> prostaglandin E(2)-mediated RANKL/osteoprotegerin regulation	Kim et al., 2010
Dentilisin	<i>T. denticola</i> dentilisin stimulates tissue-destructive cellular processes in a TLR2/MyD88/Sp1-dependent fashion	Ganther et al., 2021
FimA	The upregulation of FimA suppressed the host response to <i>P. gingivalis</i> by abrogating the proinflammatory response to subsequent TLR2 stimulation, and, therefore, increasing bacterial survival.	Bagaitkar et al., 2010
CDT	Stimulation of CDT of <i>A. actinomycetemcomitans</i> caused upregulation of RANKL.	Belibasakis et al., 2005
LTA	LTA of <i>E. faecalis</i> could increase the levels of NLRP3, caspase-1, and IL-1 $\beta$ , which resulted in bone loss.	Yin et al., 2020

LPS, lipopolysaccharide; *P. gingivalis*, *Porphyromonas gingivalis*; RANKL, receptor of nuclear factor kappa B ligand; TLR, toll-like receptor; IL, interleukin; JAG1, Jagged 1; Wnt, Wingless-integrated; CPA, capsular-like polysaccharide antigen; *A. actinomycetemcomitans*, *Aggregatibacter actinomycetemcomitans*; OPG, osteoprotegerin; Rag, Ras-related GTP-binding protein; OMP, outer membrane protein; *T. denticola*, *Treponema denticola*; NLRP3, nucleotide oligomerization domain-like receptor pyrin domain-containing 3; FimA, fimbriin; CDT, cytolethal distending toxin; LTA, lipoteichoic acid; *E. faecalis*, *enterococcus faecalis*; NF- $\kappa$ B, nuclear factor kappa B; ROS, reactive oxygen species.

such factors and metabolites cause alveolar bone loss by regulating host signal transduction. Based on current evidence, RANKL, Notch, and Wnt signaling, as well as the NLRP3 inflammasome are major pathways involved in alveolar bone loss mediated by the oral microbiota (**Figure 1**). Osteoimmunity is the bridge that spans the gap between the microbiota and the bone.

### 3.1 Signaling Pathways Related to Oral Microbiota-Mediated Alveolar Bone Remodeling

#### 3.1.1 RANKL Signaling

RANKL is the master regulator of osteoclast differentiation and function. It binds to its cognate receptor on osteoclast precursors,

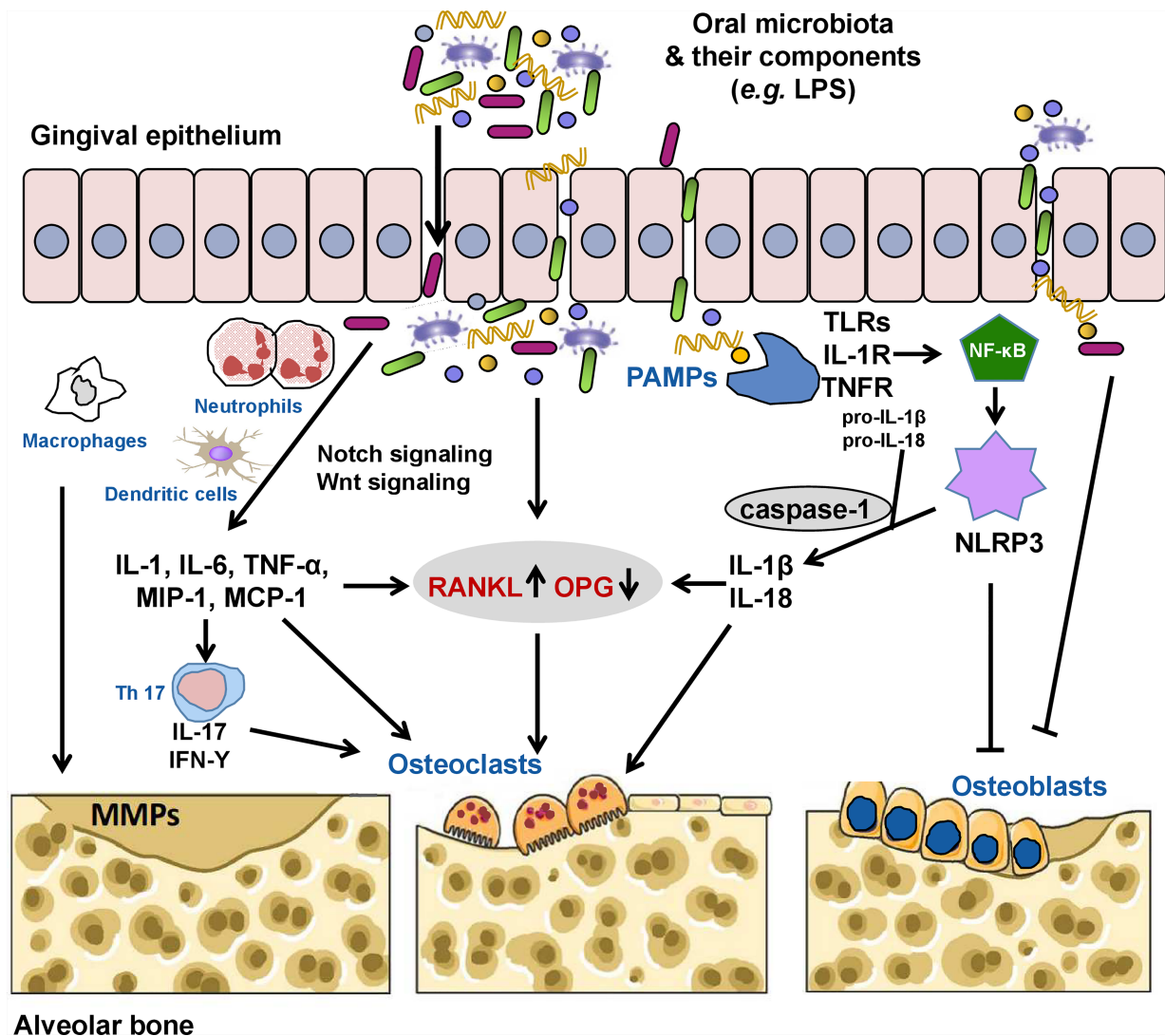


**FIGURE 1** | The oral microbiota and its components can invade the gingival epithelium through the production of proteases, thus activating receptor activator of nuclear factor kappa B (NF-κB) ligand (RANKL) signaling directly or indirectly by inducing the secretion of inflammatory cytokines (interleukin [IL]-1, IL-6, tumor necrosis factor [TNF]-α, macrophage inflammatory protein [MIP]-1, and monocyte chemoattractant protein [MCP-1]) by neutrophils, macrophages, and dendritic cells, increasing the RANKL/osteoprotegerin (OPG) ratio and contributing to alveolar bone loss by inducing osteoclast formation. Pathogenic  $T_H17$  cells stimulated by bacterial invasion evokes periodontal immune responses against these microorganisms or their metabolites while also inducing bone damage. Some pathogens (e.g., *Porphyromonas gingivalis*) and their lipopolysaccharides (LPSs) can also directly induce the activation of matrix metalloproteinases (MMPs), which mediate the degradation of the extracellular matrix. Oral pathogen-associated molecular patterns (PAMPs) such as LPS, lipoteichoic acid, and double-stranded RNA can activate the innate immune system through pattern recognition receptors, including toll-like receptors (TLRs), IL-1 receptor (IL-1R), and TNF receptor (TNFR), causing the release of NF-κB into the nucleus to initiate the expression of the nucleotide oligomerization domain-like receptor family pyrin domain-containing 3 (NLRP3) inflammasome. Activated NLRP3 cleaves pro-caspase-1 into caspase-1. Caspase-1 promotes the maturation and release of pro-IL-1β and pro-IL-18 to induce secretion of RANKL and activate osteoclasts. NLRP3 and activated caspase-1 can also promote osteoblast apoptosis. In addition, the oral microbiota and/or microbial virulence factors can inhibit the differentiation and proliferation while promoting the apoptosis of osteoblasts via various mechanisms.

inducing osteoclast differentiation and activation of bone resorption (Khosla, 2001). Osteoblasts, as well as osteocytes, also produce osteoprotegerin (OPG), a decoy receptor for RANKL, to block RANKL signaling, inhibiting osteoclast differentiation and bone resorption by mature osteoclasts (Khosla, 2001; Koide et al., 2013; Tsukasaki et al., 2020). An imbalance in the RANKL/OPG ratio is thought to deregulate bone remodeling, driving bone loss when the ratio exceeds that of normal physiology (Boyce and Xing, 2008).

Accumulating evidence has shown that RANKL signaling plays a critical role in alveolar bone loss in periodontitis (Belibasakis and Bostanci, 2012; Tsukasaki, 2021). Periodontal ligament cells, gingival epithelial cells, osteoblasts, osteocytes, and activated T and B cells are the major sources of RANKL in periodontal tissues (Kanzaki et al., 2002; Kawai et al., 2006; Nakashima et al., 2011; Usui et al., 2016). Patients with periodontitis have been shown to have an upregulated expression of RANKL in periodontal tissue, and the level of RANKL was highly correlated with the severity of periodontitis (Nagasawa et al., 2007); moreover, periodontitis-induced alveolar bone loss and osteoclast differentiation were markedly suppressed in RANKL-deficient mice (Tsukasaki et al., 2018). RANKL is also reportedly upregulated in periapical lesions and peri-implantitis sites (Duka et al., 2019; Kensara et al., 2021). It is also worth noting that OPG-knockout mice spontaneously developed severe alveolar bone loss, suggesting that not only the upregulation of RANKL, but also the downregulation and/or degradation of OPG is involved in periodontal bone loss (Koide et al., 2013). The RANKL/OPG ratio is associated with the degree of bone destruction in periodontitis (Bostanci et al., 2007), and an increased RANKL/OPG ratio may serve as a biomarker for the occurrence of periodontitis (Belibasakis and Bostanci, 2012; Tsukasaki, 2021).

Previous studies have indicated that RANKL could be activated directly by oral bacteria and their virulence factors (Belibasakis et al., 2005; Lin et al., 2011; Kassem et al., 2015). In osteoblasts, LPS of *P. gingivalis* increased the expression of RANKL via toll-like receptor 2 (TLR2) (Kassem et al., 2015). Td92 of *T. denticola* induced RANKL expression and promoted osteoclast formation via prostaglandin E(2)-dependent mechanism (Kim et al., 2010). Stimulation of gingival fibroblasts and periodontal ligament cells with cytolethal distending toxin from *A. actinomycetemcomitans* caused upregulation of RANKL (Belibasakis et al., 2005). Additionally, surface RANKL on T cells primed with *A. actinomycetemcomitans*-derived outer membrane protein 29 was essential for osteoclastogenesis (Lin et al., 2011). RANKL could also be regulated indirectly by the oral microbiota via an induced immune response. To summarize, the oral microbiota and its metabolites induce the production of inflammatory cytokines (e.g., IL-1, IL-6, and TNF- $\alpha$ ), macrophage inflammatory protein-1, and macrophage chemoattractant protein by different immune cells, including neutrophils, monocytes, macrophages, dendritic cells, T cells, and B cells, leading to the increased expression of RANKL (Brunetti et al., 2005; Rogers et al., 2007; Hung et al., 2014; Tompkins, 2016). An animal study demonstrated that activation of T cells by oral bacteria caused

RANKL-induced bone loss (Mahamed et al., 2005). Moreover, certain proteases derived from oral bacteria (e.g., gingipains of *P. gingivalis*) cleave and degrade OPG, thereby increasing the RANKL/OPG ratio and contributing to bone loss by inducing osteoclast formation (Yasuhara et al., 2009; Akiyama et al., 2014; Tsukasaki and Takayanagi, 2019). It is worth noting that osteoclast formation can also be induced by inflammatory chemokines and cytokines independent of RANKL (Hotokezaka et al., 2007; Valerio et al., 2015).

### 3.1.2 Notch Signaling

The Notch signaling pathway is considered a double-edged sword in osteoclastogenesis depending on the status of the osteoclasts and the expression of certain receptors and ligands (Pakvasa et al., 2020). However, in the context of oral microbiota-mediated alveolar bone remodeling, Notch signaling is mainly involved in alveolar bone resorption. A series of studies demonstrated that the Notch signaling pathway is in a complex relationship with proinflammatory cytokines and bone resorption regulators. Alveolar bone resorption in periodontitis and apical periodontitis is mediated through an increase in Notch receptors on the immune cell surface and stimulation of Notch-receptor intracellular domain translocation into the nucleus (Jakovljevic et al., 2019; Djinic Krasavcevic et al., 2021). Furthermore, LPS of oral bacteria can stimulate Notch signaling, thus inducing IL-6 expression in macrophages (Wongchana and Palaga, 2012). Jagged 1 is a cell surface ligand that interacts with receptors in the Notch signaling pathway. Macrophages stimulated by LPS *in vitro* exhibited increased expression of Jagged 1 (Skokos and Nussenzweig, 2007; Tsao et al., 2011). These studies provided evidence that LPS in conjunction with Notch signaling can activate cells that are involved in osteoimmunology-mediated bone loss. It will be of interest to study lineage-specific genes in the Notch-signaling-pathway knockout model to identify the role of this pathway in alveolar bone loss mediated by the oral microbiota.

### 3.1.3 Wnt Signaling

Mounting evidence indicates that Wnt signaling is essential for the control of bone mass by regulating the activity of both osteoblasts and osteoclasts. As noted above, the ratio of RANKL/OPG is key for bone resorption. Interestingly, the Wnt pathway can increase the production of OPG, decreasing the RANKL/OPG ratio and blocking RANKL-induced osteoclastogenesis (Zhong et al., 2014). The Wnt signaling pathway is involved in periodontitis, apical periodontitis, and peri-implantitis (Napimoga et al., 2014). Wnt5a is an activating ligand of non-canonical Wnt signaling pathways and plays important roles in the inflammatory response and bone development/remodeling (Zhong et al., 2014). It has been shown to enhance RANK expression in osteoclast precursors by engaging receptor tyrosine kinase-like orphan receptor 2 to activate Jun N-terminal kinase and recruiting c-Jun to the RANK gene promoter, thereby enhancing RANKL-induced osteoclastogenesis (Maeda et al., 2012). In a clinical study, the mRNA expression of Wnt5a was higher in gingival tissues from



individuals with periodontitis and peri-implantitis compared to that from healthy controls (Nanbara et al., 2012; Zhang et al., 2020). Further evidence has been derived from *in vitro* and animal studies. Wnt5a was upregulated in macrophages and monocytic cell line THP-1 following stimulation with *P. gingivalis* and LPS, respectively (Nanbara et al., 2012; Maekawa et al., 2017; Zhang et al., 2020). In macrophages, the induction of Wnt5a was dependent on lectin-type oxidized low density lipoprotein receptor-1 and TLR4. Wnt5a knockdown significantly impaired the production of IL-1 $\beta$ , macrophage chemoattractant protein 1, and matrix metalloproteinase-2 upon induction by *P. gingivalis* (Zhang et al., 2020). In THP-1 cells, this process is dependent upon NF- $\kappa$ B signaling (Nanbara et al., 2012; Maekawa et al., 2017). In a study using a rat model of apical periodontitis, inhibition of the Wnt/ $\beta$ -catenin signaling by Dickkopf-1 attenuated alveolar bone loss *via* regulation of bone coupling *in vivo* (Tan et al., 2018). Conversely, in rat bone marrow mesenchymal cells, Wnt/ $\beta$ -catenin signaling was inhibited by LPS of *P. gingivalis* and the cells exhibited decreased osteogenic potential (Tang et al., 2014). Thus, more research is required, especially in the form of *in vivo* studies, to clarify the role of Wnt signaling and related pathways in alveolar bone loss.

### 3.1.4 NLRP3 Inflammasome

The NLRP3 inflammasome is an essential component of the natural immune system (Lamkanfi and Dixit, 2014) and a critical mediator of alveolar bone loss. The reported intensity of NLRP3 expression was statistically significantly higher in tissues from patients with periodontitis than that from healthy controls (Huang et al., 2015; Xue et al., 2015). In experimental mice models, alveolar bone loss was correlated with caspase-1 activation by macrophages and elevated concentrations of IL-1 $\beta$ , which is mainly regulated by the NLRP3 inflammasome (Zang et al., 2020; Chen et al., 2021). NLRP3 knockout mice exhibited a higher bone mass and reduced osteoclast precursors and differentiation compared with wild-type mice. More importantly, an NLRP3 inflammasome inhibitor statistically significantly improved alveolar bone mass with reduced proinflammatory cytokine production and increased osteogenic gene expression in mice with periodontitis (Zang et al., 2020; Chen et al., 2021).

Many studies have been conducted to determine whether the NLRP3 inflammasome can be regulated by the oral microbiota. The NLRP3 inflammasome can recognize oral pathogen-associated molecular patterns and host-derived danger-signaling molecules, and activate the pro-inflammatory protease, caspase-1 (Yu et al., 2021). These pathogen-associated molecular patterns include LPS, peptidoglycan, and viral double-stranded RNA (Brown et al., 2011; Amari and Niehl, 2020). After activation, caspase-1 cleaves the precursors of IL-1 $\beta$  and IL-18 to produce mature cytokines (Menu and Vince, 2011). IL-1 $\beta$  further induces secretion of RANKL and activates osteoclasts, which can cause a series of inflammatory responses (Nakashima et al., 2000). Activated caspase-1 specifically recognizes and cleaves gasdermin D to mediate cell pyroptosis (Wang K. et al., 2020).

Pathogens of periapical periodontitis and periodontitis can activate NLRP3 *in vitro*. For instance, lipoteichoic acid from *Enterococcus faecalis*, the most common pathogen in periapical periodontitis, can induce the expression of NLRP3 and increase the levels of caspase-1 and IL-1 $\beta$ , thus resulting in bone loss (Yin et al., 2020). It is worth mentioning that inhibition of the NLRP3 inflammasome can effectively alleviate those effects (Yin et al., 2020). Td92, the surface protein of *T. denticola*, activates NLRP3 in macrophages and induces caspase-1-dependent cell death (Jun et al., 2012). *A. actinomycetemcomitans* can also activate NLRP3 (Zhao et al., 2014). In one study, heat-killed *A. actinomycetemcomitans* injected into the gum tissues of caspase-1-knockout mice statistically significantly decreased alveolar bone resorption in comparison with wild-type mice (Rocha et al., 2020). Furthermore, knockdown of NLRP3 using small interfering RNA in *A. actinomycetemcomitans*-infected osteoblasts attenuated apoptosis, which suggests that *A. actinomycetemcomitans* invasion of the alveolar bone surface may directly promote osteoblast apoptosis through the NLRP3 inflammasome (Zhao et al., 2014). There is also indirect evidence that differentiation of THP-1 cells into macrophage-like cells, induced by *P. gingivalis* and *F. nucleatum*, is NLRP3- and caspase-1-dependent (Kawahara et al., 2020). In MC3T3-E1 cells, stimulation with *P. gingivalis* resulted in the protein kinase R-mediated increase in NLRP3 expression *via* activation of NF- $\kappa$ B (Yoshida et al., 2017).

### 3.1.5 Gingival Solitary Chemosensory Cells

Solitary chemosensory cells (SCCs) are epithelial sentinels that utilize bitter taste receptors and coupled taste signaling elements to detect pathogen metabolites, stimulating host defenses to control the infection (O'Leary et al., 2019). Previously, our research team discovered that SCCs were present in mouse gingival junctional epithelium where they expressed several bitter taste receptors and the taste signaling elements,  $\alpha$ -gustducin, transient receptor potential cation channel subfamily M member 5, and phospholipase C  $\beta$ 2 (Zheng et al., 2019). The commensal oral microbiome was altered and natural alveolar bone loss was accelerated in  $\alpha$ -gustducin knockout mice. In a model of ligature-induced periodontitis, knockout of taste signaling molecules or the genetic absence of gingival SCCs increased the bacterial load, reduced bacterial diversity, and caused a pathogenic shift in the microbiota, leading to greater alveolar bone loss. Topical treatment with bitter denatonium to activate gingival SCCs upregulated the expression of antimicrobial peptides and ameliorated ligature-induced periodontitis in wild-type but not in  $\alpha$ -gustducin<sup>-/-</sup> mice (Zheng et al., 2019). These results demonstrated that gingival SCCs may provide a promising target for treating periodontitis by harnessing the innate immunity to regulate the oral microbiome.

## 3.2 Osteoimmunity in Alveolar Bone Loss Mediated by Oral Microbiota

Osteoimmunology has developed because of the close interplay between the immune system and bone metabolism (Rho et al., 2004). Mediation of the immune response by the oral microbiota,

especially pathogens, is critical for bone homeostasis. Dysbiosis in the oral microbial community influences the host immune response, and the immunoinflammatory reaction may shape the composition of the oral microbiota and contribute to the homeostatic relationship between microbiota and host (Hajishengallis, 2014). Oral microbiota-triggered innate and acquired immune responses are considered to be a double-edged sword in alveolar bone loss. The complement system, phagocytosis, the inducible nitric oxide synthase-mediated immune responses, and the production of antigen-specific immunoglobulins protect hosts from harmful bacteria (Jiao et al., 2014). For example, mice lacking inducible nitric oxide synthase, P-selectin, or intercellular adhesion molecule 1 are susceptible to alveolar bone loss after *P. gingivalis* infection (Baker et al., 2000; Fukada et al., 2008). However, an imbalance in the homeostasis between bacteria and host immune responses culminates in bone resorption. Bacteria possess a variety of immunostimulatory molecules, some of which induce recruitment of immune cells and others secretion of TNF- $\alpha$  and IL-1 $\beta$  from immune cells (Takeuchi and Akira, 2010). Red complex pathobionts (*P. gingivalis*, *T. denticola*, and *Tannerella forsythia*) damage the epithelial tissue by stimulating proteases that allow the translocation of immunostimulatory molecules into tissues (Saito et al., 1997; Bamford et al., 2007). In response to oral bacteria, IL-6, TNF- $\alpha$ , and IL-1 $\beta$  are secreted from neutrophils and macrophages that are recruited to damaged gingival tissues (Takeuchi and Akira, 2010). Nucleotide oligomerization domain-like receptor 1 ligands produced by certain bacteria possess the ability to recruit neutrophils that secrete inflammatory cytokines (e.g., TNF and IL-1) to alter the RANKL/OPG ratio in activated T cells, B cells, and osteoblasts, causing alveolar bone loss at damaged gingival sites (Hasegawa et al., 2006; Masumoto et al., 2006). Pathogenic T<sub>H</sub>17 cells stimulated by bacterial invasion evoke a mucosal immune response for protection against pathogens while inducing bone damage (Tsukasaki et al., 2018). Based on the accumulated evidence, we speculate that moderate immune responses induced by oral microbiota may be beneficial for alveolar bone, whereas the expression of large numbers of pro-inflammatory cytokines induced by excessive immune responses promote alveolar bone loss.

In the oral cavity, the oral microbiome, host immune system, and alveolar bone co-exist and interact. Osteomicrobiology bridges the gap between the microbiome and osteoimmunology. Osteomicrobiology and osteoimmunology are inseparable but have distinguishing characteristics. The challenge is to maintain homeostasis in the oral microbiome, moderate inflammation, and remodeling of the alveolar bone.

## 4 FACTORS THAT AFFECT ORAL MICROBIOTA-MEDIATED ALVEOLAR BONE METABOLISM

The oral microbiota is directly or indirectly responsible for most alveolar bone loss, however, the relationship is modified by

various interacting factors, including smoking, blood glucose level, estrogen concentration and probiotics. Studies in this field have provided details of the crosstalk between these factors. This section aims to offer an overview of how these factors influence oral microbiota-mediated alveolar bone metabolism.

Life events and general health conditions can affect the bone metabolism (Feres et al., 2016). For instance, obesity and hypertension have an impact on the oral microbial composition and regulate alveolar bone metabolism (Del Pinto et al., 2020; Khan et al., 2020). Smoking, diabetes mellitus (DM), and estrogen deficiency are associated with systemic bone loss, including osteoporosis and alveolar bone resorption (Weitzmann and Pacifici, 2006; Straka et al., 2015; Wang X. et al., 2020). Clinical and experimental studies have revealed a higher prevalence of periodontitis, periapical periodontitis, or peri-implantitis associated alveolar bone resorption in patients/animal models who smoke or with DM/estrogen deficiency (Duarte et al., 2004; Lima et al., 2013; Penoni et al., 2017; Gupta et al., 2020; Ford and Rich, 2021). Data from cross-sectional studies have also demonstrated that the severity of periodontitis and alveolar bone loss were positively correlated with the amount of daily smoking (Hujoel et al., 2003). The relationship of DM and periodontal disease is bidirectional, compromised management of either one would negatively affect the other one (Radaic and Kapila, 2021). Positive management of these factors exhibited beneficial effect on alveolar bone remodeling. For example, estrogen therapy is an effective method for improving alveolar bone density in post-menopausal patients with osteoporosis (Ronderos et al., 2000; Bhavsar et al., 2016).

Probiotics have been used to induce beneficial skeletal effects for it can alter the composition and/or the metabolic activity of the gut microbiota, and regulate the immune response in the host, thereby providing beneficial effects for bone health (Abboud and Papandreou, 2019; Pan et al., 2019; Schepper et al., 2020). Randomized clinical studies and animal studies demonstrated that oral administration of certain probiotics is a useful strategy for the management of periodontitis, periapical periodontitis, and peri-implantitis (Huck et al., 2020; Cosme-Silva et al., 2021; Kumar et al., 2021). Increasing evidence have shown that these factors impact the alveolar bone metabolism mainly through modulating the oral microbiota and the host immune response (osteomicrobiological modulatory effects).

### 4.1 Alter the Composition and Virulence of the Oral Microbiota

The factors can alter the composition and virulence factors of oral microbiota, thus affecting alveolar bone metabolism directly or indirectly. In smoking-related periodontitis or peri-implantitis, the microbial profile is distinct from that in non-smokers, and there are statistically significant differences in the prevalence and enrichment of disease-associated and health-compatible microorganisms (Shchipkova et al., 2010; Duan et al., 2017; Stokman et al., 2017; Naseri et al., 2020). Levels of disease-associated pathogens have been revealed to decrease following smoking cessation (Delima et al., 2010). The expression of several virulence factors of *P. gingivalis* (e.g.,



fimbrilin and Ras-related GTP-binding proteins A and B) increased after exposure to smoking, which could suppress the host response by abrogating the proinflammatory response to subsequent TLR2 stimulation, and therefore could facilitate the invasion of *P. gingivalis* into the periodontium (Bagaitkar et al., 2009). Furthermore, the expression of capsular polysaccharide is inhibited by smoking, thus promoting the colonization of *P. gingivalis* and enhancing both inter- and cross-species interaction of *P. gingivalis*, aggravating the alveolar bone loss (Zhang et al., 2019).

Hyperglycemia is able to cause dysbiosis of the oral microbiota, with a statistically significant enrichment of *Leptotrichia*, *Staphylococcus*, *Catonella*, and *Bulleidia* genera, contributing to aggravation of alveolar bone loss (Wang et al., 2019). Hintao et al. demonstrated that *T. denticola*, *Streptococcus sanguinis*, *Prevotella nigrescens*, *Staphylococcus intermedius*, and *Streptococcus oralis* were statistically significantly enriched in the supragingival plaque of individuals with type 2 DM compared with individuals without DM (Hintao et al., 2007). DM can also increase the pathogenicity of the dysbiotic oral microbiota. A study demonstrated that DM enhanced IL-17 expression and altered the oral microbiome to increase its pathogenicity (Xiao et al., 2017). Compared with the oral microbiomes of healthy mice, the pathogenic oral microbiomes of diabetic mice statistically significantly exacerbated periodontal inflammation and bone loss when transferred to GF mice (Xiao et al., 2017).

Postmenopausal women with endogenous estrogen deficiency exhibited a progressive loss in radiographic alveolar crestal height over 5 years, and that loss was associated with a change in the subgingival microbiome (LaMonte et al., 2021). The abundance of *P. gingivalis* and *T. forsythensis* were increased and were revealed to be critical in the etiology of periodontitis in postmenopausal women (Brennan et al., 2007). Cohort studies demonstrated that estrogen therapy improved periodontal probing depth and tooth mobility, with decreased levels of *P. gingivalis*, *P. intermedia*, and *T. forsythia* being detected in subgingival plaque (López-Marcos et al., 2005; Tarkkila et al., 2010). Changes in estrogen levels may cause the gums to become more susceptible to plaque, leading to a much higher risk of advanced periodontitis (Suresh and Radfar, 2004). Furthermore, estrogen-deficient conditions interfere with the oral microbiota by increasing the levels of certain bacteria in saliva and influencing the progression of periapical bone loss (Lucisano et al., 2021).

In contrast to causing oral microbiota dysbiotic, probiotics facilitate the change of abundance towards health-favoring commensals, modulating the oral microecology. Animal studies revealed that topical application of *Lactobacillus brevis* cluster of differentiation (CD) 2 attenuated alveolar bone loss, with a reduction in anaerobic bacteria and an increase in aerobic bacteria in mice (Maekawa and Hajishengallis, 2014). Oliveira et al. discovered that topical application of *Bifidobacterium lactis* HN019 reduced bone destruction, decreased the proportions of *Veillonella parvula*, *Capnocytophaga sputigena*, *E. corrodens*, and *P. intermedia*-like species, and increased the proportions of *Actinomyces* and *Streptococcus*-like species (Oliveira et al., 2017).

*In vitro* studies have demonstrated that certain probiotics exhibit inhibitory activity against endodontic pathogens (Bohora and Kokate, 2017a; Bohora and Kokate, 2017b). Probiotic *Akkermansia muciniphila* was revealed to reduce gingipain transcription by *P. gingivalis*, thereby decreasing inflammatory cell infiltration and alleviating alveolar bone loss (Huck et al., 2020). Recently, we discovered that administration of probiotics enriched butyrate-producing genera of gut microbiota, improved intestinal barrier function, and decreased gut permeability, thus preventing inflammatory alveolar bone resorption in ovariectomized rats (Jia et al., 2021).

## 4.2 Modulate the Host Immune Response

The factors could also influence the interaction between oral microbiota and alveolar bone *via* modulating the innate and adaptive host immune response. Smoking impairs chemotaxis and phagocytosis of neutrophils in the periodontal tissues and inhibits serum immunoglobulin G antibodies against periodontal pathogens, exerting a “protective” effect on pathogens (Guntsch et al., 2006; Vlachojannis et al., 2010). Furthermore, smoking indirectly modulates the oral microbiota and host immune response by inducing the generation of reactive oxygen species (ROS), which have been found to be essential for osteoclastogenesis (Matthews et al., 2011). DM altered the equilibrium of osteoclasts and osteoblasts in the alveolar bone by shaping the oral microbial balance, and by increasing the concentrations of inflammatory mediators (e.g., TNF), the RANKL/OPG ratio, advanced glycation end products, and ROS (Wu et al., 2015; Graves et al., 2019). Hyperglycemia inhibits osteoblastic differentiation as well as new bone formation, exacerbates alveolar bone resorption, and enhances peri-implant inflammation, frequently causing implant failure (Chrcanovic et al., 2014). Estrogen deficiency can also inhibit the production of cytokines triggered by dysbiotic microbiota, lower the RANKL/OPG ratio, and stimulate the production of transforming growth factor  $\beta$  by osteoblasts, resulting in a decrease in osteoclast quantity and activity (Hughes et al., 1996; Riggs, 2000). Postmenopausal estrogen deficiency induces the production of TNF- $\alpha$  and RANKL in T cells, and influences the activities of bone multicellular units, resulting in a reduction in the ratio of bone deposition by osteoblasts to bone resorption by osteoclasts, enhancing the progression of alveolar bone loss in patients with periodontitis or apical periodontitis (Lerner, 2006; D'Amelio et al., 2008). The above studies provide evidence that, smoking, DM, and estrogen deficiency exacerbate the loss of alveolar bone by promoting the invasion of pathogenic bacteria and aggravating the inflammatory response.

Contrarily, probiotics have a protective effect against alveolar bone loss by modifying immunoinflammatory parameters. *L. brevis* CD2 treatment resulted in statistically significantly less bone loss and a downregulation of TNF, IL-1 $\beta$ , IL-6, and IL-17A compared to placebo treatment (Maekawa and Hajishengallis, 2014). The group treated with *B. lactis* HN019 exhibited increased expressions of OPG and  $\beta$ -defensins, while decreased expressions of IL-1 $\beta$  and RANKL compared to the control group (Oliveira et al., 2017). Pazzini et al. also revealed that oral

supplementation with probiotic *Bacillus subtilis* was beneficial for bone remodeling by reducing the number of osteoclasts adjacent to the tooth root during orthodontic movement in mice (Pazzini et al., 2017).

Collectively, the composition of the oral microbiota and host immune response varies depending on dietary diversification, medicine used, hormonal changes, general health conditions, and age (Feres et al., 2016). Many factors could influence the osteomicrobiological modulatory effect in physiological or pathological conditions. The factors mentioned above interact with each other in antagonistic and synergistic ways to influence oral microbiota-mediated alveolar bone health. For example, estrogen depletion and streptozotocin-induced DM promoted more pronounced periodontal tissue deterioration than each did in isolation (Sasso et al., 2020). Probiotic administration has a protective effect on the mandibular bone mineral density in rats exposed to cigarette smoke inhalation (Levi et al., 2019). More studies are needed to determine the mechanisms by which these factors impact oral microbiota-mediated alveolar bone metabolism. These studies would facilitate the discovery of critical targets and the development of strategies for manipulating the microbiota to induce beneficial skeletal effects.

## 5 CRITICAL TECHNIQUES FOR ORAL OSTEOMICROBIOLOGY RESEARCH

The oral cavity harbors over 700 species, including bacteria, fungi, viruses, archaea, and protozoans, although only approximately 70% of them can be cultivated, based on the expanded Human Oral Microbiome Database (Verma et al., 2018). With the advances in rapid, low-cost sequencing technologies and next-generation sequencing-based platforms, it is possible to quantitatively characterize the composition and putative functions of microbial communities (Human Microbiome Project Consortium, 2012). 16S ribosomal DNA sequencing has greatly contributed to revealing the composition of the oral microbiome. It allows identification of bacteria at a highly accurate genus level by amplifying one or more high-variation zones, such as V1, V2, V3, and V4 regions. However, this method does not provide the full-length DNA sequence; thus, it cannot be used to distinguish species and strains, nor to identify fungi and viruses (Janda and Abbott, 2007). To overcome this drawback, whole genome sequencing, metatranscriptomics, metaproteomics, and metabolomics can be used to identify strains present in the oral microbiome, and to detect microbial genes, proteins, and metabolites that have an impact on diseases (Human Microbiome Project Consortium, 2012). Although analysis of next-generation sequencing-derived sequences remains challenging, it has greatly improved our understanding of the relationships between the oral microbiota and alveolar bone health. The importance of the microbiota has been confirmed and new insights have been gained on their effects on bone physiology (Ohlsson and Sjögren, 2018).

Animal models are also useful for studying the role of the oral microbiota in alveolar bone mass regulation. Two prominent models, GF mice and humanized mice, are of great importance for *in vivo* studies of host microbial interaction. GF mice have been employed to explore the role of oral pathobionts in dysbiosis and bone loss during periodontitis for more than half a century (Baer and Newton, 1960). The model can be used to investigate the effects of both mono-infection and polymicrobial colonization on alveolar bone. Importantly, the molecular mechanism by which the oral microbiota affects bone mass can also be demonstrated using genetically engineered GF mouse models in which selected genes are deleted or overexpressed. The most typical example is monospecies inoculation (of e.g., *P. gingivalis*) at the ligature site to evaluate the effects of infection on alveolar bone loss (Graves et al., 2008). Recently, to better reflect real world conditions, researchers introduced a polymicrobial synergy and dysbiosis model to evaluate the features of periodontal inflammation and alveolar bone loss. That model disclosed that dysbiosis of the periodontal microbiota signifies an imbalance in the relative abundance or influence of microbial species within the ecosystem compared to physiological conditions, leading to sufficient alterations in the host-microbial crosstalk to mediate destructive inflammation and bone loss (Hajishengallis and Lamont, 2012; Bowen et al., 2018). Gao et al. used *P. gingivalis*, *T. denticola*, *T. forsythia*, and *F. nucleatum* as polymicrobial oral inoculum in BALB/cByJ mice, demonstrating that it triggered statistically significant alveolar bone loss, a heightened antibody response, an elevated cytokine immune response, and a statistically significant shift in viral diversity and virome composition (Gao et al., 2020). In addition, mouse models infected with a combination of *P. gingivalis*, *A. actinomycetemcomitans*, *T. denticola*, *T. forsythia*, and *F. nucleatum* (Graves et al., 2008), or *Streptococcus gordonii*, *V. parvula*, and *F. nucleatum* (Marchesan et al., 2018), as well as other bacterial combinations (Polak et al., 2009; Settem et al., 2012; Tan et al., 2014) were developed to investigate the role of oral bacteria in alveolar bone loss *in vivo*. However, these models are imperfect imitations of the human microbial systems. Therefore, the establishment of a humanized gnotobiotic mouse model by transplantation of the oral microbiota into GF mice is necessary and will be a powerful tool for future studies.

Additionally, to study the ecology and functionality of microbial communities in a controlled yet accurate way, synthetic microbial communities have received increasing attention. Synthetic microbial communities are an emerging research field at the intersection of synthetic biology and microbiomes (Estrela et al., 2021). A synthetic microbial community is created by co-culturing two or more microbial populations under well-defined conditions. It can also include genetically engineered organisms. Synthetic microbial communities that retain the key features of their natural counterparts can act as a model system to study the ecology and function of microbial communities with the advantages of low complexity, high controllability, and good stability (Estrela et al., 2021). This approach was originally developed to provide

functional and mechanistic insights into plant-plant microbiome interactions (Liu et al., 2019). Now, it is widely used in biological treatment, focusing on fuel production, high value-added chemical synthesis, and pollutant degradation (Liu et al., 2019). Niu et al. obtained a greatly simplified synthetic bacterial community consisting of seven strains representing the most dominant phyla found in maize roots. By using a selective culture-dependent method to track the abundance of each strain, they discovered that the removal of only *Enterobacter cloacae* led to the complete loss of the community, with *Curtobacterium pusillum* taking over, suggesting that *E. cloacae* is the keystone species in their model ecosystem (Niu et al., 2017). Synthetic microbial ecologies were also proposed as simple and controllable model systems to facilitate bacteria-driven phthalic acid ester biodegradation, providing novel insights for developing effective bioremediation solutions (Hu et al., 2021).

Synthetic microbial communities, combined with systems biology (Estrela et al., 2021) and other experimental technologies, allow the prediction of the ecological stability of the communities and their key species, and thus may further advance the understanding of oral microbiota-alveolar bone relationships. Based on related studies in other fields (Liu et al., 2019), we propose the following workflow for synthetic microbial communities in osteomicrobiology: (1) sample collection: collecting dental plaque or saliva; (2) isolation: isolating single species by colony picking, limiting dilution, and cell sorting; (3) identification: identifying the culture using barcoded sequencing and Sanger sequencing; (4) culture collection: preserving bacteria using glycerol solution, and analyzing the proportion and relative abundance of available strains by comparing the bacterial reservoir constructed using natural samples; (5) correlation analysis: selecting the experimental strains according to the correlation between operational taxonomic unit abundance and phenotype, network analysis, and taxonomy; (6) functional analysis: inoculating single or multiple species into GF mice, and observing the changes in the phenotype and structure of the oral microbial community. It is worth noting that the composition of the microbial communities is critical for the services and functions they provide, and learning how to manipulate such is of great importance. Therefore, the following requirements should be considered when selecting the microbial communities: there must be variation between competing communities in terms of community traits, communities must be able to replicate, and the community trait must be heritable (Buss, 1983). Furthermore, it has recently become possible to automate synthetic microbiome design (Tran and Prindle, 2021). For example, computer-guided design has been used to select optimal microbial consortia that promote the activation of regulatory T cells in a gut microbiota-immune system model (Stein et al., 2018).

## 6 CONCLUSION

Collectively, the evidence indicates a close connection between the oral microbiota and bone health. The oral microbiota plays

important roles in post-natal jawbone development, physiological alveolar bone loss, and, particularly, pathological alveolar bone loss associated with oral diseases such as periodontitis, apical periodontitis, and peri-implantitis. Under pathological conditions, oral pathogenic microbes and microbial dysbiosis induce catabolic disruption of osteoclast-osteoblast-mediated bone remodeling, which leads to alveolar bone loss. RANKL, Notch, and Wnt signaling, as well as the NLRP3 inflammasome are major pathways involved in this process, and osteoimmunity is the key bridge between microbiota and bone. More studies are needed to identify which oral microbes contribute to alveolar bone loss and determine the underlying mechanisms by which oral microbial dysbiosis is related to alveolar bone metabolism. Synthetic microbial communities, combined with a multi-omics approach and mouse models are anticipated to provide new insights into the oral microbiota-alveolar bone relationship. In addition, many factors, such as probiotics, smoking, DM, and the estrogen concentration interact antagonistically and synergistically in influencing oral microbiota-mediated alveolar bone health. With the advances in experimental and clinical studies and the growth of personalized medicine, perhaps, in the future, such factors may be manipulated to alter the composition of the oral microbiome and effectively prevent alveolar bone loss.

Here, we propose use of the term “oral osteomicrobiology” for the rapidly emerging research field of the role of oral microbes in alveolar bone health, bridging the gaps between oral microbiology, immunology, and alveolar bone physiology or alveolar bone pathology. Oral osteomicrobiology refers to investigations on the role of the oral microbiota in alveolar bone health and disease; the mechanisms by which they regulate post-natal jawbone development as well as physiological and pathological alveolar bone loss; and the experimental methods and technologies developed for associated research.

## AUTHOR CONTRIBUTIONS

XC drafted the manuscript. XZ, CL, and XX edited and added valuable insights to the manuscript. All authors contributed to the article and approved the submitted version.

## FUNDING

This study was supported by the National Natural Science Foundation (81771099 to XX, 81870754 to XZ); the Sichuan University Postdoctoral Interdisciplinary Innovation Fund to XC; the Research and Develop Program, West China Hospital of Stomatology Sichuan University to XC (RD-02-201908); and the Research Funding from West China Hospital of Stomatology Sichuan University to XC (RCDWJS2021-16).



## REFERENCES

- Abboud, M., and Papandreou, D. (2019). Gut Microbiome, Probiotics and Bone: An Updated Mini Review. *Open Access. Maced. J. Med. Sci.* 7, 478–481. doi: 10.3889/oamjms.2019.047
- Abiko, Y., Shimizu, N., Yamaguchi, M., Suzuki, H., and Takiguchi, H. (1998). Effect of Aging on Functional Changes of Periodontal Tissue Cells. *Ann. Periodontol.* 3, 350–369. doi: 10.1902/annals.1998.3.1.350
- Akiyama, T., Miyamoto, Y., Yoshimura, K., Yamada, A., Takami, M., Suzawa, T., et al. (2014). *Porphyromonas Gingivalis*-Derived Lysine Gingipain Enhances Osteoclast Differentiation Induced by Tumor Necrosis Factor- $\alpha$  and Interleukin-1 $\beta$  But Suppresses That by Interleukin-17A: Importance of Proteolytic Degradation of Osteoprotegerin by Lysine Gingipain. *J. Biol. Chem.* 289, 15621–15630. doi: 10.1074/jbc.M113.520510
- Albus, E., Sinning, K., Winzer, M., Thiele, S., Baschant, U., Hannemann, A., et al. (2016). Milk Fat Globule-Epidermal Growth Factor 8 (MFG-E8) Is a Novel Anti-Inflammatory Factor in Rheumatoid Arthritis in Mice and Humans. *J. Bone Miner. Res.* 31, 596–605. doi: 10.1002/jbmr.2721
- Amari, K., and Niehl, A. (2020). Nucleic Acid-Mediated PAMP-Triggered Immunity in Plants. *Curr. Opin. Virol.* 42, 32–39. doi: 10.1016/j.coviro.2020.04.003
- Arimatsu, K., Yamada, H., Miyazawa, H., Minagawa, T., Nakajima, M., Ryder, M. I., et al. (2014). Oral Pathobiont Induces Systemic Inflammation and Metabolic Changes Associated With Alteration of Gut Microbiota. *Sci. Rep.* 4, 4828. doi: 10.1038/srep04828
- Baer, P. N., and Newton, W. L. (1960). Studies on Periodontal Disease in the Mouse. 3. The Germ-Free Mouse and Its Conventional Control. *Oral Surg. Oral Med. Oral Pathol.* 13, 1134–1144. doi: 10.1016/0030-4220(60)90330-3
- Bagaitkar, J., Demuth, D. R., Daep, C. A., Renaud, D. E., Pierce, D. L., and Scott, D. A. (2010). Tobacco Upregulates *P. Gingivalis* Fimbrial Proteins Which Induce TLR2 Hyposensitivity. *PLoS One* 5, e9323. doi: 10.1371/journal.pone.0009323
- Bagaitkar, J., Williams, L. R., Renaud, D. E., Bemakanakere, M. R., Martin, M., Scott, D. A., et al. (2009). Tobacco-Induced Alterations to *Porphyromonas Gingivalis*-Host Interactions. *Environ. Microbiol.* 11, 1242–1253. doi: 10.1111/j.1462-2920.2008.01852.x
- Baker, P. J., DuFour, L., Dixon, M., and Roopenian, D. C. (2000). Adhesion Molecule Deficiencies Increase *Porphyromonas Gingivalis*-Induced Alveolar Bone Loss in Mice. *Infect. Immun.* 68, 3103–3107. doi: 10.1128/iai.68.6.3103-3107.2000
- Bamford, C. V., Fenno, J. C., Jenkinson, H. F., and Dymock, D. (2007). The Chymotrypsin-Like Protease Complex of *Treponema Denticola* ATCC 35405 Mediates Fibrinogen Adherence and Degradation. *Infect. Immun.* 75, 4364–4372. doi: 10.1128/IAI.00258-07
- Belibasakis, G. N., and Bostanci, N. (2012). The RANKL-OPG System in Clinical Periodontology. *J. Clin. Periodontol.* 39, 239–248. doi: 10.1111/j.1600-051X.2011.01810.x
- Belibasakis, G. N., Johansson, A., Wang, Y., Chen, C., Kalfas, S., and Lerner, U. H. (2005). The Cytotoxic Distending Toxin Induces Receptor Activator of NF- $\kappa$ B Ligand Expression in Human Gingival Fibroblasts and Periodontal Ligament Cells. *Infect. Immun.* 73, 342–351. doi: 10.1128/IAI.73.1.342-351.2005
- Belibasakis, G. N., and Manoil, D. (2021). Microbial Community-Driven Etiopathogenesis of Peri-Implantitis. *J. Dent. Res.* 100, 21–28. doi: 10.1177/0022034520949851
- Berglundh, T., Zitzmann, N. U., and Donati, M. (2011). Are Peri-Implantitis Lesions Different From Periodontitis Lesions? *J. Clin. Periodontol.* 11, 188–202. doi: 10.1111/j.1600-051X.2010.01672.x
- Beuscher, H. U., Fallon, R. J., and Colten, H. R. (1987). Macrophage Membrane Interleukin 1 Regulates the Expression of Acute Phase Proteins in Human Hepatoma Hep 3B Cells. *J. Immunol.* 139, 1896–1901.
- Bhavsar, N. V., Trivedi, S. R., Dulani, K., Brahmbhatt, N., Shah, S., and Chaudhri, D. (2016). Clinical and Radiographic Evaluation of Effect of Risedronate 5 Mg as an Adjunct to Treatment of Chronic Periodontitis in Postmenopausal Women (12-Month Study). *Osteoporos. Int.* 27, 2611–2619. doi: 10.1007/s00198-016-3577-8
- Bohora, A., and Kokate, S. (2017a). Evaluation of the Role of Probiotics in Endodontic Treatment: A Preliminary Study. *J. Int. Soc. Prev. Community Dent.* 7, 46–51. doi: 10.4103/2231-0762.200710
- Bohora, A. A., and Kokate, S. R. (2017b). Good Bugs vs Bad Bugs: Evaluation of Inhibitory Effect of Selected Probiotics Against *Enterococcus Faecalis*. *J. Contemp. Dent. Pract.* 18, 312–316. doi: 10.5005/jp-journals-10024-2037
- Bostanci, N., Ilgenli, T., Emingil, G., Afacan, B., Han, B., Töz, H., et al. (2007). Gingival Crevicular Fluid Levels of RANKL and OPG in Periodontal Diseases: Implications of Their Relative Ratio. *J. Clin. Periodontol.* 34, 370–376. doi: 10.1111/j.1600-051X.2007.01061.x
- Bousdras, V., Aghabeigi, B., Hopper, C., and Sindet-Pedersen, S. (2006). Management of Apical Bone Loss Around a Mandibular Implant: A Case Report. *Int. J. Oral Maxillofac. Implants* 21, 439–444.
- Bowen, W. H., Burne, R. A., Wu, H., and Koo, H. (2018). Oral Biofilms: Pathogens, Matrix, and Polymicrobial Interactions in Microenvironments. *Trends Microbiol.* 26, 229–242. doi: 10.1016/j.tim.2017.09.008
- Boyce, B. F., and Xing, L. (2008). Functions of RANKL/RANK/OPG in Bone Modeling and Remodeling. *Arch. Biochem. Biophys.* 473, 139–146. doi: 10.1016/j.abb.2008.03.018
- Boyer, E., Leroyer, P., Malherbe, L., Fong, S. B., Loréal, O., Bonnaure Mallet, M., et al. (2020). Oral Dysbiosis Induced by *Porphyromonas Gingivalis* Is Strain-Dependent in Mice. *J. Oral Microbiol.* 12, 1832837. doi: 10.1080/20002297.2020.1832837
- Brennan, R. M., Genco, R. J., Hovey, K. M., Trevisan, M., and Wactawski-Wende, J. (2007). Clinical Attachment Loss, Systemic Bone Density, and Subgingival Calculus in Postmenopausal Women. *J. Periodontol.* 78, 2104–2111. doi: 10.1902/jop.2007.070155
- Brown, L. R., Roth, G. D., Hoover, D., Flanagan, V., Nielsen, A. H., and Werder, A. A. (1969). Alveolar Bone Loss in Leukemic and Nonleukemic Mice. *J. Periodontol.* 40, 725–730. doi: 10.1902/jop.1969.40.12.725
- Brown, J., Wang, H., Hajishengallis, G. N., and Martin, M. (2011). TLR-Signaling Networks: An Integration of Adaptor Molecules, Kinases, and Cross-Talk. *J. Dent. Res.* 90, 417–427. doi: 10.1177/0022034510381264
- Brunetti, G., Colucci, S., Pignataro, P., Coricciati, M., Mori, G., Cirulli, N., et al. (2005). T Cells Support Osteoclastogenesis in an *In Vitro* Model Derived From Human Periodontitis Patients. *J. Periodontol.* 76, 1675–1680. doi: 10.1902/jop.2005.76.10.1675
- Buss, L. W. (1983). Evolution, Development, and the Units of Selection. *Proc. Natl. Acad. Sci. U. S. A.* 80, 1387–1391. doi: 10.1073/pnas.80.5.1387
- Chen, Y., Yang, Q., Lv, C., Chen, Y., Zhao, W., Li, W., et al. (2021). NLRP3 Regulates Alveolar Bone Loss in Ligature-Induced Periodontitis by Promoting Osteoclastic Differentiation. *Cell. Prolif.* 54, e12973. doi: 10.1111/cpr.12973
- Chrcanovic, B. R., Albrektsson, T., and Wennerberg, A. (2014). Diabetes and Oral Implant Failure: A Systematic Review. *J. Dent. Res.* 93, 859–867. doi: 10.1177/0022034514538820
- Cosme-Silva, L., Dal-Fabbro, R., Cintra, L., Ervolino, E., Prado, A., Oliveira, D. P., et al. (2021). Dietary Supplementation With Multi-Strain Formula of Probiotics Modulates Inflammatory and Immunological Markers in Apical Periodontitis. *J. Appl. Oral Sci.* 29, e20210483. doi: 10.1590/1678-7757-2020-0483
- Costalonga, M., and Herzberg, M. C. (2014). The Oral Microbiome and the Immunobiology of Periodontal Disease and Caries. *Immunol. Lett.* 162, 22–38. doi: 10.1016/j.imlet.2014.08.017
- Curtis, M. A., Diaz, P. I., and Van Dyke, T. E. (2020). The Role of the Microbiota in Periodontal Disease. *Periodontol.* 2000 83, 14–25. doi: 10.1111/prd.12296
- D'Amelio, P., Grimaldi, A., Di Bella, S., Brianza, S., Cristofaro, M. A., Tamone, C., et al. (2008). Estrogen Deficiency Increases Osteoclastogenesis Up-Regulating T Cells Activity: A Key Mechanism in Osteoporosis. *Bone* 43, 92–100. doi: 10.1016/j.bone.2008.02.017
- Darveau, R. P., Hajishengallis, G., and Curtis, M. A. (2012). *Porphyromonas Gingivalis* as a Potential Community Activist for Disease. *J. Dent. Res.* 91, 816–820. doi: 10.1177/0022034512453589
- Delima, S. L., McBride, R. K., Preshaw, P. M., Heasman, P. A., and Kumar, P. S. (2010). Response of Subgingival Bacteria to Smoking Cessation. *J. Clin. Microbiol.* 48, 2344–2349. doi: 10.1128/JCM.01821-09
- Del Pinto, R., Pietropaoli, D., Munoz-Aguilera, E., D'Aiuto, F., Czesnikiewicz-Guzik, M., Monaco, A., et al. (2020). Periodontitis and Hypertension: Is the Association Causal? *High Blood Press Cardiovasc. Prev.* 27, 281–289. doi: 10.1007/s40292-020-00392-z
- Djinić Krasavcević, A., Nikolic, N., Mijailovic, I., Carkic, J., Milinkovic, I., Jankovic, S., et al. (2021). Impact of Notch Signalling Molecules and Bone



- Resorption Regulators on Clinical Parameters in Periodontitis. *J. Periodontol. Res.* 56, 131–138. doi: 10.1111/jre.12801
- Duan, X., Wu, T., Xu, X., Chen, D., Mo, A., Lei, Y., et al. (2017). Smoking may Lead to Marginal Bone Loss Around non-Submerged Implants During Bone Healing by Altering Salivary Microbiome: A Prospective Study. *J. Periodontol.* 88, 1297–1308. doi: 10.1902/jop.2017.160808
- Duarte, P. A., Gonçalves, P. F., Sallum, A. W., Sallum, E. A., Casati, M. Z., and Humberto Nociti, F. Jr. (2004). Effect of an Estrogen-Deficient State and its Therapy on Bone Loss Resulting From an Experimental Periodontitis in Rats. *J. Periodontol. Res.* 39, 107–110. doi: 10.1111/j.1600-0765.2004.00714.x
- Duka, M., Eraković, M., Dolicanin, Z., Stefanović, D., and Čolić, M. (2019). Production of Soluble Receptor Activator of Nuclear Factor Kappa-B Ligand and Osteoprotegerin by Apical Periodontitis Cells in Culture and Their Modulation by Cytokines. *Mediators Inflamm.* 2019, 8325380. doi: 10.1155/2019/8325380
- Estrela, S., Sánchez, Á., and Rebollada-Gómez, M. (2021). Multi-Replicated Enrichment Communities as a Model System in Microbial Ecology. *Front. Microbiol.* 12, 657467. doi: 10.3389/fmicb.2021.657467
- Farber, P. A., and Seltzer, S. (1988). Endodontic Microbiology. I. Etiology. *J. Endod.* 14, 363–371. doi: 10.1016/S0099-2399(88)80200-0
- Feres, M., Teles, F., Teles, R., Figueiredo, L. C., and Faveri, M. (2016). The Subgingival Periodontal Microbiota of the Aging Mouth. *Periodontol.* 2000 72, 30–53. doi: 10.1111/prd.12136
- Fine, D. H., Markowitz, K., Fairlie, K., Tischio-Bereski, D., Ferrendiz, J., Furgang, D., et al. (2013). A Consortium of Aggregatibacter Actinomycetemcomitans, Streptococcus Parasanguinis, and Filifactor Alocis Is Present in Sites Prior to Bone Loss in a Longitudinal Study of Localized Aggressive Periodontitis. *J. Clin. Microbiol.* 51, 2850–2861. doi: 10.1128/JCM.00729-13
- Ford, P. J., and Rich, A. M. (2021). Tobacco Use and Oral Health. *Addiction* 116, 3531–3540. doi: 10.1111/add.15513
- Fukada, S. Y., Silva, T. A., Saconato, I. F., Garlet, G. P., Avila-Campos, M. J., Silva, J. S., et al. (2008). iNOS-Derived Nitric Oxide Modulates Infection-Stimulated Bone Loss. *J. Dent. Res.* 87, 1155–1159. doi: 10.1177/154405910808701207
- Ganther, S., Radaic, A., Malone, E., Kamarajan, P., Chang, N. N., Tafolla, C., et al. (2021). Treponema Denticola Dentilisin Triggered TLR2/MyD88 Activation Upregulates a Tissue Destructive Program Involving MMPs via Sp1 in Human Oral Cells. *PLoS Pathog.* 17, e1009311. doi: 10.1371/journal.ppat.1009311
- Gao, L., Kang, M., Zhang, M. J., Reza Sailani, M., Kuraji, R., Martinez, A., et al. (2020). Polymicrobial Periodontal Disease Triggers a Wide Radius of Effect and Unique Virome. *NPJ Biofilms Microbiomes* 6, 10. doi: 10.1038/s41522-020-0120-7
- Graves, D. T., Corrêa, J. D., and Silva, T. A. (2019). The Oral Microbiota Is Modified by Systemic Diseases. *J. Dent. Res.* 98, 148–156. doi: 10.1177/0022034518805739
- Graves, D. T., Fine, D., Teng, Y. T., Van Dyke, T. E., and Hajishengallis, G. (2008). The Use of Rodent Models to Investigate Host-Bacteria Interactions Related to Periodontal Diseases. *J. Clin. Periodontol.* 35, 89–105. doi: 10.1111/j.1600-051X.2007.01172.x
- Guntsch, A., Erler, M., Preshaw, P. M., Sigusch, B. W., Klinger, G., and Glockmann, E. (2006). Effect of Smoking on Crevicular Polymorphonuclear Neutrophil Function in Periodontally Healthy Subjects. *J. Periodontol. Res.* 41, 184–188. doi: 10.1111/j.1600-0765.2005.00852.x
- Gupta, A., Aggarwal, V., Mehta, N., Abraham, D., and Singh, A. (2020). Diabetes Mellitus and the Healing of Periapical Lesions in Root Filled Teeth: A Systematic Review and Meta-Analysis. *Int. Endod. J.* 53, 1472–1484. doi: 10.1111/iej.13366
- Hajishengallis, G. (2014). Immunomicrobial Pathogenesis of Periodontitis: Keystones, Pathobionts, and Host Response. *Trends Immunol.* 35, 3–11. doi: 10.1016/j.it.2013.09.001
- Hajishengallis, G., and Lamont, R. J. (2012). Beyond the Red Complex and Into More Complexity: The Polymicrobial Synergy and Dysbiosis (PSD) Model of Periodontal Disease Etiology. *Mol. Oral Microbiol.* 27, 409–419. doi: 10.1111/j.2041-1014.2012.00663.x
- Hajishengallis, G., and Lamont, R. J. (2021). Polymicrobial Communities in Periodontal Disease: Their Quasi-Organismal Nature and Dialogue With the Host. *Periodontol.* 2000 86, 210–230. doi: 10.1111/prd.12371
- Hajishengallis, G., Liang, S., Payne, M. A., Hashim, A., Jotwani, R., Eskan, M. A., et al. (2011). Low-Abundance Biofilm Species Orchestrates Inflammatory Periodontal Disease Through the Commensal Microbiota and Complement. *Cell Host Microbe* 10, 497–506. doi: 10.1016/j.chom.2011.10.006
- Harris, W. H., and Heaney, R. P. (1969). Skeletal Renewal and Metabolic Bone Disease. *N. Engl. J. Med.* 280, 303–311. doi: 10.1056/NEJM196902062800605
- Hasegawa, M., Yang, K., Hashimoto, M., Park, J. H., Kim, Y. G., Fujimoto, Y., et al. (2006). Differential Release and Distribution of Nod1 and Nod2 Immunostimulatory Molecules Among Bacterial Species and Environments. *J. Biol. Chem.* 281, 29054–29063. doi: 10.1074/jbc.M602638200
- Hathaway-Schrader, J. D., and Novince, C. M. (2021). Maintaining Homeostatic Control of Periodontal Bone Tissue. *Periodontol.* 2000 86, 157–187. doi: 10.1111/prd.12368
- Heyman, O., Horev, Y., Koren, N., Barel, O., Aizenbud, I., Aizenbud, Y., et al. (2020). Niche Specific Microbiota-Dependent and Independent Bone Loss Around Dental Implants and Teeth. *J. Dent. Res.* 99, 1092–1101. doi: 10.1177/0022034520920577
- Hintao, J., Teanpaisan, R., Chongsuvivatwong, V., Ratarasan, C., and Dahlen, G. (2007). The Microbiological Profiles of Saliva, Supragingival and Subgingival Plaque and Dental Caries in Adults With and Without Type 2 Diabetes Mellitus. *Oral Microbiol. Immunol.* 22, 175–181. doi: 10.1111/j.1399-302X.2007.00341
- Horton, J. E., Raisz, L. G., Simmons, H. A., Oppenheim, J. J., and Mergenhagen, S. E. (1972). Bone Resorbing Activity in Supernatant Fluid From Cultured Human Peripheral Blood Leukocytes. *Science* 177, 793–795. doi: 10.1126/science.177.4051.793
- Hotokozaka, H., Sakai, E., Ohara, N., Hotokozaka, Y., Gonzales, C., Matsuo, K., et al. (2007). Molecular Analysis of RANKL-Independent Cell Fusion of Osteoclast-Like Cells Induced by TNF-Alpha, Lipopolysaccharide, or Peptidoglycan. *J. Cell. Biochem.* 101, 122–134. doi: 10.1002/jcb.21167
- Hsu, E., and Pacifici, R. (2018). From Osteoimmunology to Osteomicrobiology: How the Microbiota and the Immune System Regulate Bone. *Calcif. Tissue Int.* 102, 512–521. doi: 10.1007/s00223-017-0321-0
- Huang, X., Yang, X., Ni, J., Xie, B., Liu, Y., Xuan, D., et al. (2015). Hyperglucose Contributes to Periodontitis: Involvement of the NLRP3 Pathway by Engaging the Innate Immunity of Oral Gingival Epithelium. *J. Periodontol.* 86, 327–335. doi: 10.1902/jop.2014.140403
- Huang, W., Yang, S., Shao, J., and Li, Y. P. (2007). Signaling and Transcriptional Regulation in Osteoblast Commitment and Differentiation. *Front. Biosci.* 12, 3068–3092. doi: 10.2741/2296
- Huck, O., Mulhall, H., Rubin, G., Kizelnik, Z., Iyer, R., Perpich, J. D., et al. (2020). Akkermansia Muciniphila Reduces Porphyromonas Gingivalis-Induced Inflammation and Periodontal Bone Destruction. *J. Clin. Periodontol.* 47, 202–212. doi: 10.1111/jcpe.13214
- Hughes, D. E., Dai, A., Tiffée, J. C., Li, H. H., Mundy, G. R., and Boyce, B. F. (1996). Estrogen Promotes Apoptosis of Murine Osteoclasts Mediated by TGF-Beta. *Nat. Med.* 2, 1132–1136. doi: 10.1038/nm1096-1132
- Hujoel, P. P., del Aguila, M. A., DeRouen, T. A., and Bergström, J. (2003). A Hidden Periodontitis Epidemic During the 20th Century? *Community Dent. Oral Epidemiol.* 31, 1–6. doi: 10.1034/j.1600-0528.2003.00061.x
- Human Microbiome Project Consortium. (2012). Structure, Function and Diversity of the Healthy Human Microbiome. *Nature* 486, 207–214. doi: 10.1038/nature11234
- Hung, S. L., Lee, N. G., Chang, L. Y., Chen, Y. T., and Lai, Y. L. (2014). Stimulatory Effects of Glucose and Porphyromonas Gingivalis Lipopolysaccharide on the Secretion of Inflammatory Mediators From Human Macrophages. *J. Periodontol.* 85, 140–149. doi: 10.1902/jop.2013.130009
- Huttner, E. A., Machado, D. C., de Oliveira, R. B., Antunes, A. G., and Hebling, E. (2009). Effects of Human Aging on Periodontal Tissues. *Spec. Care Dentist.* 29, 149–155. doi: 10.1111/j.1754-4505.2009.00082.x
- Hu, R., Zhao, H., Xu, X., Wang, Z., Yu, K., Shu, L., et al. (2021). Bacteria-Driven Phthalic Acid Ester Biodegradation: Current Status and Emerging Opportunities. *Environ. Int.* 154, 106560. doi: 10.1016/j.envint.2021.106560
- Irie, K., Tomofuji, T., Ekuni, D., Fukuhara, D., Uchida, Y., Kataoka, K., et al. (2018). Age-Related Changes of CD4+ T Cell Migration and Cytokine Expression in Germ-Free and SPF Mice Periodontium. *Arch. Oral Biol.* 87, 72–78. doi: 10.1016/j.archoralbio.2017.12.007
- Jakovljevic, A., Miletic, M., Nikolic, N., Beljic-Ivanovic, K., Andric, M., and Milasin, J. (2019). Notch Signaling Pathway Mediates Alveolar Bone Resorption in Apical Periodontitis. *Med. Hypotheses* 124, 87–90. doi: 10.1016/j.mehy.2019.02.018

- Janda, J. M., and Abbott, S. L. (2007). 16s rRNA Gene Sequencing for Bacterial Identification in the Diagnostic Laboratory: Pluses, Perils, and Pitfalls. *J. Clin. Microbiol.* 45, 2761–2764. doi: 10.1128/JCM.01228-07
- Jia, X., Jia, L., Mo, L., Yuan, S., Zheng, X., He, J., et al. (2019). Berberine Ameliorates Periodontal Bone Loss by Regulating Gut Microbiota. *J. Dent. Res.* 98, 107–116. doi: 10.1177/0022034518797275
- Jiao, Y., Hasegawa, M., and Inohara, N. (2014). The Role of Oral Pathobionts in Dysbiosis During Periodontitis Development. *J. Dent. Res.* 93, 539–546. doi: 10.1177/0022034514528212
- Jia, L., Tu, Y., Jia, X., Du, Q., Zheng, X., Yuan, Q., et al. (2021). Probiotics Ameliorate Alveolar Bone Loss by Regulating Gut Microbiota. *Cell. Prolif.* 54, e13075. doi: 10.1111/cpr.13075
- Jun, H. K., Lee, S. H., Lee, H. R., and Choi, B. K. (2012). Integrin  $\alpha 5 \beta 1$  Activates the NLRP3 Inflammasome by Direct Interaction With a Bacterial Surface Protein. *Immunity* 36, 755–768. doi: 10.1016/j.immuni.2012.05.002
- Kanzaki, H., Chiba, M., Shimizu, Y., and Mitani, H. (2002). Periodontal Ligament Cells Under Mechanical Stress Induce Osteoclastogenesis by Receptor Activator of Nuclear Factor KappaB Ligand Up-Regulation via Prostaglandin E2 Synthesis. *J. Bone Miner. Res.* 17, 210–220. doi: 10.1359/jbmr.2002.17.2.210
- Kassem, A., Henning, P., Lundberg, P., Souza, P. P., Lindholm, C., and Lerner, U. H. (2015). *Porphyromonas Gingivalis* Stimulates Bone Resorption by Enhancing RANKL (Receptor Activator of NF- $\kappa$ B Ligand) Through Activation of Toll-Like Receptor 2 in Osteoblasts. *J. Biol. Chem.* 290, 20147–20158. doi: 10.1074/jbc.M115.655787
- Kawahara, Y., Kaneko, T., Yoshinaga, Y., Arita, Y., Nakamura, K., Koga, C., et al. (2020). Effects of Sulfonyleureas on Periodontopathic Bacteria-Induced Inflammation. *J. Dent. Res.* 99, 830–838. doi: 10.1177/0022034520913250
- Kawai, T., Matsuyama, T., Hosokawa, Y., Makihiro, S., Seki, M., Karimbux, N. Y., et al. (2006). B and T Lymphocytes Are the Primary Sources of RANKL in the Bone Resorptive Lesion of Periodontal Disease. *Am. J. Pathol.* 169, 987–998. doi: 10.2353/ajpath.2006.060180
- Kensara, A., Hefni, E., Williams, M. A., Saito, H., Mongodin, E., and Masri, R. (2021). Microbiological Profile and Human Immune Response Associated With Peri-Implantitis: A Systematic Review. *J. Prosthodont.* 30, 210–234. doi: 10.1111/jopr.13270
- Khan, M. S., Alasqah, M., Alammari, L. M., and Alkhaibari, Y. (2020). Obesity and Periodontal Disease: A Review. *J. Family Med. Prim. Care* 9, 2650–2653. doi: 10.4103/jfmpc.jfmpc\_283\_20
- Khosla, S. (2001). Minireview: The OPG/RANKL/RANK System. *Endocrinology* 142, 5050–5055. doi: 10.1210/endo.142.12.8536
- Kim, M., Jun, H. K., Choi, B. K., Cha, J. H., and Yoo, Y. J. (2010). Td92, an Outer Membrane Protein of *Treponema Denticola*, Induces Osteoclastogenesis via Prostaglandin E(2)-Mediated RANKL/osteoprotegerin Regulation. *J. Periodontol. Res.* 45, 772–779. doi: 10.1111/j.1600-0765.2010.01298.x
- Kitamoto, S., Nagao-Kitamoto, H., Hein, R., Schmidt, T. M., and Kamada, N. (2020). The Bacterial Connection Between the Oral Cavity and the Gut Diseases. *J. Dent. Res.* 99, 1021–1029. doi: 10.1177/0022034520924633
- Kobayashi, R., Ogawa, Y., Hashizume-Takizawa, T., and Kurita-Ochiai, T. (2020). Oral Bacteria Affect the Gut Microbiome and Intestinal Immunity. *Pathog. Dis.* 78, 1–9. doi: 10.1093/femspd/ftaa024
- Koide, M., Kobayashi, Y., Ninomiya, T., Nakamura, M., Yasuda, H., Arai, Y., et al. (2013). Osteoprotegerin-Deficient Male Mice as a Model for Severe Alveolar Bone Loss: Comparison With RANKL-Overexpressing Transgenic Male Mice. *Endocrinology* 154, 773–782. doi: 10.1210/en.2012-1928
- Komatsu, K., Shiba, T., Takeuchi, Y., Watanabe, T., Koyanagi, T., Nemoto, T., et al. (2020). Discriminating Microbial Community Structure Between Peri-Implantitis and Periodontitis With Integrated Metagenomic, Metatranscriptomic, and Network Analysis. *Front. Cell. Infect. Microbiol.* 10, 596490. doi: 10.3389/fcimb.2020.596490
- Kumar, G., Tewari, S., Tagg, J., Chikindas, M. L., Popov, I. V., and Tiwari, S. K. (2021). Can Probiotics Emerge as Effective Therapeutic Agents in Apical Periodontitis? A Review. *Probiotics Antimicrob. Proteins* 13, 299–314. doi: 10.1007/s12602-021-09750-2
- Lamkanfi, M., and Dixit, V. M. (2014). Mechanisms and Functions of Inflammasomes. *Cell* 157, 1013–1022. doi: 10.1016/j.cell.2014.04.007
- LaMonte, M. J., Andrews, C. A., Hovey, K. M., Buck, M. J., Li, L., McSkimming, D. L., et al. (2021). Subgingival Microbiome Is Associated With Alveolar Bone Loss Measured 5-Years Later in Postmenopausal Women. *J. Periodontol.* 92, 648–661. doi: 10.1002/JPER.20-0445
- Lamont, R. J., Koo, H., and Hajishengallis, G. (2018). The Oral Microbiota: Dynamic Communities and Host Interactions. *Nat. Rev. Microbiol.* 16, 745–759. doi: 10.1038/s41579-018-0089-x
- Lerner, U. H. (2006). Inflammation-Induced Bone Remodeling in Periodontal Disease and the Influence of Post-Menopausal Osteoporosis. *J. Dent. Res.* 85, 596–607. doi: 10.1177/154405910608500704
- Levi, Y., Picchi, R. N., Silva, E., Bremer Neto, H., Prado, R., Neves, A. P., et al. (2019). Probiotic Administration Increases Mandibular Bone Mineral Density on Rats Exposed to Cigarette Smoke Inhalation. *Braz. Dent. J.* 30, 634–640. doi: 10.1590/0103-6440201802862
- Liang, S., Hosur, K. B., Domon, H., and Hajishengallis, G. (2010). Periodontal Inflammation and Bone Loss in Aged Mice. *J. Periodontol. Res.* 45, 574–578. doi: 10.1111/j.1600-0765.2009.01245.x
- Lima, S. M., Grisi, D. C., Kogawa, E. M., Franco, O. L., Peixoto, V. C., Gonçalves-Júnior, J. F., et al. (2013). Diabetes Mellitus and Inflammatory Pulpal and Periapical Disease: A Review. *Int. Endod. J.* 46, 700–709. doi: 10.1111/iej.12072
- Lin, X., Han, X., Kawai, T., and Taubman, M. A. (2011). Antibody to Receptor Activator of NF- $\kappa$ B Ligand Ameliorates T Cell-Mediated Periodontal Bone Resorption. *Infect. Immun.* 79, 911–917. doi: 10.1128/IAI.00944-10
- Liu, Y. X., Qin, Y., and Bai, Y. (2019). Reductionist Synthetic Community Approaches in Root Microbiome Research. *Curr. Opin. Microbiol.* 49, 97–102. doi: 10.1016/j.mib.2019.10.010
- López-Marcos, J. F., García-Valle, S., and García-Iglesias, A. A. (2005). Periodontal Aspects in Menopausal Women Undergoing Hormone Replacement Therapy. *Med. Oral Patol. Oral Cir. Bucal* 10, 132–141.
- Luciano, M. P., da Silva, R., de Sousa Pereira, A. P., Romualdo, P. C., Feres, M., de Queiroz, A. M., et al. (2021). Alteration of the Oral Microbiota may be a Responsible Factor, Along With Estrogen Deficiency, by the Development of Larger Periapical Lesions. *Clin. Oral. Investig.* 25, 3651–3662. doi: 10.1007/s00784-020-03688-5
- Maeda, K., Kobayashi, Y., Udagawa, N., Uehara, S., Ishihara, A., Mizoguchi, T., et al. (2012). Wnt5a-Ror2 Signaling Between Osteoblast-Lineage Cells and Osteoclast Precursors Enhances Osteoclastogenesis. *Nat. Med.* 18, 405–412. doi: 10.1038/nm.2653
- Maekawa, T., and Hajishengallis, G. (2014). Topical Treatment With Probiotic *Lactobacillus Brevis* CD2 Inhibits Experimental Periodontal Inflammation and Bone Loss. *J. Periodontol. Res.* 49, 785–791. doi: 10.1111/jre.12164
- Maekawa, T., Kulwattanaporn, P., Hosur, K., Domon, H., Oda, M., Terao, Y., et al. (2017). Differential Expression and Roles of Secreted Frizzled-Related Protein 5 and the Wingless Homolog Wnt5a in Periodontitis. *J. Dent. Res.* 96, 571–577. doi: 10.1177/0022034516687248
- Mahamed, D. A., Marleau, A., Alnaeli, M., Singh, B., Zhang, X., Penninger, J. M., et al. (2005). G(-) Anaerobes-Reactive CD4+ T-Cells Trigger RANKL-Mediated Enhanced Alveolar Bone Loss in Diabetic NOD Mice. *Diabetes* 54, 1477–1486. doi: 10.2337/diabetes.54.5.1477
- Manolagas, S. C., O'Brien, C. A., and Almeida, M. (2013). The Role of Estrogen and Androgen Receptors in Bone Health and Disease. *Nat. Rev. Endocrinol.* 9, 699–712. doi: 10.1038/nrendo.2013.179
- Marchesan, J., Girnary, M. S., Jing, L., Miao, M. Z., Zhang, S., Sun, L., et al. (2018). An Experimental Murine Model to Study Periodontitis. *Nat. Protoc.* 13, 2247–2267. doi: 10.1038/s41596-018-0035-4
- Markle, J. G., Frank, D. N., Mortin-Toth, S., Robertson, C. E., Feazel, L. M., Rolfe-Kampczyk, U., et al. (2013). Sex Differences in the Gut Microbiome Drive Hormone-Dependent Regulation of Autoimmunity. *Science* 339 (6123), 1084–1088. doi: 10.1126/science.1233521
- Márton, I. J., and Kiss, C. (2000). Protective and Destructive Immune Reactions in Apical Periodontitis. *Oral Microbiol. Immunol.* 15, 139–150. doi: 10.1034/j.1399-302x.2000.150301.x
- Masumoto, J., Yang, K., Varambally, S., Hasegawa, M., Tomlins, S. A., Qiu, S., et al. (2006). Nod1 Acts as an Intracellular Receptor to Stimulate Chemokine Production and Neutrophil Recruitment *In Vivo*. *J. Exp. Med.* 203, 203–213. doi: 10.1084/jem.20051229
- Matthews, J. B., Chen, F. M., Milward, M. R., Wright, H. J., Carter, K., McDonagh, A., et al. (2011). Effect of Nicotine, Cotinine and Cigarette Smoke Extract on the Neutrophil Respiratory Burst. *J. Clin. Periodontol.* 38, 208–218. doi: 10.1111/j.1600-051X.2010.01676.x

- Meghji, S., Henderson, B., Nair, S., and Wilson, M. (1992). Inhibition of Bone DNA and Collagen Production by Surface-Associated Material From Bacteria Implicated in the Pathology of Periodontal Disease. *J. Periodontol.* 63, 736–742. doi: 10.1902/jop.1992.63.9.736
- Menu, P., and Vince, J. E. (2011). The NLRP3 Inflammasome in Health and Disease: The Good, the Bad and the Ugly. *Clin. Exp. Immunol.* 166, 1–15. doi: 10.1111/j.1365-2249.2011.04440.x
- Mishra, S., Rath, S., and Mohanty, N. (2020). Probiotics-A Complete Oral Healthcare Package. *J. Integr. Med.* 18, 462–469. doi: 10.1016/j.joim.2020.08.005
- Nagasawa, T., Kiji, M., Yashiro, R., Hormdee, D., Lu, H., Kunze, M., et al. (2007). Roles of Receptor Activator of Nuclear factor-kappaB Ligand (RANKL) and Osteoprotegerin in Periodontal Health and Disease. *Periodontol.* 2000 43, 65–84. doi: 10.1111/j.1600-0757.2006.00185.x
- Nair, P. N. (1997). Apical Periodontitis: A Dynamic Encounter Between Root Canal Infection and Host Response. *Periodontol.* 2000 13, 121–148. doi: 10.1111/j.1600-0757.1997.tb00098.x
- Nakashima, T., Hayashi, M., Fukunaga, T., Kurata, K., Oh-Hora, M., Feng, J. Q., et al. (2011). Evidence for Osteocyte Regulation of Bone Homeostasis Through RANKL Expression. *Nat. Med.* 17, 1231–1234. doi: 10.1038/nm.2452
- Nakashima, T., Kobayashi, Y., Yamasaki, S., Kawakami, A., Eguchi, K., Sasaki, H., et al. (2000). Protein Expression and Functional Difference of Membrane-Bound and Soluble Receptor Activator of NF-KappaB Ligand: Modulation of the Expression by Osteotropic Factors and Cytokines. *Biochem. Biophys. Res. Commun.* 275, 768–775. doi: 10.1006/bbrc.2000.3379
- Nanbara, H., Wara-aswapati, N., Nagasawa, T., Yoshida, Y., Yashiro, R., Bando, Y., et al. (2012). Modulation of Wnt5a Expression by Periodontopathic Bacteria. *PLoS One* 7, e34434. doi: 10.1371/journal.pone.0034434
- Napimoga, M. H., Nametala, C., da Silva, F. L., Miranda, T. S., Bossonaro, J. P., Demasi, A. P., et al. (2014). Involvement of the Wnt- $\beta$ -Catenin Signalling Antagonists, Sclerostin and Dickkopf-Related Protein 1, in Chronic Periodontitis. *J. Clin. Periodontol.* 41, 550–557. doi: 10.1111/jcpe.12245
- Naseri, R., Yaghini, J., and Feizi, A. (2020). Levels of Smoking and Dental Implants Failure: A Systematic Review and Meta-Analysis. *J. Clin. Periodontol.* 47, 518–528. doi: 10.1111/jcpe.13257
- Nguyen-Hieu, T., Borghetti, A., and Aboudharam, G. (2012). Peri-Implantitis: From Diagnosis to Therapeutics. *J. Investig. Clin. Dent.* 3, 79–94. doi: 10.1111/j.2041-1626.2012.00116.x
- Nishimura, F., Terranova, V. P., Braithwaite, M., Orman, R., Ohyama, H., Mineshiba, J., et al. (1997). Comparison of *In Vitro* Proliferative Capacity of Human Periodontal Ligament Cells in Juvenile and Aged Donors. *Oral Dis.* 3, 162–166. doi: 10.1111/j.1601-0825.1997.tb00029.x
- Niu, B., Paulson, J. N., Zheng, X., and Kolter, R. (2017). Simplified and Representative Bacterial Community of Maize Roots. *Proc. Natl. Acad. Sci. U. S. A.* 114, E2450–E2459. doi: 10.1073/pnas.1616148114
- Novince, C. M., Whitlow, C. R., Aartun, J. D., Hathaway, J. D., Poulides, N., Chavez, M. B., et al. (2017). Commensal Gut Microbiota Immunomodulatory Actions in Bone Marrow and Liver Have Catabolic Effects on Skeletal Homeostasis in Health. *Sci. Rep.* 7, 5747. doi: 10.1038/s41598-017-06126-x
- O'Leary, C. E., Schneider, C., and Locksley, R. M. (2019). Tuft Cells-Systemically Dispersed Sensory Epithelia Integrating Immune and Neural Circuitry. *Annu. Rev. Immunol.* 37, 47–72. doi: 10.1146/annurev-immunol-042718-041505
- Ohlsson, C., and Sjögren, K. (2015). Effects of the Gut Microbiota on Bone Mass. *Trends Endocrinol. Metab.* 26, 69–74. doi: 10.1016/j.tem.2014.11.004
- Ohlsson, C., and Sjögren, K. (2018). Osteomicrobiology: A New Cross-Disciplinary Research Field. *Calcif. Tissue Int.* 102, 426–432. doi: 10.1007/s00223-017-0336-6
- Okamura, H., Yamaguchi, M., and Abiko, Y. (1999). Enhancement of Lipopolysaccharide-Stimulated PGE2 and IL-1 $\beta$  Production in Gingival Fibroblast Cells From Old Rats. *Exp. Gerontol.* 34, 379–392. doi: 10.1016/s0531-5565(99)00006-6
- Oliveira, L. F., Salvador, S. L., Silva, P. H., Furlaneto, F. A., Figueiredo, L., Casarin, R., et al. (2017). Benefits of Bifidobacterium Animalis Subsp. Lactis Probiotic in Experimental Periodontitis. *J. Periodontol.* 88, 197–208. doi: 10.1902/jop.2016.160217
- Orstavik, D. (1996). Time-Course and Risk Analyses of the Development and Healing of Chronic Apical Periodontitis in Man. *Int. Endod. J.* 29, 150–155. doi: 10.1111/j.1365-2591.1996.tb01361.x
- Oz, H. S., and Ebersole, J. L. (2010). A Novel Murine Model for Chronic Inflammatory Alveolar Bone Loss. *J. Periodontol. Res.* 45, 94–99. doi: 10.1111/j.1600-0765.2009.01207.x
- Pakvasa, M., Haravu, P., Boachie-Mensah, M., Jones, A., Coalson, E., Liao, J., et al. (2020). Notch Signaling: Its Essential Roles in Bone and Craniofacial Development. *Genes Dis.* 8, 8–24. doi: 10.1016/j.gendis.2020.04.006
- Pan, H., Guo, R., Ju, Y., Wang, Q., Zhu, J., Xie, Y., et al. (2019). A Single Bacterium Restores the Microbiome Dysbiosis to Protect Bones From Destruction in a Rat Model of Rheumatoid Arthritis. *Microbiome* 7, 107. doi: 10.1186/s40168-019-0719-1
- Paster, B. J., Olsen, I., Aas, J. A., and Dewhirst, F. E. (2006). The Breadth of Bacterial Diversity in the Human Periodontal Pocket and Other Oral Sites. *Periodontol.* 2000 42, 80–87. doi: 10.1111/j.1600-0757.2006.00174.x
- Paula-Silva, F., Ribeiro-Santos, F. R., Petean, I., Manfrin Arnez, M. F., Almeida-Junior, L. A., Carvalho, F. K., et al. (2020). Root Canal Contamination or Exposure to Lipopolysaccharide Differentially Modulate Prostaglandin E2 and Leukotriene B4 Signaling in Apical Periodontitis. *J. Appl. Oral Sci.* 28, e20190699. doi: 10.1590/1678-7757-2019-0699
- Pazzini, C. A., Pereira, L. J., da Silva, T. A., Montalvany-Antonucci, C. C., Macari, S., Marques, L. S., et al. (2017). Probiotic Consumption Decreases the Number of Osteoclasts During Orthodontic Movement in Mice. *Arch. Oral Biol.* 79, 30–34. doi: 10.1016/j.archoralbio.2017.02.017
- Penoni, D. C., Fidalgo, T. K., Torres, S. R., Varela, V. M., Masterson, D., Leão, A. T., et al. (2017). Bone Density and Clinical Periodontal Attachment in Postmenopausal Women: A Systematic Review and Meta-Analysis. *J. Dent. Res.* 96, 261–269. doi: 10.1177/0022034516682017
- Philips, A., Stolarek, I., Handschuh, L., Nowis, K., Juras, A., Trzciński, D., et al. (2020). Analysis of Oral Microbiome From Fossil Human Remains Revealed the Significant Differences in Virulence Factors of Modern and Ancient *Tannerella Forsythia*. *BMC Genomics* 21, 402. doi: 10.1186/s12864-020-06810-9
- Polak, D., Wilensky, A., Shapira, L., Halabi, A., Goldstein, D., Weiss, E. I., et al. (2009). Mouse Model of Experimental Periodontitis Induced by *Porphyromonas Gingivalis/Fusobacterium Nucleatum* Infection: Bone Loss and Host Response. *J. Clin. Periodontol.* 36, 406–410. doi: 10.1111/j.1600-051X.2009.01393.x
- Pradhan-Palikhe, P., Mäntylä, P., Paju, S., Buhlin, K., Persson, G. R., Nieminen, M. S., et al. (2013). Subgingival Bacterial Burden in Relation to Clinical and Radiographic Periodontal Parameters. *J. Periodontol.* 84, 1809–1817. doi: 10.1902/jop.2013.120537
- Preshaw, P. M., Foster, N., and Taylor, J. J. (2007). Cross-Susceptibility Between Periodontal Disease and Type 2 Diabetes Mellitus: An Immunobiological Perspective. *Periodontol.* 2000 45, 138–157. doi: 10.1111/j.1600-0757.2007.00221.x
- Qiao, S., Wu, D., Wang, M., Qian, S., Zhu, Y., Shi, J., et al. (2020). Oral Microbial Profile Variation During Canine Ligature-Induced Peri-Implantitis Development. *BMC Microbiol.* 20, 293. doi: 10.1186/s12866-020-01982-6
- Radaic, A., and Kapila, Y. L. (2021). The Oralome and its Dysbiosis: New Insights Into Oral Microbiome-Host Interactions. *Comput. Struct. Biotechnol. J.* 19, 1335–1360. doi: 10.1016/j.csbj.2021.02.010
- Rho, J., Takami, M., and Choi, Y. (2004). Osteoimmunology: Interactions of the Immune and Skeletal Systems. *Mol. Cells* 17, 1–9.
- Riggs, B. L. (2000). The Mechanisms of Estrogen Regulation of Bone Resorption. *J. Clin. Invest.* 106, 1203–1204. doi: 10.1172/JCI11468
- Rocha, F., Delitto, A. E., de Souza, J., González-Maldonado, L. A., Wallet, S. M., and Rossa Junior, C. (2020). Relevance of Caspase-1 and Nlrp3 Inflammasome on Inflammatory Bone Resorption in a Murine Model of Periodontitis. *Sci. Rep.* 10, 7823. doi: 10.1038/s41598-020-64685-y
- Rogers, J. E., Li, F., Coatney, D. D., Rossa, C., Bronson, P., Krieder, J. M., et al. (2007). *Actinobacillus Actinomycetemcomitans* Lipopolysaccharide-Mediated Experimental Bone Loss Model for Aggressive Periodontitis. *J. Periodontol.* 78, 550–558. doi: 10.1902/jop.2007.060321
- Ronderos, M., Jacobs, D. R., Himes, J. H., and Pihlstrom, B. L. (2000). Associations of Periodontal Disease With Femoral Bone Mineral Density and Estrogen Replacement Therapy: Cross-Sectional Evaluation of US Adults From NHANES III. *J. Clin. Periodontol.* 27, 778–786. doi: 10.1034/j.1600-051x.2000.027010778.x
- Said, H. S., Suda, W., Nakagome, S., Chinen, H., Oshima, K., Kim, S., et al. (2014). Dysbiosis of Salivary Microbiota in Inflammatory Bowel Disease and Its



- Association With Oral Immunological Biomarkers. *DNA Res.* 21, 15–25. doi: 10.1093/dnares/dst037
- Saito, T., Ishihara, K., Kato, T., and Okuda, K. (1997). Cloning, Expression, and Sequencing of a Protease Gene From *Bacteroides Forsythus* ATCC 43037 in *Escherichia Coli*. *Infect. Immun.* 65, 4888–4891. doi: 10.1128/IAI.65.11.4888-4891.1997
- Sanz-Martin, I., Doolittle-Hall, J., Teles, R. P., Patel, M., Belibasakis, G. N., Hämmerle, C., et al. (2017). Exploring the Microbiome of Healthy and Diseased Peri-Implant Sites Using Illumina Sequencing. *J. Clin. Periodontol.* 44, 1274–1284. doi: 10.1111/jcpe.12788
- Sasso, G., Florencio-Silva, R., da Fonseca, C., Cezar, L. C., Carbonel, A., Gil, C. D., et al. (2020). Effects of Estrogen Deficiency Followed by Streptozotocin-Induced Diabetes on Periodontal Tissues of Female Rats. *J. Mol. Histol.* 51, 353–365. doi: 10.1007/s10735-020-09885-6
- Sato, K., Takahashi, N., Kato, T., Matsuda, Y., Yokoji, M., Yamada, M., et al. (2017). Aggravation of Collagen-Induced Arthritis by Orally Administered *Porphyromonas Gingivalis* Through Modulation of the Gut Microbiota and Gut Immune System. *Sci. Rep.* 7, 6955. doi: 10.1038/s41598-017-07196-7
- Sato, K., Yokoji, M., Yamada, M., Nakajima, T., and Yamazaki, K. (2018). An Orally Administered Oral Pathobiont and Commensal Have Comparable and Innocuous Systemic Effects in Germ-Free Mice. *J. Periodontol. Res.* 53, 950–960. doi: 10.1111/jre.12593
- Schepper, J. D., Collins, F., Rios-Arce, N. D., Kang, H. J., Schaefer, L., Gardinier, J. D., et al. (2020). Involvement of the Gut Microbiota and Barrier Function in Glucocorticoid-Induced Osteoporosis. *J. Bone Miner. Res.* 35, 801–820. doi: 10.1002/jbmr.3947
- Schwarzer, M., Makki, K., Storelli, G., Machuca-Gayet, I., Srutkova, D., Hermanova, P., et al. (2016). *Lactobacillus Plantarum* Strain Maintains Growth of Infant Mice During Chronic Undernutrition. *Science* 351, 854–857. doi: 10.1126/science.aad8588
- Sender, R., Fuchs, S., and Milo, R. (2016). Revised Estimates for the Number of Human and Bacteria Cells in the Body. *PLoS Biol.* 14, e1002533. doi: 10.1371/journal.pbio.1002533
- Settem, R. P., El-Hassan, A. T., Honma, K., Stafford, G. P., and Sharma, A. (2012). *Fusobacterium Nucleatum* and *Tannerella Forsythia* Induce Synergistic Alveolar Bone Loss in a Mouse Periodontitis Model. *Infect. Immun.* 80, 2436–2443. doi: 10.1128/IAI.06276-11
- Shchipkova, A. Y., Nagaraja, H. N., and Kumar, P. S. (2010). Subgingival Microbial Profiles of Smokers With Periodontitis. *J. Dent. Res.* 89, 1247–1253. doi: 10.1177/0022034510377203
- Sjögren, K., Engdahl, C., Henning, P., Lerner, U. H., Tremaroli, V., Lagerquist, M. K., et al. (2012). The Gut Microbiota Regulates Bone Mass in Mice. *J. Bone Miner. Res.* 27, 1357–1367. doi: 10.1002/jbmr.1588
- Skokos, D., and Nussenzweig, M. C. (2007). CD8- DCs Induce IL-12-Independent Th1 Differentiation Through Delta 4 Notch-Like Ligand in Response to Bacterial LPS. *J. Exp. Med.* 204, 1525–1531. doi: 10.1084/jem.20062305
- Sosroseno, W., Bird, P. S., and Seymour, G. J. (2009). Nitric Oxide Production by a Human Osteoblast Cell Line Stimulated With *Aggregatibacter Actinomycetemcomitans* Lipopolysaccharide. *Oral Microbiol. Immunol.* 24, 50–55. doi: 10.1111/j.1399-302X.2008.00475.x
- Stashenko, P., Wang, C. Y., Tani-Ishii, N., and Yu, S. M. (1994). Pathogenesis of Induced Rat Periapical Lesions. *Oral Surg. Oral Med. Oral Pathol.* 78, 494–502. doi: 10.1016/0030-4220(94)90044-2
- Stein, R. R., Tanoue, T., Szabady, R. L., Bhattarai, S. K., Olle, B., Norman, J. M., et al. (2018). Computer-Guided Design of Optimal Microbial Consortia for Immune System Modulation. *Elife* 7, e30916. doi: 10.7554/eLife.30916
- Stokman, M. A., van Winkelhoff, A. J., Vissink, A., Spijkervet, F. K., and Raghoobar, G. M. (2017). Bacterial Colonization of the Peri-Implant Sulcus in Dentate Patients: A Prospective Observational Study. *Clin. Oral Investig.* 21, 717–724. doi: 10.1007/s00784-016-1941-x
- Straka, M., Straka-Trapezanlidis, M., Deglovic, J., and Varga, I. (2015). Periodontitis and Osteoporosis. *Neuro Endocrinol. Lett.* 36, 401–406.
- Sundqvist, G. (1994). Taxonomy, Ecology, and Pathogenicity of the Root Canal Flora. *Oral Surg. Oral Med. Oral Pathol.* 78, 522–530. doi: 10.1016/0030-4220(94)90047-7
- Sundqvist, G., Johansson, E., and Sjögren, U. (1989). Prevalence of Black-Pigmented Bacteroides Species in Root Canal Infections. *J. Endod.* 15, 13–19. doi: 10.1016/S0099-2399(89)80092-5
- Suresh, L., and Radfar, L. (2004). Pregnancy and Lactation. *Oral. Surg. Oral. Med. Oral. Pathol. Oral. Radiol. Endod.* 97, 672–682. doi: 10.1016/S1079210404000861
- Tachikake-Kuramoto, M., Suzuki, J., Wang, Y., Mitsuhashi, C., and Kozai, K. (2014). Lipopolysaccharide Derived From *Aggregatibacter Actinomycetemcomitans* Inhibits Differentiation of Osteoblasts. *Pediatr. Dent. J.* 24, 83–88. doi: 10.1016/j.pdj.2014.03.004
- Takeuchi, O., and Akira, S. (2010). Pattern Recognition Receptors and Inflammation. *Cell* 140, 805–820. doi: 10.1016/j.cell.2010.01.022
- Tang, J., Wu, T., Xiong, J., Su, Y., Zhang, C., Wang, S., et al. (2015). *Porphyromonas Gingivalis* Lipopolysaccharides Regulate Functions of Bone Marrow Mesenchymal Stem Cells. *Cell. Prolif.* 48, 239–248. doi: 10.1111/cpr.12173
- Tang, Y., Zhou, X., Gao, B., Xu, X., Sun, J., Cheng, L., et al. (2014). Modulation of Wnt/ $\beta$ -Catenin Signaling Attenuates Periapical Bone Lesions. *J. Dent. Res.* 93, 175–182. doi: 10.1177/0022034513512507
- Tan, X., Huang, D., Zhou, W., Yan, L., Yue, J., Lu, W., et al. (2018). Dickkopf-1 may Regulate Bone Coupling by Attenuating Wnt/ $\beta$ -Catenin Signaling in Chronic Apical Periodontitis. *Arch. Oral Biol.* 86, 94–100. doi: 10.1016/j.archoralbio.2017.11.012
- Tani-Ishii, N., Wang, C. Y., Tanner, A., and Stashenko, P. (1994). Changes in Root Canal Microbiota During the Development of Rat Periapical Lesions. *Oral Microbiol. Immunol.* 9, 129–135. doi: 10.1111/j.1399-302x.1994.tb00048.x
- Tan, K. H., Seers, C. A., Dashper, S. G., Mitchell, H. L., Pyke, J. S., Meuric, V., et al. (2014). *Porphyromonas Gingivalis* and *Treponema Denticola* Exhibit Metabolic Symbioses. *PLoS Pathog.* 10, e1003955. doi: 10.1371/journal.ppat.1003955
- Tarkkila, L., Kari, K., Furuholm, J., Tiitinen, A., and Meurman, J. H. (2010). Periodontal Disease-Associated Micro-Organisms in Peri-Menopausal and Post-Menopausal Women Using or Not Using Hormone Replacement Therapy. A Two-Year Follow-Up Study. *BMC Oral Health* 10:10. doi: 10.1186/1472-6831-10-10
- Tatakis, D. N., Schneeberger, G., and Dziak, R. (1988). Recombinant Interleukin-1 Stimulates Prostaglandin E2 Production by Osteoblastic Cells: Synergy With Parathyroid Hormone. *Calcif. Tissue Int.* 42, 358–362. doi: 10.1007/BF02556353
- Tompkins, K. A. (2016). The Osteoimmunology of Alveolar Bone Loss. *Connect. Tissue Res.* 57, 69–90. doi: 10.3109/03008207.2016.1140152
- Tran, P., and Prindle, A. (2021). Synthetic Biology in Biofilms: Tools, Challenges, and Opportunities. *Biotechnol. Prog.* 9, e3123. doi: 10.1002/btpr.3123
- Tsao, P. N., Wei, S. C., Huang, M. T., Lee, M. C., Chou, H. C., Chen, C. Y., et al. (2011). Lipopolysaccharide-Induced Notch Signaling Activation Through JNK-Dependent Pathway Regulates Inflammatory Response. *J. Biomed. Sci.* 18, 56. doi: 10.1186/1423-0127-18-56
- Tsukasaki, M. (2021). RANKL and Osteoimmunology in Periodontitis. *J. Bone Miner. Metab.* 39, 82–90. doi: 10.1007/s00774-020-01165-3
- Tsukasaki, M., Asano, T., Muro, R., Huynh, N. C., Komatsu, N., Okamoto, K., et al. (2020). OPG Production Matters Where It Happened. *Cell. Rep.* 32:108124. doi: 10.1016/j.celrep.2020.108124
- Tsukasaki, M., Komatsu, N., Nagashima, K., Nitta, T., Pluemsakunthai, W., Shukunami, C., et al. (2018). Host Defense Against Oral Microbiota by Bone-Damaging T Cells. *Nat. Commun.* 9, 701. doi: 10.1038/s41467-018-03147-6
- Tsukasaki, M., and Takayanagi, H. (2019). Osteoimmunology: Evolving Concepts in Bone-Immune Interactions in Health and Disease. *Nat. Rev. Immunol.* 19, 626–642. doi: 10.1038/s41577-019-0178-8
- Uchida, Y., Irie, K., Fukuhara, D., Kataoka, K., Hattori, T., Ono, M., et al. (2018). Commensal Microbiota Enhance Both Osteoclast and Osteoblast Activities. *Molecules* 23, 1517. doi: 10.3390/molecules23071517
- Usui, M., Sato, T., Yamamoto, G., Okamatsu, Y., Hanatani, T., Moritani, Y., et al. (2016). Gingival Epithelial Cells Support Osteoclastogenesis by Producing Receptor Activator of Nuclear Factor Kappa B Ligand via Protein Kinase A Signaling. *J. Periodontol. Res.* 51, 462–470. doi: 10.1111/jre.12323
- Valerio, M. S., Herbert, B. A., Basilakos, D. S., Browne, C., Yu, H., and Kirkwood, K. L. (2015). Critical Role of MKP-1 in Lipopolysaccharide-Induced Osteoclast Formation Through CXCL1 and CXCL2. *Cytokine* 71, 71–80. doi: 10.1016/j.cyt.2014.08.007



- Verma, D., Garg, P. K., and Dubey, A. K. (2018). Insights Into the Human Oral Microbiome. *Arch. Microbiol.* 200, 525–540. doi: 10.1007/s00203-018-1505-3
- Vlachojannis, C., Dye, B. A., Herrera-Abreu, M., Pikdoken, L., Lerche-Sehm, J., Pretzl, B., et al. (2010). Determinants of Serum IgG Responses to Periodontal Bacteria in a Nationally Representative Sample of US Adults. *J. Clin. Periodontol.* 37, 685–696. doi: 10.1111/j.1600-051X.2010.01592.x
- Wang, K., Sun, Q., Zhong, X., Zeng, M., Zeng, H., Shi, X., et al. (2020). Structural Mechanism for GSDMD Targeting by Autoprocessed Caspases in Pyroptosis. *Cell* 180, 941–955.e20. doi: 10.1016/j.cell.2020.02.002
- Wang, X., Wang, H., Zhang, T., Cai, L., Kong, C., and He, J. (2020). Current Knowledge Regarding the Interaction Between Oral Bone Metabolic Disorders and Diabetes Mellitus. *Front. Endocrinol. (Lausanne)* 11:536. doi: 10.3389/fendo.2020.00536
- Wang, R. R., Xu, Y. S., Ji, M. M., Zhang, L., Li, D., Lang, Q., et al. (2019). Association of the Oral Microbiome With the Progression of Impaired Fasting Glucose in a Chinese Elderly Population. *J. Oral Microbiol.* 11:1605789. doi: 10.1080/20002297.2019.1605789
- Weitzmann, M. N., and Pacifici, R. (2006). Estrogen Deficiency and Bone Loss: An Inflammatory Tale. *J. Clin. Invest.* 116, 1186–1194. doi: 10.1172/JCI28550
- Wei, L., Xu, M., and Xiong, H. (2021). An Update of Knowledge on the Regulatory Role of Treg Cells in Apical Periodontitis. *Oral Dis* 27, 1356–1365. doi: 10.1111/odi.13450
- Wheeler, T. T., McArthur, W. P., Magnusson, I., Marks, R. G., Smith, J., Sarrett, D. C., et al. (1994). Modeling the Relationship Between Clinical, Microbiologic, and Immunologic Parameters and Alveolar Bone Levels in an Elderly Population. *J. Periodontol.* 65, 68–78. doi: 10.1902/jop.1994.65.1.68
- Wilson, M., Meghji, S., and Harvey, W. (1988). Effect of Capsular Material From *Haemophilus Actinomycetemcomitans* on Bone Collagen Synthesis *In Vitro*. *Microbios* 54, 181–185.
- Wongchana, W., and Palaga, T. (2012). Direct Regulation of Interleukin-6 Expression by Notch Signaling in Macrophages. *Cell. Mol. Immunol.* 9, 155–162. doi: 10.1038/cmi.2011.36
- Wu, Y. Y., Xiao, E., and Graves, D. T. (2015). Diabetes Mellitus Related Bone Metabolism and Periodontal Disease. *Int. J. Oral Sci.* 7, 63–72. doi: 10.1038/ijos.2015.2
- Xiao, E., Mattos, M., Vieira, G., Chen, S., Corrêa, J. D., Wu, Y., et al. (2017). Diabetes Enhances IL-17 Expression and Alters the Oral Microbiome to Increase Its Pathogenicity. *Cell. Host Microbe* 22, 120–128.e4. doi: 10.1016/j.chom.2017.06.014
- Xue, F., Shu, R., and Xie, Y. (2015). The Expression of NLRP3, NLRP1 and AIM2 in the Gingival Tissue of Periodontitis Patients: RT-PCR Study and Immunohistochemistry. *Arch. Oral Biol.* 60, 948–958. doi: 10.1016/j.archoralbio.2015.03.005
- Yamamoto, S., Mogi, M., Kinpara, K., Ishihara, Y., Ueda, N., Amano, K., et al. (1999). Anti-Proliferative Capsular-Like Polysaccharide Antigen From *Actinobacillus Actinomycetemcomitans* Induces Apoptotic Cell Death in Mouse Osteoblastic MC3T3-E1 Cells. *J. Dent. Res.* 78, 1230–1237. doi: 10.1177/00220345990780060601
- Yan, J., Takakura, A., Zandi-Nejad, K., and Charles, J. F. (2018). Mechanisms of Gut Microbiota-Mediated Bone Remodeling. *Gut Microbes* 9, 84–92. doi: 10.1080/19490976.2017.1371893
- Yasuhara, R., Miyamoto, Y., Takami, M., Imamura, T., Potempa, J., Yoshimura, K., et al. (2009). Lysine-Specific Gingipain Promotes Lipopolysaccharide- and Active-Vitamin D3-Induced Osteoclast Differentiation by Degrading Osteoprotegerin. *Biochem. J.* 419, 159–166. doi: 10.1042/BJ20081469
- Yin, W., Liu, S., Dong, M., Liu, Q., Shi, C., Bai, H., et al. (2020). A New NLRP3 Inflammasome Inhibitor, Dioscin, Promotes Osteogenesis. *Small* 16, e1905977. doi: 10.1002/smll.201905977
- Yoshida, K., Okamura, H., Hiroshima, Y., Abe, K., Kido, J. I., Shinohara, Y., et al. (2017). PKR Induces the Expression of NLRP3 by Regulating the NF- $\kappa$ B Pathway in *Porphyromonas Gingivalis*-Infected Osteoblasts. *Exp. Cell. Res.* 354, 57–64. doi: 10.1016/j.yexcr.2017.03.028
- Yu, C., Zhang, C., Kuang, Z., and Zheng, Q. (2021). The Role of NLRP3 Inflammasome Activities in Bone Diseases and Vascular Calcification. *Inflammation* 4, 434–449. doi: 10.1007/s10753-020-01357-z
- Zang, Y., Song, J. H., Oh, S. H., Kim, J. W., Lee, M. N., Piao, X., et al. (2020). Targeting NLRP3 Inflammasome Reduces Age-Related Experimental Alveolar Bone Loss. *J. Dent. Res.* 99, 1287–1295. doi: 10.1177/0022034520933533
- Zhang, Y., He, J., He, B., Huang, R., and Li, M. (2019). Effect of Tobacco on Periodontal Disease and Oral Cancer. *Tob. Induc. Dis.* 17, 40. doi: 10.18332/tid/106187
- Zhang, Q., Liu, J., Ma, L., Bai, N., and Xu, H. (2020). Wnt5a Is Involved in LOX-1 and TLR4 Induced Host Inflammatory Response in Peri-Implantitis. *J. Periodontol. Res.* 55, 199–208. doi: 10.1111/jre.12702
- Zhao, P., Liu, J., Pan, C., and Pan, Y. (2014). NLRP3 Inflammasome Is Required for Apoptosis of *Aggregatibacter Actinomycetemcomitans*-Infected Human Osteoblastic MG63 Cells. *Acta Histochem.* 116, 1119–1124. doi: 10.1016/j.acthis.2014.05.008
- Zheng, X., Tizzano, M., Redding, K., He, J., Peng, X., Jiang, P., et al. (2019). Gingival Solitary Chemosensory Cells Are Immune Sentinels for Periodontitis. *Nat. Commun.* 10, 4496. doi: 10.1038/s41467-019-12505-x
- Zhong, Z., Ethen, N. J., and Williams, B. O. (2014). WNT Signaling in Bone Development and Homeostasis. *Wiley Interdiscip. Rev. Dev. Biol.* 3, 489–500. doi: 10.1002/wdev.159

**Conflict of Interest:** The authors declare that the research was conducted in the absence of any commercial or financial relationships that could be construed as a potential conflict of interest.

**Publisher's Note:** All claims expressed in this article are solely those of the authors and do not necessarily represent those of their affiliated organizations, or those of the publisher, the editors and the reviewers. Any product that may be evaluated in this article, or claim that may be made by its manufacturer, is not guaranteed or endorsed by the publisher.

Copyright © 2021 Cheng, Zhou, Liu and Xu. This is an open-access article distributed under the terms of the Creative Commons Attribution License (CC BY). The use, distribution or reproduction in other forums is permitted, provided the original author(s) and the copyright owner(s) are credited and that the original publication in this journal is cited, in accordance with accepted academic practice. No use, distribution or reproduction is permitted which does not comply with these terms.



# Effect of Cavity Cleanser With Long-Term Antibacterial and Anti-Proteolytic Activities on Resin–Dentin Bond Stability

Yaping Gou\*, Wei Jin, Yanning He, Yu Luo, Ruirui Si, Yuan He, Zhongchi Wang, Jing Li and Bin Liu\*

Key Laboratory of Dental Maxillofacial Reconstruction and Biological Intelligence Manufacturing, Gansu Province, School of Stomatology, Lanzhou University, Lanzhou, China

## OPEN ACCESS

### Edited by:

Xin Xu,  
Sichuan University, China

### Reviewed by:

Jessica Kajfasz,  
University of Florida, United States  
Sang-Joon Ahn,  
University of Florida, United States

### \*Correspondence:

Yaping Gou  
gouyp@lzu.edu.cn  
Bin Liu  
liubkq@lzu.edu.cn

### Specialty section:

This article was submitted to  
Microbiome in Health and Disease,  
a section of the journal  
Frontiers in Cellular and  
Infection Microbiology

Received: 27 September 2021

Accepted: 28 October 2021

Published: 19 November 2021

### Citation:

Gou Y, Jin W, He Y, Luo Y, Si R, He Y,  
Wang Z, Li J and Liu B (2021)  
Effect of Cavity Cleanser With  
Long-Term Antibacterial and  
Anti-Proteolytic Activities on  
Resin–Dentin Bond Stability.  
Front. Cell. Infect. Microbiol. 11:784153.  
doi: 10.3389/fcimb.2021.784153

**Objective:** Secondary caries caused by oral microbiome dysbiosis and hybrid layer degradation are two important contributors to the poor resin–dentin bond durability. Cavity cleansers with long-term antimicrobial and anti-proteolytic activities are in demand for eliminating bacteria-induced secondary caries and preventing hybrid layers from degradation. The objectives of the present study were to examine the long-term antimicrobial effect and anti-proteolytic potential of poly(amidoamine) dendrimers with amino terminal groups (PAMAM-NH<sub>2</sub>) cavity cleanser.

**Methods:** Adsorption tests by attenuated total reflectance–infrared (ATR-IR) spectroscopy and confocal laser scanning microscopy (CLSM) were first performed to evaluate whether the PAMAM-NH<sub>2</sub> cavity cleanser had binding capacity to dentin surface to fulfill its relatively long-term antimicrobial and anti-proteolytic effects. For antibacterial testing, *Streptococcus mutans*, *Actinomyces naeslundii*, and *Enterococcus faecalis* were grown on dentin surfaces, prior to the application of cavity cleanser. Colony-forming unit (CFU) counts and live/dead bacterial staining were performed to assess antibacterial effects. Gelatinolytic activity within the hybrid layers was directly detected by *in situ* zymography. Adhesive permeability of bonded interface and microtensile bond strength were employed to assess whether the PAMAM-NH<sub>2</sub> cavity cleanser adversely affected resin–dentin bonding. Finally, the cytotoxicity of PAMAM-NH<sub>2</sub> was evaluated by the Cell Counting Kit-8 (CCK-8) assay.

**Results:** Adsorption tests demonstrated that the binding capacity of PAMAM-NH<sub>2</sub> on dentin surface was much stronger than that of 2% chlorhexidine (CHX) because its binding was strong enough to resist phosphate-buffered saline (PBS) washing. Antibacterial testing indicated that PAMAM-NH<sub>2</sub> significantly inhibited bacteria grown on the dentin discs as compared with the control group ( $p < 0.05$ ), which was comparable with the antibacterial activity of 2% CHX ( $p > 0.05$ ). Hybrid layers conditioned with PAMAM-NH<sub>2</sub> showed significant decrease in gelatin activity as compared with the control group. Furthermore, PAMAM-NH<sub>2</sub> pretreatment did not adversely affect resin–dentin

bonding because it did not decrease adhesive permeability and microtensile strength. CCK-8 assay showed that PAMAM-NH<sub>2</sub> had low cytotoxicity on human dental pulp cells (HDPCs) and L929.

**Conclusions:** PAMAM-NH<sub>2</sub> cavity cleanser developed in this study could provide simultaneous long-term antimicrobial and anti-proteolytic activities for eliminating secondary caries that result from a dysbiosis in the oral microbiome and for preventing hybrid layers from degradation due to its good binding capacity to dentin collagen matrix, which are crucial for the maintenance of resin–dentin bond durability.

**Keywords:** antibacterial, endogenous dentin proteases, cavity cleanser, resin–dentin bonds, poly (amidoamine) dendrimers

## 1 INTRODUCTION

Secondary caries caused by oral microbiome dysbiosis and degradation of hybrid layer *via* endogenous dentin proteases are two major challenges encountered in durable resin–dentin bond stability (Gou et al., 2018a). In contemporary minimally invasive dentistry, partial retention of caries-infected dentin is currently recommended to preserve tooth structure and avoid damage to the dental pulp complex (Thompson et al., 2008; Walsh and Brostek, 2013). Nevertheless, entrapped bacteria and their by-products through interfacial gaps between the tooth and the restoration leads to secondary caries that is described as a microbial disease that results from “a dysbiosis in the oral microbiome” (Tanner et al., 2016) and to restoration failure over time (Nyvad and Kilian, 1987; Türkün et al., 2006).

Hybrid layer degradation, caused by hydrolysis of adhesive resin (Breschi et al., 2008; Tjäderhane et al., 2013) and degradation of demineralized collagen matrices in aqueous environments (Mazzoni et al., 2015), is the other challenge in achieving durability of bonds made by resins in dentin. During the acid-etching phase of dentin bonding, endogenous dentin protease such as matrix metalloproteinases (MMPs) and cysteine cathepsins that are normally embedded within the collagen matrix by apatite crystallites become exposed and activated by acid etchants. Subsequent application of acidic resin monomers present in dentin adhesives further promotes activities of these proteases (Tay et al., 2006; Osorio et al., 2011; Frassetto et al., 2016). The activated, matrix-bound protease can progressively degrade denuded collagen fibrils within the hybrid layers, leading to deterioration of resin–dentin bonds over time (Frassetto et al., 2016).

To prolong the durability of resin–dentin interfacial bonds, the aforementioned two challenges should be concomitantly addressed. The use of cavity cleanser with antibacterial and anti-proteolytic properties is in demand. Chlorhexidine (CHX) possesses broad spectrum antibacterial (Twetman, 2004) and anti-proteolytic activities (Scaffa et al., 2012) and has been commonly used as an effective agent to disinfect dentin cavity (Ersin et al., 2008). Nevertheless, CHX is water-soluble and has weak binding affinity for the demineralized dentin collagen matrix (Slee and Tanzer, 1979; Blackburn et al., 2007). It eventually desorbs from the exposed collagen fibrils and slowly leaches out from the hybrid

layers over time, thus compromising its long-term antimicrobial and anti-proteolytic effects (Tezvergil-Mutluay et al., 2011).

Recently, poly(amidoamine) dendrimers with amino terminal groups (PAMAM-NH<sub>2</sub>) have been extensively investigated as promising antimicrobial agents due to a great number of positive charges on the protonated amino groups on their exterior (Castonguay et al., 2012; Gou et al., 2017). With numerous positively charged amino groups, PAMAM-NH<sub>2</sub> is capable of attaching to and puncturing bacteria (Mintzer et al., 2012) cell walls as well as possessing a strong affinity for the denuded dentin collagen (Liang et al., 2015). Hence, it is speculated that when PAMAM-NH<sub>2</sub> is applied to acid-etched dentin, it would strongly absorb on exposed collagen fibrils to provide relatively long-lasting antimicrobial effectiveness. However, there has been no report whether PAMAM-NH<sub>2</sub> has inhibitory effects on endogenous dentin proteases.

Accordingly, the objectives of this study were to develop a new dentin cavity cleanser containing PAMAM-NH<sub>2</sub>, to explore its effect of against bacteria grown on dentin surfaces, and to assess the enzyme activity of the resin–dentin interface using *in situ* zymography and functional enzyme activity assays. It was hypothesized that 1) the PAMAM-NH<sub>2</sub> cavity cleanser has long-term inhibitory effects on bacteria grown on dentin blocks; 2) the PAMAM-NH<sub>2</sub> cavity cleanser has inhibitory effects on soluble MMP-9 activities; 3) the PAMAM-NH<sub>2</sub> cavity cleanser has long-term inhibitory effects on endogenous dentin proteases; and 4) treatment of dentin surface with PAMAM-NH<sub>2</sub> cavity cleanser does not adversely affect dentin bond strength.

## 2 MATERIALS AND METHODS

PAMAM-NH<sub>2</sub> utilized in the present work was purchased from ChenYuan Dendrimer Technology Co., Ltd (Weihai, Shandong, China).

### 2.1 Binding Capacity of PAMAM-NH<sub>2</sub> to Demineralized Dentin

PAMAM-NH<sub>2</sub> measuring 4 mg/ml and 2% CHX were separately dropped and spread on etched dentin surface using a disposable micro brush. After 60 s of being gently air-dried at room temperature, each dentin surface was subsequently washed with

phosphate-buffered saline (PBS) three times and dried again. Attenuated total reflectance–infrared (ATR-IR) spectroscopy (Nicolet iS10, Thermo Scientific, USA) was performed and recorded before and after conditioning with PAMAM-NH<sub>2</sub> and 2% CHX, and also after washing with PBS. Each group was performed in sextuplicate. Three independent batches were conducted for the experiment.

Fluorescein isothiocyanate (FITC)-labeled PAMAM-NH<sub>2</sub> was prepared by mixing equimolar amounts of an FITC solution (in acetone) with an aqueous PAMAM-NH<sub>2</sub> solution overnight in the dark under stirring (Gou et al., 2017). FITC-labeled PAMAM-NH<sub>2</sub> (4 mg/ml, 50 µl) or FITC was respectively dropped and spread on etched dentin surface using a disposable micro brush. After 60 s, the dentin surface was washed with PBS three times, and the specimens were dried and observed by confocal laser scanning microscopy (CLSM) (Zeiss LSM700, Germany). Quantification of the green fluorescence intensity was calculated with Image-Pro Plus 6.0 (Media Cybernetics, Inc., Silver Spring, MD, USA) to represent the relative binding capacity of PAMAM-NH<sub>2</sub> to demineralized dentin. Each group was performed in sextuplicate. Three independent batches were conducted for the experiment.

## 2.2 Antibacterial Activity Testing

### 2.2.1 Bacterial Culture

*Streptococcus mutans* (ATCC 700610), *Actinomyces naeslundii* (ATCC 12104), and *Enterococcus faecalis* (ATCC 29212) were used to examine the antibacterial activities of experimental cavity cleansers. *E. faecalis* was grown aerobically in Brain Heart Infusion (BHI) broth at 37°C. *S. mutans* and *A. naeslundii* were cultured in an anaerobic atmosphere of 5% CO<sub>2</sub>, 90% N<sub>2</sub>, and 5% H<sub>2</sub> at 37°C in BHI broth. For biofilm formation, the bacteria were cultured in BHI supplemented with 1% sucrose. The bacteria were incubated for 24 h, collected by centrifugation, and rinsed three times with PBS. The bacteria were re-suspended and further diluted in BHI to a final density of  $1.0 \times 10^7$  colony-forming unit (CFU)/ml. Bacteria density was measured by a microplate reader (Beckman Coulter, Inc., Indianapolis, IN, USA) at the absorbance of 600 nm.

### 2.2.2 Minimum Inhibitory Concentration

In order to evaluate the effect of PAMAM-NH<sub>2</sub> on planktonic bacteria, the minimum inhibitory concentration (MIC) was examined by the broth microdilution method. The PAMAM-NH<sub>2</sub> solution was added in a twofold dilution series in BHI broth in 96-well microtiter plates ( $1.0 \times 10^7$  CFU/ml). After incubation overnight, bacterial growth was measured by a microplate reader at the absorbance of 600 nm. MIC value was determined as the lowest PAMAM-NH<sub>2</sub> concentration that inhibited at least 90% of bacterial growth compared with the PAMAM-NH<sub>2</sub>-free control. Each group was performed in sextuplicate. Three independent batches were performed for the experiment.

### 2.2.3 Minimum Biofilm Eradication Concentration

In a physiological state, bacteria tend to exist in biofilms. Bacteria in biofilms are less susceptible to stressful environmental conditions than in their planktonic state. Therefore, minimum biofilm eradication concentration (MBEC) was assessed to

evaluate whether PAMAM-NH<sub>2</sub> has inhibitory effects on biofilms. MBEC was assessed by microtiter plate assay. The testing was started by growing the biofilm first by incubating the suspension of *S. mutans* and *A. naeslundii* for 24 h and *E. faecalis* for 7 days at 37°C. Then, each microplate well was gently washed three times with PBS to remove unattached bacteria, and PAMAM-NH<sub>2</sub> with different concentrations was added. After that, the microplates were incubated for 24 h (*S. mutans* and *A. naeslundii*) or 7 days (*E. faecalis*) at 37°C and were rinsed with PBS. The biofilm was added with 1% of crystal violet solution and cultured at room temperature. The well was gently washed with PBS for three times to remove excess crystal violet and incubated with 95% ethanol by shaking for 15 min. The optical density at 595 nm was measured with a microplate reader (Model 3550, Bio-Rad). Each group was performed in sextuplicate. Three independent batches were conducted for the experiment.

### 2.2.4 Cell Counting Kit-8 Counts

*S. mutans*, *A. naeslundii*, or *E. faecalis* biofilm was grown on the surface of dentin discs. Each biofilm-containing dentin disc was conditioned with PAMAM-NH<sub>2</sub> and 2% CHX and kept for 60 s. The dentin blocks were gently rinsed and transferred into Petri dishes with 1 ml of PBS. The dishes were ultrasonicated to collect biofilms. The collected biofilms were cultured on BHI agar plates, and their viability was assessed by CFU counting after a serial dilution in PBS. Each group was performed in sextuplicate. Three independent batches were conducted for the experiment.

### 2.2.5 Live/Dead Bacterial Staining

*S. mutans*, *A. naeslundii*, or *E. faecalis* biofilm grown on the surface of dentin discs was treated with a LIVE/DEAD BacLight Bacterial Viability Kit (Molecular Probes, Invitrogen Corp., Carlsbad, CA, USA). Sterilized dentin blocks were incubated with each bacterium at 37°C for 24 h (*S. mutans* and *A. naeslundii*) or 7 days (*E. faecalis*) and were gently washed three times with PBS to remove unattached bacteria. Each biofilm-containing dentin disc was conditioned with PAMAM-NH<sub>2</sub> and 2% CHX by adding 100 µl of each cavity cleanser onto the dentin surface and kept for 60 s. Then the dentin blocks were treated with 2.5 µM of SYTO 9 and propidium iodide in the dark according to the instructions. Stained dentin blocks were visualized with a CLSM (LSM 780, Carl Zeiss, Oberkochen, Germany) equipped with a 20× objective lens by the channel set at excitation/emission wavelengths 480/500 nm for SYTO 9, and 590/635 nm for propidium iodide. Live bacteria are dyed green, dead bacteria are dyed red, and adjacent live and dead bacteria are shown as yellow when they are merged. Quantification of dead and live bacteria was calculated based on the value of relative green and red fluorescence by Image-Pro Plus 6.0 software. Each group was performed in sextuplicate. Three independent batches were conducted for the experiment.

## 2.3 Analysis of the Effect of PAMAM-NH<sub>2</sub> on Matrix Metalloproteinases

### 2.3.1 Inhibition of Soluble rhMMP-9

The inhibitory effects of PAMAM-NH<sub>2</sub> and 2% CHX on soluble purified recombinant human (rh) MMP-9 were assessed using purified rhMMP-9 (AS-55576) and the Sensolyte Generic MMP



assay kit (AS-72095) (all from AnaSpec Inc., CA, USA). The MMP assay kit contains an intact substrate (thiopeptolide) that is disintegrated by MMPs to release a colored product, 2-nitro-5-thiobenzoic acid.

A series of PAMAM-NH<sub>2</sub> solutions (0.5, 1, 2, 4, 8, and 16 mg/ml) were prepared as test agents. The substrate solution provided by the assay kit was prepared at 0.2 mM. In the experimental groups, the well contained 2 µl of rhMMP-9, 50 µl of substrate solution, and 10 µl of potential MMP inhibitor.

The control groups included 1) the positive control group: rhMMP-9 enzyme only without the anti-MMP agent; 2) the inhibitor control group: rhMMP-9 enzyme and MMP inhibitor (GM6001); 3) the test compound control group: assay buffer and various concentrations of PAMAM-NH<sub>2</sub> solutions; and 4) the substrate control group: assay buffer only. The reagents on the plate were shaken for 30 s to mix completely. Readings were measured every 10 min for 60 min. The intensity of color was detected using a microplate reader at 412 nm. The potency of MMP-9 inhibition by GM6001 (known MMP inhibitor) and the six concentrations of PAMAM-NH<sub>2</sub> were exhibited as percentages of the adjusted absorbance of the “positive control.” Percent inhibition of the MMP (%) was calculated as  $1 - ([A]_{\text{test compound group}} - [A]_{\text{test compound control}}) / ([A]_{\text{positive control}} - [A]_{\text{substrate control}})$ , where [A] represents the absorbance values of the wells. Each specimen was performed in sextuplicate (N = 6). Three independent batches were conducted for the experiment.

### 2.3.2 *In Situ* Zymography

Ten teeth from two cavity cleanser group were used for *in situ* zymography of the bonded interface. After being treated with 37% phosphoric acid, the dentin blocks were conditioned with each cavity cleanser for 60 s and gently air-dried. After being bonded with adhesive, a 2-mm-thick layer of flowable resin composite was placed and light-cured. After 24 h of storage in deionized water, the bonded samples were cut vertically into 1-mm-thick slabs to expose the resin–dentin interface.

The bonded slab was fixed to a glass slide and polished to approximately 50-µm thickness. The EnzChek™ Gelatinase/Collagenase Assay Kit (E-12055, Molecular Probes, Eugene, OR, USA) was employed for *in situ* zymography to identify sites of MMP activity within the hybrid layers. Briefly, the 1.0 mg/ml stock solution of self-quenched fluorescein-conjugated gelatin was diluted by adding deionized water and mixing with anti-fading agent. Then, 50 µl of the self-quenched fluorescent gelatin mixture was dropped on top of each bonded slab and covered with a coverslip. The slides were kept away from light and incubated in a humidity chamber at 37°C for 48 h.

A two-photon CLSM (LSM 780, Carl Zeiss, Thornwood, NY, USA) was used to acquire images using a 40× oil immersion objective lens, with the channels set at 488/530 nm (excitation/emission wavelengths). Green fluorescence derived from de-quenched fluorescein released from disintegrated gelatin was imaged. Sections that were 85 µm thick were acquired from different focal planes of each bonded specimen. The images were stacked and processed with ZEN 2010 software (Carl Zeiss). The image-Pro Plus 6.0 software was employed to quantify the green

fluorescence intensity. Each group was performed in sextuplicate. Three independent batches were conducted for the experiment.

## 2.4 Assessment of the Impact of PAMAM-NH<sub>2</sub> on Resin–Dentin Bonding

### 2.4.1 Adhesive Permeation of Bonded Interface

Twenty freshly extracted and intact human third molars were collected for permeability evaluation of adhesive. The dentin was sectioned at a distance of 2.5 mm away from the deepest pulpal horn using a slow-speed saw under water cooling. One drop of fluorescein sodium (Sigma-Aldrich, St Louis, MO, USA) was mixed with three drops of adhesive (Prime & Bond® NTTM) to produce a fluorescent adhesive. The bonded dentin was glued to fenestrated Perspex discs with cyanocrylate glue. The assembly was connected *via* an 18-gauge stainless steel tube to fenestrated Perspex discs. The latter was placed to a column of 0.1% green fluorescent dye solution (Alexa Fluor™ 405, excitation/emission: 401/421 nm; Thermo Fisher Scientific) oriented 20 cm above the Plexiglass block to simulate pulpal pressure. This generated water pressure through the dentinal tubules during the acid-etching process, treatment with each cavity cleanser, bonding, and resin composite buildup. The setup was kept away from light and incubated for 4 h to enable water to continue permeating the bonded interface.

After pressure perfusion, the bonded specimen was removed from the fenestrated Perspex discs and cut vertically to get a 1-mm slab containing the water perfused bonded interface. Each bonded specimen was fixed to a glass slide and polished to approximately 50-µm thickness. A two-photon CLSM was used to acquire images using a 40× oil immersion objective lens. Green fluorescence was imaged together with the red fluorescence derived from dyed adhesive. Sections that were 85 µm thick were acquired from different focal planes of each bonded specimen. The images were stacked and processed with ZEN 2010 software (Carl Zeiss). The image-Pro Plus 6.0 software was employed to quantify the dyed adhesive permeation. Each group was performed in sextuplicate. Three independent batches were conducted for the experiment.

### 2.4.2 Bond Strengths to Dentin

Thirty human third molars were collected for bond strength test. The teeth were cut 2–3 mm below the cemento-enamel junction to remove roots using water-cooled low-speed cutting saw (Isomet, Buehler Ltd., Lake Bluff, IL, USA). The occlusal enamel was removed perpendicular to the longitudinal axis of each tooth to expose flat midcoronal dentin surface. The exposed midcoronal dentin surface was polished with 600-grit silicon carbide paper under water for 60 s to produce a standardized smear layer.

Exposed dentin surfaces were randomly allocated to two groups according to the adhesives used: Prime & Bond® NT™ (PB, Dentsply DeTrey, Konstanz, Germany) and Adper™ Single Bond Plus (SBP, 3M ESPE, St. Paul, MN, USA). Each specimen was treated with 37% phosphoric acid (Uni-Etch, Bisco Inc., Schaumburg, IL, USA) for 15 s, washed with deionized water for 15 s, and air-dried for 5 s. Dentin surface from each adhesive

group was further randomly assigned to one of the following three subgroups for dentin pretreatment with PAMAM-NH<sub>2</sub>, 2% CHX, and deionized water (control) (N = 6). The etched dentin surface was pretreated with respective cavity cleanser or deionized water for 60 s and air-dried for 5 s. The adhesives were placed to the etched dentin and light-cured for 15 s with a light-curing unit. Resin composite buildups (Z250, 3 M ESPE, St. Paul, MN, USA) were constructed.

After storage in deionized water for 24 h, the bonded teeth were subsequently sectioned vertically to 0.9-mm-thick slabs using a low-speed saw under water cooling. The slabs were further cut into 0.9 mm × 0.9 mm × 8 mm long beams. Each beam was attached and stressed to failure under tension using a universal tensile testing machine (HD-B609B-S, Haida International, China). Each specimen was performed in sextuplicate. Three independent batches were conducted for the experiment.

After tensile bond strength test, the dentin side of the fractured beams was detected using a stereoscopic microscope at ×40 magnification to determine the failure mode. Failure modes were classified as adhesive failure (A), mixed failure (M, failure extending into dentin or resin composite), cohesive failure in resin composite (CC), and cohesive failure in dentin (CD).

## 2.5 Cytotoxicity Assay

Human dental pulp cells (HDPCs) and mouse fibroblast cells L929 were chosen to test the cytotoxicity of PAMAM-NH<sub>2</sub>. Freshly extracted and intact human third molars were collected, cleaned, and cut perpendicular to the longitudinal axis of each tooth to expose the pulp chamber, with the donors' written informed consent. Dental pulp tissues were gently removed by blunt non-cutting forceps and dispersed in 2 mg/ml of collagenase/dispase for 1.5 h to retrieve HDPCs at 37°C. The HDPCs and L929 were cultured in Dulbecco's Modified Eagle's Medium plus 10% heat-inactivated fetal bovine serum and 1% penicillin/streptomycin at 37°C in a humidified incubator supplemented with 5% CO<sub>2</sub>. The seeded cells were subsequently cultured until 80% confluency was achieved. Four passage cells were used for the experiment.

The cytotoxicity of PAMAM-NH<sub>2</sub> was determined by the Cell Counting Kit-8 (CCK-8) assay. Cells were seeded in a 96-well microtiter plate at a density of  $1.0 \times 10^4$  cells/well and incubated overnight. The culture medium was replaced with 100 µl of fresh culture medium containing different concentrations of PAMAM-NH<sub>2</sub>. After incubation overnight, 10 µl of CCK-8 solution was added to each well, and the microtiter plate was incubated at 37°C for 4 h, after which the absorbance at 570 nm was determined with a microplate reader (Spectra Plus, Tecan, Zurich, Switzerland). The cell viability (%) =  $([A]_{\text{test}} - [A]_{\text{blank}}) / ([A]_{\text{control}} - [A]_{\text{blank}}) \times 100\%$ , where  $[A]_{\text{test}}$ ,  $[A]_{\text{control}}$ , and  $[A]_{\text{blank}}$  represent the absorbance values of the wells with cells and PAMAM-NH<sub>2</sub>, those with cells and without PAMAM-NH<sub>2</sub>, and those without cells or PAMAM-NH<sub>2</sub>, respectively. For each sample, the average absorbance from six wells that run in parallel was calculated. Three independent batches were conducted for the experiment.

## 2.6 Statistical Analyses

Data were expressed as means and SDs. For each parameter to be analyzed, the data sets were evaluated for their normality (Shapiro–Wilk test) and equal variance assumptions (modified Levene's test) before use of parametric statistical methods. If those assumptions were not violated, the data sets were analyzed with one-factor ANOVA or one-factor repeated-measures ANOVA, depending on the parameter tested. Post-hoc comparisons were conducted using the Holm–Sidak procedures to identify statistical significance among groups. If the assumptions were violated, the data sets were non-linearly transformed to satisfy those assumptions before performing the aforementioned statistical procedures. For all tests, statistical significance was set at  $\alpha = 0.05$ .

## 3 RESULTS

### 3.1 Binding Capacity of PAMAM-NH<sub>2</sub> to Demineralized Dentin

The ATR–Fourier-transform IR (ATR-FTIR) spectra of the demineralized dentin after being conditioned with 4 mg/ml of PAMAM-NH<sub>2</sub> or 2% CHX and after being washed with PBS are shown in **Figure 1A**. The peak at  $1,000.1 \text{ cm}^{-1}$  was due to phosphate v1, v3 functional groups, which is a characteristic peak of dentin. After being conditioned with PAMAM-NH<sub>2</sub>, characteristic peaks of PAMAM-NH<sub>2</sub> were clearly detected at  $3,088.52$  to  $3,500 \text{ cm}^{-1}$  corresponding to amide vibration and at  $1,634.9 \text{ cm}^{-1}$  corresponding to amide carbonyl groups, and they are related to the number of amide groups in the branches of PAMAM-NH<sub>2</sub>. The results confirmed that PAMAM-NH<sub>2</sub> bound to the demineralized dentin. After thorough washing with PBS, these characteristic peaks of PAMAM-NH<sub>2</sub> were still apparent, which indicated that PAMAM-NH<sub>2</sub> can resist PBS washing. After being conditioned with CHX, the presence of characteristic peaks of CHX was detected, as well as C–H<sub>2</sub> stretches at  $2,948.5$  and  $2,855.0 \text{ cm}^{-1}$ , C=N vibration at  $3,319.1 \text{ cm}^{-1}$ , and para-substitution of benzene rings at  $1,631.5$  and  $1,557.0 \text{ cm}^{-1}$ . Following PBS washing, these characteristic peaks disappeared in CHX conditioning dentin surface, indicating that CHX was washed off by PBS.

FITC-labeled PAMAM-NH<sub>2</sub> and free FITC were dropped onto demineralized dentin surface. After being air-dried at room temperature, the dentin surfaces were rinsed with PBS and observed by CLSM. **Figure 1B** shows yellow-green fluorescence, which could be clearly observed for both two groups, with an intensity value of  $98.2\% \pm 4.9\%$  for the FITC-PAMAM-NH<sub>2</sub> group and  $90.5\% \pm 7.1\%$  for the FITC group (**Figure 1C**). However, little fluorescence could be detected on free FITC-coated dentin surface after PBS washing (**Figure 1B**) reaching  $26.8\% \pm 5.7\%$  fluorescence intensity, which was significantly lower than that of the FITC group before PBS washing (**Figure 1C**,  $p < 0.05$ ). In contrast, FITC-PAMAM-NH<sub>2</sub>-coated dentin retained most of the fluorescence with an intensity value of  $89.6\% \pm 3.5\%$  (**Figures 1B, C**). There was no significant difference in the fluorescence intensity in the FITC-

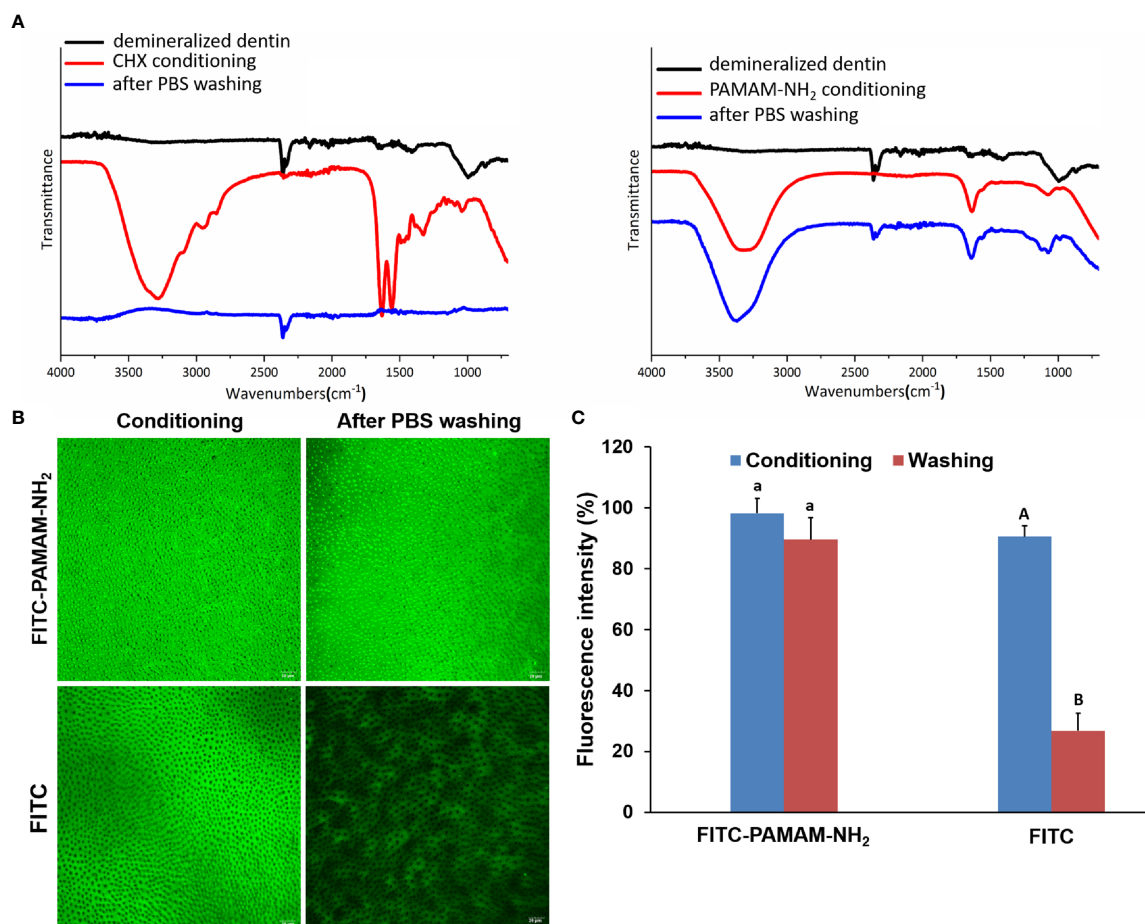


**FIGURE 1 |** The binding capacity of PAMAM-NH<sub>2</sub> to demineralized dentin. **(A)** The ATR-IR spectrum of the demineralized dentin, after conditioning with CHX or PAMAM-NH<sub>2</sub> and after washing with PBS. **(B)** The CLSM images of the demineralized dentin immobilized with FITC-labeled PAMAM-NH<sub>2</sub> or free FITC, after washing with PBS. **(C)** Bar graph of relative fluorescence intensity of the two groups. Data are means  $\pm$  SDs. Data obtained in the three groups (N = 6/group) were analyzed. For FITC-PAMAM-NH<sub>2</sub>, columns labeled with the same lowercase letters are not significantly different ( $p > 0.05$ ). For FITC, columns labeled with different uppercase letters are significantly different ( $p < 0.05$ ). ATR-IR, attenuated total reflectance-infrared; PBS, phosphate-buffered saline; CLSM, confocal laser scanning microscopy; FITC, fluorescein isothiocyanate.

PAMAM-NH<sub>2</sub> group before and after PBS washing ( $p > 0.05$ ). This result demonstrated that free FITC could not bind to the demineralized dentin surface and that PAMAM-NH<sub>2</sub> had a good binding capacity to demineralize dentin.

### 3.2 Antibacterial Activities

A microdilution method was used to assess the antibacterial activity of PAMAM-NH<sub>2</sub>. MIC values of PAMAM-NH<sub>2</sub> required to inhibit the visible growth of planktonic bacteria were 562.5, 562.5, and 750  $\mu\text{g/ml}$  for *S. mutans*, *A. naeslundii*, and *E. faecalis*. MBEC values of PAMAM-NH<sub>2</sub> on these three bacteria were 750, 1,125, and 3,500  $\mu\text{g/ml}$  (Table 1). Figure 2 shows the CFU counts of *S. mutans*, *A. naeslundii*, and *E. faecalis* biofilms after treatment with deionized water, PAMAM-NH<sub>2</sub>, or 2% CHX. For these three bacteria, control dentin blocks (without cavity cleanser) all had the highest CFU. Dentin blocks treated with the PAMAM-NH<sub>2</sub> and 2% CHX significantly reduced viable bacteria in the biofilms, compared with dentin blocks without

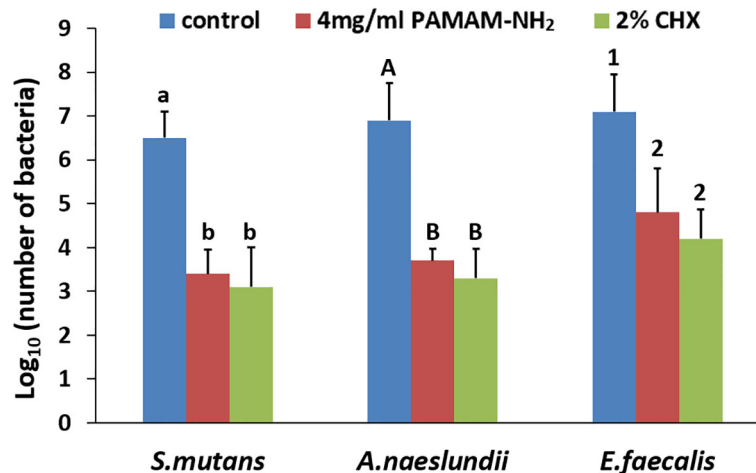
cavity cleanser ( $p < 0.05$ ). No significant difference was found between the PAMAM-NH<sub>2</sub> and the 2% CHX ( $p > 0.05$ ). These results showed that PAMAM-NH<sub>2</sub> cavity cleanser had inhibitory effects on bacteria grown on dentin blocks.

Figure 3A shows representative CLSM images of the distribution of *S. mutans*, *A. naeslundii*, and *E. faecalis* biofilms stained with live/dead stains. For all *S. mutans*, *A. naeslundii*, and *E. faecalis*, biofilms grown on control dentin blocks (without

**TABLE 1 |** MIC and MBEC values of PAMAM-NH<sub>2</sub> against *Streptococcus mutans*, *Actinomyces naeslundii*, and *Enterococcus faecalis*.

Bacteria	MIC ( $\mu\text{g/ml}$ )	MBEC ( $\mu\text{g/ml}$ )
<i>S. mutans</i>	562.5	750
<i>A. naeslundii</i>	562.5	1,125
<i>E. faecalis</i>	750	3,500

MIC, minimum inhibitory concentration; MBEC, minimum biofilm eradication concentration.



**FIGURE 2** | CFU counts of *Streptococcus mutans*, *Actinomyces naeslundii*, or *Enterococcus faecalis* grown on dentin blocks for the deionized water control and the two cavity cleansers groups. Values are mean and SDs. Data obtained in the three groups (N = 6/group) were analyzed. For each bacterium strain, columns labeled with different letters or numbers are significantly different ( $p < 0.05$ ). CFU, colony-forming unit.

cavity cleanser) consisted of primarily live bacteria, with small amounts of dead bacteria. In contrast, biofilms in the PAMAM-NH<sub>2</sub> and 2% CHX dentin blocks showed primarily dead bacteria and a higher dead/live bacteria ratio as compared with the control group ( $p < 0.05$ , **Figure 3B**), which indicates that PAMAM-NH<sub>2</sub>- and 2% CHX-pretreated dentin possessed antimicrobial activity. There was no significant difference in the antibacterial effect between the PAMAM-NH<sub>2</sub> and 2% CHX groups ( $p > 0.05$ , **Figure 3B**).

### 3.3 Inhibitory Effect of PAMAM-NH<sub>2</sub> on Matrix Metalloproteinases

The inhibitory effects of different concentrations of PAMAM-NH<sub>2</sub> on soluble MMPs are shown in **Figure 4**. The relative percentages of rhMMP-9 inhibitor by the GM6001 (kit inhibitor control) were  $97.02\% \pm 2.10\%$ . Inhibition of rhMMP-9 by PAMAM-NH<sub>2</sub> at concentrations higher than 4 mg/ml (4 to 16 mg/ml) was comparable with that of the GM6001 group (inhibitor control) ( $p > 0.05$ ). The anti-MMP activities of PAMAM-NH<sub>2</sub> at concentrations ranging from 0.5 to 2 mg/ml were significantly lower than those of the kit inhibitor control ( $p < 0.05$ ).

The *in situ* zymography technique enables screening of the relative proteolytic activities directly within dentin hybrid layers. Representative CLSM images of dentin pretreated with deionized water (control), PAMAM-NH<sub>2</sub>, and 2% CHX are shown in **Figure 5A**. **Figure 5B** summarizes the relative percentage areas of hybrid layers in the three groups that showed green fluorescence after coming in contact with the highly quenched fluorescein-conjugated gelatin. For the control dentin slabs pretreated with deionized water, an intense green fluorescence was detected within the hybrid layers, reaching  $88.3\% \pm 5.2\%$  fluorescence intensity. In contrast, the HLs in the experimental groups pretreated with 4 mg/ml of PAMAM-NH<sub>2</sub> and 2% CHX showed weak green fluorescence, with an intensity value of  $22.6\% \pm 4.1\%$  and

$18.6\% \pm 4.4\%$ , respectively. These fluorescence values were significantly lower than those of the control group ( $p < 0.05$ ). No significant difference was found between the PAMAM-NH<sub>2</sub> group and the 2% CHX group ( $p > 0.05$ ).

### 3.4 Assessment of the Impact of PAMAM-NH<sub>2</sub> on Resin–Dentin Bonding

A double-fluorescence technique was employed to evaluate the permeability of the resin–dentin interface created by the etch-and-rinse adhesive system under simulated pulpal pressure. The fluorescence representative images (separate channels; red for adhesive and green for water) of the permeability of adhesive are shown in **Figure 6A**. The adhesive infiltration data that are expressed as the relative percentage of red adhesive at the site of the dentinal tubules are presented in **Figure 6B**. In the control groups, the red adhesive sufficiently infiltrated into the dentinal tubules, as suggested by the presence of dense, branch-like resin tags at the resin–dentin interface. The relative percentages of the permeability were  $91.2\% \pm 4.9\%$ . At the bonded interface pretreated with PAMAM-NH<sub>2</sub> or 2% CHX, the shape and depth of the resin tags were analogous to those groups in the control groups, reaching  $88.5\% \pm 7.1\%$  and  $93.7\% \pm 5.8\%$  permeability, respectively. There was no significant difference among these three groups in adhesive permeability values ( $p < 0.05$ ).

Tensile bond strength for each cavity cleanser group is shown in **Figure 7**. For both commercial adhesives PB and SBP, there was no significant difference among the control (without cavity cleanser), PAMAM-NH<sub>2</sub>, and 2% CHX groups ( $p > 0.05$ ). Using PAMAM-NH<sub>2</sub> cavity cleanser before adhesive application did not adversely affect the tensile bond strength of either adhesive. The two adhesive groups had similar failure mode distribution (**Table 2**). Low bond strength values tend to fail within the adhesive. Failure modes for all test beams exhibited obvious tendency of mixed failures, with a small distribution of cohesive failure in resin composite and cohesive failure in dentin.



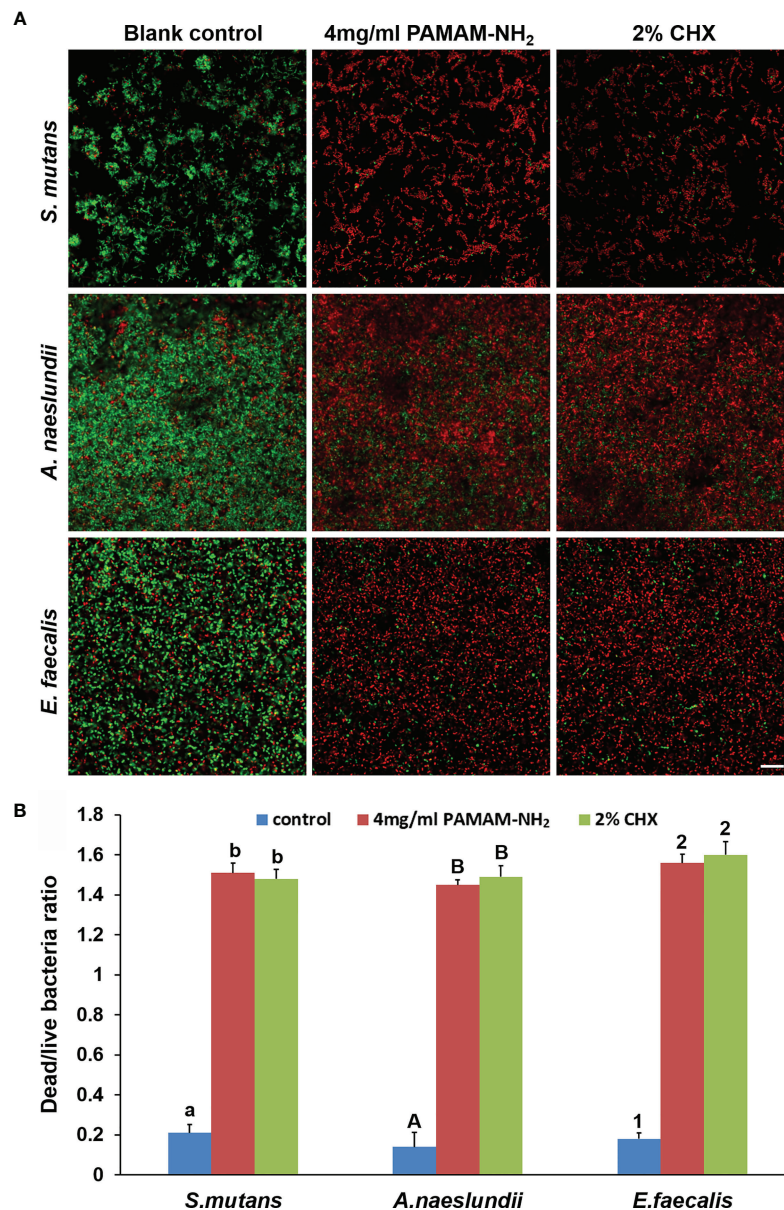


**FIGURE 3 | (A)** Representative CLSM images of *Streptococcus mutans*, *Actinomyces naeslundii*, or *Enterococcus faecalis* (live, green; dead, red) grown on dentin blocks after application of deionized water (control), and 4 mg/ml of PAMAM-NH<sub>2</sub> or 2% CHX as cavity cleansers. Bars = 20  $\mu$ m. **(B)** Bar chart of the dead/live bacteria ratio of the three groups based on analysis of the live–dead staining profiles of the dentin blocks. Values are means and SDs. Data obtained in the three groups (N = 6/group) were analyzed. For each bacterium strain, columns labeled with different letters or numbers are significantly different ( $p < 0.05$ ). CLSM, confocal laser scanning microscopy

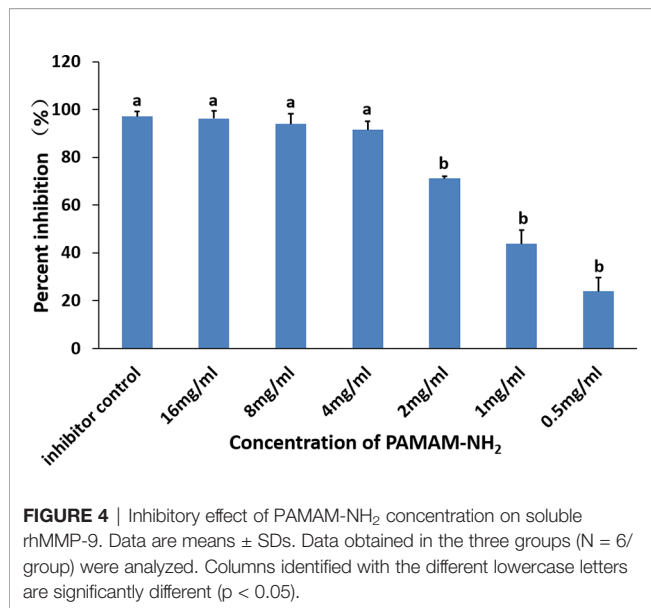
### 3.5 Cytotoxicity Assay

The cytotoxicity of PAMAM-NH<sub>2</sub> on HDPCs and L929 at various concentrations from 0.5 to 8 mg/ml was evaluated using the CCK-8 assay (Figure 8). For both cells HDPCs and L929, there was no significant difference among the groups with PAMAM-NH<sub>2</sub> at concentrations lower than 4 mg/ml (0.5 to 4 mg/ml) ( $p > 0.05$ ). Good cell viability in the range of 80%–110% was observed with PAMAM-NH<sub>2</sub> at concentrations lower than

4 mg/ml (0.5 to 4 mg/ml), which demonstrates that PAMAM-NH<sub>2</sub> has low cytotoxicity at working concentrations.

## 4 DISCUSSION

CHX is commonly recommended to be used as cavity cleanser in the clinic. Nevertheless, weak binding affinity for collagen and



the leaching-out property make CHX short-lived, thus limiting its potential clinical applications. Therefore, it is in demand to develop a new cavity cleanser with long-term antimicrobial and anti-proteolytic activities.

PAMAM-NH<sub>2</sub> dendrimer is categorized as one type of hyperbranched polymeric macromolecules and has been extensively investigated as a promising antibacterial agent (Castonguay et al., 2012; Mintzer et al., 2012). However, the dentinal tubules are filled with fluid. Intrapulpal pressure enables constant replenishment of intrinsic water from the pulp chamber to the dentin surface. Therefore, the binding capacity of PAMAM-NH<sub>2</sub> to demineralized dentin is important to fulfill its long-term antimicrobial and anti-proteolytic effects. In this study, ATR-FTIR spectroscopy and CLSM of the demineralized dentin, after being conditioned with 4 mg/ml of PAMAM-NH<sub>2</sub> or 2% CHX and after being washed with PBS, respectively, were first performed. From the present results, characteristic peaks of CHX or PAMAM-NH<sub>2</sub> were clearly observed in ATR-FTIR spectra after dentin discs were conditioned with 2% CHX or PAMAM-NH<sub>2</sub> (Figure 1A), indicating that both CHX and PAMAM-NH<sub>2</sub> could bind to the demineralized dentin surface. However, the characteristic peaks of CHX disappeared in 2% CHX conditioning dentin surface, after being washed with PBS, demonstrating that 2% CHX had a weak binding capacity to demineralized dentin surface. In contrast, PAMAM-NH<sub>2</sub>-conditioned dentin surface retained large amounts of PAMAM-NH<sub>2</sub> following washing, as suggested by the presence of the characteristic amide peaks. The results demonstrated that the binding capacity of PAMAM-NH<sub>2</sub> on demineralized dentin surface was much stronger than that of 2% CHX, and the binding was strong enough to resist PBS washing. These results were also confirmed by CLSM. CLSM images (Figure 1B) showed that the yellow-green fluorescence was visible all over the surface of the FITC-labeled PAMAM-NH<sub>2</sub> sample with an intensity value of  $89.6\% \pm 3.5\%$  (Figure 1C), while little fluorescence observed on the free FITC sample reaching  $26.8\% \pm 5.7\%$  fluorescence intensity after PBS washing. Thus, PAMAM-NH<sub>2</sub> is considered to have a better binding capacity to demineralized dentin, as it can resist PBS washing. The results

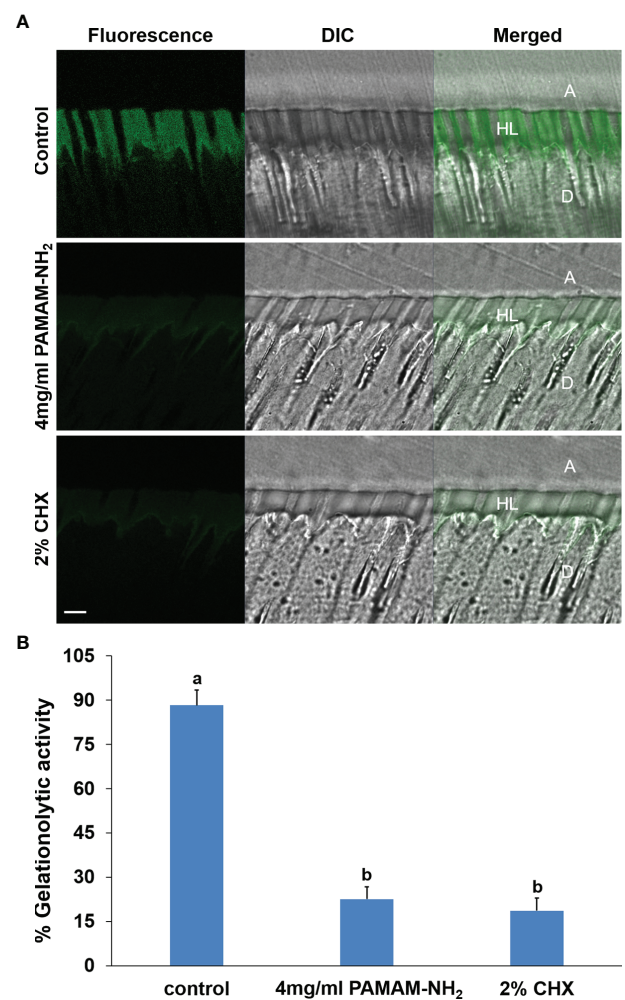
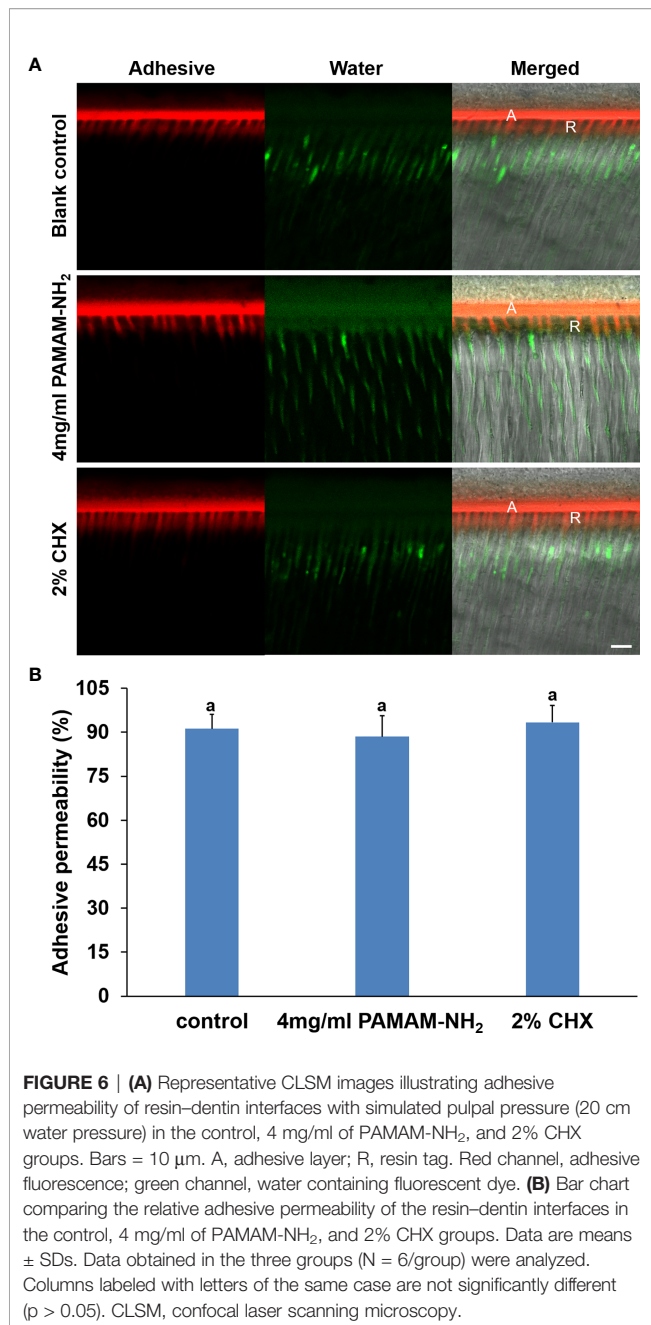


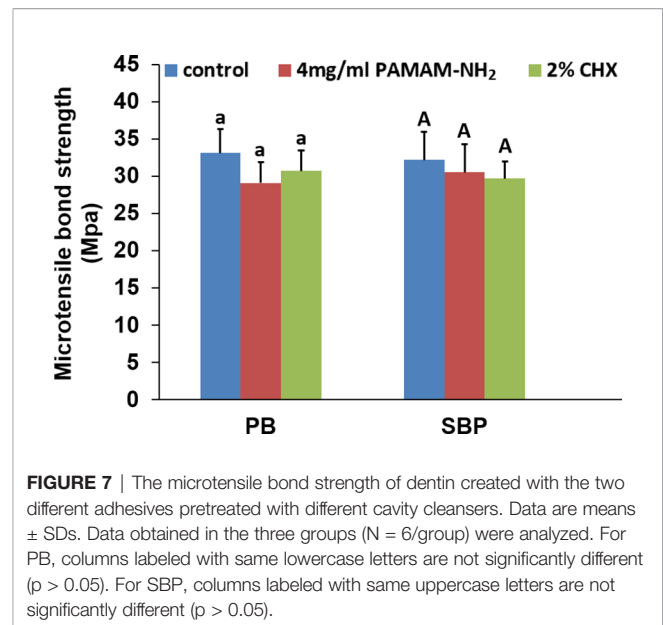
**FIGURE 5 | (A)** Representative CLSM images of *in situ* zymography performed in resin–dentin interfaces pretreated with the deionized water control, 4 mg/ml PAMAM-NH<sub>2</sub> cavity cleanser, or the 2% CHX cavity cleanser prior to adhesive application. Bars = 5  $\mu$ m. A, adhesive layer; HL, hybrid layer; D, dentin. Green channel: fluorescence derived from dequenched fluorescein released after breaking down of the highly quenched fluorescein-conjugated extrinsic gelatin source into smaller peptides. DIC, differential interference contrast image of the resin–dentin interface. **(B)** Quantified *in situ* zymography data depicting the percentage of hybrid layers that exhibit activity against extrinsic fluorescein-conjugated gelatin in the deionized water control, 4 mg/ml of PAMAM-NH<sub>2</sub> cavity cleanser, or the 2% CHX cavity cleanser. Data are means  $\pm$  SDs. Data obtained in the three groups (N = 6/group) were analyzed. Columns labeled with different lowercase letters are significantly different ( $p < 0.05$ ). CLSM, confocal laser scanning microscopy.

were consistent with a previous study, which also showed that PAMAM-NH<sub>2</sub> had a good binding capacity to the demineralized dentin (Liang et al., 2015). The stronger binding capacity of PAMAM-NH<sub>2</sub> over 2% CHX is likely attributed to its great number of functional groups. The external amine groups are positively charged groups, and the internal amide groups are negatively charged groups. These charged groups may help the molecule to bind to the collagen fibrils *via* electrostatic interactions (Liang et al., 2015). Thus, the first and third hypotheses



that “the PAMAM-NH<sub>2</sub> cavity cleanser has long-term inhibitory effects on bacteria and endogenous dentin proteases” are partially validated by the binding experiments.

Although PAMAM-NH<sub>2</sub> has been extensively investigated as a promising antibacterial agent (Castonguay et al., 2012; Mintzer et al., 2012), there are just few reports whether PAMAM-NH<sub>2</sub> has inhibitory effects on oral pathogens. *S. mutans* and *A. naeslundii* are cariogenic oral pathogens associated with secondary caries (Mo et al., 2010), which is described as a multifactorial infectious disease that is characterized by oral microbiome dysbiosis with the elevation of cariogenic bacteria (Tanner et al., 2016). *E. faecalis* is a common bacterium in filled



root canals with persistent apical periodontitis (Wang et al., 2012). Because establishment of coronal seal with composite resin is frequently performed after placement of root fillings to prevent reinfection of the obturated canal space, the antibacterial activity of PAMAM-NH<sub>2</sub> on *E. faecalis* was also evaluated (Guo et al., 2019). Therefore, these three microbes were chosen to evaluate the antibacterial properties of PAMAM-NH<sub>2</sub> cavity cleanser. From the results of antibacterial activities, the antibacterial effect of PAMAM-NH<sub>2</sub> was comparable with that of 2% CHX. Thus, the first hypothesis that “the PAMAM-NH<sub>2</sub> cavity cleanser has long-term inhibitory effects on bacteria grown on dentin blocks” is totally validated. PAMAM-NH<sub>2</sub> has a great number of positive charges on the protonated amino terminal groups on its exterior, which confers a strong affinity for bacterial surface with negative charges by electrostatic interactions. Such initial electrostatic interactions subsequently promote the disruption of anionic bacterial cell membranes and peptidoglycan, leading to leakage of cytoplasmic components and bacteria death (Castonguay et al., 2012; Mintzer et al., 2012; Gou et al., 2017). Due to its ability to damage bacteria through non-specific physical mechanisms rather than by targeting specific molecules (Wang et al., 2010), cationic PAMAM-NH<sub>2</sub> dendrimer works against not only non-resistant bacteria but also currently antibiotic-resistant strains and is less likely to contribute to the development of bacteria resistance (Xue et al., 2013).

Dental plaque is a dynamic and complex ecosystem consisting of multispecies microbial communities. The development of dental caries is closely associated with imbalance in microbial equilibrium rather than a single pathogenic species (Filoche et al., 2010). Changes in the oral environment, such as food intake or saliva flow, may trigger a shift in dental plaque, in which acidogenic/aciduric species are selectively enriched at the expense of those less aciduric commensal residents (Filoche et al., 2010; Zheng et al., 2015). These changes lead to acid accumulation



**TABLE 2** | Percentage distribution of failure modes (A: adhesive failure; M: mixed failure; CC: cohesive failure in resin composite; CD: cohesive failure in dentin).

Failure mode	Prime & Bond NT™			Adper™ Single Bond Plus		
	Control	PAMAM-NH <sub>2</sub>	CHX	Control	PAMAM-NH <sub>2</sub>	CHX
A	10	11	8	11	14	7
M	42	39	40	41	39	45
CD	3	5	8	1	1	3
CC	5	5	4	7	6	5
Total	60	60	60	60	60	60

and subsequent pH declination, thus producing dental plaque with a more cariogenic composition. Several clinical studies confirmed that the diversity of the microbiota in carious lesions could be decreased by the establishment and dominance of acidogenic/aciduric species (Costalonga and Herzberg, 2014; Kianoush et al., 2014), and a higher proportion of *S. mutans* has been observed in lesion spots (Ge et al., 2008). In our study, with the stress from the PAMAM-NH<sub>2</sub> cavity cleanser, the enriched acidogenic/aciduric species (e.g., *S. mutans* and *A. naeslundii*) were obviously inhibited and appeared to lose their dominant position, which has a potential effect in maintaining a healthy oral microbial equilibrium. Further biofilm composition studies and possible mechanism studies are required to support the potential biofilm species modulation of the presently developed bioactive PAMAM-NH<sub>2</sub> cavity cleaner.

The hybrid layer remains the weakest link within the bonded interface due to its degradation *via* endogenous dentin proteases. They become exposed and activated during the acid-etching and adhesive placement steps of contemporary bonding procedures, which contributes to the degradation of exposed collagen fibrils within the hybrid layers. Therefore, our present study also aimed to explore whether PAMAM-NH<sub>2</sub> can inhibit endogenous MMP in the dentin matrix. Soluble rhMMP-9 was employed for examining the potential inhibitory effect of PAMAM-NH<sub>2</sub> by Sensolyte assay kits. The results of the quantitative assay

demonstrated that the extent of rhMMP-9 inhibition was proportional to PAMAM-NH<sub>2</sub> concentrations. The anti-MMP-9 activities of PAMAM-NH<sub>2</sub> at concentrations higher than 4 mg/ml (4 to 16 mg/ml) were comparable with those of the GM6001 control group ( $p > 0.05$ ). Hence, the second hypothesis that “the PAMAM-NH<sub>2</sub> cavity cleanser has inhibitory effects on soluble MMP-9 activities” is validated. However, this experiment confirmed that PAMAM-NH<sub>2</sub> has inhibitory effects on exogenous rhMMP-9. Its effect on endogenous MMP-9 embedded within collagen matrix should also be investigated. In the present study, *in situ* zymography was employed to detect the proteolytic activity of the endogenous MMP-9 directly within dentin hybrid layers (Frederiks and Mook, 2004; Gou et al., 2018b). According to the concentrations of PAMAM-NH<sub>2</sub> tested from antibacterial activities and inhibitory effects on exogenous rhMMP-9, the concentration of 4 mg/ml of PAMAM-NH<sub>2</sub> was used for the following experiments. For the control groups, extensive green fluorescence was detected within the hybrid layers, indicating strong gelatinolytic activity. In contrast, dentin slabs pretreated with 4 mg/ml of PAMAM-NH<sub>2</sub> exhibited weak gelatinolytic activity within the hybrid layers after incubation for 48 h, which is significantly lower than that of the control group. Thus, the third hypothesis that “the PAMAM-NH<sub>2</sub> cavity cleanser has long-term inhibitory effects on endogenous dentin proteases” is totally validated.

Although the functional mechanism of inhibitory effects of PAMAM-NH<sub>2</sub> on dentin proteases is still not clear, several factors may have contributed to the inhibitory effect. The catalytic domains of MMPs contain cysteine-rich sites, including negatively charged glutamic acid residues (Tezvergil-Mutluay et al., 2011). PAMAM-NH<sub>2</sub> may bind electrostatically to the negatively charged glutamic acid residues with a great number of positive charges on the protonated amino groups on its exterior. This non-specific binding can change the configuration of the catalytic site of the MMPs by electrostatic interaction with the negatively charged glutamic acid residues, sterically blocking the active site and inhibiting the activation of MMPs. Additionally, amine-terminated dendritic polymers were reported as a multifunctional chelating agent for heavy metal ion removals (Mohseni et al., 2019). Accordingly, we surmise that the inhibitory effect of PAMAM-NH<sub>2</sub> on MMPs is potentially related to its potency of chelation on Zn<sup>2+</sup> and Ca<sup>2+</sup>. MMPs are a family of Zn- and Ca-dependent enzymes (Zitka et al., 2010). PAMAM-NH<sub>2</sub> may chelate Zn<sup>2+</sup> or Ca<sup>2+</sup> that can be bound to the Zn<sup>2+</sup>- and Ca<sup>2+</sup>-active sites of the catalytic domain of MMPs (Wu et al., 2019), which is also conducive to inhibiting MMP activities.

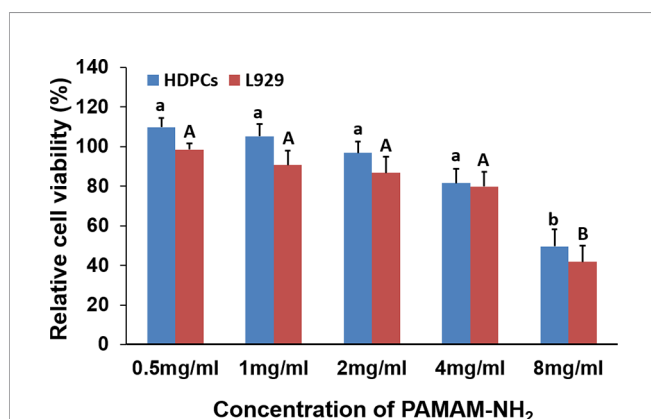


**FIGURE 8** | Cytotoxicity assay of PAMAM-NH<sub>2</sub> to HDPCs and L929 at different concentrations by CCK-8 assay. Data are means  $\pm$  SDs. Data obtained in the three groups (N = 6/group) were analyzed. For HDPCs, columns labeled with same lowercase letters are not significantly different ( $p > 0.05$ ). For L929, columns labeled with same uppercase letters are not significantly different ( $p > 0.05$ ). HDPCs, human dental pulp cells.



Adhesive infiltration into the dentinal tubules is paramount for preserving the integrity of resin–dentin bonding. To evaluate the effect of PAMAM-NH<sub>2</sub> on the adhesive permeation and morphology of the resin–dentin interface, the bonded dentin interface was observed by a double-fluorescence CLSM technique. From the present results, the resin tag shared a morphological similarity in both experimental and control groups. The quantitative analysis of permeability also demonstrated that PAMAM-NH<sub>2</sub> as a cavity cleanser did not decrease the infiltration of adhesive monomers.

The dentin tensile bond strengths were also performed to evaluate whether the application of PAMAM-NH<sub>2</sub> adversely affects the tensile bond strength of commercial adhesive. The results showed that pretreatment of dentin surface with PAMAM-NH<sub>2</sub> or 2% CHX had no adverse effect on the dentin bond strength. Thus, the fourth hypothesis that “treatment of dentin surface with PAMAM-NH<sub>2</sub> cavity cleanser does not adversely affect dentin bond strength” is validated.

In our study, the relative cell viability in the range of 80%–110% was observed with PAMAM-NH<sub>2</sub> at concentrations equal to or lower than 4 mg/ml (0.5 to 4 mg/ml), which is considered non-cytotoxic (Zou et al., 2011; International Organization for Standardization, 2009) and has potential clinical application at working concentration.

## 5 CONCLUSION

Within the limitations of the present study, it may be concluded that PAMAM-NH<sub>2</sub> cavity cleanser developed in this study could provide simultaneous long-term antimicrobial and anti-proteolytic activities for eliminating secondary caries that results from a dysbiosis in the oral microbiome and preventing hybrid layers from degradation due to its good binding capacity to dentin collagen matrix, which are crucial for the maintenance of resin–dentin bond durability. Although the price of the commercially available cavity cleaner–2% CHX may be slightly lower than that of PAMAM-NH<sub>2</sub>, long-term antibacterial and anti-proteolytic activities may give PAMAM-NH<sub>2</sub> an advantage over CHX.

## REFERENCES

- Blackburn, R. S., Harvey, A., Kettle, L. L., Manian, A. P., Payne, J. D., and Russell, S. J. (2007). Sorption of Chlorhexidine on Cellulose: Mechanism of Binding and Molecular Recognition. *J. Phys. Chem. B* 111, 8775–8784. doi: 10.1021/jp070856r
- Breschi, L., Mazzoni, A., Ruggeri, A., Cadenaro, M., Di Lenarda, R., and De Stefano Dorigo, E. (2008). Dental Adhesion Review: Aging and Stability of the Bonded Interface. *Dent. Mater.* 24, 90–101. doi: 10.1016/j.dental.2007.02.009
- Castonguay, A., Ladd, E., van de Ven, T. G. M., and Kakkar, A. (2012). Dendrimers as Bactericides. *N. J. Chem.* 36, 199–204. doi: 10.1039/C1NJ20481E
- Costalonga, M., and Herzberg, M. C. (2014). The Oral Microbiome and the Immunobiology of Periodontal Disease and Caries. *Immunol. Lett.* 162, 22–38. doi: 10.1016/j.imlet.2014.08.017
- Ersin, N. K., Aykut, A., Candan, U., Onçağ, O., Eronat, C., and Kose, T. (2008). The Effect of a Chlorhexidine Containing Cavity Disinfectant on the Clinical Performance of High-Viscosity Glass-Ionomer Cement Following ART: 24-Month Results. *Am. J. Dent.* 21, 39–43. doi: 10.1016/j.tripleo.2007.09.017

## DATA AVAILABILITY STATEMENT

The original contributions presented in the study are included in the article/supplementary material. Further inquiries can be directed to the corresponding authors.

## ETHICS STATEMENT

The studies involving human participants were reviewed and approved by Clinical Scientific Research Ethics Committee of Hospital of Stomatology, Lanzhou University. The patients/participants provided their written informed consent to participate in this study.

## AUTHOR CONTRIBUTIONS

YG contributed to the conception, design, data acquisition, analysis, and interpretation and drafted and revised the manuscript. WJ contributed to the data acquisition and interpretation and drafted the manuscript. YaH contributed to the data acquisition and analysis and drafted the manuscript. YL, RS, YuH, ZW, and JL contributed to the design, data analysis, and interpretation and drafted the manuscript. BL contributed to the data analysis and interpretation and critically revised the manuscript. All authors contributed to the article and approved the submitted version.

## FUNDING

This work was supported by the National Natural Science Foundation of China grant 82001034, Natural Science Foundation in Gansu Province of China grant 20JR10RA595, Fundamental Research Funds for the Central Universities of Lanzhou University grant lzujbky-2020-53, and School/Hospital of Stomatology, Lanzhou University grant lzukqky-2019-y15 (YG).

- Filoché, S., Wong, L., and Sissons, C. H. (2010). Oral Biofilms: Emerging Concepts in Microbial Ecology. *J. Dent. Res.* 89, 8–18. doi: 10.1177/0022034509351812
- Frassetto, A., Breschi, L., Turco, G., Marchesi, G., Di Lenarda, R., Tay, F. R., et al. (2016). Mechanisms of Degradation of the Hybrid Layer in Adhesive Dentistry and Therapeutic Agents to Improve Bond Durability—A Literature Review. *Dent. Mater.* 32, e41–e53. doi: 10.1016/j.dental.2015.11.007
- Frederiks, W. M., and Mook, O. R. (2004). Metabolic Mapping of Proteinase Activity With Emphasis on in Situ Zymography of Gelatinases: Review and Protocols. *J. Histochem. Cytochem.* 52, 711–722. doi: 10.1369/jhc.4R6251.2004
- Ge, Y., Caulfield, P. W., Fisch, G. S., and Li, Y. (2008). Streptococcus Mutans and Streptococcus Sanguinis Colonization Correlated With Caries Experience in Children. *Caries Res.* 42, 444–448. doi: 10.1159/000159608
- Gou, Y. P., Li, J. Y., Meghil, M. M., Cutler, C. W., Xu, H. H. K., Tay, F. R., et al. (2018a). Quaternary Ammonium Silane-Based Antibacterial and Anti-Proteolytic Cavity Cleanser. *Dent. Mater.* 34, 1814–1827. doi: 10.1016/j.dental.2018.10.001
- Gou, Y. P., Meghil, M. M., Pucci, C. R., Breschi, L., Pashley, D. H., Cutler, C. W., et al. (2018b). Optimizing Resin–Dentin Bond Stability Using a Bioactive

- Adhesive With Concomitant Antibacterial Properties and Anti-Proteolytic Activities. *Acta Biomater.* 75, 171–182. doi: 10.1016/j.actbio.2018.06.008
- Gou, Y. P., Yang, X., He, L. B., Xu, X. Y., Liu, Y. P., Liu, Y. B., et al. (2017). Bio-Inspired Peptide Decorated Dendrimers for a Robust Antibacterial Coating on Hydroxyapatite. *Polym. Chem.* 8, 4264–4279. doi: 10.1039/C7PY00811B
- Guo, J. M., Makvandi, P., Wei, C. C., Chen, J. H., Xu, H. K., Breschi, L., et al. (2019). Polymer Conjugation Optimizes EDTA as a Calcium-Chelating Agent That Exclusively Removes Extrafibrillar Minerals From Mineralized Collagen. *Acta Biomater.* 90, 424–440. doi: 10.1016/j.actbio.2019.04.011
- International Organization for Standardization. (2009). *ISO 10993-5: 2009 (E)*. Available at: <https://www.iso.org/obp/ui/#iso>.
- Kianoush, N., Adler, C. J., Nguyen, K. A., Browne, G. V., Simonian, M., and Hunter, N. (2014). Bacterial Profile of Dentine Caries and the Impact of pH on Bacterial Population Diversity. *PLoS One* 9, e92940. doi: 10.1371/journal.pone.0092940
- Liang, K., Yuan, H., Li, J., Yang, J., Zhou, X., He, L., et al. (2015). Remineralization of Demineralized Dentin Induced by Amine-Terminated PAMAM Dendrimer. *Macromol. Mater. Eng.* 300, 107–117. doi: 10.1002/mame.201400207
- Mazzoni, A., Tjäderhane, L., Checchi, V., Di Lenarda, R., Salo, T., Tay, F. R., et al. (2015). Role of Dentin MMPs in Caries Progression and Bond Stability. *J. Dent. Res.* 94, 241–251. doi: 10.1177/0022034514562833
- Mintzer, M. A., Dane, E. L., O'Toole, G. A., and Grinstaff, M. W. (2012). Exploiting Dendrimer Multivalency To Combat Emerging and Re-Emerging Infectious Diseases. *Mol. Pharmaceut.* 9, 342–354. doi: 10.1021/mp2005033
- Mo, S. S., Bao, W., Lai, G. Y., Wang, J., and Li, M. Y. (2010). The Microfloral Analysis of Secondary Caries Biofilm Around Class I and Class II Composite and Amalgam Fillings. *BMC. Infect. Dis.* 10:241. doi: 10.1186/1471-2334-10-241
- Mohseni, M., Akbari, S., Pajootan, E., and Mazaheri, F. (2019). Amine-Terminated Dendritic Polymers as a Multifunctional Chelating Agent for Heavy Metal Ion Removals. *Environ. Sci. Pollut. Res. Int.* 26, 12689–12697. doi: 10.1007/s11356-019-04765-3
- Nyvad, B., and Kilian, M. (1987). Microbiology of the Early Colonization of Human Enamel and Root Surfaces In Vivo. *Scand. J. Dent. Res.* 95, 369–380. doi: 10.1111/j.1600-0722.1987.tb01627.x
- Osorio, R., Yamauti, M., Osorio, E., Ruiz-Requena, M. E., Pashley, D., Tay, F., et al. (2011). Effect of Dentin Etching and Chlorhexidine Application on Metalloproteinase-Mediated Collagen Degradation. *Eur. J. Oral. Sci.* 119, 79–85. doi: 10.1111/j.1600-0722.2010.00789.x
- Scaffa, P. M., Vidal, C. M., Barros, N., Gesteira, T. F., Carmona, A. K., Breschi, L., et al. (2012). Chlorhexidine Inhibits the Activity of Dental Cysteine Cathepsins. *J. Dent. Res.* 91, 420–425. doi: 10.1177/0022034511435329
- Slee, A. M., and Tanzer, J. M. (1979). Studies on the Relative Binding Affinities of Chlorhexidine Analogs to Cation Exchange Surfaces. *J. Periodontol. Res.* 14, 213–219. doi: 10.1111/j.1600-0765.1979.tb00225.x
- Tanner, A. C., Kressler, C. A., and Faller, L. L. (2016). Understanding Caries From the Oral Microbiome Perspective. *J. Calif. Dent. Assoc.* 44, 437–446.
- Tay, F. R., Pashley, D. H., Loushine, R. J., Weller, R. N., Monticelli, F., and Osorio, R. (2006). Self-Etching Adhesives Increase Collagenolytic Activity in Radicular Dentin. *J. Endod.* 32, 862–868. doi: 10.1016/j.joen.2006.04.005
- Tezvergil-Mutluay, A., Agee, K. A., Uchiyama, T., Imazato, S., Mutluay, M. M., Cadenaro, M., et al. (2011). The Inhibitory Effects of Quaternary Ammonium Methacrylates on Soluble and Matrix-Bound MMPs. *J. Dent. Res.* 90, 535–540. doi: 10.1177/0022034510389472
- Thompson, V., Craig, R. G., Curro, F. A., Green, W. S., and Ship, J. A. (2008). Treatment of Deep Carious Lesions by Complete Excavation or Partial Removal: A Critical Review. *J. Am. Dent. Assoc.* 139, 705–712. doi: 10.14219/jada.archive.2008.0252
- Tjäderhane, L., Nascimento, F. D., Breschi, L., Mazzoni, A., Tersariol, I. L., Geraldeli, S., et al. (2013). Strategies to Prevent Hydrolytic Degradation of the Hybrid Layer-A Review. *Dent. Mater.* 29, 999–1011. doi: 10.1016/j.dental.2013.07.016
- Türkün, M., Türkün, L. S., Ergücü, Z., and Ateş, M. (2006). Is an Antibacterial Adhesive System More Effective Than Cavity Disinfectants? *Am. J. Dent.* 19, 166–170. doi: 10.1080/00016350600573191
- Twetman, S. (2004). Antimicrobials in Future Caries Control? A Review With Special Reference to Chlorhexidine Treatment. *Caries Res.* 38, 223–229. doi: 10.1159/000077758
- Walsh, L. J., and Brostek, A. M. (2013). Minimum Intervention Dentistry Principles and Objectives. *Aust. Dent. J.* 58 Suppl. 1, 3–16. doi: 10.1111/adj.12045
- Wang, B., Navath, R. S., Menjoge, A. R., Balakrishnan, B., Bellair, R., Dai, H., et al. (2010). Inhibition of Bacterial Growth and Intramniotic Infection in a Guinea Pig Model of Chorioamnionitis Using PAMAM Dendrimers. *Int. J. Pharm.* 395, 298–308. doi: 10.1016/j.ijpharm.2010.05.030
- Wang, Q. Q., Zhang, C. F., Chu, C. H., and Zhu, X. F. (2012). Prevalence of Enterococcus Faecalis in Saliva and Filled Root Canals of Teeth Associated With Apical Periodontitis. *Int. J. Oral. Sci.* 4, 19–23. doi: 10.1038/ijos.2012.17
- Wu, Q. A., Shan, T., Zhao, M., Mai, S., and Gu, L. (2019). The Inhibitory Effect of Carboxyl-Terminated Polyamidoamine Dendrimers on Dentine Host-Derived Matrix Metalloproteinases In Vitro in an Etch-and-Rinse Adhesive System. *R. Soc. Open Sci.* 6, 182104. doi: 10.1098/rsos.182104
- Xue, X., Chen, X., Mao, X., Hou, Z., Zhou, Y., Bai, H., et al. (2013). Amino-Terminated Generation 2 Poly(Amidoamine) Dendrimer as a Potential Broad-Spectrum, Nonresistance-Inducing Antibacterial Agent. *AAPS. J.* 15, 132–142. doi: 10.1208/s12248-012-9416-8
- Zheng, X., Cheng, X., Wang, L., Qiu, W., Wang, S., Zhou, Y., et al. (2015). Combinatorial Effects of Arginine and Fluoride on Oral Bacteria. *J. Dent. Res.* 94, 344–353. doi: 10.1177/0022034514561259
- Zitka, O., Kukacka, J., Krizkova, S., Huska, D., Adam, V., Masarik, M., et al. (2010). Matrix Metalloproteinases. *Curr. Med. Chem.* 17, 3751–3768. doi: 10.2174/092986710793213724
- Zou, Y., Wang, W. M., Zhu, Y. N., and Yang, W. D. (2011). In Vitro Evaluation the Cytotoxicity of Dental Bonding Agents Through CCK-8 Assay. *J. Oral. Sci. R.* 27 (8), 673–675. doi: 10.13701/j.cnki.kqxyj.2011.08.014

**Conflict of Interest:** The authors declare that the research was conducted in the absence of any commercial or financial relationships that could be construed as a potential conflict of interest.

**Publisher's Note:** All claims expressed in this article are solely those of the authors and do not necessarily represent those of their affiliated organizations, or those of the publisher, the editors and the reviewers. Any product that may be evaluated in this article, or claim that may be made by its manufacturer, is not guaranteed or endorsed by the publisher.

Copyright © 2021 Gou, Jin, He, Luo, Si, He, Wang, Li and Liu. This is an open-access article distributed under the terms of the Creative Commons Attribution License (CC BY). The use, distribution or reproduction in other forums is permitted, provided the original author(s) and the copyright owner(s) are credited and that the original publication in this journal is cited, in accordance with accepted academic practice. No use, distribution or reproduction is permitted which does not comply with these terms.



# Comparative Analysis of Salivary Mycobiome Diversity in Human Immunodeficiency Virus-Infected Patients

Shenghua Chang<sup>1†</sup>, Haiying Guo<sup>1†</sup>, Jin Li<sup>1</sup>, Yaoting Ji<sup>1</sup>, Han Jiang<sup>1</sup>, Lianguo Ruan<sup>2\*</sup> and Minquan Du<sup>1\*</sup>

<sup>1</sup> The State Key Laboratory Breeding Base of Basic Science of Stomatology (Hubei-MOST) and Key Laboratory of Oral Biomedicine Ministry of Education, School & Hospital of Stomatology, Wuhan University, Wuhan, China, <sup>2</sup> Department of Infectious Diseases Treatment, Wuhan Medical Treatment Center, Wuhan, China

## OPEN ACCESS

### Edited by:

Yulong Niu,  
Sichuan University, China

### Reviewed by:

Pengfan Zhang,  
Max Planck Institute for Plant Breeding  
Research, Germany  
Maria D'Accolti,  
University of Ferrara, Italy

### \*Correspondence:

Lianguo Ruan  
jianxing1014@foxmail.com  
Minquan Du  
duminquan@whu.edu.cn

<sup>†</sup>These authors have contributed  
equally to this work and share  
first authorship

### Specialty section:

This article was submitted to  
Microbiome in Health and Disease,  
a section of the journal  
Frontiers in Cellular  
and Infection Microbiology

**Received:** 22 September 2021

**Accepted:** 09 November 2021

**Published:** 01 December 2021

### Citation:

Chang S, Guo H, Li J, Ji Y, Jiang H,  
Ruan L and Du M (2021) Comparative  
Analysis of Salivary Mycobiome  
Diversity in Human Immunodeficiency  
Virus-Infected Patients.  
Front. Cell. Infect. Microbiol. 11:781246.  
doi: 10.3389/fcimb.2021.781246

Reports on alterations in the oral mycobiome of HIV-infected patients are still limited. This study was designed to compare the salivary mycobiome between 30 human immunodeficiency virus (HIV) infections and 30 healthy controls and explore the effect of antiretroviral therapy (ART) administration on the oral mycobiome of HIV infections. Results showed that the diversity and richness of salivary mycobiome in HIV-infected individuals were higher than those of controls ( $P < 0.05$ ). After ART, the diversity and richness of salivary mycobiome in HIV-infected patients were reduced significantly ( $P < 0.05$ ). *Candida*, *Mortierella*, *Malassezia*, *Simplicillium*, and *Penicillium* were significantly enriched in the HIV group and dramatically decreased after ART. While the relative abundance of *Verticillium*, *Issatchenkia*, and *Alternaria* significantly increased in patients with HIV after ART. Correlation analysis revealed that *Mortierella*, *Malassezia*, *Simplicillium*, and *Chaetomium* were positively correlated with viral load (VL), whereas *Thyrostroma* and *Archaeorhizomyces* were negatively related to VL and positively related to CD4<sup>+</sup> T-cell counts. All results showed that HIV infection and ART administration affected the composition of salivary mycobiome communities. Furthermore, differences of salivary mycobiome in HIV infections after ART were complex and might mirror the immune state of the body.

**Keywords:** saliva, salivary mycobiome, human immunodeficiency virus, antiretroviral therapy, high-throughput sequencing

## INTRODUCTION

Human immunodeficiency virus (HIV) infection likely results in a progressive decrease in the number and function of CD4<sup>+</sup> T lymphocytes; consequently, patients are susceptible to various opportunistic infections (Cohen et al., 2011). A high prevalence of HIV infection has been reported. There were approximately 37.6 million people living with HIV in the world at the end of 2020 and 1.5 million new infections in 2020 (Poole et al., 2013). Opportunistic infections are common among HIV-infected patients even in the era of antiretroviral therapy (ART) (Leigh et al., 2004; Aberg and Powderly, 2010). Candidiasis, pneumocystis pneumonia, and cryptococcal infections are frequently

reported (Patil et al., 2018). Among them, oral candidiasis is the most common oral infection and could be detected in the early stage of HIV infection. Moreover, the risk of suffering from oral candidiasis by HIV-infected individuals, even those who have higher CD4<sup>+</sup> T-cell counts, is higher than that by uninfected subjects (Owotade et al., 2008; Thompson et al., 2010; Hu et al., 2018); this finding can serve as a guidance for dentists to find a suspicious HIV infection (Armstrong-James et al., 2014). Oral candidiasis may also spread outside the mouth, causing candida infections in the esophagus or stomach (Hugh, 2014). Evidence has shown that similar mold and fungal communities are found in the respiratory tract, gastrointestinal tract, and mouth of HIV-infected individuals (Lijia et al., 2015; HC and GM, 2018). These findings suggested that the salivary mycobiome may play an important role in infectious diseases.

Saliva is a type of body fluid, which is nearly 50% similar to the blood, easy to collect and store (Pfaffe et al., 2011). Saliva contains human oral microorganisms, as well as DNA, RNA, proteins, and other parts, which makes it a good sample to provide information for clinical diagnosis (Zhang et al., 2016) in oral cancer (Park et al., 2009; Vidotto et al., 2010), diabetes mellitus (Abdolsamadi et al., 2014), cardiovascular disease (Zheng et al., 2014), and viral infections (Nefzi et al., 2015). Though there is a very diverse environment in saliva, the diversity of salivary microbiome is similar between individuals in short- and long-term longitudinal studies (Cameron et al., 2015; Belstrom et al., 2016; Wang et al., 2020).

In recent years, increasing studies have focused on the interaction between HIV infection and microorganisms. With the development of high-throughput sequencing technology, accumulating results have revealed significant alterations in the microbiome of the gastrointestinal tract (Ling et al., 2016), vagina (Cohen, 2016), lung (Twigg et al., 2017), and mouth (Kistler et al., 2015) in HIV-infected patients. Studies on the characteristics of the oral microbiome have also been widely performed, but most studies have focused on changes in oral bacteria. Besides, most of these studies are cross-sectional studies (Hegde et al., 2014; Li et al., 2014; Mukherjee et al., 2014; Beck et al., 2015; Kistler et al., 2015; Noguera-Julian et al., 2017), and only a few studies have investigated longitudinal variation in oral bacteria after ART administration (Navazesh et al., 2005; Li et al., 2014; Presti et al., 2018). Reports on alterations in the oral mycobiome of HIV-infected patients are still limited, and longitudinal variations are few.

In this study, next-generation sequencing (NGS) was conducted to analyze the characteristics of the salivary mycobiome in HIV-infected individuals and to further explore the variation in the salivary microbiome of HIV-infected patients after 6 months of ART administration.

## METHODS

### Subject Recruitment

Newly HIV-infected patients were recruited from Wuhan Medical Treatment Center, China, and HIV-uninfected

subjects were enrolled from the Wuhan University, China (this study was approved by the ethics committee of the School & Hospital of Stomatology, Wuhan University). HIV-infected participants were followed up for 6 months during ART administrations.

The inclusion criteria were as follows: 1) individuals were diagnosed with HIV in the past 1 year, without receiving antiretroviral therapy, or individuals were age- and gender-paired HIV-uninfected subjects; 2) participants aged over 18 years and under 60 years; 3) subjects who could cooperate and sign the informed consent forms.

The exclusion criteria were as follows: 1) subjects were diagnosed with HIV more than 1 year or with HIV in the past 1 year but received ART; 2) obvious clinical oral symptoms, including caries, periodontal disease, mucous disease, and oral surgical disease; 3) history of dental treatments in the past 6 months; 4) receiving antibiotics, immunomodulators, and probiotic treatments in the past 3 months; 5) history of infectious diseases, such as hepatitis B infection, tuberculosis infection, *Treponema pallidum* infection, and so on; 6) history of systemic diseases, such as diabetes, hypertension, and cancer; 7) history of inherited metabolic diseases and autoimmune diseases.

### Sample Collection

Subjects were instructed not to eat or drink within 1 h before sample collection. At rest, approximately 2 ml non-stimulated saliva was collected by using a 5-ml saliva collector (DNAgard® Saliva, Boykko Pharmaceutical Co. Ltd., Tokyo, Japan). Then, 1.5 ml of preservation solution was added to saliva, and they were mixed upside down for 5 s. All samples were shipped to the laboratory on dry ice and stored in a refrigerator at -80°C for further use.

### Genomic DNA Isolation and PCR Amplification

The EZNATM Mag-Bind Soil DNA Kit (OMEGA M5635-02, Norcross, GA, USA) was used to extract DNA, and Illumina nest PCR was performed to amplify the full-length Internal Transcribed Spacer (ITS) gene. The first cycling conditions were as follows: initial denaturation at 94°C for 3 min, five cycles of denaturation at 94°C for 30 s, annealing at 45°C for 1 min, elongation at 65°C for 30 s, 20 cycles of denaturation at 94°C for 20 s, annealing at 55°C for 20 s, elongation at 72°C for 30 s, and a final extension step at 72°C for 5 min. Then, 20 ng of the PCR products of each sample were used for the second PCR amplification with specific primers (ITSF: CTTGGTCA TTTAGAGGAAGTAA and ITS2R: GCTGCGTTCTTCAT CGATGC). The second cycling conditions were as follows: initial denaturation at 94°C for 3 min, five cycles of denaturation at 94°C for 20 s, annealing at 55°C for 20 s, elongation at 72°C for 30 s, and a final extension step at 72°C for 5 min. The PCR products of the second amplification were purified using Agencourt AMPure XP (Transgen, EC401-03, Beckman Coulter, Brea, CA, USA) and then were accurately quantified with a Qubit 3.0 DNA detection kit (Life Q10210, Carlsbad, CA, USA). Lastly, 20 pmol of PCR products in the



second amplification of each sample were used to sequence in Miseq2000 sequencing platform.

## Internal Transcribed Spacer rRNA Gene Sequence Analysis

The raw sequences obtained from this study were deposited into the NCBI Sequence Read Archive under the accession number PRJNA626395.

A total of 84 non-stimulated saliva samples were analyzed in this study. Prinseq (Schmieder and Edwards, 2011) was used to remove the bases with the read tail values less than 20 in each sample and cut out the N-containing sequences in reads. Then, short sequences were removed on the basis of the length threshold of 100 bp. After quality control (QC), 5,021,621 reads were obtained. The mean number of raw sequences was 59,781 (range: 35,983–78,391). The average sequence length was 240 bp. Filtered reads were processed with usearch (v.10.0) (Edgar and Flyvbjerg, 2015) in rstudio (v1.1.463) (Loraine et al., 2015). Unoise 3 (Edgar, 2018) was selected as the algorithm to remove the error results of PCR and sequencing and obtain zero-radius operational taxonomic units (zOTUs). Then, zOTUs were aligned to a reference database of known UNITE (Nilsson et al., 2015) for further analysis.

## Statistical Analysis

Chao1 and Shannon index were used to evaluate the richness and diversity of the salivary mycobiome in the three groups with the one-way analysis of variance (one-way ANOVA), and Tukey-Honestly significant difference (HSD) was used for pairwise comparisons between two groups. These results were visualized by using R vegan package (Oksanen J et al.).  $P < 0.05$  was considered statistically different. The Bray-Curtis distance was selected to perform principal coordinates analysis (PCoA), and Adonis was used to assess the difference in shared diversity among the three groups. Besides, analysis of similarities (ANOSIM) was performed to test whether the difference between groups is significantly greater than the difference in the group. One-way ANOVA and Tukey-HSD were used to compare differential abundance taxa between groups. Linear discriminant analysis (LDA) effect size (LEfSe; <http://huttenhower.sph.harvard.edu/galaxy/>) was performed to explore the fungal biomarker in each group (LDA >2). All the samples in the three groups were fed into a random forest model to determine the contribution of the salivary mycobiome in classifying the groups. Correlative analysis with Spearman's correlation coefficient was performed to analyze the relationship between the salivary mycobiome and CD4<sup>+</sup> T-cell counts and viral load (VL) (Xiao et al., 2016).

## RESULTS

### Subject Characteristics

Thirty newly HIV-infected men and 30 HIV-uninfected men were enrolled. In this study, 24 HIV-infected participants were followed up for 6 months during ART administrations. The

mean ages in Control and HIV groups were 30.07 (range: 20–45) and 30.13 (range: 20–45) years, respectively. The mean CD4<sup>+</sup> T-cell count in HIV group was 343.03 cells/ $\mu$ l (range: 20–642 cells/ $\mu$ l), and the mean VL count was 362,298 copies/ml (range: 867–8,749,628 copies/ml). After 6 months of ART administrations, the average of CD4<sup>+</sup> T-cell counts in the HIV group increased to 456.92 cells/ $\mu$ l (range: 163–873 cells/ $\mu$ l), and the average VL count decreased to 121.75 copies/ml. The demographic and clinical characteristics of the participants are shown in **Supplementary Table 1**.

### Taxonomy Analysis

After the sequences were normalized sequences, 3,587, 3,333, and 3,223 zOTUs were obtained in HIV, Control, and ART groups, respectively (**Figure 1A**). There were 2,013 zOTUs detected in HIV and Control group and 1,339 zOTUs detected in Control and ART group, respectively. Moreover, 1,018 zOTUs were shared by the three groups. These results indicated that there were similarities and differences in the composition of salivary mycobiome among the three groups, but these results should be further statistically analyzed.

Then, taxonomic assignment was performed, and 11 phyla and 306 genera were obtained. The core mycobiome was contributed by five phyla: *Ascomycota*, *Basidiomycota*, *Rozellomycota*, *Mortierellomycota*, and *Chytridiomycota* (**Figure 1B**). In our study, *Aspergillus* and *Mortierella* could be detected from all the samples. In addition, there were three other genera with a detection rate of more than 90%, including *Penicillium* (96%), *Candida* (90%), and *Issatchenkia* (90%) (**Supplementary Figure 1**).

### Alpha and Beta Diversity Analysis of the Salivary Mycobiome

Alpha diversity analysis on the zOTU level revealed that the diversity and richness of the salivary mycobiome in the HIV group were higher than those in the Control group ( $P < 0.05$ ) (**Figure 2A**). After ART, the diversity and richness of the salivary mycobiome decreased significantly ( $P < 0.05$ ) in HIV-infected individuals and were similar to those in the HIV-uninfected individuals ( $P > 0.05$ ) (**Figure 2B**).

PCoA and Adonis analysis were performed to further compare the community composition of the salivary mycobiome in the three groups. Both results revealed the differences in the mycobiome community composition among the groups (**Figure 2C**). Dramatically, the community composition of the HIV group was significantly different from that of the HIV group after 6 months of ART (ART group), but no differences were observed between the Control and ART groups (**Supplementary Table 2**). Consistent with the findings of alpha diversity analysis, these results suggested that ART did affect the community composition of the salivary mycobiome.

### Comparative Analysis of the Salivary Mycobiome Among the Three Groups

At the phylum level, the abundance of *Basidiomycota*, *Mortierellomycota*, and *Chytridiomycota* was significantly higher

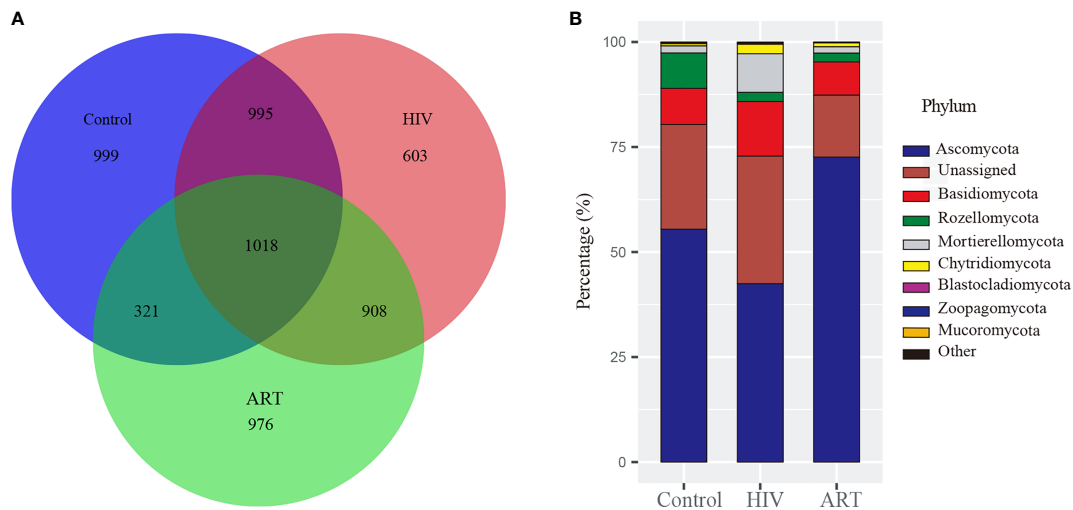


**FIGURE 1 |** Taxonomy analysis of the salivary mycobiome structure among the Control, HIV, and antiretroviral therapy (ART) groups. **(A)** Venn diagram showed the number of zero-radius operational taxonomic units (zOTUs) among the three groups. **(B)** Bar chart described the phylum distribution of the salivary mycobiome among the three groups.

in the HIV group than that in the Control and ART groups, and *Ascomycota* was more abundant in the ART group than that in the HIV and Control groups (Supplementary Table 3). A total of 22 genera with a detection rate over 20% and relative abundance over 0.5% in one dominant group were selected to perform a comparative analysis (Supplementary Table 4). Among them, the relative abundance of *Mortierella*, *Malassezia*, *Simplicillium*, *Penicillium*, and *Chaetomium* was significantly higher in the HIV group than that in the other two groups ( $P < 0.05$ ) (Figure 3A). Moreover, *Candida* was more abundant in the HIV group than in the Control and ART groups, although no statistically significant differences were observed (Figure 3A). In Figure 3B, the relative abundance of *Verticillium*, *Issatchenkia*, and *Alternaria* dramatically decreased in the HIV group compared with that in the Control group ( $P < 0.05$ ). Interestingly, the three genera were significantly enriched again in the HIV-infected subjects after 6 months of ART (HIV group vs. ART group,  $P < 0.05$ , Figure 3B; results of the comparative analysis of 11 other genera are shown in Supplementary Figure 2). These statistical results were also supported by the results of LEfSe analysis performed in the three groups (Figure 3C). These findings showed that *Mortierella*, *Malassezia*, *Simplicillium*, *Penicillium*, and *Chaetomium* were sensitive to HIV infection, and *Verticillium* and *Alternaria* were sensitive to ART.

## Random Forest Analysis

Random forest classification was analyzed to further investigate the contribution of the salivary mycobiome in classifying HIV infection and ART administration. It revealed that the most important salivary mycobiome for categorizing HIV infection was *Mortierella* (Figure 4A), and *Verticillium* was the most important fungi to categorize ART state (Figure 4B), which was also in line with the results of the comparative analysis.

## Correlation Between the Salivary Mycobiome and CD4<sup>+</sup> T-Cell Counts, Viral Load

The increased CD4<sup>+</sup> T-cell counts and decreased VL counts were predominant features of immunologic reconstitution in HIV-infected individuals after ART (Tiba et al., 2012). Correlation analysis by Spearman's correlation coefficient was performed to further analyze the relationship between salivary mycobiome and CD4<sup>+</sup> T-cell counts, VL counts (Figure 5). We found that *Mortierella*, *Malassezia*, and *Simplicillium* were positively correlated with VL, and *Verticillium*, *Alternaria*, and *Issatchenkia* were negatively correlated with VL. *Archaeorhizomyces* and *Thyrostromalt* were positively correlated with CD4<sup>+</sup> T-cell counts and negatively correlated with VL. It suggested that the community structure of saliva mycobiome of HIV-infected people had a relationship with CD4<sup>+</sup> T-cell counts and VL in the blood. It suggested that the salivary mycobiome of HIV-infected people was related to CD4<sup>+</sup> T-cell counts and VL in the blood.

## DISCUSSION

Our study reported the differences in the composition of the salivary mycobiome between patients with HIV and HIV-uninfected subjects and the effect of 6 months of ART on the salivary mycobiomes.

Previous oral mycobiome studies mainly relied on traditional isolation and culture methods (Diaz et al., 2017). However, studies have shown that less than 1% of microorganisms, including fungi, can be cultivated under laboratory conditions (Rappe and Giovannoni, 2003). Therefore, using traditional isolation and culture methods to study the relationship

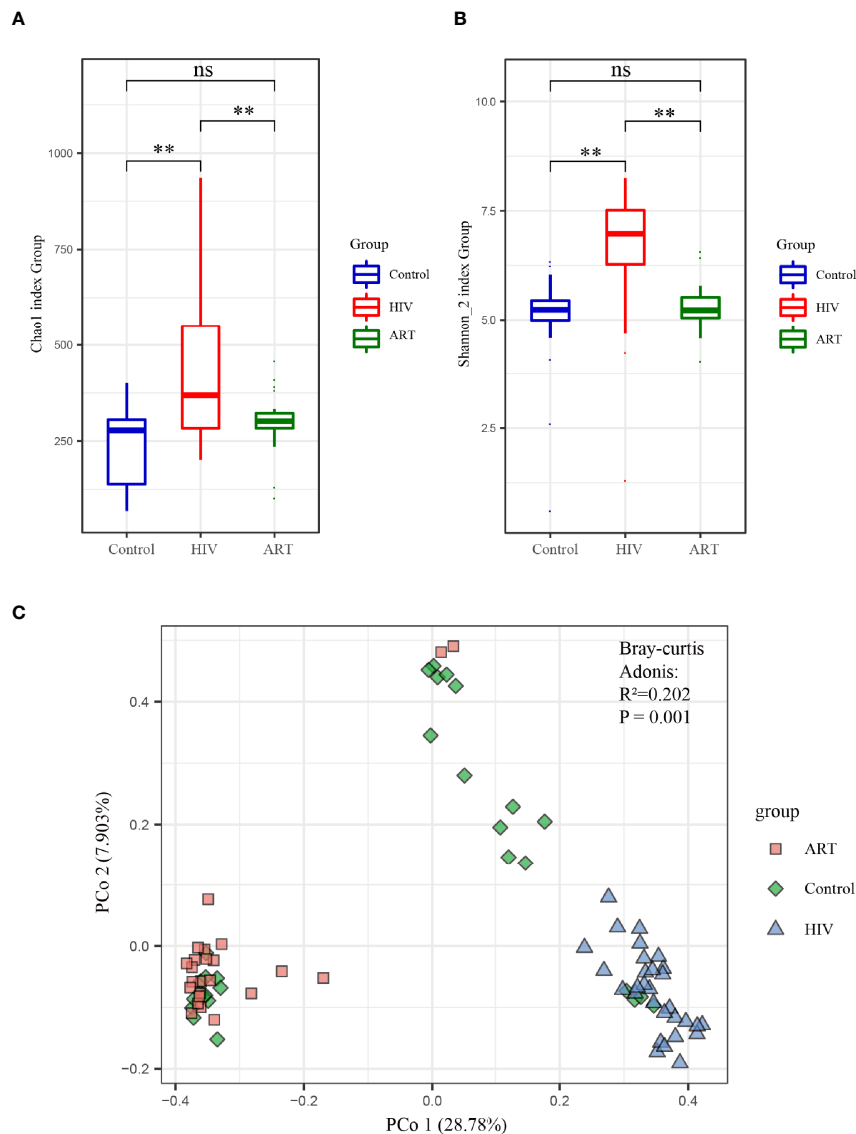


**FIGURE 2** | Alpha and beta diversity analyses of the salivary mycobiome among the three groups. **(A)** Chao1 index and **(B)** Shannon index showed the richness and evenness in the HIV, antiretroviral therapy (ART), and Control groups. **(C)** Principal coordinates analysis (PCoA) and Adonis analysis revealed the differences in the salivary mycobiome among the three groups. Blue represented the Control group, red indicated the HIV group, and green denoted the ART group. \*\* $P < 0.01$ ; ns, no significant.

between mycobiome and diseases may leave some biases. Microbial detection methods based on molecular biology techniques have emerged and expanded our understanding of oral mycobiome (Chiu and Miller, 2019).

In 2010, Ghannoum et al. (2010) used 454 pyrosequencing to analyze oral flushing samples from 20 healthy individuals and found 101 fungal genera, including 11 non-cultivable genera. Four common pathogenic fungi, including *Candida*, *Aspergillus*, *Fusarium*, and *Cryptococcus* were detected in more than 20% of subjects in this study, and these mycobiomes were also detected in our study. Apart from these fungi, *Malassezia* was a common fungus in the oral mycobiome of healthy subjects in another

study (Dupuy et al., 2014). This finding was consistent with our result, too.

Mukherjee et al. (2014) used the 454 pyrosequencing to compare the oral core fungal flora of 12 HIV-infected patients and 12 HIV-uninfected individuals and found that the oral core fungi were different between the two groups (the “core” flora were microorganisms detected in more than 20% of the subjects). Interestingly, *Candida* and *Penicillium* were common in the two groups in this study. While *Aspergillus* and *Mortierella* were detected in all the samples in our study. Besides, the frequency of *Candida*, *Epicoccum*, and *Alternaria* was much higher in the HIV group than that in the healthy group (Mukherjee et al., 2014), but

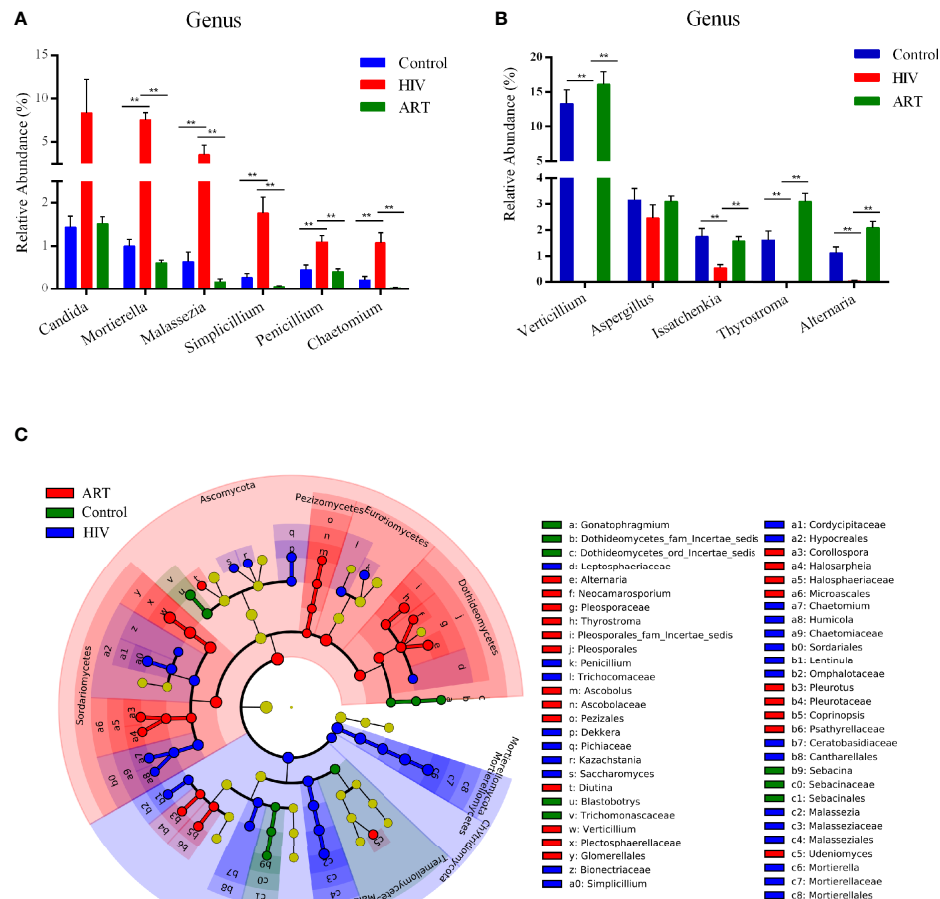


**FIGURE 3 |** Taxon comparative analysis of the salivary mycobiome among the three groups at the genus level. **(A, B)** Histogram based on the results of Tukey-HSD showed the significantly different genera among groups.  $**P < 0.01$ ,  $*P < 0.05$  (mean  $\pm$  SEM). **(C)** Linear discriminant analysis effect size (LEfSe) cladogram identified differently abundant taxa in each group. Red represented the antiretroviral therapy (ART) group-enriched taxa, blue indicated HIV group-enriched taxa, and green denoted Control group-enriched taxa.

the relative abundance of *Mortierella*, *Malassezia*, and *Penicillium* was much higher in the HIV group than that in the other group in our study. Dramatically, *Alternaria* was enriched in the control group in our study. Furthermore, only two of 22 dominant genera were not significantly different in our comparison analysis. Some differences were observed between our study and the research conducted by Mukherjee et al. (2014) because of the following: 1) the race and age of the included subjects were different; 2) the sequencing methods were different; 3) the samples were different, that is, mouth wash samples and non-stimulated whole saliva samples were selected in the two studies; 4) most of all, the characteristics of the included HIV-infected subjects were different. HIV-infected patients were newly infected within 1 past year in our study, and the body's immune system might not be severely damaged at this moment; as such, patients could not easily suffer from secondary infection. This condition was the main reason why the most common infecting genus in patients with HIV—*Candida*—was not more

enriched in HIV group compared with Control group in our study.

In addition, we explored the effect of ART on the composition of the salivary mycobiome and found that the richness and diversity of salivary mycobiome decreased after ART administration. Moreover, the composition of the salivary mycobiome in the ART group was similar to that in the Control group. Furthermore, *Verticillium*, *Archaeorhizomyces*, and *Thyrostroma* were negatively correlated with VL and positively correlated with CD4<sup>+</sup> T-cell counts. By comparison, *Saccharomyces* was positively correlated with VL and negatively correlated with CD4<sup>+</sup> T-cell counts. These results indicated that ART administration could affect the composition of the salivary mycobiome in HIV-infected patients, and some fungi were sensitive to the changes in CD4<sup>+</sup> T-cell counts and VL in the blood.

Our study had some limitations. First, the saliva samples collected from the subjects before acquiring HIV were the best



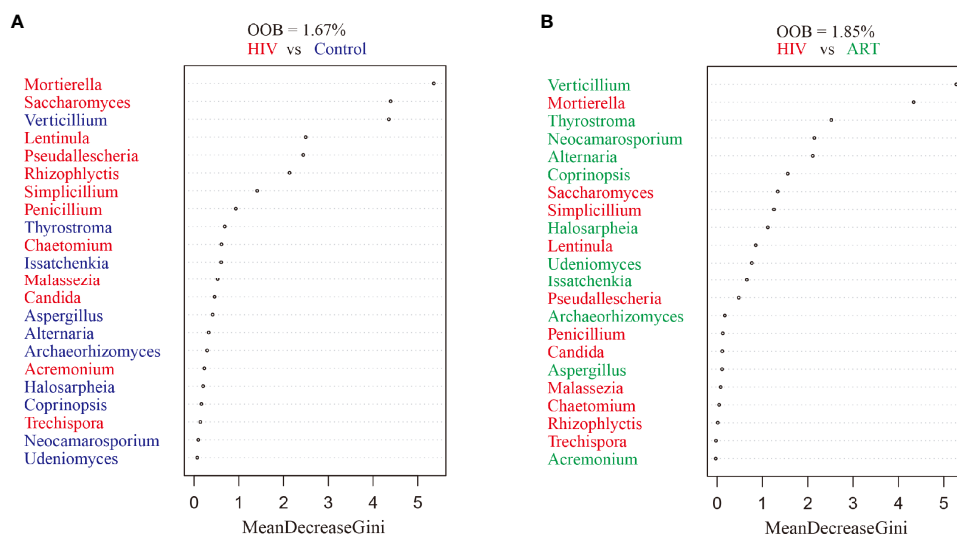


**FIGURE 4 |** Random forest analysis. Random forest analysis classification of the ranked importance of the mycobiome for classifying the samples in HIV category (patients with and without HIV infection) **(A)** and in the antiretroviral therapy (ART) category (ART or not) **(B)**. OOB, out-of-box error rate.

control. This study was limited by ethics and difficulties in collecting the samples, so saliva was obtained from HIV-uninfected subjects as the control. Second, the follow-up period was cut short because of coronavirus disease 2019 (COVID-19). Third, the sample size was not large enough. Fourth, many sequences could not be classified and annotated with the incomplete fungal ribosome database. Fifth, specific species were not detected because of the difficulties in generating

similarity thresholds to define species-level operable taxonomic units. Therefore, more cohort studies with a long follow-up period and a large sample size should be performed to further analyze the characteristics of the salivary mycobiome in HIV-infected subjects. Besides, more research is needed to improve the fungal ribosome database that should be completed. Standard methods to explore human fungal microorganisms also need to be improved.

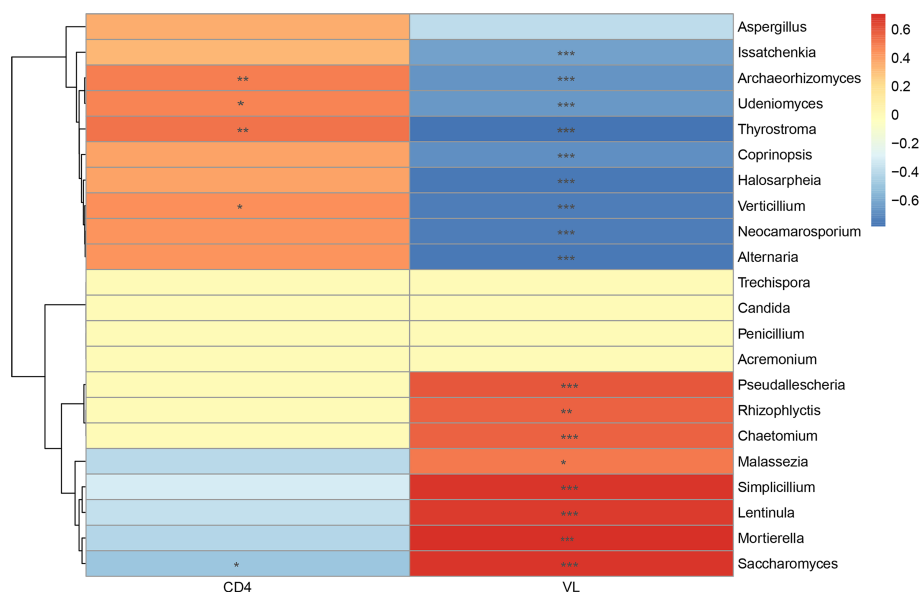


**FIGURE 5 |** Correlation analysis between the salivary mycobiome and CD4<sup>+</sup> T-cell counts and viral load (VL) in the blood. Diagram showed Spearman's correlation coefficient ( $|\rho| > 0.3$ ) with the  $P < 0.05$ . The significance is shown as flow: \* $P < 0.05$ , \*\* $P < 0.01$ , \*\*\* $P < 0.001$ .

## CONCLUSIONS

In this study, we found that HIV infection and ART administration might affect the composition of the salivary mycobiome. Furthermore, differences in the salivary mycobiome in HIV infections after ART were complex and might mirror the immune state of the body. In the future, studies should be performed on the salivary mycobiome with a large sample size and long follow-up time.

## DATA AVAILABILITY STATEMENT

The datasets presented in this study can be found in online repositories. The names of the repository/repositories and accession number(s) can be found below: <https://www.ncbi.nlm.nih.gov/>, PRJNA626395.

## ETHICS STATEMENT

The studies involving human participants were reviewed and approved by the ethics committee of the School & Hospital of Stomatology, Wuhan University. The patients/participants provided their written informed consent to participate in this study.

## REFERENCES

- Abdolsamadi, H., Goodarzi, M. T., Ahmadi Motemayel, F., Jazaeri, M., Feradmal, J., Zarabadi, M., et al. (2014). Reduction of Melatonin Level in Patients With Type II Diabetes and Periodontal Diseases. *J. Dent. Res. Dent. Clin. Dent. Prospects* 8 (3), 160–165. doi: 10.5681/joddd.2014.029
- Aberg, J., and Powderly, W. (2010). HIV: Primary and Secondary Prophylaxis for Opportunistic Infections. *BMJ Clin. Evid.* 2010, 0908.
- Armstrong-James, D., Meintjes, G., and Brown, G. D. (2014). A Neglected Epidemic: Fungal Infections in HIV/AIDS. *Trends Microbiol.* 22 (3), 120–127. doi: 10.1016/j.tim.2014.01.001
- Beck, J. M., Schloss, P. D., Venkataraman, A., Twigg, H. 3rd, Jablonski, K. A., Bushman, F. D., et al. (2015). Multicenter Comparison of Lung and Oral Microbiomes of HIV-Infected and HIV-Uninfected Individuals. *Am. J. Respir. Crit. Care Med.* 192 (11), 1335–1344. doi: 10.1164/rccm.201501-0128OC
- Belstrom, D., Holmstrup, P., Bardow, A., Kokaras, A., Fiehn, N. E., and Paster, B. J. (2016). Temporal Stability of the Salivary Microbiota in Oral Health. *PLoS One* 11 (1), e0147472. doi: 10.1371/journal.pone.0147472
- Cameron, S. J., Huws, S. A., Hegarty, M. J., Smith, D. P., and Mur, L. A. (2015). The Human Salivary Microbiome Exhibits Temporal Stability in Bacterial Diversity. *FEMS Microbiol. Ecol.* 91 (9), fiv091. doi: 10.1093/femsec/fiv091
- Chiu, C. Y., and Miller, S. A. (2019). Clinical Metagenomics. *Nat. Rev. Genet.* 20 (6), 341–355. doi: 10.1038/s41576-019-0113-7
- Cohen, J. (2016). Infectious Disease. Vaginal Microbiome Affects Hiv Risk. *Science* 353 (6297), 331. doi: 10.1126/science.353.6297.331
- Cohen, M. S., Shaw, G. M., McMichael, A. J., and Haynes, B. F. (2011). Acute HIV-1 Infection. *N. Engl. J. Med.* 364 (20), 1943–1954. doi: 10.1056/NEJMra1011874
- Diaz, P. I., Hong, B. Y., Dupuy, A. K., and Strausbaugh, L. D. (2017). Mining the Oral Mycobiome: Methods, Components, and Meaning. *Virulence* 8 (3), 313–323. doi: 10.1080/21505594.2016.1252015
- Dupuy, A. K., David, M. S., Li, L., Heider, T. N., Peterson, J. D., Montano, E. A., et al. (2014). Redefining the Human Oral Mycobiome With Improved Practices in Amplicon-Based Taxonomy: Discovery of Malassezia as a Prominent Commensal. *PLoS One* 9 (3), e90899. doi: 10.1371/journal.pone.0090899

## AUTHOR CONTRIBUTIONS

The study was conceptualized and designed by MD, SC, HG, and JL. SC and HG performed the experiments. SC analyzed the data and made figures for the article. SC and HG wrote the original draft of the article. HG, JL, YJ, HJ, and MD reviewed and revised the article. LR was the expert on HIV/AIDS, who provided and evaluated the samples of HIV infections. All authors contributed to the article and approved the submitted version.

## FUNDING

This study was supported by the National Natural Science Foundation of China (No. 81771084).

## ACKNOWLEDGMENTS

We thank all the participants for their cooperation.

## SUPPLEMENTARY MATERIAL

The Supplementary Material for this article can be found online at: <https://www.frontiersin.org/articles/10.3389/fcimb.2021.781246/full#supplementary-material>

- Edgar, R. C. (2018). Updating the 97% Identity Threshold for 16S Ribosomal RNA Otus. *Bioinf. (Oxford England)* 34 (14), 2371–2375. doi: 10.1093/bioinformatics/bty113
- Edgar, R. C., and Flyvbjerg, H. (2015). Error Filtering, Pair Assembly and Error Correction for Next-Generation Sequencing Reads. *Bioinf. (Oxford England)* 31 (21), 3476–3482. doi: 10.1093/bioinformatics/btv401
- Ghannoum, M. A., Jurevic, R. J., Mukherjee, P. K., Cui, F., Sikaroodi, M., Naqvi, A., et al. (2010). Characterization of the Oral Fungal Microbiome (Mycobiome) in Healthy Individuals. *PLoS Pathog.* 6 (1), e1000713. doi: 10.1371/journal.ppat.1000713
- Hager, C. L., and Ghannoum, M. A. (2018). The Mycobiome in HIV. *Curr. Opin. HIV AIDS* 13 (1), 69–72. doi: 10.1097/COH.0000000000000432
- Hegde, M. C., Kumar, A., Bhat, G., and Sreedharan, S. (2014). Oral Microflora: A Comparative Study in HIV and Normal Patients. *Indian J. Otolaryngol. Head Neck Surg.* 66 (Suppl 1), 126–132. doi: 10.1007/s12070-011-0370-z
- Hugh, S. (2014). Diseases of the Mouth. *Primary Care* 41 (1), 75–90. doi: 10.1016/j.pop.2013.10.011
- Hu, C., Huang, Y., Su, J., Wang, M., Zhou, Q., and Zhu, B. (2018). The Prevalence and Isolated Subtypes of BK Polyomavirus Reactivation Among Patients Infected With Human Immunodeficiency Virus-1 in Southeastern China. *Arch. Virol.* 163 (6), 1463–1468. doi: 10.1007/s00705-018-3724-y
- Kistler, J. O., Arirachakaran, P., Poovorawan, Y., Dahlen, G., and Wade, W. G. (2015). The Oral Microbiome in Human Immunodeficiency Virus (HIV)-Positive Individuals. *J. Med. Microbiol.* 64 (9), 1094–1101. doi: 10.1099/jmm.0.000128
- Leigh, J. E., Shetty, K., and Fidel, P. L. Jr. (2004). Oral Opportunistic Infections in HIV-Positive Individuals: Review and Role of Mucosal Immunity. *AIDS patient Care STDs* 18 (8), 443–456. doi: 10.1089/1087291041703665
- Lijia, C., Lucht, L., Tipton, L., Rogers, M. B., Fitch, A., Kessinger, C., et al. (2015). Topographic Diversity of the Respiratory Tract Mycobiome and Alteration in HIV and Lung Disease. *Am. J. Respir. Crit. Care Med.* 191 (8), 932–942. doi: 10.1164/rccm.201409-1583OC
- Ling, Z., Jin, C., Xie, T., Cheng, Y., Li, L., and Wu, N. (2016). Alterations in the Fecal Microbiota of Patients With HIV-1 Infection: An Observational Study in a Chinese Population. *Sci. Rep.* 6 (30673), 1–12. doi: 10.1038/srep30673

- Li, Y., Saxena, D., Chen, Z., Liu, G., Abrams, W. R., Phelan, J. A., et al. (2014). HIV Infection and Microbial Diversity in Saliva. *J. Clin. Microbiol.* 52 (5), 1400–1411. doi: 10.1128/JCM.02954-13
- Loraine, A. E., Blakley, I. C., Jagadeesan, S., Harper, J., Miller, G., and Firon, N. (2015). Analysis and Visualization of RNA-Seq Expression Data Using Rstudio, Bioconductor, and Integrated Genome Browser. *Methods Mol. Biol. (Clifton NJ)* 1284, 481–501. doi: 10.1007/978-1-4939-2444-8\_24
- Mukherjee, P. K., Chandra, J., Retuerto, M., Sikaroodi, M., Brown, R. E., Jurevic, R., et al. (2014). Oral Mycobiome Analysis of HIV-Infected Patients: Identification of *Pichia* as an Antagonist of Opportunistic Fungi. *PloS Pathog.* 10 (3), e1003996. doi: 10.1371/journal.ppat.1003996
- Navazesh, M., Mulligan, R., Pogoda, J., Greenspan, D., Alves, M., Phelan, J., et al. (2005). The Effect of HAART on Salivary Microbiota in the Women's Interagency HIV Study (WIHS). *Oral. Surgery Oral. Med. Oral. Pathol. Oral. Radiol. Endodontics* 100 (6), 701–708. doi: 10.1016/j.tripleo.2004.10.011
- Nefzi, F., Ben Salem, N. A., Khelif, A., Feki, S., Aouni, M., and Gautheret-Dejean, A. (2015). Quantitative Analysis of Human Herpesvirus-6 and Human Cytomegalovirus in Blood and Saliva From Patients With Acute Leukemia. *J. Med. Virol.* 87 (3), 451–460. doi: 10.1002/jmv.24059
- Nilsson, R. H., Tedersoo, L., Ryberg, M., Kristiansson, E., Hartmann, M., Unterseher, M., et al. (2015). A Comprehensive, Automatically Updated Fungal ITS Sequence Dataset for Reference-Based Chimera Control in Environmental Sequencing Efforts. *Microbes Environments* 30 (2), 145–150. doi: 10.1264/jsme2.ME14121
- Noguera-Julian, M., Guillen, Y., Peterson, J., Reznik, D., Harris, E. V., Joseph, S. J., et al. (2017). Oral Microbiome in HIV-Associated Periodontitis. *Medicine* 96 (12), e5821. doi: 10.1097/MD.00000000000005821
- Oksanen J., B. F., Friendly, M., et al. *Vegan: Community Ecology Package 2019*. Available at: <https://cran.r-project.org/package=vegan>.
- Owotade, F. J., Shiboski, C. H., Poole, L., Ramstead, C. A., Malvin, K., Hecht, F. M., et al. (2008). Prevalence of Oral Disease Among Adults With Primary HIV Infection. *Oral. Dis.* 14 (6), 497–499. doi: 10.1111/j.1601-0825.2007.01407.x
- Park, N. J., Zhou, H., Elashoff, D., Henson, B. S., Kastratovic, D. A., Abemayor, E., et al. (2009). Salivary MicroRNA: Discovery, Characterization, and Clinical Utility for Oral Cancer Detection. *Clin. Cancer Res.* 15 (17), 5473–5477. doi: 10.1158/1078-0432.CCR-09-0736
- Patil, S., Majumdar, B., Sarode, S. C., Sarode, G. S., and Awan, K. H. (2018). Oropharyngeal Candidosis in HIV-Infected Patients-an Update. *Front. Microbiol.* 9, 980. doi: 10.3389/fmicb.2018.00980
- Pfaffe, T., Cooper-White, J., Beyerlein, P., Kostner, K., and Punyadeera, C. (2011). Diagnostic Potential of Saliva: Current State and Future Applications. *Clin. Chem.* 57 (5), 675–687. doi: 10.1373/clinchem.2010.153767
- Poole, S., Singhrao, S. K., Kesavalu, L., Curtis, M. A., and Crean, S. (2013). Determining the Presence of Periodontopathic Virulence Factors in Short-Term Postmortem Alzheimer's Disease Brain Tissue. *J. Alzheimer's Dis.: JAD* 36 (4), 665–677. doi: 10.3233/JAD-121918
- Presti, R. M., Handley, S. A., Droit, L., Ghannoum, M., Jacobson, M., Shiboski, C. H., et al. (2018). Alterations in the Oral Microbiome in HIV-Infected Participants After Antiretroviral Therapy Administration are Influenced by Immune Status. *AIDS (London England)* 32 (10), 1279–1287. doi: 10.1097/QAD.0000000000001811
- Rappe, M. S., and Giovannoni, S. J. (2003). The Uncultured Microbial Majority. *Annu. Rev. Microbiol.* 57, 369–394. doi: 10.1146/annurev.micro.57.030502.090759
- Schmieder, R., and Edwards, R. (2011). Quality Control and Preprocessing of Metagenomic Datasets. *Bioinf. (Oxford England)* 27 (6), 863–864. doi: 10.1093/bioinformatics/btr026
- Thompson, G. R.3rd, Patel, P. K., Kirkpatrick, W. R., Westbrook, S. D., Berg, D., Erlandsen, J., et al. (2010). Oropharyngeal Candidiasis in the Era of Antiretroviral Therapy. *Oral Surg. Oral Med. Oral Pathol. Oral Radiol. Endod.* 109 (4), 488–495. doi: 10.1016/j.tripleo.2009.11.026
- Tiba, F., Nauwelaers F., Traoré, S., Traoré S., Coulibaly, B., Coulibaly, B., et al. (2012). Immune Reconstitution During the First Year of Antiretroviral Therapy of HIV-1-Infected Adults in Rural Burkina Faso. *Open AIDS J.* 6(1874-6136 (1874-6136 (Electronic)), 16–25. doi: 10.2174/1874613601206010016
- Twigg, H. L.3rd, Weinstock, G. M., and Knox, K. S. (2017). Lung Microbiome in Human Immunodeficiency Virus Infection. *Trans. Research: J. Lab. Clin. Med.* 179, 97–107. doi: 10.1016/j.trsl.2016.07.008
- Vidotto, A., Henrique, T., Raposo, L. S., Maniglia, J. V., and Tajara, E. H. (2010). Salivary and Serum Proteomics in Head and Neck Carcinomas: Before and After Surgery and Radiotherapy. *Cancer Biomark.* 8 (2), 95–107. doi: 10.3233/CBM-2011-0205
- Wang, J., Jia, Z., Zhang, B., Peng, L., and Zhao, F. (2020). Tracing the Accumulation of *In Vivo* Human Oral Microbiota Elucidates Microbial Community Dynamics at the Gateway to the GI Tract. *Gut* 69 (7), 1355–1356. doi: 10.1136/gutjnl-2019-318977
- Xiao, C., Ye, J., Esteves, R. M., and Rong, C. (2016). Using Spearman's Correlation Coefficients for Exploratory Data Analysis on Big Dataset. *Concurrency Comput. Pract. Experience* 28 (14), 3866–3878. doi: 10.1002/cpe.3745
- Zhang, C. Z., Cheng, X. Q., Li, J. Y., Zhang, P., Yi, P., Xu, X., et al. (2016). Saliva in the Diagnosis of Diseases. *Int. J. Oral. Sci.* 8 (3), 133–137. doi: 10.1038/ijos.2016.38
- Zheng, H., Li, R., Zhang, J., Zhou, S., Ma, Q., Zhou, Y., et al. (2014). Salivary Biomarkers Indicate Obstructive Sleep Apnea Patients With Cardiovascular Diseases. *Sci. Rep.* 4, 7046. doi: 10.1038/srep07046

**Conflict of Interest:** The authors declare that the research was conducted in the absence of any commercial or financial relationships that could be construed as a potential conflict of interest.

**Publisher's Note:** All claims expressed in this article are solely those of the authors and do not necessarily represent those of their affiliated organizations, or those of the publisher, the editors and the reviewers. Any product that may be evaluated in this article, or claim that may be made by its manufacturer, is not guaranteed or endorsed by the publisher.

Copyright © 2021 Chang, Guo, Li, Ji, Jiang, Ruan and Du. This is an open-access article distributed under the terms of the Creative Commons Attribution License (CC BY). The use, distribution or reproduction in other forums is permitted, provided the original author(s) and the copyright owner(s) are credited and that the original publication in this journal is cited, in accordance with accepted academic practice. No use, distribution or reproduction is permitted which does not comply with these terms.



# Protein Tyrosine and Serine/Threonine Phosphorylation in Oral Bacterial Dysbiosis and Bacteria-Host Interaction

Liang Ren, Daonan Shen, Chengcheng Liu\* and Yi Ding\*

State Key Laboratory of Oral Diseases, National Clinical Research Center for Oral Diseases, West China Hospital of Stomatology, Sichuan University, Chengdu, China

## OPEN ACCESS

### Edited by:

Jin Xiao,  
University of Rochester, United States

### Reviewed by:

Tridib Ganguly,  
University of Florida, United States  
Chenggang Wu,  
University of Texas Health Science  
Center at Houston, United States

### \*Correspondence:

Chengcheng Liu  
liuchengcheng519@163.com  
Yi Ding  
yiding2000@126.com

### Specialty section:

This article was submitted to  
Microbiome in Health and Disease,  
a section of the journal  
Frontiers in Cellular and  
Infection Microbiology

**Received:** 14 November 2021

**Accepted:** 13 December 2021

**Published:** 11 January 2022

### Citation:

Ren L, Shen D, Liu C and  
Ding Y (2022) Protein Tyrosine  
and Serine/Threonine Phosphorylation  
in Oral Bacterial Dysbiosis and  
Bacteria-Host Interaction.  
*Front. Cell. Infect. Microbiol.* 11:814659.  
doi: 10.3389/fcimb.2021.814659

The human oral cavity harbors approximately 1,000 microbial species, and dysbiosis of the microflora and imbalanced microbiota-host interactions drive many oral diseases, such as dental caries and periodontal disease. Oral microbiota homeostasis is critical for systemic health. Over the last two decades, bacterial protein phosphorylation systems have been extensively studied, providing mounting evidence of the pivotal role of tyrosine and serine/threonine phosphorylation in oral bacterial dysbiosis and bacteria-host interactions. Ongoing investigations aim to discover novel kinases and phosphatases and to understand the mechanism by which these phosphorylation events regulate the pathogenicity of oral bacteria. Here, we summarize the structures of bacterial tyrosine and serine/threonine kinases and phosphatases and discuss the roles of tyrosine and serine/threonine phosphorylation systems in *Porphyromonas gingivalis* and *Streptococcus mutans*, emphasizing their involvement in bacterial metabolism and virulence, community development, and bacteria-host interactions.

**Keywords:** oral bacteria, kinase, phosphatase, tyrosine phosphorylation, serine phosphorylation, bacterial dysbiosis

## INTRODUCTION

The oral microbiome is the second largest and most diverse microbiota in the human body, encompassing approximately 1,000 species (Lamont et al., 2018). According to the expanded Human Oral Microbiome Database (eHOMD), the oral bacteria are highly diverse, and account for the majority of oral microorganisms, composed mainly of six major phyla: Firmicutes, Bacteroidetes, Proteobacteria, Actinobacteria, Spirochaetes and Fusobacteria (Escapa et al., 2018).

**Abbreviations:** PTMs, post-translational modifications; *M. xanthus*, *Myxococcus xanthus*; *S. pneumoniae*, *Streptococcus pneumoniae*; STKs, eukaryotic serine/threonine kinases; *P. gingivalis*, *Porphyromonas gingivalis*; BY kinases, bacterial tyrosine kinases; UbK, ubiquitous bacterial kinase; *S. gordonii*, *Streptococcus gordonii*; *B. subtilis*, *Bacillus subtilis*; *E. coli*, *Escherichia coli*; *S. mutans*, *Streptococcus mutans*; Tyr kinases, tyrosine kinases; LMW-PTPs, low-molecular-weight protein tyrosine phosphatases; PTPs, eukaryotic like phosphatases; PHPs, polymerase-histidinol phosphatases; *M. tuberculosis*, *Mycobacterium tuberculosis*; PASTA, penicillin binding proteins and serine/threonine kinase associated; STPs, serine/threonine phosphatases; PPMs, metal-dependent phosphatases; PPPs, phosphoprotein phosphatases; HAD, haloacid dehalogenase; EPS, extracellular polysaccharide; NF-κB, nuclear factor-kappa B; *S. sanguinis*, *Streptococcus sanguinis*.



In healthy systems, the polymicrobial communities maintain an ecological balance *via* intermicrobial and host microbial interactions. Dysbiosis, or perturbations in the composition of commensal communities, is a driver of the host immune inflammatory response and can disrupt host tissue homeostasis, promoting oral diseases such as dental caries and periodontitis (Lamont et al., 2018; Hajishengallis and Lamont, 2021). Oral bacteria can also directly or indirectly affect a variety of systemic diseases, such as cardiovascular disease and diabetes (Hajishengallis and Chavakis, 2021). Although some controversies remain, several potential mechanisms have been proposed, including (1) bacteria entering the blood circulation, resulting in distant dissemination; (2) systemic injury by free toxins of oral bacteria; (3) stimulation of systemic inflammation by soluble antigens of oral bacteria; and (4) inducing dysbiosis of gut microbiota (Hajishengallis and Chavakis, 2021). Notably, *Porphyromonas gingivalis*, a keystone pathogen in periodontitis, expresses a variety of virulence factors (e.g., lipopolysaccharide, outer membrane vesicles and fimbriae) that facilitate its survival, spreading and disrupting the immune response (Zhang et al., 2020). The colonization of *P. gingivalis* can remodel the commensal bacterial community, thus promoting the bacterial dysbiosis and the imbalance of bacteria-host interactions. The transition from homeostatic balance to dysbiosis and imbalance plays a central role in oral microbial diseases (Lamont et al., 2018; Hajishengallis and Lamont, 2021).

Evidence has shown that post-translational modifications (PTMs) are critical processes used by oral bacteria to modify proteins and coordinate the signaling networks, and are therefore involved in the regulation of bacterial communities and bacteria-host interactions (Whitmore and Lamont, 2012). In fact, protein phosphorylation is a critical covalent protein modification in signal transduction pathways. By combining or separating small molecular phosphates with substrate amino acid residues, phosphates can be passed along these information pathways, causing a cascade of signal transduction protein alterations, thus allowing signal transmission (Low et al., 2021). This process is modulated by two families of enzymes: kinases and phosphatases (Hardie, 1990). Protein kinases and their cognate phosphatases play extensive roles in many basic physiological processes in bacteria, including signal transduction, growth control and malignant transformation, as well as in regulating bacterial pathogenicity and antibiotic resistance (Kyriakis, 2014; Shaban et al., 2020; Shamma et al., 2021). Many studies have emphasized protein phosphorylation which occurs in prokaryotes (Bonne Kohler et al., 2020). Phosphorylation of tyrosine and serine/threonine residues is the most prevalent PTM.

Pioneering investigations of the tyrosine and serine/threonine phosphorylation in bacteria began in the 1970s (Wang and Koshland, 1978; Manai and Cozzone, 1979). In the early 1990s, the first protein kinase PknL was discovered in *Myxococcus xanthus*. This enzyme shares a structural similarity with eukaryotic serine/threonine kinases (STKs) and is required for the normal development of *M. xanthus* (Muñoz-Dorado et al., 1991). Later, the first bacterial phosphatase was discovered by G A Nimmo et al. who reported that isocitrate dehydrogenase

(IDH) is regulated by phosphorylation in *Escherichia coli* (Nimmo et al., 1984; Nimmo and Nimmo, 1984). Phosphorylation systems modify bacterial proteomes, imparting cells with rapid and reversible responses to specific environmental stimuli (Janczarek et al., 2018). Evidence has indicated a close association between phosphorylation and bacterial pathogenesis. For instance, *Mycobacterium tuberculosis* can secrete the eukaryotic serine-threonine protein kinase PknG into host macrophages by blocking the transition of Rab711-GDP to Rab711-GTP in a kinase activity-dependent process, thus realizing its pathogenic potential by facilitating bacterial survival inside human macrophages (Shimizu et al., 1997; Pradhan et al., 2018). PtpA, a tyrosine phosphatase secreted by *Mycobacterium*, can also inhibit the fusion of phagosomes and lysosomes, which helps pathogens to evade host immune mechanisms (Jaiswal et al., 2019). Further evidence has been derived from *Streptococcus pneumoniae*. The tyrosine phosphatase PhpP regulates proteins phosphorylation by direct dephosphorylation of target protein and dephosphorylation of its homologous kinase StkP, thus coordinating cell wall synthesis and division of *S. pneumoniae* (Sasková et al., 2007; Osaki et al., 2009). The PhpP mutant of *S. pneumoniae* displayed insufficient cell elongation and increased sensitivity at high temperature and oxidative stress, as well as decreased genetic transformation ability (Ulrych et al., 2016).

Bacterial protein kinases and phosphatases are closely interconnected, regulating phosphate transmission and covalent modifications, and contributing to bacterial pathogenesis. However, the reciprocal relationships between oral bacterial protein tyrosine and serine/threonine phosphorylation and pathogenesis remain to be elucidated. This review focuses on two well-known oral pathogens, *Streptococcus mutans* and *P. gingivalis*, aiming to summarize the present knowledge of the structural and functional aspects of kinases and phosphatases in oral bacteria, with emphasis on the role of tyrosine and serine/threonine phosphorylation in oral bacterial dysbiosis and oral bacteria-host interactions.

## THE STRUCTURE OF BACTERIAL TYROSINE AND SERINE/THREONINE KINASES AND PHOSPHATASES

When bacteria perceive external stimulation, kinases undergo autophosphorylation and catalyze the phosphorylation, *i.e.* the transfer of the  $\gamma$ -phosphate group from nucleoside triphosphates, usually adenosine triphosphate (ATP) to other proteins (Pereira et al., 2011). Bacterial phosphatases remove the covalently linked phosphate group from the phosphorylated protein (phosphoprotein) by hydrolysis (dephosphorylation), thereby maintaining the stability of the physiological environment. Kinases and phosphatases act as switches to regulate specific signal transduction pathways (Huse and Kuriyan, 2002). In bacteria, protein kinases can be classified into five types: histidine kinases (His kinases), tyrosine kinases (Tyr kinases), arginine kinases (Arg kinases), Hanks-type Ser/Thr kinases

(STKs) (commonly known as eukaryotic-like STKs), and atypical serine kinases (Janczarek et al., 2018). Among them, Tyr kinases and STKs can phosphorylate various proteins and regulate bacterial physiology (Mijakovic et al., 2016). Compared to kinases, fewer bacterial phosphatases have been discovered and biochemically characterized. The protein phosphatase family in bacteria can be divided into four categories: phosphoprotein phosphatases (PPPs), metal-dependent phosphatases (PPMs) acting on serine/threonine residues, low-molecular-weight protein tyrosine phosphatases (LMW-PTPs), and Asp-based phosphatases (Wright and Ulijasz, 2014; Esser et al., 2016).

## Tyrosine Kinases

Protein phosphorylation on tyrosine residues is catalyzed by autophosphorylating ATP-dependent tyrosine kinases that exhibit structural and functional features similar to those of their eukaryotic counterparts. Most enzymes discovered in bacteria with tyrosine kinase activity discovered in bacterial are bacterial tyrosine kinases (BY kinases). The structure of BY kinases has been comprehensively reviewed (Whitmore and Lamont, 2012). In brief, BY kinases have a transmembrane domain and an intracellular catalytic domain (Doublet et al., 2002). The transmembrane domain interacts with other proteins through the outer membrane and affects the cellular function of

tyrosine kinase, which is critical for triggering kinase activity (Collins et al., 2006). The conservative ExxRxxR motif, canonical Walker A motif (GxxxxGK[S/T]), Walker B motif ([ilvfm](3) Dx DxR), and a tyrosine-rich cluster (Y cluster) at the C-terminal sites are common features of the BY-kinase family (Grangeasse et al., 2007). Some BY kinases have an additional Walker A' motif [(ILVFM(3)DxxP)] (Figure 1). BY kinases autophosphorylate in the Y clusters to facilitate their interaction with other proteins. The steps of signal transduction in BY-kinases are similar to those in the eukaryotic signal transduction cascade. For instance, the Tyr (569) residue of Wzc, a BY kinase of *Escherichia coli* K12, can autophosphorylate, resulting in an increased protein kinase activity (Grangeasse et al., 2002). The phosphorylation level in the tyrosine-rich cluster may affect the intensity of the interaction between BY-kinase and other proteins (Collins et al., 2006). Ptk1, which is the first discovered BY kinase in *P. gingivalis*, contains ExxRxxR, Walker A, Walker A', Walker B motifs, and a C-terminal Y cluster (Wright et al., 2014) (Figures 1, 2). All of these domains are required for kinase autophosphorylation and substrate phosphorylation activity. And Ptk1 is highly homologous to Wzc *Escherichia coli* (Figure 3). Moreover, the functional phosphor-transfer is indispensable for Ptk1-mediated control of *P. Porphyromonas gingivalis-Streptococcus gordonii* community formation and extracellular polysaccharide biosynthesis (Liu et al., 2017). The

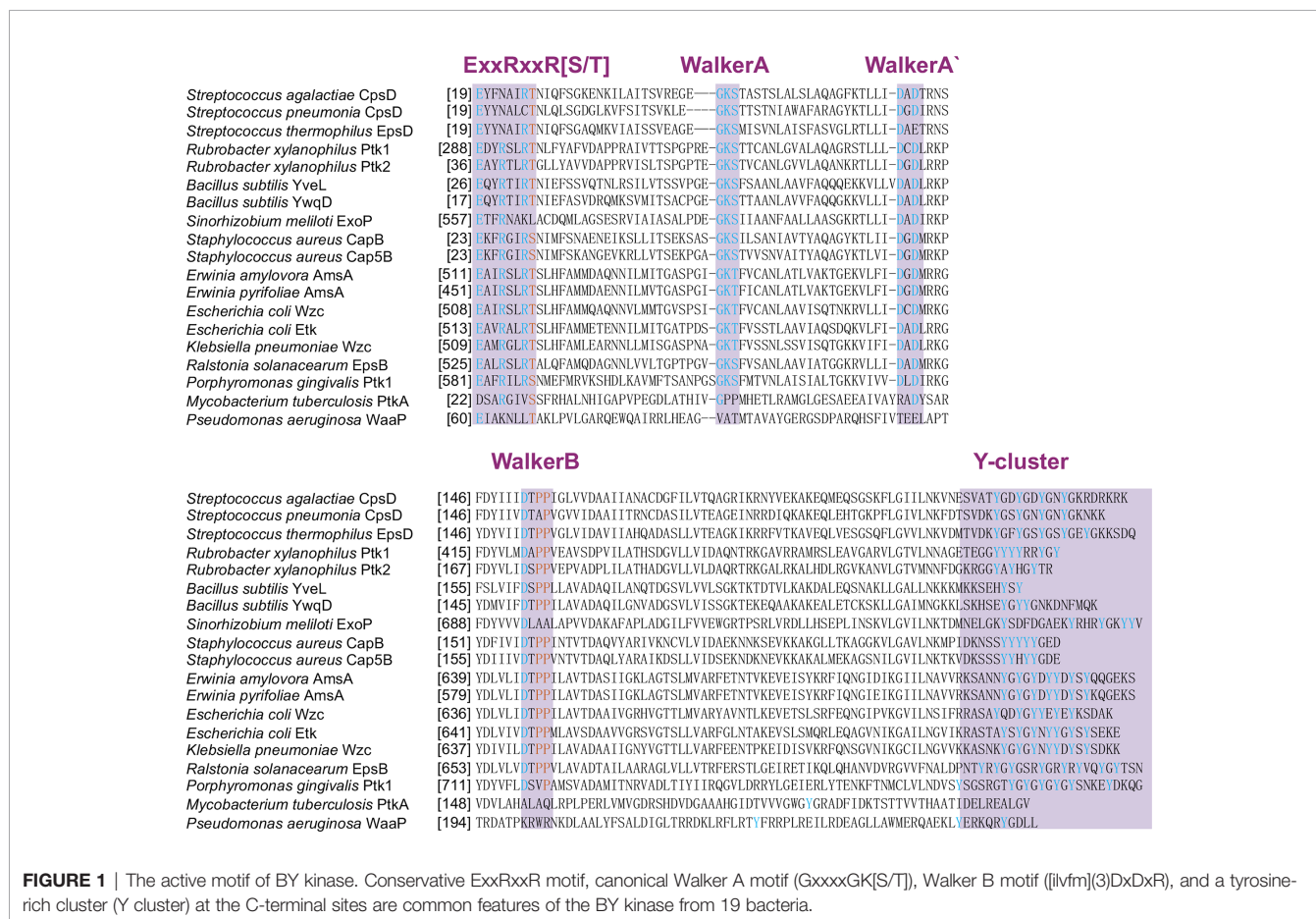


**FIGURE 1** | The active motif of BY kinase. Conservative ExxRxxR motif, canonical Walker A motif (GxxxxGK[S/T]), Walker B motif ([ilvfm](3)DxDxR), and a tyrosine-rich cluster (Y cluster) at the C-terminal sites are common features of the BY kinase from 19 bacteria.

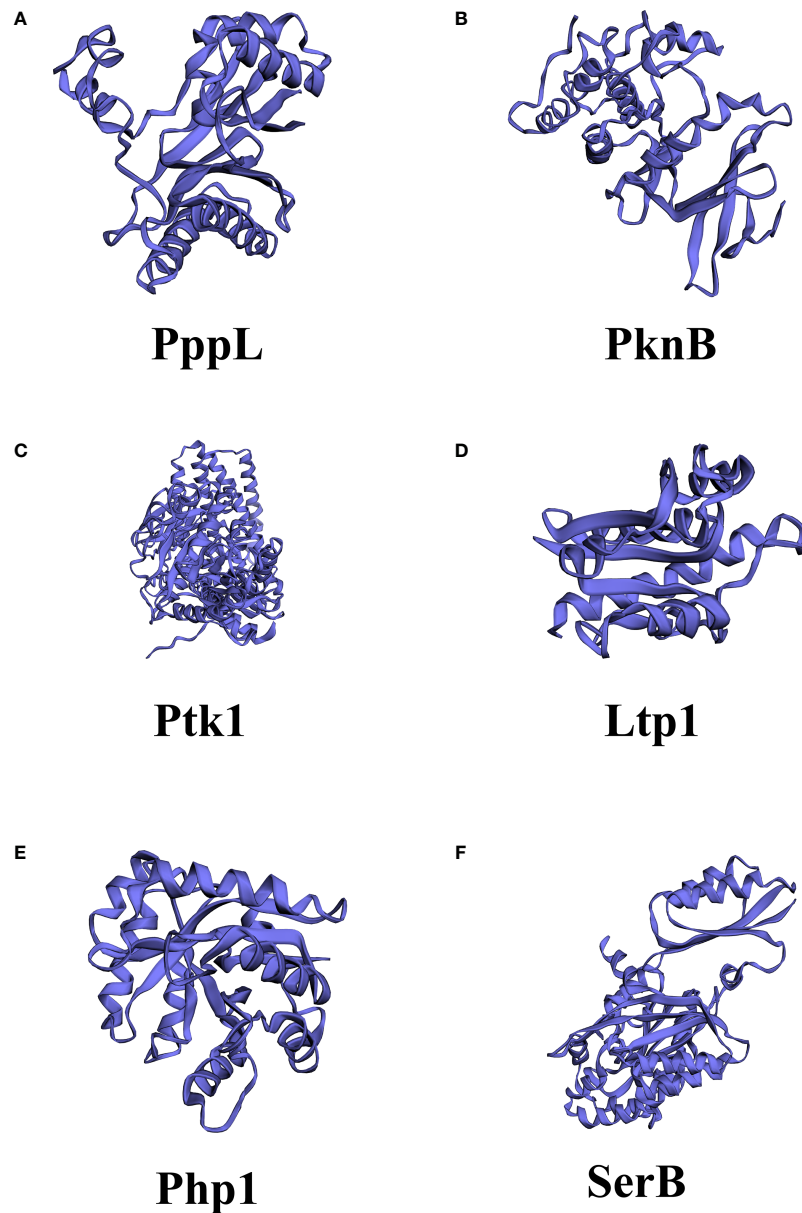


**FIGURE 2** | Different structures among kinases and phosphatase in *Streptococcus mutants* and *Porphyromonas gingivalis*. **(A)** PppL, *S. mutants* PPM family protein phosphatase; **(B)** PknB, *S. mutants* serine/threonine protein kinase; **(C)** Ptk1, *P. gingivalis* tyrosine kinase; **(D)** Ltp1, *P. gingivalis* low molecular weight protein-tyrosine phosphatase; **(E)** Php1, *P. gingivalis* PHP family tyrosine phosphatase **(F)** SerB, *P. gingivalis* Serine/threonine protein phosphatase. The structures were predicted by PHYRE2 Protein Fold Recognition Server.

ubiquitous bacterial kinase (UbK) family is a newly discovered tyrosine kinase family in oral bacteria. The UbK family was originally classified as an unknown but essential P-loop ATPase (Karst et al., 2009). A recent study revealed that the UbK family members can auto-phosphorylate and phosphorylate protein substrates on S/T and Y residues, which classifies them as dual-specific kinases (Nguyen et al., 2017). Structurally, UbK contains a conserved domain: the Walker A motif, HxDxYR, SPT/S and EW motifs. Ubk1 is a UbK family member in *P. gingivalis* that can autophosphorylate on the tyrosine and serine

residues within the HxDxYR and SPT/S domains, respectively (Perpich et al., 2021).

### Tyrosine Phosphatase

There are three categories of protein tyrosine phosphatases: eukaryotic like phosphatases (PTPs) and dual-specific phosphatases; low molecular weight protein tyrosine phosphatases (LMW-PTPs), and the less common polymerase-histidinol phosphatases (PHPs), which are often found in gram-positive bacteria (Whitmore and Lamont, 2012). Some LMW-

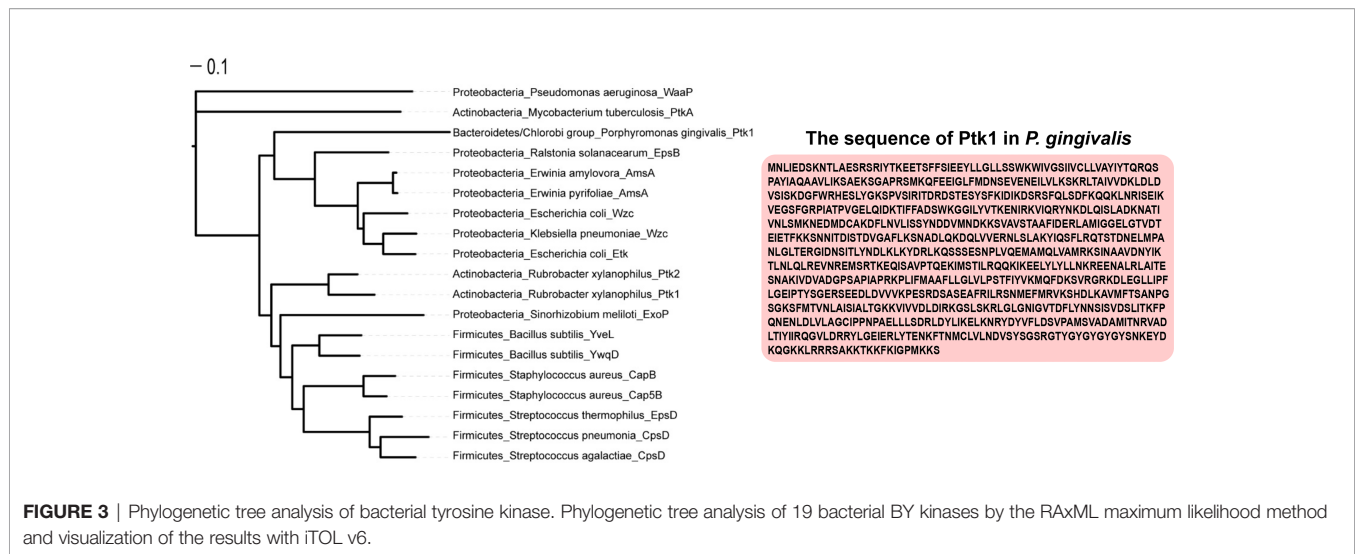


**FIGURE 3 |** Phylogenetic tree analysis of bacterial tyrosine kinase. Phylogenetic tree analysis of 19 bacterial BY kinases by the RAxML maximum likelihood method and visualization of the results with iTOL v6.

PTPs are similar to eukaryotic low molecular weight peptide, and the other part has typical characteristics of prokaryotic LMW-PTPs, such as Wzb in *E. coli* (Lescop et al., 2006). Eukaryotic and prokaryotic LMW-PTPs diverged during the evolution process. For example, there are two tyrosine phosphatases (PtpA and PtpB) in both *Staphylococcus aureus* and *Bacillus subtilis* (Soulat et al., 2002; Xu et al., 2006). PTPs, dual-specific phosphatases and LMW-PTPs utilize a common catalytic mechanism that contains the conserved signature C(x)5R motif, where cysteine and arginine residues are important for the catalytic activity. Functioning as a nucleophile, cysteine attacks the phosphorus atom of the phosphor-tyrosine residue of the substrate, while the arginine residue interacts with the phosphate moiety of the phosphor-tyrosine (Tiganis, 2002). This motif is flanked by an important aspartic acid residue, whose position varies among the families. Unlike the other members in PTPs, PHPs are divalent metal ion-dependent phosphor-tyrosine phosphatases, whose catalytic mechanism is metal-dependent (Kim et al., 2011; Standish and Morona, 2014). PHPs show optimal activity at basic pH and depend on the presence of a metal ion, especially when combined with  $Mn^{2+}$  (Mijakovic et al., 2005). This mechanism also requires an arginine residue in the active site and a nucleophilic attack by metal-bound water, even if it is dependent on metal ions (Hagelueken et al., 2009). Recently, a tyrosine phosphatase (Php1) belonging to the PHP family of *P. gingivalis* was reported by Jung et al. (2019). Php1 maintains all the invariant histidine, aspartate, and arginine residues in four conserved motifs, similar to other bacterial PHP-PTP proteins, such as in *M. xanthus* and *S. pneumoniae*, and shows high structural conservation with YwqE, a PHP-PTP in *B. subtilis* (Jung et al., 2019).

## Serine/Threonine Kinases

The first structurally characterized bacterial serine/threonine kinase was PknB in *M. tuberculosis*, which revealed a striking similarity of a two-lobe structure to the eukaryotic versions in terms of its two-lobe structure (Ortiz-Lombardia et al., 2003).

The two-lobe structure of serine/threonine kinase contains an N-terminal lobe, which is involved in the binding and orientation of an ATP molecule, whereas the C-terminal lobe is responsible for binding to the protein substrate and transferring of the phosphate group. ATP binds to a deep cleft between the two lobes. These similarities suggest that bacterial and eukaryotic STKs share conserved ATP-binding and hydrolysis mechanisms (Janczarek et al., 2018). Additional domains mediate the binding of ligands and/or protein-protein interactions, such as penicillin-binding proteins and serine/threonine kinase associated (PASTA) domains (Krupa and Srinivasan, 2005). A study analyzing *B. subtilis* revealed an interaction between PASTA motifs and peptidoglycan, the ligand of the STK receptor (Shah et al., 2008). Several *in vitro* studies have also demonstrated that PASTA motifs are able to bind  $\beta$ -lactams and peptidoglycan fragments, making STK as a cell membrane receptor that transmits information from the cell wall state to the phosphorylation target (Maestro et al., 2011; Mir et al., 2011). Importantly, STKs with PASTA motifs play a major role in the regulation of bacterial cell division and morphogenesis (Pereira et al., 2011). The activation of STKs is thought to be initiated by the binding of these neuropeptide ligands, resulting in dimerization and subsequent autophosphorylation of the cytoplasmic N-terminal kinase domain. This leads to the phosphorylation of downstream target proteins and eventually results in the modulation of transcriptional activity. This process has been confirmed in a study of *Mycobacterium tuberculosis* and *Staphylococcus aureus* (Barthe et al., 2010; Ohlsen and Donat, 2010). A topological analysis predicted PknB, the serine/threonine protein kinase of *S. mutans*, as a transmembrane protein with a catalytic domain in the cytoplasm and a C-terminal domain located extracellularly (Figure 2). Three PASTA domains are located at the C terminus (Hussain et al., 2006).

## Serine/Threonine Phosphatases

The serine/threonine phosphatase system has long been considered as an exclusive PTM in eukaryotes for a long time (Bakal and Davies, 2000), and the first reported bacterial example



was the *E. coli* tricarboxylic acid cycle enzyme isocitrate dehydrogenase (IDH) (Garnak and Reeves, 1979). Most enzymes with serine/threonine phosphatase (STP) activity are members of two structurally different families, PPMs and PPPs. A large number of identified and biochemically characterized STPs belong to the PPM family (Shi et al., 1998; Kennelly, 2002). They share a common catalytic domain consisting of 9-11 signature sequence motifs containing eight conserved amino acid residues and eight invariant residues (one Asp in motifs 1 and 2, Thr in motif 4, Gly in motifs 5 and 6, Asp and Gly in motif 8, and Asp in motif 11) (Kennelly, 2002; Zhang et al., 2004; Zhang and Shi, 2004). The phosphatase activity of STPs in the PPM family is dependent on metal status (Kamada et al., 2020). The conserved STP structure is highly parallel to the human PP2C phosphatase. The active site was surrounded by a central  $\beta$ -sandwich, with a pair of  $\alpha$ -helices in the flank, and a binuclear metal center is located within the channel of the  $\beta$ -sandwich, and two metal ions located at the base of the cleft (Shi, 2009; Pereira et al., 2011). There are some key differences between the structure of STPs and the human PP2C family, such as  $Mn^{2+}$  and  $Mg^{2+}$ ; a structural analysis revealed that bacterial enzymes have a third metal ion bound within the catalytic core (Pullen et al., 2004; Bellinzoni et al., 2007; Schlicker et al., 2008). Another difference is the lack of his62 residue in the bacterial structure, which has been shown to function as an acid that splits the phosphate oxygen bond in human PP2C (Das et al., 1996). The most remarkable structural difference corresponds to the flap subdomain. In bacteria, this region is located further away from the active site. As a mobile element, it may facilitate binding and turnover of the substrates, and introduce the specificity to the

dephosphorylation of the substrates (Pereira et al., 2011). Most serine/threonine phosphatases of the PPP family have dual specificity and can also dephosphorylate phosphor-histidine and phosphor-tyrosine residues (Wright and Ulijasz, 2014; Chen et al., 2017). PppL of *S. mutans* was the first reported oral bacterial STP (Banu et al., 2010). However, its structure requires further investigation. The haloacid dehalogenase (HAD) family phosphatase is also widespread in prokaryotes, and it is characterized by a Rossman-like fold with active motif (DxDx[V/T]) (Tribble et al., 2006). The HAD family of phosphatases uses aspartic acid as a nucleophile to form phosphatase intermediates during the phosphoryl transfer process, and absolutely requires divalent ion cofactors (Seifried et al., 2013). SerB of *P. gingivalis* is a well-studied HAD family phosphatase in oral bacteria (Table 1). SerB is secreted by *P. gingivalis* and is involved in oral bacteria-host interactions, which will be described in subsequent sections.

## THE FUNCTION OF ORAL BACTERIAL TYROSINE AND SERINE/THREONINE KINASES AND PHOSPHATASES

### Tyrosine and Serine/Threonine Kinases and Phosphatases in Bacterial Metabolism and Virulence

The first identification and characterization of tyrosine phosphorylation in bacteria appeared in 1996, when Bertrand Duclos et al. revealed the autophosphorylation of tyrosine residues

**TABLE 1** | Oral bacterial protein kinases and phosphatases.

Organism	Kinase or phosphatase	Substrates	Function	Ref
<i>S. mutans</i>	PknB <sup>a</sup> , PppL <sup>b</sup> – (Ser/Thr)		cell wall biosynthesis, cell transformation, biofilm formation, environmental stress tolerance, bacterial cariogenicity, bacteriocins production, regulation of Smu2146c, VicRK, and ComDE	(Hussain et al., 2006; Banu et al., 2010)
<i>S. mutans</i>	PknB <sup>a</sup> (Ser/Thr)	–	H <sub>2</sub> O <sub>2</sub> resistance of <i>S. mutans</i> in the interspecies competition with <i>Streptococcus sanguinis</i>	(Zhu and Kreth, 2010)
<i>P. gingivalis</i>	Ptk1 <sup>a</sup> , Ltp1 <sup>b</sup> (Tyr)	EpsD, CdhR	<i>P. gingivalis</i> - <i>S. gordonii</i> community formation, bacterial virulence, EPS production, bacterial virulence	(Maeda et al., 2008; Wright et al., 2014; Liu et al., 2017)
<i>P. gingivalis</i>	Ptk1 <sup>a</sup> , Ltp1 <sup>b</sup> (Tyr)	UDP-acetylmannosamine dehydrogenase and UDP-glucose dehydrogenase	<i>P. gingivalis</i> - <i>S. gordonii</i> community formation and EPS production	(Maeda et al., 2008; Liu et al., 2017)
<i>P. gingivalis</i>	Ptk1 <sup>a</sup> , Ltp1 <sup>b</sup> (Tyr)	PTEN	migration, proliferation, and epithelial mesenchymal transition of epithelial cells	(Liu et al., 2021)
<i>P. gingivalis</i>	Php1 <sup>b</sup>	Ptk1	EPS production and community development with <i>S. gordonii</i> under nutrient-depleted conditions	(Jung et al., 2019)
<i>P. gingivalis</i>	SerB <sup>b</sup> (Ser)	Cofilin	bacterial invasion efficiency, bacterial internalization, and survival	(Moffatt et al., 2012)
<i>P. gingivalis</i>	SerB <sup>b</sup> (Ser)	GAPDH	bacterial invasion efficiency, rearrangement of microtubules to the cell surface	(Tribble et al., 2006)
<i>P. gingivalis</i>	SerB <sup>b</sup> (Ser)	NF- $\kappa$ B RelA/p65	host inflammatory pathways and innate immunity repression, inhibition of IL-8 secretion	(Takeuchi et al., 2013)
<i>P. gingivalis</i>	Ubk1 <sup>a</sup> (Ubiquitous)	RprY	transcriptional function	(Perpich et al., 2021)

<sup>a</sup>Kinase.

<sup>b</sup>Phosphatase.

in *Acinetobacter johnsonii* (Duclos et al., 1996). Increasing evidence has demonstrated that tyrosine phosphorylation is crucial for bacterial survival and pathogenicity (Ge and Shan, 2011; Whitmore and Lamont, 2012). Studies have shown that tyrosine phosphorylation is involved in the biosynthesis and export of extracellular polysaccharides (EPS), which are key virulence factors and integral components of biofilm communities (Schwechheimer et al., 2020; Whitfield et al., 2020; Zhuang et al., 2020). Ltp1, the LMW-PTP in *P. gingivalis*, is critical for bacterial virulence, as it helps to regulate various virulence factors at multiple levels. Ltp1 controls EPS production and secretion by regulating the transcriptional activity of genes involved in K-antigen production (PG 0106-0120) and anionic polysaccharide production (PG 0435-0437) (Maeda et al., 2008). Ltp1 can also control the expression of the LuxS enzyme, which is responsible for AI-2 formation, and promote the intake of hemin, thus increasing the toxicity of *P. gingivalis* (Maeda et al., 2008; Rangarajan et al., 2017). More importantly, the secretion and activity of gingipains (Rgp and Kgp) in *P. gingivalis* was regulated by Ltp1 in distinct manner. The secretion efficiency of the Rgp has been positively correlated with the phosphatase activity of Ltp1. In contrast, the dephosphorylated Kgp shows diminished proteolytic activity (Kariu et al., 2017). Consistently, compared with parental strains, the *php1* mutant exhibited less EPS productivity and caused less alveolar bone loss in murine periodontitis models (Jung et al., 2019).

Both Ltp1 and Php1 can be phosphorylated by the tyrosine kinase Ptk1, which is also required for EPS production by *P. gingivalis* (Wright et al., 2014). The 159 and 161 tyrosine residues of Php1 can be phosphorylated by Ptk1, and the 161-residue phosphorylation may indicate a specific regulatory mechanism in

*P. gingivalis* (Jung et al., 2019). Interestingly, Ptk1 is also a substrate of Ltp1 and Php1 (Liu et al., 2017; Jung et al., 2019). These results indicated that reversible tyrosine phosphorylation of *P. gingivalis* is tightly orchestrated by the activity of tyrosine kinase (Ptk1) and tyrosine phosphatases (Ltp1 and Php1), allowing the bacteria to sense and respond to perturbations in the environment (Figure 4). Further evidence has been derived from high-throughput transposon sequencing has been used to screen the fitness of gene mutants involved in epithelial colonization in a murine abscess model (Miller et al., 2017). Either *php1* or *ptk1* mutant showed reduced fitness in the epithelial colonization model. Thus, the Ptk1-Php1 axis may be prompt the interaction of *P. gingivalis* with host epithelial barriers, functioning as a potential regulator of pathogen colonization and virulence (Miller et al., 2017). UbK1 in *P. gingivalis* can also exert its pathogenic function. Specifically, RprY, an orphan two-component system response regulator, can be phosphorylated by UbK1 on Y41 residue, affecting its transcriptional function (Shen et al., 2020; Perpich et al., 2021). The UbK in *S. mutans* has been reported associated with cell morphology and biofilm development (Bitoun et al., 2014).

STK is also essential for bacterial survival and is related to oral biofilm formation related to the oral bacterial. *S. mutans* is a major etiologic agent in dental caries, primarily because of its ability to form biofilms on the tooth surface and to ferment a variety of carbohydrates to produce organic acids (Giacaman, 2018). STK and STP systems play a pivotal role in the pathogenicity of *S. mutans* (Banu et al., 2010). *S. mutans* possesses a STK, PknB. The *pknB* mutant presented a transformation defect, reduced biofilm formation, and reduced the microbial growth rate in culture medium at pH 5.0 and sensitivity to low pH, as well as oxidative

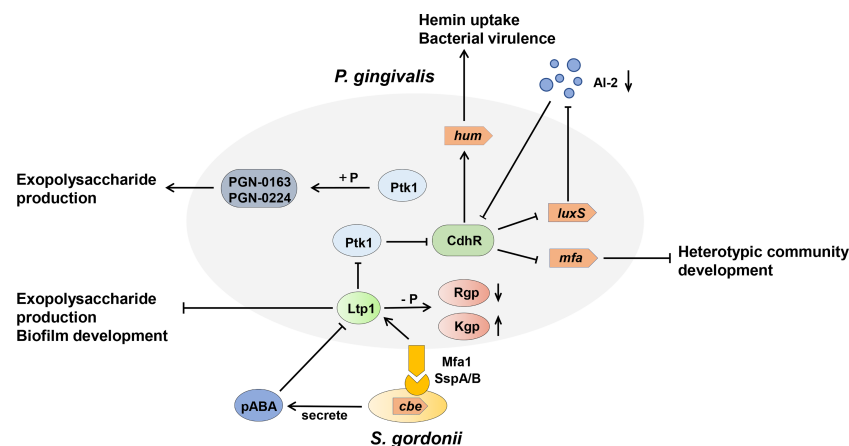


**FIGURE 4 |** Model of the tyrosine kinase-phosphatase dependent regulatory process governing *Porphyromonas gingivalis* extracellular polysaccharide production, bacterial virulence, and heterotypic community development between *Porphyromonas gingivalis* and *Streptococcus gordonii*. The interactions between *P. gingivalis* and *S. gordonii* resulting from pABA perception and direct contact of *P. gingivalis* Mfa fimbriae with *S. gordonii* Ssp proteins, which can influence Ltp1 activity, thus initiate a cascade of phosphorylation and dephosphorylation events. Ltp1 can decrease the production of exopolysaccharide and dephosphorylate gingipains Rgp and Kgp to affect colony nutrition supply. Ltp1 also dephosphorylates Ptk1 to downregulate its kinase activity, causing the upregulation of CdhR expression. CdhR represses the transcription of *luxS* and *mfa* operons to downregulate the community development of *P. gingivalis* and *S. gordonii* and promotes the transcription of the *hum* operon to increase the hum uptake and virulence of *P. gingivalis*. Lower AI-2 levels cause upregulation of CdhR and constrain the development of a heterotypic community. Conversely, protein kinase Ptk1 uses its enzyme activity to increase the production of exopolysaccharides.

and osmotic stress (van der Ploeg, 2005; Hussain et al., 2006). A whole-genome transcriptome analysis revealed that the *pknB* mutant exhibited downregulation of *SMU.1895c* and *SMU.1896c*, which are involved in bacteriocin production (van der Ploeg, 2005). The STP of *S. mutans* is encoded by the *pppL* gene located immediately downstream of *pknB*. The mutant of *pppL* and *pknB* *pppL* double mutants displayed reduced biofilm thickness and transformation defects.

## Tyrosine and Serine/Threonine Kinases and Phosphatases in Oral Bacterial Dysbiosis

Oral bacterial dysbiosis is characterized by disruption in bacterial homeostasis, caused by an imbalance in the microflora, changes in composition, and metabolic activities, which contribute to oral diseases, such as dental caries and periodontitis (Lamont et al., 2018). *P. gingivalis* acts as a critical agent by disrupting bacterial homeostasis (Mulhall et al., 2020; Xu et al., 2020). In dental plaque, *P. gingivalis* can accumulate into a heterotypic community with *S. gordonii* and utilize physiological support, while the heterotypic colonies are more virulent than *P. gingivalis* mono-species infections (Hajishengallis and Lamont, 2016; Jung et al., 2019). The mechanism of *P. gingivalis* accumulation in the *S. gordonii* matrix is due to the metabolite, 4-amino benzoate (pABA), and direct contact between *P. gingivalis* and *S. gordonii*, which is stringently regulated by the Ltp1-Ptk1 and Php1-Ptk1 axes of *P. gingivalis* (Whitmore and Lamont, 2012; Wright et al., 2014; Lamont et al., 2018; Jung et al., 2019). Ltp1 can inhibit the development of *P. gingivalis* and *S. gordonii* communities at the phenotypic level (Maeda et al., 2008). The mechanism describing how Ltp1 regulates this process was further elucidated. The results showed that Ltp1 upregulated and participated in the interspecies signal transmission after contact with streptococcal SspA or SspB surface proteins. The elevated Ltp1 resulted in dephosphorylation and inactivation of Ptk1, thus increasing the expression of community development and hemin regulator (CdhR) and suppressing the transcription of *mfa1*, which limits the development of heterotypic communities (Chawla et al., 2010). In turn, pABA secreted by *S. gordonii* could suppress the activity of Ltp1 and reverse this signaling transduction through the Ltp1-Ptk1 axis.

Ptk1 activity also converges on expression of the other fimbriae encoding genes (*fimA*). Therefore, we can speculate that Ltp1-Ptk1 affects the oral bacterial homeostasis and dysbiosis by regulating the expression of *P. gingivalis* fimbriae in a spatio-temporal dependent manner. The cognate kinase Php1-Ptk1 axis of *P. gingivalis* also participates in oral bacterial homeostasis and dysbiosis regulation via distinct mechanisms. Jung et al. demonstrated that *PhpP* mutants showed diminished heterotypic communities of *P. gingivalis* and *S. gordonii*, but had no significant effect on intraspecific communication of *P. gingivalis* (Jung et al., 2019). Php1 can also dephosphorylate Ptk1, however, the activity of Php1 is resistant to the effect of pABA secreted by *S. gordonii*. Thus, the specific mechanism by which Php1-Ptk1 regulates the heterotypic community requires further investigation.

In addition, *Streptococcus sanguinis*, an early colonizing bacterium in dental biofilm, antagonizes other streptococcus colonization and growth by secreting the virulence factor  $H_2O_2$ . Studies have shown that serine/threonine kinase PknB secreted by *S. mutans* plays a role in its tolerance to  $H_2O_2$ , which helps *S. mutans* adapt to ecological pressure and interspecific competition with *S. sanguinis* (Zhu and Kreth, 2010).

## Effect of Tyrosine and Serine/Threonine Phosphatases on Oral Bacteria-Host Interaction

Many bacteria exert their virulence by invading host cells, and the internalization and intracellular survival of bacteria are essential to their pathogenicity (Lewis et al., 2016). Lamont et al. first reported that *P. gingivalis* can invade primary cultures of gingival epithelial cells (Lamont et al., 1995). Mounting evidence supports this finding, and a series of discoveries have since demonstrated the pivotal role of tyrosine and serine/threonine phosphatases in this process (Moffatt et al., 2012; Takeuchi and Amano, 2021). The most common example of the participation of serine/threonine phosphatases in oral bacteria-host interaction is SerB in *P. gingivalis* (Figure 5). SerB can be released into host cells and directly interact with host cytoplasmic phosphoproteins, facilitating bacterial internalization (Tribble et al., 2006). The existence of SerB can ensure the invasion of host cells to the greatest extent, as SerB dephosphorylates actin cofilin, an actin depolymerizing host protein, affecting the expression of genes involved in the regulation of actin cytoskeleton dynamics and cytokine secretion (Bainbridge et al., 2010; Woo et al., 2019). Furthermore, SerB can also dephosphorylate the S536 site of NF- $\kappa$ B p65 subunit to prevent nuclear translocation of NF- $\kappa$ B. This process antagonizes the production of interleukin-8 (IL-8), leading to local chemokine paralysis (Takeuchi et al., 2013). Compared to parental strains, the SerB mutant resulted in high levels of neutrophil recruitment to gingival tissue and decreased alveolar bone destruction at both the horizontal and interproximal levels (Bainbridge et al., 2010). In summary, SerB can promote bacterial invasion of the host, allowing it to continue to exert its full pathogenic potential. Interestingly, it has very recently been reported that the tyrosine phosphatase (Ltp1) can also be secreted by *P. gingivalis* and appears in both the cytoplasm and nucleus of gingival epithelial cells (Liu et al., 2021). The secreted Ltp1 can bind to phosphatase and tensin homolog (PTEN) and dephosphorylate its Y336 residue, resulting in the degradation of PTEN. PTEN is a classic negative regulator of phosphoinositide 3-kinases/protein kinase B (PI3K/Akt). Thus, the inhibition of PTEN by Ltp1 could further activate PI3K/Akt and its downstream regulator of the cell cycle (RGCC), promoting the migration, proliferation and epithelial mesenchymal transition of epithelial cells (Liu et al., 2021) (Figure 5).

## CONCLUSION AND PERSPECTIVES

The phosphorylation system has long been considered an important signal transduction system in eukaryotes, and in recent decades, the function of kinases and phosphatases in

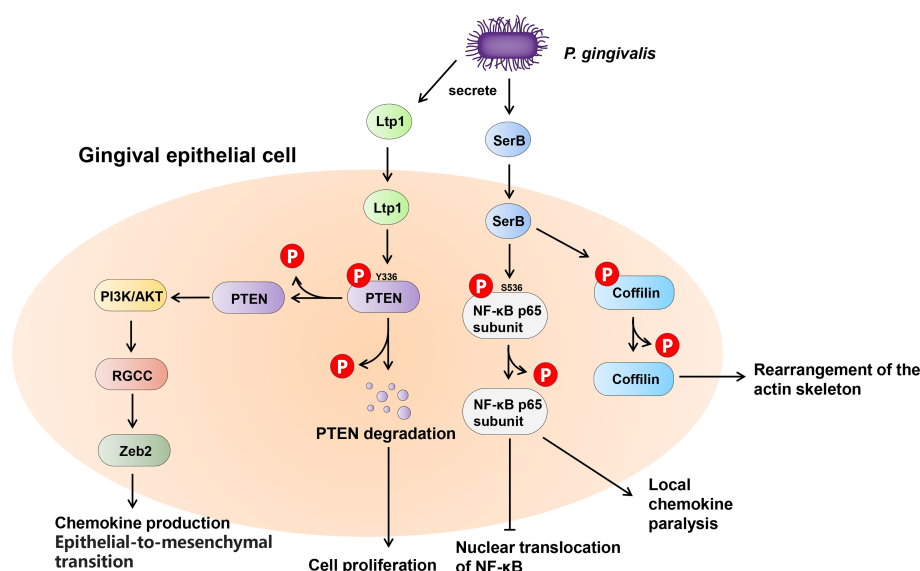


**FIGURE 5** | Schematic of the impact of phosphatases secreted by *Porphyromonas gingivalis* within the gingival epithelial cells. *P. gingivalis* secretes two phosphatases, tyrosine phosphatase Ltp1 and serine phosphatase SerB. Upon contacting the gingival epithelial cell, Ltp1 enters the cell to dephosphorylate PTEN, causing proteasomal degradation. Lower PTEN levels promote the PI3K/AKT pathway to upregulate RGCC and Zeb2. SerB dephosphorylates NF-κB and Cofilin to preserve the virulence of *P. gingivalis* and maximize the intracellular invasion of bacteria.

**TABLE 2** | Tyrosine and serine/threonine kinases and phosphatases in *S. mutants* and *P. gingivalis*.

Bacteria	Gene ID	Symbol	Function
<i>S. mutants</i> UA159	SMU_483	<i>PppL</i>	PPM family protein phosphatase (putative)
	SMU_484	<i>PknB</i>	Serine/threonine protein kinase
	SMU_65		Low molecular weight protein-tyrosine phosphatase (putative)
	SMU_646		HAD family phosphatase (putative)
	SMU_754		Serine kinase/phosphatase (putative)
	SMU_1269		Phosphoserine phosphatase (putative)
	SMU_1747c		HAD family phosphatase (putative)
	SMU_1802c		HAD family phosphatase (putative)
<i>P. gingivalis</i> ATCC 33277	PGN_1524	<i>Ptk1</i>	Tyrosine kinase
	PGN_0491	<i>Ltp1</i>	Low molecular weight protein-tyrosine phosphatase
	PGN_1525	<i>Php1</i>	PHP family tyrosine phosphatase
	PGN_0662	<i>SerB</i>	Serine/threonine protein phosphatase
	PGN_1020	<i>Ubk1</i>	Ubiquitous bacterial kinase
	PGN_1267		Phosphoserine phosphatase (putative)

prokaryotes has been gradually revealed. Yet, based on the gene homologues of bacteria, there are still many putative kinases and phosphatases that have not been studied (Table 2). The rising prevalence of antibiotic-resistant bacteria is driving research toward novel targets. With the advent of phosphor-proteomics, more phosphorylation proteins and sites can be discovered to expand the phosphorylation regulatory network (Misra et al., 2011; Mijakovic and Macek, 2012; Bäsell et al., 2014; Yagüe et al., 2019). In the future, more experiments are needed to verify the specific functions of kinases and phosphatases in oral bacteria physiology and pathogenicity, clarify mechanisms between bacteria and the host, and identify potential drug targets to treat infection, immune responses, and diseases.

## AUTHOR CONTRIBUTIONS

LR, DS and CL drafted the manuscript. CL and YD edited and added valuable insights into the manuscript. All authors approved the final manuscript and agreed to be accountable for all aspects of the work.

## FUNDING

This study was supported by the National Natural Science Foundation (grant number 82071121 to YD).



## REFERENCES

- Bainbridge, B., Verma, R. K., Eastman, C., Yehia, B., Rivera, M., Moffatt, C., et al. (2010). Role of Porphyromonas Gingivalis Phosphoserine Phosphatase Enzyme SerB in Inflammation, Immune Response, and Induction of Alveolar Bone Resorption in Rats. *Infect. Immun.* 78 (11), 4560–4569. doi: 10.1128/iai.00703-10
- Bakal, C. J., and Davies, J. E. (2000). No Longer an Exclusive Club: Eukaryotic Signalling Domains in Bacteria. *Trends Cell Biol.* 10 (1), 32–38. doi: 10.1016/s0962-8924(99)01681-5
- Banu, L. D., Conrads, G., Rehrauer, H., Hussain, H., Allan, E., and van der Ploeg, J. R. (2010). The Streptococcus Mutans Serine/Threonine Kinase, PknB, Regulates Competence Development, Bacteriocin Production, and Cell Wall Metabolism. *Infect. Immun.* 78 (5), 2209–2220. doi: 10.1128/IAI.01167-09
- Barthe, P., Mukamolova, G. V., Roumestand, C., and Cohen-Gonsaud, M. (2010). The Structure of PknB Extracellular PASTA Domain From Mycobacterium Tuberculosis Suggests a Ligand-Dependent Kinase Activation. *Structure* 18 (5), 606–615. doi: 10.1016/j.str.2010.02.013
- Bäsel, K., Otto, A., Junker, S., Zühlke, D., Rappen, G. M., Schmidt, S., et al. (2014). The Phosphoproteome and Its Physiological Dynamics in Staphylococcus Aureus. *Int. J. Med. Microbiol.* 304 (2), 121–132. doi: 10.1016/j.ijmm.2013.11.020
- Bellinzoni, M., Wehenkel, A., Shepard, W., and Alzari, P. M. (2007). Insights Into the Catalytic Mechanism of PPM Ser/Thr Phosphatases From the Atomic Resolution Structures of a Mycobacterial Enzyme. *Structure* 15 (7), 863–872. doi: 10.1016/j.str.2007.06.002
- Bitoun, J. P., Liao, S., Xie, G. G., Beatty, W. L., and Wen, Z. T. (2014). Deficiency of BrpB Causes Major Defects in Cell Division, Stress Responses and Biofilm Formation by Streptococcus Mutans. *Microbiology (Reading)* 160 (Pt 1), 67–78. doi: 10.1099/mic.0.072884-0
- Bonne Kohler, J., Jers, C., Senissar, M., Shi, L., Derouiche, A., and Mijakovic, I. (2020). Importance of Protein Ser/Thr/Tyr Phosphorylation for Bacterial Pathogenesis. *FEBS Lett.* 594 (15), 2339–2369. doi: 10.1002/1873-3468.13797
- Chawla, A., Hirano, T., Bainbridge, B. W., Demuth, D. R., Xie, H., and Lamont, R. J. (2010). Community Signalling Between Streptococcus Gordonii and Porphyromonas Gingivalis Is Controlled by the Transcriptional Regulator CdhR. *Mol. Microbiol.* 78 (6), 1510–1522. doi: 10.1111/j.1365-2958.2010.07420.x
- Chen, M. J., Dixon, J. E., and Manning, G. (2017). Genomics and Evolution of Protein Phosphatases. *Sci. Signal* 10 (474), eaag2017. doi: 10.1126/scisignal.aag1796
- Collins, R. F., Beis, K., Clarke, B. R., Ford, R. C., Hulley, M., Naismith, J. H., et al. (2006). Periplasmic Protein-Protein Contacts in the Inner Membrane Protein Wzc Form a Tetrameric Complex Required for the Assembly of Escherichia Coli Group 1 Capsules. *J. Biol. Chem.* 281 (4), 2144–2150. doi: 10.1074/jbc.M508078200
- Das, A. K., Helps, N. R., Cohen, P. T., and Barford, D. (1996). Crystal Structure of the Protein Serine/Threonine Phosphatase 2C at 2.0 Å Resolution. *EMBO J.* 15 (24), 6798–6809. doi: 10.1002/j.1460-2075.1996.tb01071.x
- Doublet, P., Grangeasse, C., Obadia, B., Vaganay, E., and Cozzzone, A. J. (2002). Structural Organization of the Protein-Tyrosine Autokinase Wzc Within Escherichia Coli Cells. *J. Biol. Chem.* 277 (40), 37339–37348. doi: 10.1074/jbc.M204465200
- Duclos, B., Grangeasse, C., Vaganay, E., Riberty, M., and Cozzzone, A. J. (1996). Autophosphorylation of a Bacterial Protein at Tyrosine. *J. Mol. Biol.* 259 (5), 891–895. doi: 10.1006/jmbi.1996.0366
- Escapa, I. F., Chen, T., Huang, Y., Gajare, P., Dewhirst, F. E., and Lemon, K. P. (2018). New Insights Into Human Nostril Microbiome From the Expanded Human Oral Microbiome Database (eHOMD): A Resource for the Microbiome of the Human Aerodigestive Tract. *mSystems* 3 (6), e00187-18. doi: 10.1128/mSystems.00187-18
- Esser, D., Hoffmann, L., Pham, T. K., Bräsen, C., Qiu, W., Wright, P. C., et al. (2016). Protein Phosphorylation and Its Role in Archaeal Signal Transduction. *FEMS Microbiol. Rev.* 40 (5), 625–647. doi: 10.1093/femsre/fuw020
- Garnak, M., and Reeves, H. C. (1979). Phosphorylation of Isocitrate Dehydrogenase of Escherichia Coli. *Science* 203 (4385), 1111–1112. doi: 10.1126/science.34215
- Ge, R., and Shan, W. (2011). Bacterial Phosphoproteomic Analysis Reveals the Correlation Between Protein Phosphorylation and Bacterial Pathogenicity. *Genomics Proteomics Bioinformatics* 9 (4-5), 119–127. doi: 10.1016/s1672-0229(11)60015-6
- Giacaman, R. A. (2018). Sugars and Beyond. The Role of Sugars and the Other Nutrients and Their Potential Impact on Caries. *Oral. Dis.* 24 (7), 1185–1197. doi: 10.1111/odi.12778
- Grangeasse, C., Cozzzone, A. J., Deutscher, J., and Mijakovic, I. (2007). Tyrosine Phosphorylation: An Emerging Regulatory Device of Bacterial Physiology. *Trends Biochem. Sci.* 32 (2), 86–94. doi: 10.1016/j.tibs.2006.12.004
- Grangeasse, C., Doublet, P., and Cozzzone, A. J. (2002). Tyrosine Phosphorylation of Protein Kinase Wzc From Escherichia Coli K12 Occurs Through a Two-Step Process. *J. Biol. Chem.* 277 (9), 7127–7135. doi: 10.1074/jbc.M110880200
- Hagelueken, G., Huang, H., Mainprize, I. L., Whitfield, C., and Naismith, J. H. (2009). Crystal Structures of Wzb of Escherichia Coli and CpsB of Streptococcus Pneumoniae, Representatives of Two Families of Tyrosine Phosphatases That Regulate Capsule Assembly. *J. Mol. Biol.* 392 (3), 678–688. doi: 10.1016/j.jmb.2009.07.026
- Hajishengallis, G., and Chavakis, T. (2021). Local and Systemic Mechanisms Linking Periodontal Disease and Inflammatory Comorbidities. *Nat. Rev. Immunol.* 21 (7), 426–440. doi: 10.1038/s41577-020-00488-6
- Hajishengallis, G., and Lamont, R. J. (2016). Dancing With the Stars: How Choreographed Bacterial Interactions Dictate Nosocomiality and Give Rise to Keystone Pathogens, Accessory Pathogens, and Pathobionts. *Trends Microbiol.* 24 (6), 477–489. doi: 10.1016/j.tim.2016.02.010
- Hajishengallis, G., and Lamont, R. J. (2021). Polymicrobial Communities in Periodontal Disease: Their Quasi-Organismal Nature and Dialogue With the Host. *Periodontol.* 2000 86 (1), 210–230. doi: 10.1111/prd.12371
- Hardie, D. G. (1990). Roles of Protein Kinases and Phosphatases in Signal Transduction. *Symp. Soc. Exp. Biol.* 44, 241–255.
- Huse, M., and Kuriyan, J. (2002). The Conformational Plasticity of Protein Kinases. *Cell* 109 (3), 275–282. doi: 10.1016/s0092-8674(02)00741-9
- Hussain, H., Branny, P., and Allan, E. (2006). A Eukaryotic-Type Serine/Threonine Protein Kinase Is Required for Biofilm Formation, Genetic Competence, and Acid Resistance in Streptococcus Mutans. *J. Bacteriol.* 188 (4), 1628–1632. doi: 10.1128/jb.188.4.1628-1632.2006
- Jaiswal, S., Chatterjee, A., Pandey, S., Lata, K., Gadi, R. K., Manda, R., et al. (2019). Mycobacterial Protein Tyrosine Kinase, PtkA Phosphorylates PtpA at Tyrosine Residues and the Mechanism Is Stalled by the Novel Series of Inhibitors. *J. Drug Target.* 27 (1), 51–59. doi: 10.1080/1061186x.2018.1473407
- Janczarek, M., Vinardell, J. M., Lipa, P., and Karaś, M. (2018). Hanks-Type Serine/Threonine Protein Kinases and Phosphatases in Bacteria: Roles in Signaling and Adaptation to Various Environments. *Int. J. Mol. Sci.* 19 (10), 2872. doi: 10.3390/ijms19102872
- Jung, Y. J., Miller, D. P., Perpich, J. D., Fitzsimonds, Z. R., Shen, D., Ohshima, J., et al. (2019). Porphyromonas Gingivalis Tyrosine Phosphatase Php1 Promotes Community Development and Pathogenicity. *mBio* 10 (5), e02004-19. doi: 10.1128/mBio.02004-19
- Kamada, R., Kudoh, F., Ito, S., Tani, I., Janairo, J. I. B., Omichinski, J. G., et al. (2020). Metal-Dependent Ser/Thr Protein Phosphatase PPM Family: Evolution, Structures, Diseases and Inhibitors. *Pharmacol. Ther.* 215, 107622. doi: 10.1016/j.pharmthera.2020.107622
- Kariu, T., Nakao, R., Ikeda, T., Nakashima, K., Potempa, J., and Imamura, T. (2017). Inhibition of Gingipains and Porphyromonas Gingivalis Growth and Biofilm Formation by Prenyl Flavonoids. *J. Periodontol. Res.* 52 (1), 89–96. doi: 10.1111/jre.12372
- Karst, J. C., Foucher, A. E., Campbell, T. L., Di Guilmi, A. M., Stroebel, D., Mangat, C. S., et al. (2009). The ATPase Activity of an 'Essential' Bacillus Subtilis Enzyme, YdiB, Is Required for Its Cellular Function and Is Modulated by Oligomerization. *Microbiology (Reading)* 155 (Pt 3), 944–956. doi: 10.1099/mic.0.021543-0
- Kennelly, P. J. (2002). Protein Kinases and Protein Phosphatases in Prokaryotes: A Genomic Perspective. *FEMS Microbiol. Lett.* 206 (1), 1–8. doi: 10.1111/j.1574-6968.2002.tb10978.x
- Kim, H. S., Lee, S. J., Yoon, H. J., An, D. R., Kim, D. J., Kim, S. J., et al. (2011). Crystal Structures of YwqE From Bacillus Subtilis and CpsB From Streptococcus Pneumoniae, Unique Metal-Dependent Tyrosine Phosphatases. *J. Struct. Biol.* 175 (3), 442–450. doi: 10.1016/j.jsb.2011.05.007
- Krupa, A., and Srinivasan, N. (2005). Diversity in Domain Architectures of Ser/Thr Kinases and Their Homologues in Prokaryotes. *BMC Genomics* 6, 129. doi: 10.1186/1471-2164-6-129

- Kyriakis, J. M. (2014). In the Beginning, There was Protein Phosphorylation. *J. Biol. Chem.* 289 (14), 9460–9462. doi: 10.1074/jbc.R114.557926
- Lamont, R. J., Chan, A., Belton, C. M., Izutsu, K. T., Vasel, D., and Weinberg, A. (1995). Porphyromonas Gingivalis Invasion of Gingival Epithelial Cells. *Infect. Immun.* 63 (10), 3878–3885. doi: 10.1128/iai.63.10.3878-3885.1995
- Lamont, R. J., Koo, H., and Hajishengallis, G. (2018). The Oral Microbiota: Dynamic Communities and Host Interactions. *Nat. Rev. Microbiol.* 16 (12), 745–759. doi: 10.1038/s41579-018-0089-x
- Lescop, E., Hu, Y., Xu, H., Hu, W., Chen, J., Xia, B., et al. (2006). The Solution Structure of Escherichia Coli Wzb Reveals a Novel Substrate Recognition Mechanism of Prokaryotic Low Molecular Weight Protein-Tyrosine Phosphatases. *J. Biol. Chem.* 281 (28), 19570–19577. doi: 10.1074/jbc.M601263200
- Lewis, A. J., Richards, A. C., and Mulvey, M. A. (2016). Invasion of Host Cells and Tissues by Uropathogenic Bacteria. *Microbiol. Spectr.* 4 (6), 4.6.38. doi: 10.1128/microbiolspec.UTI-0026-2016
- Liu, C., Miller, D. P., Wang, Y., Merchant, M., and Lamont, R. J. (2017). Structure-Function Aspects of the Porphyromonas Gingivalis Tyrosine Kinase Ptk1. *Mol. Oral. Microbiol.* 32 (4), 314–323. doi: 10.1111/omi.12173
- Liu, C., Stocke, K., Fitzsimonds, Z. R., Yakoumatos, L., Miller, D. P., and Lamont, R. J. (2021). A Bacterial Tyrosine Phosphatase Modulates Cell Proliferation Through Targeting RGCC. *PLoS Pathog.* 17 (5), e1009598. doi: 10.1371/journal.ppat.1009598
- Low, T. Y., Mohhtar, M. A., Lee, P. Y., Omar, N., Zhou, H., and Ye, M. (2021). Widening the Bottleneck of Phosphoproteomics: Evolving Strategies for Phosphopeptide Enrichment. *Mass Spectrom. Rev.* 40 (4), 309–333. doi: 10.1002/mas.21636
- Maeda, K., Tribble, G. D., Tucker, C. M., Anaya, C., Shizukuishi, S., Lewis, J. P., et al. (2008). A Porphyromonas Gingivalis Tyrosine Phosphatase Is a Multifunctional Regulator of Virulence Attributes. *Mol. Microbiol.* 69 (5), 1153–1164. doi: 10.1111/j.1365-2958.2008.06338.x
- Maestro, B., Novaková, L., Heseck, D., Lee, M., Leyva, E., Mobashery, S., et al. (2011). Recognition of Peptidoglycan and  $\beta$ -Lactam Antibiotics by the Extracellular Domain of the Ser/Thr Protein Kinase StkP From Streptococcus Pneumoniae. *FEBS Lett.* 585 (2), 357–363. doi: 10.1016/j.febslet.2010.12.016
- Manai, M., and Cozzzone, A. J. (1979). Analysis of the Protein-Kinase Activity of Escherichia Coli Cells. *Biochem. Biophys. Res. Commun.* 91 (3), 819–826. doi: 10.1016/0006-291x(79)91953-3
- Mijakovic, I., Grangeasse, C., and Turgay, K. (2016). Exploring the Diversity of Protein Modifications: Special Bacterial Phosphorylation Systems. *FEMS Microbiol. Rev.* 40 (3), 398–417. doi: 10.1093/femsre/fuw003
- Mijakovic, I., and Macek, B. (2012). Impact of Phosphoproteomics on Studies of Bacterial Physiology. *FEMS Microbiol. Rev.* 36 (4), 877–892. doi: 10.1111/j.1574-6976.2011.00314.x
- Mijakovic, I., Musumeci, L., Tautz, L., Petranovic, D., Edwards, R. A., Jensen, P. R., et al. (2005). In Vitro Characterization of the Bacillus Subtilis Protein Tyrosine Phosphatase YwqE. *J. Bacteriol.* 187 (10), 3384–3390. doi: 10.1128/jb.187.10.3384-3390.2005
- Miller, D. P., Hutcherson, J. A., Wang, Y., Nowakowska, Z. M., Potempa, J., Yoder-Himes, D. R., et al. (2017). Genes Contributing to Porphyromonas Gingivalis Fitness in Abscess and Epithelial Cell Colonization Environments. *Front. Cell Infect. Microbiol.* 7, 378. doi: 10.3389/fcimb.2017.00378
- Mir, M., Asong, J., Li, X., Cardot, J., Boons, G. J., and Husson, R. N. (2011). The Extracytoplasmic Domain of the Mycobacterium Tuberculosis Ser/Thr Kinase PknB Binds Specific Mucopeptides and Is Required for PknB Localization. *PLoS Pathog.* 7 (7), e1002182. doi: 10.1371/journal.ppat.1002182
- Misra, S. K., Milohanic, E., Aké, F., Mijakovic, I., Deutscher, J., Monnet, V., et al. (2011). Analysis of the Serine/Threonine/Tyrosine Phosphoproteome of the Pathogenic Bacterium Listeria Monocytogenes Reveals Phosphorylated Proteins Related to Virulence. *Proteomics* 11 (21), 4155–4165. doi: 10.1002/pmic.201100259
- Moffatt, C. E., Inaba, H., Hirano, T., and Lamont, R. J. (2012). Porphyromonas Gingivalis SerB-Mediated Dephosphorylation of Host Cell Cofilin Modulates Invasion Efficiency. *Cell Microbiol.* 14 (4), 577–588. doi: 10.1111/j.1462-5822.2011.01743.x
- Mulhall, H., Huck, O., and Amar, S. (2020). Porphyromonas Gingivalis, a Long-Range Pathogen: Systemic Impact and Therapeutic Implications. *Microorganisms* 8 (6), 869. doi: 10.3390/microorganisms8060869
- Muñoz-Dorado, J., Inouye, S., and Inouye, M. (1991). A Gene Encoding a Protein Serine/Threonine Kinase Is Required for Normal Development of M. Xanthus, a Gram-Negative Bacterium. *Cell* 67 (5), 995–1006. doi: 10.1016/0092-8674(91)90372-6
- Nguyen, H. A., El Khoury, T., Guiral, S., Laaberki, M. H., Candusso, M. P., Galisson, F., et al. (2017). Expanding the Kinome World: A New Protein Kinase Family Widely Conserved in Bacteria. *J. Mol. Biol.* 429 (20), 3056–3074. doi: 10.1016/j.jmb.2017.08.016
- Nimmo, G. A., Borthwick, A. C., Holms, W. H., and Nimmo, H. G. (1984). Partial Purification and Properties of Isocitrate Dehydrogenase Kinase/Phosphatase From Escherichia Coli ML308. *Eur. J. Biochem.* 141 (2), 401–408. doi: 10.1111/j.1432-1033.1984.tb08205.x
- Nimmo, G. A., and Nimmo, H. G. (1984). The Regulatory Properties of Isocitrate Dehydrogenase Kinase and Isocitrate Dehydrogenase Phosphatase From Escherichia Coli ML308 and the Roles of These Activities in the Control of Isocitrate Dehydrogenase. *Eur. J. Biochem.* 141 (2), 409–414. doi: 10.1111/j.1432-1033.1984.tb08206.x
- Ohlsen, K., and Donat, S. (2010). The Impact of Serine/Threonine Phosphorylation in Staphylococcus Aureus. *Int. J. Med. Microbiol.* 300 (2–3), 137–141. doi: 10.1016/j.ijmm.2009.08.016
- Ortiz-Lombardia, M., Pompeo, F., Boitel, B., and Alzari, P. M. (2003). Crystal Structure of the Catalytic Domain of the PknB Serine/Threonine Kinase From Mycobacterium Tuberculosis. *J. Biol. Chem.* 278 (15), 13094–13100. doi: 10.1074/jbc.M300660200
- Osaki, M., Arcondéguy, T., Bastide, A., Touriol, C., Prats, H., and Trombe, M. C. (2009). The StkP/PhpP Signaling Couple in Streptococcus Pneumoniae: Cellular Organization and Physiological Characterization. *J. Bacteriol.* 191 (15), 4943–4950. doi: 10.1128/jb.00196-09
- Pereira, S. F., Goss, L., and Dworkin, J. (2011). Eukaryote-Like Serine/Threonine Kinases and Phosphatases in Bacteria. *Microbiol. Mol. Biol. Rev.* 75 (1), 192–212. doi: 10.1128/mmb.00042-10
- Perpich, J. D., Yakoumatos, L., Johns, P., Stocke, K. S., Fitzsimonds, Z. R., Wilkey, D. W., et al. (2021). Identification and Characterization of a UbK Family Kinase in Porphyromonas Gingivalis That Phosphorylates the RprY Response Regulator. *Mol. Oral. Microbiol.* 36 (5), 258–266. doi: 10.1111/omi.12347
- Pradhan, G., Shrivastava, R., and Mukhopadhyay, S. (2018). Mycobacterial PknG Targets the Rab71 Signaling Pathway To Inhibit Phagosome-Lysosome Fusion. *J. Immunol.* 201 (5), 1421–1433. doi: 10.4049/jimmunol.1800530
- Pullen, K. E., Ng, H. L., Sung, P. Y., Good, M. C., Smith, S. M., and Alber, T. (2004). An Alternate Conformation and a Third Metal in PstP/Ppp, the M. Tuberculosis PP2C-Family Ser/Thr Protein Phosphatase. *Structure* 12 (11), 1947–1954. doi: 10.1016/j.str.2004.09.008
- Rangarajan, M., Aduse-Opoku, J., Paramonov, N. A., Hashim, A., and Curtis, M. A. (2017). Hemin Binding by Porphyromonas Gingivalis Strains Is Dependent on the Presence of A-LPS. *Mol. Oral. Microbiol.* 32 (5), 365–374. doi: 10.1111/omi.12178
- Sasková, L., Nováková, L., Basler, M., and Branny, P. (2007). Eukaryotic-Type Serine/Threonine Protein Kinase StkP Is a Global Regulator of Gene Expression in Streptococcus Pneumoniae. *J. Bacteriol.* 189 (11), 4168–4179. doi: 10.1128/jb.01616-06
- Schlicker, C., Fokina, O., Kloft, N., Grüne, T., Becker, S., Sheldrick, G. M., et al. (2008). Structural Analysis of the PP2C Phosphatase Tppha From Thermosynechococcus Elongatus: A Flexible Flap Subdomain Controls Access to the Catalytic Site. *J. Mol. Biol.* 376 (2), 570–581. doi: 10.1016/j.jmb.2007.11.097
- Schwechheimer, C., Hebert, K., Tripathi, S., Singh, P. K., Floyd, K. A., Brown, E. R., et al. (2020). A Tyrosine Phosphoregulatory System Controls Exopolysaccharide Biosynthesis and Biofilm Formation in Vibrio Cholerae. *PLoS Pathog.* 16 (8), e1008745. doi: 10.1371/journal.ppat.1008745
- Seifried, A., Schultz, J., and Gohla, A. (2013). Human HAD Phosphatases: Structure, Mechanism, and Roles in Health and Disease. *FEBS J.* 280 (2), 549–571. doi: 10.1111/j.1742-4658.2012.08633.x
- Shaban, L., Nguyen, G. T., Mecsas-Faxon, B. D., Swanson, K. D., Tan, S., and Mecsas, J. (2020). Yersinia Pseudotuberculosis YopH Targets SKAP2-Dependent and Independent Signaling Pathways to Block Neutrophil Antimicrobial Mechanisms During Infection. *PLoS Pathog.* 16 (5), e1008576. doi: 10.1371/journal.ppat.1008576
- Shah, I. M., Laaberki, M. H., Popham, D. L., and Dworkin, J. (2008). A Eukaryotic-Like Ser/Thr Kinase Signals Bacteria to Exit Dormancy in Response to Peptidoglycan Fragments. *Cell* 135 (3), 486–496. doi: 10.1016/j.cell.2008.08.039

- Shamma, F., Papavinasasundaram, K., Quintanilla, S. Y., Bandekar, A., Sassetti, C., and Boutte, C. C. (2021). Phosphorylation on PstP Regulates Cell Wall Metabolism and Antibiotic Tolerance in *Mycobacterium Smegmatis*. *J. Bacteriol.* 203 (4), e00563-20. doi: 10.1128/jb.00563-20
- Shen, D., Perpich, J. D., Stocke, K. S., Yakoumatos, L., Fitzsimonds, Z. R., Liu, C., et al. (2020). Role of the RprY Response Regulator in *P. Gingivalis* Community Development and Virulence. *Mol. Oral. Microbiol.* 35 (6), 231–239. doi: 10.1111/omi.12311
- Shi, Y. (2009). Serine/threonine Phosphatases: Mechanism Through Structure. *Cell* 139 (3), 468–484. doi: 10.1016/j.cell.2009.10.006
- Shimizu, F., Katagiri, T., Suzuki, M., Watanabe, T. K., Okuno, S., Kuga, Y., et al. (1997). Cloning and Chromosome Assignment to 1q32 of a Human cDNA (RAB7L1) Encoding a Small GTP-Binding Protein, a Member of the RAS Superfamily. *Cytogenet. Cell Genet.* 77 (3–4), 261–263. doi: 10.1159/000134591
- Shi, L., Potts, M., and Kennelly, P. J. (1998). The Serine, Threonine, and/or Tyrosine-Specific Protein Kinases and Protein Phosphatases of Prokaryotic Organisms: A Family Portrait. *FEMS Microbiol. Rev.* 22 (4), 229–253. doi: 10.1111/j.1574-6976.1998.tb00369.x
- Soulat, D., Vaganay, E., Duclos, B., Genestier, A. L., Etienne, J., and Cozzone, A. J. (2002). *Staphylococcus Aureus* Contains Two Low-Molecular-Mass Phosphotyrosine Protein Phosphatases. *J. Bacteriol.* 184 (18), 5194–5199. doi: 10.1128/jb.184.18.5194-5199.2002
- Standish, A. J., and Morona, R. (2014). The Role of Bacterial Protein Tyrosine Phosphatases in the Regulation of the Biosynthesis of Secreted Polysaccharides. *Antioxid. Redox Signal* 20 (14), 2274–2289. doi: 10.1089/ars.2013.5726
- Takeuchi, H., and Amano, A. (2021). Invasion of Gingival Epithelial Cells by *Porphyromonas Gingivalis*. *Methods Mol. Biol.* 2210, 215–224. doi: 10.1007/978-1-0716-0939-2\_21
- Takeuchi, H., Hirano, T., Whitmore, S. E., Morisaki, I., Amano, A., and Lamont, R. J. (2013). The Serine Phosphatase SerB of *Porphyromonas Gingivalis* Suppresses IL-8 Production by Dephosphorylation of NF- $\kappa$ B RelA/P65. *PLoS Pathog.* 9 (4), e1003326. doi: 10.1371/journal.ppat.1003326
- Tiganis, T. (2002). Protein Tyrosine Phosphatases: Dephosphorylating the Epidermal Growth Factor Receptor. *IUBMB Life* 53 (1), 3–14. doi: 10.1080/15216540210811
- Tribble, G. D., Mao, S., James, C. E., and Lamont, R. J. (2006). A *Porphyromonas Gingivalis* Haloacid Dehalogenase Family Phosphatase Interacts With Human Phosphoproteins and is Important for Invasion. *Proc. Natl. Acad. Sci. U. S. A.* 103 (29), 11027–11032. doi: 10.1073/pnas.0509813103
- Ulrych, A., Holečková, N., Goldová, J., Doubravová, L., Benada, O., Kofroňová, O., et al. (2016). Characterization of Pneumococcal Ser/Thr Protein Phosphatase phpP Mutant and Identification of a Novel PhpP Substrate, Putative RNA Binding Protein Jag. *BMC Microbiol.* 16 (1), 247. doi: 10.1186/s12866-016-0865-6
- van der Ploeg, J. R. (2005). Regulation of Bacteriocin Production in *Streptococcus Mutans* by the Quorum-Sensing System Required for Development of Genetic Competence. *J. Bacteriol.* 187 (12), 3980–3989. doi: 10.1128/jb.187.12.3980-3989.2005
- Wang, J. Y., and Koshland, D. E. Jr. (1978). Evidence for Protein Kinase Activities in the Prokaryote *Salmonella Typhimurium*. *J. Biol. Chem.* 253 (21), 7605–7608. doi: 10.1016/S0021-9258(17)34411-3
- Whitfield, C., Wear, S. S., and Sande, C. (2020). Assembly of Bacterial Capsular Polysaccharides and Exopolysaccharides. *Annu. Rev. Microbiol.* 74, 521–543. doi: 10.1146/annurev-micro-011420-075607
- Whitmore, S. E., and Lamont, R. J. (2012). Tyrosine Phosphorylation and Bacterial Virulence. *Int. J. Oral. Sci.* 4 (1), 1–6. doi: 10.1038/ijos.2012.6
- Woo, J. A., Liu, T., Fang, C. C., Cazzaro, S., Kee, T., LePochat, P., et al. (2019). Activated Cofilin Exacerbates Tau Pathology by Impairing Tau-Mediated Microtubule Dynamics. *Commun. Biol.* 2, 112. doi: 10.1038/s42003-019-0359-9
- Wright, D. P., and Ulijasz, A. T. (2014). Regulation of Transcription by Eukaryotic-Like Serine-Threonine Kinases and Phosphatases in Gram-Positive Bacterial Pathogens. *Virulence* 5 (8), 863–885. doi: 10.4161/21505594.2014.983404
- Wright, C. J., Xue, P., Hirano, T., Liu, C., Whitmore, S. E., Hackett, M., et al. (2014). Characterization of a Bacterial Tyrosine Kinase in *Porphyromonas Gingivalis* Involved in Polymicrobial Synergy. *Microbiologyopen* 3 (3), 383–394. doi: 10.1002/mbo3.177
- Xu, H., Xia, B., and Jin, C. (2006). Solution Structure of a Low-Molecular-Weight Protein Tyrosine Phosphatase From *Bacillus Subtilis*. *J. Bacteriol.* 188 (4), 1509–1517. doi: 10.1128/jb.188.4.1509-1517.2006
- Xu, W., Zhou, W., Wang, H., and Liang, S. (2020). Roles of *Porphyromonas Gingivalis* and its Virulence Factors in Periodontitis. *Adv. Protein Chem. Struct. Biol.* 120, 45–84. doi: 10.1016/bs.apcsb.2019.12.001
- Yagüe, P., Gonzalez-Quinonez, N., Fernández-García, G., Alonso-Fernández, S., and Manteca, A. (2019). Goals and Challenges in Bacterial Phosphoproteomics. *Int. J. Mol. Sci.* 20 (22), 5678. doi: 10.3390/ijms20225678
- Zhang, Z., Liu, D., Liu, S., Zhang, S., and Pan, Y. (2020). The Role of *Porphyromonas Gingivalis* Outer Membrane Vesicles in Periodontal Disease and Related Systemic Diseases. *Front. Cell Infect. Microbiol.* 10, 585917. doi: 10.3389/fcimb.2020.585917
- Zhang, W., and Shi, L. (2004). Evolution of the PPM-Family Protein Phosphatases in *Streptomyces*: Duplication of Catalytic Domain and Lateral Recruitment of Additional Sensory Domains. *Microbiology (Reading)* 150 (Pt 12), 4189–4197. doi: 10.1099/mic.0.27480-0
- Zhang, H., Shi, L., Li, L., Guo, S., Zhang, X., Yamasaki, S., et al. (2004). Identification and Characterization of Class 1 Integron Resistance Gene Cassettes Among *Salmonella* Strains Isolated From Healthy Humans in China. *Microbiol. Immunol.* 48 (9), 639–645. doi: 10.1111/j.1348-0421.2004.tb03473.x
- Zhuang, Z., Yang, G., Mai, Q., Guo, J., Liu, X., and Zhuang, L. (2020). Physiological Potential of Extracellular Polysaccharide in Promoting *Geobacter* Biofilm Formation and Extracellular Electron Transfer. *Sci. Total Environ.* 741:140365. doi: 10.1016/j.scitotenv.2020.140365
- Zhu, L., and Kreth, J. (2010). Role of *Streptococcus Mutans* Eukaryotic-Type Serine/Threonine Protein Kinase in Interspecies Interactions With *Streptococcus Sanguinis*. *Arch. Oral. Biol.* 55 (5), 385–390. doi: 10.1016/j.archoralbio.2010.03.012

**Conflict of Interest:** The authors declare that the research was conducted in the absence of any commercial or financial relationships that could be construed as a potential conflict of interest.

**Publisher's Note:** All claims expressed in this article are solely those of the authors and do not necessarily represent those of their affiliated organizations, or those of the publisher, the editors and the reviewers. Any product that may be evaluated in this article, or claim that may be made by its manufacturer, is not guaranteed or endorsed by the publisher.

Copyright © 2022 Ren, Shen, Liu and Ding. This is an open-access article distributed under the terms of the Creative Commons Attribution License (CC BY). The use, distribution or reproduction in other forums is permitted, provided the original author(s) and the copyright owner(s) are credited and that the original publication in this journal is cited, in accordance with accepted academic practice. No use, distribution or reproduction is permitted which does not comply with these terms.



# Raman Spectroscopy: A Potential Diagnostic Tool for Oral Diseases

Yuwei Zhang<sup>1</sup>, Liang Ren<sup>1</sup>, Qi Wang<sup>2</sup>, Zhining Wen<sup>3</sup>, Chengcheng Liu<sup>1\*</sup> and Yi Ding<sup>1\*</sup>

<sup>1</sup> State Key Laboratory of Oral Diseases, National Clinical Research Center for Oral Diseases, Department of Periodontics, West China Hospital of Stomatology, Sichuan University, Chengdu, China, <sup>2</sup> State Key Laboratory of Oral Diseases, National Clinical Research Center for Oral Diseases, Department of Prosthodontics, West China Hospital of Stomatology, Sichuan University, Chengdu, China, <sup>3</sup> College of Chemistry, Sichuan University, Chengdu, China

## OPEN ACCESS

### Edited by:

Jin Xiao,  
University of Rochester, United States

### Reviewed by:

Chiara Fabbri,  
University of Ferrara, Italy  
Fabrizia d'Apuzzo,  
University of Campania Luigi Vanvitelli,  
Italy

Nurcan Buduneli,  
Ege University, Turkey

### \*Correspondence:

Chengcheng Liu  
liuchengcheng519@163.com  
Yi Ding  
yiding2000@126.com

### Specialty section:

This article was submitted to  
Microbiome in Health and Disease,  
a section of the journal  
Frontiers in Cellular and  
Infection Microbiology

**Received:** 13 September 2021

**Accepted:** 17 January 2022

**Published:** 04 February 2022

### Citation:

Zhang Y, Ren L, Wang Q,  
Wen Z, Liu C and Ding Y (2022)  
Raman Spectroscopy: A Potential  
Diagnostic Tool for Oral Diseases.  
Front. Cell. Infect. Microbiol. 12:775236.  
doi: 10.3389/fcimb.2022.775236

Oral diseases impose a major health burden worldwide and have a profound effect on general health. Dental caries, periodontal diseases, and oral cancers are the most common oral health conditions. Their occurrence and development are related to oral microbes, and effective measures for their prevention and the promotion of oral health are urgently needed. Raman spectroscopy detects molecular vibration information by collecting inelastic scattering light, allowing a “fingerprint” of a sample to be acquired. It provides the advantages of rapid, sensitive, accurate, and minimally invasive detection as well as minimal interference from water in the “fingerprint region.” Owing to these characteristics, Raman spectroscopy has been used in medical detection in various fields to assist diagnosis and evaluate prognosis, such as detecting and differentiating between bacteria or between neoplastic and normal brain tissues. Many oral diseases are related to oral microbial dysbiosis, and their lesions differ from normal tissues in essential components. The colonization of keystone pathogens, such as *Porphyromonas gingivalis*, resulting in microbial dysbiosis in subgingival plaque, is the main cause of periodontitis. Moreover, the components in gingival crevicular fluid, such as infiltrating inflammatory cells and tissue degradation products, are markedly different between individuals with and without periodontitis. Regarding dental caries, the compositions of decayed teeth are transformed, accompanied by an increase in acid-producing bacteria. In oral cancers, the compositions and structures of lesions and normal tissues are different. Thus, the changes in bacteria and the components of saliva and tissue can be used in examinations as special markers for these oral diseases, and Raman spectroscopy has been acknowledged as a promising measure for detecting these markers. This review summarizes and discusses key research and remaining problems in this area. Based on this, suggestions for further study are proposed.

**Keywords:** Raman spectroscopy, oral microbiota, dental caries, periodontitis, oral cancer



# 1 INTRODUCTION

Oral disease is a major global public health issue, with more than 3.5 billion people suffering from chronic and progressive oral diseases worldwide. Dental caries, periodontal diseases, and oral cancers are the most prevalent and serious oral diseases. For patients, these cause a serious burden both health-wise and financially, significantly degrading the quality of life (Peres et al., 2019). In 2015, the prevalence of untreated deciduous and permanent teeth was 7.8% and 34.1%, respectively (Kassebaum et al., 2017). Severe periodontitis has been considered the sixth most common infectious disease worldwide, with 10.8% of people, i.e., 743 million, being affected in 2010 (Kassebaum et al., 2014), which increased to 1.1 billion by 2019 (Chen et al., 2021). In 2018, 177,384 people died from lip and oral cancer (Bray et al., 2018). Oral diseases also impose a great economic burden. In 2015, the direct cost of oral diseases worldwide was 356.8 billion US dollars, and the indirect cost was 187.61 billion US dollars (Righolt et al., 2018). The oral diseases mentioned above are often not detected until tissue destruction has occurred. For caries and periodontitis, the destruction of enamel, dentin, and alveolar bone is irreversible, and delayed discovery and treatment can even lead to tooth loss, affecting pronunciation, masticatory function, and aesthetics. For oral cancer, the accuracy of early diagnosis and incision directly affects the recurrence and survival rates. The current clinical detection methods remain insufficient. In terms of caries, the identification of carious dentin and healthy dentin can reduce the loss of healthy tissue during lesions removal, reduce the damage and the possibility of tooth fracture. As for periodontitis, it is known that hyperglycemia, smoking, stress, etc. are risk factors for periodontitis. Patients with risk factors or previous used concept, aggressive periodontitis, are at higher risk of periodontitis, and destruction of periodontal tissues are faster. However, the effect of these factors in the progress of periodontitis in each individual cannot be found through the existing periodontal clinical examination. Local biomarkers like the expression of local subgingival flora virulence factors and the level of some inflammatory factors in gingival crevicular fluid can warn us the risk of disease progression, while the laboratory examination is time-consuming and requires more

biological samples. Especially in large-scale epidemiological investigations, a new diagnostic tool can unify the detection standards and make the conclusions more scientific, therefore, it is more suitable for non-periodontal and non-endodontic specialist. For oral cancer, early malignant lesions are not easily diagnosed non-invasively and accurately. Delayed diagnosis makes the treatment more difficult and the prognosis is affected. Moreover, an intraoperative freezing section to determine whether the incision is clean requires a pathologist at a higher professional level. Therefore, methods for detecting lesions earlier and more sensitively could more easily avoid irreversible tissue destruction and improve the curative effect and prognosis, which are crucial to the prevention and treatment of oral diseases (Dillon et al., 2015). Raman spectra are inelastic scattering spectra based on the Raman effect, which are obtained using scattered light with a different frequency from the incident light (Raman CVK and S., 1928). Raman spectroscopy (RS) can provide fast, accurate, sensitive, and *in situ* detection analysis. It can sensitively and accurately reflect changes in material composition and structure. With the emergence of nanotechnology, advanced optical microscopes and miniaturized lasers have been developed, and problems such as weak signal, low signal-to-noise ratio, and strong autofluorescence background have also been mitigated to allow RS to be gradually applied in the biomedical field. RS has been used to detect bacteria and the compositions of cells, tissues, and biofluids, and in the past few decades it has received increasing interest for medical prognosis and diagnosis (Morris, 1999; Singh et al., 2016). It has emerged as a potential chairside microbiological diagnostic approach (Howell et al., 2011). There are obvious differences between composition and structure of dental caries and intact tooth tissues, and also between oral cancer lesions and healthy tissues. Therefore, the potential of RS in the diagnosis and prognosis of these two diseases is obvious. In the case of periodontitis, studies have shown that biomarkers in saliva can distinguish gingivitis from periodontitis (Gonchukov and Sukhinina, 2011; Hernández-Cedillo et al., 2019), and biomarkers in gingival crevicular fluid (GCF) including glycosaminoglycans and some inflammatory mediators, such as prostaglandin  $E_2$ , can detect high-risk groups of periodontal disease (Curtis et al., 1989). The changes in the composition of subgingival flora and the expression of key pathogenic bacteria virulence factors indicate the advancement or relief of periodontitis. When the target substance is specific molecule, the key information required is concentrated to several chemical bonds of the target molecule, which can be more easily extracted from RS. It can be seen that RS has the potential to assist diagnosis and improve prognosis.

Recently, many studies have suggested that RS could assist in the diagnosis and prognostic evaluation of oral diseases, such as dental caries (Almahdy et al., 2012; Yang et al., 2014; Seredin et al., 2015; Toledano et al., 2015b; Rodrigues et al., 2017), periodontal diseases, and oral cancers (Krishna et al., 2004; Panikkanvalappil et al., 2013; Krishna et al., 2014; Sahu et al., 2015; Barroso et al., 2016; Malik et al., 2017; Mian et al., 2017; Barroso et al., 2018; Xue et al., 2018). Because minor changes in quantity can be detected by RS, it has been used in detecting early caries, finding the boundaries of dentin caries, and estimating the effects of drugs on the remineralization of decalcified tooth tissues (Carvalho et al., 2013; Milly et al., 2014; Yang et al., 2014;

**Abbreviations:** SERS, surface-enhanced RS; AuNPs, Au nanoparticles; AgNPs, Ag nanoparticles; FWHM, full width at half maximum; BIMIN, biomimetic mineralization kit; QAS, quaternary ammonium salts; D<sub>2</sub>O, heavy water; WSL, white spot lesion; BAG, bioactive glass; PAA-BAG, BAG containing polyacrylic acid; PCA, principal component analysis; GCF, gingival crevicular fluid; SA, sialic acid; @IL-1 $\beta$ , interleukin-1 $\beta$ ; TNF- $\alpha$ , tumor necrosis factor- $\alpha$ ; DTNB, 5,5'-Dithiobis-(2-nitrobenzoic acid); 4-MBA, 4-mercaptobenzoic acid; OCP, octacalcium phosphate; HAP, hydroxyapatite; OSCC, oral squamous cell carcinoma; TNM classification, primary tumor, regional lymph nodes, and metastasis classification; WHO, World Health Organization; OSMF, oral submucous fibrosis; OLK, leukoplakia; OPL, oral precancerous lesion; HT, healthy tobacco users; HV, healthy volunteers; PCA-LDA, principal component analysis with linear discriminant analysis; PCA-LR, principal component analysis with logistic regression; FTIR, Fourier-transform infrared spectroscopy; SVM, support vector machine; LDA, linear discriminant analysis; QDA, quantitative discrimination analysis; PCA-QDA, principal component analysis with quantitative discrimination analysis; PCA-(h)LDA, principal component analysis with (hierarchical) linear discriminant analysis; MCR-ALS, multivariate curve resolution with alternating least squares; S100P, S100 calcium-binding protein P; LOOCV, leave-one-out cross-validation.

Adachi et al., 2015; Seredin et al., 2015; Toledano et al., 2015a; Toledano et al., 2015b; Kerr et al., 2016; Pezzotti et al., 2017; Rodrigues et al., 2017; Occhi-Alexandre et al., 2018). Interestingly, it has also been used to analyze multiple oral bacteria and differentiate saliva between patients with periodontal disease and healthy volunteers (HV) (Gonchukov et al., 2011; Kriem et al., 2020). Regarding oral cancers, many studies have focused on detecting and differentiating malignant, precancerous, benign, and normal tissues to assist diagnosis; finding an adequate surgical margin in an operation to improve the curative effect; and analyzing spectra to predict the recurrence risk (Krishna et al., 2004; Panikkanvalappil et al., 2013; Krishna et al., 2014; Sahu et al., 2015; Barroso et al., 2016; Malik et al., 2017; Mian et al., 2017; Barroso et al., 2018; Xue et al., 2018). In general, RS has the potential to assist in diagnosis and treatment as well as prognostic evaluation. The purpose of this review is to draw attention to the potential of RS in assisting clinical diagnosis and prognostic evaluation of caries, periodontitis, and oral cancer owing to its high potential for chairside detection. In this review, we focus on the application of RS to oral diseases and discuss problems that must be further explored.

## 2 RAMAN SPECTROSCOPY

### 2.1 Principle of Raman Spectroscopy

C.V. Raman and his team discovered the Raman effect in 1928 (Raman CVK and S., 1928). They proposed that when ordinary light passes through a pure medium (water or gas), a small amount of scattered light, with frequency dissimilar to that of the incident beam, is produced. This phenomenon is called Raman scattering. This occurs because when a small number of photons collide with the chemical bonds in the sample, their energy is absorbed or lost, and the frequency of the scattered light changes accordingly. Although the frequency of Raman scattering light changes rather than being dependent on the incident light frequency, the shift is related to the molecular bonds. The bands in the Raman spectra are the specific manifestations of different molecular bonds in the sample, appearing as a unique spectral “fingerprint” of every substance (Krafft and Popp, 2015).

Although RS is widely applied in biomedical fields, it still has some shortcomings, including weak signal, low signal-to-noise ratio, and strong self-fluorescent background. With the advent of nanotechnology, advanced optical microscopes, fiber optics, and miniaturized lasers, these have been combined with RS to obtain stronger Raman signals. Surface-enhanced RS (SERS), confocal RS, optical-fiber RS, Fourier-transform RS, and laser-resonance RS improve the signal-to-noise ratio by enhancing either the signal intensity or signal collection (Kong et al., 2015).

### 2.2 Related Raman Spectroscopy Detection Techniques

Combining RS with other technologies extends its application under different conditions. For instance, SERS increases the Raman signal by approximately  $10^5$ – $10^{14}$  times because of the

molecules attached to the surface of the nanostructured metal, thereby extending the capacity to detect trace substances to single molecules (Wang et al., 2014; Aditi et al., 2015). When the effector molecule is adsorbed or located in the vicinity of the metal nanostructure, Raman scattering is enhanced due to the resonant interaction of light with the surface plasmons excited by the surface of the sample atom (electromagnetic enhancement). Chemical enhancement can be observed *via* the interaction between the molecules and electrons from the surface. Further advantages of SERS include accurate spectral width, detection of multiple labels under a single-wavelength laser, and no photobleaching (Fleischmann et al., 1974; Jeanmaire and Duynes, 1977). SERS activity of  $\text{Ag}^+$  staining was found to be slightly higher than that of Au nanoparticles (AuNPs) but significantly lower than that of Ag nanoparticles (AgNPs) (Athukorale et al., 2019). Therefore, SERS is a good option for researchers to obtain bands with higher intensities. Micro-RS is a combination of RS and microscopic analysis and is considered a powerful technique. RS and optical microscopy can be effectively combined using an excitation laser with wavelengths in the visible and near-infrared regions (Delhaye and Dhamelincourt, 2010). With features of being microscopic, *in situ*, multi-phase, stable, and having high spatial resolution, it can perform point by point scanning and obtain high-resolution three-dimensional images. However, changes in the Raman spectrum baseline may mask small differences in the Raman band, which are crucial for identification in a diagnostic model. Moreover, optical-fiber RS, the combination of RS and fiber-optic probes, provides an alternative to medical diagnosis of hollow organs. Fiber-optic probes used *in vivo* must address the signal-to-noise ratio as well as the redundant Raman signal generated by the laser-transmitting fiber itself. To avoid strong background signals in the fused silica fiber in the fingerprint area ( $600$ – $1800\text{ cm}^{-1}$ ), some fiber probes have been introduced to high wavenumber regions ( $2400$ – $3800\text{ cm}^{-1}$ ) (Pavel and Nicholas, 1900). In addition, RS, which was first applied in 1986, has evolved rapidly and can be used to collect signals several times to increase the signal-to-noise ratio. In addition, irradiation of a sample with a  $1064\text{ nm}$  near-infrared laser provided by the Perkin-Elmer company greatly diminishes the fluorescent background and presents great potential for non-destructive structural analysis of chemical, biological, and biomedical samples (Nixon and Smith, 1986).

## 3 APPLICATION OF RAMAN SPECTROSCOPY FOR ORAL DISEASES

### 3.1 Dental Caries

Dental caries are characterized by demineralization of the inorganic portion and destruction of the organic substances of the teeth, including enamel, dentin, and cementum, leading to impairment of the teeth (Klokkevold, 2015). Cariogenic bacteria is a prerequisite for the occurrence of caries, which is closely related to the formation of dental biofilms on the surfaces of teeth. The organic acids produced by cariogenic bacteria result in

enamel demineralization with loss of calcium and phosphates. The first indication of dental caries is white spots on the enamel caused by demineralization (Klokkevold, 2015).

Regarding the inorganic components in tooth tissue, the iconic bands are four internal vibration modes of  $\text{PO}_4^{3-}$  at  $\nu_1 \sim 960 \text{ cm}^{-1}$ ,  $\nu_2 \sim 430 \text{ cm}^{-1}$ ,  $\nu_3 \sim 1043 \text{ cm}^{-1}$ , and  $\nu_4 \sim 590 \text{ cm}^{-1}$ , and of  $\text{CO}_3^{2-}$  at  $\sim 1070 \text{ cm}^{-1}$ . The intensities of  $\text{PO}_4^{3-}$  indicate mineralization degree, and numerous studies have adopted  $960 \text{ cm}^{-1}$  to check the demineralization. For instance, Al-Obaidi et al. constructed a Raman map based on  $960 \text{ cm}^{-1}$  intensity tooth Raman spectra for measuring the depth of the lesion based on the intensity change at  $960 \text{ cm}^{-1}$  (Al-Obaidi et al., 2019). Zhang et al. calculated the  $960 \text{ cm}^{-1}$  intensity of a carious tooth sample. Assuming that the mineral content at a normal site is 100%, they acquired the mineral content of lesions by measuring the ratio between the intensity of the lesion area and that of the normal area ( $I_{\text{lesion}}/I_{\text{normal}}$ ) (Zhang et al., 2019).  $\text{CO}_3^{2-}$  substituted  $\text{PO}_4^{3-}$  in hydroxyapatite (HAP) is a more soluble phase presented in initially decayed enamel (Seredin et al., 2015).

Besides mineral content, crystallinity is another parameter indicating tooth damage. The full width at half maximum (FWHM) at  $\sim 960 \text{ cm}^{-1}$  and  $\sim 1070 \text{ cm}^{-1}$  is often used to estimate crystallinity. The narrower the peak width, the higher the mineral crystallinity. Suzuki et al. discovered that during the process of demineralization, the scattering peaks  $\nu_1$  ( $960 \text{ cm}^{-1}$ ),  $\nu_2$  ( $430 \text{ cm}^{-1}$ ),  $\nu_3$  ( $1044 \text{ cm}^{-1}$ ), and  $\nu_4$  ( $591 \text{ cm}^{-1}$ ) corresponding to  $\text{PO}_4^{3-}$  are not shifted, while the peak width increases, indicating that the crystallinity of the enamel is impaired (Suzuki et al., 2019). Guentsch et al. calculated the FWHM of  $960 \text{ cm}^{-1}$  in an experimental biomimetic mineralization kit (BIMIN) group ( $12.2 \text{ cm}^{-1}$ ), enamel group ( $12.5 \text{ cm}^{-1}$ ), and dentin group ( $16.6 \text{ cm}^{-1}$ ), and found increased crystallinity of caries-free teeth in the BIMIN group (Guentsch et al., 2019).

For dentin, the proportion of organic components is much higher than that in enamel, and the symbolic bands of the structural alteration of collagen are involved in estimating dentin caries. Intensities of  $\sim 1655$  or  $\sim 1667 \text{ cm}^{-1}$ ,  $\sim 1246$  or  $\sim 1270 \text{ cm}^{-1}$ , and  $\sim 1450 \text{ cm}^{-1}$  are assigned to amide I, amide III, and  $\text{CH}_2$ , respectively, reflecting the structural information of collagen. In addition, the intensity ratio of amide I and phosphate  $\nu_1$  ( $I_{1650 \text{ cm}^{-1}}/I_{960 \text{ cm}^{-1}}$ ) was found to be related to the Knoop microhardness of tooth tissue, indicating that RS can be used to obtain the hardness of dentin caries as an alternative to invasive hardness testing (Alturki et al., 2020).

Previous studies have demonstrated that RS can be used for (1) detecting caries-related bacteria and early caries, (2) assessing the remineralization effect of drugs, (3) defining the margin of defective dentin, (4) exploring the effects of radiation therapy on tooth components, (5) evaluating new bonding systems, and (6) exploring the effects of quaternary ammonium salts (QAS) on cariogenic biofilms (Carvalho et al., 2013; Milly et al., 2014; Yang et al., 2014; Adachi et al., 2015; Seredin et al., 2015; Toledano et al., 2015a; Toledano et al., 2015b; Kerr et al., 2016; Pezzotti et al., 2017; Rodrigues et al., 2017; Occhi-Alexandre et al., 2018; Al-Obaidi et al., 2019; Daood et al., 2019; Guentsch et al., 2019; Hass et al., 2019; Lu et al., 2019; Miranda et al., 2019; Par et al.,

2019; Suzuki et al., 2019; Toledano et al., 2019; Zhang et al., 2019; Alturki et al., 2020; Daood et al., 2020b; Gieroba et al., 2020) (Table 1).

### 3.1.1 Application of Raman Spectroscopy for Detecting Caries-Related Bacteria and Early Caries

In dental plaque, the cariogenic bacteria are wrapped in an organic matrix of polysaccharides, proteins, and DNA, which enhances resistance to host defense and antimicrobial agents (Selwitz et al., 2007). Endogenous cariogenic bacteria (mainly *Streptococcus mutans*, *Streptococcus sobrinus*, and *Lactobacillus* spp) ferment carbohydrates and produce organic acids, resulting in local pHs below the critical value and demineralization of teeth (Featherstone, 2004; Selwitz et al., 2007).

RS can detect metabolic differences to facilitate the differentiation between biofilms. Gieroba et al. collected and analyzed Raman spectra from single biofilms of *S. mutans* CAPM 6067, *Streptococcus sanguis* ATCC 10556, and several serotypes of *S. sobrinus*. The major differences were concentrated in the region representing lipids, amides, and carbohydrates, reflecting the corresponding biological characteristics. For example, the highest and lowest amide bands in several biofilms were different, indicating different protein compositions of the biofilms and adhesive and cariogenic characteristics (Gieroba et al., 2020). Daood et al. used the changes in Raman spectra to assist in evaluating the effect of quaternary ammonium on cariogenic biofilms. With exposure to QAS, the intensity of  $484 \text{ cm}^{-1}$  in the Raman spectra, representing polysaccharides or carbohydrates, was significantly reduced, and the change was in concentration-dependent and time-dependent patterns (Daood et al., 2020a). Tao et al. focused on heavy water ( $\text{D}_2\text{O}$ ) based on single-cell Raman microspectroscopy ( $\text{D}_2\text{O}$ -Raman) and analyzed the Raman spectral region from  $2040$  to  $2300 \text{ cm}^{-1}$ , representing the C–D vibration band, to evaluate the metabolic status of the *S. mutans* UA159, *Streptococcus gordonii* ATCC10558, *S. sanguinis* ATCC10556, and *Lactobacillus fermentum* ATCC9338 oral bacteria after drug exposure. They distinguished antibiotic-sensitive and -resistant *S. mutans* (Tao et al., 2017).

The DIAGNOdent pen (Germany) is a laser pen that can detect caries *in vivo* by collecting fluorescence. To evaluate the laser pen detection capability, RS has been applied to test changes in carious teeth, and Rodrigues et al. established an enamel demineralization model *in vitro* with cattle tooth blocks and chose phosphate apatite peaks at  $\sim 960 \text{ cm}^{-1}$  to estimate demineralization (Rodrigues et al., 2017). Carvalho et al. focused on the changes in fluoridated apatite, phosphate apatite, and organic matrix in carious teeth, which present in Raman spectra as  $\sim 575 \text{ cm}^{-1}$ ,  $\sim 960 \text{ cm}^{-1}$ , and  $\sim 1450 \text{ cm}^{-1}$ , respectively. As demineralization progressed, the intensities of  $\sim 575 \text{ cm}^{-1}$  and  $\sim 960 \text{ cm}^{-1}$  declined significantly and were negatively correlated with the fluorescence detected by the DIAGNOdent pen. This proved that fluoridated apatite and phosphate apatite decreased in caries and verified the caries detection accuracy of the DIAGNOdent pen (Carvalho et al., 2013). Point-scan and wide-field Raman imaging have also been



**TABLE 1 |** Summary of RS studies on dental caries.

Sample type	Target	Year	Authors	Raman shift	Meaning of the corresponding Raman shift
<b>Detecting early caries, verifying demineralization models, and testing accuracy of other tools</b>					
Dentin	Verifying intact and decayed dentin	2018	(Occhi-Alexandre et al., 2018)	1665 cm <sup>-1</sup> ; 1453 cm <sup>-1</sup> ; 1270 cm <sup>-1</sup> ; 961 cm <sup>-1</sup>	Amide I; CH group; Amide III; Phosphate apatite
Enamel	Verifying demineralized enamel	2017	(Rodrigues et al., 2017)	~960 cm <sup>-1</sup>	Phosphate apatite
Teeth	Detecting caries	2014	(Yang et al., 2014)	–	–
Teeth	Verifying decayed teeth	2013	(Carvalho et al., 2013)	~575 cm <sup>-1</sup> ; ~960 cm <sup>-1</sup> ; ~1450 cm <sup>-1</sup>	Fluoridated apatite; Phosphate apatite; Organic matrix
<b>Evaluating the remineralization of dental caries <i>in vitro</i></b>					
Dentin	Remineralization effect of zinc-containing amalgam restoration	2019	(Toledano et al., 2019)	–	Organic and inorganic components
Enamel	Remineralization of carious enamel	2016	(Kerr et al., 2016)	960 cm <sup>-1</sup>	Phosphate apatite
Dentin	Remineralization effect of self-etching zinc-doped adhesives	2015	(Toledano et al., 2015a)	–	Organic and inorganic components
Dentin	Remineralization effect of zinc-containing amalgam loads	2015	(Toledano et al., 2015b)	–	Organic and inorganic components
Enamel	Remineralization effect of PAA-BAG and BAG on WSL	2014	(Milly et al., 2014)	433 cm <sup>-1</sup> ; 579 cm <sup>-1</sup> ; 959 cm <sup>-1</sup> ; 1043 cm <sup>-1</sup>	Phosphate apatite
<b>Distinguishing intact, infected, and affected dentin to define the margin of defective dentin precisely</b>					
Dentin	Combining fluorescence spectra with Raman spectra	2012	(Almahdy et al., 2012)	960 cm <sup>-1</sup> ; 1340 cm <sup>-1</sup>	Phosphate; Protein $\alpha$ -helices
Exploring the effects of radiation therapy on tooth components					
Dentin	Inorganic components	2019	(Campi et al., 2019)	590 cm <sup>-1</sup> ; 1070 cm <sup>-1</sup> ; 1267 cm <sup>-1</sup>	Fluoridated apatite; Phosphate apatite; Amide III
Teeth	Mineral composition; Collagen changes	2019	(Miranda et al., 2019)	1070 cm <sup>-1</sup> /960 cm <sup>-1</sup> ; 1655 or 1667 cm <sup>-1</sup> /1246 or 1270 cm <sup>-1</sup> ; 1655 or 1667 cm <sup>-1</sup> /1450 cm <sup>-1</sup> ; 2931/960 cm <sup>-1</sup>	Carbonate/Mineral; Amide I/Amide III; Amide I/CH <sub>2</sub>
Teeth	Ratio of organic to inorganic components	2019	(Lu et al., 2019)	2931/960 cm <sup>-1</sup>	Protein/Mineral
<b>Evaluating new bonding systems</b>					
Adhesive	Ratio of uncured to cured unit	2019	(Par et al., 2019)	1639 or 1640 cm <sup>-1</sup> ;	Aliphatic C=C stretching; Aromatic
		2019	(Hass et al., 2019)	1609 or 1610 cm <sup>-1</sup>	C=C stretching
<b>Exploring the effect of quaternary ammonium salts (QAS) on cariogenic biofilms</b>					
Biofilm	Effect of QAS on cariogenic biofilm changes	2020	(Daood et al., 2020b)	484 cm <sup>-1</sup> ; 960 cm <sup>-1</sup> ; 430 cm <sup>-1</sup> ; 1070 cm <sup>-1</sup>	Polysaccharide; Phosphate; Carbonate
		2019	(Daood et al., 2019)		
Biofilm	Metabolism of different biofilms	2020	(Gieroba et al., 2020)	–	–
Single cell of bacteria	Metabolic changes of single cell of bacteria after exposure to drugs	2020	(Tao et al., 2017)	2040–2300 cm <sup>-1</sup>	C–D vibration

WSL, white spot lesion; QAS, quaternary ammonium salts.

investigated for caries detection as well as application in laser pens (Yang et al., 2014). RS combined with two-dimensional (2D) charge-coupled-device cameras can be assembled into wide-field Raman imaging, which is faster for diagnosing dental caries. Additionally, to compare the penetration depth of a photosensitizer (erythrosine) on intact dentin and decayed dentin *in vitro*, RS was applied to verify the intact and decayed dentin by providing organic and inorganic information (Occhi-Alexandre et al., 2018). However, the results were mainly obtained from tooth slices *in vitro*, and to determine whether saliva and bacteria interfere with the process *in vivo* requires further investigation. In addition, Almahdy et al. collected Raman and fluorescence spectra of carious tooth tissues (Almahdy et al., 2012). Combined with three fluorescence signals (porphyrin fluorescence, putative infected dentin signal, and affected dentin signal), two Raman signals, phosphate at 960

cm<sup>-1</sup> and protein at 1340 cm<sup>-1</sup>, enabled differentiation between intact, infected, and affected dentin, indicating that vital transformations of phosphate and protein  $\alpha$ -helices are presented. More information could be obtained by investigating organic-related bands more intensively.

### 3.1.2 Raman Spectroscopy to Evaluate the Remineralization of Dental Caries *In Vitro*

Enamel is the most superficial tissue of teeth and is covered by dental plaque, which consists mainly of bacteria. When sugar and other fermentable carbohydrates reach the bacteria and produce acids, teeth demineralization begins. Conversely, when sugar consumption ceases, saliva washes away the sugars and buffers the acids. Calcium and phosphates then enter the teeth again, resulting in remineralization. Thus, a cavity occurs if demineralization overtakes remineralization over time



(Klokkevold, 2015). Kerr et al. evaluated the remineralization status of carious enamel treated with high-frequency microwave energy to sterilize and adjust pH by estimating the  $960\text{ cm}^{-1}$  intensity change (Kerr et al., 2016). For promoting enamel white spot lesion (WSL) remineralization, Raman spectra were also employed to assess the potential of bioactive glass (BAG) powder and BAG containing polyacrylic acid (PAA-BAG) (Milly et al., 2014). Four internal vibration modes of  $\text{PO}_4^{3-}$  at  $433\text{ cm}^{-1}$ ,  $579\text{ cm}^{-1}$ ,  $959\text{ cm}^{-1}$ , and  $1043\text{ cm}^{-1}$  were adopted to estimate enamel demineralization and remineralization. The intensity at  $959\text{ cm}^{-1}$  was the strongest among the four peaks.

Regarding remineralization in dentin, it is worth mentioning that Toledano et al. adopted many iconic bands to evaluate dentin changes from relative mineral concentration, crystallinity, and organic composition of dentin. Thus, the positive effects of zinc-containing amalgam mechanical loads, self-etching zinc-doped adhesives, and zinc-containing amalgam restoration on dentin remineralization before and after 24 h and after 3 weeks were clarified (Toledano et al., 2015a; Toledano et al., 2015b; Toledano et al., 2019).

### 3.2 Periodontal Diseases

Periodontitis is a chronic inflammatory disease of tooth-supporting tissues caused by pathogenic bacterial species located in the subgingival niche. Periodontal pathogens often cause the destruction of periodontal tissues, mainly by expressing toxic factors and triggering an inflammatory host response.

According to the “Keystone-Pathogen Hypothesis” (2012) (Hajishengallis et al., 2012) and polymicrobial synergy and dysbiosis model (2012) (Hajishengallis and Lamont, 2012), *Porphyromonas gingivalis* is a key periodontal pathogen, the toxic factors of which, including fimbriae, capsule, and gingipain, can destroy periodontal tissues directly and trigger an inflammatory response. In addition, it can trigger the dysbiosis of subgingival flora and finally transform into a pathogenic biofilm with higher virulence-related gene expression and stronger destructive inflammation (Curtis et al., 2020). Previous studies have reported that RS can be used for (1) detecting subgingival bacteria, (2) analyzing changes in saliva, and (3) depicting bone transformation (Table 2).

#### 3.2.1 Raman Spectroscopy to Assist in Detecting Subgingival Bacteria and Analyzing Changes of Saliva

Pioneering research began in 1999 when RS was used to detect the metabolites of periodontal bacteria. Evidence was found that an increase in spectral intensity at  $1002\text{ cm}^{-1}$  with time implies that the heme pigment is gradually accumulated on the cell surface when *P. gingivalis* is incubated on a blood plate. Moreover, *P. gingivalis* can synthesize the iron trivalent oxidation state Fe(III)PPIX with a band at  $1373\text{ cm}^{-1}$  on a horse blood plate while synthesizing the iron divalent oxidation state Fe(II)PPIX with a band at  $1359\text{ cm}^{-1}$  without horse blood. In 2003, researchers applied Mohs, Raman, and

**TABLE 2 |** Summary of RS studies on periodontal disease.

Sample type	Target	Year	Authors	Raman shift	Meaning of the corresponding Raman shift
<b>Assisting diagnosis and detection of inflammatory factors and composition changes</b>					
Periodontal ligament	Protein secondary structure	2020	(Perillo et al., 2020)	$1307\text{ cm}^{-1}$ ; $1230\text{--}1250\text{ cm}^{-1}$ ; $1240\text{--}1270\text{ cm}^{-1}$ ; $1620\text{ cm}^{-1}$ ; $1668\text{ cm}^{-1}$ ; $1680\text{ cm}^{-1}$ ; $2930\text{ cm}^{-1}$ ; $2875\text{ cm}^{-1}$ ; $2970\text{ cm}^{-1}$	$\alpha$ -helix; $\beta$ -sheet; random coil; $\beta$ -sheet or collagen $3_{10}$ -helix, $\beta$ -turn and $\beta$ -sheet secondary structure; $\text{CH}_3$ and $\text{CH}_2$
Saliva	IL-1 $\beta$ ; TNF- $\alpha$	2020	(Yang et al., 2020)	$1335\text{ cm}^{-1}$ ; $1590\text{ cm}^{-1}$	DTNB; 4-MBA
Saliva	Sialic acid	2019	(Hernández-Cedillo et al., 2019)	$1002\text{ cm}^{-1}$ , $1237\text{ cm}^{-1}$ , and $1391\text{ cm}^{-1}$ ; OR $910\text{ cm}^{-1}$ , $1171\text{ cm}^{-1}$ , and $1360\text{ cm}^{-1}$	Sialic acid
GCF	Mineral–matrix ratio; Carbonate apatite–hydroxyapatite ratio;	2014	(Jung et al., 2014)	$984\text{ cm}^{-1}$ / $1667\text{ cm}^{-1}$ ; $1088\text{ cm}^{-1}$ / $984\text{ cm}^{-1}$ ;	Phosphate/Amide I; Carbonate/Phosphate;
Saliva	Carotenoids	2011	(Gonchukov et al., 2011)	$1155\text{ cm}^{-1}$ ; $1525\text{ cm}^{-1}$	C–C; C=C
<b>Detecting metabolites of periodontal bacteria</b>					
<i>P. gingivalis</i> ATCC 33277	–	2016	(Pezzotti et al., 2016)	–	–
<i>Pr. nigrescens</i> ATCC 25261; <i>Pr. intermedia</i> ATCC 25611; <i>P. gingivalis</i> W50; Fe(III)PPIX.OH; [Fe(III)PPIX] <sub>2</sub> O	Heme pigment	2003	(Smalley et al., 2003)	$338\text{ cm}^{-1}$ ; $370\text{ cm}^{-1}$ ; $1549\text{ cm}^{-1}$ ; $1570\text{ cm}^{-1}$ ; $1580\text{ cm}^{-1}$ ; $1618\text{ cm}^{-1}$ ; $1621\text{ cm}^{-1}$	–
<b>Distinguish subgingival bacteria</b>					
<i>P. gingivalis</i> ; <i>A. actinomycetemcomitans</i> ; <i>Streptococcus</i> spp.	–	2021	(Witkowska et al., 2021)	–	–
<i>F. nucleatum</i> ; <i>S. mutans</i> ; <i>V. dispar</i> ; <i>A. naeslundii</i> ; <i>Pr. nigrescens</i>	–	2020	(Kriem et al., 2020)	–	–

UV-vis spectrophotometry to characterize the heme pigment of *Prevotella nigrescens* ATCC 25261 and *Prevotella intermedia* ATCC 25611 (Smalley et al., 2003). They also explored the changes in heme pigment under different pH conditions. In 2016, *in situ* Raman microprobe spectroscopy was used to track the metabolic changes of *P. gingivalis* on the polished surfaces of bioceramics of the antibacterial substance silicon nitride ( $\text{Si}_3\text{N}_4$ ), revealing the formation of peroxynitrite in *P. gingivalis* (Pezzotti et al., 2016).

In addition, Raman spectra can be used to distinguish different subgingival bacteria using data analysis. In 2020, Kriem et al. distinguished *Fusobacterium nucleatum*, *S. mutans*, *Veillonella dispar*, *Actinomyces naeslundii*, and *Prevotella nigrescens* with 100% accuracy in planktonic state. The accuracy of distinguishing *S. mutans*, *V. dispar*, and *A. naeslundii* single-species biofilms was 76%, and that for the others was 90% or higher (Kriem et al., 2020). Based on advanced technologies, in 2021, Witkowska et al. designed a standard Raman spectral detection process to differentiate different serotypes of *P. gingivalis*, *Aggregatibacter actinomycetemcomitans*, and *Streptococcus* spp.

The detection process applied microfluidics,  $\text{Fe}_2\text{O}_3/\text{AgNPs}$  combined with Ag/Si substrates, and successfully distinguished *P. gingivalis* from *A. actinomycetemcomitans* and *Streptococcus* spp. by principal component analysis (PCA) with an accuracy of 82–91%. They also confirmed the effectiveness of this detection system in a saliva environment (Witkowska et al., 2021). The detection process provides a feasible method for detecting periodontal pathogens in a clinical environment.

Regarding diagnosis, saliva and GCF have always been prominent as bodily fluids that can be obtained noninvasively and contain effective information as well as interfering noise. One important research approach for analyzing Raman spectra containing a large amount of information is to focus on peaks representing target substances, such as carotene, carotenoids, and sialic acid (SA).

In 2011, Gonchukov et al. collected saliva from 10 patients with periodontitis and 10 healthy subjects (Gonchukov et al., 2011). There were unique peaks in the periodontitis group at 1155 and 1525  $\text{cm}^{-1}$ , representing C–C and C=C, respectively (Darvin et al., 2010), which indicates the existence of carotenoids (Darvin et al., 2009) and proves that as the severity of the periodontal disease increases, the total antioxidant level in saliva also rises (Kim et al., 2010). In 2014, Camerlingo et al. compared the Raman spectra of GCF collected from healthy and periodontitis patients and found that the band at 1537  $\text{cm}^{-1}$ , which represents the isomerization product of the C=C group related to the degraded carotene, only appeared in the latter group (Camerlingo et al., 2014). The aforementioned studies confirm that carotenoid concentration may be beneficial in the diagnosis of periodontitis. Furthermore, SA is present in several proteins related to periodontitis (Ide et al., 2003). Hernandez-Cedillo et al. reported the potential of SA in the auxiliary diagnosis of periodontal diseases. In 2019, they collected saliva samples from patients with periodontitis or gingivitis as well as healthy controls. The peaks at 1002  $\text{cm}^{-1}$ , 1237  $\text{cm}^{-1}$ , and 1391

$\text{cm}^{-1}$  or 910  $\text{cm}^{-1}$ , 1171  $\text{cm}^{-1}$ , and 1360  $\text{cm}^{-1}$  were compared with the standard SA peaks, indicating that the concentrations of SA in each group were significantly different (Hernández-Cedillo et al., 2019). Interleukin-1 $\beta$  (IL-1 $\beta$ ) and tumor necrosis factor- $\alpha$  (TNF- $\alpha$ ) are important cytokines in periodontitis, and their concentrations in GCF are higher with periodontitis (Klokkevold, 2015). Yang et al. labeled IL-1 $\beta$  and TNF- $\alpha$  with 5,5'-Dithiobis-(2-nitrobenzoic acid) (DTNB) and 4-mercaptobenzoic acid (4-MBA), respectively, and then collected the salivary surface-enhanced Raman spectra of patients with different periodontal conditions (Yang et al., 2020). The relative area values of the IL-1 $\beta$  and TNF- $\alpha$  peaks at 1335  $\text{cm}^{-1}$  and 1590  $\text{cm}^{-1}$ , respectively, were calculated as the Raman intensity corresponding to the concentration of inflammatory factors, and significant differences were found between the three groups. The spectral characteristics of saliva reflect metabolic changes in periodontal tissues, and are of vital importance in the diagnosis of periodontitis. However, the composition of saliva is affected by many factors, such as diet and physical condition. Thus, a multi-center and large-sample study is necessary to acquire reliable spectral characteristics of different periodontal conditions.

Regarding Raman spectra of GCF, Jung et al. studied the changes in GCF composition during orthodontic tooth movement with RS. RS showed the degree of bone mineralization and accumulation of carbonate in the apatite lattice. During the alveolar bone remodeling, the mineral-matrix ratio decreased and the carbonate apatite-hydroxyapatite ratio increased. It is speculated that this results from insufficient mineralization during alveolar bone remodeling (Jung et al., 2014). Perillo et al. observed the changes in vibrational modes of proteins (amide I and amide III bands) and  $\text{CH}_2$  and  $\text{CH}_3$  modes in the periodontal ligament 2, 7, and 14 days after adding orthodontic force to obtain the molecular arrangements and conformational changes. The Raman spectra of the  $\alpha$ -helix,  $3_{10}$ -helix,  $\beta$ -turn,  $\beta$ -sheet and random coil in the amide I and amide III bands representing the secondary structure of the protein changed markedly with orthodontic tooth movement. The  $\alpha$ -helical and the intensity of the entire amide I band were reduced compared with the control periodontal ligament sample. Compared to the  $\alpha$ -helical mode, the remaining component mode of amide I became wider and stronger. The information from the Raman spectra provided quantitative insight into when and how the periodontal ligament molecular arrangement changed (Perillo et al., 2020).

### 3.2.2 Raman Spectroscopy to Depict Bone Transformation

In addition to saliva, GCF, and gingival tissue, periodontal hard tissue has also been considered for possible applications of RS. In 2019, Gatin et al. reported the application of RS to evaluate the bone differences between a periodontitis patient and a healthy patient before and after maxillary sinus lift surgery. Octacalcium phosphate (OCP) and amorphous HAP presented obvious peaks at 955–960  $\text{cm}^{-1}$ , representing immature bone. Moreover, HAP crystals and biological HAP-based bone substitutes showed

bands at  $960\text{--}965\text{ cm}^{-1}$ , representing mature bone. Based on this analysis, bone samples before surgery and 8 months after healing revealed that the two patients' samples had peaks at  $955\text{--}960\text{ cm}^{-1}$  before surgery, and only peaks at  $960\text{--}965\text{ cm}^{-1}$  presented after surgery. The broad fluorescence peaks appearing at  $800\text{--}900\text{ cm}^{-1}$  represented collagen, and the changes in specific peaks could be used to quantify the healing process (Gatin et al., 2019). Raman spectra clearly depict the transformation from immature to mature bone.

### 3.3 Oral Cancer

Oral cancers are cancerous growths in the mouth, and they are life-threatening if not diagnosed and treated early. The most common type of oral cancer is oral squamous cell carcinoma (OSCC) (Klokkevold, 2015), and biopsy is the gold standard for OSCC diagnosis. Doctors can estimate the severity of the condition according to the International Union Against Cancer's primary tumor, regional lymph nodes, and metastasis (TNM) classification and the World Health Organization (WHO) histologic grading system. To date, RS has mainly been explored for the diagnosis and classification of oral cancer. A few studies have also collected data and studied the application of RS in the treatment and prognosis of oral cancer. **Table 3** summarizes the literature on RS for oral cancer.

#### 3.3.1 Diagnosis and Classification of Oral Cancer

In 2004, Krishna et al. first studied the potential of RS for detecting oral cancer (Krishna et al., 2004). They collected Raman spectra from healthy and malignant epithelial cells and differentiated them using PCA. Subsequently, many studies have validated this conclusion. In summary, Raman spectra have been studied to (1) clarify the tumor stage and histological classification of OSCCs, (2) distinguish OSCCs from precancerous lesions and other cancers, and (3) improve the accuracy of diagnostic models.

Clarifying the tumor stage and histological classification is critical for evaluating patients' conditions and choosing the best treatment plan. Xue et al. established a diagnostic model based on the spectra of serum samples from 135 patients with OSCCs using PCA with linear discriminant analysis (PCA-LDA). The total accuracies of the diagnostic model in identifying tumors at different stages, distinguishing lymph node involvement, and distinguishing between different histological grades were 90.4%, 85.9%, and 90.4%, respectively (Xue et al., 2018). A novel SERS catheter ( $5\text{--}6\text{ }\mu\text{m}$ ) helped to successfully obtain and differentiate healthy cells, moderate OSCCs, and severe OSCCs with an accuracy of 97.84% (Madathil et al., 2019). Surprisingly, even subtypes of head and neck cancer cells could be identified by analyzing the spectra from tissue engineering models. Mian et al. successfully identified subtypes of head and neck cancer cells (Mian et al., 2017). Significant differences in the spectra were observed in the lipid content ( $2881\text{ cm}^{-1}$ ) and protein structure (amides I and III), the peaks of which are associated with several amino acids and nucleic acids ( $600\text{ cm}^{-1}$  to  $1003\text{ cm}^{-1}$ ). Therefore, doctors can choose chemotherapy or radiotherapy based on the known subtypes of cancer. In addition, Yasser et al. successfully distinguished radioresistant cell sublines (70Gy-

UPCI : SCC029B; 50Gy-UPCI : SCC029B) from parental oral cancer cell lines (UPCI : SCC029B) (Yasser et al., 2014). PCA presented a minor overlap between three clusters, indicating a large difference between three cell lines. Furthermore, Kumar et al. explored the change in differentiation efficacy during the cancer-inducing process, and the accuracy of cancer identification increased during the first 7 weeks, remained steady from 8 to 11 weeks, and exceeded 80% by the 14th week (Kumar et al., 2016).

Furthermore, RS has been found to be a powerful tool for distinguishing OSCCs from precancerous lesions. Krishna et al. studied the potential of Raman spectra obtained *in vivo* directly to differentiate malignant lesions (OSCCs, oral submucous fibrosis (OSMF) and leukoplakia (OLK)) in the oral cavity. The accuracy was 85% in HV, 89% for OSCCs, 85% for OSMF, and 82% for OLK. For spectra classified as normal and abnormal, the sensitivity and specificity were 94.2% and 94.4%, respectively (Krishna et al., 2014). However, another study reported that OSMF, OLK, and lichen planus were highly misclassified as OSCCs or habitues without lesions in the Raman spectra of sera (Dumal et al., 2020). OSCCs, verrucous carcinomas, and OLK were differentiated with 97.24% accuracy by taking thin cryosections of tissue specimens in a novel SERS catheter ( $5\text{--}6\text{ }\mu\text{m}$ ) (Madathil et al., 2019). Moreover, RS combined with cytopathology can distinguish oral precancerous lesions (OPLs), healthy tobacco users (HT), and HV (Ghosh et al., 2019). The sensitivity of the OPL group was identified as approximately 77% when analyzed spectrally, which was higher than patient-wise, with a sensitivity of approximately 70%. The main changes in the spectra of OPLs were related to nucleic acids and proteins. This is consistent with changes in protein and DNA corresponding to cellular physiological changes during poor cell proliferation (Sahu et al., 2017). Connolly et al. obtained unlabeled spectra from saliva and exfoliated cells of HV and OSCC patients using SERS and established diagnostic models using PCA-LDA and PCA with logistic regression (PCA-LR) diagnostic algorithms. Consequently, it was concluded that the saliva and exfoliated cells could identify HV and patients with OSCCs, with sensitivities of 89% and 73% and overall accuracies of 68% and 60%, respectively (Connolly et al., 2016). In brief, the accuracy of Raman spectra from exfoliated cells in differentiating diagnoses must be improved. Misclassification of Raman exfoliative cytology also indicated field cancerization changes. The higher the misclassification rate between spectra of contralateral normal tissue and tumor tissue, the more similar the exfoliated cells are (Sahu et al., 2019).

Researchers have differentiated OSCCs, other oral cancers (such as verrucous carcinoma, mucoepidermoid carcinoma, parotid pleomorphic adenoma, and Warthin's tumor) (Yan et al., 2011; Yan et al., 2015; Tan et al., 2017; Madathil et al., 2019), and cancers in other regions (such as breast, colorectal, lung, and ovarian) (Moisoiu et al., 2019). The difference in the SERS spectra of sera between OSCCs, mucoepidermoid carcinomas, and healthy humans is mainly represented by nucleic acids and proteins. The spectral differences are mainly distributed in the spectral bands represented by the specific

molecular structures of carotenoids and lipids. OSCCs were successfully distinguished from a control group with a sensitivity of 80.7% and specificity of 84.1% (Tan et al., 2017). Another study has also attempted to distinguish OSCCs from parotid pleomorphic adenomas, Warthin's tumors, and mucoepidermoid carcinomas by support vector machine (SVM) according to the SERS information of sera. The results showed that the SVM had a favorable effect on SERS spectral classification, with an accuracy of 84.1–88.3%, sensitivity of 82.2–97.4%, and specificity of 73.7–86.7%. Although this method can easily differentiate mucoepidermoid carcinoma from the other two benign tumors, it is difficult to distinguish between the two benign tumors themselves (Yan et al., 2011; Yan et al., 2015). Moisoiu et al. successfully discriminated several cancers with an accuracy of 88% for oral cancer, 76% for breast cancer, 86% for colorectal cancer, 59% for lung cancer, and 80% for ovarian cancer (Moisoiu et al., 2019). AgNP substrate enhanced the signal in serum samples and PCA-LDA differentiated spectra in different groups.

Obtaining more important information can increase the differentiation efficacy. Ghosh et al. combined Fourier-transform infrared spectroscopy (FTIR) and RS to increase the classification accuracy from 85% (FTIR) and 82% (RS) to 98% (Ghosh et al., 2019). Spectra of DNA from dehydrated cancer cells and high-wavenumber regions of spectra have attracted the attention of researchers. Panikkanvalappil et al. provided a new method for improving the accuracy of the diagnostic model. Their study found that the conformational induction of DNA from dehydrated cancer cells presents a series of unique Raman-labeled bands. According to these bands, cancer and healthy cell DNA can be distinguished. It is speculated that nucleobase damage in tumor cell DNA and subsequent changes in the electron cloud during the dehydration-driven conformational change results in a Raman spectral change (Panikkanvalappil et al., 2013). The high-wavenumber region contains more distinct information for identifying subcellular structure, i.e., the nucleus and cytoplasm, than the fingerprint region. Carvalho et al. analyzed the spectra of the nucleolus, nucleus, and cytoplasm of oral epithelial carcinomas (SCC-4), dysplasia (DOK) cell lines, and normal oral epithelial cells. The O–H bond from cell-membrane-bound water or intracellular fluid provided key information for distinguishing cell lines. The sensitivity and specificity of cytoplasm recognition were up to ~100% and 97%, respectively. Regarding nuclear recognition, the specificity was 99%. Compared to other methods, high-wavenumber regions provide more information about subcellular structures to distinguish between normal, premalignant, and malignant tissues (Carvalho et al., 2015; Carvalho et al., 2017).

In addition, improving the efficiency of the classifier can increase the distinguishing accuracy. Jeng et al. gathered the spectra from 36 normal and 44 OSCC tissues and analyzed them with PCA, followed by LDA or quantitative discrimination analysis (QDA). The accuracies of the PCA-LDA and PCA with QDA (PCA-QDA) classifiers were 81.25% (sensitivity: 77.27%, specificity: 86.11%) and 87.5% (sensitivity: 90.90%, specificity: 83.33%), respectively. PCA-QDA showed better

classification efficiency than PCA-LDA (Jeng et al., 2019). Moreover, Cals et al. adopted PCA with (hierarchical) LDA (PCA-(h)LDA) (Cals et al., 2016). Because there is a large difference between lipid, nerve, and tumor tissue, researchers first differentiated lipids and nerves from other tissues and then distinguished OSCCs from the remaining components (squamous epithelium and connective tissue, muscle, and glands). Compared to the one-step PCA-LDA model, the two-step PCA-(h)LDA model presented higher accuracy (91% accuracy; sensitivity: 100%, specificity: 78%). However, the PCA-(h)LDA model also increased the data analysis workload.

Furthermore, focusing on biomarkers is also a way to distinguish between normal and abnormal tissues. Chen et al. compared Raman spectra decomposed by multivariate curve resolution with alternating least squares (MCR-ALS) with the standard Raman spectra of keratin, a well-known molecular marker of OSCC. However, some spectra were neither divided into the OSCC group nor the normal group, and as a result, with different classification methods of suspicious samples, the sensitivity differed widely (77% or 92%) (Chen et al., 2016). Recently, Fălămaș et al. attempted to differentiate six OSCC patients from five HV by salivary Raman spectra (Fălămaș et al., 2020). They noticed that thiocyanate is not only an indicator of smokers (Tsuge et al., 2000) but also related to cancer (Shiue, 2015). The characteristic band of thiocyanate is  $2126\text{ cm}^{-1}$ , the intensity of which was higher in the cancer group than in the healthy group. The peak at  $738\text{ cm}^{-1}$  is another characteristic band of thiocyanate, contributing to the differentiation of the two groups by PCA. Fălămaș et al. also found that the peaks at 752, 884, 928, 989, and  $1047\text{ cm}^{-1}$ , representing tryptophan, collagen, proline, and glycogen, respectively, contributed to finding the biggest difference between OSCC patients and HV in salivary spectra (Fălămaș et al.). Daniel et al. also concentrated on the presence of thiocyanate at  $2108\text{ cm}^{-1}$  in the SERS spectra of saliva among smokers (Daniel et al., 2020). However, due to the small sample size, whether thiocyanate can be a potent biomarker for recognizing cancer patients requires further exploration. S100 calcium-binding protein P (S100P) mRNA has been reported as a valid salivary biomarker for oral cancer detection without periodontitis interference (Y.-S. et al., 2017). Han et al. designed a sandwich assay format consisting of oligonucleotides, AuNPs as the SERS substrate, and malachite green isothiocyanate as a reporter molecule to quantify S100P mRNA in saliva (Han et al., 2019). The concentration of S100P mRNA was three times higher in the oral cancer group than in the healthy group.

### 3.3.2 Treatment and Prognosis of Oral Cancer

The extent to which the cancerous tissue can be removed by a clinician (i.e., whether it can be completely removed or not) significantly affects the prognosis. It has been reported that the 5-year disease-free survival rate significantly declines in patients with inadequate surgical margins. Even after surgical treatment and radiotherapy or chemotherapy, malignant lesions may still recur, which directly affects the prognosis and patients' quality of life. Thus, assessing surgical margins and the potential for oral



cancer recurrence are of major importance. RS shows the application potential and unique advantages of these two aspects.

For instance, frozen section is an intraoperative choice to assess whether the surgical margin is adequate. This technique works well for soft tissues, but it is difficult to use it to assess bone edges (Nieberler et al., 2016). RS has the potential to distinguish between malignant and normal tissues. The Raman map composed of the spectra of all sites of a specimen is a candidate method for determining the surgical margins more accurately during operation. Barroso et al. found that the main factor in distinguishing a tumor from surrounding healthy tissue is water concentration (Barroso et al., 2015). Based on this, they constructed a 2D Raman map to observe the change in water concentration from tumor tissue to the surrounding healthy tissue. In 2016, Barroso et al. (Barroso et al., 2016) applied the ratio of  $3390\text{ cm}^{-1}$  (O–H stretching band of water) to  $2935\text{ cm}^{-1}$  (C–H stretching band of lipids and proteins) as an indicator of water concentration and then assigned different colors to various water concentrations for 2D Raman map construction. In the 4–6 mm transition region between the tumor and surrounding normal tissue, the water content in the tissue ranged from  $76\% \pm 8\%$  in the tumor tissue to  $54\% \pm 24\%$  in the surrounding healthy tissue. The 2D Raman map presented the water concentration transformation from the tumor tissue to the surrounding healthy tissue directly, providing valid information for clinicians to determine the surgical edge more accurately. Two years later, Barroso et al. further focused on the potential of RS to evaluate the margin of bone resection during OSCC mandibular resection (Barroso et al., 2018). They also assessed the water concentrations of healthy and tumor bone tissues (more than 3 mm from the tumor boundary), and a Mann–Whitney U-test revealed significant differences in water concentration between the two groups. Furthermore, they built a PCA-LDA model to distinguish two types of samples based on the intensity of  $2800\text{--}3050\text{ cm}^{-1}$  C–H stretching. For suspicious spectra proven by water concentration, the PCA-LDA model presented 95% accuracy (sensitivity: 95%, specificity: 87%). By assigning different colors to the tumor bone tissue and normal tissue, they completed a 2D Raman map. Therefore, Barroso et al. believed that RS is a candidate method for intraoperative surgical edge assessment. Compared to the reports from Barroso et al., Cals et al. adopted two-step PCA-(h)LDA to achieve higher accuracy (accuracy: 91%, sensitivity: 100%, specificity: 78%) (Cals et al., 2016). A 2D Raman map can also be constructed using the tumor posterior probability of each sub-site spectrum to present visual information.

RS can also sensitively detect minor changes in a sample, presenting the potential to predict the recurrence rate of oral cancer patients (Sahu et al., 2015; Malik et al., 2017). Carcinoembryonic antigen (CEA) has the potential to predict tumor recurrence, which has been confirmed in other types of cancers (Lumachi et al., 2008). The Raman spectra of sera can detect cancer-related proteins and DNA (Harris et al., 2010). In 2015, Sahu et al. reported that the Raman spectra of sera are related to OSCC recurrence (Sahu et al., 2015). They collected serum samples immediately before and 1 week after surgery. The PCA-LDA classifier could differentiate patients with or without tumor

recurrence within 2 years, and the classification effectiveness was approximately 78%. It is worth mentioning that only postoperative serum spectra are related to tumor recurrence. However, serum spectra changes cannot identify the specific location of a tumor, but as a preliminary test to screen high-risk people, they can be effective. Malik et al. applied oral mucosa to predict tumor recurrence. They analyzed the Raman spectra of malignant and contralateral normal mucosa in OSCC patients using PCA-LDA and leave-one-out cross-validation (LOOCV). They focused on misclassification, and found a relationship with recurrence 2 years post-surgery (Malik et al., 2017). They included 57 patients with OSCCs (including tongue, cheek, mandible, molar posterior pad, hard plate, and mouth cancers). Eight of 41 patients with misclassified spectra and 2 of 16 with correct spectra classification had second primary cancer or recurrence 2 years after surgery. It can be concluded that the misclassified group presented 1.5 times greater recurrence risk than the correctly classified group. Tissues have changed at the molecular level before the visible malignant change appears, and Raman spectra can detect this minor transformation. The sensitivity and specificity of the classifier were 80% and 29.7%, respectively. Although the specificity was low, it is acceptable as a preliminary screening tool, and following studies may increase the specificity by increasing the sample size.

## 4 DISCUSSION

Both dental caries and periodontal disease are chronic infectious diseases, in which bacteria and biofilms play a critical role in initiation and progression. Studies have shown that the composition of the subgingival flora and metabolism of virulence factors change significantly before periodontitis advances (Curtis et al., 2020). However, it is not easy to detect changes in the composition and metabolism of flora chairside quickly and precisely. As Raman spectra can sensitively detect changes at the molecular level, they show the potential to detect metabolic changes in bacteria and biofilms chairside. Detailed and comprehensive analysis of the metabolism of bacteria and biofilms by Raman spectra requires interpretation of the meaning and changes of each peak. The amount of information and workload is massive, and it is difficult to reverse the changes at the molecular level from this phenomenon. Focusing on the changes in key bands in the spectra, at this stage, the metabolic changes can be observed more efficiently and intuitively, such as those at  $484\text{ cm}^{-1}$  and  $2040\text{--}2300\text{ cm}^{-1}$  (Tao et al., 2017; Daood et al., 2020a). In addition, there are many reports on the application of Raman spectra to distinguish different oral bacteria, the accuracy of which can be improved by enhancing the spectral signal-to-noise ratio or applying a more distinguishable analysis method.

It is well known that mature laboratory methods such as polymerase chain reaction and western blot can identify bacteria and accurately detect changes in mRNA transcription and protein expression within hours; however, they are more suitable for the laboratory because special reagents and

instruments are required. The potential of RS is more inclined to obtaining information in a clinical environment within minutes, with the advantages of being *in situ*, non-invasive, and accurate as RS is not interfered with by water, causes no damage to the sample, and reflects the chemical bond information clearly. To tap its potential in chairside applications, researchers have made many attempts *in vitro*, including identification of bacterial species (Kriem et al., 2020), detecting bacterial metabolic changes through D<sub>2</sub>O-labeled RS (Guo et al., 2019), quorum-sensing molecules (Culhane et al., 2017), and structure of biofilms (Kriem et al., 2021). In addition, as RS can truthfully reflect information on the composition, structure, and concentration of all biological samples, it will provide a basis for obtaining more bacterial information chairside when changes in the flora and the expression of virulence factors can be obtained through RS. However, it should be noted that accurately obtaining target information from a large amount of information still requires study. In terms of hardware foundation, the only portable Raman spectrometer (Thermo Scientific™ Gemini™) is very expensive. Before a unified and standardized inspection process is established, the path to RS chairside inspection is still long. However, RS has undeniably shown strong potential to provide more microbiological information chairside or even *in situ*.

Biological samples are usually composed of proteins, lipids, nucleic acids, and inorganic substances, and various bonds make up the Raman spectra, which often causes confusion over how to extract the desired information. Samples for the diagnosis and prognosis of oral diseases include biofluids (saliva, GCF, and blood/serum), bacteria or cells, soft tissue, and hard tissue (teeth and bone). Gathering bodily fluid samples requires specific conditions and methods to avoid interfering factors. For instance, saliva samples are usually taken at 9:00 to 11:00 a.m. after mouth rinsing one to three times (Gonchukov et al., 2011; Hernández-Cedillo et al., 2019; Yang et al., 2020). Regarding GCF, the paper strips used to take samples must be carefully protected from contamination by blood or saliva, and peripheral blood samples should be taken after 10 h of overnight fasting (Xue et al., 2018). Biofluids are not usually uniformly distributed after drying and often crystallize on solid surfaces, and the spectra obtained at different sites also show large differences (Gonchukov et al., 2011). It is possible to average the spectra obtained from multiple sites for analysis and identification. It is worth mentioning that saliva contains many biomarkers, such as SA (Hernández-Cedillo et al., 2019) and carotenoids (Kim et al., 2010; Gonchukov et al., 2011) for periodontitis diagnosis, and thiocyanate (Falamas et al.; Fălămaș et al., 2020) and S100P mRNA (Han et al., 2019) for oral cancer detection.

Planktonic bacteria and cell samples are also unevenly distributed after drying, but bacterial cells are independent as a unit, unlike the uneven distribution of components in bodily fluid samples. Therefore, it is feasible to obtain Raman spectra in combination with a microscope to determine the cell distribution. It should be noted that definite and scientific culture conditions and culture time should be adopted to ensure the stability of the cell state, which is the basis for obtaining stable Raman spectra. After

biofilm formation and cell attachment, solid surfaces are formed, and the distribution disappears unevenly. Once samples form a solid plane, Raman maps can be obtained by integrating the intensities of characteristic bonds (such as O–H in high-wavenumber regions) at every site to facilitate the observation of the boundaries of different tissues and provide a basis for judging the edges of tumor tissues (Barroso et al., 2015; Barroso et al., 2016; Barroso et al., 2018). Soft tissues include epithelial, connective, adipose, glandular, and nerve tissues. Some studies have focused on biomarkers and corresponding bonds to differentiate different tissues, such as collagen in gingiva (Garnero et al., 2010; Daood et al., 2018) and keratin in squamous cell carcinoma tissue (Chen et al., 2016). Other studies have analyzed all the information in the spectra, which is complicated. Hard tissues in the oral cavity include teeth (enamel, dentin, and cement) and bone, and changes in phosphate (960 cm<sup>-1</sup>), carbonate (960 cm<sup>-1</sup>), and collagen (1655 or 1667, 1246 or 1270, and 1450 cm<sup>-1</sup>) have attracted attention for detecting caries and defining the edge of decayed tooth tissue (Toledano et al., 2015b). In bone regeneration, OCP and amorphous HAP represent immature bone, and HAP crystals representing mature bone have been used to evaluate bone transformation (Gatin et al., 2019).

There are two ways to assist the diagnosis and prognostic assessment of oral diseases using RS. One is to focus on specific biomarkers that are associated with well-known pathological changes and their corresponding bonds. The advantages of this approach are that the data analysis is simpler and the discrimination efficiency is higher. However, most biomarkers for oral cancer and periodontal disease detection are microRNA, cell-free DNA, extracellular vesicles, and cytokines (interleukin and tumor necrosis factor) (Cristaldi et al., 2019), which do not have specific bonds like SA (Hernández-Cedillo et al., 2019), carotenoids (Kim et al., 2010; Gonchukov et al., 2011), and thiocyanate (Falamas et al.; Fălămaș et al., 2020) in saliva. There are several methods to capture target biomarkers and attach labeled molecules to them, but the process is complicated. The other way is to classify the principal components of the full spectra, establish a model, and test its sensitivity and specificity. The most commonly used method for this approach is PCA-LDA+LOOCV. It is worth mentioning that MCR-ALS analysis can decompose complicated spectra into interpretable components, which are accessible to non-specialists in the spectroscopy field (Chen et al., 2016). This is a solution for nucleic acid and protein biomarkers.

RS exhibits unique potential in the biomedical field due to its high sensitivity and accuracy and low water interference and sample damage. However, only a few photons are produced in Raman scattering, the peak intensity is relatively weak, and the signal-to-noise ratio is low. Environmental factors (such as light and vibration) and the parameters selected for Raman spectra acquisition are also interfering factors. The detection sites of unevenly distributed samples (biofluids) and the focus of the microscope also affect the spectra.

The signal-to-noise ratio can be improved during the signal acquisition and data analysis stages. First, combining RS with other technologies can have a positive effect. For example, SERS enhances

**TABLE 3 |** Summary of RS studies on oral cancer.

Sample type	Sample numbers	Year	Authors	RS (spectral region; laser used)	Data analysis methodology
<b>Clarifying tumor stage, histological classification and cancer subtype</b>					
Tumor resection specimen	OSCC = 20; VC = 4; OLK = 5; N = 8	2019	(Madathil et al., 2019)	SERS; 500–1800 cm <sup>-1</sup> ; 488 nm	PCA-DA
Serum	Buccal cancer = 40; Tongue cancer = 50; Floor of mouth cancer = 45	2018	(Xue et al., 2018)	SERS; 200–1800 cm <sup>-1</sup> ; 633 nm	PCA-LDA; LOOCV
Tissue engineering models	Models = 27: N (NOF; NOK); Dysplastic (DOK; D19; D20); HNC (Cal27; SCC4; FaDu)	2017	(Mian et al., 2017)	600–1800 cm <sup>-1</sup> and 2800–3400 cm <sup>-1</sup> ; 532 nm	PCA-LDA; CA
Buccal pouch tissue	<i>Ex vivo</i> = 115; <i>In vivo</i> ; sequential = 60; <i>In vivo</i> follow-up = 6	2015	(Kumar et al., 2016)	1200–1800 cm <sup>-1</sup> ; 785 nm	PCA; PCA-LDA
Cells	Radioresistant cell sublines (70Gy-UPCI : SCC029B; 50Gy-UPCI : SCC029B); Parental oral cancer cell lines (UPCI : SCC029B)	2014	(Yasser et al., 2014)	900–1800 cm <sup>-1</sup> ; 785 nm	PCA
<b>Differentiating diagnosis between normal, precancerous lesions and cancer</b>					
Tumor resection specimen	OSCC = 20; VC = 4; OLK = 5; N = 8	2019	(Madathil et al., 2019)	SERS (catheter (5–6 μm)); 500–1800 cm <sup>-1</sup> ; 488 nm	PCA-DA
Tissue engineering models	Models = 27: N (NOF; NOK); Dysplastic cells (DOK; D19; D20); HNC (Cal27; SCC4; FaDu)	2017	(Mian et al., 2017)	600–1800 cm <sup>-1</sup> and 2800–3400 cm <sup>-1</sup>	PCA-LDA; CA
<i>In vivo</i>	OSCC = 113; OSMF = 25; OLK = 33; HV = 28	2014	(Krishna et al., 2014)	900–1750 cm <sup>-1</sup> ; 785 nm	PCA-LDA
<b>Differentiating diagnosis between different tumors (OSCC, other oral tumors and carcinomas in other systems)</b>					
Serum	HV = 39; Breast cancer = 42; Colorectal cancer = 109; Lung cancer = 33; Oral cancer = 17; Ovarian cancer = 13	2019	(Moisoiu et al., 2019)	SERS; 600–1800 cm <sup>-1</sup> ; 532 nm	PCA-LDA
Tissue frozen section	OSCC = 20; VC = 4; OLK = 5; N = 8	2019	(Madathil et al., 2019)	SERS(catheter (5–6 μm)); 500–1800 cm <sup>-1</sup> ; 488 nm	PCA-DA
Exfoliated cell	N = 13; OLK = 13; OSCC = 10	2019	(Ghosh et al., 2019)	200–2000 cm <sup>-1</sup> ; 785 nm	PCA-LDA; k-fold cross-validation
Exfoliated cell	Tumor = 16; Contralateral mucosa = 16; HT = 20	2019	(Sahu et al., 2019)	800–1800 cm <sup>-1</sup> ; 785 nm	PCA-LDA; LOOCV
Exfoliated cell	HV = 20; TH = 20; OPL = 27	2017	(Sahu et al., 2017)	800–1800 cm <sup>-1</sup> ; 785 nm	PCA-LDA
Serum	OSCC = 135; MEC = 90; HV = 145	2017	(Tan et al., 2017)	SERS; Fingerprint regions (200–1800 cm <sup>-1</sup> ); 633 nm	PCA-LDA
Saliva and exfoliated cell	Person: HV = 18; OSCC = 18; Spectra: Saliva = 180; Cell = 120	2016	(Connolly et al., 2016)	SERS; 800–1800 cm <sup>-1</sup> ; 785 nm	PCA-LDA; PCA-LR
Serum	PA = 20; WT = 21; MEC = 19; HV = 31	2015	(Yan et al., 2015)	SERS; 200–1800 cm <sup>-1</sup> ; 633 nm	SVM
Tissue section	HV = 20; PA = 20; WT = 20	2011	(Yan et al., 2011)	800–1800 cm <sup>-1</sup> ; 785 nm	SVM
<b>Obtaining more important information to elevate differentiation efficacy</b>					
Exfoliated cell	N = 13; OLK = 13; OSCC = 10;	2019	(Ghosh et al., 2019)	200–2000 cm <sup>-1</sup> ; 785 nm	PCA-LDA; k-fold cross-validation
Cells	Nucleolus, nucleus and cytoplasm: SCC-4 = 60; DOK = 60; N = 60	2017	(Carvalho et al., 2017)	2800–3600 cm <sup>-1</sup> ; 532 nm	PCA-FDA
Dehydrated cancer cell	–	2013	(Panikkanvalappil et al., 2013)	SERS; 400–2000 cm <sup>-1</sup> ; 532 nm	–
<b>Selecting better analysis methods to elevate differentiation efficacy</b>					
Tissue section	N = 36; Tumor = 44 (tongue, buccal mucosa, gingiva)	2019	(Jeng et al., 2019)	700–2000 cm <sup>-1</sup> ; 532 nm	PCA-LDA; PCA-QDA; LOOCV; k-fold cross-validation
Tumor resection specimen	OSCC = 14; N = 11	2016	(Cals et al., 2016)	400–1800 cm <sup>-1</sup> ; 785 nm	PCA-(h)LDA
<b>Focusing on biomarkers to elevate differentiation efficacy</b>					
Saliva	OSCC = 6; HV = 5	2020	(Fälämaş et al., 2020)	SERS; 600–1720 cm <sup>-1</sup> ; 785 nm	PCA
Saliva	OSCC = 3; Lymphoma = 1; Actinomyces infection = 1; HV = 3	2020	(Falamas et al.)	100–3200 cm <sup>-1</sup> ; 785 nm	PCA-LDA
Saliva	Oral dysplasia = 10; HV = 10	2020	(Daniel et al., 2020)	SERS; –	–

(Continued)

TABLE 3 | Continued

Sample type		Sample numbers	Year	Authors	RS (spectral region; laser used)	Data analysis methodology
Saliva	OSCC = 3; HV = 3		2019	(Han et al., 2019)	SERS; 1100–1700 cm <sup>-1</sup> ; 638 nm	Mann–Whitney U-test
Tissue section	OSCC = 13; N = 11		2016	(Chen et al., 2016)	800–1800 cm <sup>-1</sup> ; 488 nm	Multivariate curve resolution with alternating least squares
<b>Assessing surgical margins</b>						
Tissue resection specimen	OSCC (mandibular bone) = 20		2018	(Barroso et al., 2018)	2500–4000 cm <sup>-1</sup> ; 671 nm	PCA-LDA; Mann–Whitney U-test; ROC
Tumor resection specimen	OSCC (tongue) = 20		2016	(Barroso et al., 2016)	2500–4000 cm <sup>-1</sup> ; 671 nm	Mann–Whitney U-test
Tumor resection specimen	OSCC = 14; N = 11		2016	(Cals et al., 2016)	400–1800 cm <sup>-1</sup> ; 785 nm	PCA-(h)LDA
Tumor resection specimen	OSCC (tongue) = 14		2015	(Barroso et al., 2015)	2500–4000 cm <sup>-1</sup> ; 671 nm	Mann–Whitney U-test; ROC
<b>Predicting oral cancer recurrence</b>						
Exfoliated cell	Tumor = 16; Contralateral mucosa = 16; HT = 20		2019	(Sahu et al., 2019)	800–1800 cm <sup>-1</sup> ; 785 nm	PCA-LDA; LOOCV
<i>In vivo</i>	Tumor and contralateral normal mucosa = 99		2017	(Malik et al., 2017)	785 nm	PCA-LDA; LOOCV
Serum	Recurrence = 10; No-recurrence = 12		2015	(Sahu et al., 2015)	700–1800 cm <sup>-1</sup> ; 785 nm	PCA-LDA; LOOCV

OSCC, oral squamous cell carcinoma; N, normal; HV, healthy volunteers; TH, tobacco habit; OPL, oral premalignant conditions; HNC, head and neck cancer; VC, verrucous carcinoma; OSMF, oral submucous fibrosis; OLK, leukoplakia; MEC, mucoepidermoid carcinoma; PA, pleomorphic adenoma; WT, Warthin's tumor.

the local electric field to increase the peak intensity; micro-RS can obtain more accurate information as the signal comes from accurate sites under a microscope, reducing interference signals from other sites; and near-infrared excitation Fourier-transform RS uses Fourier-transform technology to collect signals and accumulate multiple times to improve the signal-to-noise ratio, and irradiates the sample with a 1064 nm near-infrared laser to reduce the fluorescence background. Second, data preprocessing and data analysis can improve the signal-to-noise ratio. The most commonly used data analysis method is PCA-LDA. However, PCA-QDA presents a higher accuracy than PCA-LDA (Jeng et al., 2019). Moreover, the two-step distinguishing process of PCA-(h)LDA has a higher accuracy than the one-step process of PCA-LDA (Cals et al., 2016). MCR-ALS is also an option for non-specialists in the spectroscopy field (Chen et al., 2016). Another user-friendly data analysis method for researchers with limited mathematical knowledge is worth mentioning: Inverted Discrete Wavelet Transform decomposes the Raman spectra into low-frequency (approximation) components and fluctuation (detail) components. The next layer of “approximation” and “detail” components is continuously decomposed from the previous “approximation” components. The last “approximation” and several previous “detail” components are finally integrated to filter out non-correlated signals and background signals, improving the readability of the Raman spectra (Camerlingo et al., 2008).

Third, focusing on biomarkers, such as keratin in tumor tissue (Chen et al., 2016), SA (Hernández-Cedillo et al., 2019), carotenoids (Kim et al., 2010; Gonchukov et al., 2011), thiocyanate (Falamas et al.; Fălămaș et al.), and S100P mRNA (Han et al., 2019), also increases the differentiation accuracy.

Subcellular DNA (Carvalho et al., 2017) and DNA information from dehydrated cells (Panikkanvalappil et al., 2013) also provide more valid information.

Collectively, RS has shown its ability to assist in the diagnosis and prognostic prediction of oral diseases. Its high sensitivity and accuracy and low water interference and sample damage are useful for obtaining information from not only isolated samples but also *in situ* sites, such as in detection of early caries and malignant lesions of, e.g., oral mucosa, *in vivo*. However, the collection of spectra with higher signal-to-noise ratios and selection of better data analysis methods to achieve higher accuracy are still the focus of further studies and the direction of future efforts.

## AUTHOR CONTRIBUTIONS

YZ and LR drafted the manuscript. QW and ZW provided valuable insights for the manuscript. CL and YD reviewed and edited the manuscript. All authors have approved the final version of the manuscript.

## FUNDING

This study was supported by the National Natural Science Foundation of China (grant number 82071121 to YD), Open Project of State Key Lab of Optical Technologies on Micro-Engineering and Nano-Fabrication (2021LF1007), and Sichuan University crosswise task (21H0674).



## REFERENCES

- Adachi, T., Pezzotti, G., Yamamoto, T., Ichioka, H., Boffelli, M., Zhu, W., et al. (2015). Vibrational Algorithms for Quantitative Crystallographic Analyses of Hydroxyapatite-Based Biomaterials: II, Application to Decayed Human Teeth. *Anal. Bioanal. Chem.* 407 (12), 3343–3356. doi: 10.1007/s00216-015-8539-z
- Aditi, S., Nikhila, N., Sharada, S., and C Murali, K. (2015). Recurrence Prediction in Oral Cancers: A Serum Raman Spectroscopy Study. *Analyst* 140 (7), 2294–2301. doi: 10.1039/c4an01860e
- Almahdy, A., Downey, F. C., Sauro, S., Cook, R. J., Sherriff, M., Richards, D., et al. (2012). Microbiochemical Analysis of Carious Dentine Using Raman and Fluorescence Spectroscopy. *Caries Res.* 46 (5), 432–440. doi: 10.1159/000339487
- Al-Obaidi, R., Salehi, H., Desoutter, A., Tassery, H., and Cuisinier, F. (2019). Formation and Assessment of Enamel Subsurface Lesions *In Vitro*. *J. Oral. Sci.* 61 (3), 454–458. doi: 10.2334/josnusd.18-0174
- Alturki, M., Koller, G., Almhöjd, U., and Banerjee, A. (2020). Chemo-Mechanical Characterization of Carious Dentine Using Raman Microscopy and Knoop Microhardness. *R. Soc. Open Sci.* 7 (5), 200404. doi: 10.1098/rsos.200404
- Athukorale, S., Leng, X., Xu, J. X., Perera, Y. R., Fitzkee, N. C., and Zhang, D. (2019). Surface Plasmon Resonance, Formation Mechanism, and Surface Enhanced Raman Spectroscopy of Ag(+)-Stained Gold Nanoparticles. *Front. Chem.* 7. doi: 10.3389/fchem.2019.00027
- Dillon, J. K., Brown, C. B., McDonald, T. M., Ludwig, D. C., Clark, P. J., and Leroux, B. G. How Does the Close Surgical Margin Impact Recurrence and Survival When Treating Oral Squamous Cell Carcinoma? *J. Oral. Maxillof. Surg.* 73 (6), 1182–1188. doi: 10.1016/j.joms.2014.12.014
- Barroso, E. M., Hove, I. T., Schut, T. C. B., Mast, H., and Koljenovic, S. (2018). Raman Spectroscopy for Assessment of Bone Resection Margins in Mandibulectomy for Oral Cavity Squamous Cell Carcinoma. *Eur. J. Cancer* 92, 77–87. doi: 10.1016/j.ejca.2018.01.068
- Barroso, E. M., Smits, R. W., Bakker Schut, T. C., ten Hove, I., Hardillo, J. A., Wolvius, E. B., et al. (2015). Discrimination Between Oral Cancer and Healthy Tissue Based on Water Content Determined by Raman Spectroscopy. *Anal. Chem.* 87 (4), 2419–2426. doi: 10.1021/ac504362y
- Barroso, E. M., Smits, R. W., van Lanschot, C. G., Caspers, P. J., Ten Hove, I., Mast, H., et al. (2016). Water Concentration Analysis by Raman Spectroscopy to Determine the Location of the Tumor Border in Oral Cancer Surgery. *Cancer Res.* 76 (20), 5945–5953. doi: 10.1158/0008-5472.Can-16-1227
- Bray, F., Ferlay, J., Soerjomataram, I., Siegel, R. L., Torre, L. A., and Jemal, A. (2018). Global Cancer Statistics 2018: GLOBOCAN Estimates of Incidence and Mortality Worldwide for 36 Cancers in 185 Countries. *CA Cancer J. Clin.* 68 (6), 394–424. doi: 10.3322/caac.21492
- Cals, F. L., Koljenovic, S., Hardillo, J. A., Baatenburg de Jong, R. J., Bakker Schut, T. C., and Puppels, G. J. (2016). Development and Validation of Raman Spectroscopic Classification Models to Discriminate Tongue Squamous Cell Carcinoma From Non-Tumorous Tissue. *Oral. Oncol.* 60, 41–47. doi: 10.1016/j.oraloncology.2016.06.012
- Camerlingo, C., d'Apuzzo, F., Grassia, V., Perillo, L., and Lepore, M. (2014). Micro-Raman Spectroscopy for Monitoring Changes in Periodontal Ligaments and Gingival Crevicular Fluid. *Sensors (Basel)* 14 (12), 22552–22563. doi: 10.3390/s14122552
- Camerlingo, C., Zenone, F., Perna, G., Capozzi, V., Cirillo, N., Gaeta, G. M., et al. (2008). An Investigation on Micro-Raman Spectra and Wavelet Data Analysis for Pemphigus Vulgaris Follow-Up Monitoring. *Sensors (Basel)* 8 (6), 3656–3664. doi: 10.3390/s8063656
- Campi, L. B., Lopes, F. C., Soares, L. E. S., de Queiroz, A. M., de Oliveira, H. F., Saquy, P. C., et al. (2019). Effect of Radiotherapy on the Chemical Composition of Root Dentin. *Head Neck* 41 (1), 162–169. doi: 10.1002/hed.25493
- Carvalho, F. B., Barbosa, A. F., Zanin, F. A., Brugnera Junior, A., Silveira Junior, L., and Pinheiro, A. L. (2013). Use of Laser Fluorescence in Dental Caries Diagnosis: A Fluorescence X Biomolecular Vibrational Spectroscopic Comparative Study. *Braz. Dent. J.* 24 (1), 59–63. doi: 10.1590/0103-6440201302123
- Carvalho, L. F., Bonnier, F., O'Callaghan, K., O'Sullivan, J., Flint, S., Byrne, H. J., et al. (2015). Raman Micro-Spectroscopy for Rapid Screening of Oral Squamous Cell Carcinoma. *Exp. Mol. Pathol.* 98 (3), 502–509. doi: 10.1016/j.yexmp.2015.03.027
- Carvalho, L., Bonnier, F., Tellez, C., Dos Santos, L., O'Callaghan, K., O'Sullivan, J., et al. (2017). Raman Spectroscopic Analysis of Oral Cells in the High Wavenumber Region. *Exp. Mol. Pathol.* 103 (3), 255–262. doi: 10.1016/j.yexmp.2017.11.001
- Chen, P. H., Shimada, R., Yabumoto, S., Okajima, H., Ando, M., Chang, C. T., et al. (2016). Automatic and Objective Oral Cancer Diagnosis by Raman Spectroscopic Detection of Keratin With Multivariate Curve Resolution Analysis. *Sci. Rep.* 6, 20097. doi: 10.1038/srep20097
- Chen, M. X., Zhong, Y. J., Dong, Q. Q., Wong, H. M., and Wen, Y. F. (2021). Global, Regional, and National Burden of Severe Periodontitis-2019: An Analysis of the Global Burden of Disease Study 2019. *J. Clin. Periodontol* 48 (9), 1165–1188. doi: 10.1111/jcpe.13506
- Cheng, L. Y., Jordan, L., Chen, H. S., Kang, D., Oxford, L., Plemons, J., et al. (2017). Chronic Periodontitis Can Affect the Levels of Potential Oral Cancer Salivary mRNA Biomarkers. *J. Periodontol Res.* 52 (3), 428–437. doi: 10.1111/jre.12407
- Connolly, J. M., Davies, K., Kazakeviciute, A., Wheatley, A. M., Dockery, P., Keogh, I., et al. (2016). Non-Invasive and Label-Free Detection of Oral Squamous Cell Carcinoma Using Saliva Surface-Enhanced Raman Spectroscopy and Multivariate Analysis. *Nanomedicine* 12 (6), 1593–1601. doi: 10.1016/j.nano.2016.02.021
- Cristaldi, M., Mauceri, R., Di Fede, O., Giuliana, G., Campisi, G., and Panzarella, V. (2019). Salivary Biomarkers for Oral Squamous Cell Carcinoma Diagnosis and Follow-Up: Current Status and Perspectives. *Front. Physiol.* 10. doi: 10.3389/fphys.2019.01476
- Culhane, K., Jiang, K., Neumann, A., and Pinchuk, A. O. (2017). Laser-Fabricated Plasmonic Nanostructures for Surface-Enhanced Raman Spectroscopy of Bacteria Quorum Sensing Molecules. *MRS Adv.* 2 (42), 2287–2294. doi: 10.1557/adv.2017.98
- Curtis, M. A., Diaz, P. I., and Van Dyke, T. E. (2020). The Role of the Microbiota in Periodontal Disease. *Periodontol* 2000 83 (1), 14–25. doi: 10.1111/prd.12296
- Curtis, M. A., Gillett, I. R., Griffiths, G. S., Maiden, M. F., Sterne, J. A., Wilson, D. T., et al. (1989). Detection of High-Risk Groups and Individuals for Periodontal Diseases: Laboratory Markers From Analysis of Gingival Crevicular Fluid. *J. Clin. Periodontol* 16 (1), 1–11. doi: 10.1111/j.1600-051x.1989.tb01604.x
- Daniel, A., Calado, G., Behl, I., Flint, S., Galvin, S., Healy, C., et al. (2020). “Comparative Study of Oral Dysplasia by Conventional and Surface Enhanced Raman Spectroscopy of Whole Saliva,” in *Biomedical Vibrational Spectroscopy 2020: Advances in Research and Industry* San Francisco, California, United States: Event: SPIE BiOS. Eds. W. Petrich and Z. Huang
- Daood, U., Abduljabbar, T., Al-Hamoudi, N., and Akram, Z. (2018). Clinical and Radiographic Periodontal Parameters and Release of Collagen Degradation Biomarkers in Naswar Dippers. *J. Periodontol Res.* 53 (1), 123–130. doi: 10.1111/jre.12496
- Daood, U., Burrow, M., and Yiu, C. (2019). Effect of a Novel Quaternary Ammonium Silane Cavity Disinfectant on Cariogenic Biofilm Formation. *Clin. Oral. Invest.* 24 (2), 649–661. doi: 10.1007/s00784-019-02928-7
- Daood, U., Burrow, M. F., and Yiu, C. K. Y. (2020a). Effect of a Novel Quaternary Ammonium Silane Cavity Disinfectant on Cariogenic Biofilm Formation. *Clin. Oral. Investig.* 24 (2), 649–661. doi: 10.1007/s00784-019-02928-7
- Daood, U., Matinlinna, J. P., Pichika, M. R., Nagendrababu, V., and Mak, K. K. (2020b). A Quaternary Ammonium Silane Antimicrobial Triggers Bacterial Membrane and Biofilm Destruction. *Sci. Rep.* 10 (10970). doi: 10.1038/s41598-020-67616-z
- Darvin, M. E., Gersonde, I., Albrecht, H., Meinke, M., Sterry, W., and Lademann, J. (2010). Non-Invasive *In Vivo* Detection of the Carotenoid Antioxidant Substance Lycopene in the Human Skin Using the Resonance Raman Spectroscopy. *Laser Phys. Lett.* 3 (9), 460–463. doi: 10.1002/lapl.200610032
- Darvin, M. E., Patzelt, A., Meinke, M., Sterry, W., and Lademann, J. (2009). Influence of Two Different IR Radiators on the Antioxidative Potential of the Human Skin. *Laser Phys. Lett.* 6, 3, 229–234. doi: 10.1002/lapl.200810124
- Delhaye, M., and Dhamelincourt, P. (2010). Raman Microprobe and Microscope With Laser Excitation. *J. Raman Spectrosc.* 3 (1), 33–43. doi: 10.1002/jrs.1250030105
- Dumal, S., Hole, A., Choudhary, S., Naidu, I., Bhubna, S., and Krishna, C. M. (2020). “Serum Raman Spectroscopy: Exploring Delineation of Oral Premalignant Disorders,” in *Optical Diagnostics and Sensing Xx: Toward Point-Of-Care Diagnostics*. San Francisco, California, United States. Ed. G. L. Cote

- Fălămaș, A., Rotaru, H., and Hedeșiu, M. (2020a). Surface-Enhanced Raman Spectroscopy (SERS) Investigations of Saliva for Oral Cancer Diagnosis. *Lasers Med. Sci.* 35 (6), 1393–1401. doi: 10.1007/s10103-020-02988-2
- Falamas, A., Faur, C. I., Baciut, M., Rotaru, H., Chirila, M., Pinzaru, S. C., et al (2020b). Raman Spectroscopic Characterization of Saliva for the Discrimination of Oral Squamous Cell Carcinoma. *Anal. Lett.* 54 (8), 1–13. doi: 10.1080/00032719.2020.1719129
- Featherstone, J. D. (2004). The Continuum of Dental Caries—Evidence for a Dynamic Disease Process. *J. Dent. Res.* 83, C39–C42. doi: 10.1177/154405910408301s08
- Fleischmann, M., Hendra, P. J., and McQuillan, A. J. (1974). Raman Spectra of Pyridine Adsorbed at a Silver Electrode. *Chem. Phys. Lett.* 26 (2), 163–166. doi: 10.1016/0009-2614(74)85388-1
- Garnero, P., Ferreras, M., Karsdal, M. A., Nicamhlaibh, R., Risteli, J., Borel, O., et al. (2010). The Type I Collagen Fragments ICTP and CTX Reveal Distinct Enzymatic Pathways of Bone Collagen Degradation. *J. Bone Miner. Res.* 18 (5), 859–867. doi: 10.1359/jbmr.2003.18.5.859
- Gatin, E., Nagy, P., Paun, I., Dubok, O., Bucur, V., and Windisch, P. (2019). Raman Spectroscopy: Application in Periodontal and Oral Regenerative Surgery for Bone Evaluation. *Innovation Res. Biomed.* 40 (5), 279–285. doi: 10.1016/j.irbm.2019.05.002
- Ghosh, A., Raha, S., Dey, S., Chatterjee, K., Chowdhury, A. R., and Barui, A. (2019). Chemometric Analysis of Integrated FTIR and Raman Spectra Obtained by Non-Invasive Exfoliative Cytology for the Screening of Oral Cancer. *Analyst* 144 (4), 1309–1325. doi: 10.1039/c8an02092b
- Gieroba, B., Krysa, M., Wojtowicz, K., Wiater, A., Pleszczyńska, M., Tomczyk, M., et al. (2020). The FT-IR and Raman Spectroscopies as Tools for Biofilm Characterization Created by Cariogenic Streptococci. *Int. J. Mol. Sci.* 21 (11), 3811. doi: 10.3390/ijms21113811
- Gonchukov, S. A., and Sukhinina, A. V. (2011). Periodontitis Diagnostics on the Basis of Saliva Raman Spectroscopy. *Lasers Med. Sci.* 1, S23–S24.
- Gonchukov, S., Sukhinina, A., Bakmutov, D., and Minaeva, S. (2011). Raman Spectroscopy of Saliva as a Perspective Method for Periodontitis Diagnostics. *Laser Phys. Lett.* 9 (1), 73–77. doi: 10.1002/lapl.201110095
- Guentsch, A., Fahmy, M. D., Wehrle, C., Nietzsche, S., and Krafft, C. (2019). Effect of Biomimetic Mineralization on Enamel and Dentin: A Raman and EDX Analysis. *Dental Mater.* 35 (9), 1300–1307. doi: 10.1016/j.dental.2019.05.025
- Guo, L., Ye, C., Cui, L., Wan, K., Chen, S., Zhang, S., et al. (2019). Population and Single Cell Metabolic Activity of UV-Induced VBNC Bacteria Determined by CTC-FCM and D(2)O-Labeled Raman Spectroscopy. *Environ. Int.* 130, 104883. doi: 10.1016/j.envint.2019.05.077
- Hajishengallis, G., Darveau, R. P., and Curtis, M. A. (2012). The Keystone-Pathogen Hypothesis. *Nat. Rev. Microbiol.* 10 (10), 717–725. doi: 10.1038/nrmicro2873
- Hajishengallis, G., and Lamont, R. J. (2012). Beyond the Red Complex and Into More Complexity: The Polymicrobial Synergy and Dysbiosis (PSD) Model of Periodontal Disease Etiology. *Mol. Oral. Microbiol.* 27 (6), 409–419. doi: 10.1111/j.2041-1014.2012.00663.x
- Han, S., Locke, A. K., Oaks, L. A., Cheng, Y. S. L., and Cote, G. L. (2019). Nanoparticle-Based Assay for Detection of S100P mRNA Using Surface-Enhanced Raman Spectroscopy. *J. Biomed. Optics* 24 (5), 1–9. doi: 10.1117/1.Jbo.24.5.055001
- Harris, A. T., Rennie, A., Waqar-Uddin, H., Wheatley, S. R., Ghosh, S. K., Martin-Hirsch, D. P., et al. (2010). Raman Spectroscopy in Head and Neck Cancer. *Head Neck Oncol.* 2, 26. doi: 10.1186/1758-3284-2-26
- Hass, V., Cardenas, A., Siqueira, F., Pacheco, R. R., and Loguercio, A. D. (2019). Bonding Performance of Universal Adhesive Systems Applied in Etch-And-Rinse and Self-Etch Strategies on Natural Dentin Caries. *Operative Dent.* 44 (5), 510–520. doi: 10.2341/17-252-L
- Hernández-Cedillo, A., Valdivieso, M. G. G., Hernández-Arteaga, A. C., Marín, N. P., and Navarro-Contreras, H. R. (2019). Determination of Sialic Acid Levels by Using Surface-Enhanced Raman Spectroscopy in Periodontitis and Gingivitis. *Oral. Dis.* 25 (6), 1627–1633. doi: 10.1111/odi.13141
- Howell, S. C., Haffajee, A., Pagonis, T. C., and Guze, K. A. (2011). Laser Raman Spectroscopy as a Potential Chair-Side Microbiological Diagnostic Device. *J. Endod.* 37 (7), 968–972. doi: 10.1016/j.joen.2011.03.027
- Ide, M., McPartlin, D., Coward, P. Y., Crook, M., Lumb, P., and Wilson, R. F. (2003). Effect of Treatment of Chronic Periodontitis on Levels of Serum Markers of Acute-Phase Inflammatory and Vascular Responses. *J. Clin. Periodontol.* 30 (4), 334–340. doi: 10.1034/j.1600-051x.2003.00282.x
- Jeanmaire, D. L., and Dwyne, R. P. V. (1977). Surface Raman Spectroelectrochemistry: Part I. Heterocyclic, Aromatic, and Aliphatic Amines Adsorbed on the Anodized Silver Electrode. *J. Electroanal. Chem. Interfacial Electrochem.* 84 (1), 1–20. doi: 10.1016/S0022-0728(77)80224-6
- Jeng, M. J., Sharma, M., Sharma, L., Chao, T. Y., Huang, S. F., Chang, L. B., et al. (2019). Raman Spectroscopy Analysis for Optical Diagnosis of Oral Cancer Detection. *J. Clin. Med.* 8 (9), 1313. doi: 10.3390/jcm8091313
- Jung, G. B., Kim, K. A., Han, I., Park, Y. G., and Park, H. K. (2014). Biochemical Characterization of Human Gingival Crevicular Fluid During Orthodontic Tooth Movement Using Raman Spectroscopy. *Biomed. Opt. Express* 5, 10, 3508–3520. doi: 10.1364/BOE.5.003508
- Kassebaum, N. J., Bernabé, E., Dahiya, M., Bhandari, B., Murray, C. J., and Marcenes, W. (2014). Global Burden of Severe Periodontitis in 1990–2010: A Systematic Review and Meta-Regression. *J. Dent. Res.* 93 (11), 1045–1053. doi: 10.1177/0022034514552491
- Kassebaum, N. J., Smith, A. G. C., Bernabé, E., Fleming, T. D., Reynolds, A. E., Vos, T., et al. (2017). Global, Regional, and National Prevalence, Incidence, and Disability-Adjusted Life Years for Oral Conditions for 195 Countries—2015: A Systematic Analysis for the Global Burden of Diseases, Injuries, and Risk Factors. *J. Dent. Res.* 96 (4), 380–387. doi: 10.1177/0022034517693566
- Kerr, J. E., Arndt, G. D., Byerly, D. L., Rubinovitz, R., Theriot, C. A., and Stangel, I. (2016). FT-Raman Spectroscopy Study of the Remineralization of Microwave-Exposed Artificial Caries. *J. Dent. Res.* 95 (3), 342–348. doi: 10.1177/0022034515619370
- Kim, S. C., Kim, O. S., Kim, O. J., Kim, Y. J., and Chung, H. J. (2010). Antioxidant Profile of Whole Saliva After Scaling and Root Planing in Periodontal Disease. *J. Periodontal Implant Sci.* 40 (4), 164–171. doi: 10.5051/jpis.2010.40.4.164
- Klokkevold, P. R. (2015). *Carranza's Clinical Periodontology. 12th edition* (Saunders Elsevier).
- Kong, K., Kendall, C., Stone, N., and Nottingher, I. (2015). Raman Spectroscopy for Medical Diagnostics—From *in-Vitro* Biofluid Assays to *in-Vivo* Cancer Detection. *Adv. Drug Delivery Rev.* 89, 121–134. doi: 10.1016/j.addr.2015.03.009
- Krafft, C., and Popp, J. (2015). The Many Facets of Raman Spectroscopy for Biomedical Analysis. *Anal. Bioanal. Chem.* 407 (3), 699–717. doi: 10.1007/s00216-014-8311-9
- Kriem, L. S., Wright, K., Ccahuana-Vasquez, R. A., and Rupp, S. (2020). Confocal Raman Microscopy to Identify Bacteria in Oral Subgingival Biofilm Models. *PLoS One* 15 (5), e0232912. doi: 10.1371/journal.pone.0232912
- Kriem, L. S., Wright, K., Ccahuana-Vasquez, R. A., and Rupp, S. (2021). Mapping of a Subgingival Dual-Species Biofilm Model Using Confocal Raman Microscopy. *Front. Microbiol.* 12, 729720. doi: 10.3389/fmicb.2021.729720
- Krishna, H., Majumder, S. K., Chaturvedi, P., Sidramesh, M., and Gupta, P. K. (2014). *In Vivo* Raman Spectroscopy for Detection of Oral Neoplasia: A Pilot Clinical Study. *J. Biophoton.* 7 (9), 690–702. doi: 10.1002/jbio.201300030
- Krishna, C. M., Sockalingum, G. D., Kurien, J., Rao, L., Venteo, L., Pluot, M., et al. (2004). Micro-Raman Spectroscopy for Optical Pathology of Oral Squamous Cell Carcinoma. *Appl. Spectrosc.* 58 (9), 1128–1135. doi: 10.1366/0003702041959460
- Kumar, P., Bhattacharjee, T., Ingle, A., Maru, G., and Krishna, C. M. (2016). Raman Spectroscopy of Experimental Oral Carcinogenesis: Study on Sequential Cancer Progression in Hamster Buccal Pouch Model. *Technol. Cancer Res. Treat.* 15 (5), Np60–Np72. doi: 10.1177/1533034615598622
- Lumachi, F., Basso, S. M. M., and Basso, U. (2008). “Breast Cancer Recurrence: Role of Serum Tumor Markers CEA and CA 15-3,” in *Methods of Cancer Diagnosis, Therapy and Prognosis: Breast Carcinoma*. Ed. M. A. Hayat (Dordrecht: Springer Netherlands), 109–115.
- Lu, H., Zhao, Q., Guo, J., Zeng, B., Yu, X., Yu, D., et al. (2019). Direct Radiation-Induced Effects on Dental Hard Tissue. *Radiat. Oncol.* 14 (1), 5. doi: 10.1186/s13014-019-1208-1
- Madathil, G. C., Iyer, S., Thankappan, K., Gowd, G. S., Nair, S., and Koyakutty, M. (2019). A Novel Surface Enhanced Raman Catheter for Rapid Detection, Classification, and Grading of Oral Cancer. *Adv. Healthc. Mater.* 8 (13), e1801557. doi: 10.1002/adhm.201801557
- Malik, A., Sahu, A., Singh, S. P., Deshmukh, A., Chaturvedi, P., Nair, D., et al. (2017). *In Vivo* Raman Spectroscopy-Assisted Early Identification of Potential

- Second Primary/Recurrences in Oral Cancers: An Exploratory Study. *Head Neck* 39 (11), 2216–2223. doi: 10.1002/hed.24884
- Mian, S. A., Yorucu, C., Ullah, M. S., Rehman, I. U., and Colley, H. E. (2017). Raman Spectroscopy can Discriminate Between Normal, Dysplastic and Cancerous Oral Mucosa: A Tissue-Engineering Approach. *J. Tissue Eng. Regen. Med.* 11 (11), 3253–3262. doi: 10.1002/term.2234
- Milly, H., Festy, F., Watson, T. F., Thompson, I., and Banerjee, A. (2014). Enamel White Spot Lesions can Remineralise Using Bio-Active Glass and Polyacrylic Acid-Modified Bio-Active Glass Powders. *J. Dent.* 42 (2), 158–166. doi: 10.1016/j.jdent.2013.11.012
- Miranda, R. R. D., Silva, A. C. A., Dantas, N. O., Soares, C. J., and Novais, V. R. (2019). Chemical Analysis of *In Vivo*-Irradiated Dentine of Head and Neck Cancer Patients by ATR-FTIR and Raman Spectroscopy. *Clin. Oral. Invest.* 23 (8), 3351–3358. doi: 10.1007/s00784-018-2758-6
- Moisoit, V., Stefancu, A., Gulei, D., Boitor, R., Magdo, L., Raduly, L., et al. (2019). SERS-Based Differential Diagnosis Between Multiple Solid Malignancies: Breast, Colorectal, Lung, Ovarian and Oral Cancer. *Int. J. Nanomed.* 14, 6165–6178. doi: 10.2147/ijn.S198684
- Morris, M. D. (1999). Guest Editorial: Special Section on Biomedical Applications of Vibrational Spectroscopic Imaging. *J. Biomed. Optics* 4 (1), 6. doi: 10.1117/1.429907
- Nieberler, M., Häußler, P., Kesting, M. R., Kolk, A., Deppe, H., Weirich, G., et al. Clinical Impact of Intraoperative Cytological Assessment of Bone Resection Margins in Patients With Head and Neck Carcinoma. *Ann. Surg. Oncol.* 23 (11), 3579–3586. doi: 10.1245/s10434-016-5208-1
- Nixon, D. E., and Smith, G. A. (1986). Comparison of Jarrell-Ash, Perkin-Elmer, and Modified Perkin-Elmer Nebulizers for Inductively Coupled Plasma Analysis. *Anal. Chem.* 58 (13), 2886–2888. doi: 10.1021/ac00126a069
- Occhi-Alexandre, I. G. P., Baesso, M. L., Sato, F., de Castro-Hoshino, L. V., Rosalen, P. L., Terada, R. S. S., et al. (2018). Evaluation of Photosensitizer Penetration Into Sound and Decayed Dentin: A Photoacoustic Spectroscopy Study. *Photodiagn. Photodyn. Ther.* 21, 108–114. doi: 10.1016/j.pdpdt.2017.11.008
- Panikkanvalappil, S. R., Mackey, M. A., and El-Sayed, M. A. (2013). Probing the Unique Dehydration-Induced Structural Modifications in Cancer Cell DNA Using Surface Enhanced Raman Spectroscopy. *J. Am. Chem. Soc.* 135 (12), 4815–4821. doi: 10.1021/ja400187b
- Par, M., Spanovic, N., Taubck, T. T., Attin, T., and Tarle, Z. (2019). Degree of Conversion of Experimental Resin Composites Containing Bioactive Glass 45S5: The Effect of Post-Cure Heating. *Entific Reports* 9 (1), 17245. doi: 10.1038/s41598-019-54035-y
- Pavel, M., and Nicholas, S. (1900). Prospects for the Diagnosis of Breast Cancer by Noninvasive Probing of Calcifications Using Transmission Raman Spectroscopy. *J. Biomed. Optics* 12 (2), 024008. doi: 10.1117/1.2718934
- Peres, M. A., Macpherson, L. M. D., Weyant, R. J., Daly, B., Venturelli, R., Mathur, M. R., et al. (2019). Oral Diseases: A Global Public Health Challenge. *Lancet* 394 (10194), 249–260. doi: 10.1016/s0140-6736(19)31146-8
- Perillo, L., d'Apuzzo, F., Illario, M., Laino, L., Spigna, G. D., Lepore, M., et al. (2020). Monitoring Biochemical and Structural Changes in Human Periodontal Ligaments During Orthodontic Treatment by Means of Micro-Raman Spectroscopy. *Sensors (Basel)* 20 (2), 497. doi: 10.3390/s20020497
- Pezzotti, G., Adachi, T., Gasparutti, I., Vincini, G., Zhu, W., Boffelli, M., et al. (2017). Vibrational Monitor of Early Demineralization in Tooth Enamel After *In Vitro* Exposure to Phosphoric Liquid. *Spectrochim. Acta A Mol. Biomol. Spectrosc.* 173, 19–33. doi: 10.1016/j.saa.2016.08.036
- Pezzotti, G., Bock, R. M., McEntire, B. J., Jones, E., Boffelli, M., Zhu, W., et al. (2016). Silicon Nitride Bioceramics Induce Chemically Driven Lysis in *Porphyromonas* Gingivalis. *Langmuir* 32 (12), 3024–3035. doi: 10.1021/acs.langmuir.6b00393
- Raman, C. V. K., and XXXS, K. (1928). A New Type of Secondary Radiation. *Nature (London)* 121, 501–502. doi: 10.1038/121501c0
- Righolt, A. J., Jevdjevic, M., Marcenes, W., and Listl, S. (2018). Global-, Regional-, and Country-Level Economic Impacts of Dental Diseases in 2015. *J. Dent. Res.* 97 (5), 501–507. doi: 10.1177/0022034517750572
- Rodrigues, J. A., Sarti, C. S., Assuncao, C. M., Arthur, R. A., Lussi, A., and Diniz, M. B. (2017). Evaluation of Laser Fluorescence in Monitoring Non-Cavitated Caries Lesion Progression on Smooth Surfaces *In Vitro*. *Lasers Med. Sci.* 32 (8), 1793–1800. doi: 10.1007/s10103-017-2262-2
- Sahu, A., Gera, P., Malik, A., Nair, S., Chaturvedi, P., and Krishna, C. M. (2019). Raman Exfoliative Cytology for Prognosis Prediction in Oral Cancers: A Proof of Concept Study. *J. Biophoton.* 12 (8), e201800334. doi: 10.1002/jbio.201800334
- Sahu, A., Gera, P., Pai, V., Dubey, A., Tyagi, G., Waghmare, M., et al. (2017). Raman Exfoliative Cytology for Oral Precancer Diagnosis. *J. BioMed. Opt.* 22 (11), 1–12. doi: 10.1117/1.Jbo.22.11.115003
- Sahu, A., Nandakumar, N., Sawant, S., and Krishna, C. M. (2015). Recurrence Prediction in Oral Cancers: A Serum Raman Spectroscopy Study. *Analyst* 140 (7), 2294–2301. doi: 10.1039/c4an01860e
- Selwitz, R. H., Ismail, A. I., and Pitts, N. B. (2007). Dental Caries. *Lancet* 369 (9555), 51–59. doi: 10.1016/s0140-6736(07)60031-2
- Seredin, P., Goloshchapov, D., Prutsik, T., and Ippolitov, Y. (2015). Phase Transformations in a Human Tooth Tissue at the Initial Stage of Caries. *PLoS One* 10 (4), e0124008. doi: 10.1371/journal.pone.0124008
- Shiue, I. (2015). Urinary Thiocyanate Concentrations Are Associated With Adult Cancer and Lung Problems: US NHANE-2012. *Environ. Sci. Pollut. Res. Int.* 22 (8), 5952–5960. doi: 10.1007/s11356-014-3777-8
- Singh, S. P., Ibrahim, O., Byrne, H. J., Mikkonen, J. W., Koistinen, A. P., Kullaa, A. M., et al. (2016). Recent Advances in Optical Diagnosis of Oral Cancers: Review and Future Perspectives. *Head Neck* 38, E2403–E2411. doi: 10.1002/hed.24293
- Smalley, J. W., Silver, J., Birss, A. J., Withnall, R., and Titler, P. J. (2003). The Haem Pigment of the Oral Anaerobes *Prevotella Nigrescens* and *Prevotella Intermedia* is Composed of Iron(III) Protoporphyrin IX in the Monomeric Form. *Microbiol. (Reading)* 149 (Pt 7), 1711–1718. doi: 10.1099/mic.0.26258-0
- Suzuki, S., Kataoka, Y., Kanehira, M., Kobayashi, M., Miyazaki, T., and Manabe, A. (2019). Detection of Enamel Subsurface Lesions by Swept-Source Optical Coherence Tomography. *Dent. Mater. J.* 38 (2), 303–310. doi: 10.4012/dmj.2017-404
- Tan, Y., Yan, B., Xue, L., Li, Y., Luo, X., and Ji, P. (2017). Surface-Enhanced Raman Spectroscopy of Blood Serum Based on Gold Nanoparticles for the Diagnosis of the Oral Squamous Cell Carcinoma. *Lipids Health Dis.* 16 (1), 73. doi: 10.1186/s12944-017-0465-y
- Tao, Y., Wang, Y., Huang, S., Zhu, P., Huang, W. E., Ling, J., et al. (2017). Metabolic-Activity-Based Assessment of Antimicrobial Effects by D(2)O-Labeled Single-Cell Raman Microspectroscopy. *Anal. Chem.* 89 (7), 4108–4115. doi: 10.1021/acs.analchem.6b05051
- Toledano, M., Aguilera, F. S., Osorio, E., Cabello, I., Toledano-Osorio, M., and Osorio, R. (2015a). Self-Etching Zinc-Doped Adhesives Improve the Potential of Caries-Affected Dentin to be Functionally Remineralized. *Biointerphases* 10 (3), 031002. doi: 10.1116/1.4926442
- Toledano, M., Aguilera, F. S., Osorio, E., Lopez-Lopez, M. T., Cabello, I., Toledano-Osorio, M., et al. (2015b). On Modeling and Nanoanalysis of Caries-Affected Dentin Surfaces Restored With Zn-Containing Amalgam and *In Vitro* Oral Function. *Biointerphases* 10 (4), 041004. doi: 10.1116/1.4933243
- Toledano, M., Osorio, E., Aguilera, F. S., Toledano-Osorio, M., López-López, M. T., and Osorio, R. (2019). Stored Potential Energy Increases and Elastic Properties Alterations are Produced After Restoring Dentin With Zn-Containing Amalgams. *J. Mech. Behav. BioMed. Mater.* 91, 109–121. doi: 10.1016/j.jmbbm.2018.12.002
- Tsuge, K., Kataoka, M., and Seto, Y. (2000). Cyanide and Thiocyanate Levels in Blood and Saliva of Healthy Adult Volunteers. *J. Health Sci.* 46 (5), 343–350. doi: 10.1248/jhs.46.343
- Wang, J., Lin, D., Lin, J., Yu, Y., Huang, Z., Chen, Y., et al. (2014). Label-Free Detection of Serum Proteins Using Surface-Enhanced Raman Spectroscopy for Colorectal Cancer Screening. *J. Biomed. Optics* 19 (8), 087003. doi: 10.1117/1.JBO.19.8.087003
- Witkowska, E., Łasica, A. M., Niciński, K., Potempa, J., and Kamińska, A. (2021). In Search of Spectroscopic Signatures of Periodontitis: A SERS-Based Magnetomicrofluidic Sensor for Detection of *Porphyromonas* Gingivalis and *Aggregatibacter Actinomycetemcomitans*. *ACS Sens.* 6 (4), 1621–1635. doi: 10.1021/acssensors.1c00166
- Xue, L., Yan, B., Li, Y., Tan, Y., Luo, X., and Wang, M. (2018). Surface-Enhanced Raman Spectroscopy of Blood Serum Based on Gold Nanoparticles for Tumor Stages Detection and Histologic Grades Classification of Oral Squamous Cell Carcinoma. *Int. J. Nanomed.* 13, 4977–4986. doi: 10.2147/ijn.S167996
- Yang, S., Li, B., Akkus, A., Akkus, O., and Lang, L. (2014). Wide-Field Raman Imaging of Dental Lesions. *Analyst* 139 (12), 3107–3114. doi: 10.1039/c4an00164h

- Yang, H., Zhang, M. L., Yao, L. H., Zhou, M., and Ding, Y. (2020). Surface-Enhanced Raman Scattering-Based Immunoassay of Two Cytokines in Human Gingival Crevicular Fluid Of Periodontal Disease. *J. Appl. Spectrosc.* 86 (6), 1077–1083. doi: 10.1007/s10812-020-00943-1
- Yan, B., Li, B., Wen, Z., Luo, X., Xue, L., and Li, L. (2015). Label-Free Blood Serum Detection by Using Surface-Enhanced Raman Spectroscopy and Support Vector Machine for the Preoperative Diagnosis of Parotid Gland Tumors. *BMC Cancer* 15, 650. doi: 10.1186/s12885-015-1653-7
- Yan, B., Li, Y., Yang, G., Wen, Z. N., Li, M. L., and Li, L. J. (2011). Discrimination of Parotid Neoplasms From the Normal Parotid Gland by Use of Raman Spectroscopy and Support Vector Machine. *Oral. Oncol.* 47 (5), 430–435. doi: 10.1016/j.oraloncology.2011.02.021
- Yasser, M., Shaikh, R., Chilakapati, M. K., and Teni, T. (2014). Raman Spectroscopic Study of Radioresistant Oral Cancer Sublines Established by Fractionated Ionizing Radiation. *PloS One* 9 (5), e97777. doi: 10.1371/journal.pone.0097777
- Zhang, J., Lynch, R. J. M., Watson, T. F., and Banerjee, A. (2019). Chitosan-Bioglass Complexes Promote Subsurface Remineralisation of Incipient Human Carious Enamel Lesions. *J. Dent.* 84, 67–75. doi: 10.1016/j.jdent.2019.03.006
- Conflict of Interest:** The authors declare that the research was conducted in the absence of any commercial or financial relationships that could be construed as a potential conflict of interest.
- Publisher's Note:** All claims expressed in this article are solely those of the authors and do not necessarily represent those of their affiliated organizations, or those of the publisher, the editors and the reviewers. Any product that may be evaluated in this article, or claim that may be made by its manufacturer, is not guaranteed or endorsed by the publisher.

Copyright © 2022 Zhang, Ren, Wang, Wen, Liu and Ding. This is an open-access article distributed under the terms of the Creative Commons Attribution License (CC BY). The use, distribution or reproduction in other forums is permitted, provided the original author(s) and the copyright owner(s) are credited and that the original publication in this journal is cited, in accordance with accepted academic practice. No use, distribution or reproduction is permitted which does not comply with these terms.





# The Application of Small Molecules to the Control of Typical Species Associated With Oral Infectious Diseases

## OPEN ACCESS

### Edited by:

Prasanna Neelakantan,  
The University of Hong Kong,  
Hong Kong SAR, China

### Reviewed by:

Hua Xie,  
Meharry Medical College,  
United States  
Armelia Sari Widyarman,  
Trisakti University, Indonesia  
Xuan Li,  
The University of Hong Kong,  
Hong Kong SAR, China

### \*Correspondence:

Ran Yang  
yangran@scu.edu.cn  
Xin Xu  
xin.xu@scu.edu.cn

<sup>†</sup>These authors have contributed  
equally to this work

### Specialty section:

This article was submitted to  
Microbiome in Health and Disease,  
a section of the journal  
Frontiers in Cellular and  
Infection Microbiology

**Received:** 16 November 2021

**Accepted:** 28 January 2022

**Published:** 21 February 2022

### Citation:

Yang S, Lyu X, Zhang J, Shui Y,  
Yang R and Xu X (2022) The  
Application of Small Molecules to the  
Control of Typical Species Associated  
With Oral Infectious Diseases.  
*Front. Cell. Infect. Microbiol.* 12:816386.  
doi: 10.3389/fcimb.2022.816386

Sirui Yang<sup>1,2†</sup>, Xiaoying Lyu<sup>1†</sup>, Jin Zhang<sup>1,2</sup>, Yusen Shui<sup>1</sup>, Ran Yang<sup>1,3\*</sup> and Xin Xu<sup>1,2\*</sup>

<sup>1</sup> State Key Laboratory of Oral Diseases, National Clinical Research Center for Oral Diseases, West China Hospital of Stomatology, Sichuan University, Chengdu, China, <sup>2</sup> Department of Cariology and Endodontics, West China Hospital of Stomatology, Sichuan University, Chengdu, China, <sup>3</sup> Department of Pediatric Dentistry, West China Hospital of Stomatology, Sichuan University, Chengdu, China

Oral microbial dysbiosis is the major causative factor for common oral infectious diseases including dental caries and periodontal diseases. Interventions that can lessen the microbial virulence and reconstitute microbial ecology have drawn increasing attention in the development of novel therapeutics for oral diseases. Antimicrobial small molecules are a series of natural or synthetic bioactive compounds that have shown inhibitory effect on oral microbiota associated with oral infectious diseases. Novel small molecules, which can either selectively inhibit keystone microbes that drive dysbiosis of oral microbiota or inhibit the key virulence of the microbial community without necessarily killing the microbes, are promising for the ecological management of oral diseases. Here we discussed the research progress in the development of antimicrobial small molecules and delivery systems, with a particular focus on their antimicrobial activity against typical species associated with oral infectious diseases and the underlying mechanisms.

**Keywords:** oral microbiota, small molecules, antimicrobial agents, dental plaque biofilm, dental caries, periodontal diseases

## INTRODUCTION

The oral microbiota, including more than 700 microbial species, are the most complicated microbial communities in human body (Dewhirst et al., 2010). According to the ecological plaque hypothesis, oral microbial dysbiosis leads to the occurrence of oral infectious diseases including dental caries and periodontal diseases, which seriously endanger oral and general health (Theilade, 1986).

*Streptococcus mutans* is well recognized as the major cariogenic species due to its capability of adhesion to tooth surfaces, generation of acid through sugar fermentation, and tolerance and persistence in acidic microenvironment (Hamada et al., 1984; Banas, 2004; Bowen et al., 2018). Currently, the homeostasis between pathogenic and commensal bacteria has attracted increasing attention in the etiology and pathogenesis of dental caries. Dental caries is believed to be initiated by

the imbalanced microecology and the overgrowth of acidogenic/aciduric bacteria such as *S. mutans* (Tanner et al., 2016; Samaranayake and Matsubara, 2017). In addition to caries, the microbiological etiology of periodontitis has also been indicated in recent years (Riep et al., 2009). *Porphyromonas gingivalis*, *Tannerella forsythia*, and *Treponema denticola*, commonly known as the “red complex”, are well recognized as the principal pathogens associated with periodontal destruction (Socransky et al., 1998). Currently, periodontitis is believed to be the consequence of a broadly-based dysbiotic alteration in periodontal microbiota, whereby some keystone species such as *P. gingivalis* triggers the development of this disease (Hajishengallis and Lamont, 2012). *Candida albicans* is a commensal fungal species colonizing human oral mucosal surfaces. In the immunocompromised individuals, *C. albicans* becomes opportunistic pathogen causing mucosal and disseminated infections (Metwalli et al., 2013). Intriguingly, *C. albicans* robustly interacts with oral bacteria, and this cross-kingdom interaction enhances the virulence of both fungi and bacteria, and ultimately aggravates oral diseases (Dewhirst et al., 2010; Peters et al., 2012). It has been proven that *C. albicans* is closely involved in the occurrence of various oral diseases including early childhood caries, root caries, periodontitis, endodontic infections, oral mucositis and facial space infections (Krom et al., 2014).

As an adequate plaque control by mechanical means such as brushing and flossing is difficult to achieve by most patients, mouth rinses containing antimicrobial agents are considered as an effective adjuvant measure to control dental caries (Lim and Kam, 2008; Rath and Singh, 2013). Chlorhexidine (CHX) is widely used to control oral pathogens due to its robust antimicrobial activity and broad spectrum (Jones, 1997). However, CHX has drawbacks such as taste confusions, mucosal soreness, oral microbial dysbiosis and drug resistance, which limit its long-term application (Jones, 1997; Walsh et al., 2015). Bacterial drug resistance is one of the main threats to human health (Kumar and Balbach, 2017), limiting the options of clinical treatment for oral infectious diseases (Hegstad et al., 2010). Long-term use of CHX could cause microbial resistance in microbes, including *Staphylococcus aureus*, *Enterococcus faecalis* and *Klebsiella pneumoniae* (Wang et al., 2017). Therefore, novel agents are urgently needed to control oral infectious diseases. Antimicrobial small molecules are a series of natural or synthetic bioactive compounds showing good antimicrobial activity against microbiota associated with infectious diseases (Worthington et al., 2012). Small molecules can be developed via various approaches. Drug repurposing, drug screening from existing small-molecule libraries or natural resources, and target-based designing are most common approaches to the development of small molecules that target oral microbiota and consequently benefit oral infectious disease control. In this review, we aimed to discuss the research progress in the development of antimicrobial small molecules and delivery systems, with a particular focus on: 1) their antimicrobial activity against keystone bacteria including *S. mutans*, *P. gingivalis* and *C. albicans*; 2) their inhibitory effects on the pheromones that mediate interspecies communications within polymicrobial communities; 3) the research progress in the development of

delivery systems that enhance the antimicrobial activity of small molecules in the management of oral infectious diseases.

## SMALL MOLECULES THAT INHIBIT KEYSTONE BACTERIA ASSOCIATED WITH ORAL INFECTIOUS DISEASES

### *Streptococcus mutans*

*S. mutans* is generally recognized as the key cariogenic species, particularly due to its capability of driving the shift of oral microbiota towards a more acidogenic/aciduric community that ultimately causes tooth demineralization and visible decay (Marsh, 2010).

Different small molecular antibiotics from natural products and synthetic compounds have been identified against *S. mutans*. Drug-repositioning is a commonly used approach to the identification of antimicrobial agents that inhibit *S. mutans*. Nitrofurantoin, with a mode of action similar to that of nitroimidazole, shows inhibitory activity on oral bacteria such as *S. mutans* and *Enterococcus faecalis* (Silva et al., 2014; Ang et al., 2017). Based on the antimicrobial activity of nitrofurantoin, our group synthesized and identified a compound named ZY354, a water-soluble hybrid of indolin-2-one and nitrofurantoin, which showed potent antimicrobial activity and selectivity against *S. mutans* compared with CHX (Zhang et al., 2019). Saputo et al. (2018) screened and identified 126 FDA-approved small molecules that exhibited antimicrobial activity against planktonic growth of *S. mutans*, among which 24 drugs inhibited biofilm formation, 6 drugs killed pre-existing biofilms, and 84 drugs exhibited both bacteriostatic and bactericidal effects against *S. mutans* biofilms. Napabucasin (NAP) is a phase III clinical trials anticancer drug with antibacterial activity against *Escherichia coli*, *Streptococcus faecalis*, and *Staphylococcus aureus* (Kuate et al., 2007; Kuate et al., 2011). Our group repurposed NAP against oral streptococci and found good antimicrobial activity of NAP against *S. mutans* biofilms (Kuang et al., 2020). Besides, NAP showed relatively lower antibacterial effect on oral streptococci than CHX with mild cytotoxicity on oral cells. We further redesigned and synthesized a novel small molecule based on NAP, namely LCG-N25, which exhibited potent antibacterial activity, lessened cytotoxicity, and induced no drug resistance of cariogenic *S. mutans* (Lyu et al., 2021a). Chen et al. screened approximately 2600 compounds and identified an antagonist of calcium-sensing receptor, namely NPS-2143, which exhibited antimicrobial activity against methicillin-resistant *S. aureus* (MRSA) (Chen Y et al., 2019). Further modifications of NPS-2143 yield a compound II-6s (Chen Y et al., 2019). Our group demonstrated that II-6s effectively inhibited the growth of *S. mutans*, reduced EPS production and induced no drug resistance in *S. mutans* after repeated treatment as compared to CHX, indicating its potential use in the control of dental caries (Zhang J et al., 2021).

Phenotypic screening is also a reliable approach to the identification of new antimicrobials. Antigen I/II, also known as Pac, mediates the sucrose-independent adhesion of *S. mutans* (Munro et al., 1993; Jenkinson and Demuth, 1997; Love et al., 1997),

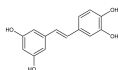
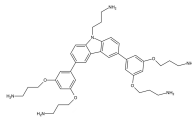
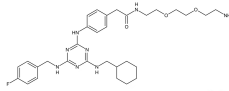
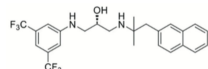
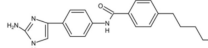
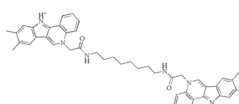
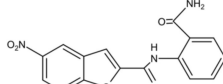
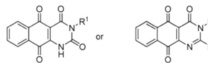
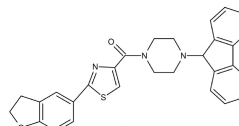
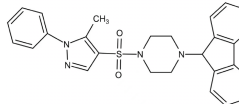
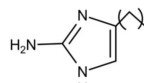
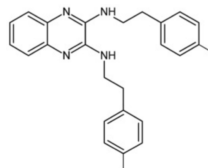
while Gtfs (GtfB, GtfC, and GtfD) mediate its sucrose-dependent adhesion (Bramstedt, 1968) and play an important role in the interspecies coaggregation and the development of oral biofilms (Bowen and Koo, 2011; Kim D et al., 2020). Rivera-Quiroga et al. performed a high-throughput screening of 883551 molecules, and identified three molecules, namely ZINC19835187 (ZI-187), ZINC19924939 (ZI-939) and ZINC 19924906 (ZI-906), which targeted antigen I/II and inhibited the adhesion of *S. mutans* with low cytotoxicity (Rivera-Quiroga et al., 2020). Wu et al. also screened and identified a molecule called 2A4, showing selectivity on *S. mutans* in multispecies biofilms via inhibiting antigens I/II and Gtfs (Liu et al., 2011). The same group also performed a structure-based virtual screening of 500,000 compounds against the GtfC catalytic domain and identified a lead compound, namely G43, which selectively bond GtfC and significantly inhibited the biofilm formation and cariogenicity of *S. mutans* (Zhang et al., 2017). They further synthesized an analog of G43, named III<sub>FI</sub>, which remarkably reduced dental caries in rats (Nijampatnam et al., 2021). Ren et al. screened 15000 molecules based on the structure of GtfC protein domain and identified a quinoxaline derivative, 2-(4-methoxyphenyl)-N-(3-[[2-(4-methoxyphenyl)ethyl]imino]-1,4-dihydro-2-quinoxalinyldene)ethanamine, which selectively bond GtfC, reduced the synthesis of insoluble glucans, inhibited *S. mutans* biofilm and reduced caries in rats (Ren et al., 2016). SrtA is membraned-bond transpeptidase that catalyzes surface protein antigen I/II, thus contributing to the biofilm formation of *S. mutans* (Lee and Boran, 2003; Krzysciak et al., 2014; Chen X et al., 2019; Wang et al., 2019). Recently, several SrtA inhibitors have been identified from either natural products or synthetic compounds (Park W et al., 2017; Song et al., 2017). Samanli et al. screened and identified a SrtA inhibitor, namely CHEMBL243796 (kurarinone), which showed better affinity to SrtA as compared to CHX (Salmanli et al., 2021). In addition to the aforementioned molecules that have been proven to inhibit antigen I/II and Gtfs, several synthetic molecules have been designed and showed antibacterial effects against *S. mutans*. Kim et al. synthesized a series of pyrimidinone or pyrimidindione-fused 1,4-naphthoquinones with antibacterial effects via pharmacophore hybridization, and some derivatives exhibited notable bacteriostatic and bactericidal effects against *S. mutans* in both resistant and sensitive strains (Kim K et al., 2020). Zhang et al. screened 100 trimetrexate (TMQ) analogs and identified 3 compounds with good selectivity against *S. mutans* (Zhang et al., 2015). Garcia et al. screened a series of 2-Aminoimidazole (2-AI) derivatives, and identified a small molecule 3F1, which specifically disturbed *S. mutans* biofilms and reduced caries in rats (Garcia et al., 2017). Besingi et al. screened and identified a benzoquinone derivative AA-861, which exhibited antibiofilm effects against *S. mutans* by targeting amyloid fibrils, an important scaffold in *S. mutans* biofilms (Besingi et al., 2017). Chen et al. also screened and identified a small molecule, namely D25, which targeted amyloid fibrils and selectively inhibited *S. mutans* biofilms (Chen et al., 2021).

Natural products and their derivatives also accounted for a large number of antimicrobial small molecules due to their structural diversity and biological activity (Davison and Brimble, 2019; Newman and Cragg, 2020). The tea polyphenols epigallocatechin

gallate (EGCG) has been identified to inhibit *S. mutans* for decades. EGCG not only inhibits planktonic bacteria but also reduces the biofilm formation of *S. mutans* by inhibiting Gtfs. In addition, EGCG can inhibit lactate dehydrogenase and F<sub>1</sub>F<sub>0</sub>-ATPase, and thus reduces the acidogenicity and aciduricity of *S. mutans* (Xu et al., 2011; Xu et al., 2012; Hairul Islam et al., 2020). A lipid-soluble green tea polyphenols which is designed based on EGCG, namely epigallocatechin-3-gallate-stearate (EGCG-S), shows an increased stability and antibiofilm activity comparable to CHX (Melok et al., 2018). Moreover, the EGCG is less cytotoxic compared with CHX, and shows anti-inflammatory effects on *S. mutans*-stimulated odontoblast-like cells (Stavroullakis et al., 2021), indicating a good prospect in the management of oral infectious diseases. Propolis and its derivatives such as apigenin and trans-trans farnesol (tt-farnesol) have been identified to show a good antimicrobial activity against *S. mutans* and exhibit notable biological activities against dental caries for decades (Koo et al., 2002; Koo et al., 2003; Cardoso et al., 2010; Veloz et al., 2016). Apigenin has been shown to inhibit Gtfs, specifically GtfB and GtfC. tt-farnesol shows anti-caries effects by reducing cell viability and destabilizing oral biofilms rather than affecting Gtfs activities (Koo et al., 2002; Koo et al., 2005; Jeon et al., 2011). Caffeic acid phenethyl ester (CAPE), another extracted compound from propolis, shows broad-spectrum antimicrobial activity against various microbes including *Enterococcus faecalis*, *S. aureus*, *Bacillus subtilis*, *Pseudomonas aeruginosa*, etc (Velazquez et al., 2007). Niu et al. showed that CAPE affected the morphology of *S. mutans* biofilms, inhibited biofilm formation and maturation and reduced EPS production (Veloz et al., 2019; Niu et al., 2020). In addition, plenty of other natural compounds have also been identified exhibiting antibacterial effects against *S. mutans*. Piceatannol, a plant-derived stilbene, can target GtfC domain and inhibit glucans production, and thus reduces *S. mutans* biofilms formation (Nijampatnam et al., 2018). Piceatannol can also inhibit F<sub>1</sub>F<sub>0</sub>-ATPase of *S. mutans*, and thus suppresses the aciduricity of *S. mutans* (Sekiya et al., 2019). In addition, curcumin, a phytopolyphenols from traditional medicine known as turmeric, and its analog desmethoxycurcumin (DMC), also show inhibitory effect on F<sub>1</sub>F<sub>0</sub>-ATPase of *S. mutans* and thus reduce its growth in acidic conditions (Sekiya et al., 2014; Nakanishi-Matsui et al., 2016; Sekiya et al., 2019). Ursolic acid, a plant-derived compound, shows inhibitory effects on EPS synthesis and biofilm formation of *S. mutans* (Kim et al., 2013; Lyu et al., 2021b). Astilbin, a flavanone compound from *Rhizoma Smilacis Glabrae* and  $\beta$ -sitosterol from kemangi, can inhibit SrtA activity and thus reduces the biofilm formation of *S. mutans* (Wang et al., 2019; Evangelina et al., 2021).

Small molecules designed for specific target is another approach to the inhibition of *S. mutans*. Charles et al. synthesized several peptides spanning residues 803-185 of antigen I/II, and identified a synthetic peptide p1025 that inhibited antigen I/II binding to salivary receptors by forming adhesion epitopes in a dose-dependent way. The effect of p1025 against *S. mutans* was relatively stable, and it was able to selectively inhibit *S. mutans* recolonization to tooth surface (Kelly et al., 1999; Younson and Kelly, 2004; Li et al., 2009). Small molecules that show inhibitory effects on *S. mutans* are summarized in **Table 1**.

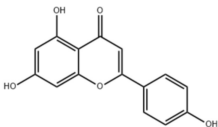
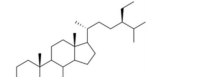
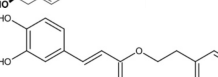
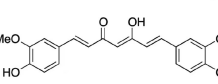
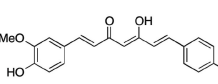
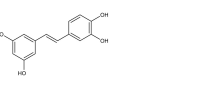
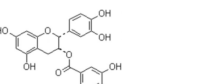
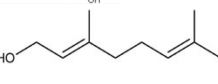
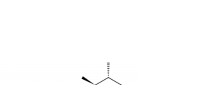
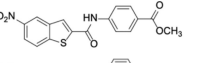
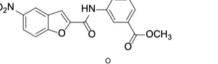
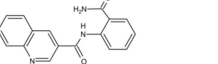
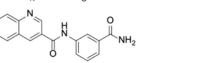
**TABLE 1 |** Small molecules that inhibit *S. mutans*.

Small molecules	Chemical structure	Mechanisms	Antimicrobial activity	Reference
Drug-repositioning				
LCG-N25		Inhibit both the planktonic cells and biofilms formation of <i>S. mutans</i>	MIC <sub>90</sub> : 0.5 µg/ml	(Lyu et al., 2021a)
MBC <sub>90</sub> : 15.6 µg/ml				
Napabucasin		Inhibit <i>S. mutans</i> biofilms	MIC <sub>90</sub> : 3.91 µg/ml MBC <sub>90</sub> : 15.63 µg/ml MBIC <sub>90</sub> : 1.95 µg/ml MBRC <sub>90</sub> : 62.5 µg/ml	(Kuang et al., 2020)
ZY354		Inhibit <i>S. mutans</i> growth and selectively inhibit the biofilm formation of <i>S. mutans</i>	MIC <sub>90</sub> : 0.24 µg/ml MBC <sub>90</sub> : 1.95 µg/ml MBIC <sub>90</sub> : 0.24 µg/ml MBRC <sub>90</sub> : 31.25 µg/ml	(Zhang et al., 2019)
II-6s		Inhibit growth and exopolysaccharides (EPS) generation of <i>S. mutans</i> ;  inhibit the demineralization of tooth enamel and induce no drug resistance in <i>S. mutans</i>	MIC <sub>90</sub> : 3.91 µg/ml MBC <sub>90</sub> : 15.63 µg/ml MBIC <sub>90</sub> : 3.91 µg/ml MBRC <sub>90</sub> : 62.5 µg/ml	(Zhang J et al., 2021)
Phenotypic screening from libraries				
Compound 3F1		Specifically disturb <i>S. mutans</i> biofilms in a mixed biofilm	MDC: 5 µM	(Garcia et al., 2017)
D25		Selectively inhibit <i>S. mutans</i> biofilms without interfering planktonic cells	Inhibit <i>S. mutans</i> biofilms at the concentration of 3.125–25 µg/mL	(Chen et al., 2021)
G43		Inhibit <i>S. mutans</i> biofilm formation by selectively binding to GtfC	Inhibit more than 85% of <i>S. mutans</i> biofilms at 12.5 µM	(Zhang et al., 2017)
Pyrimidinone or pyrimidinone-fused 1,4-naphthoquinones		Show bacteriostatic and bactericidal effects against <i>S. mutans</i> in both resistant and sensitive strains		(Kim K et al., 2020)
ZINC19835187 (ZI-187)		Inhibit <i>S. mutans</i> adhesion and biofilm formation by targeting antigens I/II	Show no inhibitory effects on <i>S. mutans</i> growth at 10–100–1000 µM	(Rivera-Quiroga et al., 2020)
ZINC19924939 (ZI-939)				
ZINC 19924906 (ZI-906)			Show inhibitory effects on adhesion than 90% at 200 µM (ZI-187 at 100 µM)	
2A4		Inhibit <i>S. mutans</i> adhesion and biofilm formation by targeting antigens I/II and glucosyltransferases (Gtfs)	MIC <sub>50</sub> : 2.0 ± 0.5 µM MBIC <sub>50</sub> : 0.94 ± 0.02 µM.	(Liu et al., 2011)
2-(4-methoxyphenyl)-N-([2-(4-methoxyphenyl)ethyl]imino)-1,4-dihydro-2-quinoxalinyldene)ethanamine		Inhibit the biofilm formation and destroy mature biofilms without killing <i>S. mutans</i> by inhibiting GtfC	Reduce 79% <i>S. mutans</i> biofilms cell viable count at 10 µg/ml	(Ren et al., 2016)
Natural products screening				

(Continued)



TABLE 1 | Continued

Small molecules	Chemical structure	Mechanisms	Antimicrobial activity	Reference
Apigenin		Inhibit Gtfs, specifically GtfB and GtfC;		(Koo et al., 2002; Koo et al., 2005)
$\beta$ -sitosterol from Kemangi		Inhibit <i>S. mutans</i> biofilm formation by inhibiting SrtA	MIC <sub>90</sub> : 25000 ppm MBC <sub>90</sub> : 50000 ppm	(Evangeline et al., 2021)
Caffeic acid phenethyl ester		Affect the thickness of <i>S. mutans</i> biofilms Inhibit biofilm formation and maturation by reducing EPS production Inhibit F1F0-ATPase and inhibit <i>S. mutans</i> growth	MIC <sub>90</sub> : 80 $\mu$ g/ml MBC <sub>90</sub> : 320 $\mu$ g/ml MBIC <sub>90</sub> : 80 $\mu$ g/ml MIC <sub>50</sub> : 6 $\mu$ M Inhibit activity of F1F0-ATPase by 74% at 30 $\mu$ M	(Velazquez et al., 2007; Veloz et al., 2019; Niu et al., 2020)
Curcumin				(Nijampatnam et al., 2018; Sekiya et al., 2019)
Desmethoxycurcumin				(Sekiya et al., 2014; Nakanishi-Matsui et al., 2016; Sekiya et al., 2019)
Piceatannol				
Epigallocatechin gallate (EGCG)		Inhibit <i>S. mutans</i> acid production, aciduricity, and biofilm formation	MIC <sub>90</sub> : 15.6 $\mu$ g/ml MBC <sub>90</sub> : 31.25 $\mu$ g/ml	(Xu et al., 2011; Xu et al., 2012; Melok et al., 2018; Hairul Islam et al., 2020; Stavroullakis et al., 2021)
Trans-trans farnesol		Disrupt membrane integrity, destabilize oral biofilms and reduce the intracellular iodophilic polysaccharides (IPS) accumulation of <i>S. mutans</i> Lipophilic moiety interaction with bacterial membrane	MIC <sub>90</sub> : 125 $\mu$ M MBC <sub>90</sub> : 500 $\mu$ M	(Koo et al., 2002; Koo et al., 2005)
Ursolic acid		Inhibit biofilm formation and maturation by reducing EPS production	MIC <sub>90</sub> : 7.8 $\mu$ g/ml MBC <sub>90</sub> : 15.6 $\mu$ g/ml	(Kim et al., 2013; Lyu et al., 2021b)
Target-base designing				
Compound III <sub>A6</sub>		Selectively bond GtfC and significantly inhibit the biofilm formation	MBIC <sub>50</sub> : 9.6 $\mu$ M	(Nijampatnam et al., 2021)
Compound III <sub>C5</sub>			MBIC <sub>50</sub> : 2.7 $\mu$ M	
Compound III <sub>F1</sub>			MBIC <sub>50</sub> : 15.3 $\mu$ M	
Compound III <sub>F2</sub>			MBIC <sub>50</sub> : 8.6 $\mu$ M	
P1025		Inhibit the adhesion and biofilm formation of <i>S. mutans</i>		(Kelly et al., 1999; Younson and Kelly, 2004; Li et al., 2009)

MIC, minimum inhibitory concentration; MBC, minimum bactericidal concentration; MBIC, minimum biofilm inhibition concentration; MBRC, minimum biofilm reduction concentration; MDC, concentration that a single dose of the small molecule needed to disperse 50% of the biofilm.

## Porphyromonas gingivalis

*P. gingivalis*, despite its relatively low abundance in the periodontal microbiota, has been well recognized as the keystone species of periodontitis (Kojima et al., 1993). *P. gingivalis* expresses Arg-specific cysteine proteinases (gingipains) that help the subversion

of recruited leukocytes, leading to uncontrolled overgrowth of other proteolytic and asaccharolytic bacteria in the microbial biofilm, which in turn elevate the complement-dependent destructive inflammation of periodontal tissue and stabilize the transition of periodontal microbiota to a disease-provoking consortium

(Hajishengallis et al., 2012; Hajishengallis, 2015). Specific inhibition of *P. gingivalis* could not only suppress its virulence to the periodontium, but also rescue the microbial dysbiosis induced by this keystone pathogen and ultimately shift the microbiota toward a community in favor of periodontal health (Hajishengallis et al., 2012).

The initial colonization of *P. gingivalis* in oral biofilms occurs in the supragingival biofilm (Wright et al., 2013). Adhesion of *P. gingivalis* to streptococci is critical for its pathogenicity. The minor fimbrial antigen (Mfa1) of *P. gingivalis* and streptococcal surface antigen I/II are involved in the interspecies adhesion (Park et al., 2005; Daep et al., 2011). Roky identified 3 small molecules, namely N7, N17 and V8 from high-throughput screening of ZINC library, that inhibited *P. gingivalis* adherence to streptococci and reduced its virulence *in vivo*. In addition, compound N17 and V8 showed low cytotoxic activity in both human and marine cells (Roky et al., 2020). Another synthetic compound PCP-III-201, firstly designed as an inhibitor that mimics the natural peptide substrate recognized by Mfa, showed marked inhibition on the adherence of *P. gingivalis* to streptococci by interfering Mfa and antigen I/II interaction, and thus disrupted the formation of mixed biofilms (Tan et al., 2018). 1,2,3-triazole-based peptidomimetics, another natural peptide substrate simulants of Mfa, exhibited inhibitory effect on *P. gingivalis* adherence to oral streptococci by inhibiting the interaction of antigen I/II and Mfa proteins (Patil et al., 2016). Similarly, “the second generation” 1,2,3-triazole-based peptidomimetics based on the first-generation diphenyloxazole were designed and showed inhibitory effect on *P. gingivalis* adherence to *S. gordonii*, indicating the potential use of triazole derivatives in the management of periodontitis (Patil et al., 2019). The major fimbriae of *P. gingivalis* is another adhesin which can bind streptococcal surface component glyceraldehyde-3-phosphate dehydrogenase (GAPDH) and mediates its adhesion to oral streptococci (Maeda et al., 2004; Daep et al., 2006). Three small molecules, namely 2A4, 2D11 and 2E11, which were screened from a library of small molecules based on the 2-aminoimidazole and 2-aminobenzimidazole scaffolds, showed inhibitory effects on *P. gingivalis* by down-regulating Mfa1 and fimA gene expression, thus inhibiting the adherence of *P. gingivalis* to oral streptococci (Wright et al., 2014).

Natural extract is another abundant resource for inhibitors against *P. gingivalis* (Abrao et al., 2021). Resveratrol, a natural compound with antimicrobial, antiviral and anticancer activities (Kolouchova et al., 2018), shows inhibitory effects on *P. gingivalis*. The minimum inhibitory concentrations (MIC) of resveratrol against *P. gingivalis* and other clinical strains are in the range of 78.12–156.25 µg/ml. Besides, resveratrol can reduce the *P. gingivalis* biofilm formation and its virulence by downregulating the expression of fimbriae (type II and IV) and proteinases (kpg and rgpA) (Kugaji et al., 2019). A study evaluated a variety of natural products from medicinal plants and identified quite a few small molecular compounds that inhibited the growth and biofilm formation of *P. gingivalis*. Intriguingly, some of the derivatives also inhibited gingipains (Kariu et al., 2017). A natural polyphenol, Quercetin (3,3',4',5,7-

pentahydroxyflavone), can inhibit gingipains activities and biofilm formation at sub-MIC concentrations. In addition, quercetin down-regulates the expression of virulence-associated genes of *P. gingivalis* (He et al., 2020). Quantum curcumin, a derivative of curcumin, shows notable inhibitory effects on planktonic cells and biofilms of *P. gingivalis*, particularly *via* inhibition of gingipain R and K (Singh et al., 2019).

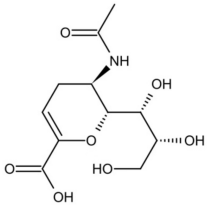
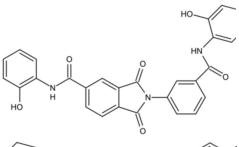
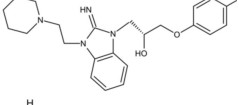
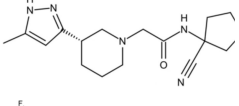
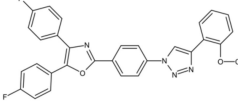
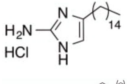
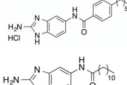
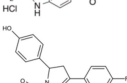
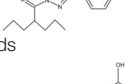
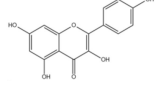
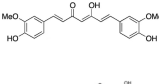
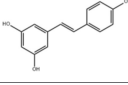
In addition, several other small molecules have also showed anti-inflammatory effects against periodontitis induced by *P. gingivalis*. Lei et al. synthesized a series of valproic acid pyrazole conjugates, and the most effective molecules 7c not only showed antibacterial effects against *P. gingivalis*, but also reduced inflammation by inhibiting TNF-α, IL-1β and IL-6 (Dong et al., 2021). A sialidase inhibitor, 2-deoxy-2,3-didehydro-N-acetylneuraminic acid (DANA), showed effects on reducing pathogenicity of *P. gingivalis* and exhibited anti-inflammatory prospect (Yu et al., 2021). Small molecules that inhibit *P. gingivalis* are summarized in **Table 2**.

## Candida albicans

*C. albicans* is an opportunistic pathogen in the oral cavity, which can cause oral fungal infections and increase the risk of oral epithelial carcinogenesis (Mayer et al., 2013). In addition, *C. albicans* robustly interacts with oral streptococci and can drive the microbial shift toward a more pathogenic microbiota that favors or aggravates the development of oral infectious diseases such as dental caries and periodontitis (Hajishengallis and Lamont, 2012).

Azoles, especially fluconazole (FLC) are the frontline treatment against fungal infections. However, with increasing drug resistance to current azole antifungals, small molecules have become a promising source for the development of novel antifungals (Kett et al., 2021). Azole antifungals inhibit sterol 14α-demethylase (CYP51), resulting in synthesis disorder of ergosterol thereby affecting cell membrane integrity. Synthetic small molecules targeting CYP51 or inhibiting the synthesis of ergosterol are common strategies to inhibit *C. albicans*. Two kinds of small molecular azole derivatives (i.e. short and extended derivatives), have shown good binding affinity to CYP51, and thus potently inhibit CYP51 activity and the growth of *C. albicans* (Binjubair et al., 2020). Drug repurposing is also a promising approach to the identification of antifungals against *C. albicans* (Ashburn and Thor, 2004). A novel 1,2,4-triazole-indole hybrid molecule, (2-(2,4-Dichlorophenyl)-3-(1H-indol-1-yl)-1-(1,2,4-1H-triazol-1-yl)propan-2-ol, namely 8g, showed a broad-spectrum activity against *Candida* with low cytotoxicity, probably due to its inhibitory effects on ergosterol synthesis and phospholipase A2-like activity (Pagniez et al., 2020). Monika et al. synthesized a series of benzoxazole derivatives showing equivalent effects to commercially used azoles, which either interacted with exogenous ergosterol or blocked the synthesis of endogenous ergosterol. Among the library of 23 benzoxazoles featuring 2-mercaptobenzoxazole with the phenacyl moiety or respective alcohols, compound 5d showed good stability and water solubility, representing a good candidate in the treatment of andida infection (Staniszewska et al., 2021a).

**TABLE 2** | Small molecules that inhibit *P. gingivalis*.

Small molecules	Chemical structure	Mechanisms	Antimicrobial activity	Reference
Synthetic molecules				
DANA		Inhibit growth and biofilm formation. Reduce expression of the <i>fimA</i> , <i>fimR</i> , and <i>fimS</i> genes and decrease gingipains activity. Inhibit TNF- $\alpha$ , IL-1 $\beta$ , and iNOS production in LPS-stimulated macrophages and prevent alveolar bone absorption and inhibited TNF- $\alpha$ and IL-1 $\beta$ production <i>in vivo</i> .	Inhibit <i>P. gingivalis</i> growth and biofilm formation at 1 mM	(Yu et al., 2021)
N7		Inhibit <i>P. gingivalis</i> adherence to streptococci and reduced its virulence		(Roky et al., 2020)
N17				
V8				
PCP-III-201		Inhibit the adherence of <i>P. gingivalis</i> to streptococci by interfering Mfa and antigen/I/I interaction, and disrupt the formation of mixed biofilms	Inhibit 50% the incorporation of <i>P. gingivalis</i> into the three-species biofilm at 15 $\mu$ M Inhibit preformed three-species biofilm in a dose-dependent way.	(Tan et al., 2018)
1,2,3-triazole-based peptidomimetics		Inhibit <i>P. gingivalis</i> adherence to <i>S. gordonii</i> by inhibiting the interaction of antigen I/I and Mfa proteins		(Patil et al., 2016; Patil et al., 2019)
2A4		Inhibit <i>P. gingivalis</i> , and downregulate Mfa1 and <i>fimA</i> gene expression	MIC <sub>90</sub> : 20 $\mu$ M	(Wright et al., 2014)
2D11			MIC <sub>50</sub> : 4.73 $\mu$ M $\pm$ 1.77	
2E11			MIC <sub>50</sub> : 6.88 $\mu$ M $\pm$ 1.45	
7c		Inhibit microorganisms responsible for periodontitis including <i>P. gingivalis</i> , and exhibit notable effects on reducing inflammation by inhibiting TNF- $\alpha$ , IL-1 $\beta$ and IL-6	MIC <sub>90</sub> : 0.05 $\mu$ g/ml	(Dong et al., 2021)
Natural Compounds				
Quercetin		Inhibit gingipains activities and biofilm formation, and down-regulate the virulence-associated gene expressions of <i>P. gingivalis</i>	MIC <sub>90</sub> : 200 $\mu$ M MBC <sub>90</sub> : 400 $\mu$ M	(He et al., 2020)
Quantum curcumin		Inhibit planktonic cells and biofilms cells of <i>P. gingivalis</i> . In addition, inhibit gingipains.		(Singh et al., 2019)
Resveratrol		Inhibit the growth of <i>P. gingivalis</i> Reduce the <i>P. gingivalis</i> biofilm formation and its virulence by downregulating the expression of fimbriae and proteinases	MIC <sub>90</sub> : 156.25 $\mu$ g/ml MBC <sub>90</sub> : 312.5 $\mu$ g/ml	(Kugaji et al., 2019)

MIC, minimum inhibitory concentration; MBC, minimum bactericidal concentration; MBIC, minimum biofilm inhibition concentration; MBRC, minimum biofilm reduction concentration.

*C. albicans* can form biofilms on the mucosal surface, which not only increase its virulence but also lead to drug resistance (Lohse et al., 2018). A study screened the Chembridge Small Molecule Diversity library containing 30,000 small molecules and identified 45 compounds which inhibited biofilm formation. Further investigation identified 4 compounds, namely CB06, CB14, CB36 and CB40, which inhibited biofilm formation and destroyed mature biofilm alone or in combination with other antifungals such as fluconazole and caspofungin (Lohse et al., 2020). Monika et al. screened 20 dibromobenzimidazole derivatives and identified a small molecule, namely 5h, which showed inhibitory effects on cell wall and reduced biofilm formation of *Candida albicans*. Besides, 5h was identified as a mitochondrial inhibitor of both *C. albicans* and *C. neoformans*, indicating its potential in the anti-fungal treatment (Staniszewska et al., 2021b).

Morphological transformation between hyphae and yeast phase in *C. albicans* is also relevant to its virulence and drug resistance (Vediyappan et al., 2013). A recent study repurposed 18 non-antifungal agents including antipsychotics, antiarrhythmics, proton pump inhibitors (PPIs), and identified 7 drugs that inhibited *C. albicans* in a dose-dependent manner, among which, chlorpromazine (CHL) and prochlorperazine (PCP) were fungicidal and the other 5 fungistatic. In addition, 3 candidate compounds, including chlorpromazine, prochlorperazine and drotaverine, inhibited germ tube formation (Kathwate et al., 2021). A high-throughput in silico study screened 584 compounds and identified 5 candidate molecules, namely U73122, disulfiram, BSK805, BIX01294, and GSKJ4, among which disulfiram showed excellent antifungal effects and inhibited 50% growth of *C. albicans* SC5314 strain at the concentration of 1mg/ml. Disulfiram also inhibited 50% growth of *C. albicans* biofilms at a concentration ranging from 32–128 mg/ml (Hao et al., 2021). A series of non-peptidic analogues of the broad-spectrum host defense peptides (HDPs) have also shown antifungal activities (Ryan et al., 2014). A compound 4 (C4) screened from HDP-mimic compound library can kill both the yeast and hyphal form of *C. albicans* at a concentration of 8 µg/ml (Menzel et al., 2017), suggesting a potential use in the control of invasive candidiasis.

*C. albicans* has several adhesins such as glutenin-like sequence (Als) family (Als1–Als7 and Als9), which mediate its adhesion to the host surface (Hoyer, 2001). Among Als family, the protein Als3 plays an important role in adhesion and hypha formation (Murciano et al., 2012). A small molecule, F2768-0318, shows inhibitory effects on the virulence factors related to adhesion and biofilm formation by inhibiting Als3 protein (Shinobu-Mesquita et al., 2020). Besides, machineries that modulate the stress responses are linked to fungal resistance. Heat shock protein 90 (Hsp90), an essential molecule in the stress responses of eukaryotes is also involved in the morphological transformation and drug resistance of *C. albicans* (Cowen and Lindquist, 2005; Taddei et al., 2014; Tiwari et al., 2015; Whitesell et al., 2019), and thus represents a promising target for the development of small molecules against Candidal infection. Yuan et al. screened 4 hsp90 inhibitors and identified a most potential compound, namely

ganetespib, which exhibited significant synergistic activity with fluconazole in both planktonic cells and biofilms. The ganetespib in combination with FLC also down-regulated the expression of azole-targeting enzyme *ERG11* and efflux pump *CDR1*, *CDR2*, and *MDR1*. The synergistic effects of ganetespib with FLC *in vivo* also indicating its potential use as an antifungal enhancer of azoles in *Candida* infections (Yuan et al., 2021).

The over-expressed drug efflux pump on the cell membrane is another common virulence trait of *C. albicans* being related to azole resistance. Development of compounds that inhibit efflux pump and increase the concentration of drugs in the cell is a classic strategy to increase fluconazole sensitivity (Coste et al., 2004; Holmes et al., 2016). Kali et al. screened 2454 small molecules against *C. auris* and identified a bis-benzodioxolylindolinone CMLD012336, a 3,3-diarylated oxindole (also called azoffluxin), which showed synergistic interaction with fluconazole against a resistant strain of *C. auris*. Mechanistically, azoffluxin increased fluconazole sensitivity in both *C. auris* and *C. albicans* by inhibiting efflux pump *CDR1* (Iyer et al., 2020). Another compound screened from a series of synthesized cyclobutene-dione (squarile) small molecules library, namely compound A, also showed inhibitory effect on MFS efflux pump CaMdr1p, and thus sensitized AD/CaMDR1 to FLC (Keniya et al., 2015). In addition, a small molecule ENOblock showed good inhibitory effects alone and in combination with FLC against *C. albicans* hypha and biofilm formation *in vivo*. Mechanistically, ENOblock interacted with CaEno1 and significantly inhibited the transglutaminase activity of CaEno1, and thus affected the growth and morphogenesis of *C. albicans* (Li et al., 2019). Small molecules that show inhibitory effects against *C. albicans* are summarized in **Table 3**.

## SMALL MOLECULES THAT INHIBIT QUORUM SENSING SYSTEM

Different microorganisms exist in oral microbiota, and the robust microbial interactions have close relationship with host health and diseases. Small molecules which disrupt microorganism interactions may rescue the microbial disequilibrium, contributing to the management of oral infectious diseases. Quorum sensing (QS) system, a mechanism of microbial interaction, involves signaling molecules that enable a cell to sense cell density (Padder et al., 2018). It relies on the production, release and recognition of self-induced signal molecules and regulates various biological behaviors including biofilm formation, microbial virulence and resistance (Papenfort and Bassler, 2016). Small signal molecules concentrated in the extracellular environment mediate QS in fungi. The mechanisms accountable for the accumulation of these molecules include passive diffusion, efflux pumps and specific transporters (Padder et al., 2018).

ComA is a critical component of *S. mutans* QS system (Havarstein et al., 1995). Ishii et al. found a compound that inhibited the peptidase domain (PEP) of ComA, thus disrupting the QS system and inhibiting biofilm formation of *S. mutans*. This compound also inhibited the PEP of *Streptococcus*



**TABLE 3** | Small molecules that inhibit *C. albicans*.

Small molecules	Chemical structure	Mechanisms	Antimicrobial activity	Reference
Drug-repositioning				
8g		Show broad-spectrum activity against <i>Candida</i> with low cytotoxicity due to its inhibitory effects on ergosterol synthesis and phospholipase A2-like activity	MIC <sub>90</sub> : 0.5 µg/ml Inhibit ergosterol production by 82% and induced production of 14a-methyl sterols at 4µg/ml	(Pagniez et al., 2020)
5d		Interact with exogenous ergosterol as well as block the synthesis of endogenous ergosterol.	MIC <sub>90</sub> : 16 µg/ml	(Staniszewska et al., 2021a)
Phenotypic screening from molecule libraries				
azofluxin		Increase fluconazole sensitivity in both <i>C. auris</i> and <i>C. albicans</i> by inhibiting efflux pump CDR1		(Iyer et al., 2020)
Compound A		Inhibit MFS efflux pump CaMdr1p	FICI<0.05	(Keniya et al., 2015)
CB06		Inhibit biofilm formation and destroy mature biofilm in combination with other antifungals	Inhibit biofilm formation in the presence of FLC at 12.5µM	(Lohse et al., 2020)
CB14		Destroy mature biofilm in the presence of caspofungin at 12.5µM		
CB36		Inhibit biofilm formation and destroy mature biofilm in the presence of caspofungin at 12.5µM		
CB40		Destroy mature biofilm in the presence of caspofungin at 12.5µM		
C4		Kill both the yeast and hyphal form of <i>C. albicans</i>	MIC <sub>90</sub> : 2 µg/ml MFC <sub>90</sub> : 8 µg/ml	(Menzel et al., 2017)
Disulfiram		Inhibit <i>C. albicans</i> planktonic cells and biofilms	MIC <sub>50</sub> : 1 mg/ml sMIC <sub>50</sub> : 32-128 mg/ml	(Hao et al., 2021)
ENOblock		Show effects alone or in combination with FLC against <i>C. albicans</i> hypha and biofilm formation <i>in vivo</i> . Interact with CaEno1 and inhibit the transglutaminase activity of CaEno1 in <i>C. albicans</i>	MIC <sub>90</sub> : 32 µg/ml FICI<0.5 ( <i>C. albicans</i> 0304103)	(Li et al., 2019)
F2768-0318		Inhibit <i>virulence factors</i> related to adhesion and biofilm formation by inhibiting Als3 protein	MIC <sub>90</sub> : 256 µg/ml MFC <sub>90</sub> : 256 µg/ml	(Shinobu-Mesquita et al., 2020)
Ganetespiob		Show synergistic activity with fluconazole in both planktonic cells and biofilms, and down-regulate the expression of azole-targeting enzyme gene <i>ERG11</i> and efflux pump genes <i>CDR1</i> , <i>CDR2</i> , and <i>MDR1</i>	FICI<0.05	(Yuan et al., 2021)
5h		Inhibit cell wall and inhibit biofilm formation. Inhibit mitochondrion in both <i>C. albicans</i> ref and <i>C. neoformans</i>	MIC <sub>50</sub> : 8 µg/ml	(Staniszewska et al., 2021b)

MIC, minimum inhibitory concentrations; MFC, minimum fungicidal concentrations; sMIC, sessile minimum inhibitory concentrations; FICI, fractional inhibitory concentration index.

*pneumoniae* and *Streptococcus. oralis* (Ishii et al., 2017). Kaur et al. synthesized a compound called 1,3-disubstituted urea derivatives, which inhibited the activity of ComA by binding to the active sites of PEP. 1,3-disubstituted urea derivatives was able to inhibit the formation of *S. mutans* biofilm alone or in combination with low concentration fluoride (Kaur et al., 2016). DMTU (1,3-di-m-tolyl-urea) is an aromatic compound showing antibiofilm effects against *Streptococcus mutans* by inhibiting its quorum sensing pathway (comDE) (Kaur et al., 2017). In addition, DMTU significantly inhibited the formation of multispecies biofilms consisting of *Streptococcus gordonii*, *Fusobacterium nucleatum*, *Porphyromonas gingivalis* and *Aggregatibacter actinomycetemcomitans* at 12.5  $\mu$ M without affecting cell viability. DMTU also down-regulated the expression of virulence genes in *P. gingivalis* such as *mfaI*, *rgpA* and *rgpB* (Kalimuthu et al., 2020).

Autoinducier-2 (AI-2) is an auto QS molecule that is produced and recognized by *S. mutans*, *S. gordonii*, *P. gingivalis* and *Fusobacterium nucleatum* (Shao and Demuth, 2010). Park et al. (Park JS et al., 2017) found that 3-(dibromomethylene) isobenzofuran-1(3H)-one derivatives inhibited the activity of AI-2 in *F. nucleatum* and reduced its biofilm formation. Another study found that D-galactose not only inhibited AI-2 activity, but also dose-dependently inhibited the biofilm formation of *F. nucleatum*, *P. gingivalis*, and *T. forsythia* (Ryu et al., 2016).

## NOVEL DRUG DELIVERY SYSTEMS OF ANTIMICROBIAL SMALL MOLECULES

Drug delivery system (DDS) is an advanced means that improves the therapeutic characteristics of conventional drugs over the last few decades. Various pharmacological properties of drugs, such as pharmacokinetics and biodistribution can be altered by using small-scale DDS such as nanoparticles (NP) and microparticles. Currently, nanotechnology has been extensively explored in DDS concerning the antimicrobial properties of drugs. The incorporation of drugs into nanoparticles and nanocomposites by physical encapsulation, adsorption, or chemical conjugation, can notably enhance the pharmacokinetics and therapeutic efficacy of the drugs in the treatment of infectious diseases as compared to their free counterparts (Zhang et al., 2010). In recent years, nano-based delivery system containing small molecular antimicrobials, either derived from natural or synthetic compounds, has attracted increasing attentions in the field of oral microbial infection control. Nowadays, since antimicrobial resistance (AMR) has been arousing global concerns in the clinical practice, a variety of innovative nanotechnologies have been applied to improve the therapeutic properties of small molecules. Antimicrobial small molecules can be conjugated with or encapsulated into various nanoparticles including organic polymers and metallic nanoparticles (MNPs), exhibiting elevated solubility (Yang et al., 2009; Nicolosi et al., 2015), biocompatibility (Wang et al., 2020) and controlled release (Barman et al., 2014), and thus benefit the control of oral infectious diseases.

## Organic Polymers

### Polysaccharides

Polysaccharides are notable for targeted drug delivery systems as natural biomaterials. Polysaccharides are inexpensive and possess promising biocompatibility and biodegradability. In the polysaccharides-based drug delivery system, the loaded agents can be absorbed into external compartments or limited within the external surface, which can augment the stability and aqueous solubility of drugs (Barclay et al., 2019). Maghsoudi et al. compared the anticariogenic activities of three curcumin-loaded polysaccharide nanoparticles including starch, alginate and chitosan. The results showed that polysaccharide nanoparticles possessed enhanced antimicrobial activities as compared to pure curcumin. Among the three curcumin-loaded polysaccharide nanoparticles, the chitosan nanoparticles showed the largest amount of release and the best anticariogenic properties particularly at lower pH (Maghsoudi et al., 2017). Jahanizadeh et al. incorporated carboxymethyl starch (CMS), a modified starch with unique negatively charged groups with chitosan to develop a novel curcumin-loaded nanocomposite. This nanocomposite showed enhanced antimicrobial and antibiofilm properties against *S. mutans*. Meanwhile, this nanocomposite had a smaller nanoscale with an average size of 35.9 nm and exhibited excellent curcumin entrapment efficiency of 91% (Jahanizadeh et al., 2017).

### Poly Lactic-Co-Glycolic Acid Copolymer

Poly lactic-co-glycolic acid (PLGA) is a synthetic polymer extensively utilized in the field of drug delivery system due to its biocompatible, biodegradable and sustained-release characteristics (Kapoor et al., 2015). Numerous PLGA-based drug delivery systems have been designed with different hydrophilic moieties such as poly ethylene glycol (PEG) or poly ethylene oxide (PEO) to increase the solubility of small molecules (Mir et al., 2017). Gürsu et al. synthesized farnesol-loaded PLGA nanoparticles to enhance the bioavailability of farnesol. PLGA chemically interacted with the OH group of farnesols, and 22.5% of the equivalent amounts of nanoparticles achieved a similar inhibitory effect against *C. albicans* (Gürsu, 2020). Ahmadi et al. modified a photoexcited orthodontic adhesive by incorporating curcumin-loaded PLGA nanoparticles and explored its anti-biofilm effects against *S. mutans*, shear bond strength (SBS) and adhesive remnant index (ARI). The results showed that the antimicrobial activity of the blue laser-7% wt. Curcumin-PLGA nanoparticles was comparable to 2% chlorhexidine. Moreover, the modified adhesive showed the highest SBS value and comparable ARI relative to the original pure adhesive (Ahmadi et al., 2020).

## Liposome

Liposome owns many critical clinical features, especially excellent biocompatibility and capability of encapsulating both hydrophilic and hydrophobic compounds (Samad et al., 2007). The most attractive feature of liposome delivery systems is enhancing pharmacokinetic properties and bactericidal activities of the new or existing drugs as well as reducing their

drugs' adverse effects (Alhariri et al., 2013). Nicolosi et al. reported that fusidic acid-loaded fusogenic liposomes increased the antimicrobial activities and broadened the antimicrobial spectrum in contrast to free drugs. The fusogenic small unilamellar vesicles may elevate the penetration of lipophilic drug into microorganisms and thus improve its antimicrobial properties (Nicolosi et al., 2015). However, the nanocarrier without being activated by specific stimuli cannot specifically reach and work in the targeting sites *in vivo*. Controlled drug release is promising for the trigger-release of liposomes in the clinical applications (Bibi et al., 2012). Mizukami et al. developed two enzyme-activity-triggered drug release systems by combining an antimicrobial peptide temporin L (TL) with surface-anionic liposomes. Protease and phosphatase were chosen as the target enzymes. For the protease-triggered system, a branched peptide that suppressed membrane-damaging activity was fabricated by modifying the cationic Lys residue of TL. As for the phosphatase-triggered system, a neutral amino acid with an anionic phosphorylated amino acid in the lipophilic region of TL was replaced. The phosphopeptides alleviated its membrane-damaging activity so that controlled release was achieved (Mizukami et al., 2017).

## Metallic Nanoparticles

Metallic nanoparticles can efficiently cope with resistant microbial strains due to its potential antimicrobial activity (Rai et al., 2017). A vast number of studies have demonstrated that silver nanoparticles have strong antimicrobial activities against various microorganisms including resistant pathogens (Rai et al., 2017). However, the toxicity of silver and many other metallic nanoparticles limits their clinical application (Mizukami et al., 2017). Yin et al. developed silver nanoparticles containing EGCG as reducing agent, which showed elevated biocompatibility than silver nitrate (AgNO<sub>3</sub>). Moreover, it also exhibited much lower MIC and MBC against *S. mutans* and potently inhibited acid and polysaccharide production (Yin et al., 2019). In contrast to other NPs, gold NPs (Au NPs) have many advantages, including controllable synthesis, versatility in surface modification, and admirable biocompatibility (Zhao et al., 2013; Yang et al., 2017). Although gold NPs usually show weak inherent antimicrobial activities (Rai et al., 2017), they can be modified or coated on different surfaces to function with antimicrobial properties. Wang, et al. synthesized a series of N-heterocyclic molecule-coated gold NPs, among which 2-mercaptoimidazole (MI)- and 3-amino-1,2,4-triazole-5-thiol (ATT)-capped Au NPs showed broad-spectrum antibiofilm activities against MDR bacteria, including MRSA and MDR *Escherichia coli* (MDR *E. coli*). These NPs directly contacted and disrupted the cell wall of microorganisms, thus less likely to induce antimicrobial resistance. Moreover, taking into account the advantages of ultrasound-assisted coating method being highly durable and able to withstand a large number of washing cycles, Wang et al. used sonochemistry to coat Au NPs on the surface of fabrics, which showed excellent antimicrobial activity (Wang et al., 2020). S. Jabir et al. also reported that a linalool loaded on glutathione-modified gold nanoparticles in spherical shape was antimicrobial against gram-positive bacteria representing a

biocompatible and less complicated and time-consuming approach to the delivery of antimicrobial small molecules (Jabir et al., 2018). Lu et al. developed a small molecule 2-mercapto-1-methylimidazole-capped Chitosan-functionalized nanocomposites whose cationic amine rendered transport of the nanocomposites towards the negatively charged bacterial cell surface. With the alliance between small Imidazol molecules and gold nanoparticles, the nanocomposites exhibited bactericidal and biofilm disruption effects against both Gram-negative *E. coli* and Gram-positive *S. aureus*. Besides, these nanocomposites can be easily synthesized with low toxicity, showing good potential in clinical applications (Jabir et al., 2018). Apart from incorporating with inherent antimicrobial small molecules, Zhao et al. incorporated a non-antimicrobial molecule 4,6-diamino-2-pyrimidinethiol (DAPT) with Au-NPs. The DAPT-decorated Au-NPs was able to inhibit most of MDR Gram-negative bacteria such as *E. coli* and MDR *Pseudomonas aeruginosa* by suppressing energy metabolism and damaging bacterial membrane (Zhao et al., 2010).

## Tetrahedral Framework Nucleic Acids

In recent years, tetrahedral framework nucleic acids (tFNAs) have attracted increasing attention due to their editability and biocompatibility (Zhang et al., 2020). Drug delivery based tFNAs has been proposed and investigated broadly over the past years (Li et al., 2021; Zhang et al., 2022). Zhang et al. synthesized tFNA/His-5, and by the modification of tFNAs, His-5 showed increased transport efficiency and improved anti-fungal effect (Zhang B et al., 2021). Moreover, Zhang et al. also developed tFNAs with a controllable conformation as a delivery vehicle for antisense oligonucleotides, which provided a better platform for the applications of antisense antibacterial therapeutics (Zhang et al., 2018). Besides, Sun et al. found tFNAs-ampicillin had a better antimicrobial effect and lower levels of drug resistance development than free ampicillin (Sun et al., 2020). However, it is doubtful that tFNAs could carry some molecules that are beyond their size and weight. Besides, attaching nucleic acids with complex secondary structures may inhibit the uptake process. Wider potential to deliver different cargos still need to be explored (Zhang et al., 2020).

## Virus-Derived Nanoparticles

Although metallic nanoparticles have been explored as nanocarriers for small molecular antimicrobials, its accumulation within human body and interactions with organs and microenvironment have aroused concerns for its potential toxicity. Metallic nanoparticles can also stimulate the expression of cytokines that generate cytotoxicity, immunotoxicity, and genotoxicity (Zazo et al., 2017). To avoid these side effects, organic nanoparticles have attracted increasing attentions. Currently, virus-derived nanoparticles (VNPs), a self-assembly-competent protein have shown advantages such as biodegradable, cost-effective and highly modifiable (Verma et al., 2018). Velázquez-Lam et al. conjugated EGCG to turnip mosaic virus (TuMV) particles, and the EGCG-TuMV VNPs not only maintained TuMV structure but also exhibited elevated antimicrobial and antibiofilm activities compared with free

EGCG. Moreover, EGCG-VNP showed a high stability after six months of being stored at 4°C. Of note, the various modifiable sites of VNPs provide the versatility for novel nanocarriers in drug delivery system (Velaázquez-Lam et al., 2020).

## CONCLUSION

Oral microbial dysbiosis is the most essential causative factor for common oral infectious diseases including dental caries and periodontal diseases. Small molecules with potent antimicrobial activity, high selectivity, and low toxicity are promising for the ecological management of oral diseases. Many small molecules have already been repurposed, screened and designed. However, many issues have yet to be solved. Although antimicrobial activities have been revealed for many small molecules, their mode of action and underlying mechanism are still unclear. The exact targets of some novel small molecules have yet to be identified. Therefore, structural modifications and optimization based on the candidates with confirmed mechanism and targets are promising. In addition, although the antimicrobial activity of small molecules against the keystone pathogens such as *S. mutans* and *P. gingivalis* has been demonstrated, their

ecological impact on the disease-provoking microbiota still needs further investigation in a more sophisticated microbial consortium and validation *in vivo*. Small molecules that disrupt microbial interactions without necessarily killing the bacteria is also promising, particularly in the light of robust advancement in the development of drug delivery system that enhances its substantivity and specificity. Finally, comprehensive evaluation of the long-term cytotoxicity *in vivo* is still needed to better translate those promising candidates to the clinical application.

## AUTHOR CONTRIBUTIONS

RY and XX conceived and designed the review. SY, XL, JZ, and YS wrote the first draft of the manuscript. RY and XX helped revise the manuscript. All authors contributed to the article and approved the submitted version.

## FUNDING

This study was supported by the National Natural Science Foundation of China (81771099, 81800989).

## REFERENCES

- Abrao, F., Silva, T. S., Moura, C. L., Ambrosio, S. R., Veneziani, R. C. S., de Paiva, R. E. F., et al. (2021). Oleoresins and Naturally Occurring Compounds of *Copaifera* Genus as Antibacterial and Antivirulence Agents Against Periodontal Pathogens. *Sci. Rep.* 11 (1), 4953. doi: 10.1038/s41598-021-84480-7
- Ahmadi, H., Haddadi-Asl, V., Ghafari, H.-A., Ghorbanzadeh, R., Mazlum, Y., and Bahador, A. (2020). Shear Bond Strength, Adhesive Remnant Index, and Anti-Biofilm Effects of a Photoexcited Modified Orthodontic Adhesive Containing Curcumin Doped Poly Lactic-Co-Glycolic Acid Nanoparticles: An *Ex-Vivo* Biofilm Model of *S. Mutans* on the Enamel Slab Bonded Brackets. *Photodiagnosis Photodyn. Ther.* 30, 101674. doi: 10.1016/j.pdpdt.2020.101674
- Alhariri, M., Azghani, A., and Omri, A. (2013). Liposomal Antibiotics for the Treatment of Infectious Diseases. *Expert Opin. Drug Deliv.* 10 (11), 1515–1532. doi: 10.1517/17425247.2013.822860
- Ang, C. W., Jarrad, A. M., Cooper, M. A., and Blaskovich, M. A. T. (2017). Nitroimidazoles: Molecular Fireworks That Combat a Broad Spectrum of Infectious Diseases. *J. Med. Chem.* 60 (18), 7636–7657. doi: 10.1021/acs.jmedchem.7b00143
- Ashburn, T. T., and Thor, K. B. (2004). Drug Repositioning: Identifying and Developing New Uses for Existing Drugs. *Nat. Rev. Drug Discov.* 3 (8), 673–683. doi: 10.1038/nrd1468
- Banas, J. A. (2004). Virulence Properties of *Streptococcus Mutans*. *Front. Biosci.* 9, 1267–1277. doi: 10.2741/1305
- Barclay, T. G., Day, C. M., Petrovsky, N., and Garg, S. (2019). Review of Polysaccharide Particle-Based Functional Drug Delivery. *Carbohydr. Polym.* 221, 94–112. doi: 10.1016/j.carbpol.2019.05.067
- Barman, S., Mukhopadhyay, S. K., Behara, K. K., Dey, S., and Singh, N. P. (2014). 1-Acetylpyrene-Salicylic Acid: Photoresponsive Fluorescent Organic Nanoparticles for the Regulated Release of a Natural Antimicrobial Compound, Salicylic Acid. *ACS Appl. Mater. Interfaces* 6 (10), 7045–7054. doi: 10.1021/am500965n
- Besingi, R. N., Wenderska, I. B., Senadheera, D. B., Cvitkovitch, D. G., Long, J. R., Wen, Z. T., et al. (2017). Functional Amyloids in *Streptococcus Mutans*, Their Use as Targets of Biofilm Inhibition and Initial Characterization of SMU\_63c. *Microbiol. (Read.)* 163 (4), 488–501. doi: 10.1099/mic.0.000443
- Bibi, S., Lattmann, E., Mohammed, A. R., and Perrie, Y. (2012). Trigger Release Liposome Systems: Local and Remote Controlled Delivery? *J. Microencapsul.* 29 (3), 262–276. doi: 10.3109/02652048.2011.646330
- Binjubaif, F. A., Parker, J. E., Warrilow, A. G., Puri, K., Braidley, P. J., Tatar, E., et al. (2020). Small-Molecule Inhibitors Targeting Sterol 14alpha-Demethylase (CYP51): Synthesis, Molecular Modelling and Evaluation Against *Candida Albicans*. *ChemMedChem* 15 (14), 1294–1309. doi: 10.1002/cmdc.202000250
- Bowen, W. H., Burne, R. A., Wu, H., and Koo, H. (2018). Oral Biofilms: Pathogens, Matrix, and Polymicrobial Interactions in Microenvironments. *Trends Microbiol.* 26 (3), 229–242. doi: 10.1016/j.tim.2017.09.008
- Bowen, W. H., and Koo, H. (2011). Biology of *Streptococcus Mutans*-Derived Glucosyltransferases: Role in Extracellular Matrix Formation of Cariogenic Biofilms. *Caries Res.* 45 (1), 69–86. doi: 10.1159/000324598
- Bramstedt, F. (1968). [Polysaccharide Synthesis Through Plaque Streptococci as an Important Factor in the Etiology of Caries]. *DDZ* 22 (11), 563–4 passim.
- Cardoso, R. L., Maboni, F., Machado, G., Alves, S. H., and de Vargas, A. C. (2010). Antimicrobial Activity of Propolis Extract Against *Staphylococcus Coagulase Positive* and *Malassezia Pachydermatis* of Canine Otitis. *Vet. Microbiol.* 142 (3–4), 432–434. doi: 10.1016/j.vetmic.2009.09.070
- Chen, Y., Ju, Y., Li, C., Yang, T., Deng, Y., and Luo, Y. (2019). Design, Synthesis, and Antibacterial Evaluation of Novel Derivatives of NPS-2143 for the Treatment of Methicillin-Resistant *S. Aureus* (MRSA) Infection. *J. Antibiot. (Tokyo)* 72 (7), 545–554. doi: 10.1038/s41429-019-0177-9
- Chen, X., Liu, C., Peng, X., He, Y., Liu, H., Song, Y., et al. (2019). Sortase A-Mediated Modification of the *Streptococcus Mutans* Transcriptome and Virulence Traits. *Mol. Oral Microbiol.* 34 (5), 219–233. doi: 10.1111/omi.12266
- Chen, Y., Cui, G., Cui, Y., Chen, D., and Lin, H. (2021). Small Molecule Targeting Amyloid Fibrils Inhibits *Streptococcus Mutans* Biofilm Formation. *AMB Express* 11 (1), 171. doi: 10.1186/s13568-021-01333-2
- Coste, A. T., Karababa, M., Ischer, F., Bille, J., and Sanglard, D. (2004). TAC1, Transcriptional Activator of CDR Genes, Is a New Transcription Factor Involved in the Regulation of *Candida Albicans* ABC Transporters CDR1 and CDR2. *Eukaryot. Cell* 3 (6), 1639–1652. doi: 10.1128/EC.3.6.1639-1652.2004
- Cowen, L. E., and Lindquist, S. (2005). Hsp90 Potentiates the Rapid Evolution of New Traits: Drug Resistance in Diverse Fungi. *Science* 309 (5744), 2185–2189. doi: 10.1126/science.1118370



- Daep, C. A., James, D. M., Lamont, R. J., and Demuth, D. R. (2006). Structural Characterization of Peptide-Mediated Inhibition of Porphyromonas Gingivalis Biofilm Formation. *Infect. Immun.* 74 (10), 5756–5762. doi: 10.1128/IAI.00813-06
- Daep, C. A., Novak, E. A., Lamont, R. J., and Demuth, D. R. (2011). Structural Dissection and *In Vivo* Effectiveness of a Peptide Inhibitor of Porphyromonas Gingivalis Adherence to Streptococcus Gordonii. *Infect. Immun.* 79 (1), 67–74. doi: 10.1128/IAI.00361-10
- Davison, E. K., and Brimble, M. A. (2019). Natural Product Derived Privileged Scaffolds in Drug Discovery. *Curr. Opin. Chem. Biol.* 52, 1–8. doi: 10.1016/j.cbpa.2018.12.007
- Dewhirst, F. E., Chen, T., Izard, J., Paster, B. J., Tanner, A. C., Yu, W. H., et al. (2010). The Human Oral Microbiome. *J. Bacteriol.* 192 (19), 5002–5017. doi: 10.1128/JB.00542-10
- Dong, L., Fang, L., Dai, X., Zhang, J., Wang, J., and Xu, P. (2021). Antibacterial and Anti-Inflammatory Activity of Valproic Acid-Pyrazole Conjugates as a Potential Agent Against Periodontitis. *Drug Dev. Res.* doi: 10.1002/ddr.21851
- Evangelina, I. A., Herdiyati, Y., Laviana, A., Rikmasari, R., Zubaedah, C., Anisah, et al. (2021). Bio-Mechanism Inhibitory Prediction of Beta-Sitosterol From Kemangi (*Ocimum Basilicum* L.) as an Inhibitor of MurA Enzyme of Oral Bacteria: *In Vitro* and *In Silico* Study. *Adv. Appl. Bioinform. Chem.* 14, 103–115. doi: 10.2147/AABC.S301488
- Garcia, S. S., Blackledge, M. S., Michalek, S., Su, L., Ptacek, T., Eipers, P., et al. (2017). Targeting of Streptococcus Mutans Biofilms by a Novel Small Molecule Prevents Dental Caries and Preserves the Oral Microbiome. *J. Dent. Res.* 96 (7), 807–814. doi: 10.1177/0022034517698096
- Gürsu, B. Y. (2020). Potential Antibiofilm Activity of Farnesol-Loaded Poly (DL-Lactide-Co-Glycolide)(PLGA) Nanoparticles Against Candida Albicans. *J. Anal. Sci. Technol. Health Care* 11 (1), 1–10.
- Hairul Islam, M. I., Arokiyaraj, S., Kuralarasana, M., Senthil Kumar, V., Hari Krishnan, P., Saravanan, S., et al. (2020). Inhibitory Potential of EGCG on Streptococcus Mutans Biofilm: A New Approach to Prevent Cariogenesis. *Microb. Pathog.* 143, 104129. doi: 10.1016/j.micpath.2020.104129
- Hajishengallis, G. (2015). Periodontitis: From Microbial Immune Subversion to Systemic Inflammation. *Nat. Rev. Immunol.* 15 (1), 30–44. doi: 10.1038/nri3785
- Hajishengallis, G., Darveau, R. P., and Curtis, M. A. (2012). The Keystone-Pathogen Hypothesis. *Nat. Rev. Microbiol.* 10 (10), 717–725. doi: 10.1038/nrmicro2873
- Hajishengallis, G., and Lamont, R. J. (2012). Beyond the Red Complex and Into More Complexity: The Polymicrobial Synergy and Dysbiosis (PSD) Model of Periodontal Disease Etiology. *Mol. Oral. Microbiol.* 27 (6), 409–419. doi: 10.1111/j.2041-1014.2012.00663.x
- Hamada, S., Koga, T., and Ooshima, T. (1984). Virulence Factors of Streptococcus Mutans and Dental Caries Prevention. *J. Dent. Res.* 63 (3), 407–411. doi: 10.1177/00220345840630031001
- Hao, W., Qiao, D., Han, Y., Du, N., Li, X., Fan, Y., et al. (2021). Identification of Disulfiram as a Potential Antifungal Drug by Screening Small Molecular Libraries. *J. Infect. Chemother.* 27 (5), 696–701. doi: 10.1016/j.jiac.2020.12.012
- Havarstein, L. S., Diep, D. B., and Nes, I. F. (1995). A Family of Bacteriocin ABC Transporters Carry Out Proteolytic Processing of Their Substrates Concomitant With Export. *Mol. Microbiol.* 16 (2), 229–240. doi: 10.1111/j.1365-2958.1995.tb02295.x
- He, Z. Y., Zhang, X., Song, Z. C., Li, L., Chang, H. S., Li, S. L., et al. (2020). Quercetin Inhibits Virulence Properties of Porphyromonas Gingivalis in Periodontal Disease. *Sci. Rep.* 10 (1), 18313. doi: 10.1038/s41598-020-74977-y
- Hegstad, K., Langsrud, S., Lunestad, B. T., Scheie, A. A., Sunde, M., and Yazdankhah, S. P. (2010). Does the Wide Use of Quaternary Ammonium Compounds Enhance the Selection and Spread of Antimicrobial Resistance and Thus Threaten Our Health? *Microb. Drug Resist.* 16 (2), 91–104. doi: 10.1089/mdr.2009.0120
- Holmes, A. R., Cardno, T. S., Strouse, J. J., Ivniński-Steele, I., Keniya, M. V., Lackovic, K., et al. (2016). Targeting Efflux Pumps to Overcome Antifungal Drug Resistance. *Future Med. Chem.* 8 (12), 1485–1501. doi: 10.4155/fmc-2016-0050
- Hoyer, L. L. (2001). The ALS Gene Family of Candida Albicans. *Trends Microbiol.* 9 (4), 176–180. doi: 10.1016/S0966-842X(01)01984-9
- Ishii, S., Fukui, K., Yokoshima, S., Kumagai, K., Beniyama, Y., Kodama, T., et al. (2017). High-Throughput Screening of Small Molecule Inhibitors of the Streptococcus Quorum-Sensing Signal Pathway. *Sci. Rep.* 7 (1), 4029. doi: 10.1038/s41598-017-03567-2
- Iyer, K. R., Camara, K., Daniel-Ivad, M., Trilles, R., Pimentel-Elardo, S. M., Fossen, J. L., et al. (2020). An Oxindole Efflux Inhibitor Potentiates Azoles and Impairs Virulence in the Fungal Pathogen Candida Auris. *Nat. Commun.* 11 (1), 6429. doi: 10.1038/s41467-020-20183-3
- Jabir, M. S., Taha, A. A., and Sahib, U. I. (2018). Linalool Loaded on Glutathione-Modified Gold Nanoparticles: A Drug Delivery System for a Successful Antimicrobial Therapy. *Artif. Cells Nanomedicine Biotechnol. Adv.* 46 (sup2), 345–355. doi: 10.1080/21691401.2018.1457535
- Jahanizadeh, S., Yazdian, F., Marjani, A., Omidi, M., and Rashedi, H. (2017). Curcumin-Loaded Chitosan/Carboxymethyl Starch/Montmorillonite Bio-Nanocomposite for Reduction of Dental Bacterial Biofilm Formation. *Int. J. Biol. Macromol.* 105, 757–763. doi: 10.1016/j.ijbiomac.2017.07.101
- Jenkinson, H. F., and Demuth, D. R. (1997). Structure, Function and Immunogenicity of Streptococcal Antigen I/II Polypeptides. *Mol. Microbiol.* 23 (2), 183–190. doi: 10.1046/j.1365-2958.1997.2021577.x
- Jeon, J. G., Pandit, S., Xiao, J., Gregoire, S., Falsetta, M. L., Klein, M. I., et al. (2011). Influences of Trans-Trans Farnesol, a Membrane-Targeting Sesquiterpenoid, on Streptococcus Mutans Physiology and Survival Within Mixed-Species Oral Biofilms. *Int. J. Oral. Sci.* 3 (2), 98–106. doi: 10.4248/IJOS11038
- Jones, C. G. (1997). Chlorhexidine: Is It Still the Gold Standard? *Periodontol.* 2000 15, 55–62. doi: 10.1111/j.1600-0757.1997.tb00105.x
- Kalimuthu, S., Cheung, B. P. K., Yau, J. Y. Y., Shanmugam, K., Solomon, A. P., and Neelakantan, P. (2020). A Novel Small Molecule, 1,3-Di-M-Tolyl-Urea, Inhibits and Disrupts Multispecies Oral Biofilms. *Microorganisms* 8 (9), 1261. doi: 10.3390/microorganisms8091261
- Kapoor, D. N., Bhatia, A., Kaur, R., Sharma, R., Kaur, G., and Dhawan, S. (2015). PLGA: A Unique Polymer for Drug Delivery. *Ther. Deliv.* 6 (1), 41–58. doi: 10.4155/tde.14.91
- Kariu, T., Nakao, R., Ikeda, T., Nakashima, K., Potempa, J., and Imamura, T. (2017). Inhibition of Gingipains and Porphyromonas Gingivalis Growth and Biofilm Formation by Prenyl Flavonoids. *J. Periodontol. Res.* 52 (1), 89–96. doi: 10.1111/jre.12372
- Kathwate, G. H., Shinde, R. B., and Mohan Karuppayil, S. (2021). Non-Antifungal Drugs Inhibit Growth, Morphogenesis and Biofilm Formation in Candida Albicans. *J. Antibiot. (Tokyo)* 74 (5), 346–353. doi: 10.1038/s41429-020-00403-0
- Kaur, G., Balamurugan, P., and Princy, S. A. (2017). Inhibition of the Quorum Sensing System (ComDE Pathway) by Aromatic 1,3-Di-M-Tolylurea (DMTU): Cariostatic Effect With Fluoride in Wistar Rats. *Front. Cell Infect. Microbiol.* 7, 313. doi: 10.3389/fcimb.2017.00313
- Kaur, G., Balamurugan, P., Uma Maheswari, C., Anitha, A., and Princy, S. A. (2016). Combinatorial Effects of Aromatic 1,3-Disubstituted Ureas and Fluoride on *In Vitro* Inhibition of Streptococcus Mutans Biofilm Formation. *Front. Microbiol.* 7, 861. doi: 10.3389/fmicb.2016.00861
- Kelly, C. G., Younson, J. S., Hikmat, B. Y., Todryk, S. M., Czisch, M., Haris, P. I., et al. (1999). A Synthetic Peptide Adhesion Epitope as a Novel Antimicrobial Agent. *Nat. Biotechnol.* 17 (1), 42–47. doi: 10.1038/5213
- Keniya, M. V., Fleischer, E., Klinger, A., Cannon, R. D., and Monk, B. C. (2015). Inhibitors of the Candida Albicans Major Facilitator Superfamily Transporter Mdr1p Responsible for Fluconazole Resistance. *PLoS One* 10 (5), e0126350. doi: 10.1371/journal.pone.0126350
- Kett, S., Pathak, A., Turillazzi, S., Cavalieri, D., and Marvasi, M. (2021). Antifungals, Arthropods and Antifungal Resistance Prevention: Lessons From Ecological Interactions. *Proc. Biol. Sci.* 288 (1944), 20202716. doi: 10.1098/rspb.2020.2716
- Kim, S., Song, M., Roh, B. D., Park, S. H., and Park, J. W. (2013). Inhibition of Streptococcus Mutans Biofilm Formation on Composite Resins Containing Ursolic Acid. *Restor. Dent. Endod.* 38 (2), 65–72. doi: 10.5395/rde.2013.38.2.65
- Kim, D., Barraza, J. P., Arthur, R. A., Hara, A., Lewis, K., Liu, Y., et al. (2020). Spatial Mapping of Polymicrobial Communities Reveals a Precise Biogeography Associated With Human Dental Caries. *Proc. Natl. Acad. Sci. U.S.A.* 117 (22), 12375–12386. doi: 10.1073/pnas.1919099117
- Kim, K., Kim, D., Lee, H., Lee, T. H., Kim, K. Y., and Kim, H. (2020). New Pyrimidinone-Fused 1,4-Naphthoquinone Derivatives Inhibit the Growth of Drug Resistant Oral Bacteria. *Biomedicines* 8 (6), 160. doi: 10.3390/biomedicines8060160

- Kojima, T., Yasui, S., and Ishikawa, I. (1993). Distribution of Porphyromonas Gingivalis in Adult Periodontitis Patients. *J. Periodontol.* 64 (12), 1231–1237. doi: 10.1902/jop.1993.64.12.1231
- Kolouchova, I., Matatkova, O., Paldrychova, M., Kodes, Z., Kvasnickova, E., Sigler, K., et al. (2018). Resveratrol, Pterostilbene, and Baicalein: Plant-Derived Anti-Biofilm Agents. *Folia Microbiol. (Praha)* 63 (3), 261–272. doi: 10.1007/s12223-017-0549-0
- Koo, H., Rosalen, P. L., Cury, J. A., Park, Y. K., and Bowen, W. H. (2002). Effects of Compounds Found in Propolis on Streptococcus Mutans Growth and on Glucosyltransferase Activity. *Antimicrob. Agents Chemother.* 46 (5), 1302–1309. doi: 10.1128/AAC.46.5.1302-1309.2002
- Koo, H., Hayacibara, M. F., Schobel, B. D., Cury, J. A., Rosalen, P. L., Park, Y. K., et al. (2003). Inhibition of Streptococcus Mutans Biofilm Accumulation and Polysaccharide Production by Apigenin and Tt-Farnesol. *J. Antimicrob. Chemother.* 52 (5), 782–789. doi: 10.1093/jac/dkg449
- Koo, H., Schobel, B., Scott-Anne, K., Watson, G., Bowen, W. H., Cury, J. A., et al. (2005). Apigenin and Tt-Farnesol With Fluoride Effects on S. Mutans Biofilms and Dental Caries. *J. Dent. Res.* 84 (11), 1016–1020. doi: 10.1177/154405910508401109
- Krom, B. P., Kidwai, S., and Ten Cate, J. M. (2014). Candida and Other Fungal Species: Forgotten Players of Healthy Oral Microbiota. *J. Dent. Res.* 93 (5), 445–451. doi: 10.1177/0022034514521814
- Krzysciak, W., Jurczak, A., Koscielniak, D., Bystrowska, B., and Skalniak, A. (2014). The Virulence of Streptococcus Mutans and the Ability to Form Biofilms. *Eur. J. Clin. Microbiol. Infect. Dis.* 33 (4), 499–515. doi: 10.1007/s10096-013-1993-7
- Kuang, X., Yang, T., Zhang, C., Peng, X., Ju, Y., Li, C., et al. (2020). Repurposing Napabucasin as an Antimicrobial Agent Against Oral Streptococcal Biofilms. *BioMed. Res. Int.* 2020, 8379526. doi: 10.1155/2020/8379526
- Kuete, V., Eyong, K. O., Folefoc, G. N., Beng, V. P., Hussain, H., Krohn, K., et al. (2007). Antimicrobial Activity of the Methanolic Extract and of the Chemical Constituents Isolated From Newbouldia laevis. *Pharmazie* 62 (7), 552–556.
- Kuete, V., Alibert-Franco, S., Eyong, K. O., Ngameni, B., Folefoc, G. N., Nguemaving, J. R., et al. (2011). Antibacterial Activity of Some Natural Products Against Bacteria Expressing a Multidrug-Resistant Phenotype. *Int. J. Antimicrob. Agents* 37 (2), 156–161. doi: 10.1016/j.ijantimicag.2010.10.020
- Kugaji, M. S., Kumbar, V. M., Peram, M. R., Patil, S., Bhat, K. G., and Diwan, P. V. (2019). Effect of Resveratrol on Biofilm Formation and Virulence Factor Gene Expression of Porphyromonas Gingivalis in Periodontal Disease. *APMIS* 127 (4), 187–195. doi: 10.1111/apm.12930
- Kumar, A., and Balbach, J. (2017). Targeting the Molecular Chaperone SlyD to Inhibit Bacterial Growth With a Small Molecule. *Sci. Rep.* 7, 42141. doi: 10.1038/srep42141
- Lee, S. F., and Boran, T. L. (2003). Roles of Sortase in Surface Expression of the Major Protein Adhesin P1, Saliva-Induced Aggregation and Adherence, and Cariogenicity of Streptococcus Mutans. *Infect. Immun.* 71 (2), 676–681. doi: 10.1128/IAI.71.2.676-681.2003
- Li, L., Zhang, T., Xu, J., Wu, J., Wang, Y., Qiu, X., et al. (2019). The Synergism of the Small Molecule ENOblock and Fluconazole Against Fluconazole-Resistant Candida Albicans. *Front. Microbiol.* 10, 2071. doi: 10.3389/fmicb.2019.02071
- Li, Y., Gao, S., Shi, S., Xiao, D., Peng, S., Gao, Y., et al. (2021). Tetrahedral Framework Nucleic Acid-Based Delivery of Resveratrol Alleviates Insulin Resistance: From Innate to Adaptive Immunity. *Nano-Micro. Lett.* 13 (1), 86. doi: 10.1007/s40820-021-00711-6
- Lim, K. S., and Kam, P. C. (2008). Chlorhexidine—Pharmacology and Clinical Applications. *Anaesth. Intensive Care* 36 (4), 502–512. doi: 10.1177/0310057X0803600404
- Liu, C., Worthington, R. J., Melander, C., and Wu, H. (2011). A New Small Molecule Specifically Inhibits the Cariogenic Bacterium Streptococcus Mutans in Multispecies Biofilms. *Antimicrob. Agents Chemother.* 55 (6), 2679–2687. doi: 10.1128/AAC.01496-10
- Li, M. Y., Wang, J., and Lai, G. Y. (2009). Effect of a Dentifrice Containing the Peptide of Streptococcal Antigen I/II on the Adherence of Mutans Streptococcus. *Arch. Oral. Biol.* 54 (11), 1068–1073. doi: 10.1016/j.archoralbio.2009.08.004
- Lohse, M. B., Ennis, C. L., Hartooni, N., Johnson, A. D., and Nobile, C. J. (2018). Development and Regulation of Single- and Multi-Species Candida Albicans Biofilms. *Nat. Rev. Microbiol.* 16 (1), 19–31. doi: 10.1038/nrmicro.2017.107
- Lohse, M. B., Gulati, M., Johnson, A. D., and Nobile, C. J. (2020). A Screen for Small Molecules to Target Candida Albicans Biofilms. *J. Fungi (Basel)* 7 (1), 9. doi: 10.3390/jof7010009
- Love, R. M., McMillan, M. D., and Jenkinson, H. F. (1997). Invasion of Dental Tubules by Oral Streptococci Is Associated With Collagen Recognition Mediated by the Antigen I/II Family of Polypeptides. *Infect. Immun.* 65 (12), 5157–5164. doi: 10.1128/iai.65.12.5157-5164.1997
- Lyu, X., Li, C., Zhang, J., Wang, L., Jiang, Q., Shui, Y., et al. (2021a). A Novel Small Molecule, LCG-N25, Inhibits Oral Streptococcal Biofilm. *Front. Microbiol.* 12, 654692. doi: 10.3389/fmicb.2021.654692
- Lyu, X., Wang, L., Shui, Y., Jiang, Q., Chen, L., Yang, W., et al. (2021b). Ursolic Acid Inhibits Multi-Species Biofilms Developed by Streptococcus Mutans, Streptococcus Sanguinis, and Streptococcus Gordonii. *Arch. Oral. Biol.* 125, 105107. doi: 10.1016/j.archoralbio.2021.105107
- Maeda, K., Nagata, H., Yamamoto, Y., Tanaka, M., Tanaka, J., Minamino, N., et al. (2004). Glyceraldehyde-3-Phosphate Dehydrogenase of Streptococcus Oralis Functions as a Coadhesin for Porphyromonas Gingivalis Major Fimbriae. *Infect. Immun.* 72 (3), 1341–1348. doi: 10.1128/IAI.72.3.1341-1348.2004
- Maghsoudi, A., Yazdian, F., Shahmoradi, S., Ghaderi, L., Hemati, M., and Amoabediny, G. (2017). Curcumin-Loaded Polysaccharide Nanoparticles: Optimization and Anticariogenic Activity Against Streptococcus Mutans. *Mater. Sci. Eng.: C* 75, 1259–1267. doi: 10.1016/j.msec.2017.03.032
- Marsh, P. D. (2010). Microbiology of Dental Plaque Biofilms and Their Role in Oral Health and Caries. *Dent. Clin. North Am.* 54 (3), 441–454. doi: 10.1016/j.cden.2010.03.002
- Mayer, F. L., Wilson, D., and Hube, B. (2013). Candida Albicans Pathogenicity Mechanisms. *Virulence* 4 (2), 119–128. doi: 10.4161/viru.22913
- Melok, A. L. (2018). Green Tea Polyphenol Epigallocatechin-3-Gallate-Stearate Inhibits the Growth of Streptococcus Mutans: A Promising New Approach in Caries Prevention. *Dent. J. (Basel)* 6 (3), 38. doi: 10.3390/dj6030038
- Menzel, L. P., Chowdhury, H. M., Masso-Silva, J. A., Ruddick, W., Falkovsky, K., Vorona, R., et al. (2017). Potent In Vitro and In Vivo Antifungal Activity of a Small Molecule Host Defense Peptide Mimic Through a Membrane-Active Mechanism. *Sci. Rep.* 7 (1), 4353. doi: 10.1038/s41598-017-04462-6
- Metwalli, K. H., Khan, S. A., Krom, B. P., and Jabra-Rizk, M. A. (2013). Streptococcus Mutans, Candida Albicans, and the Human Mouth: A Sticky Situation. *PLoS Pathog.* 9 (10), e1003616. doi: 10.1371/journal.ppat.1003616
- Mir, M., Ahmed, N., and ur Rehman, A. (2017). Recent Applications of PLGA Based Nanostructures in Drug Delivery. *Colloids Surf. B: Biointerfaces* 159, 217–231. doi: 10.1016/j.colsurfb.2017.07.038
- Mizukami, S., Kashibe, M., Matsumoto, K., Hori, Y., and Kikuchi, K. (2017). Enzyme-Triggered Compound Release Using Functionalized Antimicrobial Peptide Derivatives. *Chem. Sci. (Royal Soc. Chem.: 2010)* 8 (4), 3047–3053. doi: 10.1039/c6sc04435b
- Munro, G. H., Evans, P., Todryk, S., Buckett, P., Kelly, C. G., and Lehner, T. (1993). A Protein Fragment of Streptococcal Cell Surface Antigen I/II Which Prevents Adhesion of Streptococcus Mutans. *Infect. Immun.* 61 (11), 4590–4598. doi: 10.1128/iai.61.11.4590-4598.1993
- Murciano, C., Moyes, D. L., Runglall, M., Tobouti, P., Islam, A., Hoyer, L. L., et al. (2012). Evaluation of the Role of Candida Albicans Agglutinin-Like Sequence (Als) Proteins in Human Oral Epithelial Cell Interactions. *PLoS One* 7 (3), e33362. doi: 10.1371/journal.pone.0033362
- Nakanishi-Matsui, M., Sekiya, M., and Futai, M. (2016). ATP Synthase From Escherichia Coli: Mechanism of Rotational Catalysis, and Inhibition With the Epsilon Subunit and Phytopolyphenols. *Biochim. Biophys. Acta* 1857 (2), 129–140. doi: 10.1016/j.bbabo.2015.11.005
- Newman, D. J., and Cragg, G. M. (2020). Natural Products as Sources of New Drugs Over the Nearly Four Decades From 01/1981 to 09/2019. *J. Nat. Prod.* 83 (3), 770–803. doi: 10.1021/acs.jnatprod.9b01285
- Nicolosi, D., Cupri, S., Genovese, C., Tempera, G., Mattina, R., and Pignatello, R. (2015). Nanotechnology Approaches for Antibacterial Drug Delivery: Preparation and Microbiological Evaluation of Fusogenic Liposomes Carrying Fusidic Acid. *Int. J. Antimicrob. Agents* 45 (6), 622–626. doi: 10.1016/j.ijantimicag.2015.01.016
- Nijampatnam, B., Zhang, H., Cai, X., Michalek, S. M., Wu, H., and Velu, S. E. (2018). Inhibition of Streptococcus Mutans Biofilms by the Natural Stilbene

- Piceatannol Through the Inhibition of Glucosyltransferases. *ACS Omega* 3 (7), 8378–8385. doi: 10.1021/acsomega.8b00367
- Nijampatnam, B., Ahirwar, P., Pukkanasut, P., Womack, H., Casals, L., Zhang, H., et al. (2021). Discovery of Potent Inhibitors of Streptococcus Mutans Biofilm With Antivirulence Activity. *ACS Med. Chem. Lett.* 12 (1), 48–55. doi: 10.1021/acsmchemlett.0c00373
- Niu, Y., Wang, K., Zheng, S., Wang, Y., Ren, Q., Li, H., et al. (2020). Antibacterial Effect of Caffeic Acid Phenethyl Ester on Cariogenic Bacteria and Streptococcus Mutans Biofilms. *Antimicrob. Agents Chemother.* 64 (9), e00251–20. doi: 10.1128/AAC.00251-20
- Padder, S. A., Prasad, R., and Shah, A. H. (2018). Quorum Sensing: A Less Known Mode of Communication Among Fungi. *Microbiol. Res.* 210, 51–58. doi: 10.1016/j.micres.2018.03.007
- Pagniez, F., Lebouvier, N., Na, Y. M., Ourliac-Garnier, I., Picot, C., Le Borgne, M., et al. (2020). Biological Exploration of a Novel 1,2,4-Triazole-Indole Hybrid Molecule as Antifungal Agent. *J. Enzyme Inhib. Med. Chem.* 35 (1), 398–403. doi: 10.1080/14756366.2019.1705292
- Papenfort, K., and Bassler, B. L. (2016). Quorum Sensing Signal-Response Systems in Gram-Negative Bacteria. *Nat. Rev. Microbiol.* 14 (9), 576–588. doi: 10.1038/nrmicro.2016.89
- Park, Y., Simionato, M. R., Sekiya, K., Murakami, Y., James, D., Chen, W., et al. (2005). Short Fimbriae of Porphyromonas Gingivalis and Their Role in Coadhesion With Streptococcus Gordonii. *Infect. Immun.* 73 (7), 3983–3989. doi: 10.1128/IAI.73.7.3983-3989.2005
- Park, W., Ahn, C. H., Cho, H., Kim, C. K., Shin, J., and Oh, K. B. (2017). Inhibitory Effects of Flavonoids From Spatholobus Suberectus on Sortase A and Sortase A-Mediated Aggregation of Streptococcus Mutans. *J. Microbiol. Biotechnol.* 27 (8), 1457–1460. doi: 10.4014/jmb.1704.04001
- Park, J. S., Ryu, E. J., Li, L., Choi, B. K., and Kim, B. M. (2017). New Bicyclic Brominated Furanones as Potent Autoinducer-2 Quorum-Sensing Inhibitors Against Bacterial Biofilm Formation. *Eur. J. Med. Chem.* 137, 76–87. doi: 10.1016/j.ejmech.2017.05.037
- Patil, P. C., Tan, J., Demuth, D. R., and Luzzio, F. A. (2016). 1,2,3-Triazole-Based Inhibitors of Porphyromonas Gingivalis Adherence to Oral Streptococci and Biofilm Formation. *Bioorg. Med. Chem.* 24 (21), 5410–5417. doi: 10.1016/j.bmc.2016.08.059
- Patil, P. C., Tan, J., Demuth, D. R., and Luzzio, F. A. (2019). 'Second-Generation' 1,2,3-Triazole-Based Inhibitors of Porphyromonas Gingivalis Adherence to Oral Streptococci and Biofilm Formation. *Medchemcomm.* 10 (2), 268–279. doi: 10.1039/c8md00405f
- Peters, B. M., Ovchinnikova, E. S., Krom, B. P., Schlecht, L. M., Zhou, H., Hoyer, L. L., et al. (2012). Staphylococcus Aureus Adherence to Candida Albicans Hyphae Is Mediated by the Hyphal Adhesin Als3p. *Microbiol. (Read.)* 158 (Pt 12), 2975–2986. doi: 10.1099/mic.0.062109-0
- Rai, M., Ingle, A. P., Pandit, R., Paralikar, P., Gupta, I., Chaud, M. V., et al. (2017). Broadening the Spectrum of Small-Molecule Antibacterials by Metallic Nanoparticles to Overcome Microbial Resistance. *Int. J. Pharm.* 532 (1), 139–148. doi: 10.1016/j.ijpharm.2017.08.127
- Rath, S. K., and Singh, M. (2013). Comparative Clinical and Microbiological Efficacy of Mouthwashes Containing 0.2% and 0.12% Chlorhexidine. *Dent. Res. J. (Isfahan)* 10 (3), 364–369.
- Ren, Z., Cui, T., Zeng, J., Chen, L., Zhang, W., Xu, X., et al. (2016). Molecule Targeting Glucosyltransferase Inhibits Streptococcus Mutans Biofilm Formation and Virulence. *Antimicrob. Agents Chemother.* 60 (1), 126–135. doi: 10.1128/AAC.00919-15
- Riep, B., Edesi-Neuss, L., Claessen, F., Skarabis, H., Ehmke, B., Flemmig, T. F., et al. (2009). Are Putative Periodontal Pathogens Reliable Diagnostic Markers? *J. Clin. Microbiol.* 47 (6), 1705–1711. doi: 10.1128/JCM.01387-08
- Rivera-Quiroga, R. E., Cardona, N. M., Padilla, L., Rivera, W., Rocha-Roa, C., and Diaz De Rienzo, M. A. (2020). In Silico Selection and In Vitro Evaluation of New Molecules That Inhibit the Adhesion of Streptococcus Mutans Through Antigen I/II. *Int. J. Mol. Sci.* 22 (1), 377. doi: 10.3390/ijms22010377
- Roky, M., Tan, J., Sztukowska, M. N., Trent, J. O., and Demuth, D. R. (2020). Identification of Small-Molecule Inhibitors Targeting Porphyromonas Gingivalis Interspecies Adherence and Determination of Their In Vitro and In Vivo Efficacies. *Antimicrob. Agents Chemother.* 64 (11), e00884–20. doi: 10.1128/AAC.00884-20
- Ryan, L. K., Freeman, K. B., Masso-Silva, J. A., Falkovsky, K., Aloyouny, A., Markowitz, K., et al. (2014). Activity of Potent and Selective Host Defense Peptide Mimetics in Mouse Models of Oral Candidiasis. *Antimicrob. Agents Chemother.* 58 (7), 3820–3827. doi: 10.1128/AAC.02649-13
- Ryu, E. J., Sim, J., Sim, J., Lee, J., and Choi, B. K. (2016). D-Galactose as an Autoinducer 2 Inhibitor to Control the Biofilm Formation of Periodontopathogens. *J. Microbiol.* 54 (9), 632–637. doi: 10.1007/s12275-016-6345-8
- Salmanli, M., Tatar Yilmaz, G., and Tuzuner, T. (2021). Investigation of the Antimicrobial Activities of Various Antimicrobial Agents on Streptococcus Mutans Sortase A Through Computer-Aided Drug Design (CADD) Approaches. *Comput. Methods Programs BioMed.* 212, 106454. doi: 10.1016/j.cmpb.2021.106454
- Samad, A., Sultana, Y., and Aqil, M. (2007). Liposomal Drug Delivery Systems: An Update Review. *Curr. Drug Deliv.* 4 (4), 297–305. doi: 10.2174/156720107782151269
- Samaranayake, L., and Matsubara, V. H. (2017). Normal Oral Flora and the Oral Ecosystem. *Dent. Clin. North Am.* 61 (2), 199–215. doi: 10.1016/j.cden.2016.11.002
- Saputo, S., Faustoferri, R. C., and Quivey, R. G. Jr. (2018). Vitamin D Compounds Are Bactericidal Against Streptococcus Mutans and Target the Bacitracin-Associated Efflux System. *Antimicrob. Agents Chemother.* 62 (1), e01675–17. doi: 10.1128/AAC.01675-17
- Sekiya, M., Chiba, E., Satoh, M., Yamakoshi, H., Iwabuchi, Y., Futai, M., et al. (2014). Strong Inhibitory Effects of Curcumin and Its Demethoxy Analog on Escherichia Coli ATP Synthase F1 Sector. *Int. J. Biol. Macromol.* 70, 241–245. doi: 10.1016/j.ijbiomac.2014.06.055
- Sekiya, M., Izumisawa, S., Iwamoto-Kihara, A., Fan, Y., Shimoyama, Y., Sasaki, M., et al. (2019). Proton-Pumping F-ATPase Plays an Important Role in Streptococcus Mutans Under Acidic Conditions. *Arch. Biochem. Biophys.* 666, 46–51. doi: 10.1016/j.abb.2019.03.014
- Shao, H., and Demuth, D. R. (2010). Quorum Sensing Regulation of Biofilm Growth and Gene Expression by Oral Bacteria and Periodontal Pathogens. *Periodontol.* 2000 52 (1), 53–67. doi: 10.1111/j.1600-0757.2009.00318.x
- Shinobu-Mesquita, C. S., Martins, E., Junior, J. B., de Souza Bonfim-Mendonça, P., Felipe, M. S. S., Kioshima, E. S., et al. (2020). In Vitro and In Vivo Activity of a Possible Novel Antifungal Small Molecule Against Candida Albicans. *J. Mycol. Med.* 30 (2), 100939. doi: 10.1016/j.mycmed.2020.100939
- Silva, A. R., Santos, E. B., Pinto, S. C., Gomes, J. C., Vaz, I. P., and Carvalho, M. F. (2014). Antimicrobial Effect and Transdental Diffusion of New Intracanal Formulations Containing Nitrofurantoin or Doxycycline. *Braz. Dent. J.* 25 (5), 425–429. doi: 10.1590/0103-6440201302338
- Singh, A. K., Yadav, S., Sharma, K., Firdaus, Z., Aditi, P., Neogi, K., et al. (2019). Quantum Curcumin Mediated Inhibition of Gingivitis and Mixed-Biofilm of Porphyromonas Gingivalis Causing Chronic Periodontitis (Vol 82018). *Rsc. Adv.* 9 (1), 91–91, pg 40426. doi: 10.1039/c8ra90104j
- Socransky, S. S., Haffajee, A. D., Cugini, M. A., Smith, C., and Kent, R. L. Jr. (1998). Microbial Complexes in Subgingival Plaque. *J. Clin. Periodontol.* 25 (2), 134–144. doi: 10.1111/j.1600-051X.1998.tb02419.x
- Song, M., Teng, Z., Li, M., Niu, X., Wang, J., and Deng, X. (2017). Epigallocatechin Gallate Inhibits Streptococcus Pneumoniae Virulence by Simultaneously Targeting Pneumolysin and Sortase A. *J. Cell Mol. Med.* 21 (10), 2586–2598. doi: 10.1111/jcmm.13179
- Staniszewska, M., Kuryk, L., Gryciuk, A., Kawalec, J., Rogalska, M., Baran, J., et al. (2021a). In Vitro Anti-Candida Activity and Action Mode of Benzoxazole Derivatives. *Molecules* 26 (16), 5008. doi: 10.3390/molecules26165008
- Staniszewska, M., Kuryk, L., Gryciuk, A., Kawalec, J., Rogalska, M., Baran, J., et al. (2021b). The Antifungal Action Mode of N-Phenacyldibromobenzimidazoles. *Molecules* 26 (18), 5463. doi: 10.3390/molecules26185463
- Stavroulakis, A. T., Goncalves, L. L., Levesque, C. M., Kishen, A., and Prakki, A. (2021). Interaction of Epigallocatechin-Gallate and Chlorhexidine With Streptococcus Mutans Stimulated Odontoblast-Like Cells: Cytotoxicity, Interleukin-1beta and Co-Species Proteomic Analyses. *Arch. Oral. Biol.* 131, 105268. doi: 10.1016/j.archoralbio.2021.105268
- Sun, Y., Li, S., Zhang, Y., Li, Q., Xie, X., Zhao, D., et al. (2020). Tetrahedral Framework Nucleic Acids Loading Ampicillin Improve the Drug Susceptibility Against Methicillin-Resistant Staphylococcus Aureus. *ACS Appl. Mater. Interfaces* 12 (33), 36957–36966. doi: 10.1021/acsmi.0c11249
- Taddei, M., Ferrini, S., Giannotti, L., Corsi, M., Manetti, F., Giannini, G., et al. (2014). Synthesis and Evaluation of New Hsp90 Inhibitors Based on a 1,4,5-Trisubstituted 1,2,3-Triazole Scaffold. *J. Med. Chem.* 57 (6), 2258–2274. doi: 10.1021/jm401536b



- Tan, J., Patil, P. C., Luzzio, F. A., and Demuth, D. R. (2018). *In Vitro* and *In Vivo* Activity of Peptidomimetic Compounds That Target the Periodontal Pathogen *Porphyromonas Gingivalis*. *Antimicrob. Agents Chemother.* 62 (7), e00400\*–18. doi: 10.1128/AAC.00400-18
- Tanner, A. C., Kressler, C. A., and Faller, L. L. (2016). Understanding Caries From the Oral Microbiome Perspective. *J. Calif. Dent. Assoc.* 44 (7), 437–446.
- Theilade, E. (1986). The Non-Specific Theory in Microbial Etiology of Inflammatory Periodontal Diseases. *J. Clin. Periodontol.* 13 (10), 905–911. doi: 10.1111/j.1600-051X.1986.tb01425.x
- Tiwari, S., Thakur, R., and Shankar, J. (2015). Role of Heat-Shock Proteins in Cellular Function and in the Biology of Fungi. *Biotechnol. Res. Int.* 132635. doi: 10.1155/2015/132635
- Vediappan, G., Dumontet, V., Pelissier, F., and d'Enfert, C. (2013). Gymnemic Acids Inhibit Hyphal Growth and Virulence in *Candida Albicans*. *PLoS One* 8 (9), e74189. doi: 10.1371/journal.pone.0074189
- Velaázquez-Lam, E., Imperial, J., and Ponz, F. (2020). Polyphenol-Functionalized Plant Viral-Derived Nanoparticles Exhibit Strong Antimicrobial and Antibiofilm Formation Activities. *ACS Appl. Bio Mater.* 3 (4), 2040–2047. doi: 10.1021/acsabm.9b01161
- Velazquez, C., Navarro, M., Acosta, A., Angulo, A., Dominguez, Z., Robles, R., et al. (2007). Antibacterial and Free-Radical Scavenging Activities of Sonoran Propolis. *J. Appl. Microbiol.* 103 (5), 1747–1756. doi: 10.1111/j.1365-2672.2007.03409.x
- Veloz, J. J., Alvear, M., and Salazar, L. A. (2019). Antimicrobial and Antibiofilm Activity Against *Streptococcus Mutans* of Individual and Mixtures of the Main Polyphenolic Compounds Found in Chilean Propolis. *BioMed. Res. Int.* 2019, 7602343. doi: 10.1155/2019/7602343
- Veloz, J. J., Saavedra, N., Alvear, M., Zambrano, T., Barrientos, L., and Salazar, L. A. (2016). Polyphenol-Rich Extract From Propolis Reduces the Expression and Activity of *Streptococcus Mutans* Glucosyltransferases at Subinhibitory Concentrations. *BioMed. Res. Int.* 2016, 4302706. doi: 10.1155/2016/4302706
- Verma, D., Gulati, N., Kaul, S., Mukherjee, S., and Nagaich, U. (2018). Protein Based Nanostructures for Drug Delivery. *J. Pharm.* 2018, 9285854. doi: 10.1155/2018/9285854
- Walsh, T., Oliveira-Neto, J. M., and Moore, D. (2015). Chlorhexidine Treatment for the Prevention of Dental Caries in Children and Adolescents. *Cochrane Database Syst. Rev.* 4, CD008457. doi: 10.1002/14651858.CD008457.pub2
- Wang, S., Wang, H., Ren, B., Li, H., Weir, M. D., Zhou, X., et al. (2017). Do Quaternary Ammonium Monomers Induce Drug Resistance in Cariogenic, Endodontic and Periodontal Bacterial Species? *Dent. Mater.* 33 (10), 1127–1138. doi: 10.1016/j.dental.2017.07.001
- Wang, J., Shi, Y., Jing, S., Dong, H., Wang, D., and Wang, T. (2019). Astilbin Inhibits the Activity of Sortase A From *Streptococcus Mutans*. *Molecules* 24 (3), 465. doi: 10.3390/molecules24030465
- Wang, L., Natan, M., Zheng, W., Zheng, W., Liu, S., Jacobi, G., et al. (2020). Small Molecule-Decorated Gold Nanoparticles for Preparing Antibiofilm Fabrics. *Nanoscale Adv.* 2 (6), 2293–2302. doi: 10.1039/D0NA00179A
- Whitesell, L., Robbins, N., Huang, D. S., McLellan, C. A., Shekhar-Guturja, T., LeBlanc, E. V., et al. (2019). Structural Basis for Species-Selective Targeting of Hsp90 in a Pathogenic Fungus. *Nat. Commun.* 10 (1), 402. doi: 10.1038/s41467-018-08248-w
- Worthington, R. J., Richards, J. J., and Melander, C. (2012). Small Molecule Control of Bacterial Biofilms. *Org. Biomol. Chem.* 10 (37), 7457–7474. doi: 10.1039/c2ob25835h
- Wright, C. J., Burns, L. H., Jack, A. A., Back, C. R., Dutton, L. C., Nobbs, A. H., et al. (2013). Microbial Interactions in Building of Communities. *Mol. Oral Microbiol.* 28 (2), 83–101. doi: 10.1111/omi.12012
- Wright, C. J., Wu, H., Melander, R. J., Melander, C., and Lamont, J. (2014). Disruption of Heterotypic Community Development by *Porphyromonas Gingivalis* With Small Molecule Inhibitors. *Mol. Oral Microbiol.* 29 (5), 185–193. doi: 10.1111/omi.12060
- Xu, X., Zhou, X. D., and Wu, C. D. (2011). The Tea Catechin Epigallocatechin Gallate Suppresses Cariogenic Virulence Factors of *Streptococcus Mutans*. *Antimicrob. Agents Chemother.* 55 (3), 1229–1236. doi: 10.1128/AAC.01016-10
- Xu, X., Zhou, X. D., and Wu, C. D. (2012). Tea Catechin Epigallocatechin Gallate Inhibits *Streptococcus Mutans* Biofilm Formation by Suppressing Gtf Genes. *Arch. Oral Biol.* 57 (6), 678–683. doi: 10.1016/j.archoralbio.2011.10.021
- Yang, D., Pornpattananakul, D., Nakatsuji, T., Chan, M., Carson, D., Huang, C.-M., et al. (2009). The Antimicrobial Activity of Liposomal Lauric Acids Against *Propionibacterium Acnes*. *Biomaterials* 30 (30), 6035–6040. doi: 10.1016/j.biomaterials.2009.07.033
- Yang, X., Yang, J., Wang, L., Ran, B., Jia, Y., Zhang, L., et al. (2017). Pharmaceutical Intermediate-Modified Gold Nanoparticles: Against Multidrug-Resistant Bacteria and Wound-Healing Application via an Electrospun Scaffold. *ACS Nano* 11 (6), 5737–5745. doi: 10.1021/acsnano.7b01240
- Yin, I. X., Yu, O. Y., Zhao, I. S., Mei, M. L., Li, Q.-L., Tang, J., et al. (2019). Developing Biocompatible Silver Nanoparticles Using Epigallocatechin Gallate for Dental Use. *Arch. Oral Biol.* 102, 106–112. doi: 10.1016/j.archoralbio.2019.03.022
- Younson, J., and Kelly, C. (2004). The Rational Design of an Anti-Caries Peptide Against *Streptococcus Mutans*. *Mol. Divers.* 8 (2), 121–126. doi: 10.1023/B:MODI.0000025655.93643.f8
- Yuan, R., Tu, J., Sheng, C., Chen, X., and Liu, N. (2021). Effects of Hsp90 Inhibitor Ganetespib on Inhibition of Azole-Resistant *Candida Albicans*. *Front. Microbiol.* 12, 680382. doi: 10.3389/fmicb.2021.680382
- Yu, S., Fan, X., Zheng, S., Lin, L., Liu, J., Pan, Y., et al. (2021). The Sialidase Inhibitor, DANA, Reduces *Porphyromonas Gingivalis* Pathogenicity and Exerts Anti-Inflammatory Effects: An *In Vitro* and *In Vivo* Experiment. *J. Periodontol.* 92 (2), 286–297. doi: 10.1002/JPER.19-0688
- Zazo, H., Millán, C. G., Colino, C. I., and Lanao, J. M. (2017). “Applications of Metallic Nanoparticles in Antimicrobial Therapy,” in *In Antimicrobial Nanoarchitectonics* (Elsevier), 411–444.
- Zhang, L., Kuang, X., Zhou, Y., Yang, R., Zhou, X., Peng, X., et al. (2010). Development of Nanoparticles for Antimicrobial Drug Delivery. *Curr. Med. Chem.* 17 (6), 585–594. doi: 10.2174/092986710790416290
- Zhang, Q., Nguyen, T., McMichael, M., Velu, S. E., Zou, J., Zhou, X., et al. (2015). New Small-Molecule Inhibitors of Dihydrofolate Reductase Inhibit *Streptococcus Mutans*. *Int. J. Antimicrob. Agents* 46 (2), 174–182. doi: 10.1016/j.ijantimicag.2015.03.015
- Zhang, Q., Nijampatnam, B., Hua, Z., Nguyen, T., Zou, J., Cai, X., et al. (2017). Structure-Based Discovery of Small Molecule Inhibitors of Cariogenic Virulence. *Sci. Rep.* 7 (1), 5974.
- Zhang, Y., Ma, W., Zhu, Y., Shi, S., Li, Q., Mao, C., et al. (2018). Inhibiting Methicillin-Resistant *Staphylococcus Aureus* by Tetrahedral DNA Nanostructure-Enabled Antisense Peptide Nucleic Acid Delivery. *Nano Lett.* 18 (9), 5652–5659. doi: 10.1021/acs.nanolett.8b02166
- Zhang, C., Kuang, X., Zhou, Y., Peng, X., Guo, Q., Yang, T., et al. (2019). A Novel Small Molecule, ZY354, Inhibits Dental Caries-Associated Oral Biofilms. *Antimicrob. Agents Chemother.* 63 (5), e02414–18. doi: 10.1128/AAC.02414-18
- Zhang, T., Tian, T., Zhou, R., Li, S., Ma, W., Zhang, Y., et al. (2020). Design, Fabrication and Applications of Tetrahedral DNA Nanostructure-Based Multifunctional Complexes in Drug Delivery and Biomedical Treatment. *Nat. Protoc.* 15 (8), 2728–2757. doi: 10.1038/s41596-020-0355-z
- Zhang, J., Kuang, X., Zhou, Y., Yang, R., Zhou, X., Peng, X., et al. (2021). Antimicrobial Activities of a Small Molecule Compound II-6s Against Oral *Streptococci*. *J. Oral Microbiol.* 13 (1), 1909917. doi: 10.1080/20002297.2021.1909917
- Zhang, B., Qin, X., Zhou, M., Tian, T., Sun, Y., Li, S., et al. (2021). Tetrahedral DNA Nanostructure Improves Transport Efficiency and Anti-Fungal Effect of Histatin 5 Against *Candida Albicans*. *Cell Prolif.* doi: 10.1111/cpr.13020
- Zhang, M., Zhang, X., Tian, T., Zhang, Q., Wen, Y., Zhu, J., et al. (2022). Anti-Inflammatory Activity of Curcumin-Loaded Tetrahedral Framework Nucleic Acids on Acute Gouty Arthritis. *Bioact. Mater.* 8, 368–380. doi: 10.1016/j.bioactmat.2021.06.003
- Zhao, Y., Tian, Y., Cui, Y., Liu, W., Ma, W., and Jiang, X. (2010). Small Molecule-Capped Gold Nanoparticles as Potent Antibacterial Agents That Target Gram-Negative Bacteria. *J. Am. Chem. Soc.* 132 (35), 12349–12356. doi: 10.1021/ja1028843
- Zhao, Y., Chen, Z., Chen, Y., Xu, J., Li, J., and Jiang, X. (2013). Synergy of non-Antibiotic Drugs and Pyrimidinethiol on Gold Nanoparticles Against Superbugs. *J. Am. Chem. Soc.* 135 (35), 12940–12943. doi: 10.1021/ja4058635

**Conflict of Interest:** The authors declare that the research was conducted in the absence of any commercial or financial relationships that could be construed as a potential conflict of interest.

**Publisher's Note:** All claims expressed in this article are solely those of the authors and do not necessarily represent those of their affiliated organizations, or those of the publisher, the editors and the reviewers. Any product that may be evaluated in



this article, or claim that may be made by its manufacturer, is not guaranteed or endorsed by the publisher.

Copyright © 2022 Yang, Lyu, Zhang, Shui, Yang and Xu. This is an open-access article distributed under the terms of the Creative Commons Attribution License

(CC BY). The use, distribution or reproduction in other forums is permitted, provided the original author(s) and the copyright owner(s) are credited and that the original publication in this journal is cited, in accordance with accepted academic practice. No use, distribution or reproduction is permitted which does not comply with these terms.



# Influence of Fluoride-Resistant *Streptococcus mutans* Within Antagonistic Dual-Species Biofilms Under Fluoride *In Vitro*

Keke Zhang<sup>1†</sup>, Yangfan Xiang<sup>1†</sup>, Youjian Peng<sup>2</sup>, Fengyu Tang<sup>1</sup>, Yanfan Cao<sup>1</sup>, Zhenjie Xing<sup>1</sup>, Yejian Li<sup>1</sup>, Xiangyan Liao<sup>1</sup>, Yan Sun<sup>1</sup>, Yan He<sup>3\*</sup> and Qingsong Ye<sup>1,2\*</sup>

<sup>1</sup> School and Hospital of Stomatology, Wenzhou Medical University, Wenzhou, China, <sup>2</sup> Center of Regenerative Medicine, Renmin Hospital of Wuhan University, Wuhan, China, <sup>3</sup> Tianyou Hospital, Wuhan University of Science and Technology, Wuhan, China

## OPEN ACCESS

### Edited by:

Yulong Niu,  
Sichuan University, China

### Reviewed by:

Cheng Zhao,  
University of Washington,  
United States

Adline Princy Solomon,  
SASTRA University, India

### \*Correspondence:

Qingsong Ye  
qingsongye@hotmail.com  
Yan He  
helen-1101@hotmail.com

<sup>†</sup>These authors have contributed  
equally to this work and share  
first authorship

### Specialty section:

This article was submitted to  
Microbiome in Health and Disease,  
a section of the journal  
Frontiers in Cellular and  
Infection Microbiology

**Received:** 25 October 2021

**Accepted:** 20 January 2022

**Published:** 28 February 2022

### Citation:

Zhang K, Xiang Y, Peng Y, Tang F, Cao Y, Xing Z, Li Y, Liao X, Sun Y, He Y and Ye Q (2022) Influence of Fluoride-Resistant *Streptococcus mutans* Within Antagonistic Dual-Species Biofilms Under Fluoride *In Vitro*. *Front. Cell. Infect. Microbiol.* 12:801569. doi: 10.3389/fcimb.2022.801569

The widespread application of fluoride, an extremely effective caries prevention agent, induces the generation of fluoride-resistant strains of opportunistic cariogenic bacteria such as fluoride-resistant *Streptococcus mutans* (*S. mutans*). However, the influence of this fluoride-resistant strain on oral microecological homeostasis under fluoride remains unknown. In this study, an antagonistic dual-species biofilm model composed of *S. mutans* and *Streptococcus sanguinis* (*S. sanguinis*) was used to investigate the influence of fluoride-resistant *S. mutans* on dual-species biofilm formation and pre-formed biofilms under fluoride to further elucidate whether fluoride-resistant strains would influence the anti-caries effect of fluoride from the point of biofilm control. The ratio of bacteria within dual-species biofilms was investigated using quantitative real-time PCR and fluorescence *in situ* hybridization. Cristal violet staining, scanning electron microscopy imaging, and 3-(4,5-dimethylthiazol-2-yl)-2,5-diphenyl-2H-tetrazolium bromide assay were used to evaluate biofilm biomass, biofilm structure, and metabolic activity, respectively. Biofilm acidogenicity was determined using lactic acid and pH measurements. The anthrone method and exopolysaccharide (EPS) staining were used to study the EPS production of biofilms. We found that, in biofilm formation, fluoride-resistant *S. mutans* occupied an overwhelming advantage in dual-species biofilms under fluoride, thus showing more biofilm biomass, more robust biofilm structure, and stronger metabolic activity (except for 0.275 g/L sodium fluoride [NaF]), EPS production, and acidogenicity within dual-species biofilms. However, in pre-formed biofilms, the advantage of fluoride-resistant *S. mutans* could not be fully highlighted for biofilm formation. Therefore, fluoride-resistant *S. mutans* could influence the anti-caries effect of fluoride on antagonistic dual-species biofilm formation while being heavily discounted in pre-formed biofilms from the perspective of biofilm control.

**Keywords:** fluoride-resistant *Streptococcus mutans*, *Streptococcus sanguinis*, antagonistic dual-species biofilm, biofilm homeostasis, cariogenic virulence, dental caries

## INTRODUCTION

Caries is a disease of chronic and progressive destruction of the hard tissue of teeth caused by multiple factors, including bacteria (Mathur and Dhillon, 2018). In the United States, for example, caries prevalence indicated that about 45.8% of children aged 2–19 years old had experienced dental caries in primary and permanent dentitions, while 57% of adults had experienced dental caries (Fleming and Afful, 2018; Brandfass et al., 2019). With the growing sugar intake becoming a global issue, the incidence of dental caries has increased rapidly and has a profound impact on the general health of individuals (Van Loveren, 2019). Over 1,000 different microbial species, also known as oral biofilms, have been identified within the dental plaque (Dewhirst et al., 2010). The caries ecological hypothesis proposed by Phil D. Marsh suggested that there was a balance in the microecology of oral plaque (Marsh et al., 2015). Dental caries result from the disruption of homeostasis in this microecology. Excessive sugar intake and reduced salivary production contribute to the decrease in pH in oral biofilms. Consecutively, acid-tolerant and acid-producing bacteria would survive and strengthen acid production, thus causing the occurrence of demineralization and the development of caries (Marsh et al., 2015).

Fluoride, such as sodium fluoride (NaF), acidulated fluorophosphates (APF), and stannous fluoride (SnF<sub>2</sub>), is commonly used to prevent the development of caries. They are used in clinical anti-caries applications, including toothpaste, mouthwash, gel, varnishes, and tooth-filling materials that release ionic fluoride (Anusavice et al., 2005; Pitts et al., 2017). Fluoride enhances the acid resistance of teeth by inhibiting demineralization and enhancing remineralization and also inhibits the growth and metabolism of bacteria by suppressing the activities of enzymes such as enolase and ATPase (Ten Cate, 2004; Oh et al., 2017). When the pH of the extracellular environment decreases, protons (H<sup>+</sup>) and fluoride (F<sup>-</sup>) from fluoride materials diffuse into bacterial cells and exist as hydrogen fluoride (HF) in the cytoplasm (Marquis et al., 2003). This influx of HF both directly and indirectly affects the growth and cariogenicity of bacteria (Liao et al., 2017). The protective effect of fluoride on the enamel was observed at 0.02 mg/L fluoride, and fluoride significantly reduced the number of *Streptococcus mutans* (*S. mutans*) at a concentration starting from 0.25 g/L. *S. mutans* is one of the main opportunistic cariogenic bacteria, and its virulence factors are acid production, acid tolerance, and adhesion (Liu et al., 2015).

However, the widespread application of fluoride induces the generation of fluoride-resistant strains, including opportunistic cariogenic bacteria such as fluoride-resistant *S. mutans*. As early as 1980, transient fluoride-resistant *S. mutans* strains were isolated from the plaque of radiation-induced xerostomia patients who were treated daily with preventive NaF gel (Streckfuss et al., 1980). Laboratory-induced and characteristically stable (at least 50 generations) fluoride-resistant *S. mutans* were used to study their phenotypes and fluoride-resistant mechanisms (Liao et al., 2017). This type of fluoride-resistant *S. mutans* is generally able to withstand fluoride concentrations three times higher than its

wild strains (Liao et al., 2017). Some studies have reported the phenotypic characteristics of fluoride-resistant strains, such as the stability of fluoride resistance, fitness, growth, acidogenicity, and cariogenicity. These results showed that there are many significant differences in these phenotypic characteristics between the fluoride-resistant strains and their wild strains, such as higher fluoride resistance, higher acid tolerance, lower growth, and some controversial cariogenic characteristics (Van Loveren et al., 1991; Zhu et al., 2012; Liao et al., 2015; Cai et al., 2017; Liao et al., 2017; Liao et al., 2018; Lee et al., 2021). These genetic stability differences could be caused by genetic mutations, as revealed by gene sequencing (Liao et al., 2015; Liao et al., 2018; Lee et al., 2021). Although the complete mechanism of *S. mutans* fluoride resistance needs to be further studied, some genes or genetic loci have been found to be responsible for the fluoride resistance of *S. mutans* (Liao et al., 2016; Men et al., 2016; Murata and Hanada, 2016; Tang et al., 2019; Lu et al., 2020; Yu et al., 2020). However, the ecological effects of fluoride-resistant *S. mutans* remain unknown.

Accumulating evidence indicates that there is a competitive and antagonistic relationship between *S. mutans* and *S. sanguinis* (Marsh and Zaura, 2017). A significant association has been reported between the *S. mutans* and *S. sanguinis* ratio and severe early childhood caries in dental plaque (Mitrakul et al., 2016). The presence of *S. sanguinis* had a negative relationship with the occurrence of dental caries. Kreth et al. reported that *S. sanguinis* could produce hydrogen peroxide to inhibit *S. mutans* (Kreth et al., 2008). *S. mutans* can suppress the adhesion of *S. sanguinis* through mutacin production (Valdebenito et al., 2018). The balance between these two strains represents the equilibrium of dental plaque to some extent (Sun et al., 2019; Du et al., 2021). However, there have been no studies on the influence of fluoride-resistant *S. mutans* on oral microecological homeostasis under fluoride. The present study used an antagonistic dual-species biofilm model composed of *S. mutans* and *S. sanguinis* to investigate the influence of fluoride-resistant *S. mutans* on microbial flora under fluoride. We hypothesized that, under the screening effect of fluoride, fluoride-resistant *S. mutans* might gain a survival advantage within antagonistic dual-species biofilms, which destroys the ecological balance of oral biofilms and leads to the occurrence and development of dental caries. Eventually, it would influence the anti-caries effect of fluoride. This *in vitro* study was designed to verify this hypothesis.

## MATERIALS AND METHODS

### Bacterial Strains and Growth Conditions

*S. mutans* UA159 and *S. sanguinis* ATCC 10556 were obtained from the School and Hospital of Stomatology, Wenzhou Medical University. Fluoride-resistant *S. mutans* was induced *in vitro* as previously described, with modifications (Zhu et al., 2012). Briefly, an overnight bacterial suspension was inoculated on a brain heart infusion (BHI, Oxoid, Basingstoke, UK) agar plate containing 0.5 g/L NaF for 48 h growth, where a single colony of

*S. mutans* was picked and passaged on BHI agar without NaF for 50 generations. The fluoride-resistant characteristics of *S. mutans* were confirmed on BHI solid medium with 0.5 g/L NaF. BHI medium was used for bacterial amplification, and BHI with 1% sucrose (BHIS) was used for biofilm formation. The growth conditions were 37°C and 5% CO<sub>2</sub>.

## Biofilm Culture

In this study, we characterized fluoride-resistant *S. mutans* in biofilm formation and in pre-formed biofilms under fluoride. For biofilm formation, overnight bacterial suspensions of one or two species were diluted 50-fold into BHIS containing 0, 0.275, and 1.25 g/L NaF (0.275 and 1.25 g/L NaF were the fluoride content in regular and prescription toothpaste, respectively, after 3-fold dilution) and incubated for 24 h (Nassar and Gregory, 2017). For the pre-formed biofilm assay, after 24 h of biofilm formation without fluoride, the culture medium was replaced with fresh BHIS with different concentrations of NaF and incubated for another 24 h.

The groups in this experiment were divided into single-species biofilms of *S. mutans* wild-type strain (*S.m* WT), single-species biofilms of fluoride-resistant *S. mutans* (*S.m* FR), single-species biofilms of *S. sanguinis* (*S.s*), dual-species biofilms of the wild type of *S. mutans* strain and *S. sanguinis* (*S.m* WT + *S.s*), and dual-species biofilms of fluoride-resistant *S. mutans* and *S. sanguinis* (*S.m* FR + *S.s*). Each group was treated with different fluoride concentrations, which included control, low (0.275 g/L), and high concentrations (1.25 g/L).

## Crystal Violet Staining

The biomass of the biofilm was determined using crystal violet (CV) staining (Zhu et al., 2021). Biofilms in 96-well plates were washed with phosphate-buffered saline (PBS) and fixed with methanol for 15 min. Air-dried biofilms were stained with 100 µl of 0.1% crystal violet solution for 30 min and washed with PBS. Images of the stained biofilms were captured using a stereo microscope (Nikon SMZ800, Nikon Corporation, Japan). Next, they were dissolved in 200 µl of 33% acetic acid with shaking for 15 min, and the absorbance was measured at 590 nm using a microplate reader (SpectraMax M5, Molecular Devices, USA).

## Metabolic Activity

For metabolic activity assessment, biofilms growing on round glass wafers were washed with PBS to remove planktonic bacteria and stained with 1 ml 0.5% 3-(4,5-dimethylthiazol-2-yl)-2,5-diphenyl-2H-tetrazolium bromide (MTT) solution (dissolved in PBS) for 1 h. Subsequently, the wafers were transferred to a new plate with dimethyl sulfoxide (1 ml per well). Thereafter, the plate was shaken for 30 min to completely dissolve the crystals. A 200-µl aliquot of the solution was measured at 540 nm using a microplate reader (SpectraMax M5, Molecular Devices, USA).

## Lactic Acid and pH Measurement

Lactic acid and pH measurements were conducted to monitor acid production (Sun et al., 2019). Biofilms in wafers were first washed with cysteine peptone water and then cultured in

buffered peptone water (BPW) containing 0.2% sucrose (1 ml/well) for 3 h to allow acid production. Lactic dehydrogenase was used to quantify lactate concentrations in the BPW solution. The absorbance was read at 340 nm, and standard curves were generated using a lactic acid standard.

For pH measurement, the supernatant of the biofilms was measured using a pH meter (Mettler Toledo Instruments Co., Ltd., Shanghai, China).

## Scanning Electron Microscopy Imaging

SEM imaging was performed to observe the morphology and structure of the biofilms (Liu et al., 2013). Biofilms were fixed with 2.5% glutaraldehyde and dehydrated using an ethanol gradient (50, 60, 70, 80, 90, and 95% and absolute ethyl alcohol) for 30 min at each concentration. Dry biofilms were sputter-coated with gold-palladium for observation using SEM at ×2,000 magnification (Hitachi, Tokyo, Japan).

## Water-Insoluble Exopolysaccharide Measurement

The water-insoluble EPS of biofilms was measured using the anthrone method (Sun et al., 2021). Briefly, the biofilms were collected, washed twice with sterile water, and resuspended in 0.4 M NaOH. After centrifugation, 200 µl of the suspension was mixed with 600 µl of anthrone reagent and incubated at 95°C for 6 min. The absorbance was monitored at 625 nm using a microplate reader (SpectraMax M5, Molecular Devices, USA). Standard curves were prepared using dextran standard.

## Confocal Laser Scanning Microscopy Assay

To observe the EPS production in biofilms, fluorescence staining was conducted (Liu et al., 2013). Alexa Fluor-647 dextran conjugate (Molecular Probes, Invitrogen Corp., Carlsbad, CA, USA) was added to the culture medium at the beginning of biofilm formation to label the EPSs. At the end of biofilm formation, the biofilms were stained with SYTO 9 (Molecular Probes, Invitrogen Corp., Carlsbad, CA, USA) for total bacteria measurement. Random fields were selected, and images were captured using a ×60 oil immersion lens with a confocal laser scanning microscope (Nikon Corporation, Tokyo, Japan).

## Quantitative Real-time PCR Assay

To determine the ratio of *S. mutans* and *S. sanguinis* in dual-species biofilms, TB Green Premix Ex Taq™ II kit (Takara Bio Inc., Otsu, Japan) was used for qRT-PCR analysis. The total DNA of dual-species biofilms was extracted using Rapid Bacterial Genomic DNA Isolation Kit (Sangon Biotech, Shanghai, China). The primers used in this study were the same as those previously described (Huang et al., 2015) (Supplementary Table 1). A total of 20 µl of reaction mixture contained 10.0 µl 2× TB Green Premix Ex Taq II, 0.8 µl forward primer, 0.8 µl reverse primer, 2.0 µl cDNA, and 6.4 µl sterilized distilled water. We used a LightCycler 96 instrument (Roche Diagnostics, Basel, Switzerland) and programmed the system for 30 s of pre-denaturation at 95°C, followed by 40 cycles of 5-s



denaturation at 95°C, 30 s annealing at 55°C, and 30-s extension at 72°C. The standard curves of *S. mutans* and *S. sanguinis* were generated based on the known quantities of bacteria by CFU count.

## Fluorescence *In Situ* Hybridization

FISH was used to observe the proportion of bacterial components in the dual-species biofilms. Briefly, after washing with PBS twice, the biofilms on the wafers were fixed with 4% paraformaldehyde for 6 h. Lysozyme was used to lyse the cell wall. The biofilms were then dehydrated with gradient ethanol and dried at 46°C for 10 min. Specific fluorescent probes (Supplementary Table 2) were used to stain *S. mutans* and *S. sanguinis* within dual-species biofilms (Zheng et al., 2013). A confocal laser scanning microscope (Nikon Corporation, Tokyo, Japan) was used to capture the FISH results using a ×60 oil immersion lens.

## Statistical Analysis

All experiments were repeated independently at least thrice. One-way analysis of variance was performed, and statistical significance was set at  $p < 0.05$  using SPSS software (version 24.0; SPSS Inc., Chicago, IL, USA).

## RESULTS

### Fluoride-Resistant *S. mutans* Obtained Remarkable Competitive Advantage Within Dual-Species Biofilms During Biofilm Formation While Not in Pre-Formed Biofilms Under NaF

The ratio of *S.m* and *S.s* in dual-species biofilms was analyzed using FISH and qRT-PCR (Figure 1). We found that *S.s* had an advantage (more than 50%) in competition with *S.m* WT and FR without fluoride in biofilm formation. In the fluoride-free group, *S.m* FR accounted for 11.72% of dual-species biofilms, while *S.m* WT accounted for 31.93%. However, with the addition of NaF, the proportion of *S.m* FR (over 90%) was much higher than that of *S.s*, occupying a dominant position in dual-species biofilms. However, the ratio of *S.m* WT (less than 50%) maintained a previous trend with the effect of NaF. Surprisingly, in the pre-formed biofilm, *S.m* FR did not gain advantage over *S.s* under NaF-like biofilm formation, and the proportion of *S.m* WT was higher than that of *S.s* in all experimental groups in the pre-formed biofilm.

### NaF Had Different Effects on Biofilm Formation and Pre-formed Biofilm Even in WT Strains

Using CV staining, we compared the biomass of different biofilms under NaF treatment (Figure 2). During the biofilm formation of single-species biofilms, *S.m* FR showed a stronger biofilm-forming ability than both *S.m* WT and *S.s* under NaF and even formed a robust biofilm at 1.25 g/L NaF (Figure 2A).

For the biofilm formation of dual-species, *S.m* FR + *S.s* also showed observably improved biofilm formation capability under NaF (Figure 2B). However, NaF had a little anti-biofilm effect on both *S.m* FR and *S.m* WT in pre-formed biofilms (Figure 2C). The pre-formed *S.s* biofilms did not show strong resistance as two *S.m* strains under NaF and its biofilm biomass were reduced significantly under 1.25 g/L NaF (Figure 2C). In the pre-formed dual-species biofilm, both types of dual-species biofilms withstood NaF stress and only decreased by 19.77 and 36.93% for *S.m* WT + *S.s* and 5.57 and 24.13% for *S.m* FR + *S.s* under 0.275 and 1.25 g/L NaF, respectively (Figure 2D). The SEM results also showed a similar tendency in which FR strain-related biofilms acquired survival advantage at 1.25 g/L NaF during biofilm formation, thus forming a more robust biofilm than that of the WT biofilms (Figure 3). However, the fluoride resistance advantage of *S.m* FR was not highlighted in the pre-formed biofilms (Figure 3).

### Biofilm Formation and Pre-formed Biofilm Showed Different Susceptibilities to NaF in Metabolic Activity Even When *S.ms* Was Compared to its Fluoride-Resistant Strain-Related Biofilms

The MTT assay was used to detect the metabolic activity of the biofilms (Figure 4). In general, NaF suppressed the metabolic activity of biofilms, while this inhibitory effect was different between biofilm formation and pre-formed biofilms. At 0.275 g/L NaF, all *S.m* and its containing groups showed greater metabolic activity than the fluoride-resistant and *S.s* strains. During biofilm formation, either *S.m* FR or *S.m* FR + *S.s* involving dual-species biofilm showed a higher metabolic activity than the other groups under NaF at 1.25 g/L (Figures 4A, B). Similar to the CV results in pre-formed biofilms, although NaF showed a suppressive effect on metabolic activity in a strain-, species-, and dose-dependent manner, all pre-formed biofilms could still sustain biofilm even at 1.25 g/L NaF (Figures 4C, D). There were no obvious differences between *S.m* WT and *S.m* FR as well as their involved dual-species biofilms at 1.25 g/L NaF (Figures 4C, D).

### Fluoride-Resistant *S.m*-Related Biofilms Produce More EPS Than WT Strain Under Fluoride

EPS staining (Figure 5) and the anthrone method (Figure 6) were used to measure biofilm EPS production. The biofilm formation results showed that fluoride-resistant strain-related biofilms produced less EPS than WT strains without fluoride, while there was more EPS under fluoride (Figures 5A and 6A, B). In pre-formed biofilms, the results were disparate (Figures 5B and 6C, D). Although fluoride-resistant *S.m*-related biofilms synthesized more EPS at 0.275 mg/L, there were no significant differences between fluoride-resistant *S.m*-related biofilms and their WT biofilms at 1.25 g/L (Figures 6C, D). Analogous results of EPS production were also confirmed by the SEM images (Figure 3).

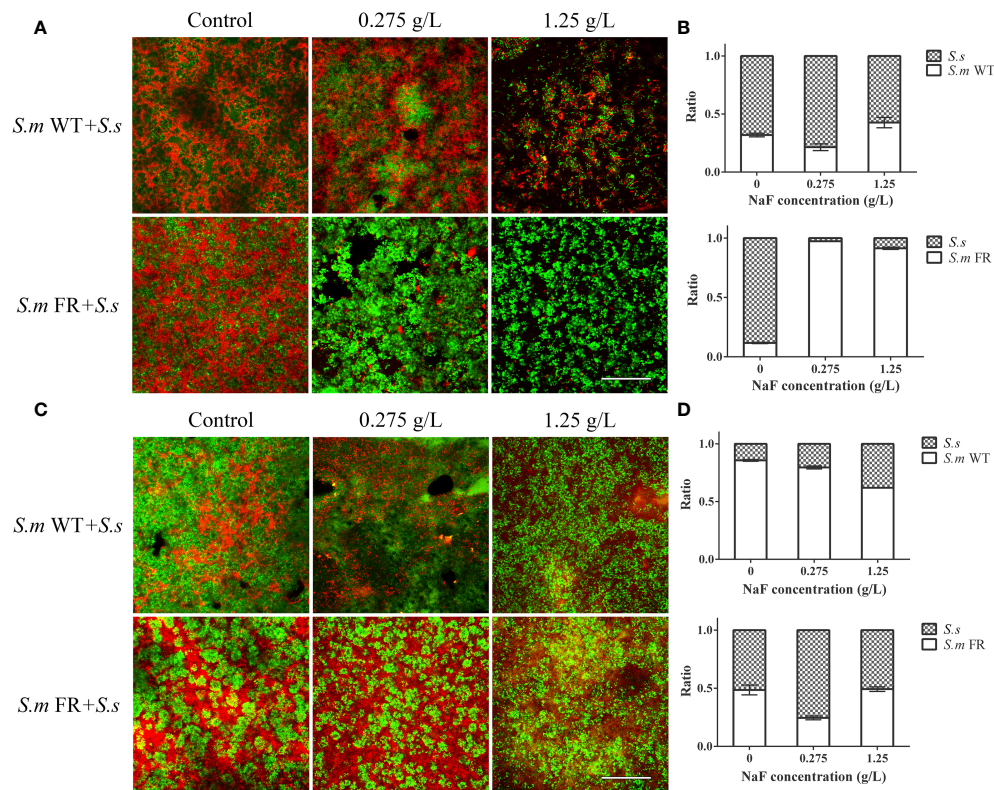


**FIGURE 1** | The composition of dual-species biofilm was monitored using fluorescence *in situ* hybridization (FISH) and qRT-PCR. **(A)** FISH images of 24-h dual-species biofilm in biofilm formation. **(B)** Composition of dual-species biofilm based on qRT-PCR in biofilm formation. **(C)** FISH images of pre-formed biofilms. **(D)** Composition of dual-species pre-formed biofilm based on qRT-PCR. *S. m* was labeled in green, while *S. sanguinis* was in red. Size marker equals 60  $\mu$ m.

## Fluoride-Resistant *S. m*-Related Biofilms Had Lower Supernatant pH Than Wild-Type Strains in All NaF-Containing Groups Except in Pre-Formed Biofilms at High NaF

In total, NaF treatment resulted in a higher pH of the biofilm supernatant (Figure 7). During biofilm formation, *S. m* WT and *S. m* WT + *S. s* had a lower pH than *S. m* FR and *S. m* FR + *S. s* without NaF (Figures 7A, B). However, the opposite was observed with the addition of NaF, as *S. m* FR and *S. m* FR + *S. s* had a lower pH (Figures 7A, B). In pre-formed biofilms, *S. m* FR and *S. m* FR + *S. s* had a lower pH than *S. m* WT and *S. m* WT + *S. s* only at 0.275 mg/L (Figures 7C, D).

## Fluoride-Resistant Strain-Related Biofilms Showed Stronger Lactic Acid Production Under High Fluoride Concentration in Biofilm Formation While Not in Pre-Formed Biofilms

Lactic acid production in the two models of biofilms, biofilm formation and pre-formed biofilms, was also detected. The lactic acid measurements showed that the production of lactic acid by fluoride resistance was inhibited by 0.275 g/L (Figures 8A, B). At 1.25 g/L, the lactic acid production of *S. m* FR and *S. m* FR + *S. s*

was much higher than that of *S. m* WT and *S. m* WT + *S. s* in biofilm formation (Figures 8A, B). Surprisingly, in the pre-formed biofilm, *S. m* FR and *S. m* FR + *S. s* produced less lactic acid than *S. m* WT and *S. m* WT + *S. s* under NaF (Figures 8C, D).

## DISCUSSION

The present study investigated whether fluoride-resistant *S. mutans* would influence oral microecological homeostasis under fluoride in an antagonistic dual-species biofilm model to further investigate whether fluoride-resistant strains would influence the anti-caries effect of fluoride. A dual-species biofilm composed of *S. mutans* and *S. sanguinis* was chosen, as homeostasis of this dual-species biofilm used in our study could also represent dental plaque balance to a certain degree. Both dual-species biofilm formation and pre-formed biofilm were monitored, and our results showed that fluoride-resistant *S. mutans* influenced the composition, biomass, structure, metabolic activity, acid production, and EPS production of dual-species biofilms when compared with wild-type biofilms under NaF. Fluoride-resistant *S. mutans* had a survival advantage and stronger cariogenic potency in dual-species biofilm formation under NaF but could not highlight its fluoride-

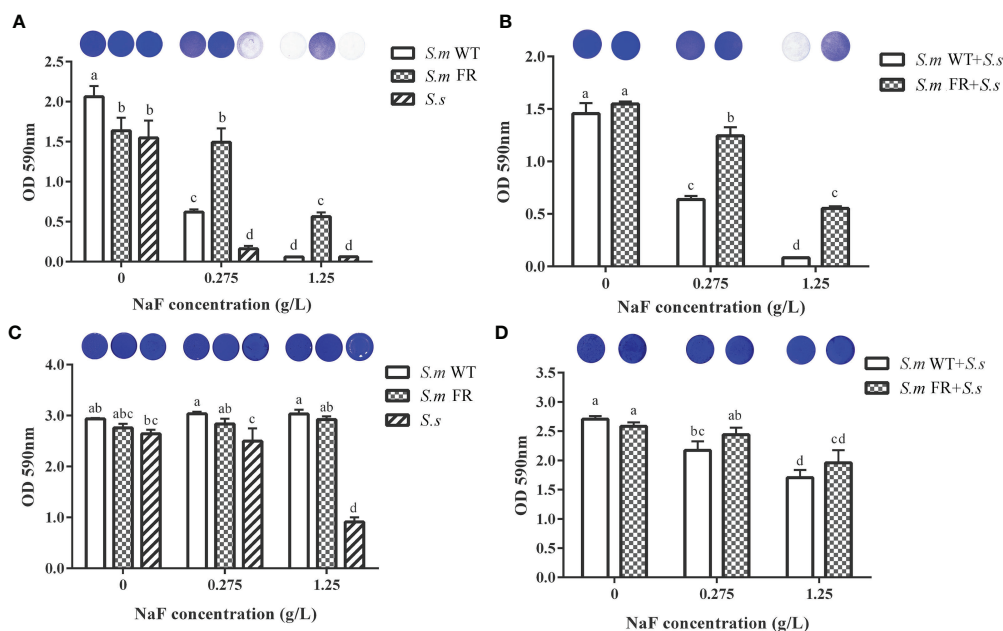


**FIGURE 2** | Biomass measured using crystal violet staining. **(A)** Single-species biofilm formation. **(B)** Dual-species biofilm formation. **(C)** Pre-formed single-species biofilms. **(D)** Pre-formed dual-species biofilms. The same letters indicate no statistical difference, and different letters indicate a significant difference between groups ( $P < 0.05$ ).

resistant superiority thoroughly in pre-formed dual-species biofilms under NaF.

The lower ratio of the fluoride-resistant strain within the dual-species biofilm without NaF compared to its wild strain

might be partly attributed to the slow growth rate of the fluoride-resistant strain in our study (data not shown). The slow growth rate of the fluoride-resistant strain was consistent with previous reports, which might have resulted from bacterial-deficient

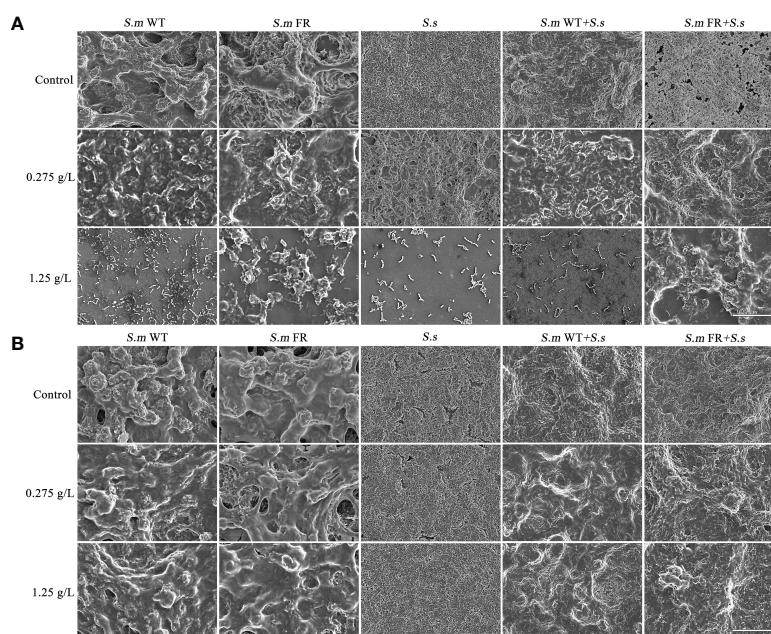


**FIGURE 3** | SEM images of the structure of biofilm in different NaF concentrations at  $\times 2,000$  magnification. **(A)** Biofilm formation. **(B)** Pre-formed biofilms. Size marker equals  $20\ \mu\text{m}$ .



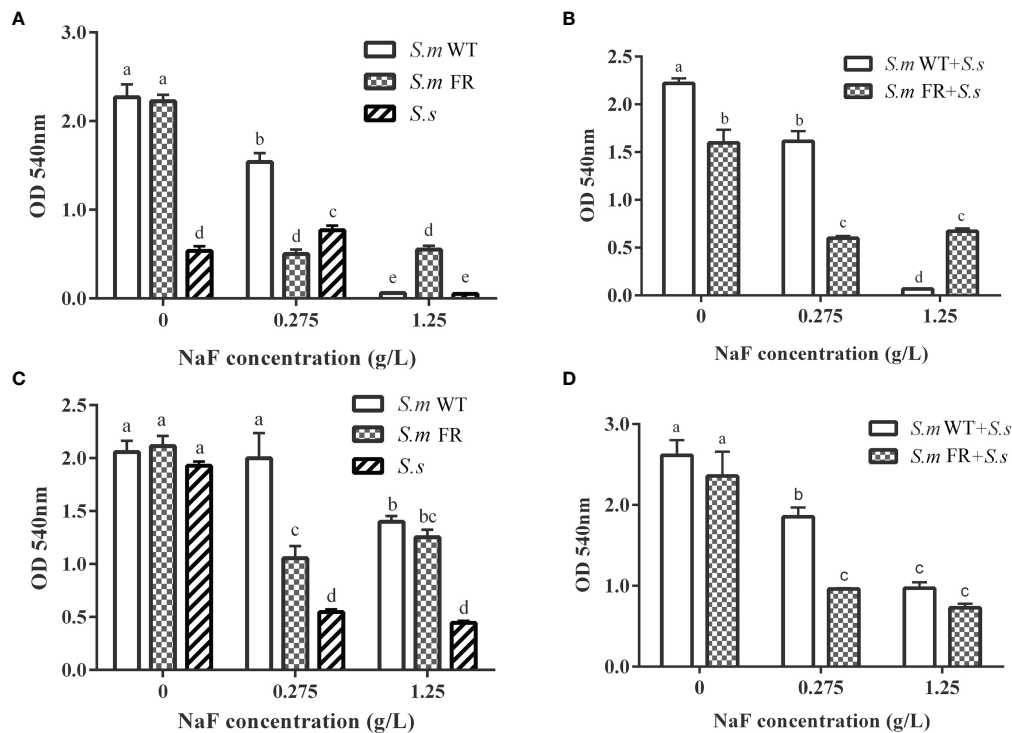


**FIGURE 4 |** Metabolic activity measured using MTT assay. **(A)** Single-species biofilm formation. **(B)** Dual-species biofilm formation. **(C)** Pre-formed single-species biofilms. **(D)** Pre-formed dual-species biofilms. The same letters indicate no statistical difference, and different letters indicate a significant difference between groups ( $P < 0.05$ ).

carbohydrate uptake (Liao et al., 2015; Lee et al., 2021). The ratio of either *S. mutans* or its fluoride-resistant dual-species was raised without NaF with the development of biofilm when compared between 24 and 48 h, which was confirmed by FISH and qRT-PCR. This tendency was similar to a previous study on the association between *S. mutans* and *S. sanguinis*. It has been reported that the level of *S. mutans* is lower than that of *S. sanguinis* in the initial biofilm and higher in the mature biofilm (Mitrakul et al., 2016). However, in line with our expectations, the fluoride-resistant *S. mutans* was at an advantage in competition with *S. sanguinis* with the addition of NaF in biofilm formation owing to its fluoride-resistant properties, which could be supported by the biomass and metabolic activity of single-species biofilm formation. Surprisingly, in the pre-formed biofilm, the trend was completely different, as fluoride-resistant *S. mutans* did not achieve a competitive advantage within dual-species biofilms. The different outcomes of fluoride-resistant *S. mutans* within dual-species biofilms between biofilm formation and pre-formed biofilms under NaF might be explained as follows: NaF was added at the beginning of biofilm formation, and its screening effect on bacterioplankton was effective immediately, resulting in a survival advantage of the fluoride-resistant strain. Once dominant in biofilms, *S. mutans* produces more acid and creates an environment conducive to its own growth, thus taking an advantage over *S. sanguinis* (Takahashi and Nyvad, 2011).

Nevertheless, in preformed biofilms, NaF was added after 24-h formed biofilms. The biofilms are more resistant to drugs than planktonic bacteria as reported previously (Stewart and Costerton, 2001). Owing to the resistance of mature biofilms to drugs, the survival advantage of the fluoride-resistant strain under NaF was almost entirely covered in the pre-formed biofilm.

Fluoride can influence the adherence of *S. mutans*, a dominant cariogenic virulence (Shani et al., 2000). It has been reported that fluoride-resistant strains retain more adherence ability under fluoride (Men et al., 2016). EPS plays an important role in the stability of biofilms and adhesion to tooth surfaces (Flemming and Wingender, 2010). In biofilm formation, the EPS production of dual-species biofilms of fluoride-resistant *S. mutans* was lower than that of the wild strain without NaF. However, under fluoride, the EPS production of dual-species biofilms containing fluoride-resistant *S. mutans* was significantly higher than that of the wild strain, which was the same as that of the single-species biofilms. In pre-formed biofilms, fluoride-resistant *S. mutans*-related biofilms only produced more EPS at 0.275 g/L NaF. EPS is known to help bacteria increase the resistance of biofilms to escape antibiotic drugs and immune responses (Đapa et al., 2013). More EPS accumulation may enhance the resistance and adherence of biofilms and even cause higher cariogenicity. This could partly explain why pre-formed biofilms were more resistant to NaF. As a major factor in cariogenicity, glucosyltransferases (Gtfs) play a critical role in



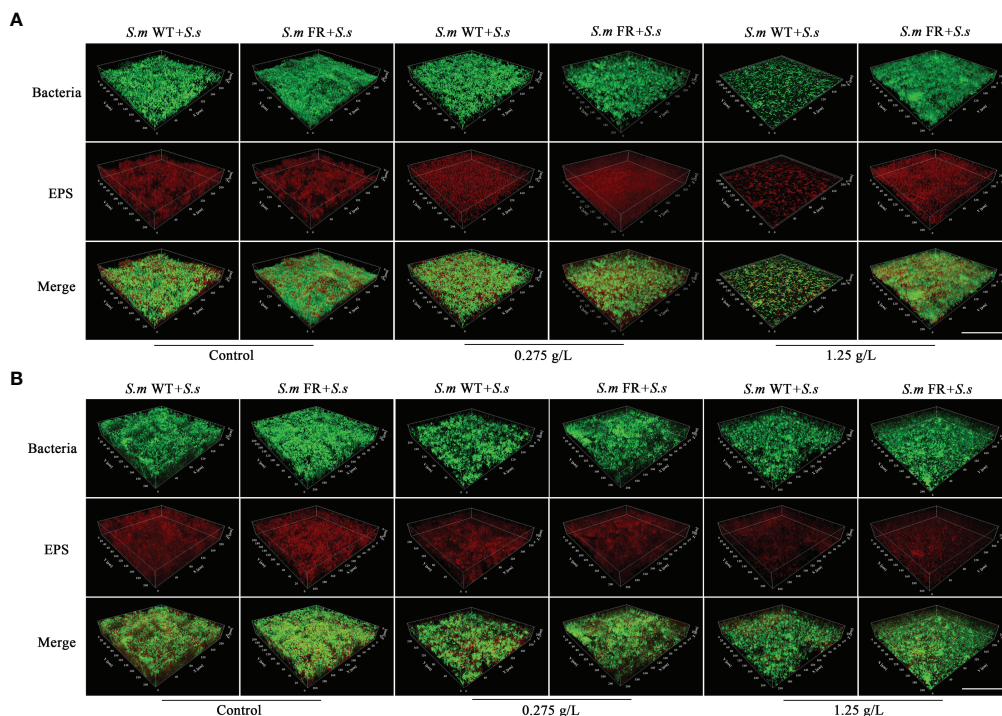


**FIGURE 5** | Representative confocal images of EPS staining in different NaF concentrations. **(A)** Dual-species biofilm formation. **(B)** Pre-formed dual-species biofilms. Total bacterial cells were labeled with SYTO 9 (green) and exopolysaccharide with Alexa Fluor 647 (red). Size marker equals 100  $\mu$ m.

EPS formation (Bowen and Koo, 2011). However, previous studies found that there was no inhibition of Gtfs activity of the *S. mutans* wild strain by fluoride (Pandit et al., 2011; Guo et al., 2014). Whether the Gtfs activity of our fluoride-resistant *S. mutans* was suppressed by NaF needs to be further investigated. We were unaware whether there was a direct relationship between fluoride resistance acquisition and EPS production as shown in single-species biofilm results without NaF. The survival advantage of fluoride-resistant *S. mutans* made a significant contribution to the EPS production of its dual-species biofilms during biofilm formation.

Acid production is also an important factor in cariogenic virulence. In general, NaF had an inhibitory effect on acid production in biofilms, whether in single or dual species, according to our data, which was consistent with a previous report (Liao et al., 2017). At present, there is no unified conclusion about the variation in acid production ability of wild-type *S. mutans* compared with fluoride-resistant *S. mutans*. Some studies found that fluoride-resistant *S. mutans* had a weaker acid production ability, while others found it to be stronger when compared to its related wild strain, and further studies found that there was no significant difference between these two strains (Eisenberg et al., 1985; Van Loveren et al., 1991; Hoelscher and Hudson, 1996; Cai et al., 2017; Lee et al., 2021). This diversity might be derived from different culture conditions and bacterial strains and induced by fluoride-resistant strains. In our study, fluoride-resistant *S. mutans*-related biofilms had a lower supernatant pH than the wild-type strains in all NaF-containing groups except in

pre-formed biofilms at high NaF, indicating a greater cariogenic potential. This result may partly result from the suppression effect of NaF on acid production. During the lactic acid production process without NaF, fluoride-resistant *S. mutans*-related biofilms showed stronger lactic acid production under a high fluoride concentration in biofilm formation, but not in pre-formed biofilms. Lactic acid production was derived from carbohydrate metabolism (Krzyściak et al., 2014). The lactic acid result may be partly attributed to the stronger resistance to NaF in pre-formed biofilm, including the wild-type ones, resulting in an entirely different trend of biofilm metabolic activity when compared to that of biofilm formation, which would further influence lactic acid production. In addition, biofilm composition also contributed to the observed difference, as *S. sanguinis* produced less acid than *S. mutans* and its fluoride-resistant strain within the biofilm. The inconformity between pH and lactic acid results originated from the methods used. For lactic acid measurement, after 24 h of biofilm formation or treatment of pre-formed biofilm with NaF for another 24 h, the resulting biofilms were used for lactic acid production without fluoride. For pH, the culture medium contained fluoride for 24 h in both the biofilm formation and pre-formed biofilms. We hypothesize that the acidogenicity of the fluoride-resistant strain in our study was higher than that of wild strains under fluoride in biofilm formation, which is consistent with previous studies of single-species biofilms (Van Loveren et al., 1991; Hoelscher and Hudson, 1996; Sheng and Liu, 2000). However, this preponderance could not be observed in the pre-formed biofilms.

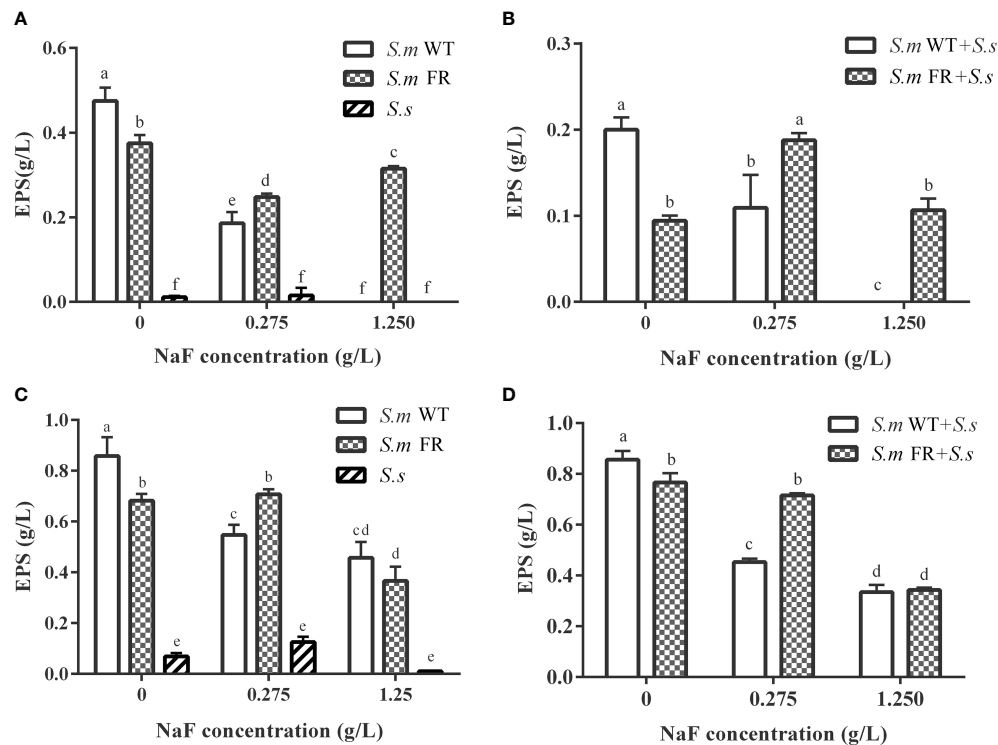


**FIGURE 6** | Water-insoluble exopolysaccharide measured using anthrone method. **(A)** Single-species biofilm formation. **(B)** Dual-species biofilm formation. **(C)** Pre-formed single-species biofilms. **(D)** Pre-formed dual-species biofilms. The same letters indicate no statistical difference, and different letters indicate a significant difference between groups ( $P < 0.05$ ).

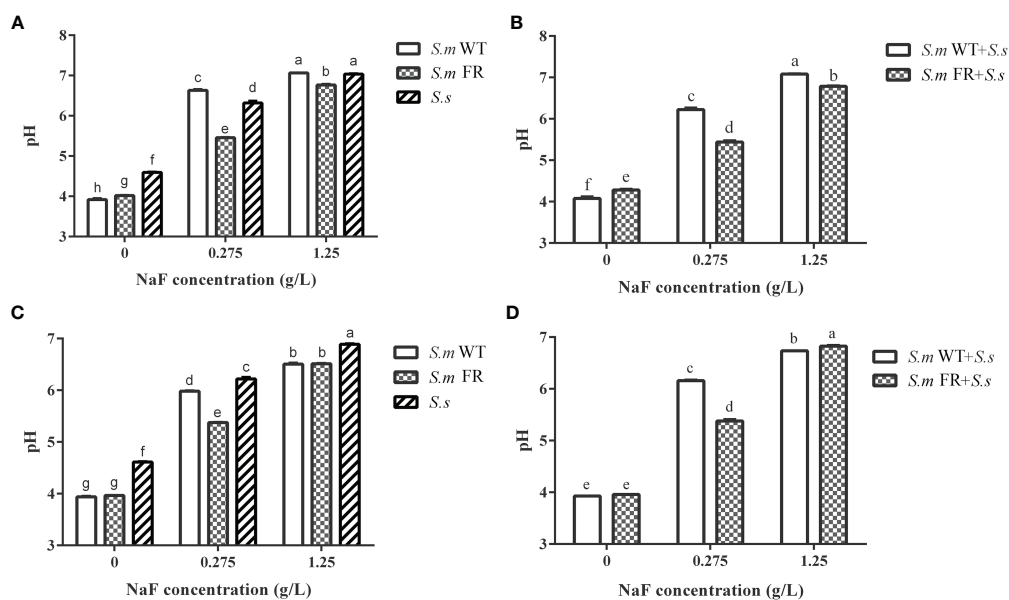


**FIGURE 7** | pH of culture supernatant of biofilm. **(A)** Single-species biofilm formation. **(B)** Dual-species biofilm formation. **(C)** Pre-formed single-species biofilms. **(D)** Pre-formed dual-species biofilms. The same letters indicate no statistical difference, and different letters indicate a significant difference between groups ( $P < 0.05$ ).

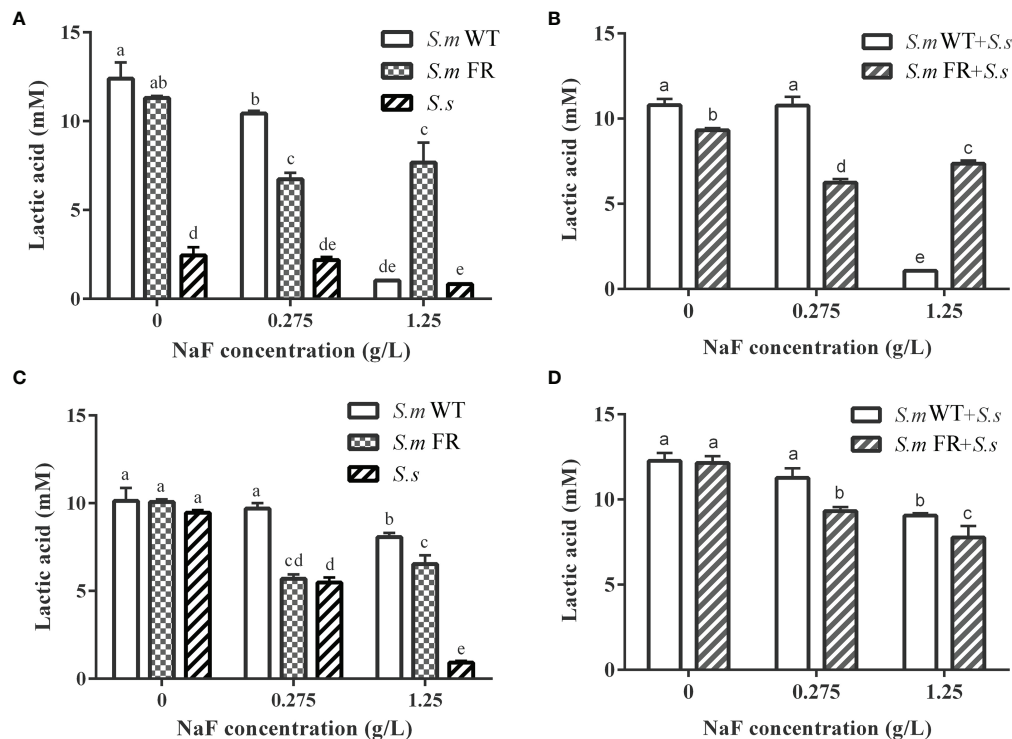


**FIGURE 8** | Lactic acid production of biofilms. **(A)** Single-species biofilm formation. **(B)** Dual-species biofilm formation. **(C)** Pre-formed single-species biofilms. **(D)** Pre-formed dual-species biofilms. The same letters indicate no statistical difference, and different letters indicate a significant difference between groups ( $P < 0.05$ ).

Although the balance between *S. mutans* and *S. sanguinis* could represent the dental plaque equilibrate to some extent, dental plaque is intricate (Sun et al., 2019). Further studies need to be conducted using saliva or *in vivo* biofilms to evaluate the impact of fluoride-resistant strains on the micro-ecology of dental plaque. In addition, studies on the use of more clinically isolated fluoride-resistant strains, including *S. mutans*, were encouraged, as lab-induced fluoride-resistant strains might provide different results from clinical isolates. There is no doubt that a comprehensive understanding of the fluoride-resistant mechanism would inspire more methods to control these fluoride-resistant opportunistic cariogenic bacteria. Drug resistance is a worldwide crisis, especially in the post-antibiotic era. To inhibit biofilm formation containing drug-resistant bacteria, controlling drug-resistant strains should be considered; otherwise, it would occupy an absolute ecological advantage, as in our study. The pre-formed biofilms were more resistant than biofilms during formation in our study, just as reported before (Angelopoulou et al., 2020). Dispersal molecules might be a route to consider, which could trigger biofilm degradation and disperse pre-formed biofilms to the bacterioplankton state and thus could control it by inhibiting biofilm formation (Fleming and Rumbaugh, 2017). Moreover, although fluoride had less impact on controlling fluoride-resistant *S. mutans* biofilms, especially in biofilm formation, whether fluoride-resistant *S. mutans* would finally disrupt homeostasis between demineralization and remineralization

remains to be further studied. Fluoride could inhibit demineralization and enhance remineralization, with the exception of the antibacterial effect.

In summary, this study investigated the effect of fluoride-resistant *S. mutans* on microecological homeostasis using an antagonistic dual-species biofilm model under fluoride. Under the screening effect of fluoride, fluoride-resistant *S. mutans* gained a survival advantage within antagonistic dual-species biofilms during biofilm formation, thus disrupting the ecological balance. Fluoride-resistant *S. mutans* also exhibited stronger cariogenic virulence, including acidogenicity and EPS production, which might further influence the anti-caries effect of fluoride from the perspective of biofilm control. However, in pre-formed biofilms, even wild-type *S. mutans* containing dual-species biofilms showed strong resistance, and the advantage of fluoride-resistant *S. mutans* could not be fully highlighted for biofilm formation. However, this does not mean that fluoride is invalid for fluoride-resistant strains. Inhibition of biofilm biomass, metabolism, acidogenicity, and EPS production was found within biofilms under NaF.

## DATA AVAILABILITY STATEMENT

The original contributions presented in the study are included in the article/Supplementary Material. Further inquiries can be directed to the corresponding authors.

## AUTHOR CONTRIBUTIONS

QY and YH designed this project. KZ and YX conducted experiments and acquired the data. YP, FT, YX, YC, and ZX analyzed and interpreted the data. QY, YH, YL, and XL polished the language. KZ and YX wrote the main manuscript text. KZ and YS acquired funding. All authors contributed to the article and approved the submitted version.

## FUNDING

This study was supported by the National Natural Science Foundation of China (grant no. 82001041), Zhejiang Provincial Natural Science Foundation of China (grant no. LGF20H140001

and LGF19H140004), and Wenzhou Technology Bureau Project (grant no. Y20190487).

## ACKNOWLEDGMENTS

We thank Yi Zheng and Yuqin Zhu from the School of Laboratory Medicine and Life Science, Wenzhou Medical University and Zhejiang Provincial Key Laboratory for Medical Genetics for their confocal laser scanning microscopy support.

## SUPPLEMENTARY MATERIAL

The Supplementary Material for this article can be found online at: <https://www.frontiersin.org/articles/10.3389/fcimb.2022.801569/full#supplementary-material>

## REFERENCES

- Angelopoulou A., Field D., Pérez-Ibarreche M., Warda A. K., Hill C., and Ross R. P. (2020). Vancomycin and Nisin A Are Effective Against Biofilms of Multi-Drug Resistant *Staphylococcus Aureus* Isolates From Human Milk. *PLoS One* 15, e0233284. doi: 10.1371/journal.pone.0233284
- Anusavice K. J., Zhang N. Z., and Shen C. (2005). Effect of CaF<sub>2</sub> Content on Rate of Fluoride Release From Filled Resins. *J. Dent. Res.* 84, 440–444. doi: 10.1177/154405910508400508
- Bowen W. H., and Koo H. (2011). Biology of *Streptococcus Mutans*-Derived Glucosyltransferases: Role in Extracellular Matrix Formation of Cariogenic Biofilms. *Caries Res.* 45, 69–86. doi: 10.1159/000324598
- Brandfass J. T., Ulano A. C., Nickerson J. P., and Bazylewicz M. P. (2019). Dental Caries on CT in the ER Population: Prevalence and Reporting Practices. *Emerg. Radiol.* 26, 263–267. doi: 10.1007/s10140-018-01663-y
- Cai Y., Liao Y., Brandt B. W., Wei X., Liu H., Crielaard W., et al. (2017). The Fitness Cost of Fluoride Resistance for Different *Streptococcus Mutans* Strains in Biofilms. *Front. Microbiol.* 8, 1630. doi: 10.3389/fmicb.2017.01630
- Dapa T., Leuzzi R., Ng Y. K., Baban S. T., Adamo R., Kuehne S. A., et al. (2013). Multiple Factors Modulate Biofilm Formation by the Anaerobic Pathogen *Clostridium Difficile*. *J. Bacteriol.* 195, 545–555. doi: 10.1128/JB.01980-12
- Dewhirst F. E., Chen T., Izard J., Paster B. J., Tanner A. C., Yu W. H., et al. (2010). The Human Oral Microbiome. *J. Bacteriol.* 192, 5002–5017. doi: 10.1128/JB.00542-10
- Du Q., Ren B., He J., Peng X., Guo Q., Zheng L., et al. (2021). *Candida Albicans* Promotes Tooth Decay by Inducing Oral Microbial Dysbiosis. *ISME J.* 15, 894–908. doi: 10.1038/s41396-020-00823-8
- Eisenberg A. D., Wegman M. R., Oldershaw M. D., and Curzon M. E. (1985). Effect of Fluoride, Lithium or Strontium on Acid Production by Pelleted Human Dental Plaque. *Caries Res.* 19, 454–457. doi: 10.1159/000260881
- Fleming E., and Aful J. (2018). Prevalence of Total and Untreated Dental Caries Among Youth: United States 2015–2016. *NCHS Data Brief*, 1–8.
- Fleming D., and Rumbaugh K. P. (2017). Approaches to Dispersing Medical Biofilms. *Microorganisms* 5, 15. doi: 10.3390/microorganisms5020015
- Flemming H. C., and Wingender J. (2010). The Biofilm Matrix. *Nat. Rev. Microbiol.* 8, 623–633. doi: 10.1038/nrmicro2415
- Guo L., Ying Y., Hong X., Zhang R., Yang Y., Hu T., et al. (2014). A Preliminary Study of Exogenous Dextranase and NaF Directly Influence *Streptococcus Mutans* Glucosyltransferase Activity. *J. Pure Appl. Microbiol.* 8, 21–28.
- Hoelscher G. L., and Hudson M. C. (1996). Characterization of an Unusual Fluoride-Resistant *Streptococcus Mutans* Isolate. *Curr. Microbiol.* 32, 156–161. doi: 10.1007/s002849900028
- Huang R., Zhang J., Yang X. F., and Gregory R. L. (2015). PCR-Based Multiple Species Cell Counting for *In Vitro* Mixed Culture. *PLoS One* 10, e0126628. doi: 10.1371/journal.pone.0126628
- Kreth J., Zhang Y., and Herzberg M. C. (2008). Streptococcal Antagonism in Oral Biofilms: *Streptococcus sanguinis* and *Streptococcus gordonii* Interference and LGF19H140004), and Wenzhou Technology Bureau Project (grant no. Y20190487).
- Krzyściak W., Jurczak A., Kościelniak D., Bystrowska B., and Skalniak A. (2014). The Virulence of *Streptococcus mutans* and the Ability to Form Biofilms. *Eur. J. Clin. Microbiol. Infect. Dis.* 33, 499–515. doi: 10.1007/s10096-013-1993-7
- Lee H. J., Song J., and Kim J. N. (2021). Genetic Mutations That Confer Fluoride Resistance Modify Gene Expression and Virulence Traits of *Streptococcus mutans*. *Microorganisms* 9 (4), 849. doi: 10.3390/microorganisms9040849
- Liao Y., Brandt B. W., Li J., Crielaard W., Van Loveren C., and Deng D. M. (2017). Fluoride Resistance in *Streptococcus mutans*: A Mini Review. *J. Oral. Microbiol.* 9, 1344509. doi: 10.1080/20002297.2017.1344509
- Liao Y., Brandt B. W., Zhang M., Li J., Crielaard W., van Loveren C., et al. (2016). A Single Nucleotide Change in the Promoter Mutp Enhances Fluoride Resistance of *Streptococcus mutans*. *Antimicrob. Agents Chemother.* 60, 7509–7512. doi: 10.1128/AAC.01366-16
- Liao Y., Chen J., Brandt B. W., Zhu Y., Li J., Van Loveren C., et al. (2015). Identification and Functional Analysis of Genome Mutations in a Fluoride-Resistant *Streptococcus mutans* Strain. *PLoS One* 10, e0122630. doi: 10.1371/journal.pone.0122630
- Liao Y., Yang J., Brandt B. W., Li J., Crielaard W., van Loveren C., et al. (2018). Genetic Loci Associated With Fluoride Resistance in *Streptococcus mutans*. *Front. Microbiol.* 9, 3093. doi: 10.3389/fmicb.2018.03093
- Liu C., Niu Y., Zhou X., Zhang K., Cheng L., Li M., et al. (2013). Hyperosmotic Response of *Streptococcus mutans*: From Microscopic Physiology to Transcriptomic Profile. *BMC Microbiol.* 13, 275. doi: 10.1186/1471-2180-13-275
- Liu C., Niu Y., Zhou X., Zheng X., Wang S., Guo Q., et al. (2015). *Streptococcus Mutans* Copes With Heat Stress by Multiple Transcriptional Regulons Modulating Virulence and Energy Metabolism. *Sci. Rep.* 5, 12929. doi: 10.1038/srep12929
- Lu M., Xiang Z., Gong T., Zhou X., Zhang Z., Tang B., et al. (2020). Intrinsic Fluoride Tolerance Regulated by a Transcription Factor. *J. Dent. Res.* 99, 1270–1278. doi: 10.1177/0022034520927385
- Marquis R. E., Clock S. A., and Mota-Meira M. (2003). Fluoride and Organic Weak Acids as Modulators of Microbial Physiology. *FEMS Microbiol. Rev.* 26, 493–510. doi: 10.1111/j.1574-6976.2003.tb00627.x
- Marsh P. D., Head D. A., and Devine D. A. (2015). Ecological Approaches to Oral Biofilms: Control Without Killing. *Caries Res.* 49 (Suppl 1), 46–54. doi: 10.1159/000377732
- Marsh P. D., and Zaura E. (2017). Dental Biofilm: Ecological Interactions in Health and Disease. *J. Clin. Periodontol.* 44 (Suppl 18), S12–S22. doi: 10.1111/jcpe.12679
- Mathur V. P., and Dhillon J. K. (2018). Dental Caries: A Disease Which Needs Attention. *Indian J. Pediatr.* 85, 202–206. doi: 10.1007/s12098-017-2381-6
- Men X., Shibata Y., Takeshita T., and Yamashita Y. (2016). Identification of Anion Channels Responsible for Fluoride Resistance in Oral Streptococci. *PLoS One* 11, e0165900. doi: 10.1371/journal.pone.0165900



- Mitrakul K., Vongsawan K., Sriutai A., and Thosathan W. (2016). Association Between *S. Mutans* and *S. Sanguinis* in Severe Early Childhood Caries and Caries-Free Children a Quantitative Real-Time PCR Analysis. *J. Clin. Pediatr. Dent.* 40, 281–289. doi: 10.17796/1053-4628-40.4.281
- Murata T., and Hanada N. (2016). Contribution of Chloride Channel Permease to Fluoride Resistance in *Streptococcus Mutans*. *FEMS Microbiol. Lett.* 363, fnw101. doi: 10.1093/femsle/fnw101
- Nassar H. M., and Gregory R. L. (2017). Biofilm Sensitivity of Seven *Streptococcus Mutans* Strains to Different Fluoride Levels. *J. Oral. Microbiol.* 9, 1328265. doi: 10.1080/20002297.2017.1328265
- Oh H. J., Oh H. W., Lee D. W., Kim C. H., Ahn J. Y., Kim Y., et al. (2017). Chronologic Trends in Studies on Fluoride Mechanisms of Action. *J. Dent. Res.* 96, 1353–1360. doi: 10.1177/0022034517717680
- Pandit S., Kim J. E., Jung K. H., Chang K. W., and Jeon J. G. (2011). Effect of Sodium Fluoride on the Virulence Factors and Composition of *Streptococcus Mutans* Biofilms. *Arch. Oral. Biol.* 56, 643–649. doi: 10.1016/j.archoralbio.2010.12.012
- Pitts N. B., Zero D. T., Marsh P. D., Ekstrand K., Weintraub J. A., Ramos-Gomez F., et al. (2017). Dental Caries. *Nat. Rev. Dis. Primers* 3, 17030. doi: 10.1038/nrdp.2017.30
- Shani S., Friedman M., and Steinberg D. (2000). The Anticariogenic Effect of Amine Fluorides on *Streptococcus Sobrinus* and Glucosyltransferase in Biofilms. *Caries Res.* 34, 260–267. doi: 10.1159/000016600
- Sheng J., and Liu Z. (2000). Induction of Fluoride-Resistant Mutant of *S. Mutans* and the Measurement of Its Acidogenesis *In Vitro*. *Zhonghua Kou Qiang Yi Xue Za Zhi* 35, 95–98.
- Stewart P. S., and Costerton J. W. (2001). Antibiotic Resistance of Bacteria in Biofilms. *Lancet* 358, 135–138. doi: 10.1016/S0140-6736(01)05321-1
- Streckfuss J. L., Perkins D., Horton I. M., Brown L. R., Dreizen S., and Graves L. (1980). Fluoride Resistance and Adherence of Selected Strains of *Streptococcus Mutans* to Smooth Surfaces After Exposure to Fluoride. *J. Dent. Res.* 59, 151–158. doi: 10.1177/00220345800590021501
- Sun Y., Jiang W., Zhang M., Zhang L., Shen Y., Huang S., et al. (2021). The Inhibitory Effects of Ficin on *Streptococcus Mutans* Biofilm Formation. *BioMed. Res. Int.* 2021, 6692328. doi: 10.1155/2021/6692328
- Sun Y., Pan Y., Sun Y., Li M., Huang S., Qiu W., et al. (2019). Effects of Norspermidine on Dual-Species Biofilms Composed of *Streptococcus Mutans* and *Streptococcus Sanguinis*. *BioMed. Res. Int.* 2019, 1950790. doi: 10.1155/2019/1950790
- Takahashi N., and Nyvad B. (2011). The Role of Bacteria in the Caries Process: Ecological Perspectives. *J. Dent. Res.* 90, 294–303. doi: 10.1177/0022034510379602
- Tang B., Gong T., Zhou X., Lu M., Zeng J., Peng X., et al. (2019). Deletion of Cas3 Gene in *Streptococcus Mutans* Affects Biofilm Formation and Increases Fluoride Sensitivity. *Arch. Oral. Biol.* 99, 190–197. doi: 10.1016/j.archoralbio.2019.01.016
- Ten Cate J. M. (2004). Fluorides in Caries Prevention and Control: Empiricism or Science. *Caries Res.* 38, 254–257. doi: 10.1159/000077763
- Valdebenito B., Tullume-Vergara P. O., González W., Kreth J., and Giacaman R. A. (2018). In Silico Analysis of the Competition Between *Streptococcus Sanguinis* and *Streptococcus Mutans* in the Dental Biofilm. *Mol. Oral. Microbiol.* 33, 168–180. doi: 10.1111/omi.12209
- Van Loveren C. (2019). Sugar Restriction for Caries Prevention: Amount and Frequency. Which Is More Important? *Caries Res.* 53, 168–175. doi: 10.1159/000489571
- Van Loveren C., Van De Plassche-Simons Y. M., De Soet J. J., De Graaff J., and Ten Cate J. M. (1991). Acidogenesis in Relation to Fluoride Resistance of *Streptococcus Mutans*. *Oral. Microbiol. Immunol.* 6, 288–291. doi: 10.1111/j.1399-302X.1991.tb00494.x
- Yu J., Wang Y., Han D., Cao W., Zheng L., Xie Z., et al. (2020). Identification of *Streptococcus Mutans* Genes Involved in Fluoride Resistance by Screening of a Transposon Mutant Library. *Mol. Oral. Microbiol.* 35, 260–270. doi: 10.1111/omi.12316
- Zheng X., Zhang K., Zhou X., Liu C., Li M., Li Y., et al. (2013). Involvement of gshAB in the Interspecies Competition Within Oral Biofilm. *J. Dent. Res.* 92, 819–824. doi: 10.1177/0022034513498598
- Zhu J., Liu J., Li Z., Xi R., Li Y., Peng X., et al. (2021). The Effects of Nonnutritive Sweeteners on the Cariogenic Potential of Oral Microbiome. *BioMed. Res. Int.* 2021, 9967035. doi: 10.1155/2021/9967035
- Zhu L., Zhang Z., and Liang J. (2012). Fatty-Acid Profiles and Expression of the fabM Gene in a Fluoride-Resistant Strain of *Streptococcus Mutans*. *Arch. Oral. Biol.* 57, 10–14. doi: 10.1016/j.archoralbio.2011.06.011

**Conflict of Interest:** The authors declare that the research was conducted in the absence of any commercial or financial relationships that could be construed as a potential conflict of interest.

**Publisher's Note:** All claims expressed in this article are solely those of the authors and do not necessarily represent those of their affiliated organizations, or those of the publisher, the editors and the reviewers. Any product that may be evaluated in this article, or claim that may be made by its manufacturer, is not guaranteed or endorsed by the publisher.

Copyright © 2022 Zhang, Xiang, Peng, Tang, Cao, Xing, Li, Liao, Sun, He and Ye. This is an open-access article distributed under the terms of the Creative Commons Attribution License (CC BY). The use, distribution or reproduction in other forums is permitted, provided the original author(s) and the copyright owner(s) are credited and that the original publication in this journal is cited, in accordance with accepted academic practice. No use, distribution or reproduction is permitted which does not comply with these terms.



# Porphyromonas gingivalis Induces Increases in Branched-Chain Amino Acid Levels and Exacerbates Liver Injury Through *livh/livk*

Leng Wu<sup>1,2†</sup>, Rui Shi<sup>1,3†</sup>, Huimin Bai<sup>1</sup>, Xingtong Wang<sup>4</sup>, Jian Wei<sup>2</sup>, Chengcheng Liu<sup>1\*</sup> and Yafei Wu<sup>1\*</sup>

## OPEN ACCESS

### Edited by:

Jin Xiao,  
University of Rochester, United States

### Reviewed by:

J. Christopher Fenno,  
University of Michigan, United States  
Qingyuan Guo,  
Qingdao University Medical College,  
China  
Alexandra Tsigarida,  
University of Rochester, United States

### \*Correspondence:

Chengcheng Liu  
liuchengcheng519@163.com  
Yafei Wu  
yfw1110@163.com

<sup>†</sup>These authors have contributed  
equally to this work

### Specialty section:

This article was submitted to  
Microbiome in Health and Disease,  
a section of the journal  
Frontiers in Cellular and  
Infection Microbiology

**Received:** 14 September 2021

**Accepted:** 17 February 2022

**Published:** 10 March 2022

### Citation:

Wu L, Shi R, Bai H, Wang X,  
Wei J, Liu C and Wu Y (2022)  
Porphyromonas gingivalis Induces  
Increases in Branched-Chain Amino  
Acid Levels and Exacerbates  
Liver Injury Through *livh/livk*.  
Front. Cell. Infect. Microbiol. 12:776996.  
doi: 10.3389/fcimb.2022.776996

<sup>1</sup> State Key Laboratory of Oral Diseases, National Clinical Research Center for Oral Diseases, West China Hospital of Stomatology, Department of Periodontics, Sichuan University, Chengdu, China, <sup>2</sup> Department of Stomatology, Tongji Hospital, Tongji Medical College, Huazhong University of Science and Technology, Wuhan, China, <sup>3</sup> Department of Periodontics and Oral Mucosal Diseases, The Affiliated Stomatology Hospital of Southwest Medical University, Luzhou, China, <sup>4</sup> Department of Hematology, Cancer Center, The First Hospital of Jilin University, Changchun, China

*Porphyromonas gingivalis*, a keystone periodontal pathogen, has emerged as a risk factor for systemic chronic diseases, including non-alcoholic fatty liver disease (NAFLD). To clarify the mechanism by which this pathogen induces such diseases, we simultaneously analyzed the transcriptome of intracellular *P. gingivalis* and infected host cells via dual RNA sequencing. Pathway analysis was also performed to determine the differentially expressed genes in the infected cells. Further, the infection-induced notable expression of *P. gingivalis livk* and *livh* genes, which participate in branched-chain amino acid (BCAA) transfer, was also analyzed. Furthermore, given that the results of recent studies have associated NAFLD progression with elevated serum BCAA levels, which reportedly, are upregulated by *P. gingivalis*, we hypothesized that this pathogen may induce increases in serum BCAA levels and exacerbate liver injury via *livh/livk*. To verify this hypothesis, we constructed *P. gingivalis livh/livk*-deficient strains ( $\Delta livk$ ,  $\Delta livh$ ) and established a high-fat diet (HFD)-fed murine model infected with *P. gingivalis*. Thereafter, the kinetic growth and exopolysaccharide (EPS) production rates as well as the invasion efficiency and *in vivo* colonization of the mutant strains were compared with those of the parental strain. The serum BCAA and fasting glucose levels of the mice infected with either the wild-type or mutant strains, as well as their liver function were also further investigated. It was observed that *P. gingivalis* infection enhanced serum BCAA levels and aggravated liver injury in the HFD-fed mice. Additionally, *livh* deletion had no effect on bacterial growth, EPS production, invasion efficiency, and *in vivo* colonization, whereas the  $\Delta livk$  strain showed a slight decrease in invasion efficiency and *in vivo* colonization. More importantly, however, both the  $\Delta livk$  and  $\Delta livh$  strains showed impaired ability to upregulate serum BCAA levels or exacerbate liver injury in HFD-fed mice. Overall, these results suggested that *P. gingivalis* possibly aggravates NAFLD progression in HFD-fed

mice by increasing serum BCAA levels, and this effect showed dependency on the bacterial BCAA transport system.

**Keywords:** *Porphyromonas gingivalis*, branched-chain amino acids, non-alcoholic fatty liver disease, dual RNA-sequencing, *livh*, *livk*

## INTRODUCTION

Globally, non-alcoholic fatty liver disease (NAFLD), with a prevalence of approximately 25%, is one of the most common liver diseases (Younossi et al., 2018), and reportedly, it has as one of its pathological features, the excessive accumulation of triglyceride in the liver, owing to metabolic alterations (Zhang et al., 2018a). It has also been observed that this disease can develop into reversible steatosis and non-alcoholic steatohepatitis (NASH), which is a more serious form of NAFLD that shows potential progression to liver cirrhosis or cancer (Friedman et al., 2018). The mechanisms by which NAFLD develops and progresses are extremely complicated. Thus, it has been suggested that several potential risk factors, such as diabetes mellitus and obesity, can lead to its aggravation (Buzzetti et al., 2016; Friedman et al., 2018). Further, increasing evidence from cross-sectional studies, as well as longitudinal and experimental studies, has shown the existence of an association between periodontitis and NAFLD (Weintraub et al., 2019; Chen et al., 2020; Hatasa et al., 2021). Specifically, periodontitis, which is an inflammatory disease that is initiated by the dysbiosis of oral flora, is characterized by the destruction of alveolar bone and connective tissues around the teeth (Liu et al., 2017b; Lu et al., 2020; Hajishengallis and Lamont, 2021). It has also been suggested that *Porphyromonas gingivalis*, a gram-negative anaerobe, is the most important pathogenic bacterium in periodontitis (Lamont et al., 2018; Liu et al., 2021). Furthermore, *P. gingivalis* possesses a plurality of virulence factors that invade periodontal tissues and subsequently enter blood circulation and disseminate into the whole body, increasing the risk of several systemic diseases, notably diabetes, cardiovascular diseases, rheumatoid arthritis, Alzheimer's disease, and NAFLD (Potempa et al., 2017; Nakahara et al., 2018; Mei et al., 2020; Fitzsimonds et al., 2021). Previous studies have shown that *P. gingivalis* infection aggravates liver inflammation and fibrosis in NASH mouse

model induced by high-fat diet (HFD) (Furusho et al., 2013; Nagasaki et al., 2020). Recently, Nagasaki et al. also reported that the elimination of *P. gingivalis*-odontogenic infection inhibits liver inflammation and fibrosis of NASH (Nagasaki et al., 2021). Thus, the mechanisms by which *P. gingivalis* infection leads to liver injury have attracted our attention.

Branched-chain amino acids ( BCAAs), which include leucine, isoleucine, and valine, are essential amino acids that mediate the regulation of important hepatic metabolic signaling pathways, such as insulin signaling and glucose regulation (Zhang et al., 2018b). Multiple studies have revealed that elevated circulating BCAA levels are strongly associated with obesity and diabetes, which are the most well-known risk factors for NAFLD (McCormack et al., 2013; Menni et al., 2013; Lynch and Adams, 2014; Nakamura et al., 2014), and in several recent studies, the relationship between BCAAs and NAFLD progression has been demonstrated (Cook et al., 2015; Zhang et al., 2016; Zhao et al., 2020). In particular, the downregulated expression of hepatic BCAA-degrading enzymes has been identified as a hallmark of NAFLD (Mardinoglu et al., 2014; Lake et al., 2015). Moreover, it has also been observed that patients with NASH show higher hepatic BCAA levels than patients with simple steatosis (Lake et al., 2015), and in addition to BCAA-degrading deficiency and fat accumulation in the liver, it has been reported that serum BCAA levels are positively correlated with the severity of NAFLD (Kalhan et al., 2011; Gaggini et al., 2018; Grzych et al., 2020). Recently, Zhao et al. found that BCAAs supplementation in HFD-mice could disrupt hepatic glucose and lipid metabolism and aggravate liver insulin resistance *via* negatively regulating hepatic Akt2 signaling. BCAAs supplementation led to mTORC1-dependent insulin receptor substrate activation, which then block insulin-mediated Akt activation. On the other hand, BCAAs supplementation could inhibit mTORC2 signaling, and subsequently induce Akt2 ubiquitination and degradation *via* promoting the binding of Mül1 and Akt2 (Zhao et al., 2020).

Humans do not synthesize BCAAs, and elevated human serum BCAA levels are strongly associated with gut microbiota (Pedersen et al., 2016). Notably, *Prevotella copri* and *Bacteroides vulgatus*, which have a high potential for BCAA biosynthesis and a low potential for BCAA import, have been identified as the major contributors to increased BCAA levels in humans (Pedersen et al., 2016). Interestingly, a recent study also demonstrated that *P. gingivalis* enhances serum BCAA levels *via* BCAA biosynthesis and consequently, induces insulin resistance in HFD-fed mice (Tian et al., 2020). Furthermore, genetic analysis and transport studies have revealed that the leucine-isoleucine-valine (LIV) system, a member of the ATP-binding cassette (ABC) superfamily of transporters, is required

**Abbreviations:** NAFLD, non-alcoholic fatty liver disease; NASH, non-alcoholic steatohepatitis; HFD, high-fat diet; BCAAs, branched-chain amino acids; EPS, exopolysaccharide; LIV, leucine-isoleucine-valine; ABC, adenosine 5'-triphosphate binding cassette; TSB, trypticase soy broth; HUVEC, human umbilical vein endothelial cells; PBS, phosphate buffered solution; DEGs, differentially expressed genes; FDR, false discovery rate; FC, fold-change; KEGG, Kyoto Encyclopedia of Genes and Genomes; GO, Gene Ontology; FITC, fluorescein isothiocyanate isomer-I; NC, normal chew; CMC, carboxymethyl cellulose; ALT, alanine transaminase; AST, aspartate aminotransferase; ANOVA, analysis of variance; SD, standard deviation. PCA, principal component analysis; PC1, first principal component; HIF-1, hypoxia inducible factor 1; qRT-PCR, quantitative reverse transcription PCR; qPCR, quantitative polymerase chain reaction; CSLM, confocal laser scanning microscopy; FBG, fasting blood glucose.

for BCAA transport (Ribardo and Hendrixson, 2011). Therefore, the aim of the present study was to comprehensively analyze the transcriptomes of intracellular *P. gingivalis* and endothelial cells infected by *P. gingivalis* to clarify the mechanism by which this pathogen exacerbates liver injury.

## MATERIALS AND METHODS

### Bacteria and Cell Culture

*P. gingivalis* ATCC 33277 was cultured anaerobically in trypticase soy broth (TSB) or on TSB-blood agar plates supplemented with 1 g/L yeast extract, 5 µg/mL hemin, and 1 µg/mL menadione at 37°C. When needed, erythromycin (10 µg/mL) was added to the medium to eliminate isogenic mutants. Human umbilical vein endothelial cells (HUVECs) (EA. hy926) were maintained in Dulbecco's modified Eagle's medium with fetal bovine serum (10%) (Millipore Sigma, St. Louis, MO, USA) and penicillin/streptomycin (1%) at 37°C in a 5% CO<sub>2</sub> atmosphere (Wang et al., 2017). The PCR fusion technique and electroporation were utilized to generate the *P. gingivalis* BCAA ABC transporter permease (*livh*)-deficient strain ( $\Delta$ *livh*) and the ABC-type BCAA transport system periplasmic component (*livk*)-deficient strain ( $\Delta$ *livk*) via homologous recombination, as described in **Figure S1** (Wright et al., 2014). The primers used for mutant construction and confirmation are shown in **Table S1**. The mutants were confirmed via PCR and DNA sequencing (**Figure S1**).

HUVECs were seeded in 6-well plates and cultured to 80% confluence. After washing with phosphate-buffered saline (PBS), cells were infected with *P. gingivalis* at a multiplicity of infection of 100 for 2 h at 37°C in 5% CO<sub>2</sub>, unless otherwise stated. Non-adherent bacteria were removed by washing with PBS, and the cell-adherent bacteria were killed using gentamicin (300 µg/mL) and metronidazole (200 µg/mL) for 1 h at 37°C in 5% CO<sub>2</sub> (Moffatt et al., 2012). For RNA isolation, the cells were washed with PBS and lysed using TRIzol<sup>®</sup> reagent (Invitrogen, Carlsbad, CA, USA).

### Dual RNA Sequencing

Total RNA was extracted using TRIzol<sup>®</sup> reagent (Invitrogen, Carlsbad, CA, USA) according to protocols provided by the manufacturer. Further, genomic DNA was removed using the commercially available DNase I system (Qiagen, Germantown, PA, USA), and RNA concentration was measured by determining the A260/A280 ratio using a Nanodrop 2000 system (ThermoFisher, Waltham, MA, USA). RNA integrity was verified via 1.5% agarose gel electrophoresis, and qualified RNAs were quantified using a Qubit 3.0 fluorometer with a Qubit<sup>™</sup> RNA Broad Range Assay Kit (ThermoFisher, Waltham, MA). Furthermore, the RNA samples were analyzed at the Huayin Genome Research Facility (Huayin Health Medical Group Co, Wuhan, China) to determine ribosomal RNA (rRNA) depletion and subsequent RNA sequencing, and rRNA was removed using a Ribo-off rRNA Depletion Kit (Vazyme Biotech Co., Nanjing, China) for humans (Catalog No. N406)

and/or bacteria (catalog NO. N407). Additionally, cDNA libraries for Illumina<sup>®</sup> sequencing were generated using the KC-Digital<sup>™</sup> Stranded mRNA Library Prep Kit (Illumina, San Diego, CA, USA). The library products corresponding to 200–250 bps were then enriched, quantified, and sequenced using a Nova-seq 6000 sequencer (Illumina, San Diego, CA, USA) (Westermann et al., 2016; Westermann et al., 2017; Westermann and Vogel, 2018).

Trimmomatic version 0.36 was used to pre-process raw sequencing data to remove low-quality reads and trim adaptor sequences. To eliminate duplication bias introduced during library preparation and sequencing, the clean reads were first clustered according to the unique molecular identifier sequences, the reads in the same cluster were then compared via pairwise alignment to generate new sub-clusters based on sequence identity (>95%), and multiple sequence alignments were conducted to acquire one consensus sequence for each sub-cluster. De-duplicated consensus sequences were then mapped to the human or *P. gingivalis* ATCC 33277 genome using STAR 2.5.3a. Feature Counts (Subread-1.5.1; Bioconductor) was used for counting reads mapped to the exon regions of each gene, after which the number of reads per kilobase million was calculated. Further, the edgeR package v3.12.1 was used to identify differentially expressed genes (DEGs) between the infected group and control group. Genes with false discovery rate (FDR) P-values < 0.05 and absolute log<sub>2</sub>FC value ≥ 1 were considered as differentially expressed. Principal-component analysis was conducted via the function rda in the Vegan package in R. Kyoto Encyclopedia of Genes and Genomes (KEGG) enrichment analysis was conducted after the DEGs were identified using the KEGG orthology-based annotation system. Thereafter, to statistically test the results of the enrichment analysis, a hypergeometric test was performed; a cutoff P-value of 0.05 was applied for the identification of the enriched KEGG pathways (Nuss et al., 2017; Westermann and Vogel, 2018). Gene Ontology (GO) enrichment analysis for DEGs was carried out by the R/Bioconductor package clusterProfiler, and P < 0.05 was set as the threshold level to determine the significance of the GO terms (Yu et al., 2012).

### Quantitative Reverse Transcription PCR (qRT-PCR)

For the gene expression assay, total mRNA was extracted as mentioned above and reverse transcribed into cDNA using the PrimeScript RT reagent Kit (Takara Bio, Kusatsu, Japan). qRT-PCR was then performed using the SYBR<sup>®</sup> Premix Ex Taq<sup>™</sup> II Kit (Takara Bio, Kusatsu, Japan) or via TaqMan Fast Universal Master Mix and TaqMan gene expression assay (ThermoFisher, Waltham, MA, USA) using an Applied Biosystems 7300 system (Foster City, CA, USA) (Liu et al., 2021). PCR amplification was performed as follows: 95°C for 5 min, and 40 cycles at 95°C for 15 s, 56°C for 15 s and 72°C for 15 s, and melting curve analysis. Relative mRNA expression was quantified through the comparative 2<sup>-ΔΔCT</sup> method with GAPDH as the internal control (Liu et al., 2015). The mRNA expression levels of *livk*



and *livh* were measured using 16S rRNA as an internal reference based on the primers listed in **Table S1**.

### Growth Curves of *P. gingivalis*

The overnight culture of *P. gingivalis* was diluted to an optical density at 600 nm (OD<sub>600</sub>) of 0.1 using fresh medium, and then anaerobically cultured at 37°C. The OD<sub>600</sub> of the bacterial culture was then measured at 2-h intervals for 24 h using a spectrophotometer (Multiskan GO; Thermo Scientific, Inc., Waltham, MA, USA). The experiments were each repeated three times, and growth curves were generated.

### Invasion Assays

Invasion experiments were set up as mentioned in 2.1 except that HUVECs were seeded in 12-well plates ( $2.0 \times 10^5$  cells per well) and cultured to 60% confluence. After antibiotic treatment, the cells were washed with PBS and then lysed with sterile distilled water (1 mL per well). The lysates were diluted and plated on TSB-blood agar. After incubation anaerobically at 37°C for 10 days, the number of bacterial colonies on TSB-Blood agar was counted to determine invasion efficiency, which was expressed as the percentage of the initial inoculum recovered (Moffatt et al., 2012).

### Exopolysaccharide (EPS) Level Detection

The amount of EPS produced by *P. gingivalis* was determined using fluorescent lectins, as described previously (Liu et al., 2017a). Briefly, *P. gingivalis* cells were labeled with Syto-17 (Thermo Fisher, Waltham, MA, USA) and deposited on glass coverslips, while the polysaccharides were labeled with concanavalin A-fluorescein isothiocyanate isomer-I (FITC) and wheat germ agglutinin-FITC ( $100 \mu\text{g mL}^{-1}$ ) for 30 min at room temperature. Thereafter, images were collected *via* laser scanning confocal microscopy (SP8; Leica, Germany) and analyzed using Volocity software version 6.3 (PerkinElmer, Waltham, MA, USA).

### Animal Studies

All the animal procedures applied in the present study were approved by the Ethics Committee of Tongji Hospital, Tongji Medical College, Huazhong University of Science and Technology and the Ethics Committee of West China Hospital of Stomatology, Sichuan University (WCHSIRB-D-2017-071). C57BL/6 mice (male, five-week-old) were housed in specific pathogen-free facilities, and after one week of environmental acclimation, the mice were randomly assigned into five groups of 5 mice each as follows: normal chow (NC) control, HFD, *P. gingivalis* WT infection with HFD (WT + HFD), *P. gingivalis*  $\Delta\text{livh}$  infection with HFD ( $\Delta\text{livh}$  + HFD), and *P. gingivalis*  $\Delta\text{livk}$  infection with HFD ( $\Delta\text{livk}$  + HFD). The mice in the HFD group and NC group were administered Research Diet No. D12492 and No. D12450J, respectively (**Table S2**). After 12 weeks, the mice were euthanized, and liver and sera samples were harvested. Further, blood samples were drawn *via* cardiac puncture using non-anticoagulant vacuum tubes and 23G1 needles (Tian et al., 2020).

Mice in the *P. gingivalis* infection groups were inoculated with  $1 \times 10^9$  bacteria in 100  $\mu\text{L}$  PBS with 2% carboxymethyl cellulose (CMC) (Kuboniwa et al., 2017). Infection was repeated once every 3 days for 8 weeks. Conversely, mice in the NC and HFD groups were inoculated with PBS containing 2% CMC as controls. The body weights of the mice were measured at baseline and at the end of the experiment.

### Quantification of *P. gingivalis* in Liver Tissue

Total DNA was isolated from aliquots of liver samples, and the copy number of the *P. gingivalis* genome in the liver DNA samples was determined *via* qPCR using the Wizard<sup>®</sup> Genomic DNA Purification Kit (Promega, Madison, WI, USA) and the SYBR<sup>®</sup> Premix Ex Taq<sup>™</sup> II Kit (Takara Bio, Kusatsu, Japan). *P. gingivalis*-specific primers are listed in **Table S1**. Amplification reactions were performed using the following cycling parameters: 95°C for 5 min, 40 cycles at 95°C for 10 s, 60°C for 15 s, and 72°C for 15 s. The corresponding copy numbers were calculated using a standard curve (**Figure S2**), generated as previously described (Kuboniwa et al., 2017).

### Glucose, Alanine Transaminase (ALT), Aspartate Aminotransferase (AST), and BCAA Levels in Blood

The mice were fasted for 6 h prior to blood sample collection for the determination of fasting blood glucose (FBG) levels. Specifically, after the fasting, blood samples were collected from the tail vein of the mice and FBG levels were measured using a glucometer (Roche, Basel, Switzerland). Serum was collected after centrifuging the blood samples at  $1,000 \times g$  for 10 min at 4°C and stored at -80°C until further analysis. Serum AST and ALT levels were also measured using AST and ALT activity assay kits, respectively (Millipore Sigma, St. Louis, MO, USA), while serum BCAA levels were determined using BCAA assay kits (Abcam, Cambridge, MA, USA).

### Statistical Analysis

Statistical analysis was performed using GraphPad Prism software version 7.0 (San Diego, CA, USA). Unpaired two-tailed Student's t-tests were used to assess differences between groups, while analysis of variance (ANOVA) with Tukey's test was carried out for multiple comparisons to analyze datasets with more than two groups. Statistical significance was set at  $P < 0.05$ . Further, the results were presented as mean  $\pm$  standard deviation (mean  $\pm$  SD).

## RESULTS

### Upregulation of Bacterial Genes Related to BCAA Transport Within Endothelial Cells

Principal component analysis (PCA) was used to determine the distances between *P. gingivalis* transcriptomes within endothelial cells and the free culture medium. Specifically, the first principal

component (PC1), which showed the largest variance (43.8%), separated intracellular *P. gingivalis* and *P. gingivalis* in the culture medium (Figure 1A). Additionally, intracellular *P. gingivalis* showed a total of 573 DEGs compared with the control bacteria, and of these DEGs, 304 and 269 were upregulated and downregulated, respectively (Figure 1B). The complete list of the DEGs corresponding to intracellular *P. gingivalis* is shown in Table S3. GO analysis revealed that upregulated genes were significantly enriched in the GO terms amino acid biosynthetic and metabolic processes (Figure 1C). Interestingly, ABC transporter genes, which are critical for the virulence of *P. gingivalis*, were also significantly upregulated in intracellular bacteria (Table S3). Further analysis of the expression levels of PGN\_RS06330 (BCAA ABC transporter permease, *livh*) and PGN\_RS06345 (ABC-type BCAA transport system periplasmic component, *livk*) via qRT-PCR confirmed that the expression levels of *livh* and *livk* increased significantly in intracellular *P. gingivalis* (Figure 1D). Adaptation through horizontal gene transfer, which is mediated by *tra* gene homologs (Tribble et al., 2007), is regarded as an important process that is required for the survival of *P. gingivalis* within its host. In this regard, it was observed that *P. gingivalis traA*, *traI*, *traG*, *traN*, *traJ*, *traO*, *traQ*, *traM*, and *traP* genes were significantly upregulated in HUVECs compared with levels in the culture

medium (Table S3). Further, HcpR, which is necessary for the growth of *P. gingivalis* with nitrite and nitric oxide, was also upregulated (Table S3).

## Role of *livh/livk* in Bacterial Growth, Invasion, and EPS Production

To explore the role of *livh/livk* in *P. gingivalis*, we further assessed the effect of *livh/livk* deficiency on bacterial growth, invasion, and EPS production *in vitro*. The construction of the growth curve of *P. gingivalis* showed that the growth rates of either the *livh* or *livk* mutant strains were comparable to that of the parental strain (Figure 2A). Additionally, the invasion efficiency of the  $\Delta livk$  strain was confirmed using an invasion assay (Figure 2B). However, no significant difference in invasion efficiency was observed between the  $\Delta livh$  and WT strains (Figure 2B). Moreover, EPS production often plays an important role in biofilm communities developing. Therefore, to assess the role of *livh/livk* in EPS production, *P. gingivalis* was labeled with Syto-17, and EPS was stained with fluorescently labeled lectin concanavalin A and wheat germ agglutinin (Figure 2C). Thereafter, the level of EPS was normalized to that of *P. gingivalis*, and it was observed that the rates of production of EPS in  $\Delta livh$  and  $\Delta livk$  were not significantly different from those in the parental strain (Figure 2D).

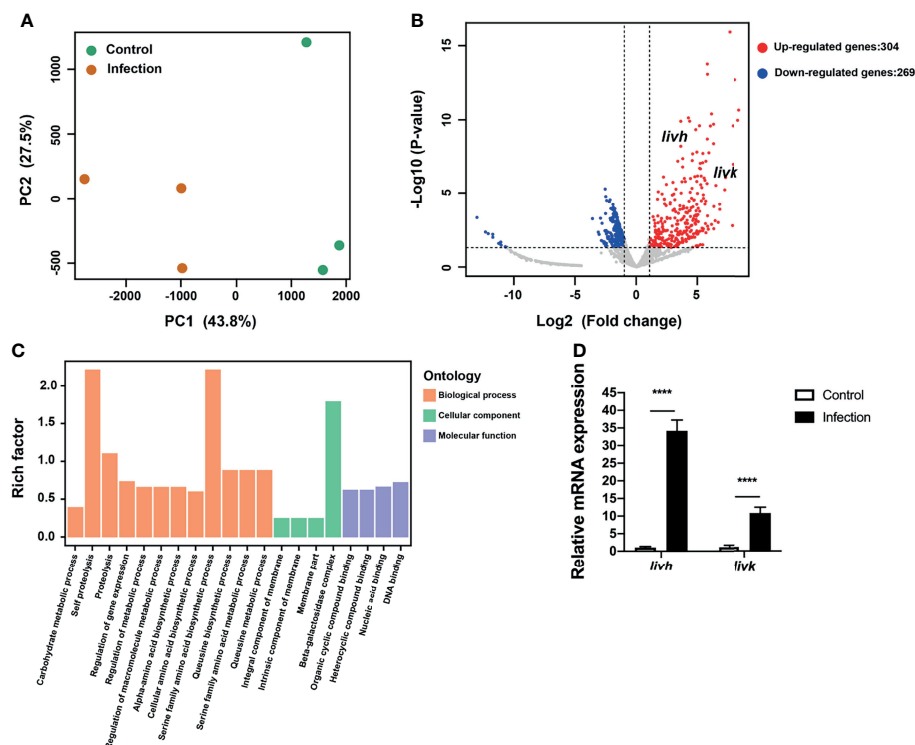


**FIGURE 1 |** Transcriptional profiling of *P. gingivalis* in HUVECs. **(A)** Transcriptional patterns of intracellular *P. gingivalis* (infection) and *P. gingivalis* culture in the medium (control) showing clear divergence as determined via PCA. **(B)** Volcano plot of differentially expressed genes. **(C)** Bar plots of enriched GO terms of upregulated genes in intracellular *P. gingivalis*. **(D)** Detection of the expression levels of *livh* and *livk* in *P. gingivalis*. FC of the expression level of each gene in intracellular *P. gingivalis* (infection) relative to that in the *P. gingivalis* culture medium (control). HUVECs, human umbilical vein endothelial cells; PCA, principal component analysis; FC, fold change. The results presented are the average of three independent experiments and are presented as mean  $\pm$  SD; \*\*\*\* $P \leq 0.0001$ .

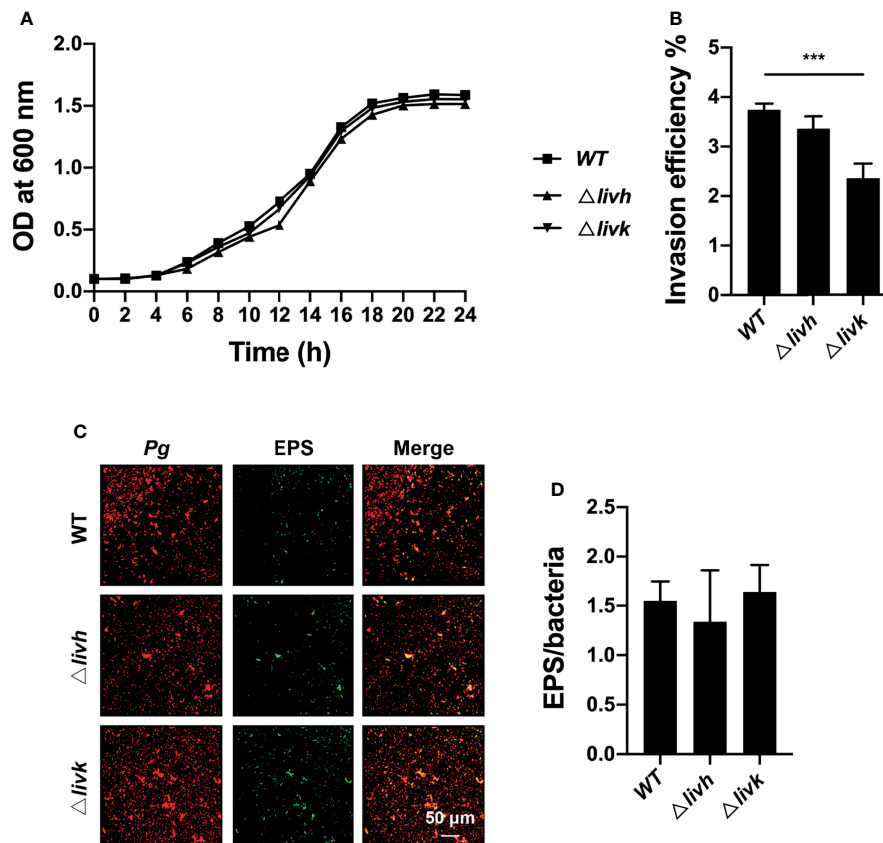


**FIGURE 2 |** Role of *livh/livk* in the growth, invasion efficiency, and EPS production of *P. gingivalis*. **(A)** Growth curve of *P. gingivalis* ATCC 33277 WT,  $\Delta livh$ , and  $\Delta livk$  strain. **(B)** Invasion efficiency of *P. gingivalis*  $\Delta livh/\Delta livk$  compared with that of the parental strain. **(C)** Representative CSLM images of EPS (green) labeled with FITC-labeled concanavalin A and wheat germ agglutinin and *P. gingivalis* (red) wild-type,  $\Delta livh$  and  $\Delta livk$ . Scale bar = 50  $\mu$ m. **(D)** Quantitative determination of EPS using Volocity software version 6.3. CSLM, confocal laser scanning microscopy, EPS, exopolysaccharide, FITC, fluorescein isothiocyanate isomer-I. The results are the average of three independent experiments and are presented as mean  $\pm$  SD, \*\*\* $P \leq 0.001$ .

## Eukaryotic Targets of *P. gingivalis* Enriched in the NAFLD Pathway

To gain insight into the pathways corresponding to the endothelial cells targeted by bacteria, we analyzed the DEGs and enriched KEGG pathways corresponding to HUVECs challenged with *P. gingivalis*. It was observed that the transcriptional landscapes of the infected and uninfected HUVECs showed two independent clusters, indicating distinct gene expression patterns (Figure 3A). Additionally, a total of 838 DEGs were detected in *P. gingivalis*-infected HUVECs compared with their uninfected counterparts, and of these, 297 and 541 genes were upregulated and downregulated, respectively (Figure 3B). The complete list of DEGs corresponding to the HUVECs is shown in Table S4. Further, we annotated the DEGs identified during the comparison of the infected and uninfected HUVECs based on the KEGG pathway. It was observed that both the upregulated and downregulated genes were enriched in pathways associated with chronic systemic diseases, including Parkinson's disease, Huntington's disease, NAFLD, and Alzheimer's disease (Figures 3C, D). However, only the

upregulated DEGs were found to be enriched in the taste transduction, metabolic, and hypoxia inducible factor 1 (HIF-1) signaling pathways (Figure 2C). Moreover, the downregulated DEGs were also enriched in pyrimidine metabolism, purine metabolism, RNA transport, RNA polymerase, viral carcinogenesis, transcriptional misregulation in cancer, systemic lupus erythematosus, and alcoholism pathways (Figure 3D). To corroborate the involvement of NAFLD-related genes in HUVECs challenged with *P. gingivalis*, the expression levels of *MTCO2*, *MTCO3*, *UQCRB*, and *NDUFB10* were detected via qRT-PCR (Table 1). Consistent with the dual RNA sequencing results, *MTCO2* and *MTCO3* were significantly upregulated, whereas *UQCRB* and *NDUFB10* were significantly downregulated in cells infected with *P. gingivalis* (Figure 3E).

## Bacteria Induces Increases in Circulating BCAA Levels and Liver Injury via *livh/livk*

To clarify the potential effect of *P. gingivalis* infection on NAFLD, an HFD-fed mouse model was used to confirm the transmission of *P. gingivalis* in the liver, and detect the effect of

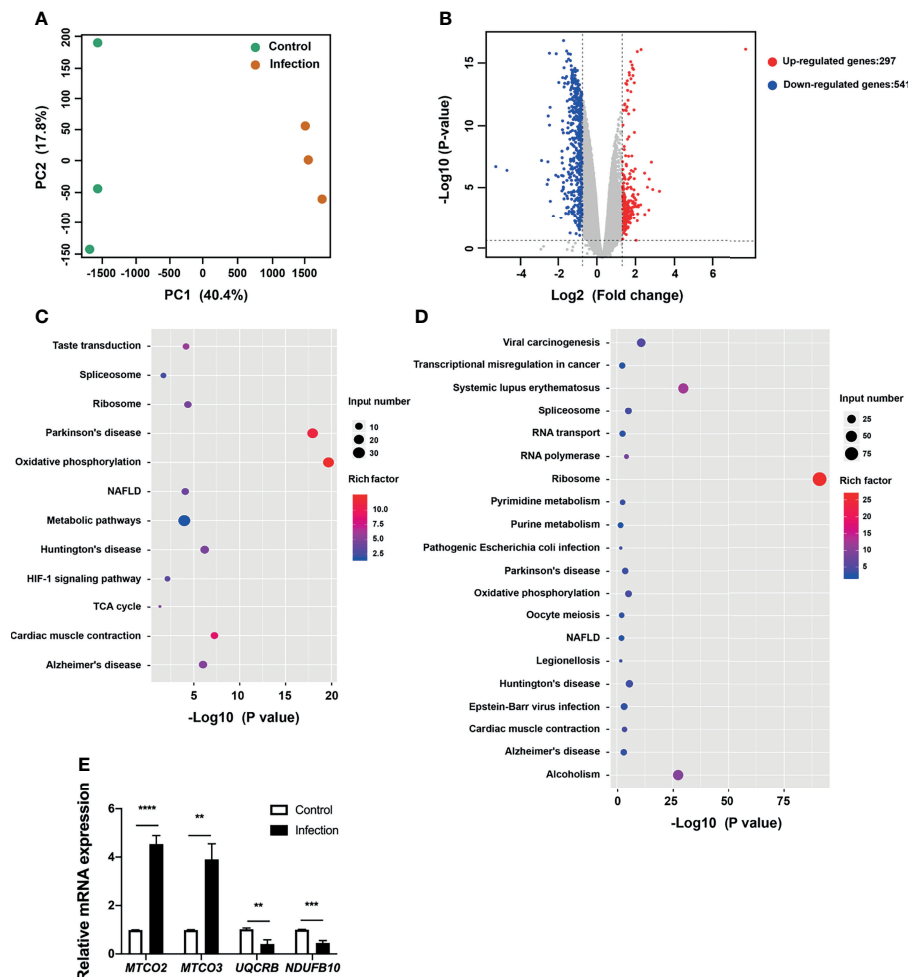


**FIGURE 3** | Transcriptional pattern of HUVECs in response to *P. gingivalis* infection. **(A)** Transcriptional pattern of HUVECs infected with *P. gingivalis* (infection) and uninfected cells (control) showing clear divergence as determined via PCA. **(B)** Volcano plot of differentially expressed genes in HUVECs. **(C)** KEGG analysis of upregulated genes in HUVECs during infection. **(D)** KEGG analysis of downregulated genes in HUVECs during infection. **(E)** Validation of RNA sequencing data via qRT-PCR. The expression of *MTCO2*, *MTCO3*, *UQCRCB*, and *NDUFB10* in endothelial cells. FC of the expression of each gene in HUVECs infected with *P. gingivalis* relative to that corresponding to uninfected cells. HUVECs, human umbilical vein endothelial cells; PCA, principal component analysis; FC, fold change; KEGG, Kyoto Encyclopedia of Genes and Genomes. The results are the average of three independent experiments and are presented as mean  $\pm$  SD. \*\* $P \leq 0.01$ ; \*\*\* $P \leq 0.001$ ; \*\*\*\* $P \leq 0.0001$ .

bacterial infection on circulating BCAA levels, FBG levels, and liver function. As expected, at the end of the experiment, it was observed that the HFD induced an increase in the body weight of the mice, which were unaffected by infection with *P. gingivalis* (Table S5). Additionally, the serum levels of FBG, ALT, and AST, as well as the AST/ALT ratios were significantly elevated in mice fed HFD compared with those in mice fed NC (Figure S3), suggesting that HFD resulted in impaired liver function in the mice. Consistent with the results of previous studies, *P. gingivalis* was detected in the liver tissue of WT + HFD mice (Figure 4A). Further, *P. gingivalis* infection also induced increased serum ALT and AST levels, elevated the AST/ALT ratio, and resulted in higher FBG levels in the HFD-fed mice, confirming that *P. gingivalis* can aggravate HFD-induced liver injury (Figures 4B–E).

Circulating BCAAs participate in the regulation of liver function, and *livh/livk* has been annotated as a BCAA ABC transporter permease or ABC-type BCAA transport system periplasmic component of *P. gingivalis*. Therefore, we measured serum BCAA levels in mice infected with different strains of *P. gingivalis*. The results showed that *P. gingivalis* infection induced increases in BCAA levels in HFD-fed mice (Figure 4F). However, this was compromised by either  $\Delta livh$  or  $\Delta livk$  (Figure 4F). Given that the reduced invasion efficiency of the  $\Delta livk$  strain was confirmed via an invasion assay (Figure 2B), we further investigated the effect of  $\Delta livh$  or  $\Delta livk$  deficiency on *P. gingivalis* liver transmission. We observed that the liver of HFD-fed mice contained less  $\Delta livk$  than the parental strain (Figure 4A). Interestingly, FBG, ALT, and AST levels, as well as the AST/ALT ratios in both the  $\Delta livh$  + HFD and  $\Delta livk$  + HFD



**TABLE 1 |** Differentially expressed genes of the NAFLD pathway between infected and uninfected human umbilical vein endothelial cells ( $|\log_2 FC| \geq 1$  and  $FDR \leq 0.05$ ).

Gene Symbol	Log <sub>2</sub> FC	FDR
MT-CYB	1.532528324	2.03E-12
MTCO3P12	1.294580426	9.23E-11
MIR6723	1.362691234	7.13E-06
MT-CO2	1.442745846	5.75E-12
MT-CO1	1.434791085	2.72E-11
MT-CO3	1.230595848	2.39E-10
MTCO1P2	1.174011287	0.002827059
CDC42P6	-1.784905872	9.93E-06
COX4I1	-1.35886734	2.67E-12
COX6C	-1.202149761	1.21E-10
NDUFA8	-1.083056922	5.67E-08
UQCRLH	-1.636421338	2.29E-08
UQCRB	-1.186605753	4.31E-10
NDUFB10	-1.283988953	7.11E-11
UQCR10	-1.215371564	8.66E-07
NDUF55	-1.496650718	8.89E-12
COX7B	-1.488988881	2.36E-10

groups were significantly lower than those in the WT + HFD group. This notwithstanding, the  $\Delta livh$  + HFD and  $\Delta livk$  + HFD groups showed no significant difference (Figures 4B–E).

## DISCUSSION

This study provides the transcriptional landscape of intracellular *P. gingivalis* as well as that of endothelial cells infected by this bacterium based on dual RNA sequencing. A comparison of the transcriptional profiles of the intracellular bacteria and the free-cultured bacteria cells revealed that *P. gingivalis* infection enhances the expression of BCAA ABC transporter permease (*livh*) and ABC-type BCAA transport system periplasmic component (*livk*) genes to facilitate their survival in host cells. Additionally, both *livh* and *livk* were identified as components of the LIV system, and were found to be responsible for the transport of BCAAs. By analyzing mutants with the deletion of individual genes, we observed that the growth rates of either  $\Delta livh$  or  $\Delta livk$  strains as well as the rate of EPS production in *P. gingivalis*-infected cells were comparable to those in the parental strain. Interestingly,  $\Delta livk$  showed impaired invasion efficiency and *in vivo* colonization. A previous study also showed that *livk*, but not *livh*, is required for commensal colonization by *Campylobacter jejuni* (Ribardo and Hendrixson, 2011). Thus, a possible explanation for this observation is that *livk* may bind to amino acids other than BCAAs, whose transport is required for bacterial survival *in vivo*. To understand different invasion and colonization of  $\Delta livk$  and  $\Delta livh$  mutants, further study such as analyzing the transcriptional profiles of these mutants in HUVEC's is needed.

Further, transcriptional profiling together with KEGG pathway analysis of HUVECs revealed that *P. gingivalis* induced the differential expression of NAFLD-related genes (e.g., *MTCO2*, *MTCO3*, *UQCRB*, and *NDUFB10*). NAFLD is a condition in which excess fat, not related to alcohol use, is stored in the liver. Further, NAFLD and its progressive inflammatory form, NASH,

represent a growing cause of chronic liver injury (Huang et al., 2021), and increasing evidence suggests the existence of a correlation between *P. gingivalis* and NAFLD (Ding et al., 2019). Yoneda et al. first observed that the detection rate of *P. gingivalis* in the saliva is significantly higher in NAFLD patients than that in healthy controls (46.7% vs. 21.7%, odds ratio: 3.16) (Yoneda et al., 2012). Furusho et al. also reported the detection of *P. gingivalis* in 21 out of 40 liver biopsy specimens from NASH patients. They also reported that *P. gingivalis*-positive cases showed significantly higher fibrosis scores than *P. gingivalis*-negative cases (Furusho et al., 2013). Consistent with these previous findings, Nakahara et al. recently identified a significant correlation between NAFLD progression and the titer of serum antibodies against *P. gingivalis* (Nakahara et al., 2018).

Dual RNA-seq has the potential to provide novel insights into the host–pathogen interaction *via* simultaneously determining the transcriptomes of host and pathogen. However, dual RNA-seq is complex experiments. Factors such as heterogeneity in cell populations and infection, differences in transcriptome stabilization, RNA extraction, library preparation, and sequencing may induce batch effects. To obtain accurate representative genomes of the host and pathogen, high sequencing depth is required. Besides, dual RNA-seq crucially depends on proper statistical analysis to determine DEGs during infection. Currently, three popular analysis, EdgeR, DESeq2 and limma/voom, perform well. DESeq generally appears to be more conservative and edgeR more liberal in its p-value calculations. In this study, the unique molecular identifier sequences were introduced to optimize the de-duplication, and DEGs was identified using the edgeR package. In addition to the validation of the sequencing results through qRT-PCR for *in vitro* infection,  $\Delta livk$  and  $\Delta livh$  mutants was constructed and *in vivo* experiments were performed to demonstrate our hypothesis.

Animal studies have also shown that *P. gingivalis* accelerates NAFLD progression in HFD-fed mice. Specifically, Kuraji et al. showed that experimental periodontitis induced by *P. gingivalis* leads to the progression of NASH. It has also been reported that increased levels of endotoxins resulting from *P. gingivalis* infection possibly contribute to NASH progression (Kuraji et al., 2016). Nakahara et al. also observed that fibrosis and steatosis are more severe in HFD-fed mice infected with *P. gingivalis* than in mice without *P. gingivalis* infection, and their further metabolome analysis suggested that the alteration in fatty acid metabolism seems to play a considerable role in the fibrosis progression of NAFLD (Nakahara et al., 2018). Moreover, in HFD-fed mice, intravenous injection of sonicated *P. gingivalis* aggravates NAFLD and changes the expression levels of genes associated with lipid and glucose metabolism in the liver (Sasaki et al., 2018). Mechanistically, *P. gingivalis* odontogenic infection possibly aggravates NASH *via* the upregulation of the lipopolysaccharide and toll-like receptor pathway and free fatty acid-induced NOD-, LRR-, and pyrin domain-containing protein 3 inflammasome activation (Furusho et al., 2013). In this study, we identified LIV as a novel mechanism by which *P. gingivalis* induces increases in BCAA levels and exacerbates liver injury in HFD-fed mice. This finding is consistent with an earlier study, which showed that elevated circulating BCAA levels are

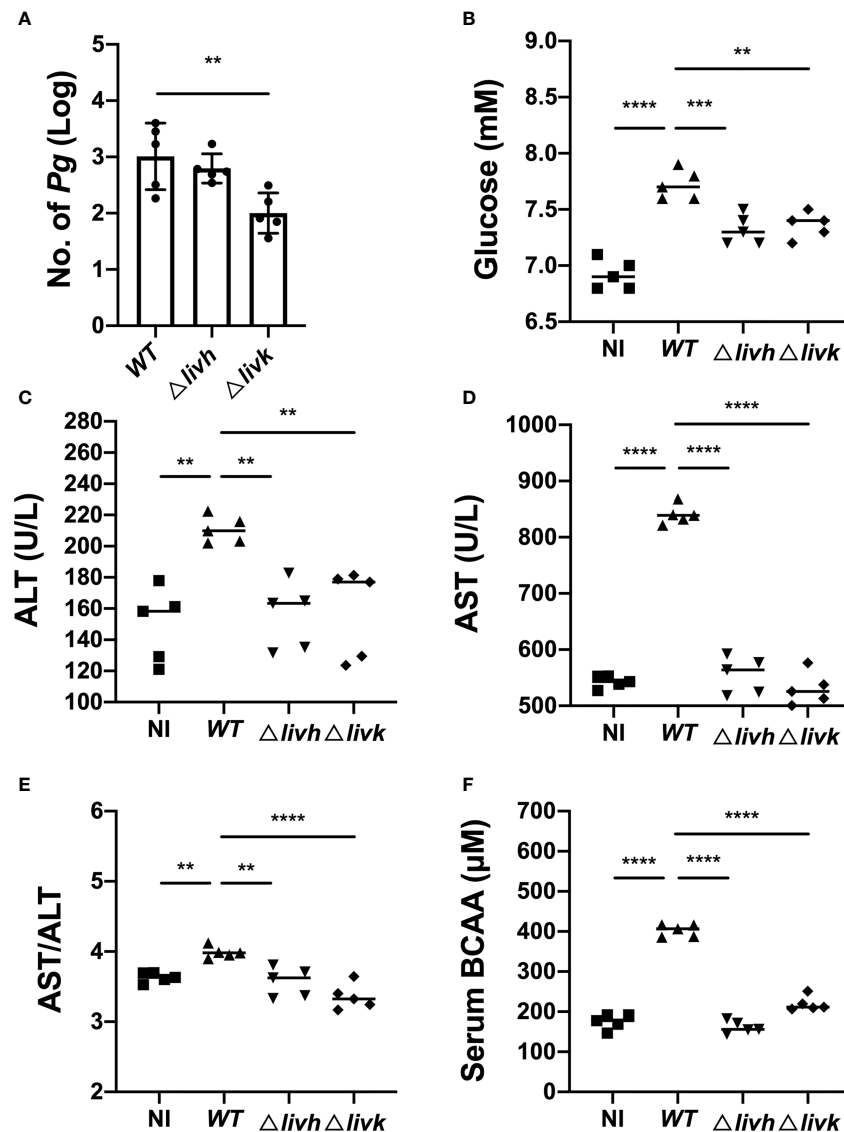


**FIGURE 4** | Influence of *P. gingivalis* infection on circulating BCAA levels and liver function. Six-week-old male C57BL/6 mice were infected with  $1 \times 10^9$  *P. gingivalis* in 100  $\mu$ L of PBS containing 2% CMC for 8 weeks. The NC and HFD groups were mock-treated with PBS containing 2% CMC. Four weeks after infection, the mice were euthanized, and liver and serum samples were harvested. **(A)** Colonization of *P. gingivalis* WT,  $\Delta livh$ , and  $\Delta livk$  detected via qPCR in the liver tissues of HFD-fed mice. Sera samples from mice were assayed for BCAA and FBG levels, and for the determination of selected liver-specific biochemistries. **(B)** Glucose level, **(C)** ALT level, **(D)** AST level, **(E)** AST/ALT ratio, and **(F)** BCAA level. CMC, carboxymethyl cellulose; BCAA, branched-chain amino acid; NC, normal chow, HFD, high-fat diet. All data represent the mean  $\pm$  SD for five mice per group. \*\* $P \leq 0.01$ ; \*\*\* $P \leq 0.001$ ; \*\*\*\* $P \leq 0.0001$ .

significantly related to metabolic diseases, such as insulin resistance and NAFLD (Sunny et al., 2015). It has also been reported that periodontal infection with *P. gingivalis* results in increased circulating BCAA levels and aggravates insulin resistance in mice fed HFD (Tian et al., 2020). Moreover, BCAA aminotransferase deficiency reduces *P. gingivalis*-induced serum BCAA levels and insulin resistance in mice fed HFD (Tian et al., 2020). However, the data from this study should be interpreted with some caution. The repeated oral administration of *P. gingivalis* has also been shown to result in the alteration of gut microbiota, which reportedly, is associated

with elevated serum BCAA levels (Saad et al., 2016; Yoon, 2016; Sato et al., 2017). Possibly, mice can also ingest plenty *P. gingivalis* that can affect gut microbiota. Therefore, we could not rule out the possibility that the oral administration of *P. gingivalis* possibly led to changes in gut microbiota characteristics, thus indirectly affecting serum BCAA levels. Moreover, whether *P. gingivalis* accelerates liver injury by enhancing the levels of circulating BCAAs still needs to be further confirmed *in vivo*.

Although this study as well as others showed that *P. gingivalis* induced upregulation of BCAA serum levels in mice,

the underlying mechanism is still unclear. Reportedly, BCAA biosynthesis and transportation are key factors in the modulation of bacteria-related intracellular and extracellular BCAA concentrations (Cai et al., 2020; Wendisch, 2020). The overexpression of BCAA-related synthetic pathway genes and BCAA importer genes as well as the deletion of BCAA exporter genes can result in the accumulation of bacterial intracellular BCAAs (Chen et al., 2015; Zhu et al., 2018; Cai et al., 2020). For instance, it has been observed that *Bacillus licheniformis* DW2 YhdG acts as an exporter of BCAAs, and the deletion of the *ydhG* gene improves intracellular BCAA accumulation, while overexpression of the importer genes, *yvbW* and *braB*, increases and decreases intracellular and extracellular BCAA concentrations, respectively (Cai et al., 2020). According to KEGG database, *P. gingivalis* possesses a biosynthetic pathway and transport system (LivKHGMF) of BCAA. *PGN\_RS05180* encodes branched-chain amino acid aminotransferase (BCAT), a key enzyme of BCAA synthesis. Multiple sequence alignments show that *P. gingivalis* BCAT contains the conserved domains and active catalytic site of bacterial branched-chain amino acid transaminase. Tian et al. found that  $\Delta bcac$  strain loses this ability to increase plasma level of BCAAs. Moreover, *P. copri* and *B. vulgatus*, the major contributors to increased BCAA levels in humans, have a high potential for BCAA biosynthesis. The amino acid sequences of BCAT in *P. gingivalis*, *P. copri* and *B. vulgatus* are highly homologous. These findings suggest that *P. gingivalis* has a strong BCAA synthesis. Intriguingly, the results of this study showed an obvious upregulation of two components of the BCAA transportation system (*livk* and *livh*) of intercellular *P. gingivalis*, as well as different expression levels for the genes associated with the NAFLD pathway in HUVECs infected with *P. gingivalis*. More importantly, we observed that both *livh* and *livk* deletion reduced the ability of *P. gingivalis* to induce increases in serum BCAA, ALT, and AST levels in mice fed HFD. Thus, we speculated that the LIV system of *P. gingivalis* may aggravate NAFLD and NASH by inducing increases in circulating BCAA levels. It is likely that *P. gingivalis* elevate BCAA serum levels through biosynthesizing BCAAs, and then exporting the biosynthesized BCAAs to extracellular environments such as blood circulation. However, it is still unclear whether the effects of *P. gingivalis* on BCAA levels and liver injury are related to specific components of the LIV system. Therefore, the effects of LIV, especially *livh* and *livk*, on BCAA levels and NAFLD signaling pathways still require further investigation. For instance, comparing the intracellular and extracellular BCAA concentrations in *P. gingivalis* mutants ( $\Delta bcac$ ,  $\Delta livk$  and  $\Delta livh$ ) under various stresses is needed to validate the role of BCAT and LIV system of *P. gingivalis* in modulating its intracellular and extracellular BCAA concentrations, as well as to explore the regulators of BCAA synthesis and transportation.

## DATA AVAILABILITY STATEMENT

The original contributions presented in the study are included in the article/Supplementary Material. The RNA sequencing data

are deposited in Gene Expression Omnibus (GEO) database under the accession number GSE184085 (<https://www.ncbi.nlm.nih.gov/geo/query/acc.cgi?acc=GSE184085>). Further inquiries can be directed to the corresponding author.

## ETHICS STATEMENT

All the animal procedures applied in the present study were approved by the Ethics Committee of Tongji Hospital, Tongji Medical College, Huazhong University of Science and Technology and the Ethics Committee of West China Hospital of Stomatology, Sichuan University (WCHSIRB-D-2017-071). And this has been stated in Line 378-382.

## AUTHOR CONTRIBUTIONS

LW and RS contributed to the study conception and design, data acquisition, analysis, and interpretation, and in the drafting the of the manuscript. HB, XW, and JW contributed to data acquisition, analysis, and interpretation. CL and YW contributed to the study conception and design, data acquisition, analysis, and interpretation, and the drafting and critical revision of the manuscript. All the authors approved the final version of the manuscript and agreed to be accountable for all aspects of the work.

## FUNDING

This study was supported by the National Natural Science Foundation of China (grant number 82170970 to YW; grant number 81600871 to CL).

## SUPPLEMENTARY MATERIAL

The Supplementary Material for this article can be found online at: <https://www.frontiersin.org/articles/10.3389/fcimb.2022.776996/full#supplementary-material>

**Supplementary Figure 1** | Construction and confirmation of *P. gingivalis*  $\Delta livh$  and  $\Delta livk$  strain.

**Supplementary Figure 2** | qPCR standard curve of *P. gingivalis*.

**Supplementary Figure 3** | Effect of HFD on liver function. Serum (A) glucose, (B) ALT, (C) AST levels, and (D) AST/ALT ratio in HFD-fed mice were compared with those in NC-fed mice. HFD, high-fat diet; NC, normal chow. \*\* $P \leq 0.01$ ; \*\*\* $P \leq 0.001$ ; \*\*\*\* $P \leq 0.0001$ .

**Supplementary Table 2** | The compositions of D12492 and D12450J.

**Supplementary Table 3** | Differentially expressed genes of intracellular *P. gingivalis* compared with *P. gingivalis* cultured in medium.

**Supplementary Table 4** | Differentially expressed genes of human umbilical vein endothelial cells (HUVECs) infected with *P. gingivalis* compared with uninfected HUVECs.

## REFERENCES

- Buzzetti, E., Pinzani, M., and Tsochatzis, E. A. (2016). The Multiple-Hit Pathogenesis of Non-Alcoholic Fatty Liver Disease (NAFLD). *Metabolism* 65, 1038–1048. doi: 10.1016/j.metabol.2015.12.012
- Cai, D., Zhu, J., Li, Y., Li, L., Zhang, M., Wang, Z., et al. (2020). Systematic Engineering of Branch Chain Amino Acid Supply Modules for the Enhanced Production of Bacitracin From *Bacillus Licheniformis*. *Metab. Eng. Commun.* 11, e00136. doi: 10.1016/j.mec.2020.e00136
- Chen, C., Li, Y., Hu, J., Dong, X., and Wang, X. (2015). Metabolic Engineering of *Corynebacterium Glutamicum* ATCC13869 for L-Valine Production. *Metab. Eng.* 29, 66–75. doi: 10.1016/j.ymben.2015.03.004
- Chen, Y., Yang, Y. C., Zhu, B. L., Wu, C. C., Lin, R. F., and Zhang, X. (2020). Association Between Periodontal Disease, Tooth Loss and Liver Diseases Risk. *J. Clin. Periodontol* 47, 1053–1063. doi: 10.1111/jcpe.13341
- Cook, J. R., Langlet, F., Kido, Y., and Accili, D. (2015). Pathogenesis of Selective Insulin Resistance in Isolated Hepatocytes. *J. Biol. Chem.* 290, 13972–13980. doi: 10.1074/jbc.M115.638197
- Ding, L. Y., Liang, L. Z., Zhao, Y. X., Yang, Y. N., Liu, F., Ding, Q. R., et al. (2019). Porphyromonas Gingivalis-Derived Lipopolysaccharide Causes Excessive Hepatic Lipid Accumulation via Activating NF-kappaB and JNK Signaling Pathways. *Oral Dis.* 25, 1789–1797. doi: 10.1111/odi.13153
- Fitzsimonds, Z. R., Liu, C., Stocke, K. S., Yakoumatos, L., Shumway, B., Miller, D. P., et al. (2021). Regulation of Olfactomedin 4 by *Porphyromonas Gingivalis* in a Community Context. *ISME J.* 15, 2627–2642. doi: 10.1038/s41396-021-00956-4
- Friedman, S. L., Neuschwander-Tetri, B. A., Rinella, M., and Sanyal, A. J. (2018). Mechanisms of NAFLD Development and Therapeutic Strategies. *Nat. Med.* 24, 908–922. doi: 10.1038/s41591-018-0104-9
- Furusho, H., Miyauchi, M., Hyogo, H., Inubushi, T., Ao, M., Ouhara, K., et al. (2013). Dental Infection of *Porphyromonas Gingivalis* Exacerbates High Fat Diet-Induced Steatohepatitis in Mice. *J. Gastroenterol.* 48, 1259–1270. doi: 10.1007/s00535-012-0738-1
- Gaggini, M., Carli, F., Rosso, C., Buzzigoli, E., Marietti, M., Della Latta, V., et al. (2018). Altered Amino Acid Concentrations in NAFLD: Impact of Obesity and Insulin Resistance. *Hepatology* 67, 145–158. doi: 10.1002/hep.29465
- Grzych, G., Vonghia, L., Bout, M. A., Weyler, J., Verrijken, A., Dirinck, E., et al. (2020). Plasma BCAA Changes in Patients With NAFLD Are Sex Dependent. *J. Clin. Endocrinol. Metab.* 105, dgaa175. doi: 10.1210/clinem/dgaa175
- Hajishengallis, G., and Lamont, R. J. (2021). Polymicrobial Communities in Periodontal Disease: Their Quasi-Organismal Nature and Dialogue With the Host. *Periodontol* 2000 86, 210–230. doi: 10.1111/prd.12371
- Hatasa, M., Yoshida, S., Takahashi, H., Tanaka, K., Kubotsu, Y., Ohsugi, Y., et al. (2021). Relationship Between NAFLD and Periodontal Disease From the View of Clinical and Basic Research, and Immunological Response. *Int. J. Mol. Sci.* 22 (7), 3728. doi: 10.3390/ijms22073728
- Huang, D. Q., El-Serag, H. B., and Loomba, R. (2021). Global Epidemiology of NAFLD-Related HCC: Trends, Predictions, Risk Factors and Prevention. *Nat. Rev. Gastroenterol. Hepatol.* 18, 223–238. doi: 10.1038/s41575-020-00381-6
- Kalhan, S. C., Guo, L., Edmison, J., Dasarthy, S., McCullough, A. J., Hanson, R. W., et al. (2011). Plasma Metabolomic Profile in Nonalcoholic Fatty Liver Disease. *Metabolism* 60, 404–413. doi: 10.1016/j.metabol.2010.03.006
- Kuboniwa, M., Houser, J. R., Hendrickson, E. L., Wang, Q., Alghamdi, S. A., Sakanaka, A., et al. (2017). Metabolic Crosstalk Regulates *Porphyromonas Gingivalis* Colonization and Virulence During Oral Polymicrobial Infection. *Nat. Microbiol.* 2, 1493–1499. doi: 10.1038/s41564-017-0021-6
- Kuraji, R., Ito, H., Fujita, M., Ishiguro, H., Hashimoto, S., and Numabe, Y. (2016). *Porphyromonas Gingivalis* Induced Periodontitis Exacerbates Progression of Non-Alcoholic Steatohepatitis in Rats. *Clin. Exp. Dent. Res.* 2, 216–225. doi: 10.1002/cre2.41
- Lake, A. D., Novak, P., Shipkova, P., Aranibar, N., Robertson, D. G., Reily, M. D., et al. (2015). Branched Chain Amino Acid Metabolism Profiles in Progressive Human Nonalcoholic Fatty Liver Disease. *Amino Acids* 47, 603–615. doi: 10.1007/s00726-014-1894-9
- Lamont, R. J., Koo, H., and Hajishengallis, G. (2018). The Oral Microbiota: Dynamic Communities and Host Interactions. *Nat. Rev. Microbiol.* 16, 745–759. doi: 10.1038/s41579-018-0089-x
- Liu, C., Miller, D. P., Wang, Y., Merchant, M., and Lamont, R. J. (2017a). Structure-Function Aspects of the *Porphyromonas Gingivalis* Tyrosine Kinase Ptk1. *Mol. Oral. Microbiol.* 32, 314–323. doi: 10.1111/omi.12173
- Liu, C., Mo, L., Niu, Y., Li, X., Zhou, X., and Xu, X. (2017b). The Role of Reactive Oxygen Species and Autophagy in Periodontitis and Their Potential Linkage. *Front. Physiol.* 8, 439. doi: 10.3389/fphys.2017.00439
- Liu, C., Niu, Y., Zhou, X., Xu, X., Yang, Y., Zhang, Y., et al. (2015). Cell Cycle Control, DNA Damage Repair, and Apoptosis-Related Pathways Control Pre-Ameloblasts Differentiation During Tooth Development. *BMC Genomics* 16, 592. doi: 10.1186/s12864-015-1783-y
- Liu, C., Stocke, K., Fitzsimonds, Z. R., Yakoumatos, L., Miller, D. P., and Lamont, R. J. (2021). A Bacterial Tyrosine Phosphatase Modulates Cell Proliferation Through Targeting RGCC. *PLoS Pathog.* 17, e1009598. doi: 10.1371/journal.ppat.1009598
- Lu, L., Yakoumatos, L., Ren, J., Duan, X., Zhou, H., Gu, Z., et al. (2020). JAK3 Restrains Inflammatory Responses and Protects Against Periodontal Disease Through Wnt3a Signaling. *FASEB J.* 34, 9120–9140. doi: 10.1096/fj.201902697RR
- Lynch, C. J., and Adams, S. H. (2014). Branched-Chain Amino Acids in Metabolic Signalling and Insulin Resistance. *Nat. Rev. Endocrinol.* 10, 723–736. doi: 10.1096/fj.201902697RR
- Mardinoglu, A., Agren, R., Kampf, C., Asplund, A., Uhlen, M., and Nielsen, J. (2014). Genome-Scale Metabolic Modelling of Hepatocytes Reveals Serine Deficiency in Patients With Non-Alcoholic Fatty Liver Disease. *Nat. Commun.* 5, 3083. doi: 10.1038/ncomms4083
- McCormack, S. E., Shaham, O., McCarthy, M. A., Deik, A. A., Wang, T. J., Gerszten, R. E., et al. (2013). Circulating Branched-Chain Amino Acid Concentrations Are Associated With Obesity and Future Insulin Resistance in Children and Adolescents. *Pediatr. Obes.* 8, 52–61. doi: 10.1111/j.2047-6310.2012.00087.x
- Mei, F., Xie, M., Huang, X., Long, Y., Lu, X., Wang, X., et al. (2020). *Porphyromonas Gingivalis* and Its Systemic Impact: Current Status. *Pathogens* 9, 944. doi: 10.3390/pathogens9110944
- Menni, C., Fauman, E., Erte, I., Perry, J. R., Kastenmuller, G., Shin, S. Y., et al. (2013). Biomarkers for Type 2 Diabetes and Impaired Fasting Glucose Using a Nontargeted Metabolomics Approach. *Diabetes* 62, 4270–4276. doi: 10.2337/db13-0570
- Moffatt, C. E., Inaba, H., Hirano, T., and Lamont, R. J. (2012). *Porphyromonas Gingivalis* SerB-Mediated Dephosphorylation of Host Cell Cofilin Modulates Invasion Efficiency. *Cell Microbiol.* 14, 577–588. doi: 10.1111/j.1462-5822.2011.01743.x
- Nagasaki, A., Sakamoto, S., Arai, T., Kato, M., Ishida, E., Furusho, H., et al. (2021). Elimination of *Porphyromonas Gingivalis* Inhibits Liver Fibrosis and Inflammation in NASH. *J. Clin. Periodontol.* 48 (10), 1367–1378. doi: 10.1111/jcpe.13523
- Nagasaki, A., Sakamoto, S., Chea, C., Ishida, E., Furusho, H., Fujii, M., et al. (2020). Odontogenic Infection by *Porphyromonas Gingivalis* Exacerbates Fibrosis in NASH via Hepatic Stellate Cell Activation. *Sci. Rep.* 10, 4134. doi: 10.1038/s41598-020-60904-8
- Nakahara, T., Hyogo, H., Ono, A., Nagaoki, Y., Kawaoka, T., Miki, D., et al. (2018). Involvement of *Porphyromonas Gingivalis* in the Progression of Non-Alcoholic Fatty Liver Disease. *J. Gastroenterol.* 53, 269–280. doi: 10.1007/s00535-017-1368-4
- Nakamura, H., Jinzu, H., Nagao, K., Noguchi, Y., Shimba, N., Miyano, H., et al. (2014). Plasma Amino Acid Profiles Are Associated With Insulin, C-Peptide and Adiponectin Levels in Type 2 Diabetic Patients. *Nutr. Diabetes* 4, e133. doi: 10.1038/nutd.2014.32
- Nuss, A. M., Beckstette, M., Pimenova, M., Schmuhl, C., Opitz, W., Pisano, F., et al. (2017). Tissue Dual RNA-Seq Allows Fast Discovery of Infection-Specific Functions and Riboregulators Shaping Host-Pathogen Transcriptomes. *Proc. Natl. Acad. Sci. U. S. A.* 114, E791–E800. doi: 10.1073/pnas.1613405114
- Pedersen, H. K., Gudmundsdottir, V., Nielsen, H. B., Hyotylainen, T., Nielsen, T., Jensen, B. A., et al. (2016). Human Gut Microbes Impact Host Serum Metabolome and Insulin Sensitivity. *Nature* 535, 376–381. doi: 10.1038/nature18646
- Potempa, J., Mydel, P., and Koziel, J. (2017). The Case for Periodontitis in the Pathogenesis of Rheumatoid Arthritis. *Nat. Rev. Rheumatol* 13, 606–620. doi: 10.1038/nrrheum.2017.132



- Ribardo, D. A., and Hendrixson, D. R. (2011). Analysis of the LIV System of *Campylobacter* Jejuni Reveals Alternative Roles for LivJ and LivK in Commensalism Beyond Branched-Chain Amino Acid Transport. *J. Bacteriol* 193, 6233–6243. doi: 10.1128/JB.05473-11
- Saad, M. J., Santos, A., and Prada, P. O. (2016). Linking Gut Microbiota and Inflammation to Obesity and Insulin Resistance. *Physiol. (Bethesda)* 31, 283–293. doi: 10.1152/physiol.00041.2015
- Sasaki, N., Katagiri, S., Komazaki, R., Watanabe, K., Maekawa, S., Shiba, T., et al. (2018). Endotoxemia by *Porphyromonas* Gingivalis Injection Aggravates Non-Alcoholic Fatty Liver Disease, Disrupts Glucose/Lipid Metabolism, and Alters Gut Microbiota in Mice. *Front. Microbiol.* 9, 2470. doi: 10.3389/fmicb.2018.02470
- Sato, K., Takahashi, N., Kato, T., Matsuda, Y., Yokoji, M., Yamada, M., et al. (2017). Aggravation of Collagen-Induced Arthritis by Orally Administered *Porphyromonas* *Gingivalis* Through Modulation of the Gut Microbiota and Gut Immune System. *Sci. Rep.* 7, 6955. doi: 10.1038/s41598-017-07196-7
- Sunny, N. E., Kalavalapalli, S., Bril, F., Garrett, T. J., Nautiyal, M., Mathew, J. T., et al. (2015). Cross-Talk Between Branched-Chain Amino Acids and Hepatic Mitochondria Is Compromised in Nonalcoholic Fatty Liver Disease. *Am. J. Physiol. Endocrinol. Metab.* 309, E311–E319. doi: 10.1152/ajpendo.00161.2015
- Tian, J., Liu, C., Zheng, X., Jia, X., Peng, X., Yang, R., et al. (2020). *Porphyromonas* *Gingivalis* Induces Insulin Resistance by Increasing BCAA Levels in Mice. *J. Dent. Res.* 99, 839–846. doi: 10.1177/0022034520911037
- Tribble, G. D., Lamont, G. J., Progulski-Fox, A., and Lamont, R. J. (2007). Conjugal Transfer of Chromosomal DNA Contributes to Genetic Variation in the Oral Pathogen *Porphyromonas* *Gingivalis*. *J. Bacteriol* 189, 6382–6388. doi: 10.1128/JB.00460-07
- Wang, H. X., Gao, X. W., Ren, B., Cai, Y., Li, W. J., Yang, Y. L., et al. (2017). Comparative Analysis of Different Feeder Layers With 3T3 Fibroblasts for Culturing Rabbits Limbal Stem Cells. *Int. J. Ophthalmol.* 10, 1021–1027. doi: 10.18240/ijo.2017.07.01
- Weintraub, J. A., Lopez Mitnik, G., and Dye, B. A. (2019). Oral Diseases Associated With Nonalcoholic Fatty Liver Disease in the United States. *J. Dent. Res.* 98, 1219–1226. doi: 10.1177/0022034519866442
- Wendisch, V. F. (2020). Metabolic Engineering Advances and Prospects for Amino Acid Production. *Metab. Eng.* 58, 17–34. doi: 10.1016/j.ymben.2019.03.008
- Westermann, A. J., Barquist, L., and Vogel, J. (2017). Resolving Host-Pathogen Interactions by Dual RNA-Seq. *PLoS Pathog.* 13, e1006033. doi: 10.1371/journal.ppat.1006033
- Westermann, A. J., Forstner, K. U., Amman, F., Barquist, L., Chao, Y., Schulte, L. N., et al. (2016). Dual RNA-Seq Unveils Noncoding RNA Functions in Host-Pathogen Interactions. *Nature* 529, 496–501. doi: 10.1038/nature16547
- Westermann, A. J., and Vogel, J. (2018). Host-Pathogen Transcriptomics by Dual RNA-Seq. *Methods Mol. Biol.* 1737, 59–75. doi: 10.1007/978-1-4939-7634-8\_4
- Wright, C. J., Xue, P., Hirano, T., Liu, C., Whitmore, S. E., Hackett, M., et al. (2014). Characterization of a Bacterial Tyrosine Kinase in *Porphyromonas* *Gingivalis* Involved in Polymicrobial Synergy. *Microbiologyopen* 3, 383–394. doi: 10.1002/mbo3.177
- Yoneda, M., Naka, S., Nakano, K., Wada, K., Endo, H., Mawatari, H., et al. (2012). Involvement of a Periodontal Pathogen, *Porphyromonas* *Gingivalis* on the Pathogenesis of Non-Alcoholic Fatty Liver Disease. *BMC Gastroenterol.* 12, 16. doi: 10.1186/1471-230X-12-16
- Yoon, M. S. (2016). The Emerging Role of Branched-Chain Amino Acids in Insulin Resistance and Metabolism. *Nutrients* 8 (7), 405. doi: 10.3390/nu8070405
- Younossi, Z., Anstee, Q. M., Marietti, M., Hardy, T., Henry, L., Eslam, M., et al. (2018). Global Burden of NAFLD and NASH: Trends, Predictions, Risk Factors and Prevention. *Nat. Rev. Gastroenterol. Hepatol.* 15, 11–20. doi: 10.1038/nrgastro.2017.109
- Yu, G., Wang, L. G., Han, Y., and He, Q. Y. (2012). ClusterProfiler: An R Package for Comparing Biological Themes Among Gene Clusters. *OMICS* 16, 284–287. doi: 10.1089/omi.2011.0118
- Zhang, F., Hu, Z., Li, G., Huo, S., Ma, F., Cui, A., et al. (2018a). Hepatic CREBZF Couples Insulin to Lipogenesis by Inhibiting Insig Activity and Contributes to Hepatic Steatosis in Diet-Induced Insulin-Resistant Mice. *Hepatology* 68, 1361–1375. doi: 10.1002/hep.29926
- Zhang, Z. Y., Monleon, D., Verhamme, P., and Staessen, J. A. (2018b). Branched-Chain Amino Acids as Critical Switches in Health and Disease. *Hypertension* 72, 1012–1022. doi: 10.1161/HYPERTENSIONAHA.118.10919
- Zhang, F., Zhao, S., Yan, W., Xia, Y., Chen, X., Wang, W., et al. (2016). Branched Chain Amino Acids Cause Liver Injury in Obese/Diabetic Mice by Promoting Adipocyte Lipolysis and Inhibiting Hepatic Autophagy. *EbioMedicine* 13, 157–167. doi: 10.1016/j.ebiom.2016.10.013
- Zhao, H., Zhang, F., Sun, D., Wang, X., Zhang, X., Zhang, J., et al. (2020). Branched-Chain Amino Acids Exacerbate Obesity-Related Hepatic Glucose and Lipid Metabolic Disorders via Attenuating Akt2 Signaling. *Diabetes* 69, 1164–1177. doi: 10.2337/db19-0920
- Zhu, J., Cai, D., Xu, H., Liu, Z., Zhang, B., Wu, F., et al. (2018). Enhancement of Precursor Amino Acid Supplies for Improving Bacitracin Production by Activation of Branched Chain Amino Acid Transporter BrnQ and Deletion of Its Regulator Gene Lrp in *Bacillus Licheniformis*. *Synth Syst. Biotechnol.* 3, 236–243. doi: 10.1016/j.synbio.2018.10.009

**Conflict of Interest:** The authors declare that the research was conducted in the absence of any commercial or financial relationships that could be construed as a potential conflict of interest.

**Publisher's Note:** All claims expressed in this article are solely those of the authors and do not necessarily represent those of their affiliated organizations, or those of the publisher, the editors and the reviewers. Any product that may be evaluated in this article, or claim that may be made by its manufacturer, is not guaranteed or endorsed by the publisher.

Copyright © 2022 Wu, Shi, Bai, Wang, Wei, Liu and Wu. This is an open-access article distributed under the terms of the Creative Commons Attribution License (CC BY). The use, distribution or reproduction in other forums is permitted, provided the original author(s) and the copyright owner(s) are credited and that the original publication in this journal is cited, in accordance with accepted academic practice. No use, distribution or reproduction is permitted which does not comply with these terms.



# Probiotic Species in the Management of Periodontal Diseases: An Overview

Yuwei Zhang<sup>1</sup>, Yi Ding<sup>1</sup> and Qiang Guo<sup>2\*</sup>

<sup>1</sup> State Key Laboratory of Oral Diseases, National Clinical Research Center for Oral Diseases, Department of Periodontics, West China Hospital of Stomatology, Sichuan University, Chengdu, China, <sup>2</sup> State Key Laboratory of Oral Diseases, National Clinical Research Center for Oral Diseases, West China Hospital of Stomatology, Sichuan University, Chengdu, China

## OPEN ACCESS

### Edited by:

Jin Xiao,  
University of Rochester, United States

### Reviewed by:

Jessica Scofield,  
University of Alabama at Birmingham,  
United States  
Feng Chen,  
Peking University, China  
Pei-Hui Ding,  
Zhejiang University, China

### \*Correspondence:

Qiang Guo  
guoqiang2014@scu.edu.cn

### Specialty section:

This article was submitted to  
Microbiome in Health and Disease,  
a section of the journal  
Frontiers in Cellular and  
Infection Microbiology

**Received:** 31 October 2021

**Accepted:** 25 February 2022

**Published:** 25 March 2022

### Citation:

Zhang Y, Ding Y and Guo Q (2022)  
Probiotic Species in the Management  
of Periodontal Diseases: An Overview.  
Front. Cell. Infect. Microbiol. 12:806463.  
doi: 10.3389/fcimb.2022.806463

Periodontal diseases are one of the most common chronic inflammatory diseases of the oral cavity, which are initiated and sustained by pathogenic plaque biofilms. Central to modern periodontology is the idea that dysbiosis of periodontal microecology and disorder of host inflammatory response gives rise to degradation of periodontal tissues together, which eventually leads to tooth loss, seriously affecting the life quality of patients. Probiotics were originally used to treat intestinal diseases, while in recent years, extensive studies have been exploring the utilization of probiotics in oral disease treatment and oral healthcare. Probiotic bacteria derived from the genera *Lactobacillus*, *Bifidobacterium*, *Streptococcus*, and *Weissella* are found to play an effective role in the prevention and treatment of periodontal diseases via regulating periodontal microbiota or host immune responses. Here, we review the research status of periodontal health-promoting probiotic species and their regulatory effects. The current issues on the effectiveness and safety of probiotics in the management of periodontal diseases are also discussed at last. Taken together, the use of probiotics is a promising approach to prevent and treat periodontal diseases. Nevertheless, their practical use for periodontal health needs further research and exploration.

**Keywords:** probiotic, periodontal disease, periodontopathogen, microecological balance, immunoregulation

## PROBIOTIC AND ORAL HEALTH

The term “probiotic” was put forward by Lilly and Stillwell in 1965, defined as “growth-promoting factors produced by microorganisms” (Lilly and Stillwell, 1965). Since then, the definition of “probiotic” has changed several times until the WHO and the Food and Agriculture Organization of the United States (FAO) in 2002 came up with a new definition that was generally accepted: probiotics are “living microorganisms that can have a beneficial effect on the host when taken in sufficient doses” (Hill et al., 2014). The origins of probiotics could be traced back to ancient Roman records, and Plinius Secundus Maior recorded that fermented milk products are beneficial to stomach healing. In the early 20th century, Elie Metchnikoff, a Nobel laureate, recorded in “The Prolongation of Life” that Bulgarians lived longer than others because they drank fermented milk (Metchnikoff, 1907). Through the study of human gut flora, he concluded that harmful products of some bacteria could be a reason for aging, and he recommended milk fermented by *Lactobacillus* to prevent the harmful effects of bacterial products.

Probiotics were originally used to treat intestinal diseases. Studies have shown that they could help control intestinal infections, relieve constipation and diarrhea, improve lactose intolerance, etc. (Lourenshattingh and Viljoen, 2001). The beneficial effects of probiotics defined by WHO and FAO are not only on the intestines but also on other body systems. In fact, many probiotics have been demonstrated to play a role in maintaining a healthy urogenital system and fighting against cancers, diabetes, obesity, and allergies (Waigankar and Patel, 2011; Sunita et al., 2012; Kang et al., 2013; Takeda et al., 2014; Kahouli et al., 2015). In recent decades, extensive studies also explored the application of probiotics in oral disease treatment and oral healthcare. Currently, it is found that probiotics contributing to oral health are concentrated in the genera *Lactobacillus*, *Bifidobacterium*, *Streptococcus*, and *Weissella*, as well as certain scattered species like *Bacillus subtilis* and *Saccharomyces cerevisiae*. Several strains of *Lactobacillus reuteri*, *Lactobacillus brevis*, *Streptococcus salivarius*, etc., have been commercially produced as oral health-promoting probiotics, all of which are microorganisms isolated from the oral cavity (Allaker and Stephen, 2017; Mahasneh and Mahasneh, 2017). Effects of probiotics on improving oral health have been observed in common oral diseases such as dental caries, periodontal diseases, oral candida infection, and halitosis (Ince et al., 2015; Ohshima et al., 2016; Yoo et al., 2019; Sivamaruthi et al., 2020).

## PERIODONTAL DISEASES

Periodontal diseases are chronic inflammatory diseases that destroy bone and gum tissues that support the teeth, of which gingivitis and periodontitis are the most common types. Gingivitis is a mild form of periodontal disease, but the progression of untreated gingivitis can lead to more serious periodontitis by creating deep periodontal pockets that could cause teeth to loosen or lead to tooth loss, which has a marked impact on patients' life. It is reported that as of 2019, there are 1.1 billion patients with severe periodontitis worldwide, and the prevalence of severe periodontitis has increased by 8.44% from 1990 to 2019 (Chen et al., 2021). Dental plaque, which is a microbial biofilm that forms on the teeth and gingiva, is thought to be the initial factor of periodontal diseases. The understanding of the pathogenicity of dental plaque biofilms has evolved over time, and several hypotheses were proposed in history, from the "Specific Plaque Hypothesis" (1976) (Loesche, 1976), the "Non-Specific Plaque Hypothesis" (1986) (Theilade, 1986), to the "Ecological Plaque Hypothesis" (1994) (Marsh, 1994). Modern periodontology, however, not only focuses on the pathogenicity of dental plaque biofilms but also emphasizes the interaction between oral microbes and the host. In recent years, the "Keystone-Pathogen Hypothesis" (KPH) (2012) and polymicrobial synergy and dysbiosis (PSD) model (2012) have attracted wide attention. The KPH (Hajishengallis et al., 2012) proposed that certain low-abundance periodontopathogens such as *Porphyromonas gingivalis* could weaken the bactericidal effect

of the host immune system and promote host inflammatory response, thus destroying the host-microbe homeostasis and balance of periodontal microecosystem that finally lead to the occurrence of periodontal diseases. The PSD model (Hajishengallis and Lamont, 2012) emphasized that the synergistic effect between polymicrobial communities and the host inflammatory response disorder caused periodontal diseases, and moreover, the ecological imbalance and inflammatory response could reinforce each other and constitute the actual driving factors of diseases. In fact, subversion of host immunity by dysbiotic periodontal microbiota not only gives rise to periodontal diseases but also contributes to systemic inflammation (Hajishengallis, 2015).

Studies on oral microorganisms show that there are more than 700 bacterial species colonizing the mouth (Kumar et al., 2005). However, only a few bacteria are proved to initiate and advance periodontal diseases, such as *P. gingivalis*, *Aggregatibacter actinomycetemcomitans*, *Tannerella forsythia*, *Prevotella intermedia*, and *Fusobacterium nucleatum* (Hajishengallis et al., 2012). When reviewing the studies focusing on the action of probiotics in managing periodontal diseases, we noticed that the majority referred to four periodontopathogens, namely, *P. gingivalis* (chronic periodontitis), *A. actinomycetemcomitans* (aggressive periodontitis), *P. intermedia* (pregnancy gingivitis, moderate and severe gingivitis, acute necrotizing gingivitis, and chronic periodontitis), and *F. nucleatum* (chronic periodontitis and acute necrotizing ulcerative gingivitis), indicating that periodontal probiotics are often related with or applied to specific periodontal diseases driven by them. With the help of various virulence factors that cause direct destruction to periodontal tissues or stimulate host cells to activate a wide range of inflammatory responses (Figure 1), these pathogens destroy the host-microbe homeostasis and cause or promote the occurrence and development of multiple periodontal diseases (Zhao et al., 2012; Jaffar et al., 2016; Zhao et al., 2019; Ishikawa et al., 2020; Moman et al., 2020; Ding et al., 2021; Jansen et al., 2021).

## APPLICATION OF PROBIOTICS IN MANAGING PERIODONTAL DISEASES

There is an increasing interest in the use of probiotics in periodontal therapy and periodontal care. The existing published studies have revealed that probiotics could effectively inhibit periodontopathogens and improve various clinical indices related to periodontal health, including plaque index (PI), gingival index (GI), bleeding on probing (BOP), periodontal pocket depth (PPD), clinical attachment loss (CAL), and gingival crevicular fluid (GCF) volume, as well as inflammation-associated biochemical markers, such as interleukin (IL)-1 $\beta$ , matrix metalloproteinase (MMP)-8, and tissue inhibitor of metalloproteinase (TIMP)-1. Although there are various forms of probiotics applied in managing periodontal diseases, such as tablets, mouthwash, and toothpaste, probiotics commercialized

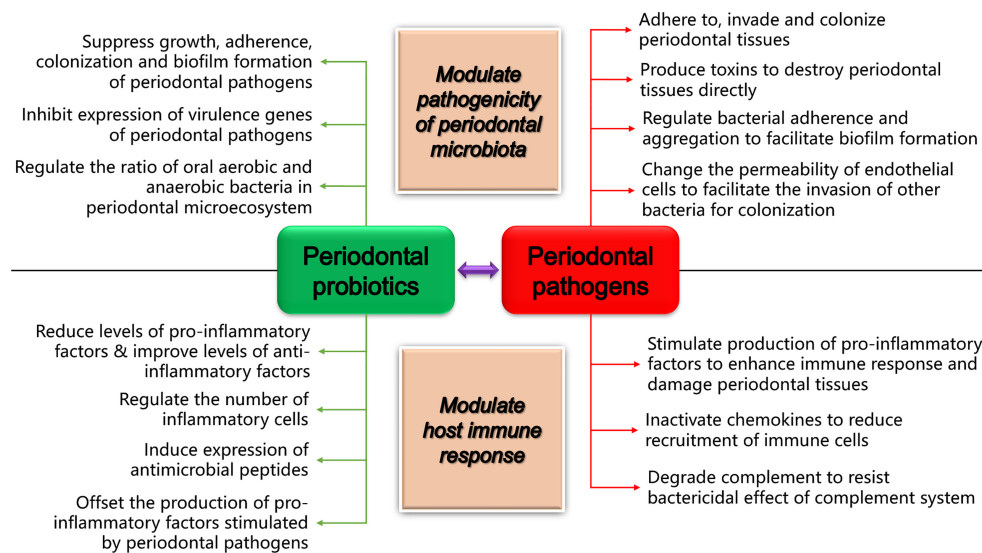


**FIGURE 1** | How periodontal probiotics and pathogens play their roles in regulating periodontal health and disease. The diagram shows the primary mechanisms of periodontopathogens and probiotics in regulating periodontal microbiota and host immune responses, respectively.

and studied in periodontal therapy are usually made into tablets, while probiotics in the forms of mouthwash and toothpaste are often applied in periodontal health care.

## Periodontal Health Care

Some studies have focused on the role of probiotics in periodontal care. Amizic et al. found that probiotic toothpaste could prevent caries and periodontal diseases more effectively than non-probiotic toothpaste, and the capacity of the toothpaste to inhibit bacteria was even better than that of mouthwash. It was speculated that toothpaste could contact the tooth surface for a longer time, and it would be easy to enter gingival sulcus with the help of a toothbrush (Amizic et al., 2017). However, the study of Alkaya et al. (2016) had a different conclusion. Forty patients with gingivitis were recruited and divided into 2 groups, using placebo or experimental probiotic *B. subtilis*-, *Bacillus megaterium*-, and *Bacillus pumilus*-containing toothpaste, mouthwash, and toothbrush cleaner for 8 weeks. After evaluation of PI, GI, PPD, and BOP at baseline and 8 weeks, it was reported that there was no intergroup difference detected, suggesting that genetically distinct probiotics perhaps have different effects on periodontal health.

## An Adjuvant Therapy for Periodontal Non-Surgical Treatment

Some researchers have evaluated the short-term and long-term effects of probiotics as a supplementary therapy for periodontal non-surgical treatment. For example, in the study of Kuru et al. (2017), 51 periodontal healthy volunteers were first given non-surgical periodontal therapy, and 7 days later (baseline), they were randomized into two groups receiving yogurt containing either placebo or *Bifidobacterium animalis* subsp. *lactis* DN-173010 for 28 days, followed by a 5-day non-brushing period. PI,

GI, BOP, PPD, GCF volume, and total amount and concentration of IL-1 $\beta$  in GCF were measured on days 0 (baseline), 28, and 33. It was reported that there was no intergroup difference detected on day 0 and day 28. However, after plaque accumulation, all parameters in the probiotic group were significantly better than those in the placebo group on day 33, indicating that the short-term use of probiotics has a positive effect on plaque accumulation and gingival inflammatory parameters, even without oral hygiene measures. The long-term clinical benefits of probiotic were proved by Ince et al. Thirty patients with chronic periodontitis were randomly given either *L. reuteri*-containing lozenge or placebo twice a day after scaling and root planing (SRP) for 3 weeks, and clinical parameters were collected at baseline and on days 21, 90, 180, and 360 after SRP. It was found that the probiotic group's PI, GI, BOP, and PPD were much better than those of the placebo group at all time points. Decreased MMP-8 and increased TIMP-1 levels in GCF were found to be significant up to day 180. From day 90, mean values of attachment gain were significantly higher in the probiotic group (Ince et al., 2015). In a meta-analysis about the effects of using probiotics as the supplemental therapy after periodontal non-surgical treatment for 42–360 days, Kumar et al. concluded that probiotics could help reduce CAL significantly in moderately deep periodontal pockets. However, the three of four studies included for meta-analysis showed significant heterogeneity, though the risk of bias was low (Kumar and Madurantakam, 2017). Studies have suggested that short-term and long-term applications of probiotics can achieve certain clinical benefits, but relevant studies are not enough, and limited probiotics are involved.

As for peri-implant disease, some studies on the effect of *L. reuteri* ATCC PTA 5289 and DSM 17938 as adjuvant therapy to mechanical debridement revealed the potential of probiotics in



treating peri-implant mucositis. Using *L. reuteri* for at least 30 days relieved PI, GI, PPD, and BOP in peri-implant mucositis and reduced the concentrations of IL-1 $\beta$ , IL-6, and IL-8 in GCF (Flichy-Fernández et al., 2015; Galofré et al., 2018). Moreover, compared to mechanical debridement followed by rinsing with 0.12% chlorhexidine (CHX), utilization of *L. reuteri* did not make a difference (Peña et al., 2019). However, with respect to implantitis, only one study reported significant PD and BOP improvement in 90 days after mechanical treatment and *L. reuteri* application (Galofré et al., 2018). *L. reuteri* might improve PI, but the subgingival microbial community of the implant was not changed markedly (Galofré et al., 2018; Tada et al., 2018; Laleman et al., 2020).

## Alternatives to Antimicrobials

Because of the overuse of antimicrobial drugs, antimicrobial resistance becomes serious day by day. Therefore, there is an urgent need to find alternatives to antimicrobials. In this background, Shah et al. compared the effects of probiotics and antibiotics as the supplemental therapies of periodontal non-surgical treatment (Shah and Gujjari, 2017). They recruited 18 patients with aggressive periodontitis and divided them into 3 groups after SRP, which were given *L. brevis* CD2, *L. brevis* CD2 with doxycycline, or doxycycline alone for 14 days. PI, GI, PPD, CAL, and salivary levels of *Lactobacillus* and *A. actinomycetemcomitans* were measured at baseline, 14 days, 2 months, and 5 months. It was reported that GI in all the three groups was significantly improved at 5 months, and the intergroup results were also statistically significant. Besides, *L. brevis* CD2 showed a similar effect to doxycycline, but a synergistic effect was not detected when the probiotic and doxycycline were given simultaneously. It was concluded that *L. brevis* CD2 could be used as an alternative to antibiotics to treat aggressive periodontitis, without the risk of promoting antibiotic resistance.

The broad-spectrum bactericide CHX is widely used in dental clinical therapy. In a study comparing effects of CHX, probiotics, and herbs, 45 healthy volunteers were randomly divided into three groups and used CHX mouthwash, probiotic mouthwash, or herbal mouthwash for 14 days. The probiotic mouthwash contained *Lactobacillus acidophilus*, *Lactobacillus rhamnosus*, *Bifidobacterium longum*, *Saccharomyces boulardii*; the herbal mouthwash contained Belleric Myrobalan (*Bibhitaki*), Betel (*Nagavalli*), and Meswak (*Salvadora Persica*). PI, GI, and Oral Hygiene Index-Simplified (OHI-S) were collected on days 0, 7, and 14. The effects of all three types of mouthwash were demonstrated to be similar, and there were few side effects reported, suggesting that both probiotic mouthwash and herbal mouthwash are effective substitutes for CHX mouthwash (Deshmukh et al., 2017).

## PERIODONTAL HEALTH-PROMOTING PROBIOTIC SPECIES AND THEIR REGULATORY EFFECTS

The mechanisms of probiotics promoting periodontal health have not been fully elucidated. Nevertheless, a considerable

amount of research results from clinical trials, animal experiments, and *in vitro* experiments have revealed that probiotics confer periodontal-health benefits upon the host by regulating periodontal microbiota or immune responses *via* various mechanisms (Figure 1). Specifically, regulatory effects of various periodontal health-promoting probiotics, which mainly belong to genera *Lactobacillus*, *Bifidobacterium*, *Streptococcus*, and *Weissella*, as well as the emerging recombinant probiotics, have been widely observed (Table 1). For the genera *Lactobacillus* and *Streptococcus*, probiotic species whose periodontal health-modulating effects were reported by at least three research articles in the past 5 years are chosen as the typical and important periodontal health-promoting probiotics in their genera to introduce here, as listed in Table 1.

### *Lactobacillus*

*Lactobacillus* is a type of gram-positive facultative anaerobic or obligate anaerobic bacteria that widely colonize the human digestive system, urinary system, and reproductive system. Probiotics derived from the genus *Lactobacillus* have been used in the prevention and treatment of numerous gastrointestinal tract disorders, urogenital diseases, vaginal infection, atopic disease, food hypersensitivity, and oral diseases like dental caries, periodontal diseases, and oral candida infection (Lebeer et al., 2008; Ishikawa et al., 2015; James et al., 2016). The genus *Lactobacillus* contributes the majority of the current known periodontal health-promoting probiotic species.

### *Lactobacillus acidophilus*

The studies of periodontal health-promoting *L. acidophilus* are concentrated on *in vitro* experiments. *L. acidophilus* plays an important role in the inhibition of *P. gingivalis* growth *in vitro* and regulation of the interaction between *P. gingivalis* and gingival epithelial cells (GEC) (Zhao et al., 2011; Zhao et al., 2012; Zhao et al., 2019). *L. acidophilus* ATCC 4356 could offset the pro-inflammatory process induced by *P. gingivalis* ATCC 33277 at both protein and mRNA levels and could antagonize the regulatory effects of *P. gingivalis* on the proliferation and apoptosis of GEC in a dose-dependent manner (Zhao et al., 2012; Zhao et al., 2019). Recently, *L. acidophilus* LA5 was observed to downregulate multiple virulence factors of *P. gingivalis*, such as the fimbriae encoding genes *mfa1* and *fimA* in *P. gingivalis* ATCC 33277 and *mfa1* in *P. gingivalis* W83, the gingipains encoding genes *kgp* and *rgpA*, and the quorum-sensing gene *luxS* in ATCC 33277 or W83 interacting with GECs (Ishikawa et al., 2020).

*L. acidophilus* ATCC 4356 also shows its universal regulatory effects on different *F. nucleatum* strains, *via* inhibiting the expression of virulence factors and the adhesion ability of *F. nucleatum* or reducing the levels of cytokines in oral epithelial cells stimulated by *F. nucleatum*. It is worth noting that live and heat-killed *L. acidophilus* ATCC 4356 have similar adhesion ability to KB and HOK cells, and both forms do not affect the viability of cells (Ding et al., 2021). The live *L. acidophilus* ATCC 4356 has been proved to decrease the production of IL-6 in KB cells activated by *F. nucleatum* ATCC 10953 (Kang et al., 2011). In a recent study, the heat-

**TABLE 1 |** The regulatory effects of known probiotic species promoting periodontal health.

Genus/type	Species	Regulate immune responses	Regulate periodontal microbiota
<b>Lactobacillus</b>	<i>Lactobacillus acidophilus</i>	<ol style="list-style-type: none"> <li>1. Reduce <i>Porphyromonas gingivalis</i>-induced pro-inflammatory IL-1<math>\beta</math> and IL-6/8 production in KB cells (<i>in vitro experiment</i>) (Zhao et al., 2012)</li> <li>2. Reduce the <i>Fusobacterium nucleatum</i>-induced pro-inflammatory IL-6/8 production in KB and HOK cells (<i>in vitro experiment</i>) (Kang et al., 2011; Ding et al., 2021)</li> <li>3. Antagonize the regulatory effect on the proliferation and apoptosis stimulated by <i>P. gingivalis</i> (<i>in vitro experiment</i>) (Zhao et al., 2019)</li> </ol>	<ol style="list-style-type: none"> <li>1. Inhibit the growth of <i>P. gingivalis</i> (<i>in vitro experiment</i>) (Zhao et al., 2011)</li> <li>2. Co-aggregate with <i>F. nucleatum</i> to interfere with adhesion and invasion (<i>in vitro experiment</i>) (Ding et al., 2021)</li> <li>3. Downregulate the virulence-associated factors (<i>mfa1</i>, <i>fimA</i>, <i>kpg</i>, <i>rgpA</i>, and <i>luxS</i>) of <i>P. gingivalis</i> (<i>in vitro experiment</i>) (Ishikawa et al., 2020)</li> <li>4. Downregulate the adhesion-associated factors (<i>fap2</i>) of <i>F. nucleatum</i> (<i>in vitro experiment</i>) (Ding et al., 2021)</li> <li>5. Downregulate the virulence-associated factors (<i>LtxA</i>, <i>CdtB</i>, <i>dspB</i>, and <i>katA</i>) of <i>Aggregatibacter actinomycetemcomitans</i> (<i>in vitro experiment</i>) (Ishikawa et al., 2021)</li> <li>6. Degrade <i>A. actinomycetemcomitans</i> biofilms by producing enzymes such as lipase (<i>in vitro experiment</i>) (Jaffar et al., 2016)</li> </ol>
	<i>Lactobacillus brevis</i>	Produce arginine deiminase to reduce the level of pro-inflammatory factors (TNF- $\alpha$ , IL-1 $\beta$ , IL-6, and IL-17) ( <i>animal experiment</i> ) (Maekawa and Hajishengallis, 2014)	<ol style="list-style-type: none"> <li>1. Promote a higher ratio between aerobic and anaerobic bacteria in ligature-associated microbiota (<i>animal experiment</i>) (Maekawa and Hajishengallis, 2014)</li> <li>2. Inhibit <i>A. actinomycetemcomitans</i> in saliva (<i>clinical trial</i>) (Shah and Gujjari, 2017)</li> <li>3. Inhibit the growth and biofilm formation of <i>Prevotella melaninogenica</i> (<i>in vitro experiment</i>) (Shah and Gujjari, 2017)</li> </ol>
	<i>Lactobacillus casei</i>	Reduce the <i>F. nucleatum</i> -induced pro-inflammatory IL-6 production in oral epithelial cells ( <i>in vitro experiment</i> ) (Kang et al., 2011)	<ol style="list-style-type: none"> <li>1. Reduce the abundance of <i>P. gingivalis</i>, <i>A. actinomycetemcomitans</i>, and <i>P. intermedia</i> in subgingival plaque (<i>clinical trial</i>) (Imran et al., 2015)</li> <li>2. Degrade <i>A. actinomycetemcomitans</i> biofilms by producing enzymes such as lipase (<i>in vitro experiment</i>) (Jaffar et al., 2016)</li> </ol>
	<i>Lactobacillus fermentum</i>	Reduce the <i>F. nucleatum</i> -induced pro-inflammatory IL-6 production in oral epithelial cells ( <i>in vitro experiment</i> ) (Kang et al., 2011)	<ol style="list-style-type: none"> <li>1. Degrade <i>A. actinomycetemcomitans</i> biofilms by producing enzymes such as lipase (<i>in vitro experiment</i>) (Jaffar et al., 2016)</li> <li>2. Inhibit the growth of <i>P. gingivalis</i>, <i>P. intermedia</i>, and <i>A. actinomycetemcomitans</i> (<i>in vitro experiment</i>) (Terai et al., 2015)</li> </ol>
	<i>Lactobacillus gasseri</i>	<ol style="list-style-type: none"> <li>1. Raise the level of mBD14 mRNA in gingiva, tongue, and saliva (<i>animal experiment</i>) (Kobayashi et al., 2017)</li> <li>2. Decrease the mRNA levels of IL-6 and TNF-<math>\alpha</math> in gingiva infected by <i>P. gingivalis</i> (<i>animal experiment</i>) (Kobayashi et al., 2017)</li> </ol>	<ol style="list-style-type: none"> <li>1. Reduce the expression of <i>LtxA</i> and <i>CdtB</i> exotoxins by <i>A. actinomycetemcomitans</i> (<i>in vitro experiment</i>) (Nissen et al., 2014)</li> <li>2. Inhibit the growth of <i>P. gingivalis</i> and <i>P. intermedia</i> (<i>in vitro experiment</i>) (Terai et al., 2015)</li> <li>3. Decrease the colonization of <i>P. gingivalis</i> in gingiva (<i>animal experiment</i>) (Kobayashi et al., 2017)</li> </ol>
	<i>Lactobacillus reuteri</i>	<ol style="list-style-type: none"> <li>1. Reduce the <i>F. nucleatum</i>-induced pro-inflammatory cytokine IL-6 production in KB cells (<i>in vitro experiment</i>) (Kang et al., 2011)</li> <li>2. Raise the hemocyte density in <i>Galleria mellonella</i> infected by <i>P. gingivalis</i>, upregulating immune responses (<i>animal experiment</i>) (Geraldo et al., 2020; Santos et al., 2020)</li> <li>3. Reduce the level of MMP-8 and increase the level of TIMP-1 (<i>clinical trial</i>) (Ince et al., 2015)</li> <li>4. Inhibit the expression of pro-inflammatory factors (TNF-<math>\alpha</math>, IL-1<math>\beta</math>, and IL-17) (<i>clinical trial</i>) (Szkardkiewicz et al., 2014)</li> </ol>	<ol style="list-style-type: none"> <li>1. Inhibit the growth of <i>P. gingivalis</i>, <i>P. intermedia</i>, <i>A. actinomycetemcomitans</i>, and <i>F. nucleatum</i> depending on B12, presence of anaerobiosis, and substrate glycerol (<i>in vitro experiment</i>) (Geraldo et al., 2020; Santos et al., 2020; Jansen et al., 2021)</li> <li>2. Inhibit <i>P. gingivalis</i> in saliva, supragingival plaque and subgingival plaque, and <i>P. intermedia</i> in saliva (<i>clinical trial</i>) (Invernici et al., 2018)</li> <li>3. Reduce the load of <i>P. gingivalis</i> in peri-implant mucositis (<i>clinical trial</i>) (Gallofré et al., 2018)</li> </ol>
	<i>Lactobacillus rhamnosus</i>	Reduce the number of TRAP-positive cells and infiltrating inflammatory cells ( <i>animal experiment</i> ) (Gatej et al., 2018)	<ol style="list-style-type: none"> <li>1. Inhibit the growth of <i>P. gingivalis</i>, <i>A. actinomycetemcomitans</i>, and <i>F. nucleatum</i> (<i>in vitro experiment</i>) (Moman et al., 2020)</li> <li>2. Reduce the biofilm biomass and viable counts in biofilm of <i>A. actinomycetemcomitans</i> by releasing</li> </ol>

(Continued)

TABLE 1 | Continued

Genus/type	Species	Regulate immune responses	Regulate periodontal microbiota
			postbiotics ( <i>in vitro experiment</i> ) (Ishikawa et al., 2021).
			3. Downregulate the virulence-associated factors ( <i>LtxA</i> , <i>CdtB</i> , <i>dspB</i> , and <i>katA</i> ) of <i>A. actinomycetemcomitans</i> ( <i>in vitro experiment</i> ) (Ishikawa et al., 2021)
	<i>Lactobacillus salivarius</i>	–	1. Inhibit <i>A. actinomycetemcomitans</i> in saliva and GCF ( <i>clinical trial</i> ) (Sajedinejad et al., 2017)
			2. Reduce the expression of <i>LtxA</i> and <i>CdtB</i> exotoxins by <i>A. actinomycetemcomitans</i> ( <i>in vitro experiment</i> ) (Nissen et al., 2014)
	<i>Lactobacillus johnsonii</i> , <i>Lactobacillus fructosum</i> , <i>Lactobacillus delbrueckii</i> subsp. <i>casei</i>	–	Degrade <i>A. actinomycetemcomitans</i> biofilms by producing enzymes such as lipase ( <i>in vitro experiment</i> ) (Jaffar et al., 2016)
<b>Bifidobacterium</b>	<i>Bifidobacterium animalis</i> subsp. <i>lactis</i>	1. Increase the expression of anti-inflammatory factors (IL-10, TGF- $\beta$ 1, OPG, and $\beta$ -defensins) and reduce the expression of pro-inflammatory factors (TNF- $\alpha$ , IL-1 $\beta$ , IL-6, CINC, and RANKL) in gingival tissues of experimental periodontitis ( <i>animal experiment</i> ) (Oliveira et al., 2017; Ricoldi et al., 2017; Silva et al., 2021) 2. Reduce the expression of IL-1 $\beta$ and the ratio of RANKL/OPG in gingival tissues of rats with periodontitis and metabolic syndrome ( <i>animal experiment</i> ) (Silva et al., 2021) 3. Reduce IL-1 $\beta$ in GCF ( <i>clinical trial</i> ) (Kuru et al., 2017) 4. Raise the expression of $\beta$ -defensin, TLR4, and CD4 in gingiva ( <i>clinical trial</i> ) (Invernici et al., 2020)	1. Inhibit the growth of <i>P. gingivalis</i> , <i>P. intermedia</i> , <i>A. actinomycetemcomitans</i> , and <i>F. nucleatum</i> ( <i>in vitro experiment</i> ) (Invernici et al., 2020) 2. Reduce the adhesion of <i>P. gingivalis</i> to buccal epithelial cells ( <i>in vitro experiment</i> ) (Invernici et al., 2020) 3. Antagonize the biofilm formation of <i>F. nucleatum</i> and <i>P. gingivalis</i> ( <i>in vitro experiment</i> ) (Argandoña Valdez et al., 2021) 4. Change the ratio between aerobic and anaerobic bacteria and the proportion of subgingival community in animal models ( <i>animal experiment</i> ) (Oliveira et al., 2017; Ricoldi et al., 2017) 5. Reduce the level of <i>P. gingivalis</i> , <i>Treponema denticola</i> , <i>Fusobacterium nucleatum vincentii</i> , and <i>A. actinomycetemcomitans</i> in deep periodontal pockets, saliva, and dental plaque ( <i>clinical trial</i> ) (Alanzi et al., 2018; Invernici et al., 2018)
<b>Streptococcus</b>	<i>Streptococcus salivarius</i>	Inhibit the expression of IL-6 and IL-8 induced by <i>P. gingivalis</i> , <i>A. actinomycetemcomitans</i> , and <i>F. nucleatum</i> in gingival fibroblasts ( <i>in vitro experiment</i> ) (Adam et al., 2011; MacDonald et al., 2021).	1. Inhibit the growth of <i>P. gingivalis</i> , <i>P. intermedia</i> , <i>A. actinomycetemcomitans</i> , and <i>F. nucleatum</i> ( <i>in vitro experiment</i> ) (Moman et al., 2020; Jansen et al., 2021) 2. Inhibit the adhesion of <i>A. actinomycetemcomitans</i> , <i>P. gingivalis</i> , and <i>P. intermedia</i> ( <i>in vitro experiment</i> ) (Sliepen et al., 2008; Van Hoogmoed et al., 2008; Sliepen et al., 2009)
	<i>Streptococcus dentisani</i>	Increase the secretion of IL-10 and decline the level of IFN- $\gamma$ induced by <i>F. nucleatum</i> in HGF-1 ( <i>in vitro experiment</i> ) (Esteban-Fernandez et al., 2019)	1. Change cell wall structure of <i>P. intermedia</i> and induce cell lysis of <i>F. nucleatum</i> ( <i>in vitro experiment</i> ) (López-López et al., 2017) 2. Suppress <i>F. nucleatum</i> and <i>P. gingivalis</i> growth and attachment to HGF-1 ( <i>in vitro experiment</i> ) (López-López et al., 2017)
	<i>Streptococcus cristatus</i>	Reduce the <i>F. nucleatum</i> -induced pro-inflammatory IL-8 production in oral epithelial cells ( <i>in vitro experiment</i> ) (Zhang et al., 2008)	1. Produce arginine deiminase ArcA to inhibit fimbrial gene ( <i>fimA</i> ) expression and biofilm formation of <i>P. gingivalis</i> ( <i>in vitro experiment</i> ) (Xie et al., 2000; Xie et al., 2007) 2. Inhibit adhesion and colonization of <i>A. actinomycetemcomitans</i> ( <i>in vitro experiment</i> ) (Sliepen et al., 2008)
	<i>Streptococcus gordonii</i> , <i>Streptococcus sanguinis</i> , <i>Streptococcus mitis</i>	–	1. Reduce fimbrial gene ( <i>mfa1</i> ) expression of <i>P. gingivalis</i> ( <i>in vitro experiment</i> ) (Xie et al., 2000; Xie et al., 2007) 2. Inhibit adhesion and colonization of <i>A. actinomycetemcomitans</i> , <i>P. gingivalis</i> , and <i>P. intermedia</i> on hard surfaces or epithelial cells ( <i>in vitro experiment</i> ) (Xie et al., 2000; Xie et al., 2007)

(Continued)

TABLE 1 | Continued

Genus/type	Species	Regulate immune responses	Regulate periodontal microbiota
<b>Weissella</b>	<i>Weissella cibaria</i>	<ol style="list-style-type: none"> <li>1. Reduce the <i>F. nucleatum</i>-induced pro-inflammatory cytokine (IL-6 and IL-8) production in KB cells (<i>in vitro experiment</i>) (Kang et al., 2011)</li> <li>2. Inhibit NF-<math>\kappa</math>B activation and NO production in response to periodontopathogen stimulation in macrophages (<i>in vitro experiment</i>) (Kim et al., 2020b)</li> <li>3. Reduce both the production of pro-inflammatory (TNF-<math>\alpha</math>, IL-1<math>\beta</math>, IL-6) and anti-inflammatory (IL-10) cytokines (<i>animal experiment</i>) (Kim et al., 2020a)</li> </ol>	<p><i>vitro experiment</i>) (Teughels et al., 2007; Sliepen et al., 2008; Van Hoogmoed et al., 2008)</p> <ol style="list-style-type: none"> <li>1. Co-aggregate with <i>F. nucleatum</i>, <i>T. denticola</i>, and <i>P. gingivalis</i> and inhibit the growth of <i>F. nucleatum</i> and <i>P. gingivalis</i> (<i>in vitro experiment</i>) (Kang et al., 2006b; Jang et al., 2016)</li> <li>2. Interfere with the adhesion of <i>F. nucleatum</i> (<i>in vitro experiment</i>) (Kang et al., 2011)</li> <li>3. Produce acid, H<sub>2</sub>O<sub>2</sub>, and N-acetylmuramidase to inhibit <i>F. nucleatum</i>, <i>P. gingivalis</i>, and <i>P. intermedia</i> (<i>in vitro experiment</i>) (Lim et al., 2018)</li> <li>4. Reduce the amount of plaque and <i>F. nucleatum</i>, <i>P. gingivalis</i>, <i>P. intermedia</i>, and <i>T. forsythia</i> levels in the oral cavity and <i>P. gingivalis</i> level in gingival tissues (<i>animal experiment</i>) (Do et al., 2019; Kim et al., 2020a)</li> <li>5. Reduce <i>F. nucleatum</i> in GCF (clinical trial) (Kang et al., 2020).</li> </ol>
<b>Recombinant probiotics</b>	Recombinant <i>Lactobacillus paracasei</i> Recombinant <i>L. acidophilus</i>	–  Express FomA to induce the production of antibodies against FomA protein and prevent the infection of <i>F. nucleatum</i> and its co-aggregated <i>P. gingivalis</i> ( <i>in vitro experiment</i> ) (Ma et al., 2013)	Express single-chain antibody fragments against RgpA gingipain to co-aggregate with <i>P. gingivalis</i> and kill it ( <i>in vitro experiment</i> ) (Marcotte et al., 2006) Present similar antibacterial activity and antibiotic sensitivity to the wild <i>L. acidophilus</i> , and its adhesive ability was improved ( <i>in vitro experiment</i> ) (Ma et al., 2018)

GCF, gingival crevicular fluid; OPG, osteoprotegerin.

killed *L. acidophilus* ATCC 4356 was observed to downregulate the expression of IL-6/8 in KB and HOK cells activated by *F. nucleatum* ATCC 23726, co-aggregate with *F. nucleatum* ATCC 23726 and ATCC 25586, and inhibit the expression of their virulence factor *fap2* involved in adhesion and invasion, thus interfering *F. nucleatum* self-aggregation and adhesion to epithelial cells, which is another way to inhibit *F. nucleatum* infecting oral epithelial cells in addition to competing for adhesion sites (Ding et al., 2021). The heat-killed *L. acidophilus* ATCC 4356 drew interest, as it could avoid drug resistance and dysbacteriosis and could be more safe (Ding et al., 2021).

It was reported that live *L. acidophilus* JCM1021 could degrade biofilms of *A. actinomycetemcomitans* Y4 (more than 90%), and SUNY75 and OMZ 534 (more than 50%) by lipase and other hydrolases (Jaffar et al., 2016). Ishikawa et al. further revealed part of the mechanisms in *A. actinomycetemcomitans* (serotype b, JP2 clone) biofilm degradation with cell-free pH-neutralized supernatants (CFS) of *L. acidophilus* LA5 and NCFM (Ishikawa et al., 2021). *L. acidophilus* LA5 CFS could reduce the number of planktonic bacteria, as well as biofilm biomass and viable counts in biofilm by releasing postbiotics, which can assist antibiotics in removing *A. actinomycetemcomitans*, as bacteria in biofilm are difficult to eliminate. Besides, *L. acidophilus* LA5 CFS could downregulate the expression of vital virulence factors leukocyte toxin (*LtxA*) and cytolethal distending toxin (*CdtB*) related to evading host defenses. Another strain, *L. acidophilus* NCFM CFS, could decrease biofilm biomass and viable counts in biofilm by postbiotics but downregulate the transcription of *dspB*, hindering its application to control periodontitis.

Moreover, both *L. acidophilus* LA5 and NCFM downregulated *katA*, a gene encoding catalase, attenuating the resistance of oxidative stress of *A. actinomycetemcomitans*.

### *Lactobacillus reuteri*

Many *in vitro* experiments proved the inhibitory effects of *L. reuteri* on periodontopathogens, which is probably attributed to its specific by-products, such as reuterin, which is a non-protein broad-spectrum antibiotic and could suppress the growth of many gram-positive/negative bacteria, yeast, and fungi (Stevens et al., 2011). *L. reuteri* ATCC PTA 5289 is a good inhibitor of many periodontopathogens, including *P. gingivalis* ATCC 33277, *P. intermedia* ATCC 25611, and *F. nucleatum* ATCC 25586, except for *A. actinomycetemcomitans* ATCC 33384 (Jansen et al., 2021). As for the forms of the probiotics, both live *L. reuteri* PTA 5289 and DSM 17938 and their CFS showed inhibition on *P. gingivalis* ATCC 33277 and *F. nucleatum* ATCC 25586, while only the live form of the two *L. reuteri* attenuated the growth of *A. actinomycetemcomitans* ATCC 29522 *in vitro* (Geraldo et al., 2020; Santos et al., 2020). Another subspecies, *L. reuteri* ATCC 55730, also inhibited the growth of *F. nucleatum* ATCC 10953, *P. gingivalis* ATCC 33277, and *A. actinomycetemcomitans* ATCC 33384 and protected HOK cells infected by periodontal pathogens from death (Moman et al., 2020). Besides, exopolysaccharide (EPS) produced by *L. reuteri* DSM 17938 benefits its adhesion to epithelial cells to compete with pathogenic bacteria for adhesion sites (Kšonžeková et al., 2016). In another *in vitro* experiment, *L. reuteri* KCTC 3594 was shown to inhibit the secretion of IL-6 induced by *F. nucleatum* in KB cells (Kang et al., 2011).



In clinical trials, application of *L. reuteri* inhibited *P. gingivalis* in saliva, supragingival plaque and subgingival plaque, and *P. intermedia* in saliva (Invernici et al., 2018). However, for peri-implant diseases, *L. reuteri* DSM 17938 and PTA 5289, could only reduce the load of *P. gingivalis* in patients with peri-implant mucositis (Galofré et al., 2018). In animal experiments, the live *L. reuteri* DSM 17938 and PTA 5289 could raise the hemocyte density in *Galleria mellonella* infected by *P. gingivalis* ATCC 33277, thereby upregulating immune responses (Geraldo et al., 2020; Santos et al., 2020). The clinical trials also proved the immunomodulatory effects of *L. reuteri* such as regulating the imbalance between MMP and TIMP (Ince et al., 2015) or reducing the production of pro-inflammatory cytokines (tumor necrosis factor- $\alpha$  (TNF- $\alpha$ ), IL-1 $\beta$ , and IL-17) (Szkaradkiewicz et al., 2014), which could contribute to relieving inflammatory response and reducing periodontal tissues destruction.

### ***Lactobacillus rhamnosus***

*In vitro* experiments, *L. rhamnosus* could inhibit several vital periodontopathogens and downregulate the virulence factors about biofilm formation and immune escape in *A. actinomycetemcomitans* (Moman et al., 2020; Ishikawa et al., 2021). *L. rhamnosus* ATCC 53103 could inhibit the growth of *F. nucleatum* ATCC 10953, *P. gingivalis* ATCC 33277, and *A. actinomycetemcomitans* ATCC 33384 *in vitro* and could protect HOK cells infected by periodontal pathogens from death (Moman et al., 2020). *L. rhamnosus* Lr32 and HN001 CFS could reduce the biofilm biomass and viable counts in the biofilm of *A. actinomycetemcomitans* (serotype b, JP2 clone) by releasing postbiotics to facilitate antibiotics removing this pathogen (Ishikawa et al., 2021). Besides, *L. rhamnosus* Lr32 CFS could downregulate the expression of *LtxA* and *CdtB* to interfere with the process of evading host defenses. Both *L. rhamnosus* Lr32 and HN001 downregulated *kataA*, damaging the resistance of oxidative stress of *A. actinomycetemcomitans*. However, it was observed that *L. rhamnosus* HN001 CFS upregulated the transcription of *dspB* to degrade EPS of the biofilm but raised the transcription of *LtxA*, thus hindering its application to control periodontitis (Ishikawa et al., 2021). *L. rhamnosus* could also regulate *in vivo* immune responses. *L. rhamnosus* GG reduced inflammatory cell, osteoclast, and TRAP-positive cell number in periodontal tissues in a mouse model of experimental periodontitis (Gatej et al., 2018).

### ***Bifidobacterium***

*Bifidobacterium* is a type of gram-positive anaerobic bacteria that could be found in the human intestines, vagina, oral cavity, and breast milk. *Bifidobacterium* probiotics have been proved to relieve multiple intestinal diseases such as irritable bowel syndrome and constipation (Agrawal et al., 2009) and inflammatory bowel disease (Kim et al., 2007), improve lactose intolerance (He et al., 2008), prevent infectious diarrhea (Qiao et al., 2002), and reduce incidence and duration of respiratory infections (Jungersen et al., 2014) and exhibit anticancer effects (You et al., 2004). They also play a role in controlling oral infectious diseases including periodontal

diseases (Ricoldi et al., 2017) and oral candida infection (Ishikado et al., 2007).

### ***Bifidobacterium animalis* subsp. *lactis***

Recent studies have evaluated the effects of the *B. animalis* subsp. *lactis* (*B. lactis*) on periodontopathogens. In *in vitro* experiments, *B. lactis* ATCC 27673 antagonized the biofilm formation of *F. nucleatum* ATCC 25585 and *P. gingivalis* ATCC 33277 after co-incubating for 168 h, without interfering with the growth of *Streptococcus oralis* (Argandoña Valdez et al., 2021). *B. lactis* HN019 not only inhibits *P. gingivalis* W83, *P. intermedia* ATCC 25611, *F. nucleatum* ATCC 25586, and *A. actinomycetemcomitans* ATCC 33393 but also significantly reduces the adhesion of *P. gingivalis* W83 to buccal epithelial cells (Invernici et al., 2020). In animal experiments, *B. lactis* could also regulate the ratio between aerobic and anaerobic bacteria, as reported in the study of Ricoldi et al. (2017). Oliveira et al. had a consistent conclusion in their study since they found that the *B. lactis* HN019 treatment resulted in lower proportions of *P. intermedia*-like species in subgingival plaque of EP animals (Oliveira et al., 2017). In clinical trials, when *B. lactis* HN019 was taken for 30 days, *P. gingivalis*, *Treponema denticola*, and *F. nucleatum vincentii* were reduced markedly in deep periodontal pockets ( $\geq 7$  mm) (Invernici et al., 2018). *B. lactis* BB-12 combined with *L. rhamnosus* GG could decrease *F. nucleatum* and *A. actinomycetemcomitans* in saliva and dental plaque as well as *P. gingivalis* in dental plaque, and the amounts of bacteria in saliva become lower (Alanzi et al., 2018).

*B. lactis* HN019 is observed to regulate immune responses in animal experiments and clinical trials. Oliveira et al. reported that the EP-*B. lactis* HN019 group presented higher levels of osteoprotegerin (OPG) and  $\beta$ -defensins as well as lower levels of IL-1 $\beta$  and receptor activator of nuclear factor-kappa B (NF- $\kappa$ B) ligand (RANKL) than the EP-only group (Oliveira et al., 2017). *B. lactis* HN019 application could markedly decrease the levels of IL-1 $\beta$  and the ratio of RANKL/OPG in rats with periodontitis and metabolic syndrome and could downregulate the expression of TNF- $\alpha$  and IL-6 in rats only with periodontitis (Silva et al., 2021). In clinical trials, when *B. lactis* HN019 was taken for 30 days, 4 weeks, or 15 days after SRP, the mean ratios between the levels of IL-1 $\beta$  or IL-6 and those at baseline in GCF were lower than those in groups without *B. lactis* HN019; fewer osteoclasts, increased expression of anti-inflammatory factors (IL-10 and TGF- $\beta$ 1), and reduced expression of IL-1 $\beta$  and cytokine-induced neutrophil chemoattractant (CINC) were also induced (Kuru et al., 2017; Ricoldi et al., 2017; Invernici et al., 2018). *B. lactis* HN019 treatment as adjuvant therapy of SRP for 30 days could obviously raise the expression of  $\beta$ -defensin-3, toll-like receptor 4 (TLR4), and cluster of differentiation (CD)-4 in gingiva (Invernici et al., 2020).

### ***Streptococcus***

*Streptococcus* is a type of gram-positive, aerobic to facultatively anaerobic bacteria that is a member of the normal flora of the human mouth and intestines. Some *Streptococcus* spp. are identified as sources of invasive infections in humans that range from subacute to acute or even chronic, while others

have been proved their health benefits in improving digestive problems such as ulcerative colitis (Ohland and Macnaughton, 2010) and antibiotic-associated diarrhea (Correa et al., 2005), regulating immunity (Dargahi et al., 2020) and treating various oral diseases including dental caries (Di Pierro et al., 2015), periodontal diseases (López-López et al., 2017; Esteban-Fernandez et al., 2019), oral candida infection (Ishijima et al., 2012) and halitosis (Jamali et al., 2016).

### ***Streptococcus salivarius***

The regulatory effects of *S. salivarius* on many periodontopathogens have been observed *in vitro* experiments. *S. salivarius* M18 shows stable inhibition to common periodontopathogens, including *P. gingivalis* ATCC 33277, *P. intermedia* ATCC 25611, *F. nucleatum* ATCC 25586, and *A. actinomycetemcomitans* ATCC 33384 (Jansen et al., 2021). Another strain *S. salivarius* K12 shows distinct inhibitory effects on *P. intermedia* ATCC 25611, *A. actinomycetemcomitans* ATCC 33384, *F. nucleatum* ATCC 10953, and *P. gingivalis* ATCC 33277 (Moman et al., 2020; Jansen et al., 2021). *S. salivarius* K12 could raise the viability of HOK cells infected by *P. gingivalis* and *F. nucleatum*, thus increasing the defense capability of epithelium (Moman et al., 2020). Apart from M18 and K12, *S. salivarius* TOVE could cause 1.5% and 71.3% reduction of *A. actinomycetemcomitans* adhesion by pre-colonization of glass coverslips (Sliepen et al., 2008) or epithelial cells (Sliepen et al., 2009), as well as inhibiting the adhesion of *P. gingivalis* and *P. intermedia* (Van Hoogmoed et al., 2008).

*S. salivarius* probiotic strains are also found to regulate immune responses *in vitro* experiments. *S. salivarius* K12 and M18 could inhibit immune activation by periodontopathogens and reduce the levels of IL-6/8 in human gingival fibroblasts stimulated by *A. actinomycetemcomitans*, *P. gingivalis*, and *F. nucleatum* when *S. salivarius* is co-incubated with pathogens and fibroblasts simultaneously or *S. salivarius* is pretreated with fibroblasts before infection (Adam et al., 2011; MacDonald et al., 2021).

### ***Weissella***

*Weissella* is a type of gram-positive facultative anaerobes that are classified from the genus *Lactobacillus* and occur in a great variety of habitats, including human saliva, breast milk, intestines, feces, vagina, and skin. Among them, there are opportunistic pathogens as well as probiotic bacteria with beneficial effects such as antibacterial activities (Srionnual et al., 2007), antifungal activities (Quattrini et al., 2020), and immunoregulation (Lee et al., 2013). Certain probiotic *Weissella* such as *Weissella cibaria* strains have been shown to play a role in inhibiting dental caries, halitosis, and periodontal diseases (Kang et al., 2006a; Kang et al., 2006b; Jang et al., 2016; Do et al., 2019; Kim et al., 2020a).

### ***Weissella cibaria***

Some *W. cibaria* strains have shown strong antibacterial activities against periodontopathogens *in vitro* experiments. Kang et al. found that *W. cibaria* CMU, CMS2, and CMS3 co-

aggregated most strongly with *F. nucleatum*, the proliferation of which was decreased by 5-log cycles as a result (Kang et al., 2006b). Jang et al. obtained a consistent result, as 95% *P. gingivalis* and *F. nucleatum* were inhibited because of co-aggregation with *W. cibaria* CMU (Jang et al., 2016). It can be inferred that co-aggregation with *W. cibaria* does not interfere with the colonization of periodontal pathogens but suppresses their growth. *W. cibaria* CFS was also found to be against pathogens, which is mainly related to acidic pH, the presence of hydroxyl, and the secretion of specific proteins with antimicrobial activities (Lim et al., 2018). Organic acids, including lactic acid, acetic acid, citric acid, fatty acids, and oleic acid, could interfere with the basic metabolism of the pathogens and inhibit the growth of *P. gingivalis* KCTC 5352, *F. nucleatum* KCTC 2488, and *P. intermedia* ATCC 25611. Besides, hydrogen peroxide (H<sub>2</sub>O<sub>2</sub>) in CFS could suppress *P. gingivalis* and *P. intermedia*, and *W. cibaria* CMU could produce the most H<sub>2</sub>O<sub>2</sub> in commercial probiotics for oral healthcare (Lim et al., 2018). On the other hand, the bacteriocin-like compounds (BLCs) of CFS, *N*-acetylmuramidase, were only against the *P. gingivalis* effectively by binding to cell walls and causing lysis (Lim et al., 2018). In animal experiments, the application of *W. cibaria* significantly lowered the amount of plaque; the level of *F. nucleatum*, *P. gingivalis*, *P. intermedia*, and *T. forsythia* in the oral cavity; and the level of *P. gingivalis* in gingival tissues (Do et al., 2019; Kim et al., 2020a). A recent clinical trial indicated that taking *W. cibaria* CMU for 8 weeks significantly reduced *F. nucleatum* in GCF (Kang et al., 2020), corresponding to its strong co-aggregation ability with *F. nucleatum* *in vitro* (Kang et al., 2006b).

*W. cibaria* was also observed to regulate the inflammatory response *in vitro* experiments. *W. cibaria* CMU could reduce the production of IL-6 and IL-8 in KB cells activated by *F. nucleatum*, as well as the cell attachment of *F. nucleatum*, while the viability and co-aggregation of *W. cibaria* CMU may not play an essential role in this process (Kang et al., 2011). The anti-inflammatory activity of *W. cibaria* CMU is related to inhibiting NF- $\kappa$ B activation in response to periodontopathogen stimulation and NO production. In RAW 264.7 macrophages stimulated by formalin-inactivated *A. actinomycetemcomitans* ATCC 3338, *W. cibaria* CMU downregulated the expression of inducible NO synthase (iNOS) and the mRNA of IL-1 $\beta$  and IL-6 to reduce NO production. The inhibition of NF- $\kappa$ B inhibitor  $\alpha$  (I $\kappa$ B $\alpha$ ) kinase (IKK) phosphorylation, I $\kappa$ B $\alpha$  degradation, and the nuclear translocation of p65 were also observed in *W. cibaria* CMU-treated RAW 264.7 macrophages (Kim et al., 2020b). In animal models, *W. cibaria* CMU decreased the level of both pro-inflammatory (TNF- $\alpha$ , IL-1 $\beta$ , and IL-6) and anti-inflammatory (IL-10) cytokines (Kim et al., 2020a).

### **Recombinant Probiotics**

In addition to the application of conventional forms, such as the live, heat-killed, freeze-dried probiotics and the probiotics CFS, recombinant probiotics produced by genetic engineering could express more diverse antibacterial substances and present an enhanced antibacterial activity. A recombinant *Lactobacillus*

*paracasei* strain was constructed by Marcotte et al. to express single-chain antibody fragments (scFv) against RgpA gingipain, a virulence factor of *P. gingivalis*, to co-aggregate with *P. gingivalis*; the antibacterial activity of *L. paracasei* was not damaged. It is worth mentioning that co-aggregation may facilitate the colonization of *P. gingivalis* via *L. paracasei* adhesion, but the pathogen may be killed by the locally high concentration of antibacterial substances secreted by *L. paracasei* (Marcotte et al., 2006). In 2013, Ma et al. reported a recombinant *L. acidophilus*, some wild strains of which have shown periodontal beneficial characteristics, expressing *F. nucleatum* outer membrane protein FomA. The recombinant *L. acidophilus* strain could stimulate the antibodies against FomA protein to prevent the infection of *F. nucleatum* and its co-aggregated pathogens such as *P. gingivalis* in periodontal tissues (Ma et al., 2013). Animal studies proved that oral administration of the recombinant *L. acidophilus* reduced the infection by *F. nucleatum* and *P. gingivalis* (Ma et al., 2013). Particularly, the recombinant *L. acidophilus* presents a similar antibacterial activity and antibiotic sensitivity to the wild *L. acidophilus*, and its adhesive ability is further improved (Ma et al., 2018). In these studies, the genome of parent probiotics is modified by genetic engineering techniques to construct recombinant strains of probiotic with new genetic characteristics, providing a new idea for the development and application of probiotics.

## ISSUES IN CURRENT APPLICATION OF PERIODONTAL HEALTH-RELATED PROBIOTICS

### Effectiveness

Although a multitude of studies have suggested that probiotics are beneficial to periodontal health, the effectiveness of probiotics in managing periodontal disease and health is still controversial. Even in studies that used the same probiotic bacteria, the observed improvements in clinical measurements, inflammation, and microbiota related to periodontal diseases are not consistent. The causes of the conflicting observations and conclusions on the effectiveness of probiotics in different periodontal-health research are complicated and diverse.

Multiple factors are considered to affect the results of probiotic research, such as probiotic species or strains, administration dosage or modes, sample size, the combination of different probiotics, and reaction time. In a randomized controlled clinical trial of Laleman et al. (2015), 48 periodontitis patients were included, divided evenly into two groups after SRP (baseline), and then given either a placebo or a probiotic tablet containing *S. oralis* KJ3, *Streptococcus uberis* KJ2, and *Streptococcus rattus* JH145 twice a day for 12 weeks. No significant difference in clinical indices including PPD, BOP, and CAL could be detected between the probiotic group and the control group at the baseline, 12-week, or 24-week time points. Nevertheless, a *post hoc* power analysis conducted by them revealed that eight times more patients were needed to show a

statistically significant intergroup difference for PPD at 12 weeks. The results of the study indicate that sample size is a non-negligible factor that affects the observations of probiotic studies. In addition, for different probiotic strains, the effective dose and the best application mode should be considered first when studying the effects of probiotics in modulating periodontal health. Inappropriate dose or mode in applying probiotics may result in the failure in obtaining expected outcomes and correct conclusions. However, the problem is that up to now, there are not enough references to determine effective dose and application mode for numerous probiotic strains. As for the combination of probiotics, *L. reuteri* DSM 17938 could regulate *L. reuteri* ATCC PTA 5289 to stabilize its antibacterial activity (Jansen et al., 2021). The antibacterial activity of *P. gingivalis* is related to the double or triple combination of *B. longum*, *B. lactis*, and *Bifidobacterium infantis*. The growth of *P. gingivalis* was inhibited by 41.8% with exposure to *B. longum* with *B. lactis* and 50.1% to triple combination (Argandoña Valdez et al., 2021). Besides, reaction time is another factor, as 11.3% *F. nucleatum* was shown to be suppressed at 24 h after exposure to probiotics, and growth inhibition rates rose to 18.4%–51.6% until 72 h (Argandoña Valdez et al., 2021). Thus, the combination manner of probiotics and action time also affect the effectiveness of judgment. Consequently, sometimes, it is difficult for researchers to scientifically assess the effectiveness of probiotics.

Experimental design and evaluation indices selected of a study also have an important impact on the understanding of probiotic effectiveness. For example, in some studies, it is concluded that probiotic treatment was not able to significantly improve the clinical symptoms of periodontal diseases, which may be partly attributed to the inappropriate selection of evaluation indices. As observed by Montero et al. in a study evaluating the efficacy of the adjunctive use of probiotics on gingivitis (Montero et al., 2017), gingivitis subjects were recruited and administered with tablets containing placebo or the probiotic combination of *Lactobacillus plantarum*, *L. brevis*, and *Pediococcus acidilactici* for 6 weeks. Their results showed no significant differences in the average GI between the placebo and probiotic groups. When focusing on the change in the number of sites with higher GI scores (GI = 3 at baseline), a significantly higher reduction was observed in the probiotic group. In other words, the average GI may be not the optimum evaluation index for probiotic intervention in the study, because the improvement effect of probiotics on sites with severe inflammation was diluted by other sites when calculating the mean value of GI.

Sometimes, it is reported that although the clinical parameters are improved by probiotics, periodontal microbiota and related inflammatory factors do not show detectable differences. Keller et al. found that after treating moderate-gingivitis patients with tablets containing a mix of *L. rhamnosus* PB01, DSM 14869 and *Lactobacillus curvatus* EB10, and DSM 32307 for 4 weeks, BOP and GCF volume were obviously improved, while all the selected cytokines (IL-1 $\beta$ , IL-6, IL-8, IL-10, and TNF- $\alpha$ ) in GCF and the salivary microbiome were unaffected by the intervention (Keller et al., 2017). The researchers speculated that cytokine



concentrations in GCF of some samples were lower than the detectable levels and thus could not be analyzed and evaluated. In addition, subgingival plaques were not collected in the study for microbial diversity and abundance analysis, which may be one of the reasons for not observing microbial alterations.

What is particularly noteworthy is that a recent study on intestinal colonization by probiotics suggested that the effectiveness of probiotics might vary from person to person. Through using endoscopy to collect flora at multiple intestine sites to analyze the flora composition of volunteers who were given probiotic supplements, Zmora et al. found that humans featured person-, region-, and strain-specific mucosal colonization patterns of probiotics, hallmarked by predictive pretreatment microbiome and host features (Zmora et al., 2018). Consequently, probiotic interventions are likely to exert differential influences on different individuals, which is thought to possibly explain the high variability in probiotic effects on the host or gut microbiome observed in different studies. Since periodontal diseases are related to original periodontal microbiota and host immunity, differential colonization resistance and responsiveness of individuals to probiotics may also exist and impact the research results observed with probiotic use in periodontal diseases.

## Safety

With the deepening of probiotic research and the recognition of more potential probiotic species and strains, there has been growing concern about the safety of probiotics, in particular, when applied to humans with the purpose of managing diseases and improving health. In fact, there are some studies reporting that probiotics have limited benefits to the body and may even be harmful to health (De Groote et al., 2005; Doron and Snyderman, 2015). It has been recommended by the WHO/FAO working group to conduct a series of safety assessments of probiotics including antibiotic resistance, toxin production, potential hemolysis, metabolic activities, and side effects in humans and post-market surveillance of commercial consumers (Araya et al., 2002). Classical probiotics such as some *Lactobacillus* and *Bifidobacterium* species that have a long history of use in fermented foods or dairy products are generally recognized as safe (Kang et al., 2019). However, there are no adequate systematic safety studies, and indeed, complications of probiotic use occur sometimes. Some studies have revealed that treatment with probiotics caused bacteremia, including the most commonly used *Lactobacillus* spp. (De Groote et al., 2005). Despite no existing evidence of the occurrence of bacteremia induced by probiotic use in periodontal therapy or care, people with damaged periodontal tissues or tooth bleeding after SRP seem to be susceptible to bacterial invasion, and therefore such a possibility could not be ruled out.

The application of probiotics may have unexpected impacts on host immune responses and microecology. Recently, Suez et al. (2018) evaluating the probiotic impact on post-antibiotic reconstitution of the intestinal host-microbiome homeostasis showed that antibiotic treatment enhanced human gut mucosal colonization by probiotics, and more importantly, compared to spontaneous post-antibiotic recovery, probiotics significantly

delayed rather than aided in gut microbiome and host transcriptome reconstitution. It was noticed that probiotic presence led to elevated transcription levels of certain inflammatory mediators and antimicrobial peptides, which may affect the restoration of the original intestinal flora. In many probiotic-periodontal disease studies, probiotics were attempted to be used as adjuvant therapy after non-surgical periodontal therapy. However, it is reminded by this study that probiotic use may influence or even interfere with periodontal microbiome recolonization and restoration of periodontal microecological balance after removal of dental plaques by periodontal non-surgical treatment.

Collectively, these findings suggest that studies on periodontal health-promoting probiotics need to focus more on the safety in use, although there are few relevant adverse events reported. Just as the effects of probiotics depend on strain traits, each probiotic strain would be anticipated to have a different safety profile. Thus, it is quite essential to verify the identities, phenotypic characteristics, and non-pathogenicity of different probiotics for safe use in humans (Kang et al., 2019). Furthermore, it is proposed that perhaps the safety of a commercially available probiotic product depends not only on the probiotic organism but also on the other constituents of the product, whether in food or medicinal formulation (Doron and Snyderman, 2015). This highlights the importance of systematic and persistent assessment of probiotic products by researchers in the overall process of probiotic research, development, and application.

## CONCLUDING REMARKS AND FUTURE PERSPECTIVES

The emergence of probiotics provides more options for the prevention and treatment of periodontal diseases. Different from antibiotics and bactericides that are widely used in clinical practice, probiotics generally play a role in periodontal therapy and healthcare through regulating host immune function and restoring the balance of periodontal microecology. Consequently, probiotics have unique advantages and considerable potential in application to maintain periodontal health.

Different probiotic species exert their periodontal health-regulatory effects through diverse mechanisms such as competition for adhesion sites to epithelial cells, antagonism against growth, biofilm formation and virulence expression of periodontopathogens, and influence on host immune responses. Currently, the majority of known periodontal health-promoting probiotics is derived from the classical probiotic genera *Lactobacillus* and *Bifidobacterium* and seems to be more effective and safe when applied in human health management. Nevertheless, taking account of the controversy on effectiveness and concerns on safety, these probiotics, as well as probiotics derived from other genera or remodeled by genetic engineering techniques, need more investigation to support their role in periodontal therapy and care.



The studies on probiotic use in the intestine have highlighted a need for developing personalized probiotic approaches according to the host individual's flora and immune status so that probiotics could better colonize and play a more effective role in promoting health. In order to ensure universal and persistent efficacy, such a personalized strategy should also be considered and developed when applying probiotics in the prevention and treatment of periodontal diseases. Furthermore, a diverse combination of different probiotic species and probiotic strains is probably one of the major development directions for probiotic application, which may provide combinational or synergistic effects on regulating host microbiota and immunity, especially when considering the high complexity of subgingival plaques and the presence of various oral environmental stress factors. Genetic engineering would provide more ideas and possibilities for probiotic research and development. The probiotic function could be further enhanced and improved by directional genetic modifications on existing probiotics that

strengthen or remold their immunoregulation capabilities, antimicrobial activities against periodontopathogens, adaptive capacities to the oral environment, etc.

## AUTHOR CONTRIBUTIONS

YZ and QG conceptualized the review. YZ drafted the manuscript, and QG edited the manuscript, with YD providing critical revisions. All authors contributed significantly and read and approved the final manuscript.

## FUNDING

This work was supported by grants from the Youth Science Fund Project of the National Natural Science Foundation of China (No. 81500842) and the Science and Technology Department of Sichuan Province (No. 2021YJ0133).

## REFERENCES

- Adam, E., Jindal, M., Seney, S., Summers, K., Hamilton, D., Hatibović-Kofman, S., et al. (2011). Streptococcus Salivarius K12 and M18 Probiotics Reduce Periodontal Pathogen-Induced Inflammation. In: *IADR General Session 2011*. (San Diego, California, United States)
- Agrawal, A., Houghton, L. A., Morris, J., Reilly, B., Guyonnet, D., Goupil Feuillat, N., et al. (2009). Clinical Trial: The Effects of a Fermented Milk Product Containing Bifidobacterium Lactis DN-173 010 on Abdominal Distension and Gastrointestinal Transit in Irritable Bowel Syndrome With Constipation. *Aliment. Pharmacol. Ther.* 29, 104–114. doi: 10.1111/j.1365-2036.2008.03853.x
- Alanzi, A., Honkala, S., Honkala, E., Varghese, A., Tolvanen, M., and Söderling, E. (2018). Effect of Lactobacillus Rhamnosus and Bifidobacterium Lactis on Gingival Health, Dental Plaque, and Periodontopathogens in Adolescents: A Randomised Placebo-Controlled Clinical Trial. *Benef Microbes* 9, 593–602. doi: 10.3920/BM2017.0139
- Alkaya, B., Laleman, I., Keceli, S., Ozelik, O., Cenk, H. M., and Teughels, W. (2016). Clinical Effects of Probiotics Containing Bacillus Species on Gingivitis: A Pilot Randomized Controlled Trial. *J. Periodontol. Res.* 52 (3), 497–504. doi: 10.1111/jre.12415
- Allaker, R. P., and Stephen, A. S. (2017). Use of Probiotics and Oral Health. *Curr. Oral. Health Rep.* 4, 309–318. doi: 10.1007/s40496-017-0159-6
- Amizic, I. P., Cigić, L., Gavić, L., Radić, M., and Barišić, I. G. (2017). Antimicrobial Efficacy of Probiotic-Containing Toothpastes: An *In Vitro* Evaluation. *Med. Glas.* 14, 139–144. doi: 10.17392/870-16
- Araya, M., Morelli, L., Reid, G., Sanders, M., Stanton, C., Pineiro, M., et al. (2002). "Guidelines for the Evaluation of Probiotics in Food," *Joint FAO/WHO Working Group Report*. (London Ontario, Canada), 1–11.
- Argandoña Valdez, R. M., Ximenez-Fyvie, L. A., Caiiffa, K. S., Rodrigues Dos Santos, V., Gonzales Cervantes, R. M., Almaguer-Flores, A., et al. (2021). Antagonist Effect of Probiotic Bifidobacteria on Biofilms of Pathogens Associated With Periodontal Disease. *Microb. Pathog.* 150, 104657. doi: 10.1016/j.micpath.2020.104657
- Chen, M. X., Zhong, Y. J., Dong, Q. Q., Wong, H. M., and Wen, Y. F. (2021). Global, Regional, and National Burden of Severe Periodontitis 1990–2019: An Analysis of the Global Burden of Disease Study 2019. *J. Clin. Periodontol.* 48 (9), 1165–1188. doi: 10.1111/jcpe.13506
- Correa, N. B. O., Peret, L. A., Penna, F. J., Lima, R., and Nicoli, J. R. (2005). A Randomized Formula Controlled Trial of Bifidobacterium Lactis and Streptococcus Thermophilus for Prevention of Antibiotic-Associated Diarrhea in Infants. *J. Clin. Gastroenterol.* 39, 385–389. doi: 10.1097/01.mcg.0000159217.47419.5b
- Dargahi, N., Johnson, J., and Apostolopoulos, V. (2020). Streptococcus Thermophilus Alters the Expression of Genes Associated With Innate and Adaptive Immunity in Human Peripheral Blood Mononuclear Cells. *PLoS One* 15 (2), e0228531. doi: 10.1371/journal.pone.0228531
- De Groote, M. A., Frank, D. N., Dowell, E., Glode, M. P., and Pace, N. R. (2005). Lactobacillus Rhamnosus GG Bacteremia Associated With Probiotic Use in a Child With Short Gut Syndrome. *Pediatr. Infect. Dis. J.* 24, 278. doi: 10.1097/01.inf.0000154588.79356.e6
- Deshmukh, M. A., Dodamani, A. S., Karibasappa, G., Khairnar, M. R., Naik, R. G., and Jadhav, H. C. (2017). Comparative Evaluation of the Efficacy of Probiotic, Herbal and Chlorhexidine Mouthwash on Gingival Health: A Randomized Clinical Trial. *J. Clin. Diagn. Res.* 11, ZC13. doi: 10.7860/JCDR/2017/23891.9462
- Ding, Q., Sun, X., Cao, S., Zhao, C., Wang, Y., and Wang, X. (2021). Heat-Killed Lactobacillus Acidophilus Mediates Fusobacterium Nucleatum Induced Pro-Inflammatory Responses in Epithelial Cells. *FEMS Microbiol. Lett.* 368 (5), fnaa160. doi: 10.1093/femsle/fnaa160
- Di Piero, F., Zanvit, A., Nobili, P., Rizzo, P., and Fornaini, C. (2015). Cariogram Outcome After 90 Days of Oral Treatment With Streptococcus Salivarius M18 in Children at High Risk for Dental Caries: Results of a Randomized, Controlled Study. *Clin. Cosmet. Investig. Dent.* 7, 107–113. doi: 10.2147/CCIDE.S93066
- Do, K.-H., Park, H.-E., Kang, M., Kim, J.-T., Yeu, J.-E., and Lee, W.-K. (2019). Effects of Weissella Cibaria CMU on Halitosis and Calculus, Plaque, and Gingivitis Indices in Beagles. *J. Vet. Dent.* 36 (2), 135–142. doi: 10.1177/0898756419872562
- Doron, S., and Snyderman, D. R. (2015). Risk and Safety of Probiotics. *Clin. Infect. Dis.* 60 Suppl 2, S129–S134. doi: 10.1093/cid/civ085
- Esteban-Fernandez, A., Ferrer, M. D., Zorraquin-Pena, I., Lopez-Lopez, A., Moreno-Arribas, M. V., and Mira, A. (2019). *In Vitro* Beneficial Effects of Streptococcus Dentisani as Potential Oral Probiotic for Periodontal Diseases. *J. Periodontol.* 90, 1346–1355. doi: 10.1002/JPER.18-0751
- Flichy-Fernández, A. J., Ata-Ali, J., Alegre-Domingo, T., Candel-Martí, E., Ata-Ali, F., Palacio, J. R., et al. (2015). The Effect of Orally Administered Probiotic Lactobacillus Reuteri-Containing Tablets in Peri-Implant Mucositis: A Double-Blind Randomized Controlled Trial. *J. Periodontol. Res.* 50, 775–785. doi: 10.1111/jre.12264
- Galofré, M., Palao, D., Vicario, M., Nart, J., and Violant, D. (2018). Clinical and Microbiological Evaluation of the Effect of Lactobacillus Reuteri in the

- Treatment of Mucositis and Peri-Implantitis: A Triple-Blind Randomized Clinical Trial. *J. Periodontol. Res.* 53, 378–390. doi: 10.1111/jre.12523
- Gatej, S. M., Marino, V., Bright, R., Fitzsimmons, T. R., Gully, N., Zilm, P., et al. (2018). Probiotic Lactobacillus Rhamnosus GG Prevents Alveolar Bone Loss in a Mouse Model of Experimental Periodontitis. *J. Clin. Periodontol.* 45 (2), 204–212. doi: 10.1111/jcpe.12838
- Geraldo, B. M. C., Batalha, M. N., Milhan, N. V. M., Rossoni, R. D., Scorroni, L., and Anbinder, A. L. (2020). Heat-Killed Lactobacillus Reuteri and Cell-Free Culture Supernatant Have Similar Effects to Viable Probiotics During Interaction With Porphyromonas Gingivalis. *J. Periodontol. Res.* 55, 215–220. doi: 10.1111/jre.12704
- Hajishengallis, G. (2015). Periodontitis: From Microbial Immune Subversion to Systemic Inflammation. *Nat. Rev. Immunol.* 15, 30–44. doi: 10.1038/nri3785
- Hajishengallis, G., Darveau, R. P., and Curtis, M. A. (2012). The Keystone-Pathogen Hypothesis. *Nat. Rev. Microbiol.* 10, 717–725. doi: 10.1038/nrmicro2873
- Hajishengallis, G., and Lamont, R. J. (2012). Beyond the Red Complex and Into More Complexity: The Polymicrobial Synergy and Dysbiosis (PSD) Model of Periodontal Disease Etiology. *Mol. Oral. Microbiol.* 27, 409–419. doi: 10.1111/j.2041-1014.2012.00663.x
- He, T., Priebe, M. G., Zhong, Y., Huang, C., Harmsen, H. J., Raangs, G. C., et al. (2008). Effects of Yogurt and Bifidobacteria Supplementation on the Colonic Microbiota in Lactose-Intolerant Subjects. *J. Appl. Microbiol.* 104, 595–604. doi: 10.1111/j.1365-2672.2007.03579.x
- Hill, C., Guarner, F., Reid, G., Gibson, G. R., Merenstein, D. J., Pot, B., et al. (2014). Expert Consensus Document. The International Scientific Association for Probiotics and Prebiotics Consensus Statement on the Scope and Appropriate Use of the Term Probiotic. *Nat. Rev. Gastroenterol. Hepatol.* 11, 506–514. doi: 10.1038/nrgastro.2014.66
- Imran, F., Das, S., Padmanabhan, S., Rao, R., Suresh, A., and Bharath, D. (2015). Evaluation of the Efficacy of a Probiotic Drink Containing Lactobacillus Casei on the Levels of Periodontopathic Bacteria in Periodontitis: A Clinico-Microbiological Study. *Indian J. Dental Res.* 26, 462. doi: 10.4103/0970-9290.172033
- Ince, G., Gursoy, H., Ipci, S. D., Cakar, G., Emekli-Alturfan, E., and Yilmaz, S. (2015). Clinical and Biochemical Evaluation of Lozenges Containing Lactobacillus Reuteri as an Adjunct to Non-Surgical Periodontal Therapy in Chronic Periodontitis. *J. Periodontol.* 86, 746–754. doi: 10.1902/jop.2015.140612
- Invernici, M. M., Furlaneto, F., Salvador, S. L., Ouwehand, A. C., Salminen, S., Mantzari, A., et al. (2020). Bifidobacterium Animalis Subsp Lactis HN019 Presents Antimicrobial Potential Against Periodontopathogens and Modulates the Immunological Response of Oral Mucosa in Periodontitis Patients. *PLoS One* 15, e0238425. doi: 10.1371/journal.pone.0238425
- Invernici, M. M., Salvador, S. L., Silva, P. H. F., Soares, M. S. M., Casarin, R., Palioto, D. B., et al. (2018). Effects of Bifidobacterium Probiotic on the Treatment of Chronic Periodontitis: A Randomized Clinical Trial. *J. Clin. Periodontol.* 45, 1198–1210. doi: 10.1111/jcpe.12995
- Ishijima, S. A., Hayama, K., Burton, J. P., Reid, G., Okada, M., Matsushita, Y., et al. (2012). Effect of Streptococcus Salivarius K12 on the *In Vitro* Growth of Candida Albicans and Its Protective Effect in an Oral Candidiasis Model. *Appl. Environ. Microbiol.* 78, 2190–2199. doi: 10.1128/AEM.07055-11
- Ishikado, A., Suido, H., Sato, T., and Makino, T. *Preventive/therapeutic Agent for Diseases Associated With Candida Infection, Such as Allergy, Atopic Dermatitis, Periodontal Disease, Comprises Bifidobacterium Fermented Product of Plant Chosen From Brassicaceae Plant and Carrot*, WO2007086573-A1 WOJP051465 30 Jan 2007 JP2007556044-X JP556044 30 Jan 2007 JP5328158-B2 JP556044 30 Jan 2007.
- Ishikawa, K. H., Bueno, M. R., Kawamoto, D., Simionato, M. R. L., and Mayer, M. P. A. (2021). Lactobacilli Postbiotics Reduce Biofilm Formation and Alter Transcription of Virulence Genes of Aggregatibacter Actinomycetemcomitans. *Mol. Oral. Microbiol.* 36, 92–102. doi: 10.1111/omi.12330
- Ishikawa, K. H., Mayer, M. P., Miyazima, T. Y., Matsubara, V. H., Silva, E. G., Paula, C. R., et al. (2015). A Multispecies Probiotic Reduces Oral Candida Colonization in Denture Wearers. *J. Prosthodont. Implant Esthet. Reconstr. Dent.* 24, 194–199. doi: 10.1111/jopr.12198
- Ishikawa, K. H., Mita, D., Kawamoto, D., Nicoli, J. R., Albuquerque-Souza, E., Lorenzetti Simionato, M. R., et al. (2020). Probiotics Alter Biofilm Formation and the Transcription of Porphyromonas Gingivalis Virulence-Associated Genes. *J. Oral. Microbiol.* 12, 1805553. doi: 10.1080/20002297.2020.1805553
- Jaffar, N., Ishikawa, Y., Mizuno, K., Okinaga, T., and Maeda, T. (2016). Mature Biofilm Degradation by Potential Probiotics: Aggregatibacter Actinomycetemcomitans versus Lactobacillus spp. *PLoS One* 11, e0159466. doi: 10.1371/journal.pone.0159466
- Jamali, Z., Aminabadi, N. A., Samiei, M., Deljavan, A. S., Shokravi, M., and Shirazi, S. (2016). Impact of Chlorhexidine Pretreatment Followed by Probiotic Streptococcus Salivarius Strain K12 on Halitosis in Children: A Randomised Controlled Clinical Trial. *Oral. Health Prev. Dent.* 14, 305–313. doi: 10.3290/johpd.a36521
- James, K. M., Macdonald, K. W., Chanyi, R. M., Cadieux, P. A., and Burton, J. P. (2016). Inhibition of Candida Albicans Biofilm Formation and Modulation of Gene Expression by Probiotic Cells and Supernatant. *J. Med. Microbiol.* 65, 328. doi: 10.1099/jmm.0.000226
- Jang, H. J., Kang, M. S., Yi, S. H., Hong, J. Y., and Hong, S. P. (2016). Comparative Study on the Characteristics of Weissella Cibaria CMU and Probiotic Strains for Oral Care. *Molecules* 21 (12), 1752. doi: 10.3390/molecules21121752
- Jansen, P. M., Abdelbary, M. M. H., and Conrads, G. (2021). A Concerted Probiotic Activity to Inhibit Periodontitis-Associated Bacteria. *PLoS One* 16, e0248308. doi: 10.1371/journal.pone.0248308
- Jungersen, M., Wind, A., Johansen, E., Christensen, J. E., Stuer-Lauridsen, B., and Eskesen, D. (2014). The Science Behind the Probiotic Strain Bifidobacterium Animalis Subsp. Lactis BB-12(R). *Microorganisms* 2, 92–110. doi: 10.3390/microorganisms2020092
- Kahouli, I., Malhotra, M., AlaouiJamali, M., and Prakash, S. (2015). In-Vitro Characterization of the Anti-Cancer Activity of the Probiotic Bacterium Lactobacillus Fermentum NCIMB 5221 and Potential Against Colorectal Cancer. *J. Cancer Sci. Ther.* 07 (7). doi: 10.4172/1948-5956.1000354
- Kang, M. S., Chung, J., Kim, S. M., Yang, K. H., and Oh, J. S. (2006a). Effect of Weissella Cibaria Isolates on the Formation of Streptococcus Mutans Biofilm. *Caries Res.* 40, 418–425. doi: 10.1159/000094288
- Kang, M. S., Kim, B. G., Chung, J., Lee, H. C., and Oh, J. S. (2006b). Inhibitory Effect of Weissella Cibaria Isolates on the Production of Volatile Sulphur Compounds. *J. Clin. Periodontol.* 33, 226–232. doi: 10.1111/j.1600-051X.2006.00893.x
- Kang, M. S., Lee, D. S., Lee, S. A., Kim, M. S., and Nam, S. H. (2020). Effects of Probiotic Bacterium Weissella Cibaria CMU on Periodontal Health and Microbiota: A Randomised, Double-Blind, Placebo-Controlled Trial. *BMC Oral. Health* 20, 243. doi: 10.1186/s12903-020-01231-2
- Kang, M., Lim, H.-S., Kim, S.-M., Lee, H., and Oh, J.-S. (2011). Effect of Weissella Cibaria on Fusobacterium Nucleatum-Induced Interleukin-6 and Interleukin-8 Production in KB Cells. *J. Bacteriol. Virol.* 41, 9. doi: 10.4167/jbv.2011.41.1.9
- Kang, M., Yeu, and Hong, (2019). Safety Evaluation of Oral Care Probiotics Weissella Cibaria CMU and CMS1 by Phenotypic and Genotypic Analysis. *Int. J. Mol. Sci.* 20, 2693. doi: 10.3390/ijms20112693
- Kang, J. H., Yun, S. I., Park, M. H., Park, J. H., Jeong, S. Y., and Park, H. O. (2013). Anti-Obesity Effect of Lactobacillus Gasseri BNR17 in High-Sucrose Diet-Induced Obese Mice. *PLoS One* 8, e54617. doi: 10.1371/journal.pone.0054617
- Keller, M. K., Brandsborg, E., Holmström, K., and Twetman, S. (2017). Effect of Tablets Containing Probiotic Candidate Strains on Gingival Inflammation and Composition of the Salivary Microbiome: A Randomised Controlled Trial. *Benef. Microbes* 9 (3), 487–494. doi: 10.3920/BM2017.0104
- Kim, J. W., Jung, B. H., Lee, J. H., Yoo, K. Y., Lee, H., Kang, M. S., et al. (2020a). Effect of Weissella Cibaria on the Reduction of Periodontal Tissue Destruction in Mice. *J. Periodontol.* 91 (10), 1367–1374. doi: 10.1002/JPER.19-0288
- Kim, N., Kunisawa, J., Kwon, M. N., Eog Ji, G., and Kiyono, H. (2007). Oral Feeding of Bifidobacterium Bifidum (BGN4) Prevents CD4(+) CD45RB(high) T Cell-Mediated Inflammatory Bowel Disease by Inhibition of Disordered T Cell Activation. *Clin. Immunol.* 123, 30–39. doi: 10.1016/j.clim.2006.11.005
- Kim, M. J., You, Y. O., Kang, J. Y., Kim, H. J., and Kang, M. S. (2020b). Weissella Cibaria CMU Exerts an Anti-Inflammatory Effect by Inhibiting Aggregatibacter Actinomycetemcomitans-Induced Nf- $\kappa$ b Activation in Macrophages. *Mol. Med. Rep.* 22, 4143–4150. doi: 10.3892/mmr.2020.11512
- Kobayashi, R., Kobayashi, T., Sakai, F., Hosoya, T., Yamamoto, M., and Kurita-Ochiai, T. (2017). Oral Administration of Lactobacillus Gasseri SBT2055 is Effective in Preventing Porphyromonas Gingivalis-Accelerated Periodontal Disease. *Sci. Rep.* 7 (1), 545. doi: 10.1038/s41598-017-00623-9.

- Kšonežková, P., Bystrický, P., Vlčková, S., Pätöprstý, V., Pulzová, L., Mudroňová, D., et al. (2016). Exopolysaccharides of *Lactobacillus Reuteri*: Their Influence on Adherence of *E. Coli* to Epithelial Cells and Inflammatory Response. *Carbohydr. Polym.* 141, 10–19. doi: 10.1016/j.carbpol.2015.12.037
- Kumar, P. S., Griffen, A. L., Moeschberger, M. L., and Leys, E. J. (2005). Identification of Candidate Periodontal Pathogens and Beneficial Species by Quantitative 16s Clonal Analysis. *J. Clin. Microbiol.* 43, 3944–3955. doi: 10.1128/JCM.43.8.3944-3955.2005
- Kumar, S., and Madurantakam, P. (2017). Limited Evidence Shows Short-Term Benefit of Probiotics When Used as an Adjunct to Scaling and Root Planing in the Treatment of Chronic Periodontitis. *Evid. Based Dent.* 18, 109–110. doi: 10.1038/sj.ebd.6401270
- Kuru, B. E., Laleman, I., Yalınzoğlu, T., Kuru, L., and Teughels, W. (2017). The Influence of a *Bifidobacterium Animalis* Probiotic on Gingival Health: A Randomized Controlled Clinical Trial. *J. Periodontol.* 88, 1115–1123. doi: 10.1902/jop.2017.170213
- Laleman, I., Pauwels, M., Quirynen, M., and Teughels, W. (2020). The Usage of a Lactobacilli Probiotic in the non-Surgical Therapy of Peri-Implantitis: A Randomized Pilot Study. *Clin. Oral. Implants Res.* 31, 84–92. doi: 10.1111/clr.13555
- Laleman, I., Yilmaz, E., Ozelik, O., Haytac, C., Pauwels, M., Herrero, E. R., et al. (2015). The Effect of a Streptococci Containing Probiotic in Periodontal Therapy: A Randomized Controlled Trial. *J. Clin. Periodontol.* 42, 1032–1041. doi: 10.1111/jcpe.12464
- Lebeer, S., Vanderleyden, J., and De Keersmaecker, S. C. (2008). Genes and Molecules of Lactobacilli Supporting Probiotic Action. *Microbiol. Mol. Biol. Rev.* 72, 728–764, Table of Contents. doi: 10.1128/MMBR.00017-08
- Lee, W., Cho, S. M., Kim, M., Ko, Y. G., Yong, D., and Lee, K. (2013). Weissella Confusa Bacteremia in an Immune-Competent Patient With Underlying Intramural Hematomas of the Aorta. *Ann. Lab. Med.* 33, 459–462. doi: 10.3343/alm.2013.33.6.459
- Lilly, D. M., and Stillwell, R. H. (1965). Probiotics: Growth-Promoting Factors Produced by Microorganisms. *Science* 147, 747–748. doi: 10.1126/science.147.3659.747
- Lim, H. S., Yeu, J. E., Hong, S. P., and Kang, M. S. (2018). Characterization of Antibacterial Cell-Free Supernatant From Oral Care Probiotic Weissella Cibaria, CMU. *Molecules* 23 (8), 1984. doi: 10.3390/molecules23081984
- Loesche, W. J. (1976). Chemotherapy of Dental Plaque Infections. *Oral. Sci. Rev.* 9, 65–107.
- López-López, A., Camelo-Castillo, A., Ferrer, M. D., Simon-Soro, and Mira, A. (2017). Health-Associated Niche Inhabitants as Oral Probiotics: The Case of *Streptococcus Dentisani*. *Front. Microbiol.* 8, 379. doi: 10.3389/fmicb.2017.00379
- Lourenshattingh, A., and Viljoen, B. C. (2001). Yogurt as Probiotic Carrier Food. *Int. Dairy J.* 11, 1–17. doi: 10.1016/S0958-6946(01)00036-X
- Macdonald, K. W., Chanyi, R. M., Macklaim, J. M., Cadieux, P. A., Reid, G., and Burton, J. P. (2021). Streptococcus Salivarius Inhibits Immune Activation by Periodontal Disease Pathogens. *BMC Oral. Health* 21, 245. doi: 10.1186/s12903-021-01606-z
- Ma, L., Ding, Q., Feng, X., and Li, F. (2013). The Protective Effect of Recombinant FomA-Expressing Lactobacillus; Acidophilus Against Periodontal Infection. *Inflammation* 36, 1160–1170. doi: 10.1007/s10753-013-9651-x
- Maekawa, T., and Hajishengallis, G. (2014). Topical Treatment With Probiotic Lactobacillus Brevis CD2 Inhibits Experimental Periodontal Inflammation and Bone Loss. *J. Periodontol. Res.* 49, 785. doi: 10.1111/jre.12164
- Mahasneh, S. A., and Mahasneh, A. M. (2017). Probiotics: A Promising Role in Dental Health. *Dent. J. (Basel)* 5 (4), 26. doi: 10.3390/dj5040026
- Ma, L., Li, F., Zhang, X., and Feng, X. (2018). Biochemical Characterization of a Recombinant Lactobacillus Acidophilus Strain Expressing Exogenous FomA Protein. *Arch. Oral. Biol.* 92, 25–31. doi: 10.1016/j.archoralbio.2018.04.016
- Marcotte, H., Köll-Klais, P., Hultberg, A., Zhao, Y., Gmür, R., Mändar, R., et al. (2006). Expression of Single-Chain Antibody Against RgpA Protease of Porphyromonas Gingivalis in Lactobacillus. *J. Appl. Microbiol.* 100, 256–263. doi: 10.1111/j.1365-2672.2005.02786.x
- Marsh, P. D. (1994). Microbial Ecology of Dental Plaque and its Significance in Health and Disease. *Adv. Dent. Res.* 8, 263–271. doi: 10.1177/08959374940080022001
- Metchnikoff, E. (1907). *The Prolongation of Life: Optimistic Studies* Vol. 31 (Berlin, Germany: Nabu Press), 133.
- Moman, R., O'Neill, C. A., Ledger, R. G., Cheesapcharoen, T., and McBain, A. J. (2020). Mitigation of the Toxic Effects of Periodontal Pathogens by Candidate Probiotics in Oral Keratinocytes, and in an Invertebrate Model. *Front. Microbiol.* 11, 999. doi: 10.3389/fmicb.2020.00999
- Montero, E., Iniesta, M., Rodrigo, M., Marin, M. J., Figuero, E., Herrera, D., et al. (2017). Clinical and Microbiological Effects of the Adjunctive Use of Probiotics in the Treatment of Gingivitis: A Randomized Controlled Clinical Trial. *J. Clin. Periodontol.* 44 (7), 708–716. doi: 10.1111/jcpe.12752
- Nissen, L., Sgorbati, B., Biavati, B., and Belibasakis, G. N. (2014). Lactobacillus Salivarius and L-Gasserii Down-Regulate Aggregatibacter Actinomycetemcomitans Exotoxins Expression. *Ann. Microbiol.* 64, 611–617. doi: 10.1007/s13213-013-0694-x
- Ohland, C. L., and Macnaughton, W. K. (2010). Probiotic Bacteria and Intestinal Epithelial Barrier Function. *Am. J. Physiol. Gastrointest. Liver Physiol.* 298, G807–G819. doi: 10.1152/ajpgi.00243.2009
- Ohshima, T., Kojima, Y., Seneviratne, C. J., and Maeda, N. (2016). Therapeutic Application of Synbiotics, a Fusion of Probiotics and Prebiotics, and Biogenics as a New Concept for Oral Candida Infections: A Mini Review. *Front. Microbiol.* 7, 10. doi: 10.3389/fmicb.2016.00010
- Oliveira, L. F., Salvador, S. L., Silva, P. H., Furlaneto, F. A., Figueiredo, L., Casarin, R., et al. (2017). Benefits of Bifidobacterium Animalis Subsp. Lactis Probiotic in Experimental Periodontitis. *J. Periodontol.* 88, 197–208. doi: 10.1902/jop.2016.160217
- Peña, M., Barallat, L., Vilarrasa, J., Vicario, M., Violant, D., and Nart, J. (2019). Evaluation of the Effect of Probiotics in the Treatment of Peri-Implant Mucositis: A Triple-Blind Randomized Clinical Trial. *Clin. Oral. Investig.* 23, 1673–1683. doi: 10.1007/s00784-018-2578-8
- Qiao, H., Duffy, L. C., Griffiths, E., Dryja, D., Leavens, A., Rossman, J., et al. (2002). Immune Responses in Rhesus Rotavirus-Challenged BALB/c Mice Treated With Bifidobacteria and Prebiotic Supplements. *Pediatr. Res.* 51, 750–755. doi: 10.1203/00006450-200206000-00015
- Quattrini, M., Korcari, D., Ricci, G., and Fortina, M. G. (2020). A Polyphasic Approach to Characterize Weissella Cibaria and Weissella Confusa Strains. *J. Appl. Microbiol.* 128, 500–512. doi: 10.1111/jam.14483
- Ricoldi, M. S. T., Furlaneto, F., Oliveira, L. F. F., Teixeira, G. C., Pischiotini, J. P., Moreira, A. L. G., et al. (2017). Effects of the Probiotic Bifidobacterium Animalis Subsp. Lactis on the non-Surgical Treatment of Periodontitis. A Histomorphometric, Microtomographic and Immunohistochemical Study in Rats. *PLoS One* 12, e0179946. doi: 10.1371/journal.pone.0179946
- Sajedinejad, N., Paknejad, M., Houshmand, B., Sharafi, H., Jelodar, R., Zahiri, H. S., et al. (2017). Lactobacillus Salivarius NK02: A Potent Probiotic for Clinical Application in Mouthwash. *Probiotics Antimicrob. Proteins* 10 (3), 485–495. doi: 10.1007/s12602-017-9296-4
- Santos, T. A., Scorzoni, L., Correia, R., Junqueira, J. C., and Anbinder, A. L. (2020). Interaction Between Lactobacillus Reuteri and Periodontopathogenic Bacteria Using *In Vitro* and *In Vivo* (G. Mellonella) Approaches. *Pathog. Dis.* 78 (8), ftaa044. doi: 10.1093/femspd/ftaa044
- Shah, M. P., and Gujjari, S. K. (2017). Long-Term Effect of Lactobacillus Brevis CD2 (Inersan®) and/or Doxycycline in Aggressive Periodontitis. *J. Indian Soc. Periodontol.* 21, 341–343. doi: 10.4103/jisp.jisp\_215\_17
- Silva, G. A., Moreira, A. L. G., Silva, P. H. F., Salvador, S. L., Casarin, R. C. V., Vicente, R. M., et al. (2021). The Use of Probiotics can Reduce the Severity of Experimental Periodontitis in Rats With Metabolic Syndrome: An Immunoenzymatic and Microtomographic Study. *J. Periodontol.* 93 (2), e1–12. doi: 10.1002/JPER.21-0285
- Sivamaruthi, B. S., Kesika, P., and Chaiyasut, C. (2020). A Review of the Role of Probiotic Supplementation in Dental Caries. *Probiotics Antimicrob. Proteins* 12 (4), 1300–1309. doi: 10.1007/s12602-020-09652-9
- Sliepen, I., Hofkens, J., Van, E. M., Quirynen, M., and Teughels, W. (2008). Aggregatibacter Actinomycetemcomitans Adhesion Inhibited in a Flow Cell. *Oral. Microbiol. Immunol.* 23, 520–524. doi: 10.1111/j.1399-302X.2008.00456.x
- Sliepen, I., Van Esche, M., Loozen, G., Van Eldere, J., Quirynen, M., and Teughels, W. (2009). Interference With Aggregatibacter Actinomycetemcomitans: Colonization of Epithelial Cells Under Hydrodynamic Conditions. *Oral. Microbiol. Immunol.* 24, 390–395. doi: 10.1111/j.1399-302X.2009.00531.x

- Srionnual, S., Yanagida, F., Lin, L. H., Hsiao, K. N., and Chen, Y. S. (2007). Weissellicin 110, a Newly Discovered Bacteriocin From *Weissella Cibaria* 110, Isolated From Plaa-Som, a Fermented Fish Product From Thailand. *Appl. Environ. Microbiol.* 73, 2247–2250. doi: 10.1128/AEM.02484-06
- Stevens, M., Vollenweider, S., Lacroix, C., and Zurich, E. T. H. (2011). *The Potential of Reuterin Produced by Lactobacillus Reuteri as a Broad Spectrum Preservative in Food*. (Sawston. Cambridge, United Kingdom: Woodhead Publishing), 129–160.
- Suez, J., Zmora, N., Zilberman-Schapira, G., Mor, U., Dori-Bachash, M., Bashiardes, S., et al. (2018). Post-Antibiotic Gut Mucosal Microbiome Reconstitution Is Impaired by Probiotics and Improved by Autologous FMT. *Cell* 174, 1406–1423.e1416. doi: 10.1016/j.cell.2018.08.047
- Sunita, G., Mallapa, R. H., Kumar, S. A., and Kumar, B. V. (2012). Probiotics for Human Health –New Innovations and Emerging Trends. *Gut Pathog.* 4, 15–15. doi: 10.1186/1757-4749-4-15
- Szkaradkiewicz, A. K., Stopa, J., and Karpiński, T. M. (2014). Effect of Oral Administration Involving a Probiotic Strain of *Lactobacillus Reuteri* on Pro-Inflammatory Cytokine Response in Patients With Chronic Periodontitis. *Arch. Immunol. Ther. Exp.* 62, 495–500. doi: 10.1007/s00005-014-0277-y
- Tada, H., Masaki, C., Tsuka, S., Mukaibo, T., Kondo, Y., and Hosokawa, R. (2018). The Effects of *Lactobacillus Reuteri* Probiotics Combined With Azithromycin on Peri-Implantitis: A Randomized Placebo-Controlled Study. *J. Prosthodont. Res.* 62, 89–96. doi: 10.1016/j.jpor.2017.06.006
- Takeda, S., Hidaka, M., Yoshida, H., Takeshita, M., Kikuchi, Y., Tsend-Ayush, C., et al. (2014). Antiallergic Activity of Probiotics From Mongolian Dairy Products on Type I Allergy in Mice and Mode of Antiallergic Action. *J. Funct. Foods* 9, 60–69. doi: 10.1016/j.jff.2014.04.013
- Tera, T., Okumura, T., Imai, S., Nakao, M., Yamaji, K., Ito, M., et al. (2015). Screening of Probiotic Candidates in Human Oral Bacteria for the Prevention of Dental Disease. *PloS One* 10, e0128657. doi: 10.1371/journal.pone.0128657
- Teughels, W., Kinder, H. S., Sliepen, I., Pauwels, M., Van, E. J., Cassiman, J. J., et al. (2007). Bacteria Interfere With A. Actinomycetemcomitans Colonization. *J. Dental Res.* 86, 611–617. doi: 10.1177/154405910708600706
- Theilade, E. (1986). The non-Specific Theory in Microbial Etiology of Inflammatory Periodontal Diseases. *J. Clin. Periodontol.* 13, 905–911. doi: 10.1111/j.1600-051X.1986.tb01425.x
- Van Hoogmoed, C. G., Geertsema-Doornbusch, G. I., Teughels, W., Quirynen, M., Busscher, H. J., and van der Mei, H. C. (2008). Reduction of Periodontal Pathogens Adhesion by Antagonistic Strains. *Oral. Microbiol. Immunol.* 23, 43–48. doi: 10.1111/j.1399-302X.2007.00388.x
- Waigankar, S. S., and Patel, V. (2011). Role of Probiotics in Urogenital Healthcare. *J. Midlife Health* 2, 5–10. doi: 10.4103/0976-7800.83253
- Xie, H., Cook, G. S., Costerton, J. W., Bruce, G., Rose, T. M., and Lamont, R. J. (2000). Intergeneric Communication in Dental Plaque Biofilms. *J. Bacteriol.* 182, 7067–7069. doi: 10.1128/JB.182.24.7067-7069.2000
- Xie, H., Lin, X., Wang, B. Y., Wu, J., and Lamont, R. J. (2007). Identification of a Signalling Molecule Involved in Bacterial Intergeneric Communication. *Microbiology* 153, 3228–3234. doi: 10.1099/mic.0.2007/009050-0
- Yoo, J. I., Shin, I. S., Jeon, J. G., Yang, Y. M., Kim, J. G., and Lee, D. W. (2019). The Effect of Probiotics on Halitosis: A Systematic Review and Meta-Analysis. *Probiotics Antimicrob. Proteins* 11, 150–157. doi: 10.1007/s12602-017-9351-1
- You, H. J., Oh, D. K., and Ji, G. E. (2004). Anticarcinogenic Effect of a Novel Chiroinositol-Containing Polysaccharide From *Bifidobacterium Bifidum* Bgn4. *FEMS Microbiol. Lett.* 240, 131–136. doi: 10.1016/j.femsle.2004.09.020
- Zhang, G., Chen, R., and Rudney, J. D. (2008). *Streptococcus Cristatus* Attenuates *Fusobacterium Nucleatum*-Induced Interleukin-8 Expression in Oral Epithelial Cells. *J. Periodontal Res.* 43, 408–416. doi: 10.1111/j.1600-0765.2007.01057.x
- Zhao, J.-J., Feng, X.-P., Zhang, X.-L., and Le, K.-Y. (2012). Effect of *Porphyromonas Gingivalis* and *Lactobacillus Acidophilus* on Secretion of IL1B, IL6, and IL8 by Gingival Epithelial Cells. *Inflammation* 35, 1330–1337. doi: 10.1007/s10753-012-9446-5
- Zhao, J. J., Jiang, L., Zhu, Y. Q., and Feng, X. P. (2019). Effect of *Lactobacillus Acidophilus* and *Porphyromonas Gingivalis* on Proliferation and Apoptosis of Gingival Epithelial Cells. *Adv. Med. Sci.* 64, 54–57. doi: 10.1016/j.advms.2018.04.008
- Zhao, J. J., Ke-Yi, L. E., Feng, X. P., and Li, M. (2011). Antagonistic Effects of *Lactobacillus Acidophilus* and *Bifidobacterium Adolescents* on Periodontalpathogens *In Vitro*. *Shanghai J. Stomatol.* 20, 364–367.
- Zmora, N., Zilberman-Schapira, G., Suez, J., Mor, U., Dori-Bachash, M., Bashiardes, S., et al. (2018). Personalized Gut Mucosal Colonization Resistance to Empiric Probiotics Is Associated With Unique Host and Microbiome Features. *Cell* 174, 1388–1405.e1321. doi: 10.1016/j.cell.2018.08.041

**Conflict of Interest:** The authors declare that the research was conducted in the absence of any commercial or financial relationships that could be construed as a potential conflict of interest.

**Publisher's Note:** All claims expressed in this article are solely those of the authors and do not necessarily represent those of their affiliated organizations, or those of the publisher, the editors and the reviewers. Any product that may be evaluated in this article, or claim that may be made by its manufacturer, is not guaranteed or endorsed by the publisher.

Copyright © 2022 Zhang, Ding and Guo. This is an open-access article distributed under the terms of the Creative Commons Attribution License (CC BY). The use, distribution or reproduction in other forums is permitted, provided the original author(s) and the copyright owner(s) are credited and that the original publication in this journal is cited, in accordance with accepted academic practice. No use, distribution or reproduction is permitted which does not comply with these terms.





# Oral Microbiota-Host Interaction Mediated by Taste Receptors

Hao Dong<sup>1†</sup>, Jiaxin Liu<sup>1,2†</sup>, Jianhui Zhu<sup>3,4</sup>, Zhiyan Zhou<sup>1,2</sup>, Marco Tizzano<sup>5</sup>, Xian Peng<sup>1</sup>, Xuedong Zhou<sup>1,2</sup>, Xin Xu<sup>1,2\*</sup> and Xin Zheng<sup>1,2\*</sup>

<sup>1</sup> State Key Laboratory of Oral Diseases and National Clinical Research Center for Oral Diseases, West China Hospital of Stomatology, Sichuan University, Chengdu, China, <sup>2</sup> Department of Cariology and Endodontics, West China Hospital of Stomatology, Sichuan University, Chengdu, China, <sup>3</sup> Stomatology Hospital, School of Stomatology, Zhejiang University School of Medicine, Hangzhou, China, <sup>4</sup> Clinical Research Center for Oral Diseases of Zhejiang Province, Key Laboratory of Oral Biomedical Research of Zhejiang Province, Cancer Center of Zhejiang University, Hangzhou, China, <sup>5</sup> Basic and Translation Sciences, Penn Dental Medicine, University of Pennsylvania, Philadelphia, PA, United States

## OPEN ACCESS

### Edited by:

Kangmin Duan,  
University of Manitoba, Canada

### Reviewed by:

Manoj Reddy Medapati,  
University of Manitoba, Canada  
Nisha Singh,  
University of Manitoba, Canada

### \*Correspondence:

Xin Zheng  
zxzdg@126.com  
Xin Xu  
xin.xu@scu.edu.cn

<sup>†</sup>These authors have contributed  
equally to this work and share  
first authorship

### Specialty section:

This article was submitted to  
Microbiome in Health and Disease,  
a section of the journal  
Frontiers in Cellular and  
Infection Microbiology

**Received:** 26 October 2021

**Accepted:** 07 March 2022

**Published:** 29 March 2022

### Citation:

Dong H, Liu J, Zhu J, Zhou Z,  
Tizzano M, Peng X, Zhou X, Xu X  
and Zheng X (2022) Oral  
Microbiota-Host Interaction  
Mediated by Taste Receptors.  
Front. Cell. Infect. Microbiol. 12:802504.  
doi: 10.3389/fcimb.2022.802504

Taste receptors, originally identified in taste buds, function as the periphery receptors for taste stimuli and play an important role in food choice. Cohort studies have revealed that single nucleotide polymorphisms of taste receptors such as T1R1, T1R2, T2R38 are associated with susceptibility to oral diseases like dental caries. Recent studies have demonstrated the wide expression of taste receptors in various tissues, including intestinal epithelia, respiratory tract, and gingiva, with an emerging role of participating in the interaction between mucosa surface and microorganisms via monitoring a wide range of metabolites. On the one hand, individuals with different oral microbiomes exhibited varied taste sensitivity, suggesting a potential impact of the oral microbiota composition on taste receptor function. On the other hand, animal studies and *in vitro* studies have uncovered that a variety of oral cells expressing taste receptors such as gingival solitary chemosensory cells, gingival epithelial cells (GECs), and gingival fibroblasts can detect bacterial signals through bitter taste receptors to trigger host innate immune responses, thus regulating oral microbial homeostasis. This review focuses on how taste receptors, particularly bitter and sweet taste receptors, mediate the oral microbiota-host interaction as well as impact the occurrence and development of oral diseases. Further studies delineating the role of taste receptors in mediating oral microbiota-host interaction will advance our knowledge in oral ecological homeostasis establishment, providing a novel paradigm and treatment target for the better management of dental infectious diseases.

**Keywords:** taste receptor, oral microbiota, innate immunity, periodontitis, dental caries, diet

## INTRODUCTION

Taste is triggered by signals from the oral sensory structures known as taste buds, which are stimulated by tastants and then conveyed to the central gustatory nervous system (Small, 2012; von Molitor et al., 2021). Various tastes including sweet, bitter, umami, sour, and salt are mainly perceived by specific taste receptors located at taste buds, which help the host to discriminate

between nutrients and poisonous and harmful substances (Margolskee, 1993; Roper, 2013). General health may be impaired by dysfunctional or diseased states of taste receptors. Past studies have well illustrated that gustatory sensitivity is influenced by single nucleotide polymorphisms (SNPs) of taste receptors and leads to different food preferences, which contribute to varied oral microbiota and disease susceptibility in the host (Chamoun et al., 2018b).

Recent studies have found that taste receptors are not only distributed in cells within taste buds, but are also expressed on a variety of cell types both orally and extra-orally, such as tuft cells, airway smooth muscle cells, macrophages, and so on (Deshpande et al., 2010; Sbarbati et al., 2010; Grassin-Delyle et al., 2019). Meanwhile, studies on taste receptors both on and off the taste buds support the view that taste receptors play an essential role as chemoreceptors in diverse non-gustatory physiological and pathological processes (Lee et al., 2014; Schneider et al., 2019; Gopallawa et al., 2021). Taking the oral taste receptors as an example, on the one hand, taste receptors detect various metabolites and other toxins derived from the oral microbiota, contributing to the establishment of the host immune response and the maintenance of homeostasis (Gil et al., 2015; Zheng et al., 2019; Medapati et al., 2021b). On the other hand, the perceptive capacity of taste receptors is in turn shaped by the oral microbiota (Solemdal et al., 2012; Zhu et al., 2021). Studies in other tissues have yielded similar findings (Tizzano et al., 2010; Deckmann and Kummer, 2016). The investigation of how taste receptors are involved in the interaction between host and oral microbiota will facilitate a thorough understanding of the chemosensory function of taste receptors, which is of great significance for the elucidation of the association between taste receptors and oral diseases. Accordingly, the role of taste receptors in regulating oral health and disease states will be discussed in this review, with a focus on the impact of genotypic and phenotypic changes in receptors on the composition of the oral microbiota, as well as the key role of taste receptors mediating innate immune responses in oral microbiota-host interaction.

## MOLECULAR MECHANISMS OF TASTE SIGNAL TRANSDUCTION

Taste receptors are chemosensory receptors that exist in both taste buds and extra-gustatory tissues (Chandrashekar et al., 2006; Carey and Lee, 2019). Five widely accepted and fundamental tastes (sweet, umami, salt, sour, bitter) are initiated from these taste receptors (Lindemann, 2001). In recent studies, kokumi and fat are likely to be potential candidates for new basic tastes (Khan et al., 2019; Rhyu et al., 2020; Hichami et al., 2021). The receptors, including multiple members of the G protein-coupled receptor (GPCR) superfamily and some ionic channels, put different specificity to stimuli (Nuemket et al., 2017; Teng et al., 2019; Ahmad and Dalziel, 2020). In practical terms, sweet means consuming carbohydrates as vital energy source, salt indicates ingestion of sodium, and

umami promotes detecting amino acids, which are respectively indispensable for energy metabolism, ionic homeostasis and building proteins (Yamaguchi and Ninomiya, 2000; Dias et al., 2012; Laffitte et al., 2014). Sour, which perceives rotten food, and bitter, which implicate a variety of toxic substances such as alkaloids and cyanogenic glycosides, are revolting tastes (Glendinning, 1994; Huang et al., 2008). Therefore, sour and bitter tastes promote the establishment of early warning against the intake of underlying toxins.

Bitter, sweet and umami taste signals are supposed to converge on a common intracellular signaling transduction in the Type II cells. Bitter, sweet, umami tastes are activated by GPCRs, which are seven-transmembrane proteins of two main classes. GPCRs that detect sweet and umami stimuli are named as taste receptor family 1 member (T1R) (Zhao et al., 2003), and those that transduce bitter compounds are named as taste receptor family 2 member (T2R) (Chandrashekar et al., 2000). When activated by corresponding stimuli, G protein coupled to these taste receptors is resolved into  $G_{\beta\gamma}$  subunit and  $G_{\alpha}$  subunit including  $G_{\alpha}$ -gustducin,  $G_{\alpha14}$  and  $G_{\alpha i}$  (McLaughlin et al., 1992; Huang et al., 1999; Tizzano et al., 2008). With further hydrolysis of  $G_{\beta\gamma}$ ,  $G_{\beta3}$  and  $G_{\gamma13}$  can be formed, which stimulates phospholipase C $\beta$ 2 (PLCB2) to increase intracellular  $Ca^{2+}$  levels (Zhang et al., 2007).  $G_{\alpha}$  subunit is considered to influence cyclic adenosine monophosphate (cAMP) signaling (Clapp et al., 2008). When bitter and umami receptors are activated by tastants,  $G_{\alpha}$  subunit diminishes intracellular cAMP levels, which inhibits activity of protein kinase A. As a result, it weakens the inhibition of protein kinase A on the PLCB2-IP $_3$  pathway, and further promotes the release of  $Ca^{2+}$  in the endoplasmic reticulum. When sweet receptors are activated by tastants,  $G_{\alpha}$  subunit increases intracellular cAMP levels, which enhances the activity of protein kinase A and inhibits  $K^+$  channels, thereby promoting extracellular  $Ca^{2+}$  influx. At last, elevated intracellular  $Ca^{2+}$  levels promote the opening of transient receptor potential cation channel subfamily M member 5 (TRPM5), which is an ion channel that results in membrane depolarization and causes action potential followed by the release of ATP (**Figure 1**) (Iwata et al., 2014).

Sour taste receptors are located in a subset of taste receptor cells, the Type III cells, on the tongue and palate epithelium (Chandrashekar et al., 2006). Recent studies have demonstrated that sour taste is initiated by a proton-selective channel Otopetrin-1 (OTOP1), which is a 24 transmembrane protein (Tu et al., 2018; Zhang et al., 2019). Up to date, OTOP1 and other otopetrin family members are supposed to be the only voltage-insensitive and proton-selective ionic channels (Teng et al., 2019), which may explain how Type III cells are activated by small changes in proton levels and tolerate much more massive changes in other ion levels when in food intake. The increasing intracellular proton levels mediated by OTOP1, on one hand, proximately change the membrane potential (Zhang et al., 2019), on the other hand, subsequently block  $K_{IR}2.1$ , a member of inward-rectifier  $K^+$  channels, to generate membrane depolarization (Ye et al., 2016). However, how OTOP1 gates and passes through protons and whether there

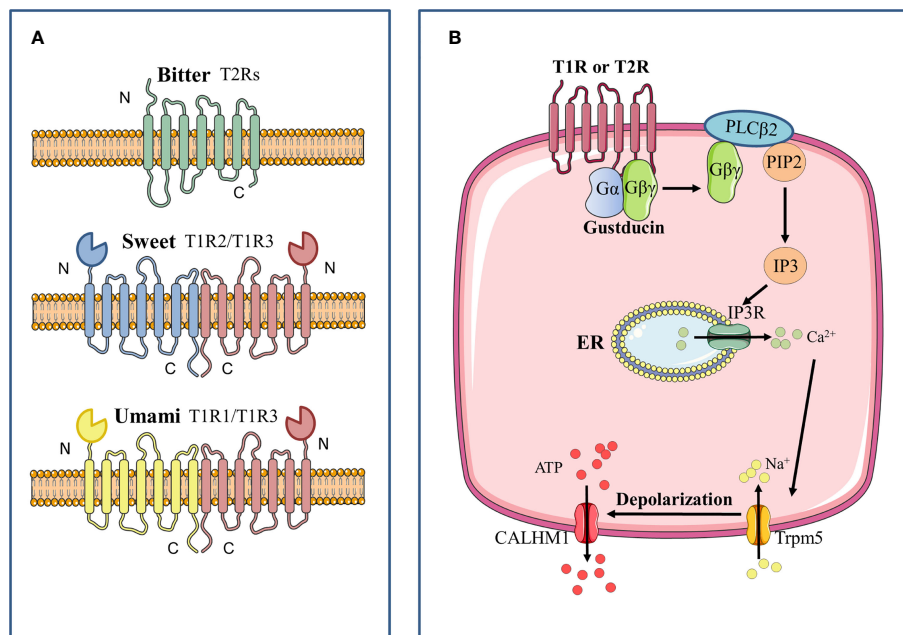


**FIGURE 1** | Signal transduction pathway of bitter, sweet, and umami GPCRs. **(A)** Bitter, sweet and umami receptors are all G-protein coupled-receptors. Bitter receptors are composed of T2Rs, while sweet (T1R2/T1R3) and umami (T1R2/T1R3) receptors are composed of T1Rs, which are characterized by a large N terminal domain that forms a Venus flytrap structure. **(B)** After stimulation of the taste receptor, the downstream G $\beta\gamma$  complex is mobilized, which then activates phospholipase C isoform  $\beta 2$  (PLC $\beta 2$ ) to induce the production of inositol 1,4,5-trisphosphate (IP3). IP3 then activates the IP3 receptor (IP3R), an intracellular ion channel that allows the release of Ca $^{2+}$  from the endoplasmic reticulum (ER), resulting in an increase in intracellular Ca $^{2+}$ . The complex of transient receptor potential cation channel subfamily M member 5 (TRPM5) is then activated and triggers the inward Na $^{+}$  diffusion. The depolarization causes activation of the complex of calcium homeostasis modulator 1 (CALHM1) channels, thus resulting in the release of ATP as the neurotransmitter.

are other elements in sour taste transduction remain to be solved in the future.

Salty taste in most mammals is divided into two pathways: appetitive salt taste and high-salt taste. Animals and humans adapt easily to appetitive salty taste in a low concentration (<100 mM) (Heck et al., 1984). This appetite is likely to meet the host requirement of Na $^{+}$  to maintain an ionic homeostasis. By comparison, high-salt taste (>300 mM) is significantly aversive (Oka et al., 2013), which indicates a reflex that protects individuals against hypernatremia and dehydration. Appetitive salt taste is activated by epithelial sodium channels (ENaC), a heterotrimer consisted of  $\alpha$ ,  $\beta$  and  $\gamma$  subunits (Canessa et al., 1994), in some taste cells within fungiform papillae (Nomura et al., 2020). With the access of Na $^{+}$  through ENaC, it causes a membrane depolarization driving action potentials. Notably, there is no change in intracellular Ca $^{2+}$  levels with the generation of action potentials in the ENaC $^{+}$  taste cells. ATP is released by calcium homeostasis modulator 1 (CALHM1) and CALHM3 subunits which are switched on under depolarization. Some studies have indicated that activation of a high-salt taste is associated with some types of bitter and sour taste cells in the foliate papillae and circumvallate papillae (Kretz et al., 1999; Lewandowski et al., 2016). However, there are no specific receptors and well-defined salty transduction signaling that have been demonstrated to function with high-salt taste.

## GENETIC VARIATION OF TASTE RECEPTORS CORRELATED WITH ORAL DISEASES

Varied dietary patterns among individuals are influenced by differences in taste perception abilities, thus shaping different oral health status. Genetic variations in certain genes associated with sweet, bitter, umami, salt, and sour tastes have been shown to correlate with taste function in varying degrees, and are thought to be potentially relevant affectors of oral disease susceptibility (Table 1) (Chamoun et al., 2018b).

### Sweet Taste Receptors

The perception of sweet taste is mediated by a heterodimer receptor composed of T1R2 and T1R3 together (Li et al., 2002). Various kinds of sweet taste compounds are detected by the T1R2/T1R3 sweet taste receptor, such as natural sugars, nonnutritive sweeteners, sweet-tasting proteins, and so on (Chandrashekar et al., 2006). The activation of the sweet taste receptor initiates intracellular signal transduction, mediating the regulation of the production and secretion of physiologically significant hormones and proteins like insulin and glucagon-like peptide-1 (GLP-1) (Kojima and Nakagawa, 2011; Kyriazis et al., 2012). Moreover, the sweet taste is a source of hedonic liking and greatly influences people's dietary choices (Jayasinghe et al., 2017).

**TABLE 1 |** SNPs of taste receptors correlated with oral diseases.

	Gene	SNP ID	Outcome	Reference
Sweet	TAS1R2:	rs35874116	Individuals with Ile191Val consumed fewer sugars as well as faced a lower risk of developing dental caries compared with Ile homozygotes. The Ile/Val and Ile/Ile genotypes appeared with a lower carbohydrate intake compared with the Val/Val genotype among the population of West Mexico. Children with Ile191Val were more frequently affected by caries than the common Ile allele. TAS1R3 gene rs307355 polymorphism has been found to be an independent risk factor for dental caries experience and to have increased the risk of caries.	(Eny et al., 2010; Kulkarni et al., 2013; Haznedaroğlu et al., 2015) (Ramos-Lopez et al., 2016)
	18854899T > C			
	TAS1R3:			
	-1572C > T			
Bitter	TAS2R38:	rs713598	The PAV (taster) haplotype was protective against dental caries.	(Wendell et al., 2010)
	145G > C	rs1726866	PROP non-tasters presented with significantly increased caries risk than PROP tasters.	(Öter et al., 2011)
	(A49P)	rs10246939	PAV/PAV homozygosity had the strongest ability to induce T2R38 expression when stimulated by <i>S. mutans</i> whereas AVI/AVI changed little.	(Gil et al., 2015)
	785T > C (V262A)			
Umami	886T > C (I296V)	rs17492553	"Super-tasters" CC homozygotes tend to have a lower risk of dental caries prevalence.	(Rawal et al., 2013)
	TAS1R1:			
	6576401C > T			

Disruption or loss of sweet taste receptor function would cause a wide range of health problems including metabolic disorders and oral diseases (Murovets et al., 2015; Smith et al., 2016).

Specifically, differences in the capacity of sweet taste receptors are associated with their genetic variation (Garcia-Bailo et al., 2009). SNPs of T1R2 and T1R3 determine sweet taste perception thresholds and the degree of sweet food preference and consumption (Jayasinghe et al., 2017). Eny et al. pointed out Ile191Val (rs35874116) variations in T1R2 were associated with different sugar intake, as Val allele carriers consumed fewer sugars compared with the Ile homozygotes (Eny et al., 2010). A recent study conducted in a Mexican population reported that a higher carbohydrate intake, as well as the risk of hypertriglyceridemia (HTG), was found in the Val/Val genotype individuals versus the Ile/Val and Ile/Ile genotypes (Ramos-Lopez et al., 2016). In addition, the studies of T1R3 revealed the association between SNPs and sweet taste sensitivity as well (Fushan et al., 2009; Murovets et al., 2020).

As aforementioned, SNPs of sweet taste receptors lead to differences in dietary sugar intake (Garcia-Bailo et al., 2009). The ingested carbohydrates are metabolized to produce acid in the oral biofilm made up of microorganisms that adhere to the tooth surface (Bradshaw and Lynch, 2013). When the pH of the tooth surface falls below 5.5, minerals are lost from the tooth surface faster than remineralization, which ultimately leads to dental caries. Put simply, sweet taste receptor gene polymorphisms shape the risk of caries by altering sweet food preferences. Studies conducted by Kulkarni et al. and Haznedaroglu et al. concluded that individuals who hold an Ile191Val polymorphism consumed fewer sugars with a lower risk of developing dental caries, while Ile homozygotes whose carbohydrate intake are higher showed more frequent high-risk caries experience (>8 caries) (Kulkarni et al., 2013; Haznedaroglu et al., 2015). These conclusions are consistent with most of the other studies (Eny et al., 2010; Ramos-Lopez et al., 2016). However, one study reported an opposite finding that children who carried the Val allele were more frequently

affected by caries than the common Ile allele (Izakovicova Holla et al., 2015). One possible explanation is that differences in race, environment, and food culture among populations are also involved in the effect of sweet taste receptor SNPs on dietary choices as well as the risk of caries. Another possibility is that the different genotypes of taste receptors not merely determine the sensitivity of taste perception, but are also involved in the oral microbiota-host interaction through other mechanisms.

Additionally, the increased intake of sugar caused by T1R2/T1R3 SNPs also modifies the oral microecological environment, leading to the alteration of the composition of oral microflora. A recent study revealed that children with low sensitivity to sweet taste presented with a higher incidence of dental caries mainly due to their more frequent consumption of sweet food, who also appeared to contain an increased presence of cariogenic *Streptococcus mutans* (*S. mutans*) (Jurczak et al., 2020). Altered microbial diversity occurs after a sugar-rich diet, which greatly increases the presence of cariogenic species, mediating the further development of caries (Tanner et al., 2018).

## Bitter Taste Receptors

Human detects numerous different bitter tastes through 25 types of T2Rs, while T2R38 plays the most vital role that genetically controls the perception capacity of bitter taste (Kim et al., 2003; Dong et al., 2009). Bitter taste receptors often work in conjunction with sweet taste receptors to influence our diet. Simply as people with high sweetness sensitivity reduce their intake of sweet food, people with high bitter sensitivity often tend to avoid bitter food. However, reduced intake of bitter foods such as antioxidant-rich vegetables and fruits may lead to a higher risk of cardiovascular disease or cancer (Basson et al., 2005; Roura et al., 2016).

The bitter taste sensation of agonists PTC and PROP is mediated by their combination with T2R38 (Kim et al., 2003; Bufe et al., 2005). Three SNPs of T2R38 caused by different combinations of amino acid substitutions respectively at positions 49 (Pro49Ala, rs713598), 262 (Ala262Val, rs1726866), and 296 (Val296Ile, rs10246939) mainly regulated



the diverse senses of bitter taste (Kim et al., 2003). Homozygous for the PAV haplotype are characterized by a stronger perception of bitterness than the average person and are called “super-tasters”, while those homozygous for the AVI haplotype manifest as “non-tasters” whose sense of bitter taste are less sensitive. The performance of heterozygotes is intermediate (Bartoshuk et al., 1994).

Various studies have confirmed that some undesirable diet may be attributed to the “supertaster” phenotype and have further linked the effects of bitter taste receptor SNPs leading to food preferences to health-disease transformation. Wendell et al. reported that the PAV (taster) haplotype is proven to be protective against dental caries (Wendell et al., 2010). The result of a subsequent study by Öter et al. confirmed this surprising view, as PROP non-tasters presented with significantly increased caries risk than PROP tasters (Öter et al., 2011). Interestingly, the capacity of T2R38 expression stimulated by *S. mutans* exhibits a polarity. PAV/PAV homozygosity had the strongest ability to induce T2R38 expression whereas AVI/AVI changed little (Gil et al., 2015). However, the theory that taste receptor mediates food selection fails to explain this phenomenon, as “super-tasters” have a stronger perception of bitterness and tend to consume less healthful bitter foods, yet they have a lower risk of caries and a lower abundance of pathogenic bacteria. This suggests the presence of pathogenic factors independent of taste receptor-mediated food selection. Further studies are needed to elucidate the pathogenesis involved.

In addition, several bitter taste receptors other than T2R38 have recently been shown to be as well involved in interactions with the oral flora and induction of disease. A recent study uncovered the novel role of bitter taste receptor T2R14 in detecting *S. mutans* and mediating innate immune defense in GECs (Medapati et al., 2021b). Moreover, CA6 gene polymorphisms were associated with *S. mutans* colonization, oral microbiota composition and the risk of dental caries, which were linked to bitter taste and smell perception (Esberg et al., 2019).

## Other Taste Receptors

Umami taste is initiated and enhanced through the heterodimer T1R1/T1R3 (Zhao et al., 2003). The primary umami taste substance is free l-glutamate, a compound that we are familiar with its another form called monosodium glutamate (MSG) (Ikeda, 2002). Two SNPs caused the substitutions of amino acid in the T1R1 respectively at positions 110 (Ala110Val, rs41278020) and 372 (Ala372Thr, rs34160967) are associated with sensitivity in umami taste (Raliou et al., 2009). An intronic SNP (rs17492553) in T1R1 is related to taste intensity in sweet, bitter, salty and sour (Rawal et al., 2013). CC homozygotes appeared to possess stronger taste intensity as “super-tasters” than that in TT homozygotes from rs17492553 groups. Similar to the trend in rs17492553 that in rs34160967, GG groups are stronger in overall taste intensity than that in AA/AG groups (Rawal et al., 2013). A recent study conducted in a Brazilian pre-adolescent population has shown that rs17492553 in T1R1 was relevant to dental caries prevalence. “Super-tasters” CC homozygotes tend to have a lower risk of dental caries

prevalence. The impact of SNPs in other taste receptors such as ENaC and OTOP1 on taste perception and oral disease susceptibility has remained obscure.

## REGULATION OF TASTE RECEPTORS ON ORAL MICROBIOTA-HOST INTERACTION

Since its discovery, the associations between taste receptors and oral diseases have been extensively studied. The prevailing notion is that the SNPs of taste receptors enable the host to perceive various tastes differently, which influenced dietary choices and host oral microbiome, regulating the host’s metabolism along with internal environmental homeostasis and ultimately mediating the reciprocal transition between health and disease states. Meanwhile, as we noted previously, food selection conducted by taste receptors SNPs fails to explain the full range of disease events. Several recent studies have focused on revealing how the taste receptor acts as a chemoreceptor to engage in signal transduction and immune responses in the oral cavity, which provides fresh insights into the role that taste receptors play in oral diseases. The latest relevant advancements are presented and summarized below, providing fresh perspectives on how taste receptors interact with oral microbiota to manage oral health status.

### Taste-Shaped Diet Impacts Host Metabolism and Microbial Homeostasis

As previously mentioned, the differential perceptive capacity of taste receptors due to SNPs influences individual food preferences. Recent studies have confirmed that taste preferences for sweet, bitter, sour and salt are affected genetically in part and have an impact on food and beverage choices (Chamoun et al., 2018a; Eriksson et al., 2019; Chamoun et al., 2021). Ample research evidence suggests that diet is one of the most important factors influencing human health and that different dietary patterns greatly regulate host metabolism and microbial homeostasis. For example, a high-fat diet in healthy adults leads to altered gut microbiota, including higher levels of *Alistipes* and *Bacteroides* species and a decrease in *Faecalibacterium* species, as well as increased faecal metabolites p-resol and indole, which are implicated in a higher risk of cardiovascular and metabolic disturbances (Wan et al., 2019). Some researchers have also suggested that microbiota can in turn alter dietary patterns by manipulating host taste perception (Cattaneo et al., 2019b). Overall, taste perception could be involved in host-microbiota interaction by influencing dietary patterns.

Further, impairment or loss of taste function poses a systemic and multilayered risk to people, rather than solely oral diseases. As a consequence of altered taste perception, many foods may be averted owing to the difficulty in appreciating the diet, thus shifting people towards unhealthy eating habits and potentially leading to serious consequences (Chamoun et al., 2018b). For instance, an increase in salt taste recognition threshold may lead

people to consume more salt to improve food palatability, thereby elevating their risk of cardiovascular diseases (Pilic and Mavrommatis, 2018; Tapanee et al., 2021). Notably, a national health survey in the US reported that participants who met the recommendations of the Healthy Eating Index (HEI-2015) scores were at a lower risk of developing untreated coronal caries than those who did not conform to the recommendations (Kaye et al., 2020). In addition, shifted taste perception has also been proven to be correlated with depression and anxiety (Esposito et al., 2021).

In addition, taste receptors are associated with the regulation of body metabolism and internal environmental homeostasis. Several studies have revealed the secretory function of taste receptors in the gastrointestinal tract. For example, TAS2Rs regulate intestinal anion secretion to protect the host from ingesting dietary toxins (Glendinning, 1994). Smith et al. proved that intestinal sweet taste receptors modulate gut hormone responses and glucose absorption, as glucose-dependent stimulation of intestinal T1R2/T1R3 chemo-sensors on L-cells enhances glucose absorption through GLP-2-mediated activation of GLUT2 transporter in enterocytes (Smith et al., 2018). Serrano et al. subsequently found that T1R2 gene variant Ile191Val causes a partial loss of function and results in reduced glucose excursions during an OGTT, which is independent of the variations in beta-cell function or insulin sensitivity (Serrano et al., 2021). Additionally, bitter taste receptors have also been revealed of the function to evoke airway smooth muscle relaxation *via* localized calcium flux, predicting the potential role in counteracting asthmatic bronchoconstriction (Deshpande et al., 2010). Recent studies have also found that older carriers of variant rs236514 (A) of the *KCNJ2* gene, which is located in Type III sour-sensing taste cells and affects sour perception thresholds, have a higher preference for acid and lower energy intake, along with an increased risk of mild-to-severe cognitive impairment (Chamoun et al., 2018b; Ferraris et al., 2021a; Ferraris et al., 2021b).

## Microbiota Modulate the Perceptive Capacity of Taste Receptors

Significant relationships between oral microbiota composition and taste sensitivity were found recently. A study conducted by Solemdal et al. in acutely hospitalized elderly showed reduced taste ability in patients with poor oral hygiene such as caries activity, among whom patients with high *Lactobacillus* growth had the most significant impairment in sour taste (Solemdal et al., 2012). This result may be in relation to the adaptation of sour taste perception due to acid produced by bacteria and the increased sour taste threshold. Cattaneo et al. revealed a significant difference among subjects with varied responsiveness to PROP in terms of the relative abundance of some taxa (Cattaneo et al., 2019a). Subjects characterized by greater PROP responsiveness showed overrepresentation mainly in five bacterial genera, including *Actinomyces*, *Oribacterium*, *Solobacterium*, *Catonella* and *Campylobacter*. Their further study also found that specific bacterial taxa mainly composed of *Clostridiales* and *Bacteroidales* may influence host sensitivity to

salt and acid, as these taxa were negatively correlated with perceived taste thresholds for salt and acid (Cattaneo et al., 2019b). Similarly, Feng et al. reported that elevated proportions of *Actinomyces* and *Firmicutes* in the saliva were associated with reduced taste sensitivity, whereas increased taste sensitivity resulted from higher proportions of *Bacteroides* in the tongue film (Feng et al., 2018). Besides, a study by Besnard et al. demonstrated that the low-fat tasters showed greater oral bacterial diversity and a high *Bacteroides/Lactobacillus* ratio which significantly promotes host inflammation compared to the high-fatty tasters (Besnard et al., 2020). Impairment of oral fat perception may form a feedback loop with such a pro-inflammatory bacterial community composition, as obesity-induced inflammation has been shown to damage taste buds in mice and reduce fatty taste sensitivity in human (Jilani et al., 2017; Kaufman et al., 2018). Our latest study as well illustrated that bacterial lipopolysaccharide-induced alternative splicing of the mouse sweet taste receptor T1R2, thus contributing to a significant upregulation of its non-functional isoform expression and inhibition of sweet taste perception (Zhu et al., 2021). It can be hypothesized that these impaired or non-functional isoforms of taste receptors would similarly lack the ability to detect and mediate the elimination of pathogens.

There are several possible interpretations of the perceptive changes in taste receptors owing to the growth of specific oral bacteria. One possibility lies in the ability of oral bacteria to modulate the food preferences of the host. Microbes in the gastrointestinal tract have shown a potential role in manipulating host diet by regulating chemoreceptor expression (van de Wouw et al., 2017). This is in line with the recent study which indicated that higher relative abundance of oral *Clostridia* is associated with increased total energy, fat and protein intake as well as reduced fiber consumption, while *Proteobacteria phylum* and *Prevotella genus* exhibited the reverse correlation (Cattaneo et al., 2019b). Another plausible explanation rests on the fact that bacterial metabolites of the compounds can activate or modulate host taste perception. For instance, host sensitivity to sucrose is correlated with the sucrose catabolism of different oral bacteria *in vivo* (Gardner et al., 2020; Sedghi et al., 2021). Some specific intraoral bacteria like *Porphyromonas gingivalis* (*P. gingivalis*) are capable of utilizing salivary glutamates so as to modulate their concentration, ultimately affecting the taste perception (Takahashi, 2015). Consistent findings were observed in investigations that examined the impacts of different oral microbiota on the metabolism and aroma perception of cysteine conjugates as well as glycosides (Starkenmann et al., 2008; Parker et al., 2020). Furthermore, oral microbiota also modulates host chemosensation by altering taste receptor density, which is attributed to the ability of certain microorganisms to mediate the secretion of inflammatory factors by host cells and trigger inflammation. On the one hand, the immune response can diminish taste perception through damaging taste buds (Wang et al., 2009; Cohn et al., 2010). On the other hand, several studies have also demonstrated that taste receptors themselves have varying degrees of responsiveness to microorganisms and are directly engaged in

the host immune regulation (Gil et al., 2015; Zheng et al., 2019). We elaborate below on the latest progress in studying the participation of taste receptors in the host immune response.

## Taste Receptors Implicated in the Host Immune Response to Microorganisms

As previously stated, taste receptors act as chemoreceptors that not only sense chemicals known as tastants to initiate taste signals, but also recognize microorganisms such as bacteria and activate downstream signaling cascades, thereby contributing to innate host defense and the maintenance of microbial homeostasis (Lee et al., 2014; Gil et al., 2015; Jaggupilli et al., 2018). In the past, great progress has been made on the involvement of taste receptors in extraoral organs such as airways and gastrointestinal tract in host innate immunity and microbial regulation, while the role of taste receptors in the oral cavity in mediating microbiota-host interaction is minimally known. A number of recent studies have yielded new light on

oral taste receptors that detect bacterial signals and subsequently coordinate immune responses (**Figure 2**).

Taste receptors have been detected to be expressed on a variety of tissues and cells, and are known to be engaged in host immunity (Workman et al., 2015; Bloxham et al., 2020; Welcome, 2020). Expression of bitter receptors is observed in immune cells such as monocytes and neutrophils, which aids in the recognition of bacterial quorum sensing molecules (QSMs) and facilitates the innate immune response to disease (Maurer et al., 2015). T2Rs (mainly T2R38 and T2R14) in airway epithelial cells specifically bind to the *Pseudomonas aeruginosa* derived QSMs acyl homoserine lactones (AHLs) and initiates the host immune response, activating chemotaxis of immune cells and promoting the secretion of antimicrobial peptides (AMPs) as well as inflammatory factors (Hariri et al., 2017; Freund et al., 2018; Jaggupilli et al., 2018). In addition, the mechanism of T2R participation in the immune response has been further revealed by the work of Gopallawa et al. in macrophages (Gopallawa et al., 2021).

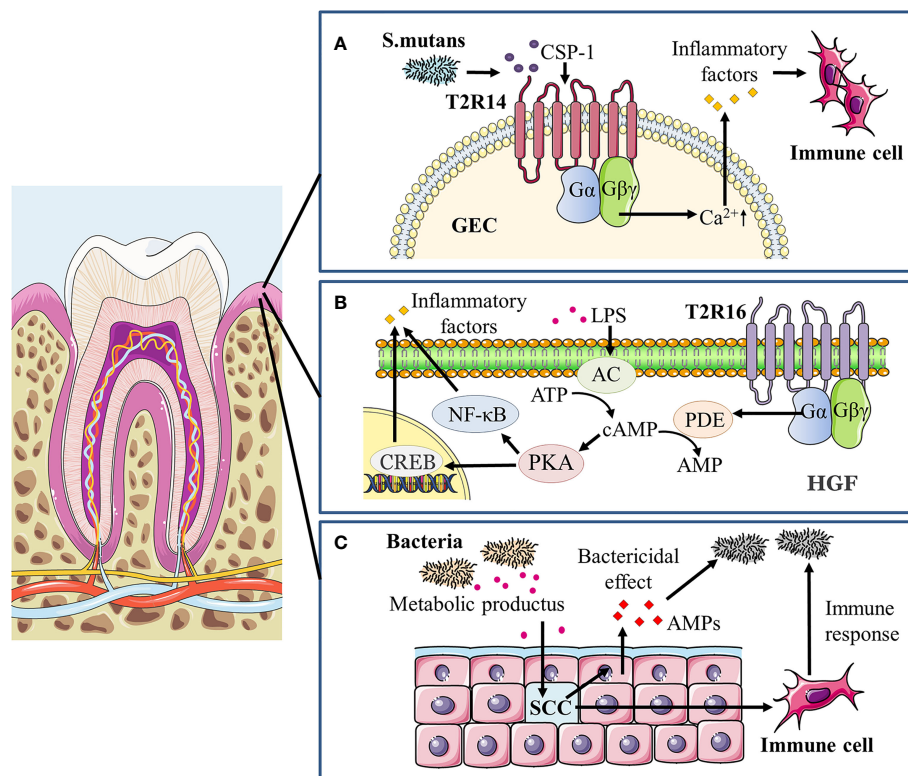


**FIGURE 2 |** Taste receptors modulate oral immune response to microorganisms. **(A)** In gingiva epithelial cells (GECs) treated with *S. mutans* competence stimulating peptide-1 (CSP-1), a vigorous increase in intracellular calcium mobilization and secretion of cytokines/chemokines including IL-6, IL-8 and TNF- $\alpha$  occurred primarily through the T2R14-G $\beta\gamma$ -PLC $\beta$  pathway, recruiting immune cells and mediating the immune response to pathogens. **(B)** LPS can induce a significant dose- and time-dependent increase in adenylate cyclase (AC) activity and thereafter elevates intracellular cAMP levels, positively affecting NF- $\kappa$ B activity through its major effector protein kinase A (PKA) and stimulating inflammatory responses. In addition, the cAMP/PKA/cAMP response element binding protein (CREB) signaling pathway may promote the LPS-induced release of pro-inflammatory cytokines, including IL-6, IL-33, and TNF- $\alpha$ . In human gingival fibroblasts (HGFs), agonist-stimulated T2R16 mobilizes downstream  $\alpha$ -gustducin to activate the phosphodiesterase (PDE) that hydrolyzes cAMP, thereby reducing intracellular cAMP levels and alleviating the LPS-induced inflammation as well as tissue injury. **(C)** Taste receptors of gingival solitary chemosensory cells (gSCCs) activated by bacterial metabolites would stimulate epithelial cells to release antimicrobial peptides (AMPs) as a direct bactericidal effect and also recruit immune cells to modulate the oral immune response.



Bitter taste metabolite from bacteria stimulates bitter taste receptors and activates calcium signaling, leading to activation of nitric oxide synthase (NOS) isoforms with nitric oxide (NO) production. NO may upregulate phagocytosis of macrophages via several mechanisms (Jun et al., 1996). Simultaneously, bacterial co-stimulation of macrophages and T2Rs also enhanced phagocytosis by reducing cAMP when cAMP levels were elevated from baseline. Interestingly, sweet taste may regulate innate immunity in reverse to bitter taste signals. Lee et al. demonstrated that T1R2/3 receptors activated by sugars or bacterial d-amino acids could inhibit T2R-dependent calcium signaling and downstream AMP secretion of adjoining epithelial cells, diminishing the immune response to microbial bitter products (Lee et al., 2014; Lee et al., 2017). Furthermore, T2Rs activation can also induce anti-inflammatory effects as antagonizing lipopolysaccharide (LPS)-provoked production of inflammatory mediators in human peripheral mononuclear blood cells and lung macrophages (Tran et al., 2018; Grassin-Delyle et al., 2019). The anti-inflammatory activity of T2Rs was likewise associated with SNPs, as the functional PAV haplotype T2R38 receptor exhibited significant inhibition of TNF- $\alpha$  release after agonist stimulation compared to the non-functional AVI/AVI diplotype (Tran et al., 2018).

Studies in the oral cavity have expanded the role of taste receptors, especially bitter taste receptors, in the recognition of oral pathogenic microorganisms and modulation of oral microbial homeostasis. Gil et al. showed that the T2R38 gene polymorphism in the oral cavity determined the degree of innate immune response induced by oral bacteria (Gil et al., 2015). T2R38 mRNA expression in GECs carrying PAV/PAV genotype increased significantly when stimulated with *S. mutans*, while AVI/AVI genotype showed little change. Human  $\beta$ -defensin-2 (hBD-2) and IL-1 $\alpha$  secretion after the stimulation of *S. mutans* was decreased in PAV/PAV cell line after the T2R38 knockdown. The result agrees with Wendell et al. who reported that the PAV haplotype of T2R38 exhibited a protective effect against caries in primary dentition, whereas the AVI haplotype posed a higher risk of suffering from caries (Wendell et al., 2010). In the same study by Gil et al., an opposite result was found for stimulation from *P. gingivalis* or *Fusobacterium nucleatum*, as the expression of T2R38 was significantly upregulated in the GECs of AVI/AVI genotype, while no significant changes were observed in PAV/PAV or PAV/AVI genotype (Gil et al., 2015). This suggests that different pathogenic bacteria may act through different signaling pathways to stimulate taste receptors and elicit subsequent immune responses in the organism. The study by Medapati and his colleagues then uncovered an emerging role of T2R14 in recognizing oral *S. mutans* with activation of innate immune response in GECs (Medapati et al., 2021b). T2R14 in GECs mediates calcium signaling and secretion of pro-inflammatory cytokines upon recognition of competence stimulating peptide-1 (CSP-1) secreted by *S. mutans*, as well as attracting differentiated HL-60 immune cells (dHL-60). A subsequent study by Medapati et al. further pointed out that T2R14 may mediate the internalization of *Staphylococcus aureus* (*S. aureus*) in GECs through activating p21-activated kinase 1 associated actin and F-actin, and enhanced hBD-2 secretion that

inhibits *S. aureus* (Medapati et al., 2021a). However, the knockdown of T2R14 alone does not affect the level of the internalization of *S. mutans* and the secretion of hBD-2 in GECs. It is interesting to observe that T2R14-dependent inhibition of *S. aureus* occurred when GECs were treated with CSP-1 from *S. mutans*. This hints that bitter receptor-mediated bactericidal effects may be one of the important mechanisms by which *S. mutans* overcome competition with commensal bacteria in the oral cavity. Of note, study evidence also suggests that bitter taste receptors may similarly assume a repressive role against inflammation development in the oral cavity. Our recent work unveiled that the bitter agonist salicin decreased LPS-induced cAMP accumulation in human gingival fibroblasts in a T2R16-dependent manner, and subsequently suppressed the expression of inflammatory cytokines along with NF- $\kappa$ B activation (Zhou et al., 2021). The simultaneous function of T2Rs in mediating the secretion of antimicrobial substances and preventing excessive inflammatory responses prompted its potential use as a target for the treatment of periodontitis.

Impairment of taste receptors, which are crucial for the host to detect bacteria and mediate regulation oral homeostasis, can lead to overgrowth of pathogenic microorganisms and disease progression. Our study on gingival solitary chemosensory cells (gSCCs) showed that knockout of taste signaling molecules increases bacterial load as well as pathogenicity, ultimately exacerbating periodontitis (Zheng et al., 2019). GSCCs are found in the mouse gingival junctional epithelium, utilizing bitter taste receptors and coupled taste transduction elements to detect bacterial components and modulate immune responses.  $\alpha$ -gustducin-null (*Gnat3*<sup>-/-</sup>) mice which knocked out one of the taste signaling receptors altered the oral microbiome, resulting in greater alveolar bone loss. Meanwhile, topical treatment of bitter denatonium benzoate in wildtype mice could alleviate periodontitis by upregulating the expression of antimicrobial peptides, which was abolished in *Gnat3*<sup>-/-</sup> mice. This is coherent with past studies in nasal SCCs (Tizzano et al., 2010; Lee et al., 2014). One plausible hypothesis is that the lack of taste signaling in gSCCs causes insufficient antimicrobial peptides secretion and dysbiosis of microbiota, increasing the risk of periodontitis. These outcomes suggest that taste signaling plays a key role in host oral immune modulation.

## CONCLUSION

There is now substantial evidence to support that multiple taste receptors are expressed on different cells in the oral cavity to detect bacterial metabolites and distinguish pathogenic from commensal bacteria, playing a critical role in host regulation of oral microbial homeostasis as well as oral health (Zheng et al., 2019). For instance, recent studies in GECs have shown that the expressed bitter taste receptors T2R14 and T2R38 detect various bacterial QSMs or metabolites through different pathways, with the secretion of AMPs to remove pathogenic bacteria (Gil et al., 2015; Medapati et al., 2021b). Functional alterations in taste receptors can also occur as a result of oral microbiota and disease (Zhu et al., 2021). Targeting taste receptors may be a promising



alternative therapy to treat oral diseases caused by specific pathogens without antibiotics.

In parallel, numerous studies have described the influence of host genetic polymorphisms on susceptibility to oral diseases (Piekoszewska-Ziętek et al., 2017; Kozak et al., 2020). Similarly, taste receptor SNPs not only determine the distinct taste perception capacities and thus affect food preferences, but also shape the recognition of microbial metabolites, leading to different levels of immune defense in response to specific oral microbes (Chisini et al., 2021). Taste receptor genotypic and phenotypic variations may have potential implications in predicting susceptibility to oral disease and the efficacy of therapy, thereby facilitating the development of personalized treatment based on individual receptor genotypes.

However, current research on the non-gustatory perceptive functions of taste receptors in the oral cavity is still limited, with many crucial questions awaiting further explanations. To name a few, are sour or salt taste receptors in oral likewise engaged in the detection and response to bacterial metabolites? Are there any differences in the transduction pathways between gustatory perception and non-gustatory perception functions? Furthermore, the present understanding of the links and mechanisms between the taste receptor SNPs and oral microbiota as well as diseases is still far from enough. We look forward to further studies on taste receptors to reveal their key role as chemoreceptors in host-pathogen interactions both in oral and systemic settings.

## REFERENCES

- Ahmad, R., and Dalziel, J. E. (2020). G Protein-Coupled Receptors in Taste Physiology and Pharmacology. *Front. Pharmacol.* 11. doi: 10.3389/fphar.2020.587664
- Bartoshuk, L. M., Duffy, V. B., and Miller, I. J. (1994). PTC/PROP Tasting: Anatomy, Psychophysics, and Sex Effects. *Physiol. Behav.* 56 (6), 1165–1171. doi: 10.1016/0031-9384(94)90361-1
- Basson, M. D., Bartoshuk, L. M., Dichello, S. Z., Panzini, L., Weiffenbach, J. M., and Duffy, V. B. (2005). Association Between 6-N-Propylthiouracil (PROP) Bitterness and Colonic Neoplasms. *Digestive Dis. Sci.* 50 (3), 483–489. doi: 10.1007/s10620-005-2462-7
- Besnard, P., Christensen, J. E., Bernard, A., Simoneau-Robin, I., Collet, X., Verges, B., et al. (2020). Identification of an Oral Microbiota Signature Associated With an Impaired Orosensory Perception of Lipids in Insulin-Resistant Patients. *Acta Diabetol.* 57 (12), 1445–1451. doi: 10.1007/s00592-020-01567-9
- Bloxham, C. J., Foster, S. R., and Thomas, W. G. (2020). A Bitter Taste in Your Heart. *Front. Physiol.* 11. doi: 10.3389/fphys.2020.00431
- Bradshaw, D. J., and Lynch, R. J. M. (2013). Diet and the Microbial Aetiology of Dental Caries: New Paradigms. *Int. Dental J.* 63 Suppl 2, 64–72. doi: 10.1111/idj.12082
- Bufe, B., Breslin, P. A. S., Kuhn, C., Reed, D. R., Tharp, C. D., Slack, J. P., et al. (2005). The Molecular Basis of Individual Differences in Phenylthiocarbamide and Propylthiouracil Bitterness Perception. *Curr. Biol.: CB* 15 (4), 322–327. doi: 10.1016/j.cub.2005.01.047
- Canessa, C. M., Schild, L., Buell, G., Thorens, B., Gautschi, I., Horisberger, J. D., et al. (1994). Amiloride-Sensitive Epithelial Na<sup>+</sup> Channel is Made of Three Homologous Subunits. *Nature* 367 (6462), 463–467. doi: 10.1038/367463a0
- Carey, R. M., and Lee, R. J. (2019). Taste Receptors in Upper Airway Innate Immunity. *Nutrients* 11 (9), 2017. doi: 10.3390/nu11092017
- Cattaneo, C., Gargari, G., Koirala, R., Laureati, M., Riso, P., Guglielmetti, S., et al. (2019a). New Insights Into the Relationship Between Taste Perception and Oral Microbiota Composition. *Sci. Rep.* 9 (1), 3549. doi: 10.1038/s41598-019-40374-3

## AUTHOR CONTRIBUTIONS

Conceptualization: XX, XZ, and MT. Writing original draft: HD, JL, JZ, ZZ. Writing, review, and editing: XP, XDZ, XZ, XX, and MT. funding acquisition: XX and XZ. All authors contributed to the article and approved the submitted version.

## FUNDING

This work was supported by the National Natural Science Foundation of China (81900995 to XZ, 81771099 to XX), the China Postdoctoral Science Foundation (2020M673266 to XZ), and the Research funding for talents developing, West China Hospital of Stomatology Sichuan University (RCDWJS2020-11 to XZ); the National Institute of Dental and Craniofacial Research (NIDCR) (R01DC028979 to MT), and National Institute on Deafness and Other Communication Disorders (NIDCD) (R01DC016598 to MT).

## ACKNOWLEDGMENTS

Figures were produced with the assistance of Servier Medical Art (<https://smart.servier.com/>).

- Cattaneo, C., Riso, P., Laureati, M., Gargari, G., and Pagliarini, E. (2019b). Exploring Associations Between Interindividual Differences in Taste Perception, Oral Microbiota Composition, and Reported Food Intake. *Nutrients* 11 (5), 1167. doi: 10.3390/nu11051167
- Chamoun, E., Carroll, N. A., Duizer, L. M., Qi, W., Feng, Z., Darlington, G., et al. (2018a). The Relationship Between Single Nucleotide Polymorphisms in Taste Receptor Genes, Taste Function and Dietary Intake in Preschool-Aged Children and Adults in the Guelph Family Health Study. *Nutrients* 10 (8), 990. doi: 10.3390/nu10080990
- Chamoun, E., Liu, A. S., Duizer, L. M., Feng, Z., Darlington, G., Duncan, A. M., et al. (2021). Single Nucleotide Polymorphisms in Sweet, Fat, Umami, Salt, Bitter and Sour Taste Receptor Genes are Associated With Gustatory Function and Taste Preferences in Young Adults. *Nutr. Res. (New York N.Y.)* 85, 40–46. doi: 10.1016/j.nutres.2020.12.007
- Chamoun, E., Mutch, D. M., Allen-Vercos, E., Buchholz, A. C., Duncan, A. M., Spriet, L. L., et al. (2018b). A Review of the Associations Between Single Nucleotide Polymorphisms in Taste Receptors, Eating Behaviors, and Health. *Crit. Rev. Food Sci. Nutr.* 58 (2), 194–207. doi: 10.1080/10408398.2016.1152229
- Chandrashekar, J., Hoon, M. A., Ryba, N. J. P., and Zuker, C. S. (2006). The Receptors and Cells for Mammalian Taste. *Nature* 444 (7117), 288–294. doi: 10.1038/nature05401
- Chandrashekar, J., Mueller, K. L., Hoon, M. A., Adler, E., Feng, L., Guo, W., et al. (2000). T2Rs Function as Bitter Taste Receptors. *Cell* 100 (6), 703–711. doi: 10.1016/S0092-8674(00)80706-0
- Chisini, L. A., Cademartori, M. G., Conde, M. C. M., Costa, F. D. S., Salvi, L. C., Tovo-Rodrigues, L., et al. (2021). Single Nucleotide Polymorphisms of Taste Genes and Caries: A Systematic Review and Meta-Analysis. *Acta Odontol. Scand.* 79 (2), 147–155. doi: 10.1080/00016357.2020.1832253
- Clapp, T. R., Trubey, K. R., Vandenbeuch, A., Stone, L. M., Margolskee, R. F., Chaudhari, N., et al. (2008). Tonic Activity of Galpha-Gustducin Regulates Taste Cell Responsivity. *FEBS Lett.* 582 (27), 3783–3787. doi: 10.1016/j.febslet.2008.10.007
- Cohn, Z. J., Kim, A., Huang, L., Brand, J., and Wang, H. (2010). Lipopolysaccharide-Induced Inflammation Attenuates Taste Progenitor Cell

- Proliferation and Shortens the Life Span of Taste Bud Cells. *BMC Neurosci.* 11, 72. doi: 10.1186/1471-2202-11-72
- Deckmann, K., and Kummer, W. (2016). Chemosensory Epithelial Cells in the Urethra: Sentinels of the Urinary Tract. *Histochem. Cell Biol.* 146 (6), 673–683. doi: 10.1007/s00418-016-1504-x
- Deshpande, D. A., Wang, W. C. H., McIlmoyle, E. L., Robinett, K. S., Schillinger, R. M., An, S. S., et al. (2010). Bitter Taste Receptors on Airway Smooth Muscle Bronchodilate by Localized Calcium Signaling and Reverse Obstruction. *Nat. Med.* 16 (11), 1299–1304. doi: 10.1038/nm.2237
- Dias, A. G., Rousseau, D., Duizer, L., Cockburn, M., Chiu, W., Nielsen, D., et al. (2012). Genetic Variation in Putative Salt Taste Receptors and Salt Taste Perception in Humans. *Chem. Senses* 38 (2), 137–145. doi: 10.1093/chemse/bjs090
- Dong, D., Jones, G., and Zhang, S. (2009). Dynamic Evolution of Bitter Taste Receptor Genes in Vertebrates. *BMC Evol. Biol.* 9, 12. doi: 10.1186/1471-2148-9-12
- Eny, K. M., Wolever, T. M., Corey, P. N., and El-Sohemy, A. (2010). Genetic Variation in TAS1R2 (Ile191Val) is Associated With Consumption of Sugars in Overweight and Obese Individuals in 2 Distinct Populations. *Am. J. Clin. Nutr.* 92 (6), 1501–1510. doi: 10.3945/ajcn.2010.29836
- Eriksson, L., Esberg, A., Haworth, S., Holgerson, P. L., and Johansson, I. (2019). Allelic Variation in Taste Genes Is Associated With Taste and Diet Preferences and Dental Caries. *Nutrients* 11 (7), 1491. doi: 10.3390/nu11071491
- Esberg, A., Haworth, S., Brunius, C., Lif Holgerson, P., and Johansson, I. (2019). Carbonic Anhydrase 6 Gene Variation Influences Oral Microbiota Composition and Caries Risk in Swedish Adolescents. *Sci. Rep.* 9 (1), 452–452. doi: 10.1038/s41598-018-36832-z
- Espósito, C. M., Ceresa, A., and Buoli, M. (2021). The Association Between Personality Traits and Dietary Choices: A Systematic Review. *Adv. Nutr. (Bethesda Md.)* 12 (4), 1149–1159. doi: 10.1093/advances/nmaa166
- Feng, Y., Licandro, H., Martin, C., Septier, C., Zhao, M., Neyraud, E., et al. (2018). The Associations Between Biochemical and Microbiological Variables and Taste Differ in Whole Saliva and in the Film Lining the Tongue. *BioMed. Res. Int.* 2018, 2838052. doi: 10.1155/2018/2838052
- Ferraris, C., Turner, A., Scarlett, C., Veysey, M., Lucock, M., Bucher, T., et al. (2021a). Association Between Sour Taste SNP -Rs236514, Diet Quality and Mild Cognitive Impairment in an Elderly Cohort. *Nutrients* 13 (3), 719. doi: 10.3390/nu13030719
- Ferraris, C., Turner, A., Scarlett, C. J., Veysey, M., Lucock, M., Bucher, T., et al. (2021b). Sour Taste SNP -Rs236514 and Differences in Nutrient Intakes and Metabolic Health Markers in the Elderly. *Front. Nutr.* 8. doi: 10.3389/fnut.2021.701588
- Freund, J. R., Mansfield, C. J., Doghramji, L. J., Adappa, N. D., Palmer, J. N., Kennedy, D. W., et al. (2018). Activation of Airway Epithelial Bitter Taste Receptors by Quinolones Modulates Calcium, Cyclic-AMP, and Nitric Oxide Signaling. *J. Biol. Chem.* 293 (25), 9824–9840. doi: 10.1074/jbc.RA117.001005
- Fushan, A. A., Simons, C. T., Slack, J. P., Manichaikul, A., and Drayna, D. (2009). Allelic Polymorphism Within the TAS1R3 Promoter is Associated With Human Taste Sensitivity to Sucrose. *Curr. Biol.: CB* 19 (15), 1288–1293. doi: 10.1016/j.cub.2009.06.015
- Garcia-Bailo, B., Toguri, C., Eny, K. M., and El-Sohemy, A. (2009). Genetic Variation in Taste and its Influence on Food Selection. *Omic: J. Integr. Biol.* 13 (1), 69–80. doi: 10.1089/omi.2008.0031
- Gardner, A., So, P. W., and Carpenter, G. H. (2020). Intraoral Microbial Metabolism and Association With Host Taste Perception. *J. Dental Res.* 99 (6), 739–745. doi: 10.1177/0022034520917142
- Gil, S., Coldwell, S., Drury, J. L., Arroyo, F., Phi, T., Saadat, S., et al. (2015). Genotype-Specific Regulation of Oral Innate Immunity by T2R38 Taste Receptor. *Mol. Immunol.* 68 (2 Pt C), 663–670. doi: 10.1016/j.molimm.2015.10.012
- Glendinning, J. I. (1994). Is the Bitter Rejection Response Always Adaptive? *Physiol. Behav.* 56 (6), 1217–1227. doi: 10.1016/0031-9384(94)90369-7
- Gopallawa, I., Freund, J. R., and Lee, R. J. (2021). Bitter Taste Receptors Stimulate Phagocytosis in Human Macrophages Through Calcium, Nitric Oxide, and Cyclic-GMP Signaling. *Cell. Mol. Life Sci.: CMLS* 78 (1), 271–286. doi: 10.1007/s00018-020-03494-y
- Grassin-Delyle, S., Salvator, H., Mantov, N., Abrial, C., Brollo, M., Faisy, C., et al. (2019). Bitter Taste Receptors (TAS2Rs) in Human Lung Macrophages: Receptor Expression and Inhibitory Effects of TAS2R Agonists. *Front. Physiol.* 10. doi: 10.3389/fphys.2019.01267
- Hariri, B. M., McMahon, D. B., Chen, B., Freund, J. R., Mansfield, C. J., Doghramji, L. J., et al. (2017). Flavones Modulate Respiratory Epithelial Innate Immunity: Anti-Inflammatory Effects and Activation of the T2R14 Receptor. *J. Biol. Chem.* 292 (20), 8484–8497. doi: 10.1074/jbc.M116.771949
- Haznedaroglu, E., Koldemir-Gündüz, M., Bakır-Coşkun, N., Bozkuş, H. M., Çağatay, P., Süsleyici-Duman, B., et al. (2015). Association of Sweet Taste Receptor Gene Polymorphisms With Dental Caries Experience in School Children. *Caries Res.* 49 (3), 275–281. doi: 10.1159/000381426
- Heck, G. L., Mierison, S., and DeSimone, J. A. (1984). Salt Taste Transduction Occurs Through an Amiloride-Sensitive Sodium Transport Pathway. *Science (New York N.Y.)* 223 (4634), 403–405. doi: 10.1126/science.6691151
- Hichami, A., Khan, A. S., and Khan, N. A. (2021). Cellular and Molecular Mechanisms of Fat Taste Perception. *Handb. Exp. Pharmacol.* 6, 1–24. doi: 10.1007/164\_2021\_437
- Huang, Y. A., Maruyama, Y., Stimac, R., and Roper, S. D. (2008). Presynaptic (Type III) Cells in Mouse Taste Bud Sense Sour (Acid) Taste. *J. Physiol.* 586 (12), 2903–2912. doi: 10.1113/jphysiol.2008.151233
- Huang, L., Shanker, Y. G., Dubauskaite, J., Zheng, J. Z., Yan, W., Rosenzweig, S., et al. (1999). Ggamma13 Colocalizes With Gustducin in Taste Receptor Cells and Mediates IP3 Responses to Bitter Denatonium. *Nat. Neurosci.* 2 (12), 1055–1062. doi: 10.1038/15981
- Ikedo, K. (2002). New Seasonings. *Chem. Senses* 27 (9), 847–849. doi: 10.1093/chemse/27.9.847
- Iwata, S., Yoshida, R., and Ninomiya, Y. (2014). Taste Transductions in Taste Receptor Cells: Basic Tastes and Moreover. *Curr. Pharm. Design* 20 (16), 2684–2692. doi: 10.2174/13816128113199990575
- Izakovicova Holla, L., Borilova Linhartova, P., Lucanova, S., Kastovsky, J., Musilova, K., Bartosova, M., et al. (2015). GLUT2 and TAS1R2 Polymorphisms and Susceptibility to Dental Caries. *Caries Res.* 49 (4), 417–424. doi: 10.1159/000430958
- Jaggupilli, A., Singh, N., Jesus, V. C. D., Duan, K., and Chelikani, P. (2018). Characterization of the Binding Sites for Bacterial Acyl Homoserine Lactones (AHLs) on Human Bitter Taste Receptors (T2Rs). *ACS Infect. Dis.* 4 (7), 1146–1156. doi: 10.1021/acsinfecdis.8b00094
- Jayasinghe, S. N., Kruger, R., Walsh, D. C. I., Cao, G., Rivers, S., Richter, M., et al. (2017). Is Sweet Taste Perception Associated With Sweet Food Liking and Intake? *Nutrients* 9 (7), 750. doi: 10.3390/nu9070750
- Jilani, H., Ahrens, W., Buchecker, K., Russo, P., and Hebestreit, A. (2017). Association Between the Number of Fungiform Papillae on the Tip of the Tongue and Sensory Taste Perception in Children. *Food Nutr. Res.* 61 (1), 1348865. doi: 10.1080/16546628.2017.1348865
- Jun, C. D., Han, M. K., Kim, U. H., and Chung, H. T. (1996). Nitric Oxide Induces ADP-Ribosylation of Actin in Murine Macrophages: Association With the Inhibition of Pseudopodia Formation, Phagocytic Activity, and Adherence on a Laminin Substratum. *Cell. Immunol.* 174 (1), 25–34. doi: 10.1006/cimm.1996.0290
- Jurczak, A., Jamka-Kasprzyk, M., Bębenek, Z., Staszczek, M., Jagielski, P., Kościelniak, D., et al. (2020). Differences in Sweet Taste Perception and Its Association With the Cariogenic Profile in Preschool Children With Caries. *Nutrients* 12 (9), 2592. doi: 10.3390/nu12092592
- Kaufman, A., Choo, E., Koh, A., and Dando, R. (2018). Inflammation Arising From Obesity Reduces Taste Bud Abundance and Inhibits Renewal. *PLoS Biol.* 16 (3), e2001959. doi: 10.1371/journal.pbio.2001959
- Kaye, E. A., Sohn, W., and Garcia, R. I. (2020). The Healthy Eating Index and Coronal Dental Caries in US Adults: National Health and Nutrition Examination Survey 2011–2014. *J. Am. Dental Assoc. (1939)* 151 (2), 78–86. doi: 10.1016/j.adaj.2019.09.009
- Khan, A. S., Murtaza, B., Hichami, A., and Khan, N. A. (2019). A Cross-Talk Between Fat and Bitter Taste Modalities. *Biochimie* 159, 3–8. doi: 10.1016/j.biochi.2018.06.013
- Kim, U.-K., Jorgenson, E., Coon, H., Leppert, M., Risch, N., and Drayna, D. (2003). Positional Cloning of the Human Quantitative Trait Locus Underlying Taste Sensitivity to Phenylthiocarbamide. *Science (New York N.Y.)* 299 (5610), 1221–1225. doi: 10.1126/science.1080190
- Kojima, I., and Nakagawa, Y. (2011). The Role of the Sweet Taste Receptor in Enterendocrine Cells and Pancreatic  $\beta$ -Cells. *Diabetes Metab. J.* 35 (5), 451–457. doi: 10.4093/dmj.2011.35.5.451

- Kozak, M., Dabrowska-Zamojcin, E., Mazurek-Mochol, M., and Pawlik, A. (2020). Cytokines and Their Genetic Polymorphisms Related to Periodontal Disease. *J. Clin. Med.* 9 (12), 4045. doi: 10.3390/jcm9124045
- Kretz, O., Barbry, P., Bock, R., and Lindemann, B. (1999). Differential Expression of RNA and Protein of the Three Pore-Forming Subunits of the Amiloride-Sensitive Epithelial Sodium Channel in Taste Buds of the Rat. *J. Histochem. Cytochem.* 47 (1), 51–64. doi: 10.1177/002215549904700106
- Kulkarni, G. V., Chng, T., Eny, K. M., Nielsen, D., Wessman, C., and El-Sohemy, A. (2013). Association of GLUT2 and TAS1R2 Genotypes With Risk for Dental Caries. *Caries Res.* 47 (3), 219–225. doi: 10.1159/000345652
- Kyriazis, G. A., Soundarapandian, M. M., and Tyrberg, B. (2012). Sweet Taste Receptor Signaling in Beta Cells Mediates Fructose-Induced Potentiation of Glucose-Stimulated Insulin Secretion. *Proc. Natl. Acad. Sci. U. S. A.* 109 (8), E524–E532. doi: 10.1073/pnas.1115183109
- Laffitte, A., Neiers, F., and Briand, L. (2014). Functional Roles of the Sweet Taste Receptor in Oral and Extraoral Tissues. *Curr. Opin. Clin. Nutr. Metab. Care* 17 (4), 379–385. doi: 10.1097/MCO.0000000000000058
- Lee, R. J., Hariri, B. M., McMahon, D. B., Chen, B., Doghramji, L., Adappa, N. D., et al. (2017). Bacterial D-Amino Acids Suppress Sinusoidal Innate Immunity Through Sweet Taste Receptors in Solitary Chemosensory Cells. *Sci. Signaling* 10 (495), eaam7703. doi: 10.1126/scisignal.aam7703
- Lee, R. J., Kofonow, J. M., Rosen, P. L., Siebert, A. P., Chen, B., Doghramji, L., et al. (2014). Bitter and Sweet Taste Receptors Regulate Human Upper Respiratory Innate Immunity. *J. Clin. Invest.* 124 (3), 1393–1405. doi: 10.1172/JCI72094
- Lewandowski, B. C., Sukumaran, S. K., Margolskee, R. F., and Bachmanov, A. A. (2016). Amiloride-Insensitive Salt Taste Is Mediated by Two Populations of Type III Taste Cells With Distinct Transduction Mechanisms. *J. Neurosci.* 36 (6), 1942–1953. doi: 10.1523/JNEUROSCI.2947-15.2016
- Lindemann, B. (2001). Receptors and Transduction in Taste. *Nature* 413 (6852), 219–225. doi: 10.1038/35093032
- Li, X., Staszewski, L., Xu, H., Durick, K., Zoller, M., and Adler, E. (2002). Human Receptors for Sweet and Umami Taste. *Proc. Natl. Acad. Sci. U. S. A.* 99 (7), 4692–4696. doi: 10.1073/pnas.072090199
- Margolskee, R. F. (1993). The Molecular Biology of Taste Transduction. *BioEssays: News Rev. Mol. Cell. Dev. Biol.* 15 (10), 645–650. doi: 10.1002/bies.950151003
- Maurer, S., Wabnitz, G. H., Kahle, N. A., Stegmaier, S., Prior, B., Giese, T., et al. (2015). Tasting *Pseudomonas Aeruginosa* Biofilms: Human Neutrophils Express the Bitter Receptor T2R38 as Sensor for the Quorum Sensing Molecule N-(3-Oxododecanoyl)-L-Homoserine Lactone. *Front. Immunol.* 6. doi: 10.3389/fimmu.2015.00369
- McLaughlin, S. K., McKinnon, P. J., and Margolskee, R. F. (1992). Gustducin is a Taste-Cell-Specific G Protein Closely Related to the Transducins. *Nature* 357 (6379), 563–569. doi: 10.1038/357563a0
- Medapati, M. R., Bhagirath, A. Y., Singh, N., Schroth, R. J., Bhullar, R. P., Duan, K., et al. (2021a). Bitter Taste Receptor T2R14 Modulates Gram-Positive Bacterial Internalization and Survival in Gingival Epithelial Cells. *Int. J. Mol. Sci.* 22 (18), 9920. doi: 10.3390/ijms22189920
- Medapati, M. R., Singh, N., Bhagirath, A. Y., Duan, K., Triggs-Raine, B., Batista, E. L., et al. (2021b). Bitter Taste Receptor T2R14 Detects Quorum Sensing Molecules From Cariogenic *Streptococcus Mutans* and Mediates Innate Immune Responses in Gingival Epithelial Cells. *FASEB J.* 35 (3), e21375. doi: 10.1096/fj.202000208R
- Murovets, V. O., Bachmanov, A. A., and Zolotarev, V. A. (2015). Impaired Glucose Metabolism in Mice Lacking the Tas1r3 Taste Receptor Gene. *PLoS One* 10 (6), e0130997. doi: 10.1371/journal.pone.0130997
- Murovets, V. O., Lukina, E. A., Sozontov, E. A., Andreeva, J. V., Khropycheva, R. P., and Zolotarev, V. A. (2020). Allelic Variation of the Tas1r3 Taste Receptor Gene Affects Sweet Taste Responsiveness and Metabolism of Glucose in F1 Mouse Hybrids. *PLoS One* 15 (7), e0235913. doi: 10.1371/journal.pone.0235913
- Nomura, K., Nakanishi, M., Ishidate, F., Iwata, K., and Taruno, A. (2020). All-Electrical Ca-Independent Signal Transduction Mediates Attractive Sodium Taste in Taste Buds. *Neuron* 106 (5), 816–829.e6. doi: 10.1016/j.neuron.2020.03.006
- Nuemket, N., Yasui, N., Kusakabe, Y., Nomura, Y., Atsumi, N., Akiyama, S., et al. (2017). Structural Basis for Perception of Diverse Chemical Substances by T1r Taste Receptors. *Nat. Commun.* 8, 15530. doi: 10.1038/ncomms15530
- Oka, Y., Butnaru, M., von Buchholtz, L., Ryba, N. J. P., and Zuker, C. S. (2013). High Salt Recruits Aversive Taste Pathways. *Nature* 494 (7438), 472–475. doi: 10.1038/nature11905
- Öter, B., Ulukapı, I., Ulukapı, H., Topçuoğlu, N., and Cildir, S. (2011). The Relation Between 6-N-Propylthiouracil Sensitivity and Caries Activity in Schoolchildren. *Caries Res.* 45 (6), 556–560. doi: 10.1159/000332432
- Parker, M., Onetto, C., Hixson, J., Bilogrevic, E., Schueth, L., Pisaniello, L., et al. (2020). Factors Contributing to Interindividual Variation in Retronasal Odor Perception From Aroma Glycosides: The Role of Odorant Sensory Detection Threshold, Oral Microbiota, and Hydrolysis in Saliva. *J. Agric. Food Chem.* 68 (38), 10299–10309. doi: 10.1021/acs.jafc.9b05450
- Piekoszewska-Ziętek, P., Turska-Szybka, A., and Olczak-Kowalczyk, D. (2017). Single Nucleotide Polymorphism in the Aetiology of Caries: Systematic Literature Review. *Caries Res.* 51 (4), 425–435. doi: 10.1159/000476075
- Pilic, L., and Mavrommatis, Y. (2018). Genetic Predisposition to Salt-Sensitive Normotension and its Effects on Salt Taste Perception and Intake. *Br. J. Nutr.* 120 (7), 721–731. doi: 10.1017/S0007114518002027
- Raliou, M., Wiencis, A., Pillias, A. M., Planchais, A., Eloit, C., Boucher, Y., et al. (2009). Nonsynonymous Single Nucleotide Polymorphisms in Human Tas1r1, Tas1r3, and Mglur1 and Individual Taste Sensitivity to Glutamate. *Am. J. Clin. Nutr.* 90 (3), 789S–799S. doi: 10.3945/ajcn.2009.27462P
- Ramos-Lopez, O., Panduro, A., Martinez-Lopez, E., and Roman, S. (2016). Sweet Taste Receptor TAS1R2 Polymorphism (Val191Val) Is Associated With a Higher Carbohydrate Intake and Hypertriglyceridemia Among the Population of West Mexico. *Nutrients* 8 (2), 101. doi: 10.3390/nu8020101
- Rawal, S., Hayes, J. E., Wallace, M. R., Bartoshuk, L. M., and Duffy, V. B. (2013). Do Polymorphisms in the TAS1R1 Gene Contribute to Broader Differences in Human Taste Intensity? *Chem. Senses* 38 (8), 719–728. doi: 10.1093/chemse/bjt040
- Rhyu, M.-R., Song, A.-Y., Kim, E.-Y., Son, H.-J., Kim, Y., Mummalaneni, S., et al. (2020). Kokumi Taste Active Peptides Modulate Salt and Umami Taste. *Nutrients* 12 (4), 1198. doi: 10.3390/nu12041198
- Roper, S. D. (2013). Taste Buds as Peripheral Chemosensory Processors. *Semin. Cell Dev. Biol.* 24 (1), 71–79. doi: 10.1016/j.semcdb.2012.12.002
- Roura, E., Foster, S., Winklebach, A., Navarro, M., Thomas, W., Campbell, K., et al. (2016). Taste and Hypertension in Humans: Targeting Cardiovascular Disease. *Curr. Pharm. Design* 22 (15), 2290–2305. doi: 10.2174/1381612822666160216151545
- Sbarbati, A., Bramanti, P., Benati, D., and Merigo, F. (2010). The Diffuse Chemosensory System: Exploring the Iceberg Toward the Definition of Functional Roles. *Prog. Neurobiol.* 91 (1), 77–89. doi: 10.1016/j.pneurobio.2010.01.010
- Schneider, C., O'Leary, C. E., and Locksley, R. M. (2019). Regulation of Immune Responses by Tuft Cells. *Nat. Rev. Immunol.* 19 (9), 584–593. doi: 10.1038/s41577-019-0176-x
- Sedghi, L., DiMassa, V., Harrington, A., Lynch, S. V., and Kapila, Y. L. (2021). The Oral Microbiome: Role of Key Organisms and Complex Networks in Oral Health and Disease. *Periodontol.* 2000 87 (1), 107–131. doi: 10.1111/prd.12393
- Serrano, J., Seflova, J., Park, J., Pribadi, M., Sanematsu, K., Shigemura, N., et al. (2021). The Ile191Val is a Partial Loss-of-Function Variant of the TAS1R2 Sweet-Taste Receptor and is Associated With Reduced Glucose Excursions in Humans. *Mol. Metab.* 54, 101339. doi: 10.1016/j.molmet.2021.101339
- Small, D. M. (2012). Flavor is in the Brain. *Physiol. Behav.* 107 (4), 540–552. doi: 10.1016/j.physbeh.2012.04.011
- Smith, K. R., Hussain, T., Karimian Azari, E., Steiner, J. L., Ayala, J. E., Pratley, R. E., et al. (2016). Disruption of the Sugar-Sensing Receptor T1R2 Attenuates Metabolic Derangements Associated With Diet-Induced Obesity. *Am. J. Physiol. Endocrinol. Metab.* 310 (8), E688–E698. doi: 10.1152/ajpendo.00484.2015
- Smith, K., Karimian Azari, E., LaMoia, T. E., Hussain, T., Vargova, V., Karolyi, K., et al. (2018). T1R2 Receptor-Mediated Glucose Sensing in the Upper Intestine Potentiates Glucose Absorption Through Activation of Local Regulatory Pathways. *Mol. Metab.* 17, 98–111. doi: 10.1016/j.molmet.2018.08.009
- Solemdal, K., Sandvik, L., Willumsen, T., Mowe, M., and Hummel, T. (2012). The Impact of Oral Health on Taste Ability in Acutely Hospitalized Elderly. *PLoS One* 7 (5), e36557. doi: 10.1371/journal.pone.0036557
- Starkenmann, C., Le Calvé, B., Niclass, Y., Cayeux, I., Beccucci, S., and Troccaz, M. (2008). Olfactory Perception of Cysteine-S-Conjugates From Fruits and Vegetables. *J. Agric. Food Chem.* 56 (20), 9575–9580. doi: 10.1021/jf801873h
- Takahashi, N. (2015). Oral Microbiome Metabolism: From “Who Are They?” to “What Are They Doing?” *J. Dental Res.* 94 (12), 1628–1637. doi: 10.1177/0022034515606045



- Tanner, A. C. R., Kressirer, C. A., Rothmiller, S., Johansson, I., and Chalmers, N. I. (2018). The Caries Microbiome: Implications for Reversing Dysbiosis. *Adv. Dental Res.* 29 (1), 78–85. doi: 10.1177/0022034517736496
- Tapanee, P., Tidwell, D. K., Schilling, M. W., Peterson, D. G., and Tolar-Peterson, T. (2021). Genetic Variation in Taste Receptor Genes (1, 1) and Its Correlation With the Perception of Saltiness in Normotensive and Hypertensive Adults. *Int. J. Hypertension* 2021, 5559831. doi: 10.1155/2021/5559831
- Teng, B., Wilson, C. E., Tu, Y.-H., Joshi, N. R., Kinnamon, S. C., and Liman, E. R. (2019). Cellular and Neural Responses to Sour Stimuli Require the Proton Channel Otop1. *Curr. Biol.: CB* 29 (21), 3647–3656.e5. doi: 10.1016/j.cub.2019.08.077
- Tizzano, M., Dvoryanchikov, G., Barrows, J. K., Kim, S., Chaudhari, N., and Finger, T. E. (2008). Expression of Galphal4 in Sweet-Transducing Taste Cells of the Posterior Tongue. *BMC Neurosci.* 9, 110. doi: 10.1186/1471-2202-9-110
- Tizzano, M., Gulbransen, B. D., Vandenbeuch, A., Clapp, T. R., Herman, J. P., Sibhatu, H. M., et al. (2010). Nasal Chemosensory Cells Use Bitter Taste Signaling to Detect Irritants and Bacterial Signals. *Proc. Natl. Acad. Sci. U. S. A.* 107 (7), 3210–3215. doi: 10.1073/pnas.0911934107
- Tran, H. T. T., Herz, C., Ruf, P., Stetter, R., and Lamy, E. (2018). Human T2R38 Bitter Taste Receptor Expression in Resting and Activated Lymphocytes. *Front. Immunol.* 9. doi: 10.3389/fimmu.2018.02949
- Tu, Y.-H., Cooper, A. J., Teng, B., Chang, R. B., Artiga, D. J., Turner, H. N., et al. (2018). An Evolutionarily Conserved Gene Family Encodes Proton-Selective Ion Channels. *Science (New York N.Y.)* 359 (6379), 1047–1050. doi: 10.1126/science.aao3264
- van de Wouw, M., Schellekens, H., Dinan, T. G., and Cryan, J. F. (2017). Microbiota-Gut-Brain Axis: Modulator of Host Metabolism and Appetite. *J. Nutr.* 147 (5), 727–745. doi: 10.3945/jn.116.240481
- von Molitor, E., Riedel, K., Krohn, M., Hafner, M., Rudolf, R., and Cesetti, T. (2021). Sweet Taste Is Complex: Signaling Cascades and Circuits Involved in Sweet Sensation. *Front. Hum. Neurosci.* 15. doi: 10.3389/fnhum.2021.667709
- Wang, H., Zhou, M., Brand, J., and Huang, L. (2009). Inflammation and Taste Disorders: Mechanisms in Taste Buds. *Ann. New York Acad. Sci.* 1170, 596–603. doi: 10.1111/j.1749-6632.2009.04480.x
- Wan, Y., Wang, F., Yuan, J., Li, J., Jiang, D., Zhang, J., et al. (2019). Effects of Dietary Fat on Gut Microbiota and Faecal Metabolites, and Their Relationship With Cardiometabolic Risk Factors: A 6-Month Randomised Controlled-Feeding Trial. *Gut* 68 (8), 1417–1429. doi: 10.1136/gutjnl-2018-317609
- Welcome, M. O. (2020). The Bitterness of Genitourinary Infections: Properties, Ligands of Genitourinary Bitter Taste Receptors and Mechanisms Linking Taste Sensing to Inflammatory Processes in the Genitourinary Tract. *Eur. J. Obstet. Gynecol. Reprod. Biol.* 247, 101–110. doi: 10.1016/j.ejogrb.2020.02.015
- Wendell, S., Wang, X., Brown, M., Cooper, M. E., DeSensi, R. S., Weyant, R. J., et al. (2010). Taste Genes Associated With Dental Caries. *J. Dental Res.* 89 (11), 1198–1202. doi: 10.1177/0022034510381502
- Workman, A. D., Palmer, J. N., Adappa, N. D., and Cohen, N. A. (2015). The Role of Bitter and Sweet Taste Receptors in Upper Airway Immunity. *Curr. Allergy Asthma Rep.* 15 (12), 72. doi: 10.1007/s11882-015-0571-8
- Yamaguchi, S., and Ninomiya, K. (2000). Umami and Food Palatability. *J. Nutr.* 130 (4), 921S–926S. doi: 10.1093/jn/130.4.921S
- Ye, W., Chang, R. B., Bushman, J. D., Tu, Y.-H., Mulhall, E. M., Wilson, C. E., et al. (2016). The K<sup>+</sup> Channel KIR2.1 Functions in Tandem With Proton Influx to Mediate Sour Taste Transduction. *Proc. Natl. Acad. Sci. U. S. A.* 113 (2), E229–E238. doi: 10.1073/pnas.1514282112
- Zhang, J., Jin, H., Zhang, W., Ding, C., O'Keefe, S., Ye, M., et al. (2019). Sour Sensing From the Tongue to the Brain. *Cell* 179 (2), 392–402.e15. doi: 10.1016/j.cell.2019.08.031
- Zhang, Z., Zhao, Z., Margolskee, R., and Liman, E. (2007). The Transduction Channel TRPM5 is Gated by Intracellular Calcium in Taste Cells. *J. Neurosci.* 27 (21), 5777–5786. doi: 10.1523/JNEUROSCI.4973-06.2007
- Zhao, G. Q., Zhang, Y., Hoon, M. A., Chandrashekar, J., Erlenbach, I., Ryba, N. J., et al. (2003). The Receptors for Mammalian Sweet and Umami Taste. *Cell* 115 (3), 255–266. doi: 10.1016/s0092-8674(03)00844-4
- Zheng, X., Tizzano, M., Redding, K., He, J., Peng, X., Jiang, P., et al. (2019). Gingival Solitary Chemosensory Cells are Immune Sentinels for Periodontitis. *Nat. Commun.* 10 (1), 4496. doi: 10.1038/s41467-019-12505-x
- Zhou, Z., Xi, R., Liu, J., Peng, X., Zhao, L., Zhou, X., et al. (2021). TAS2R16 Activation Suppresses LPS-Induced Cytokine Expression in Human Gingival Fibroblasts. *Front. Immunol.* 12. doi: 10.3389/fimmu.2021.726546
- Zhu, J. H., Zheng, X., Peng, X., Xu, X., Margolskee, R., and Zhou, X. D. (2021). Regulation Effect of Lipopolysaccharide on the Alternative Splicing and Function of Sweet Taste Receptor T1R2. *Hua Xi Kou Qiang Yi Xue Za Zhi* 39 (4), 469–474. doi: 10.7518/hxkq.2021.04.015

**Conflict of Interest:** The authors declare that the research was conducted in the absence of any commercial or financial relationships that could be construed as a potential conflict of interest.

**Publisher's Note:** All claims expressed in this article are solely those of the authors and do not necessarily represent those of their affiliated organizations, or those of the publisher, the editors and the reviewers. Any product that may be evaluated in this article, or claim that may be made by its manufacturer, is not guaranteed or endorsed by the publisher.

Copyright © 2022 Dong, Liu, Zhu, Zhou, Tizzano, Peng, Zhou, Xu and Zheng. This is an open-access article distributed under the terms of the Creative Commons Attribution License (CC BY). The use, distribution or reproduction in other forums is permitted, provided the original author(s) and the copyright owner(s) are credited and that the original publication in this journal is cited, in accordance with accepted academic practice. No use, distribution or reproduction is permitted which does not comply with these terms.



# Frontiers in Cellular and Infection Microbiology

Investigates how microorganisms interact with their hosts

Explores bacteria, fungi, parasites, viruses, endosymbionts, prions and all microbial pathogens as well as the microbiota and its effect on health and disease in various hosts.

## Discover the latest Research Topics

[See more →](#)

### Frontiers

Avenue du Tribunal-Fédéral 34  
1005 Lausanne, Switzerland  
[frontiersin.org](https://frontiersin.org)

### Contact us

+41 (0)21 510 17 00  
[frontiersin.org/about/contact](https://frontiersin.org/about/contact)

